BINDING SERVICES
Tel +44 (0)29 2087 4949
Fax +44 (0)29 20371921
e-mail bindery@cardiff.ac.uk

Synthesis and evaluation of inhibitors against vitamin D_3 and all-*trans* retinoic acid metabolising enzymes as potential therapy for androgen-independent prostate cancer

Sook Wah Yee

A thesis submitted in accordance with the conditions governing candidates for the degree of Philosophiae Doctor (PhD)

2005

Medicinal Chemistry Division, Welsh School of Pharmacy, Cardiff University

ProQuest LLC
789 East Eisenhower Parkway
P.O. Box 1346
Ann Arbor, MI 48106-1346

Declaration

This work has not previously been accepted in substance for any degree and is not being concurrently submitted in candidature for any degree.

Signed 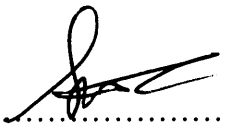 (candidate)

Date 14 Oct 2005

STATEMENT 1

This thesis is the result of my own investigations, except where otherwise stated.

Other sources are acknowledged by footnotes giving explicit references. A bibliography is appended.

Signed 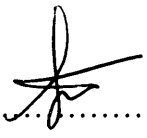 (candidate)

Date 14 Oct 2005

STATEMENT 2

I hereby give consent for my thesis, if accepted, to be available for photocopying and for inter-library loan, and for the title and summary to be made available to outside organisations.

Signed 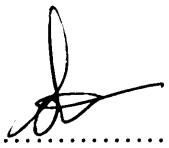 (candidate)

Date 14 Oct 2005

献给我致爱的父母亲—抗癌的勇士

To my mother and father for their enormous courage and strength in fighting cancer

Acknowledgements

I am grateful to many people whom I have benefited from and who have contributed in different ways to the progress and development of this thesis. The person whom I am indebted to is my great supervisor, Dr. Claire Simons, who has always been very encouraging and supportive throughout my thesis, and has given me all the opportunities to experience and to explore in this stimulating and interesting research. Secondly, I would like to thank the Tenovus Cancer Research cell culture group, Dr. Bronwen A.J. Evans, Mrs. Carole Elford, Dr. Moray J. Campbell, Dr. Marc Le Borgne, Dr. Michael P. Coogan and Dr. Liling Ooi, for their valuable guidance and collaborations. Thirdly, I would like to thank all my friends, colleagues and the staff members in the Redwood building, for the pleasant company and interesting thoughts and ideas. I would like to extend my sincere gratitude to Dr. Kenneth T. Wann for his valuable support from the beginning of my stay in UK (eight years in total). I would also like to acknowledge the ORS Awards Scheme for a United Kingdom Scholarship. Finally, and most important, I wish to thank my mother and father, to whom this thesis is dedicated. Their constant love, inspiration and encouragement are immeasurable. Their strong will power in fighting and surviving cancer has always given me the motivation and enthusiasm in wanting to find a cure for cancer.

Abstract

The majority of prostate cancer patients demonstrate good initial responses to surgical castration and/or hormonal therapy. Unfortunately, hormonal therapy is not capable of producing durable responses in the majority of the patients who subsequently develop androgen-independent prostate cancer (AIPC). New effective therapies are needed in the management of AIPC patients.

One potential therapeutic strategy is to employ a differentiating agent to suppress prostate cancer cell proliferation. 1α,25-Dihydroxyvitamin D_3 (1α,25-$(OH)_2$-D_3) and all-*trans* retinoic acid (ATRA) have differentiating and anti-proliferative effects on prostate cancer cells. However, the use of 1α,25-$(OH)_2$-D_3 and ATRA is limited by the induction of the cytochrome P450 enzymes. The P450 enzymes that are responsible for the catabolism of 1α,25-$(OH)_2$-D_3 and ATRA are cytochrome 24 (CYP24) and 26 (CYP26) respectively. ATRA is also metabolised by other P450 4-hydroxylase enzymes in the liver. Therefore, a drug which can prolong the action of 1α,25-$(OH)_2$-D_3 or ATRA by inhibiting the P450 enzymes could have potential use in the treatment of AIPC.

Three series of novel compounds were synthesised in an attempt to probe for the key binding residues in the enzymes. The preparation of the rat kidney mitochondria and rat liver microsome enzymes were described herein to study the inhibition of the 25-hydroxyvitamin D_3 and ATRA metabolism respectively using the synthesised compounds. In addition, cancer cell-lines (MCF-7 and DU-145) were also used to study the inhibition of the 25-hydroxyvitamin D_3 and ATRA metabolism using the synthesised compounds. Reverse-transcriptase-polymerase chain reaction (RT-PCR) analysis was carried out to demonstrate the presence of CYP24 and CYP26 mRNA in the cancer cell-lines. Some of the synthesised compounds described herein show improved activities compared with ketoconazole and/or liarozole in these *in vitro* assays. Molecular docking studies using the homology model of CYP26 was carried out to investigate the binding of the substrate, ATRA and the synthesised compounds at the active site.

Furthermore, the anti-proliferative effects of some synthesised compounds, both alone and in combination with 1α,25-$(OH)_2$-D_3 in human prostate cancer cells (DU-145 and PC-3) were examined. The effects of ketoconazole and one of the synthesised compounds were further investigated to examine their effects, both alone and in combination with 1α,25-$(OH)_2$-D_3 on the vitamin D_3 target genes in DU-145 and PC-3 by real-time quantitative RT-PCR.

List of conference abstracts and papers

The following titles have been presented either as a conference abstract or paper. The full conference abstracts (**1 – 5**) and papers (**6 – 8**) can be seen in **Appendix 2**.

1. Design and synthesis of benzofuran derivatives as CYP24 inhibitors for androgen-independent prostate cancer.
   Poster presentation. European Conference of the Pharmaceutical Chemistry Group of the Atlantic Arc (GP2A), October 2003, La Rochelle, France.
2. Design and synthesis of P450 enzyme inhibitors as differentiating agent for androgen-independent prostate cancer.
   Oral presentation. International Symposium of Medicinal Chemistry, August 2004, Copenhagen, Denmark.
3. Synthesis and evaluation of tetralone derivatives: P450 enzyme inhibitors as differentiating agents for the treatment of hormone-refractory prostate cancer. *Oral and poster presentation. British Pharmaceutical Conference, September 2004, Manchester, UK.*
4. Synthesis and evaluation of retinoic acid metabolism blocking agents (RAMBAs) as indirect differentiating agents for cancer therapeutics.
   Oral presentation. American Chemical Society national meeting, March 2005, San Diego, USA.
5. Design and assessment of novel inhibitors of CYP24 to enhance VDR signalling in androgen-independent prostate cancer cells.
   Poster presentation. NCRI (National Cancer Research Institute) Conference, October 2005, Birmingham, UK.
6. Yee S.W. and Simons C. (2004) Synthesis and CYP24 inhibitory activity of 2-substituted-3,4-dihydro-2*H*-naphthalen-1-one (tetralone) derivatives. *Bioorg. Med. Chem. Lett.*, **14**, 5651-5654.
7. Yee S.W., Jarno, L., Gomaa M.S., Elford, C., Ooi, L.L., Coogan, M.P., McClelland, R., Nicholson, R.I., Evans, B.A.J., Brancale, A. and Simons, C. (2005) Novel tetralone-derived retinoic acid metabolism blocking agents (RAMBAs): Synthesis and *in vitro* evaluation with liver microsomal and MCF-7 CYP26A1 cell assays. *J. Med. Chem.*, accepted for publication.
8. Yee S.W., Campbell M.J. and Simons C (2005) Inhibition of Vitamin D_3 metabolism enhances VDR signalling in androgen-independent prostate cancer cells. *J. Steroid Biochem. Molec. Biol.*, in manuscript.

Contents

Abbreviations

Abbreviation	Distribution
25-(OH)-D_3	25-Hydroxyvitamin D_3
1α,25-$(OH)_2$-D_3	1α,25-Dihydroxyvitamin D_3 (Calcitriol)
24,25-$(OH)_2$-D_3	24,25-Dihydroxyvitamin D_3
1α,24, 25-$(OH)_3$-D_3	1α,24,25-Trihydroxyvitamin D_3
ACTH	Andrenocorticotrophic hormone
AIPC	Androgen-independent prostate cancer [synonym: hormone-refractory prostate cancer (HRPC)]
AR	Androgen receptor
ARE	Androgen response element
ATRA	All-*trans* retinoic acid
BPH	Benign prostatic hyperplasia
CDI	1,1'-Carbonyldiimidazole
cDNA	Complementary deoxyribose nucleic acid
CRH	Corticotrophin-releasing hormone
CSCC	Cholesterol side-chain cleavage
CYP1α	Cytochrome P450 1α-hydroxylase
CYP24	Cytochrome P450 24-hydroxylase
DCM	Dichloromethane
DES	Diethylstibestrol
DHEA	Dehydroepiandrosterone
DHT	Dihydrotestosterone
DMF	Dimethyl formamide
DMSO	Dimethyl sulfoxide
DNA	Deoxyribonucleic acid
DRE	Digital rectal examination
EI	Electron ionisation
ES	Electron spray
EtOAc	Ethyl acetate

EtOH	Ethanol
FBS	Foetal bovine serum
FCS	Foetal calf serum
FDA	Food and drug admistration
FSH	Follicle-stimulating hormone
GADD45α	Growth-arrest and DNA-damage gene
GH	Growth hormone
HPLC	High performance liquid chromatography
HMBC	Heteronuclear multiple bond coherence
HRMS	High resolution mass spectrum
HRPC	Hormone-refractory prostate cancer [synonym: androgen-independent prostate cancer (AIPC)]
HSD	Hydroxysteroid dehydrogenase
HSQC	Heteronuclear single quantum coherence
LH	Luteinising hormone
LHRH	Luteinising hormone-releasing hormone
MeOH	Methanol
MOE	Molecular operating environment
MS	Mass spectrometry
NADPH	Nicotinamide-adenine dinucleotide phosphate (reduced form)
n.m.r.	Nuclear magnetic resonance
PBS	Phosphate buffer saline
PCR	Polymerase chain reaction
PDB	Protein data bank
PSA	Prostatic specific antigen
PTH	Parathyroid hormone
qPCR	Real-time quantitative RT-PCR
RA	Retinoic acid
RAMBA	Retinoic acid metabolism blocking agent
r.t.	Room temperature
RT	Reverse transcriptase

S-FCS	Steroid-depleted foetal calf serum
THF	Tetrahydrofuran
t.l.c.	Thin layer chromatography
TNM	Tumour node metastases
TRUS	Transrectal ultrasound
VDR	Vitamin D receptor
VDRE	Vitamin D response element
v/v	volume/volume
wRPMI	Phenol-red free RPMI media

CHAPTER 1

Introduction

1. Introduction

1.1 Prostate cancer and treatment

1.1.1 Incidence

Prostate cancer, is the most common cancer among males in the USA, with an estimated 232,090 new cases and 30,350 deaths for 2005 alone, *i.e.* 1 in 6 men (Jemal *et al.*, 2005). Prostate cancer was the sixth most common cancer in the world (Parkin, 2004) and third most common cancer in men in Europe (Bhandari *et al.*, 2005), with some 156,000 new cases in 1995 (Bray *et al.*, 2002).

1.1.2 The prostate gland

The prostate gland is an organ situated just below the bladder and in front of the rectum (**Figure 1.1.1**). It plays a role in producing the fluid that transports semen during ejaculation. The size and shape of the prostate gland are variable, but it is usually about 2 – 3 inches in diameter and the weight of a normal adult prostate is approximately 20 g (Griffin, 2000).

The prostate gland is composed of tall columnar secretory epithelial cells and stromal cells. The epithelial and stromal cells interact closely to maintain the normal function of the prostate gland (DeMarzo *et al.*, 2003).

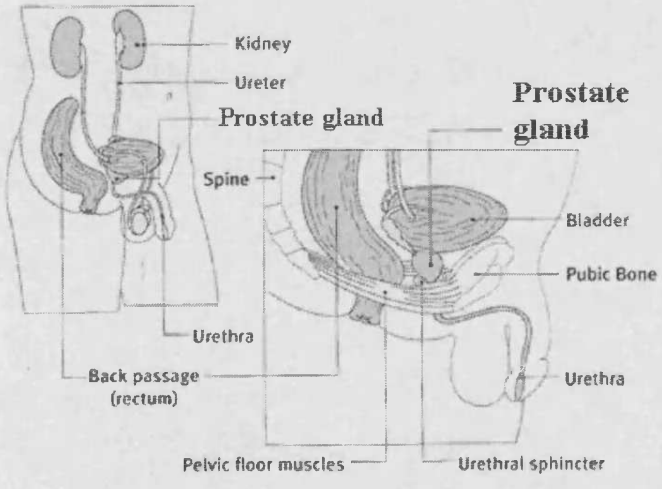

Figure 1.1.1. The location of the prostate gland in males (Christie Hospital NHS Trust, 2003).

1.1.3 Risk factors of prostate cancer

1.1.3.1 Age

Prostate cancer is a disease associated with increasing age, with 78 % cases are in men aged 65 years or above (Parkin, 2004). Autopsy studies reveal that the majority of men over 80 years old have areas of malignant tissue in their prostate glands; most die with it, not of it (Selley *et al.*, 1997c).

1.1.3.2 Race

Prostate cancer incidence and mortality rates vary widely between ethnic groups (Sasagawa and Nakada, 2001). Both incidence and mortality data reveal that the incidence of clinical prostate cancer is low in Asian men and higher in Scandinavian men (Boring *et al.*, 1992). Incidence rates vary 120-fold between Chinese men and African-American men living in San Francisco (Pienta and Esper, 1993). It is unclear if this is based on genetic or environmental factors; however, migration studies demonstrate that men tend to take on the risk for their host countries. An example of this is, Japanese-Americans show higher mortality rates when compared with the mortality rates in Japan (Cook *et al.*, 1999). The possible explanation for differences in the incidence and mortality of prostate cancer is the dietary differences between ethnicities (Muir *et al.*, 1991; Yu *et al.*, 1991).

1.1.3.3 Diet

There has been considerable interest in evaluating the link between diet and prostate cancer, particularly dietary fat and vitamins.

Dietary fat is most frequently associated with prostate cancer. Rose and colleagues have shown a positive correlation between the mortality rate for prostate cancer and animal fat consumption by country (Rose *et al.*, 1986). Several other studies also confirmed this relationship between high dietary fat and increased prostate cancer risk (Heshmat *et al.*, 1985; Mettlin *et al.*, 1989; Mills *et al.*, 1989; Slattery *et al.*, 1990; Snowdon *et al.*, 1984).

The n-3 and n-6 polyunsaturated fatty acids have been shown in laboratory studies to have beneficial and risk factors, respectively, for several kinds of malignancy including prostate (Bagga *et al.*, 1997; Gann *et al.*, 1994; Harvei *et al.*, 1997). Epidemiological data reported by Terry's group indicated that fish fat consumption lowers the risk of prostate cancer (Terry *et al.*, 2001). Persons who consume fish (including salmon, herring and mackerel which contain a high amount of n-3 fatty acid)

had a lower relative risk of prostate cancer either diagnosed or cancer death compared with persons who consumed less fish (Terry *et al.*, 2001). The n-3 fatty acid is thought to influence cellular proliferation, the immune system and the potential of a tumour to invade locally and metastasise (Karmali, 1987).

Vitamins and supplement which have been shown by epidemiology or laboratory study to have protective effects on prostate cancer are as following and have been reviewed in detail by few authors (Heshmat *et al.*, 1985; Willis and Wians Jr., 2003).

- Vitamin A (Cohen *et al.*, 2000; Giovannucci, 1999)
- Vitamin E and D (Heinonen *et al.*, 1998; Klein, 2005; Schwartz and Hulka, 1990)
- Phytoestrogens (Adlercreutz, 2002; Jacobsen *et al.*, 1998; Klein, 2005; Shirai *et al.*, 2002; Wang *et al.*, 2002).

The role of vitamin A and vitamin D_3 in prostate cancer will be discussed in section **1.6** of this chapter.

1.1.3.4 Family history and genetic factors

Several studies reveal a positive association between family history and prostate cancer risk (Goldgar *et al.*, 1994; Steinberg *et al.*, 1990). The risk for the first degree relative of a man diagnosed with prostate cancer is 2 - 3 fold compared with the risk of a man with no family history (Steinberg *et al.*, 1990).

Researchers at the National Center for Human Genome Research, The Johns Hopkins University and Umeå University, Sweden, have identified the location of the first major gene that predisposes men to prostate cancer. They reported the localisation of a major susceptibility locus for prostate cancer (*HPC*1) to chromosome 1 (band q24-25). This international study involved 91 families with at least three first degree relatives with prostate cancer (Smith *et al.*, 1996).

The two main genetic studies which demonstrated the gene that are associated with the risk and progression of prostate cancer are:

- Vitamin D receptor gene polymorphism (Habuchi *et al.*, 2000; Ingles *et al.*, 1997; Taylor *et al.*, 1996). Two separate epidemiology studies involved white and black men in the United States (Ingles *et al.*, 1997) and the Japanese group (Habuchi *et al.*, 2000) revealed that inherited polymorphisms in the VDR gene may be linked with prostate cancer risk.

- The polymorphic CAG repeat sequence in the androgen receptor gene. A few research groups have found that men with short CAG repeat lengths had a higher risk of prostate cancer (Giovannucci *et al.*, 1997; Ingles *et al.*, 1997; Irvine *et al.*, 1995). Coetzee and Ross postulated that a short CAG repeat lengths is associated with a higher level of androgen receptor transactivation function, therefore possibly resulting in a higher risk of prostate cancer (Coetzee and Ross, 1994).

1.1.3.5 Hormones

Steroid hormones play important role in the growth of the normal prostate epithelium and in the development of prostatic cancer. This is widely supported by the fact that: (**1**) prostate cancer does not occur in eunuchs and the incidence is very low in castrated men (Pienta and Esper, 1993); (**2**) the incidence of microscopic, latent prostate cancer show a very close correlation with increasing age (Wilding, 1995); (**3**), orchiectomy and anti-androgen therapy play a vital role in the first-line treatment of prostate cancer (McLeod, 2003).

1.1.4 Diagnosis and screening of prostate cancer

Early diagnosis of prostate cancer could provide improved prognostic factors and could lower the mortality and morbidity rate (Selley *et al.*, 1997c). Patients with prostate cancer will complain of having nocturia, increase in urination frequency and urgency, which is a result of urinary tract obstruction due to the enlarged prostate gland (Selley *et al.*, 1997a). Patients can be asymptomatic during the early stage, therefore screening for prostate cancer by the Prostate-Specific Antigen (PSA) testing is very important.

The first stage of diagnosis of prostate cancer is to measure serum PSA level and to carry out a Digital Rectal Examination (DRE). If there are suspicious findings from either of these tests, transrectal ultrasound technology will be used to allow histological confirmation of the presence of prostate cancer (Selley *et al.*, 1997a).

1.1.4.1 PSA test

PSA is a glycoprotein which is secreted by prostate epithelium (Garnick, 1993). PSA is found mainly in the semen, and a small amount is present in the blood serum. An immuno-assay method is used to measure the PSA level (Garnick, 1993). Most men have levels under 4 ng/mL in the blood (Garnick, 1993). The PSA level is

raised after ejaculation, after prostate biopsy, surgery, prostatitis and also in patients with benign prostatic hyperplasia and prostate cancer (Frankel *et al.*, 2003). Therefore, PSA measurement should always be carried out before prostate biopsy (Garnick, 1993).

Although PSA testing is not specific for prostate cancer, it is a quick and easy diagnostic tool for screening and staging of prostate cancer (Frankel *et al.*, 2003). Moreover, PSA testing is important in patient undergoing prostate cancer treatment, as the patient's PSA level can be an indicator as to how well the treatment is working for the patient (Selley *et al.*, 1997c).

1.1.4.2 Digital rectal examination (DRE)

DRE is a common diagnostic and screening test for prostate cancer. During the examination, the doctor inserts the finger into the rectum to examine whether there is the presence of an abnormal mass in the prostate gland (Selley *et al.*, 1997a). Similarly to PSA testing, DRE is also used for screening, diagnostic and clinical staging of prostate cancer.

1.1.4.3 Transrectal ultrasound (TRUS)

This is used in the diagnosis and clinical staging of prostate cancer. The doctor will use transrectal ultrasound (TRUS) to guide the biopsy needle through the wall of the rectum and into several areas of the prostate gland to remove samples of prostate tissues. Samples obtained allow accurate histologic grades of the sample neoplasm by the pathologist (Selley *et al.*, 1997a).

1.1.5 Staging of prostate cancer

1.1.5.1 Pathologic evaluation

Pathologists grade the prostate cancers according to the Gleason system. The pathologist determines the differentiation of the tumour cells (Selly *et al.*, 1997b). Gleason grade ranging from 1 to 5 divides the prostate cancer into 5 different histologic patterns. Gleason grade 1 represent well-differentiated prostate cancer (*i.e.* least aggressive), whereas Gleason grade 5 represent poorly-differentiated or anaplastic lesion (*i.e.* most aggressive tumour cells). A grade is assigned in two different areas that best describe the cancerous cells/tissues. These two grades are added together to give the Gleason score, ranging from 2 to 10. Scores of below 7 tend to have better prognosis (Selly *et al.*, 1997b).

1.1.5.2 Clinical evaluation

The most commonly used staging system for prostate cancer is called the TNM System of the American Joint Committee on Cancer (AJCC) (Selly *et al.*, 1997b). The TNM system applies to both clinical as well as pathological staging (see **Box 1**). This system describes the extent of the primary tumour (T stage), whether or not the cancer has spread to nearby lymph nodes (N stage) and the absence or presence of distant metastasis (M stage) (Selly *et al.*, 1997b). Once this is determined, this is then combined with the Gleason score to give the stage grouping (**Box 1**), ranging from **Stage 0** to **Stage IV**.

Box 1.1. The staging system for prostate cancer: the TNM system of the American Joint Committee on Cancer (AJCC). Permission granted from AJCC (American Joint Committee on Cancer, 1992).

Primary Tumour (T)

TX Primary tumour cannot be assessed

T0 No evidence of primary tumour

T1 Clinically inapparent tumour not palpable or visible by imaging
- **T1a** Tumour incidental histologic finding in 5 % or less of tissue resected
- **T1b** Tumour incidental histologic finding in more than 5 % of tissue resected
- **T1c** Tumour identified by needle biopsy (*e.g.*, because of elevated PSA)

T2 Tumour confined within the prostate*
- **T2a** Tumour involves half of a lobe or less
- **T2b** Tumour involves more than half of a lobe, but not both lobes
- **T2c** Tumour involves both lobes

T3 Tumour extends through the prostatic capsule**

T4 Tumour is fixed or invades adjacent structures other than the seminal vesicles
- **T4a** Tumour invades any of: bladder neck, external sphincter, or rectum
- **T4b** Tumour invades levator muscles and/or fixed to the pelvic wall

***Note**: Tumour found in one or both lobes by needle biopsy, but not palpable or visible by imaging, is classified as **T1c**.

****Note**: Invasion into the prostatic apex or into (but not beyond) the prostatic capsule is not classified as **T3**, but as **T2**.

Regional Lymph Nodes (N)

NX Regional lymph nodes cannot be assessed

N0 No regional lymph node metastasis

N1 Metastasis in a single lymph node, 2 cm or less in greatest dimension

N2 Metastasis in a single lymph node, more than 2 cm but not more than 5 cm in greatest dimension; or multiple lymph node metastases, none more than 5 cm in greatest dimension

N3 Metastasis in lymph node more than 5 cm in greatest dimension

Distant Metastasis (M)

MX Presence of distant metastasis cannot be assessed
M0 No distant metastasis

M1 Distant metastasis
- **M1a** Nonregional lymph node(s)
- **M1b** Bone(s)
- **M1c** Other site(s)

Histopathologic Grade (G)

GX Grade cannot be assessed

G1 Well differentiated (slight anaplasia)

G2 Moderately differentiated (moderate anaplasia)

G3-4 Poorly differentiated or undifferentiated (marked anaplasia)

Stage Grouping

Stage 0	T1a	N0	M0	G1
Stage I	T1a	N0	M0	G2, G3-4
	T1b	N0	M0	Any G
	T1c	N0	M0	Any G
	T1	N0	M0	Any G
Stage II	T2	N0	M0	Any G
Stage III	T3	N0	M0	Any G
Stage IV	T4	N0	M0	Any G
	Any T	N1	M0	Any G
	Any T	N2	M0	Any G
	Any T	N3	M0	Any G
	Any T	Any N	M1	Any G

1.1.6 Treatment and management of prostate cancer

The clinical management and treatment depend on the prostate cancer disease, patients' life expectancy and patients' health conditions. The National Comprehensive Cancer Network has developed detailed cancer treatment guidelines for prostate cancer health professionals (Scherr *et al.*, 2003). Recent reviews on the management and treatment of prostate cancer according to stages has been published by various authors (Garnick, 1993; Jani and Hellman, 2003; Selley *et al.*, 1997a). The potential benefits and risks of the treatment options should always be considered. The five main types of treatments are described below.

1.1.6.1 Radical prostatectomy

Prostatectomy involves surgical removal of the entire prostate gland and some of the surrounding tissue. During the surgical procedure, the surgeon can assess the pathological disease of the patient, *i.e.* to assess the extention to which the cancer has spread. This could guide the physicians decision whether to give any other adjuvant therapy to the patients (Ohori *et al.*, 1995). Radical retropubic prostatectomy, radical perinial prostatectomy and radical laproscopic prostatectomy are the three different types of radical prostatectomy. Radical retropubic prostatectomy involves skin incision in the lower abdomen to allow the removal of the whole prostate gland and the seminal vesicles. Complications associated with radical retropubic prostatectomy are intraoperative bleeding and postoperative complication, for examples, urinary incontinence and impotence (Catalona *et al.*, 1999; Lepor *et al.*, 2001; Stanford *et al.*, 2000). Radical perinial prostatectomy and radical laproscopic prostatectomy have not achieved widespread use due to a lack of evidence of the long term efficacy.

1.1.6.2 Radiation therapy

Radiation therapy is used to kill cancer cells by high energy particles can be divided into two main types, namely the external-beam radiotherapy and brachytherapy.

External-beam radiation therapy

The use of external-beam radiation therapy has been studied and carried out extensively for early-stage and locally advanced prostate cancer. External-beam radiation therapy has undergone a technological revolution and, has shown promising success rate and reduction of side effects (Hanlon and Hanks, 2000; Shipley *et al.*, 1999; Zagars *et al.*, 1997; Zietman *et al.*, 1995). The two newer form of external-beam radiation therapy, namely the three-dimensional conformal radiation therapy (3DCRT) and the intensity-modulate radiation therapy (IMRT) minimizes the dose of radiation reaching normal tissues while delivering high dose to the cancer cells to minimize complications (Pollack *et al.*, 2000; Zelefsky *et al.*, 2001).

Brachytherapy

Brachytherapy involves the use of small radioactive pellets that are implanted directly into the prostate gland. Transrectal ultrasound, CT scans or MRI is used to guide the placement of the radioactive material. The use of this treatment for early-stage prostate cancer is positive and its use can achieve disease-free survival comparable with

those of radical prostatectomy and external-beam radiotherapy (Jani and Hellman, 2003). The two main types of brachytherapy are the low-dose rate using low energy radioactive sources (Iodine-125 or Palladium-103) and the high-dose rate using high dose radioactive source (Iridium-192) (Vicini *et al.*, 1999). Brachytherapy provides a more localised dose distribution compared with external-beam radiation therapy (Vicini *et al.*, 1999). In the external-beam radiation therapy, the beam needs to transverse across normal tissues, such as, the bladder and rectum in order to reach the prostate. As a result, brachytherapy provides a lower incidence of rectal and neurovascular side-effects (Merrick *et al.*, 2000; Merrick *et al.*, 2001; Potters *et al.*, 2001).

Overall, radiation therapy is a non-invasive method, with no anaesthesia risk. It is suitable in patients who would not be able to tolerate prostatectomy (Jani and Hellman, 2003).

Although the results were positive in the use of external-beam radiation therapy (Koper *et al.*, 1999) and brachytherapy (Martinez *et al.*, 2001; Vicini *et al.*, 1999), there is a lack of randomized trials comparing radiotherapy with surgery for prostate cancer (Fletcher and Theodorescu, 2005).

1.1.6.3 Hormone therapy

Surgery and radiation therapy is the mainstay of treatment for early-stage prostate cancer. Whereas, treatment for locally or advanced disease rely on hormonal therapies to suppress the testosterone production (Scherr *et al.*, 2003). The available hormonal therapies could be divided into 4 groups, which will be discussed in detail here.

Oestrogen therapy

Oestrogen therapy in the form of diethylstilbestrol (DES) (**Figure 1.1.2**) was the earliest form of treatment for advanced prostate cancer in the 1980s (Scherr *et al.*, 2002). DES is the first non-steroidal compound with potent oestrogenic activity (Dodds *et al.*, 1938).

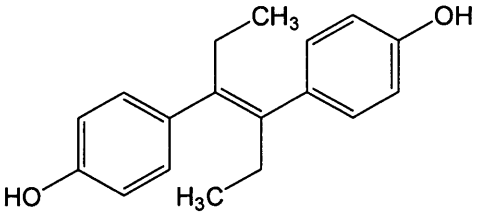

Figure 1.1.2. The chemical structure of *trans*-diethylstilbestrol.

DES has an effect on suppressing the production of testosterone by suppression of pituitary luteinising hormone (LH) secretion from the pituitary gland (Malkowicz, 2001). Moreover, DES can increase the level of sex-hormone-binding globulin (SHBG), increase pituitary prolactin secretion and decrease testosterone production in the testes (Malkowicz, 2001). DES also gives a direct cytotoxic effect in prostate cancer *in vitro* through cell cycle control and apoptosis mechanism (Robertson *et al.*, 1996).

The use of DES has fallen out of favour due to the unfavourable side-effects (Zagars *et al.*, 1988). The most complicated side-effects are cardiovascular side-effects, for example, myocardial infarction and deep vein thrombosis (Malkowicz, 2001); gynaecomastia, nipple tenderness and breast pain (Stege, 2000). Unlike other hormonal therapy, DES offers additional benefits besides suppressing testosterone production, *i.e.*, it does not cause bone loss and therefore has no potential of leading to osteoporosis (Scherr *et al.*, 2002).

Luteinising Hormone-Releasing Hormone (LHRH) Agonists

Luteinising Hormone-Releasing Hormone (LHRH) was first isolated by Schally's group (Schally *et al.*, 2000) from porcine hypothalamic extracts. They demonstrated that this decapeptide (**Figure 1.1.3**) is responsible for the release of luteinising hormone (LH).

It was found that substitution of the amino acids in the basic LHRH structure, resulted in LHRH analogues with potent agonist activity. Paradoxically, it was found that these LHRH agonists decrease, rather than increase both the LH and testosterone levels and that they were very effective in reducing the serum testosterone levels (McLeod, 2003). The mode of action of LHRH agonist is to downregulate the LHRH receptors at the pituitary level, thus decreasing the release of testosterone (Limonta *et al.*, 2001). A recent review anticipated that LHRH may exert direct anti-proliferative and apoptotic effects in prostate cancer cells (Kraus *et al.*, 2005).

The use of LHRH analogues could initially lead to transient elevations in testosterone and dihydrotestosterone levels (Schellhammer, 2001) which is known as "tumour flare". This manifestation of tumour flare may be prevented by 14 to 28 days administration of an antiandrogen drug, such as bicalutamide (Anon, 2005; Dalesio *et al.*, 2000).

LHRH analogues have an increasing role in locally advanced and metastatic prostate cancer (Scherr *et al.*, 2003). There are 4 different LHRH agonist currently available in United Kingdom for the treatment of prostate cancer (Anon, 2005). Common side-effects from LHRH agonist are hot flushes, loss of libido, weight gain, gynaecomastia and osteoporosis (Schally *et al.*, 2000; Seidenfeld *et al.*, 2000).

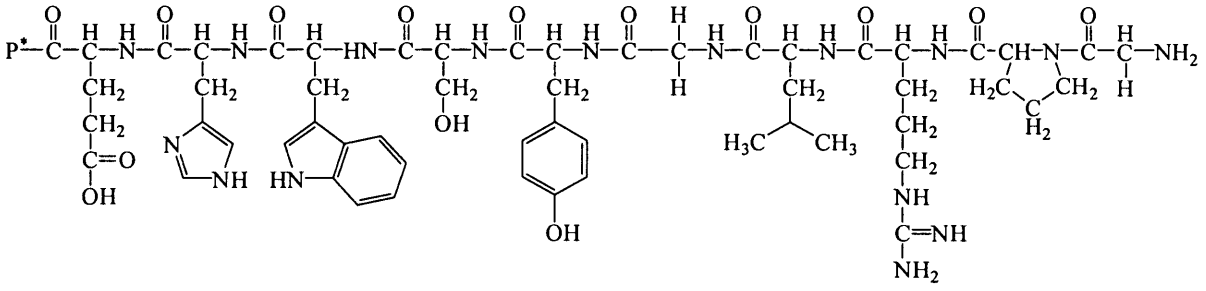

Glutamic Acid — Histidine — Tryptophan — Serine — Tyrosine — Glycine — Leucine — Arginine — Proline — Glycine

P^* = Amino acid-associated protein

Figure 1.1.3. The 10 amino acid sequence of LHRH (Ojeda and McCann, 2000).

Anti-androgen therapy

Anti-androgen drugs, for example, flutamide, bicalutamide (Casodex®) and cyproterone acetate (**Figure 1.1.4**), are used in patients with locally advanced disease (Kolvenbag *et al.*, 2001). The function of anti-androgens is to block the androgen receptor and thus prevent the natural androgen substrate from binding to the androgen receptor. Androgen plays an important role in the pathology of prostate cancer by inducing growth of the prostate cancer cells (Debes and Tindall, 2002).

Monotherapy with 150 mg bicalutamide (Casodex®) has shown an equivalent effect to castration in patients with non-metastatic disease (Abrahamsson, 2001; Iversen *et al.*, 2000; Kolvenbag *et al.*, 2001). However, anti-androgens are not recommended in conjunction with surgical castration (Eisenberger *et al.*, 1998). The side-effects profile for bicalutamide is better in terms of quality-of-life related to sexual interest and physical capacity (Kolvenbag *et al.*, 2001; Seidenfeld *et al.*, 2000).

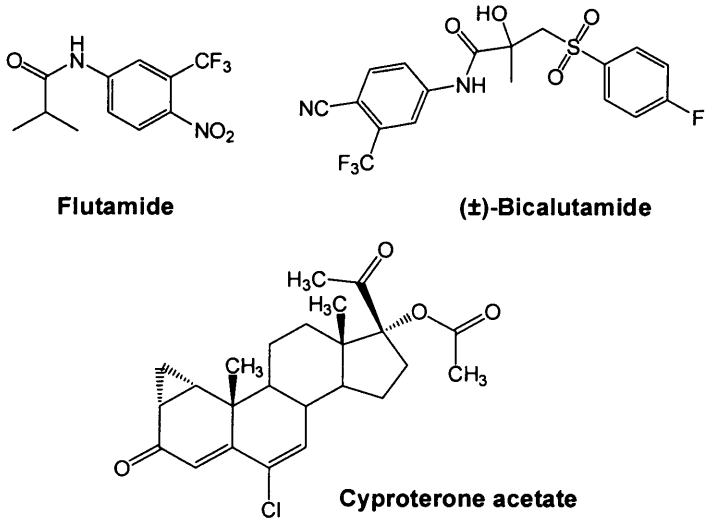

Figure 1.1.4. The chemical structure of the anti-androgen drugs used in locally advanced prostate cancer.

Combined androgen blockade

This therapy involves the combination of an anti-androgen with an LHRH agonist to block androgen synthesis as well as preventing the binding of circulating androgen to the receptors. The use of LHRH analogues alone cannot block the androgen produced by the adrenal gland as the androgen produced from the adrenal gland is controlled by andrenocorticotropic hormone (ACTH). Therefore the use of the combined androgen blockade is to stop the action of the adrenal androgens (Chamberlain *et al.*, 1997a; Dalesio *et al.*, 2000).

1.1.6.4 Chemotherapy

Although more than 85 % of patients with metastatic disease will respond to hormonal therapy, unfortunately, the prostate tumours eventually develop into androgen-independent type. One of the options for these patients with androgen-independent prostate cancer (AIPC) is to use cytotoxic therapy (Berry, 2005; Oh and Kandoff, 1998). The use of mitoxantrone (similar structure to the anthracycline, **Figure 1.15**) plus low dose of prednisolone was approved by Food and Drug Administration (FDA) for patients with AIPC in the 1990s (Moore *et al.*, 1994). It exerts its cytotoxic effect through intercalating between adjacent base pairs of DNA (Skladanowski and Konopa, 2000).

Taxanes, paclitaxel, docetaxel and estramustine were also initiated to test their feasibility and therapeutic potential (Wit de, 2005). In estramustine, oestradiol-17β-phosphate is linked to a nitrogen mustard via a carbamate ester linkage (**Figure 1.1.5**). It

was designed for the purpose of releasing the mustard to the cancer cells, which acts as an alkylating agent, by cleavage of the linkage. However, it was found in *in vivo* and *in vitro* experiments that the mechanism involves the inhibition of microtubule function and mitosis (Hartley-Asp, 1984; Moraga *et al.*, 1992).

Recently two independent randomized studies have demonstrated that docetaxel-based chemotherapy (*i.e* docetaxel plus prednisolone or docetaxel plus estramustine) improves the overall survival of patients with AIPC (Petrylak *et al.*, 2004; Tannock *et al.*, 2004).

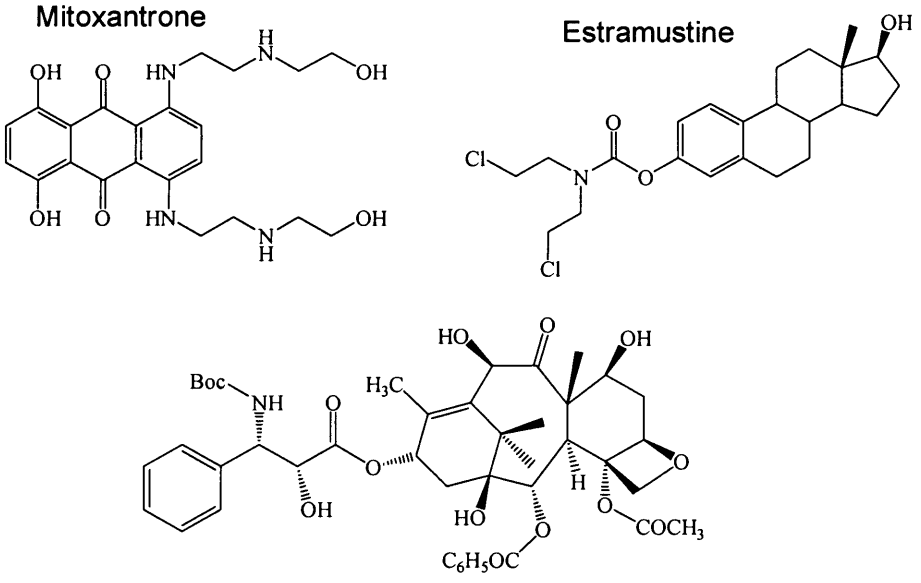

Figure 1.1.5. The chemical structure of the commonly used cytotoxic agents for AIPC.

1.1.6.5 Watchful waiting

This form of management only applies to asymptomatic patients with localised prostate cancer. As the growth of prostate cancer is often very slow, watchful waiting may be the form of prostate cancer management, and more preferable if the patient's life expectancy is less than 10 years. Patients will have regular check-ups which involve PSA testing and DRE (Chamberlain *et al.*, 1997b).

1.1.6.6 New therapy

There are a few promising research areas being investigated as alternative treatments for patients who have developed resistance to the standard androgen-ablation therapy. The American Cancer Society (http://www.cancer.org) has a very useful website to inform patients and health professionals regarding new clinical trials and new

treatments available. Some new approaches and novel agents targeting proteins involved in angiogenesis or cell cycle pathway and other small molecules that target specific signaling pathways have been discussed and reviewed in recent articles (Bhandari *et al.*, 2005; Harris and Reese, 2001; Morris and Scher, 2002; van der Poel, 2004).

1.2 Androgens and prostate cancer

1.2.1 Biosynthesis of steroid hormones

The adrenal cortex, testis and ovary are the major tissues involve in the biosynthesis of steroid hormones. There are three major categories of steroid hormones (**Figure 1.2.2**):

- Mineralocorticoids – These are important for maintaining the body's sodium and potassium content. Synthesis mainly occurs in the mitochondria and endoplasmic reticulum of the adrenal cortex.
- Glucocorticoids – These are important for maintaining the body's carbohydrate reserves. Synthesis mainly occurs in the mitochondria and endoplasmic reticulum of the adrenal cortex.
- Androgens – *e.g.* testosterone and oestrogens, are responsible for the development of male and female secondary sex characteristics respectively. Synthesis mainly occurs in the testis (for testosterone) and ovary (for oestrogens).

Steroid hormones are synthesised *via* the steroidogenic pathways from the steroidal precursor cholesterol (**Figure 1.2.1**). Biosynthesis of the various steroid hormones involves P450 isozymes that are localised in steroidogenic tissues. P450 isozymes catalyse the oxygenation of carbons at position 3, 11, 17, 18 and 21, as depicted in **Figure 1.2.2**.

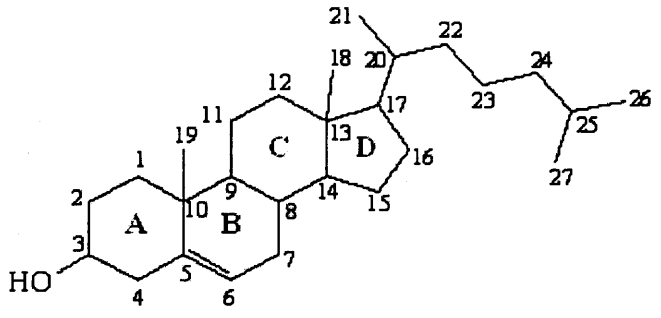

Figure 1.2.1. Chemical structure of cholesterol and the steroid numbering system.

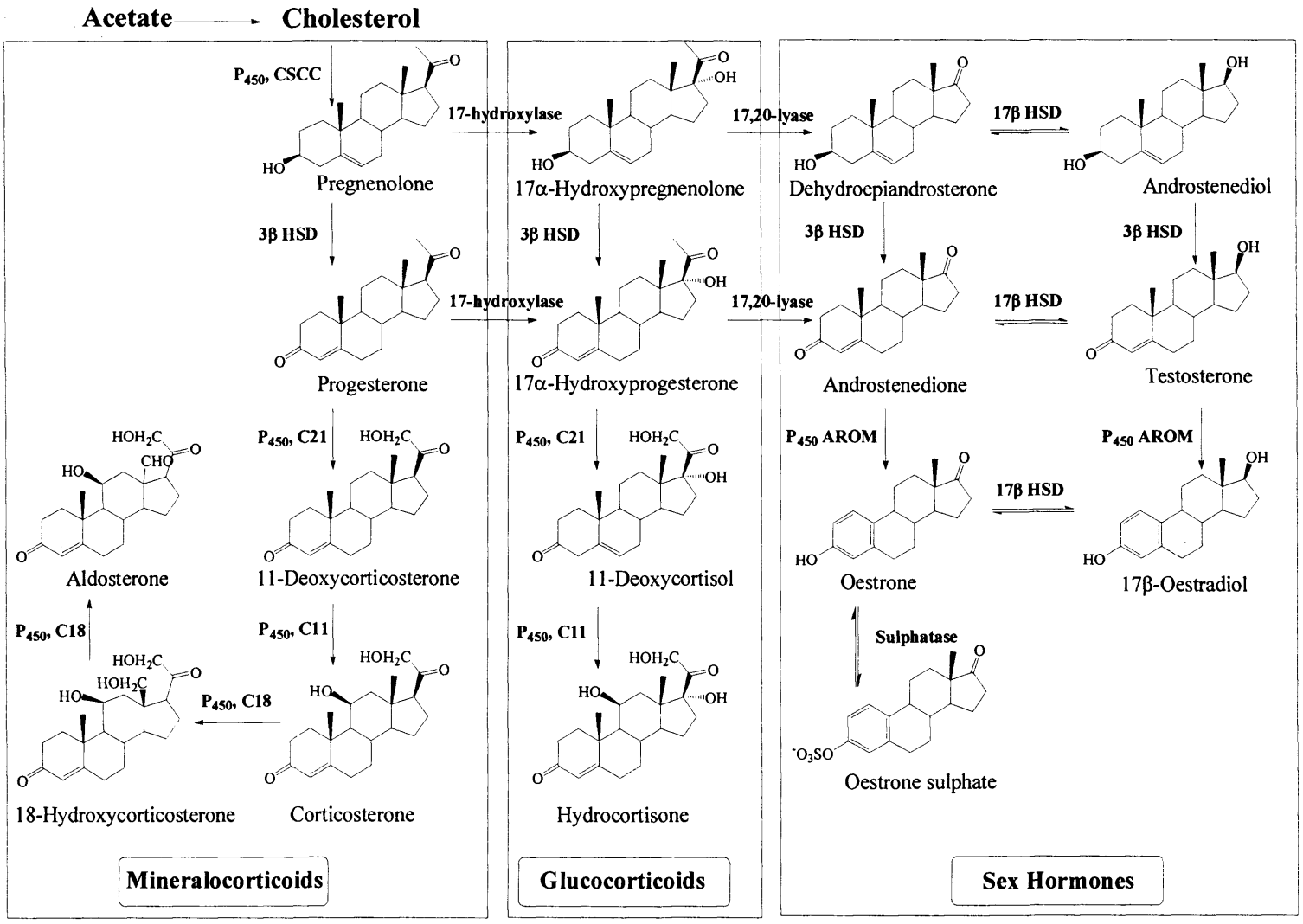

Figure 1.2.2. Biosynthesis of the mineralocorticoids, glucocorticoids and sex hormones (*i.e.* androgens and oestrogens).
Notes: P_{450}, CSCC = cholesterol side-chain cleavage enzyme; 3β-HSD = 3β-hydroxysteroid dehydrogenase; 17β-HSD = 17β-hydroxysteroid dehydrogenase.

1.2.2 Biosynthesis and regulation of androgens

Androgens play an important role during: (**1**) male sexual differentiation; (**2**) development and maintenance of the male secondary characteristics and (**3**) spermatogenesis (Mooradian *et al.*, 1987). The testes produce 90 – 95 % of circulating androgens (Preslock, 1980).

Let's first look at the pathway of androgen production and the example shown here will involve the prostate gland as the target tissue (**Figure 1.2.3**).

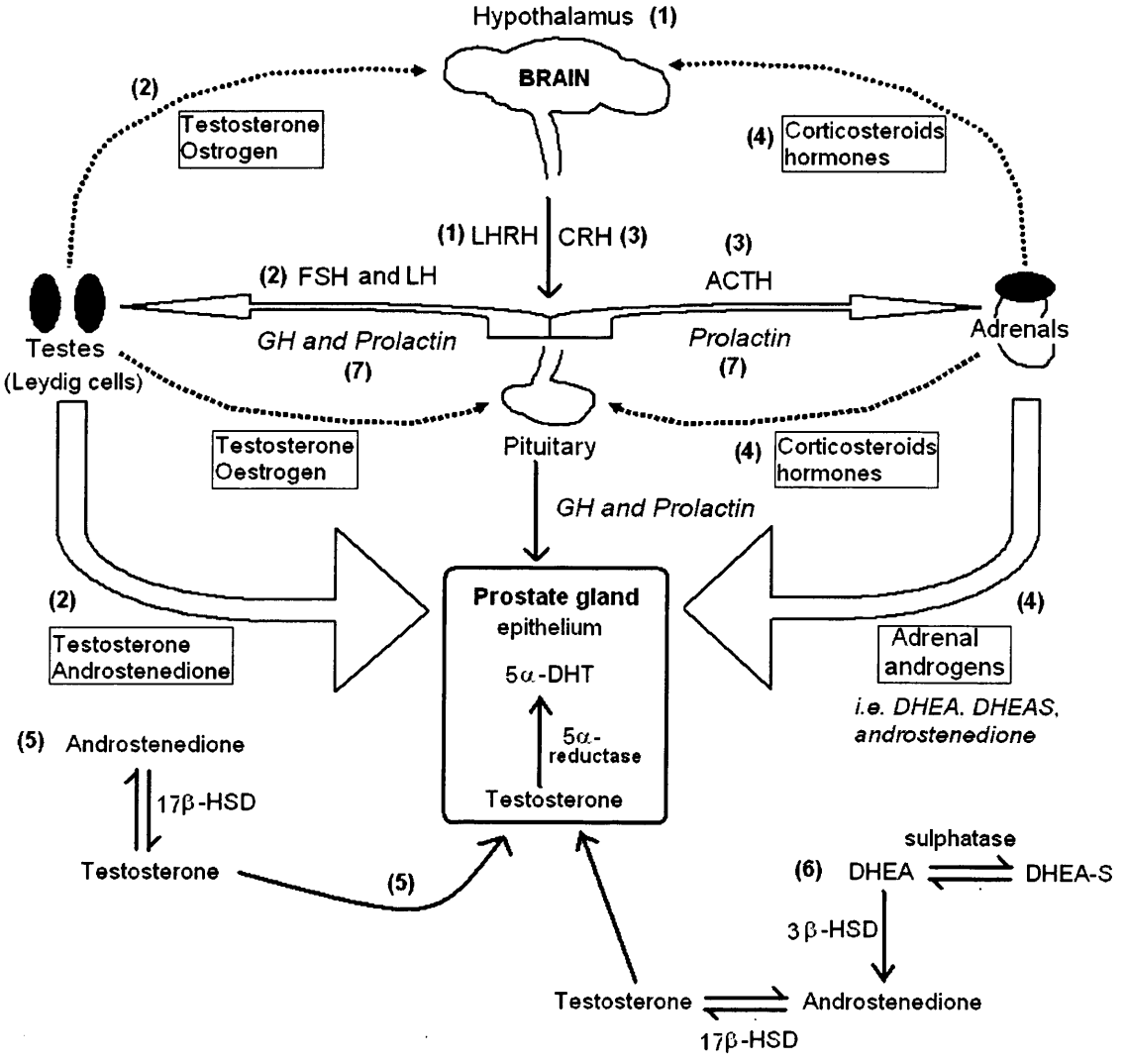

Figure 1.2.3. The regulation of androgen synthesis involving the prostate gland. The broken line indicates negative feedback loop. Abbreviations: LHRH = Luteinising hormone-releasing hormone; CRH = Corticotrophin-releasing hormone; ACTH = Adrenocorticotrophic hormone; LH = Luteinising hormones; FSH = Follicle-stimulating hormone; GH = Growth hormone; DHEA = Dehydroepiandrosterone.
The diagram has been adapted from Galbraith and Duchesne (Galbraith and Duchesne, 1997).

Referring to the numbering in **Figure 1.2.3**:

(1) The hypothalamus in the brain produces LHRH and secretes these hormones into the hypophyseal portal circulation to reach the anterior pituitary (Kraus *et al.*, 2005).

(2) FSH and LH released from the pituitary gland stimulate Leydig cells to secrete testosterone. Secretion of these pituitary hormones is controlled by the negative feedback loop (depicted as broken lines in the figure) (Goodman, 1994b)

(3) The hypothalamus produces and secretes CRH which then stimulate the release of ACTH from the pituitary gland (Goodman, 1994a).

(4) ACTH then stimulates the adrenal gland, which covers the superior surface of the kidney, to produce three different kinds of corticosteroid hormones, namely aldosterone, hydrocortisone and adrenal androgens. The adrenal androgens include: androstenedione, DHEA and DHEA sulphate. Secretion of these corticosteroid hormones is also controlled by the negative feedback loop.

(5) The testosterone which is released from the Leydig cells of the testes will be taken up by the prostate gland epithelium. In the prostate cells, testosterone is converted to 5α-dihydrotestosterone (5α-DHT), by 5α-reductase. 5α-DHT is the most active androgen, with a higher affinity for the androgen receptor than does testosterone (Berrevoets *et al.*, 2002).

(6) The adrenal androgens released from adrenal gland will also have an effect on the growth of the prostate cells. DHEA can be converted into androstenedione and then to testosterone by two non-cytochrome P450 enzymes 3β-hydroxysteroid dehydrogenase (3β-HSD) and 17β-hydroxysteroid dehydrogenase (17β-HSD) respectively (also **Figure 1.2.2**). The process described above can either occur in the plasma or in the prostate cell itself, as the prostate cell is able to take up and metabolise the adrenal androgens (Harper *et al.*, 1974).

(7) GH and prolactin are hormones that are synthesised and stored in the pituitary gland. The production of androgens from the testis and adrenal gland can be influenced by these two hormones. Prolactin can act with LH to stimulate testosterone secretion from the testes and can increase the adrenal androgen production (Galbraith and Duchesne, 1997).

1.2.3 Androgen receptor

Testosterone circulating in the blood is largely bound to albumin and sex-hormone-binding globulin (SHBG), and small fractions dissolved freely in the serum. The freely dissolved testosterone enters the target cells (*e.g.* prostate cells) where it either directly, or after conversion to 5α-DHT, binds to the androgen receptor (**Figure 1.2.4**). The androgen receptor (AR) is a member of the nuclear receptor superfamily (Griffin, 2000; Mangelsdorf *et al.*, 1995). Vitamin D_3 and retinoic acid receptors are also members of this nuclear receptor superfamily, these receptors will be discussed in section **1.5** in more detail.

ARs are found in the nucleus in the unbound state. The binding of androgen (testosterone or 5α-DHT) to the AR binding domain induces the formation of an AR homodimer complex. The DNA binding domain (DBD) of the receptor then binds to the androgen-responsive elements (AREs) in the promoter regions of target genes (Debes and Tindall, 2002). This will then allow transcription of target genes, such as genes that are involved in the control and regulation of prostate cell growth.

ARs are present in many parts of the body, however, the male accessory organs, e.g. prostate, genital skin and seminal vesicles have a higher concentration.

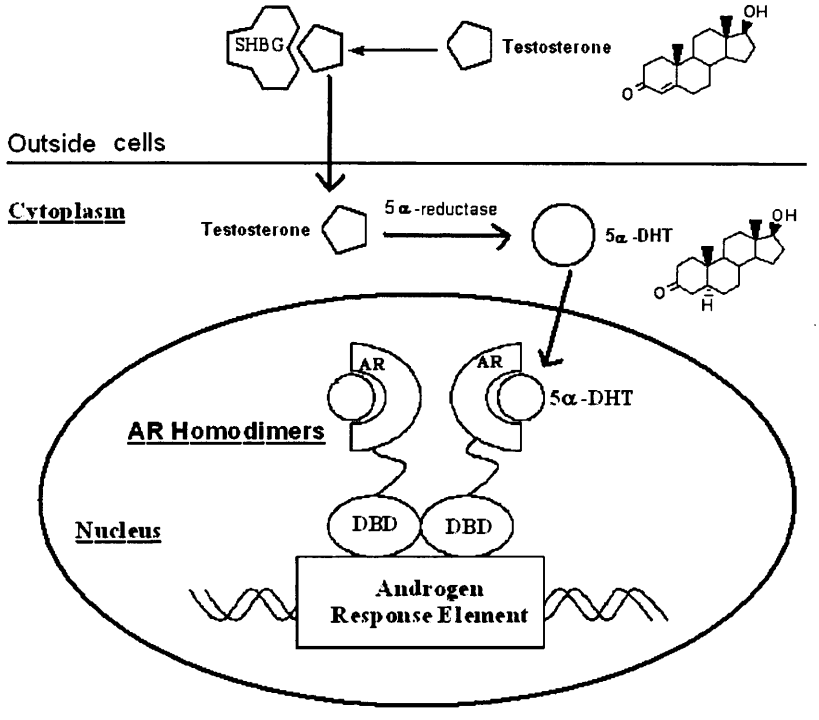

Figure 1.2.4. The mode of action of androgen in the androgen-responsive cells, *e.g.* prostate cell. Abbreviations: SHBG = Sex hormone binding globulin; AR = Androgen receptor; DBD = DNA binding domain; 5α-DHT = 5α-dihydrotestosterone.

1.2.4 Prostate cancer aetiology

Many risk factors are associated to the growth of prostate cancer cells, as discussed in section **1.1.3**.

Huggins and Hodges (Huggins *et al.*, 1941) discovered that androgens are required for the development, growth and maintenance of both the normal and carcinoma prostate (Montie and Pienta, 1994). Androgen regulates the development of prostate cancer through interaction with the androgen receptor. Changes to the androgen receptor is one of the main factor that contribute to the aetiology of prostate cancer (Debes and Tindall, 2002).

Genetic changes to the somatic and inherited genes have been associated with the molecular changes towards prostate cancer. The changes or mutation in certain genes *e.g. tumour suppressor genes*, could result in changes towards the rate of apoptosis, cell differentiation and cell proliferation (DeMarzo *et al.*, 2003).

Tissue growth factors play an important role in maintaining the growth and development of prostate cancer cells, namely, epidermal growth factor (EGF), insulin-like growth factor (IGF), transforming growth factor (TGF) and fibroblast growth factor (FGF). The functions of each growth factor will not be discussed in this thesis, however, it is important to note that these growth factors are implicated in the pathogenesis of many cancers including prostate cancer (Dowling and Risbridger, 2000; Russell *et al.*, 1998).

1.2.5 The aetiology of androgen-independent prostate cancer

During the long term androgen deprivation, the tumour cells lose the capacity to undergo apoptosis and do not depend on androgen for growth and survival (Brinkmann, 2001; Feldman and Feldman, 2001). At this stage, patient is said to have androgen-independent prostate cancer (AIPC), *i.e.* progression of prostate cancer despite continued androgen ablation. AIPC is also called, hormone-refractory prostate cancer (HRPC). Patients with AIPC will not respond to the hormonal therapy, and this is manifested by the increasing PSA levels, worsening of symptoms and progressive disease on imaging studies (Bhandari *et al.*, 2005). The possible mechanisms by which AIPC occurs were reviewed by Feldman's group (Feldman and Feldman, 2001) and Galbraith and Duchesne (Galbraith and Duchesne, 1997) and are summarised below:

- ***Mutations to the androgen receptor gene***

  Mutation to the androgen receptor gene could allow the androgen receptors to continue to stimulate the growth of prostate cancer cells in the absence of androgen binding to the receptor.

- ***Altered expression of the androgen receptor***

  The levels of androgen receptor expression are high in AIPC patients as detected by semi-quantitative polymerase chain reaction (PCR) analysis and by immunohistochemistry.

- ***Overamplification of the androgen receptor gene***

  This may occur in patients treated with androgen ablation therapy. This overamplification potentially allows the prostate cancer cells to be more sensitive even at low concentrations of androgen.

- ***Mutations in oncogenes or tumour suppressor genes***

  Experiments using prostate cancer cell-lines and primary cultures have shown that the cells can become androgen-independent by activation of proto-oncogenes, *e.g. Ras*; or inactivation of tumour suppressor genes, *e.g. Rb1*; or overexpression of anti-apoptotic gene, *e.g. bcl-2.*

- ***Growth factors***

  The growth factors, *e.g.* the epidermal growth factor (EGF), insulin-like growth factor (IGF), transforming growth factors (TGF) and fibroblast growth factor (FGF) are up-regulated in AIPC. In the androgen deprived environment, as a result of the androgen ablation therapy, the prostate cancer cells depend on the growth factors to grow. In this androgen deprived environment, clonal selection of androgen-independent cells from a heterogenous population of androgen-dependent and androgen-independent cells could occur.

1.2.6 Conclusions

So far, we have looked at the epidemiology, risk factors, treatment, aetiology of prostate cancer. In the next few chapters, the role of the vitamin D_3 and the retinoids, in the differentiation and proliferation of prostate cancer cells, will be discussed. The biosynthesis of vitamin D_3 and retinoids, and especially the enzymes that metabolise retinoids and vitamin D_3, will be discussed in further details in section **1.7**.

1.3 Vitamin D_3

Vitamin D_3 metabolites are involved in a wide array of biological responses, including calcium homeostasis, immunology, cell differentiation and regulation of gene transcription (Bouillon et al., 1995; Ylikomi et al., 2002). The principal mediator in this host of cellular processes, is the hormone 1α,25-dihydroxyvitamin D_3 (1α,25-$(OH)_2$-D_3), also known as calcitriol. The chemistry, pharmacology and clinical implications of 1α,25-$(OH)_2$-D_3 will be discussed in this section.

1.3.1 The vitamin D_3 endocrine system

1.3.1.1 Metabolism and production of vitamin D_3 metabolites

In the presence of ultraviolet light, 7-dehydrocholesterol is catalysed into previtamin D_3 in the human skin. This precursor is rapidly transformed by a rearrangement of double bonds to form vitamin D_3 (**Figure 1.3.1**).

The next step that occurs in the liver, involves hydroxylation of vitamin D_3 at carbon 25 to give 25-hydroxyvitamin D_3 (25-(OH)-D_3) by vitamin D_3-25-hydroxylase (CYP27A1). Further processing occurs in the kidney which involves the enzyme 25-hydroxyvitamin D_3-1α-hydroxylase (CYP1α, also known as CYP27B1) that introduces a hydroxyl group at the α-position of carbon 1 of the A ring to produce 1α,25-dihydroxyvitamin D_3 (1α,25-$(OH)_2$- D_3) which is the hormonally active metabolite. The enzyme 25-hydroxyvitamin D_3-24-hydroxylase (CYP24) in the kidney, is involved in the catabolism of 25-(OH)-D_3 and 1α,25-$(OH)_2$-D_3 to 24,25-dihydroxyvitamin D_3 (24,25-$(OH)_2$-D_3) and 1α,24,25-dihydroxyvitamin D_3 (1α,24,25-$(OH)_2$-D_3) respectively (**Figure 1.3.1**).

The degradation of 1α,25-$(OH)_2$-D_3 to form calcitrioic acid, involves several steps catalysed by the CYP24 enzyme via the C-24 oxidation pathway (**Figure 1.3.1**).

The three vitamin D_3 hydroxylases mentioned above have been isolated and cloned. Based on their sequence-alignment (Chen et al., 1993; Guo et al., 1993; Monkawa et al., 1997), they were found to contain heme-binding and functional domains typical of cytochrome P450 heme protein enzyme (Ghazarian *et al.*, 1974; Ghazarian *et al.*, 1973; Jones *et al.*, 1998).

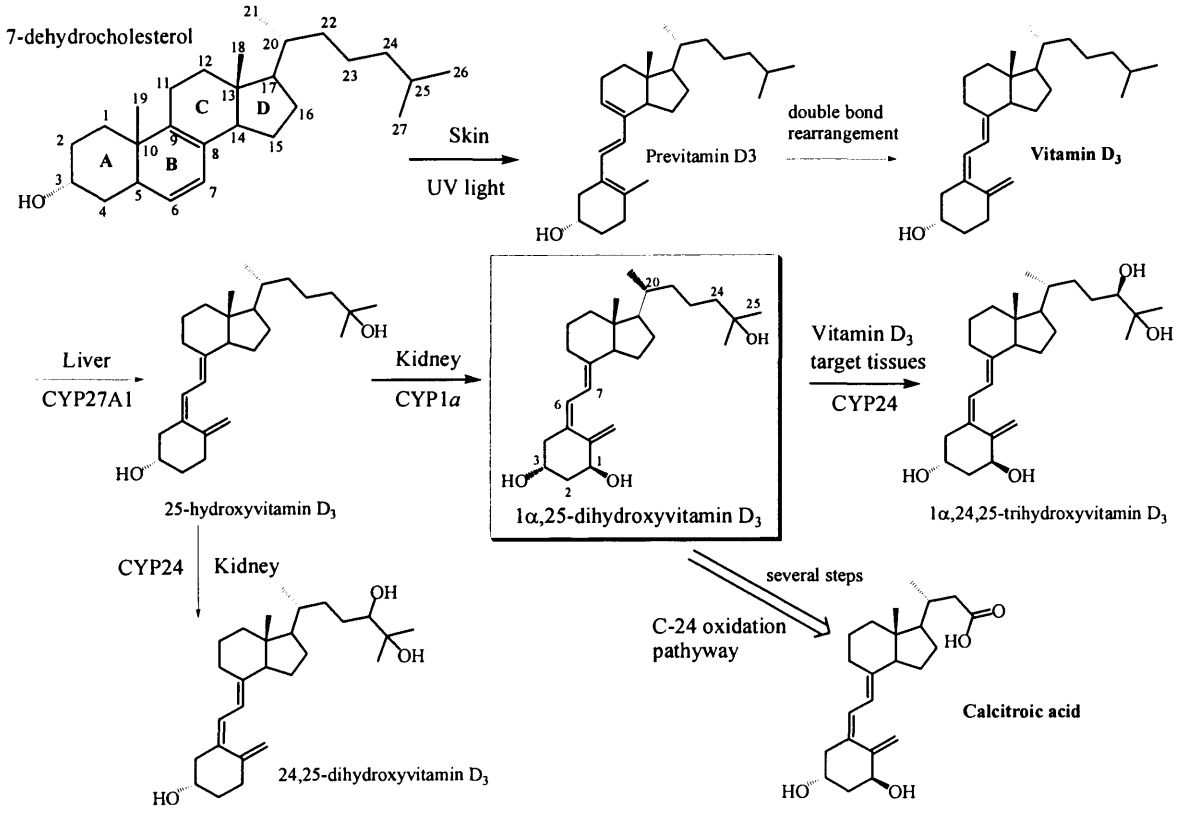

Figure 1.3.1. The biosynthesis and metabolism of vitamin D_3.

1.3.1.2 Tissue distribution of vitamin D_3 hydroxylases and regulation of vitamin D_3

It was established by radiolabeled vitamin D_3 that the major tissue for expression of CYP27A1 is the liver (Ponchon et al., 1969). There has been some controversy over whether this enzyme is found in the mitochondrial or microsomal fractions of the liver (Jones et al., 1998; Omdahl et al., 2002).

Kidney is the major endocrine organ for 1α,25-$(OH)_2$-D_3 synthesis and it is the preferred site for CYP1α and CYP24 expression. It is now recognized that many tissues in the body express CYP1α, including prostate, colon, skin and osteoblast, in order to synthesise 1α,25-$(OH)_2$-D_3 locally (Schwartz et al., 1998; Tangpricha et al., 2001). CYP1α is expressed in both the proximal and distal convoluted tubules and the enzyme is attached to the inner mitochondrial membrane of the kidney (Omdahl et al., 2003). Similarly, it was original thought that CYP24 was located exclusively in the kidney to metabolise 25-(OH)-D_3 to 24,25-$(OH)_2$-D_3. Many metabolites of 1α,25-$(OH)_2$-D_3 were later isolated from plasma including 1α,24,25-$(OH)_2$-D_3 (Holick et al., 1973). Subsequently, it was shown that 24-hydroxylase is omnipresent as it is expressed in many target tissues expressing vitamin D_3 receptors, including kidney, intestine,

fibroblast, cartilage and many more (Gamblin *et al.*, 1985; Lou *et al.*, 2003; Omdahl *et al.*, 1972).

The synthesis of 25-(OH)-D_3 by the liver appears to be loosely regulated, whereas, the synthesis and degradation of 1α,25-$(OH)_2$-D_3 are tightly regulated by specific cytochrome P450 enzymes, i.e. CYP1α and CYP24 (Omdahl et al., 2003) (**Figure 1.3.2**).

1α,25-$(OH)_2$-D_3, like other steroid hormones, is a negative feedback inhibitor. High plasma level of 1α,25-$(OH)_2$-D_3 exerts via its short feedback loop to suppress CYP1α. The parathyroid gland is a site of high localisation of 1α,25-$(OH)_2$-D_3 (Hughes and Haussler, 1978). 1α,25-$(OH)_2$-D_3 reduces parathyroid gland proliferation and parathyroid hormone (PTH) production by suppressing transcription of the parathyroid gene (Jones et al., 1998).

Moreover, 1α,25-$(OH)_2$-D_3 stimulates 24-hydroxylation to cause catabolism of 1α,25-$(OH)_2$-D_3 through a vitamin D_3 receptor (VDR)-dependent mechanism. This phenomenon predominates in the kidney but also occurs in all 1α,25-$(OH)_2$-D_3 target cells (Haussler et al., 1998).

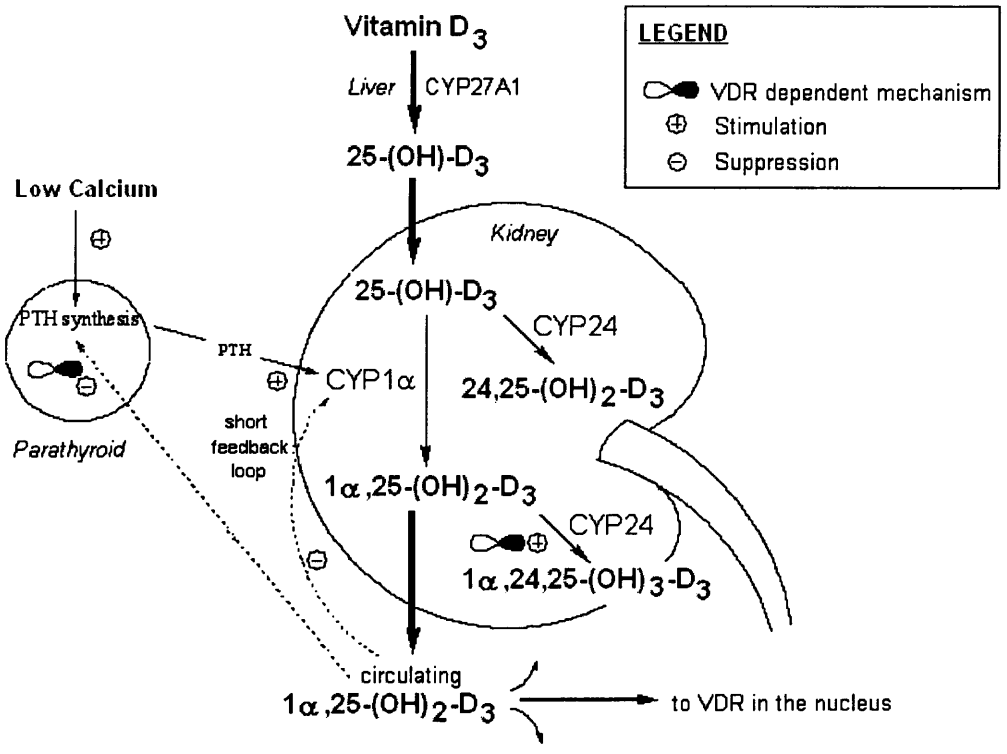

Figure 1.3.2. The regulation of the 1α,25-$(OH)_2$-D_3.

1.3.1.3 Role of vitamin D_3 in homeostasis

The classic role of 1α,25-$(OH)_2$-D_3 is to maintain normal development of the skeleton and maintenance of calcium homeostasis. Since the discovery of the physiological action of vitamin D_3 in preventing bony diseases like rickets and osteomalacia (DeLuca, 1988), it became clear that the role of 1α,25-$(OH)_2$-D_3 is to increase plasma calcium and phosphorus to mineralize skeleton to prevent bone diseases. The 1α,25-$(OH)_2$-D_3 hormone does this by (Ettinger and DeLuca, 1996; Reichel et al., 1989) (**Figure 1.3.3**):-

- Stimulating intestinal transport of calcium and phosphorus
- Reabsorption of calcium in the renal distal tubule
- Increasing bone resorption (i.e. mobilisation of bone calcium)

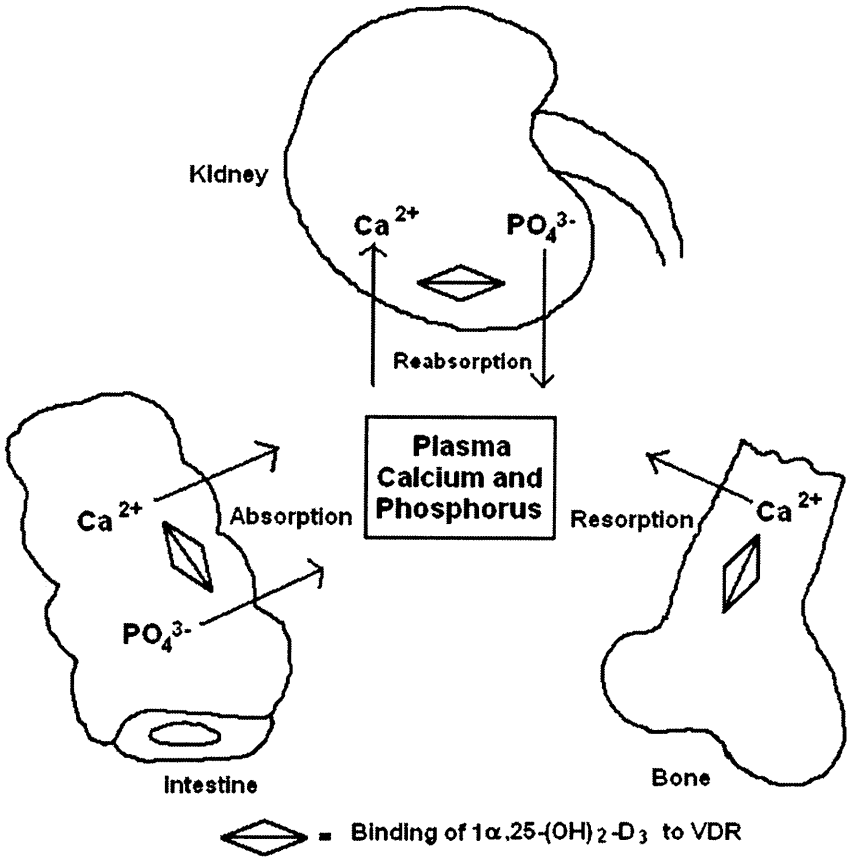

Figure 1.3.3. The role of 1α,25-$(OH)_2$-D_3 in homeostasis.

Besides the classical role of 1α,25-$(OH)_2$-D_3 in homeostasis, the role of 1α,25-$(OH)_2$-D_3 in restoring the normal balance of proliferation and differentiation of prostate cancer cells will be discussed in section **1.6**.

1.3.2 The chemistry of the vitamin D_3

Many synthetic routes are carried out to synthesise 1α,25-$(OH)_2$-D_3 and its analogues. The Hoffman-La Roche group (Baggiolini *et al.*, 1986; Baggiolini *et al.*, 1982) was the first to achieve total synthesis of 1α,25-$(OH)_2$-D_3. It gives flexibility for producing side chain modifications and other analogues based on this method. However, the disadvantage is that it takes 5 steps to produce the A-ring fragment, phosphine oxide, (**I**) and 9 steps to produce the C and D ring fragment, trimethylsilyl ether, (**II**) (**Figure 1.3.4**). The final steps involves a Horner-Wittig reaction between the phosphine oxide (**I**) and the CD-ring ketone (**II**) [**Figure 1.3.4**] followed by deprotection to produce 1α,25-$(OH)_2$-D_3.

The more popular approaches employed in industry involve the preparation of crystalline 1α,25$(OH)_2D_3$ from 25-hydroxycholesterol through an efficient 8-step synthesis (Barton *et al.*, 1973).

There are many other methods being employed to synthesise1α,25-$(OH)_2$-D_3. There are a few good reviews describing the chemical synthesis of vitamin D_3 compounds in greater detail (Barton et al., 1973; Dai and Posner, 1994; Lythgoe, 1980).

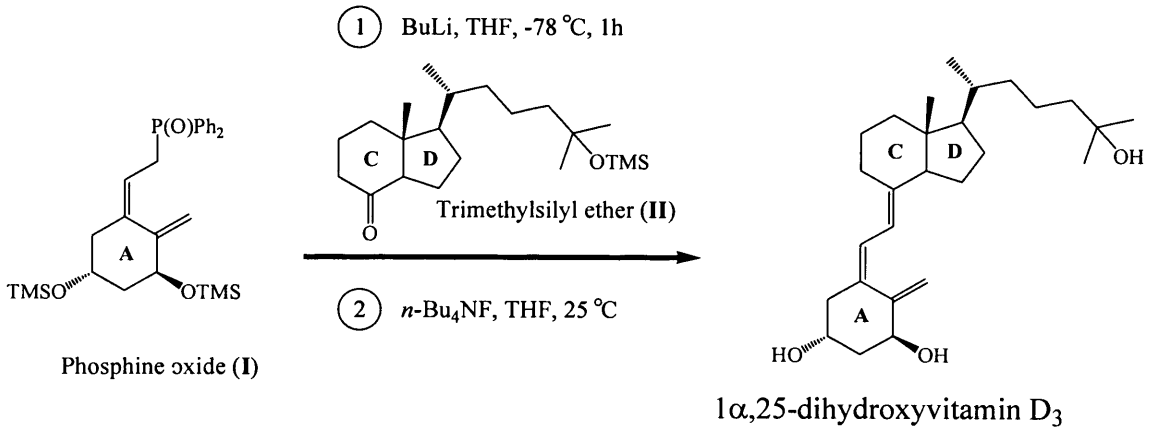

Figure 1.3.4. Horner-Wittig reaction between the phosphine oxide (**I**) and the trimethylsilyl ether (**II**).

1.3.3 Therapeutic uses of vitamin D_3 analogues

Hundreds of vitamin D_3 analogues have been synthesised and biological activity has been evaluated (Bouillon *et al.*, 1995; Jones *et al.*, 1998). These analogues show alterations to the A, B and/or CD rings of 1α,25-$(OH)_2$-D_3. These vitamin D_3 analogues have been used clinically to target diseases such as bone disease (osteoporosis), skin disease (psoriasis) and as hormonal therapy (hypoparathyroidism).

One of the 1α,25-$(OH)_2$-D_3 analogues that is in clinical use for the local treatment of psoriatic plaques is Calcipotriol (Dovonex®), formulated as a topical treatment (**Figure 1.3.5**).

Vitamin D_3 compounds are formulated either on their own or with calcium carbonate, used as a supplement product for patients with vitamin D_3 deficiency due to intestinal malabsorption or chronic liver disease (Anon, 2005). The products ergocalciferol (vitamin D_2), alfacalcidol (1α-hydroxyvitamin D_3), calcitriol (1α,25-dihydroxyvitamin D_3), colecalciferol (vitamin D_3) and dihydrotachysterol (**Figure 1.3.5**) are listed in the British National Formulary 2004 (Anon, 2005). Calcitriol is also licensed for the management of postmenopausal osteoporosis.

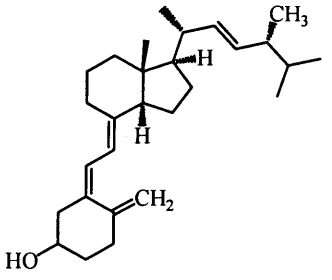

Ergocalciferol (Vitamin D_2)

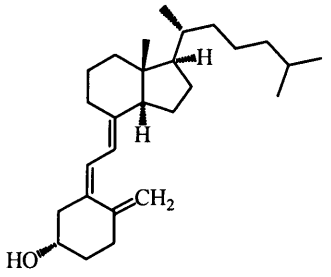

Colecalciferol (Vitamin D_3)

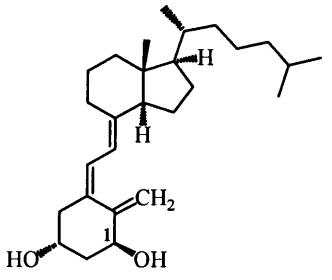

Alfacalcidol
(1α-hydroxycholecalciferol or
1α-hydroxyvitamin D_3)

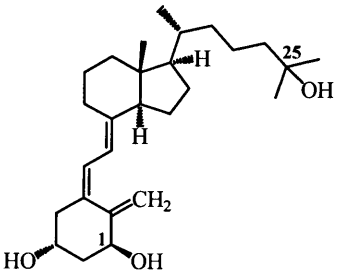

Calcitriol
(1α,25-dihydroxycholecalciferol or
1α,25-dihydroxyvitamin D_3)

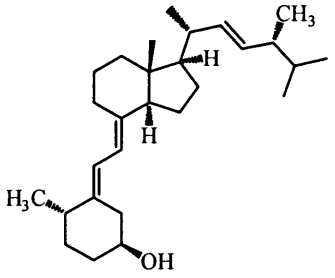

Dihydrotachysterol

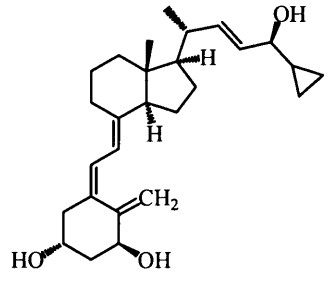

Calcipotriol (Dovonex®)

Figure 1.3.5. Chemical structures of vitamin D analogues in clinical use.

1.4 The retinoids

Similarly to the active metabolite of vitamin D_3, 1α,25-$(OH)_2$-D_3, retinoic acid also plays an important role in development, differentiation and homeostatsis in our body (Chambon, 1996). In this section, the chemistry, biology and role of retinoic acid will be discussed.

1.4.1 Biosynthesis, metabolism and regulation of the retinoids

The term retinoids refers to the natural forms and the many synthetic analogues of retinol (also known as vitamin A), retinal and retinoic acid (RA). The main dietary sources of vitamin A are provitamin A carotenoids from vegetables (carrots, spinach and broccoli); preformed retinyl esters and retinol from animal origin (liver and fish oil) (Blomhoff *et al.*, 1992). Provitamin A carotenoids are chemically converted into retinol in the liver and intestine by oxidative cleavage of carotenoids (Blaner and Olson, 1994). Retinol is then bound to the cellular retinol binding protein (CRBP). The resulting CRBP-retinol complex serves as a substrate for two different microsomal enzymes:

- Lecithin:retinol acyl transferase (LRAT), which catalyse the esterification of retinol to retinyl esters. Retinyl ester is the storage form of retinol in many tissues *e.g.* small intestine, liver, skin, eye, testis *etc.* (Blomhoff *et al.*, 1992; Napoli, 1996) (**Figure 1.4.1**).
- Retinol dehydrogenase, which catalyses the oxidation of retinol to retinaldehyde. This is the rate limiting step in the oxidative formation of RA (Blaner and Olson, 1994; Blomhoff *et al.*, 1992; Chen *et al.*, 2000b; Napoli, 1996) (**Figure 1.4.1**).

The metabolism of retinaldehyde to all-*trans* retinoic acid (ATRA) is mediated mainly by dehydrogenase but it can also be metabolised by cytochrome P450 enzymes, namely the CYPs 1A1, 1A2 and 3A4 in human (Zhang *et al.*, 2000). Metabolites of ATRA generated *in vivo* include 13-*cis*-RA (Tang and Russell, 1990), 9-*cis*-RA (Heyman *et al.*, 1992), 4-hydroxy-RA, 4-oxo-RA and other polar metabolites (**Figure 1.4.1**). There are many different cytochrome P450 isozymes (section **1.7.4**) that are able to metabolise RA to inactive metabolites, namely, 4-hydroxy-RA, 4-oxo-RA and the subsequent polar inactive metabolites. Robert *et al.* (Roberts *et al.*, 1979) reported that the formation of these metabolites in the hamster intestine and liver microsome homogenates required NADPH and oxygen and was strongly inhibited by carbon monoxide. Moreover, Van Wauwe *et al.* also showed that liarozole, which is a known

P450 inhibitor, enhanced endogenous RA plasma concentrations (Van Wauwe *et al.*, 1992).

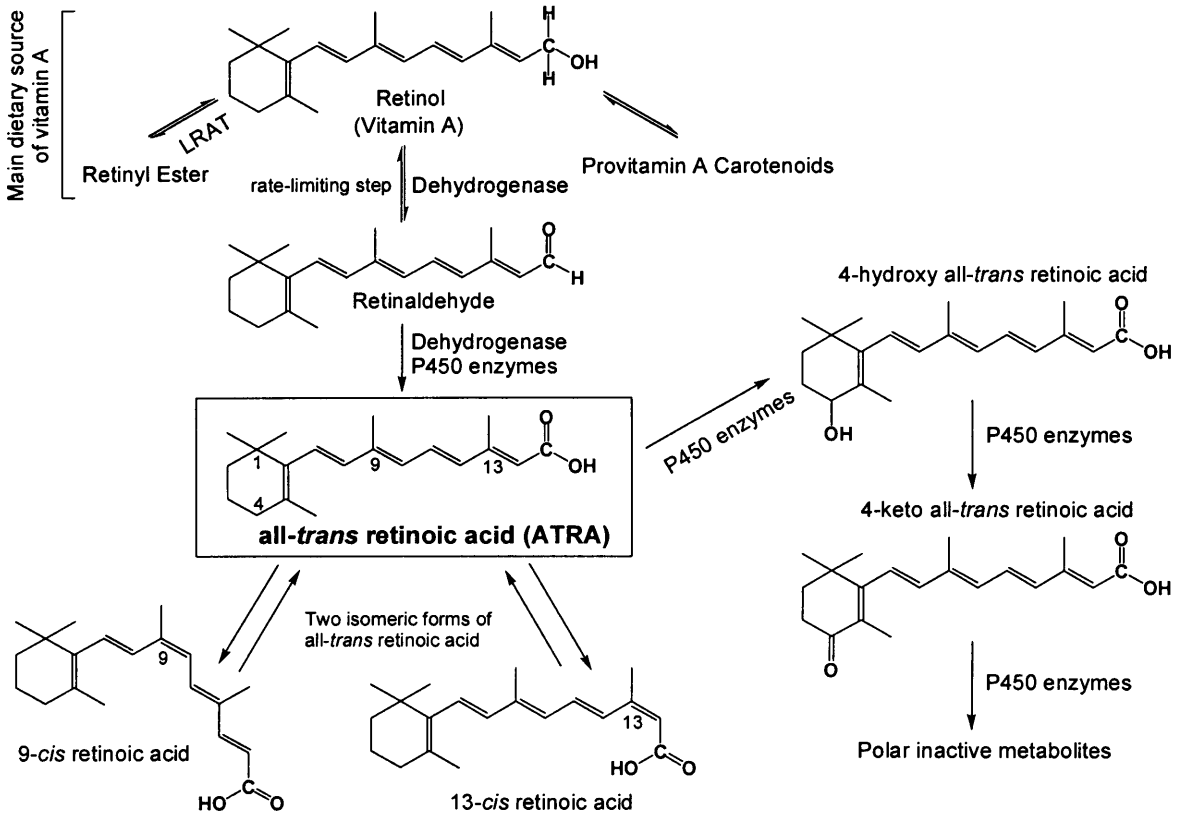

Figure 1.4.1. Biosynthesis and metabolism of all-*trans* retinoic acid.

There are several proteins which play key roles in ATRA homeostasis [reviewed in Ross *et al.* (Ross, 2003; Ross *et al.*, 2001)] :

- The cellular retinol binding protein (CRBP), facilitates retinol uptake, and allows retinol to bind to lecithin:retinol acyl transferase (LRAT) for storage as retinyl ester (Ong, 1994). [**Figure 1.4.2**, (**1**)]
- Lecithin:retinol acyl transferase (LRAT) has a crucial role in diverting retinol away from oxidative activation, therefore preventing ATRA biosynthesis. ATRA can cause a strong induction of LRAT and hence a reduction in the conversion of retinol to ATRA (Kurlandsky *et al.*, 1996). [**Figure 1.4.2**, (**2**)]
- The cellular retinoic acid binding protein (CRABP) which facilitates the retinoic acid uptake, and allows ATRA bind to cytochrome P450 hydroxylase for inactivation (Fiorella and Napoli, 1991). Thus, the binding of ATRA to CRABP decreases the elimination half-life of RA. [**Figure 1.4.2**, (**3**)]

- Cytochrome P450RAI (Retinoic Acid Inducible) (designated as CYP26) appears to be the novel cytochrome P450 hydroxylase enzyme expressed in numerous tissues, and is rapidly induced by ATRA (White *et al.*, 1997). [**Figure 1.4.2, (4)**]

CYP26A1 has been cloned from zebra fish (White *et al.*, 1996), mouse (Abu-Abed *et al.*, 1998) and man (White *et al.*, 1997). The hydroxylation of ATRA by CYP26 produces polar metabolites, *i.e.* hydroxyl or keto metabolites of ATRA, which are less bioactive than ATRA. After the discovery of P450RAI-1 (CYP26A1) by the White group (White *et al.*, 1997), they identified another two members of CYP26, namely the P450RAI-2 (CYP26B1) and P450RAI-3 (CYP26C1) (Taimi *et al.*, 2004). ATRA is the preferred substrate for all the three members of CYP26, except for CYP26C1 which can metabolise both ATRA and 9-*cis* RA (Taimi *et al.*, 2004).

The recent information and advances of retinoid biosynthesis, transport and regulation are well reviewed in book and journal articles (Blaner and Olson, 1994; Blomhoff *et al.*, 1992; Napoli, 1996; Ross *et al.*, 2001).

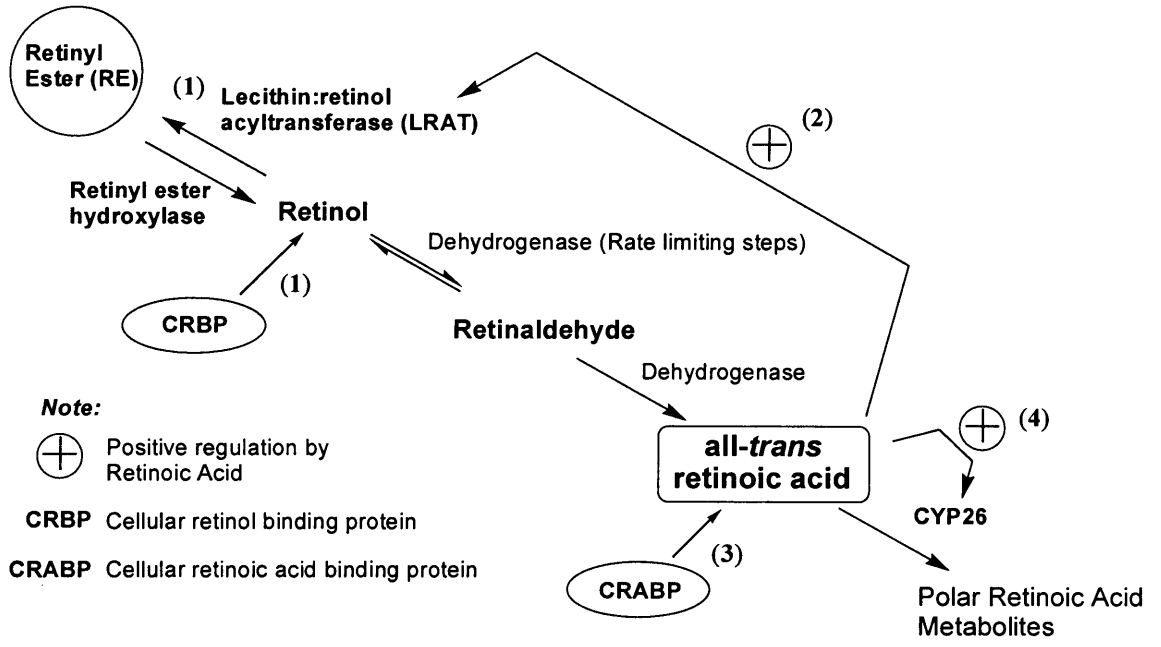

Figure 1.4.2.Regulation of retinoic acid homeostasis. LRAT and CYP26 play a crucial role in the down-regulation of ATRA biosynthesis.

1.4.2 The chemistry of the retinoids

Well over 1000 new retinoids have been synthesised, and they have been studied in *in vitro* and *in vivo* assays. These are summarised in the edited book by Sporn *et al.* (Dawson and Hobbs, 1994). The purpose of the wide range of synthetic retinoid analogues is to provide reference samples for metabolic studies and samples for biological investigation. Secondly, it is to develop retinoids with reduced toxicity, while

maintaining or enhancing activity as chemotherapeutic agents (Ralhan and Kaur, 2003), *i.e.* to improve the therapeutic index of a retinoid compound.

Rosenberger's group at the Hoffmann-La Roche first reported the total synthesis of 4-hydroxy- and 4-keto-retinoic acid (Rosenberger, 1982). Since then, many analogues have been synthesised by modification of the ring, the lipophilic chain and modification of the ring and chain. A few exciting results have been noticed by these modifications producing novel synthesised retinoids (**Figure 1.4.3**), for examples:

- Modification of the lipophilic chain of ATRA: *e.g.* Polyenyl benzoic acids (**1**) – this benzoic acid-terminated retinoid had high activity in cell differentiation assays, reported by Sporn and Newton's group (Dawson and Hobbs, 1994).
- Modification of the lipophilic chain and the aromatic ring of ATRA: *e.g.* stilbenecarboxylic acids (**2**) and aryl naphthalenylcarboxylic acid (**3**) – these synthetic classes of retinoids were first reported by the Loeliger group (Dawson and Hobbs, 1994; Gollnick *et al.*, 1990).
- Totally new series of synthetic retinoids – compounds (**4** and **5**), have been shown to have the biological activity of ATRA. The chalcone class of retinoids (**4**) and retinoids having an amide spacer (**5**) were prepared by Shudo and co-workers (Kagechika *et al.*, 1988; Kagechika *et al.*, 1989). These compounds have been reported to differentiate the human myeloid leukaemia cell line (HL-60) (Dawson and Hobbs, 1994).

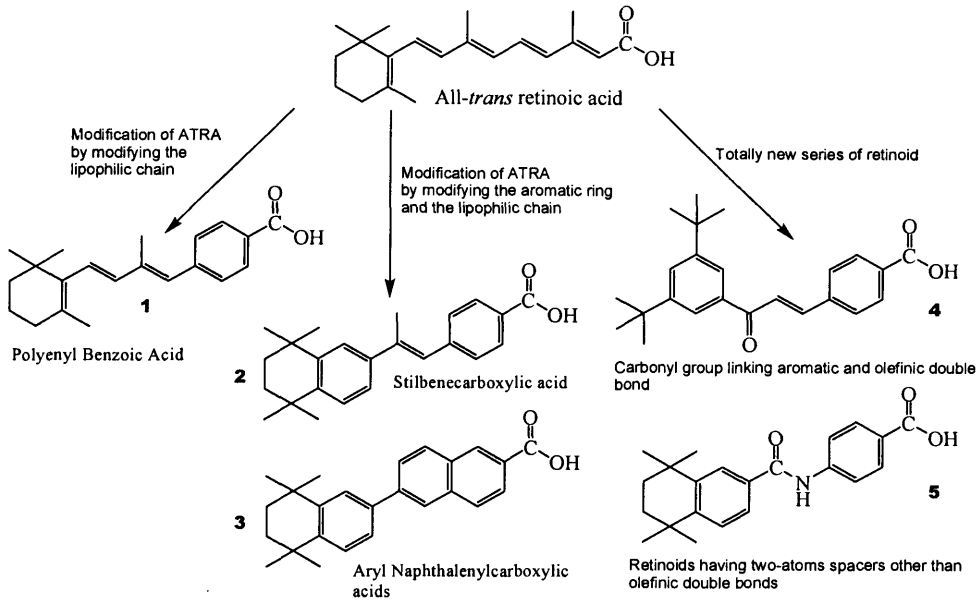

Figure 1.4.3. Examples of retinoid analogues with modified lipophilic chain and/or aromatic ring of the ATRA (**1** – **3**) and totally new series of retinoids (**4** and **5**) with the biological activity of ATRA.

1.4.3 Therapeutic uses of the retinoids

Tretinoin (all-*trans* retinoic acid) became the first synthetic retinoid. Out of the many synthesised retinoids, there are only three retinoids that have become prescription-only medicine in the United Kingdom: Tretinoin, Isotretinoin and Acitretin (Anon, 2005). This is summarised in **Figure 1.4.4** and **Table 1.4.1**.

Strong evidence exists between retinoic acid and cell differentiation and anti-proliferation as demonstrated in both normal and malignant cells as reviewed in a few articles (Hill and Grubbs, 1992; Lotan, 1980). Moreover, synthetic retinoids have been shown to be useful and effective in the prevention of carcinogenesis in laboratory animals as supported by a substantial body of literature (Hill and Grubbs, 1992; Lotan, 1980; Moon *et al.*, 1994). Promising results have been demonstrated in the treatment of acute promyelocytic leukaemia (APL) with ATRA (Chen *et al.*, 1991; Huang *et al.*, 1988). ATRA is licensed for use in patients previously untreated for APL, as well as those who have relapsed after standard chemotherapy or who are refractory to standard chemotherapy (Anon, 2005).

The use of these synthetic retinoids in dermatology has been beneficial and was reviewed by G.L. Peck (Peck, 1982; Peck and DiGiovanna, 1994). The drug of choice for severe cystic acne is isotretinoin, whereas, acitretin is the drug of choice for the treatment of psoriasis and related disorders of keratinisation (Gollnick *et al.*, 1990; Goodman, 1984).

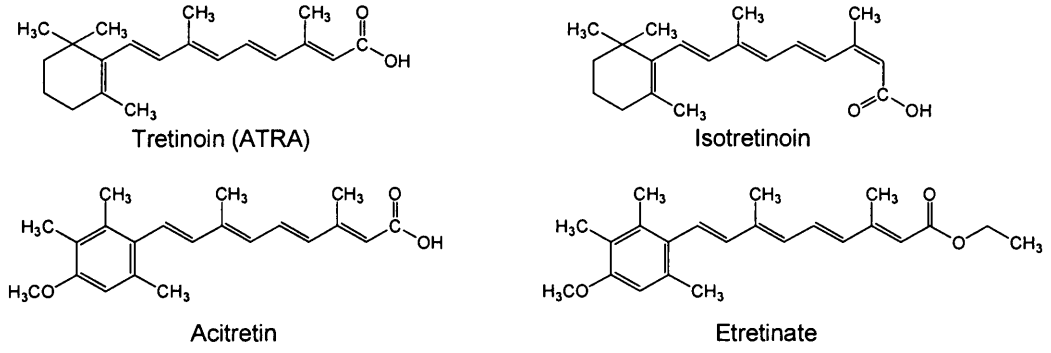

Figure 1.4.4. Chemical structures of synthetic retinoids in clinical use.

Table 1.4.1. Therapeutic application of some of the retinoids which are currently used clinically.

Retinoid	Brand name	Dosage form	Application
Tretinoin (All-*trans* Retinoic Acid)	Vesanoid®	capsule	Acute promyelocytic leukaemia
	Retin-A®	cream and gel	Acne
Isotretinoin (13-*cis* Retinoic Acid)	Roaccutane®	capsule	Acne
	Isotrex®	gel	Acne
Acitretin (metabolite of Etretinate)	Neotigason®	capsule	Severe extensive psoriasis

1.5 The nuclear receptor superfamily

Steroids, thyroid hormones, RA and 1α,25-$(OH)_2$-D_3 are lipophilic compounds that are able to permeate the plasma membrane and nuclear membrane to interact with its own receptor in the nucleus. These intracellular nuclear receptors for these lipophilic ligands function as a direct regulator of gene trancription (Evans, 1988; Lodish *et al.*, 2003; Mangelsdorf *et al.*, 1995). The nuclear receptors for RA and 1α,25-$(OH)_2$-D_3 will be discussed in this section.

1.5.1 Vitamin D_3 receptor (VDR), Retinoic acid receptor (RAR) and Retinoid X receptor (RXR)

The advance in molecular biology has led to the identification of the amino acid sequence and cloning of the nuclear receptors.

- Petkovitch's group and Giguere's group independently isolated the human retinoic acid receptor (RAR) in 1987 (Giguere *et al.*, 1987; Petkovich *et al.*, 1987).
- Baker *et al.* successfully cloned and isolated the human vitamin D_3 receptor (VDR) in 1988 (Baker *et al.*, 1988).
- Mangelsdorf *et al.* identified retinoid X receptor (RXR) in 1990 (Mangelsdorf *et al.*, 1990). 9-*cis* RA was later identified as the ligand for RXR (Rowe, 1997).

RAR, RXR and VDR are members of the nuclear receptor superfamily and they all share a common domain structure (Mangelsdorf *et al.*, 1995) [**Figure 1.5.1**].

Androgen receptor, as discussed in section **1.2.3**, is also a member of the nuclear receptor superfamily. These nuclear receptors are characterised by:

- ligand-binding domain (**LBD**), which is the binding recognition site for the ligand, *i.e.* retinoic acid or 1α,25-$(OH)_2$-D_3.
- DNA-binding domain (**DBP**), which targets the receptor to specific DNA sequences known as the nuclear receptor response element.

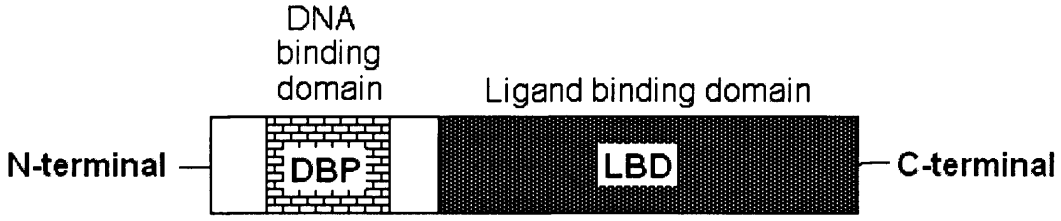

Figure 1.5.1. The common domain structure of the nuclear receptor.

RXR is identified as a cofactor, as it is required by several members of the nuclear receptor superfamily, *e.g.* VDR and RAR, for transcriptional activation. RXR forms a heterodimer with VDR or RAR, and in the presence of the ligand, *i.e.* 1α,25-$(OH)_2$-D_3, ATRA or 9-*cis* RA, transcription is then initiated through specific response elements, *i.e.* VDRE or RARE (**Figure 1.5.2** and **Figure 1.5.3**, **A**) (Allenby *et al.*, 1993; Jones *et al.*, 1998). RXR can also form a homodimer (i.e. RXR/RXR) on interaction with 9-*cis* RA with RXR (Mangelsdorf and Evans, 1995) and interact with the retinoid X response element (RXRE) to initiate transcription of target genes (**Figure 1.5.3**, **B**).

ATRA which is bound to CRABP, is either, hydroxylated by cytochrome P-450 to 4-hydroxy-RA, which has weak biological activity, or translocated to the nucleus where it can bind to its nuclear receptor, RAR (**Figure 1.5.3**). The retinoic acid receptors (RARs) and retinoid X receptors (RXRs) are each composed of three subtypes (α, β and γ). The RAR family (RAR α, β and γ) is activated by both ATRA and by 9-*cis* RA (Mangelsdorf *et al.*, 1995), whereas, the RXR family (RXR α, β and γ) is activated only by 9-*cis* RA (Heyman *et al.*, 1992).

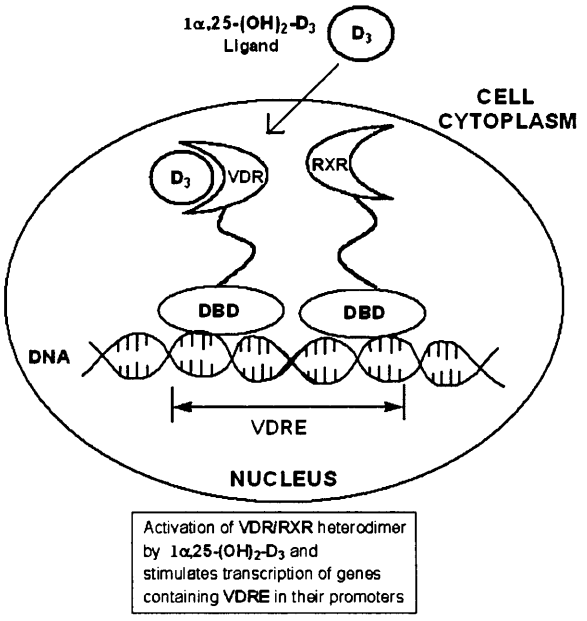

Figure 1.5.2. Vitamin D_3 receptor (VDR) forms a heterodimer with retinoid X receptor (RXR) in the nucleus. The DNA binding domain (DBD) bind to the specific DNA sequence known as the response element (VDRE).

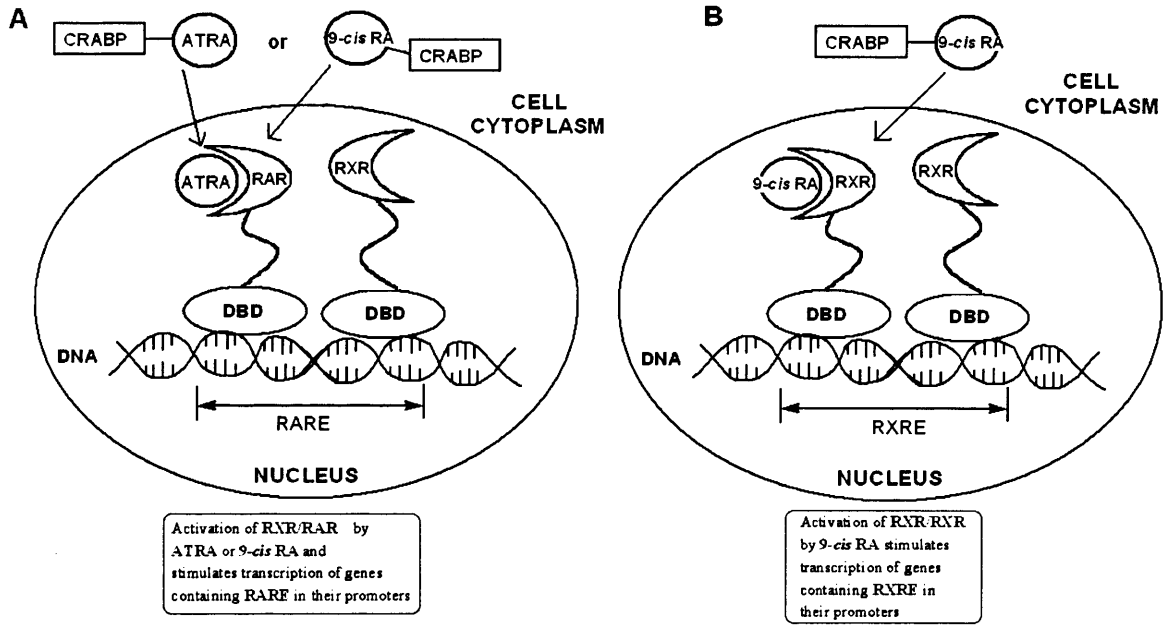

Figure 1.5.3. The binding of ATRA or 9-*cis* RA to the RAR (**A**) or 9-*cis* RA to the RXR (**B**) nuclear receptors in the nucleus. The DNA binding domain (DBD) bind to the specific DNA sequence known as the response element (RARE or RXRE).

VDR, RXR and RAR have been identified in many cells, including:

- Keratinocytes (Fisher and Voorhees, 1996)
- Colon (Giuliano *et al.*, 1991; Sonneveld *et al.*, 1998)
- Breast (Koike *et al.*, 1997; Sonneveld *et al.*, 1998)

- Prostate (Blutt *et al.*, 1997; Campbell *et al.*, 1998; Kivineva *et al.*, 1998; Peehl *et al.*, 1994; Richter *et al.*, 2002)

The presence of these receptors in various tissues allow 1α,25-$(OH)_2$-D_3 and RA to directly regulate gene expression by binding to its nuclear receptors within the target cells. The transcription of the genes have many effects on a variety of biological processes in the cells, including homeostasis, proliferation, differentiation and apoptosis (Bouillon *et al.*, 1995; Gudas *et al.*, 1994). The role of 1α,25-$(OH)_2$-D_3 and RA in cell differentiation and cell anti-proliferation will be discussed in the following section **1.6**.

1.6 The role of vitamin D_3 and retinoids in prostate cancer

Epidemiologic studies have indicated a strong link between incidence of prostate cancer and vitamin D_3 and RA. Examples of such studies are as follows:

- Low level of circulating 1α,25-$(OH)_2$-D_3 which was co-related with the risk of prostate cancer (Schwartz and Hulka, 1990).
- An inverse correlation between mortality due to prostate cancer and exposure to ultraviolet light, which is the principal source of vitamin D_3 (Hanchette and Schwartz, 1992; John *et al.*, 2004).
- A positive association between latitude and prostate cancer mortality (Luscombe *et al.*, 2001).
- Vitamin A intake is inversely related to the risk of prostate cancer (Kolonel *et al.*, 1987; Pasquali *et al.*, 1996).

1α,25-$(OH)_2$-D_3 and retinoids (which include natural and synthetic RA analogues) have been widely investigated *in vitro* (Zhao *et al.*, 1999) and *in vivo* (Culine *et al.*, 1999; Osborne *et al.*, 1995) in controlling prostate cancer progression. The advance in genetic screening methods allowed researchers to use cDNA microarray technology to understand and to investigate the regulation of gene expression by 1α,25-$(OH)_2$-D_3 and retinoids (Peehl *et al.*, 2004; van der Spek *et al.*, 2003; White, 2004).

1.6.1 Anti-proliferative effects of 1α,25-$(OH)_2$-D_3 and retinoids in prostate cancer cells

1α,25-$(OH)_2$-D_3 and RA play crucial roles in the prostate cancer cell cycle which results in anti-proliferation of the prostate cancer cells. Proliferating cells continuously undergo the process of the cell cycle as illustrated in **Figure 1.6.1**. Whereas, non-proliferating cells will leave the cell cycle in G_1 phase and will enter the

resting/quiescent phase. There are many types of proteins/genes that help control cell growth and proliferation, *e.g.* tumour suppressor gene (*e.g. p53*, *Rb* gene), anti-apoptotic protein (*e.g. bcl-2*) and cyclin-dependent kinases (CDK).

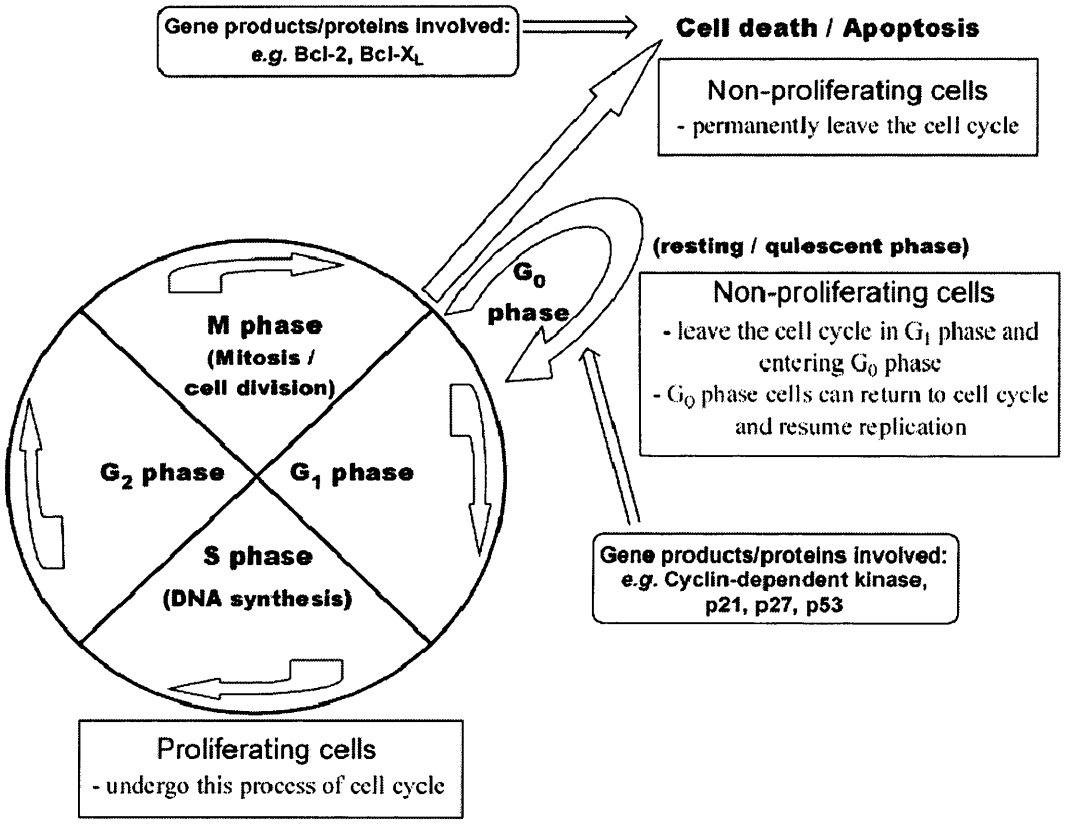

Figure 1.6.1. The cell cycle of the proliferating cells. The gene products/proteins that are involved in apoptosis and cell-cycle arrest (G_0 phase) are shown here.

It has been shown by a few research groups that 1α,25-$(OH)_2$-D_3 and its analogues inhibit the growth (anti-proliferation effect) of normal prostatic epithelial cells, primary cultures of prostate cancer cells, and many different types of prostate cancer cell lines, by:

- Increasing the expression of CDK inhibitor $p21^{waf1/cip1}$ (Campbell *et al.*, 1997; Johnson *et al.*, 2002; Yang and Burnstein, 2003) and $p27^{kip1}$ (Campbell *et al.*, 1997). $p21^{waf1/cip1}$ and $p27^{kip1}$ belong to the VDR target genes, therefore, 1α,25-$(OH)_2$-D_3 exerts its anti-proliferative effects on the cancer cells by binding to the VDR resulting in transcription of the $p21^{waf1/cip1}$ and $p27^{kip1}$ genes (Freedman, 1999).
- Decreasing CDK2 activity leading to a decrease in phosphorylation of retinoblastoma protein (*Rb*) resulting in the prostate cancer cell to arrest in the G_0/G_1 phase (Zhuang and Burnstein, 1998).

The anti-proliferative effects of retinoids have been studied on normal prostatic epithelial cells (Peehl *et al.*, 1993), primary cultures of prostate cancer cells (Igawa *et al.*, 1994; Peehl *et al.*, 1993), prostate cancer cell lines (de Vos *et al.*, 1997; Fong *et al.*, 1993; Koshiuka *et al.*, 2000; Peehl *et al.*, 1993) and in rat primary and metastatic prostate carcinoma (Pollard *et al.*, 1991; Slawin *et al.*, 1993). Liang *et al.* observed the cell growth inhibition and S-phase arrest by a novel synthetic retinoid, CD437, in LNCaP and PC-3 cells, was associated with upregulation of $p21^{waf1/cip1}$ mRNA levels (Liang *et al.*, 1999).

1.6.2 Apoptotic effects of 1α,25-$(OH)_2$-D_3 and retinoids in prostate cancer cells

1α,25-$(OH)_2$-D_3 was found to induce apoptosis in prostate cancer cell lines by down-regulation of the VDR target genes, *bcl*-2 and *bcl*-X_L, the two anti-apoptotic proteins (Blutt *et al.*, 2000a; Guzey *et al.*, 2002).

The apoptotic effect of retinoids, for example, 4-HPR (**Figure 1.4.5**), have been examined in androgen-dependent and androgen-independent prostate cancer cell lines by some groups (Gao *et al.*, 1999; Liang *et al.*, 1999; Shen *et al.*, 1999; Sun *et al.*, 1999). The apoptotic effect of 4-HPR in LNCaP cells, is due to the decrease in *bcl*-2 expression and increase of *bax* gene expression, these effects are associated with apoptosis induction (Shen *et al.*, 1999).

1.6.3 Pro-differentiation effects of 1α,25-$(OH)_2$-D_3 and retinoids in prostate cancer cells

The effect of 1α,25-$(OH)_2$-D_3 on differentiation of prostate cancer cell lines has been shown, by up-regulating the androgen receptor and increasing the secretion of prostate-specific antigen (PSA) in LNCaP cells (Zhao and Feldman, 2001; Zhao *et al.*, 1999). The increasing PSA expression by 1α,25-$(OH)_2$-D_3 may be considered differentiation marker for epithelial prostate cells (Krishnan *et al.*, 2003).

The effect of RA in differentiation of prostate cancer tissues has been examined by Kelly *et al.* (Kelly *et al.*, 2000). The group investigated the histological changes of the tumour biopsy specimens of androgen-independent patients who were treated with ATRA. The increase in prostate-specific membrane antigen (PMSA) expression after treatment with ATRA indicated the tumour cells changed from metastatic to a high-grade phenotype.

1.6.4 Synergistic effects of 1α,25-$(OH)_2$-D_3 and retinoids in prostate cancer cells

Since the discovery that vitamin D_3 receptor (VDR) acts as a heterodimer with RXR (Mangelsdorf *et al.*, 1995), it was suggested that there may be functional interactions between 1α,25-$(OH)_2$-D_3 and RA. Not surprisingly, there have been accumulated evidences that these two agents act synergistically or have additive differentiating and anti-proliferative effects in several cell types (James *et al.*, 1995; Miyaura *et al.*, 1985) including prostate cancer cell-lines (Campbell *et al.*, 1998; Peehl *et al.*, 1995).

1α,25-$(OH)_2$-D_3 and 9-*cis* RA has been found to act synergistically by:

- Inhibiting the growth of prostate cancer cells causing accumulation of cells in G_1 phase (Blutt *et al.*, 1997; Elstner *et al.*, 1999)
- Inducing androgen receptor in LNCaP prostate cancer cells (Zhao *et al.*, 1999)

Despite these positive results in prostate cancer cell-lines, there are no studies showing synergistic or beneficial effects using both 1α,25-$(OH)_2$-D_3 and RA *in vivo*.

1.6.5 Clinical studies of vitamin D_3 and retinoids in prostate cancer

Besides the current clinical use of vitamin D_3 analogues mentioned in section **1.3.3**, a number of research groups are synthesising and investigating vitamin D_3 analogues for the desirable anti-proliferative and pro-differentiating activities in prostate (Blutt *et al.*, 2000b; Campbell *et al.*, 1997; Chen *et al.*, 2000c), colon (Cross *et al.*, 1991), and other cancer (Prudencio *et al.*, 2001). One of the vitamin D_3 analogues, EB1089 (**Figure 1.6.2**), has been extensively studied in various cancer cell-lines (Akutsu *et al.*, 2001; Prudencio *et al.*, 2001).

However, in order to develop vitamin D_3 analogues as effective chemotherapeutic agents, these analogues should possess desirable anti-proliferative and pro-differentiating activities rather than undesirable calcemic activity (Campbell and Koeffler, 1997). Many different types of non- or less- calcemic vitamin D analogues have been investigated for their effects on prostate cancer cell proliferation and differentiation *in vitro*. Examples of these are (**Figure 1.6.2, i – iv**):

- 19-nor-hexafluoride vitamin D_3 (**i**) (Campbell *et al.*, 1997)
- 20-cyclopropyl-vitamin D_3 (**ii**) analogues (Koike *et al.*, 1999)
- 19-nor-1α,25-dihydroxyvitamin D_2 (**iii**) (Chen *et al.*, 2000c)
- 5,6-trans-16-ene vitamin D_3 (**iv**) analogues (Hisatake *et al.*, 1999)

To date there have been two clinical trials of using calcitriol (1α,25-$(OH)_2$-D_3) for human prostate cancer. A small trial in 14 men with AIPC failed to show an objective response in any patient, but in two there were declines in PSA levels of 25 % and 45 % (Osborne *et al.*, 1995). In another study (Gross *et al.*, 1998), 7 patients with early recurrent prostate cancer after radical prostatectomy or radiotheraphy were treated with calcitriol, all patients showed a statistically significant decline in the rate of PSA increase. In both of these studies doses of calcitriol were limited by hypercalcemia and hypercalciuria. A recent review by Trump *et al.* (Trump *et al.*, 2004) discussed the use of combination therapy of 1α,25-$(OH)_2$-D_3 and other chemotherapeutic agent(s), *e.g.* dexamethasone, carboplatin or taxanes in AIPC. Intermittent use of 1α,25-$(OH)_2$-D_3 to reduce toxicity has showed positive results in Phase I and II clinical studies for AIPC (Beer, 2003; Trump *et al.*, 2004).

Phase I and II study have been carried out to evaluate the efficacy of the vitamin D_2, 1α-hydroxyvitamin D_2 (1α-OH-D_2) [**Figure 1.6.2**, **(v)**], in patients with AIPC (Liu *et al.*, 2002; Liu *et al.*, 2003). Although the results were encouraging, further investigations are necessary to elucidate the mechanism and effect of 1α-OH-D_2.

The Phase II study of ATRA have demonstrated mild to moderate efficacy in AIPC (Culine *et al.*, 1999; Trump *et al.*, 1997), despite the anti-proliferative, pro-differentiative and apoptotic effects shown *in vitro*. Culine *et al.* (Culine *et al.*, 1999) reported that the use of ATRA has minimal activity in AIPC. However, it is not known whether this moderate efficacy of RA is due to toxicity or rapid metabolism of RA in the body which results in under dosing.

The RA analogue, *N*-(4-hydroxyphenyl)-retinamide (4-HPR), also known as fenretinide (**Figure 1.6.2**, **(vi)**), has been studied for its effect in malignant (DU-145, PC-3) (Igawa *et al.*, 1994; Sharp *et al.*, 2001) and non-malignant (RWPE and WPE) prostate cancer cell lines (Sharp *et al.*, 2001). 4-HPR has also demonstrated a benefit in both prevention and progression in prostate cancer rat models (Pienta *et al.*, 1993; Pollard *et al.*, 1991). However, the use of 4-HPR in clinical trials to treat prostate cancer has shown limited effect.

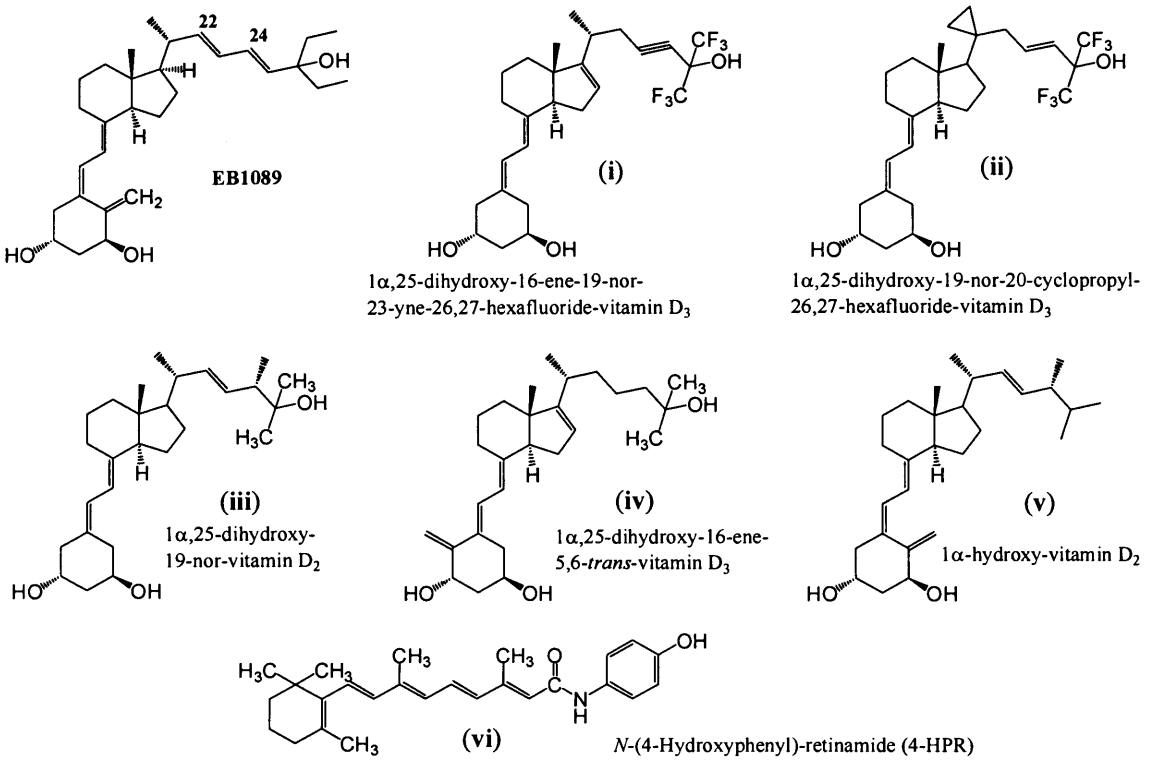

Figure 1.6.2. Vitamin D_2 and D_3 analogues and retinoid with promising in vitro activity or in clinical trials.

1.7 The properties of the vitamin D_3 and retinoic acid hydroxylase enzymes

1.7.1 General features of the hydroxylase enzymes

The hydroxylase enzymes that are involved in the metabolism of 25-hydroxyvitamin D_3 (CYP1α and CYP24) and retinoic acid (CYP26 and other non-specific cytochrome P450 4-hydroxylases present in the liver) are members of the cytochrome P450 superfamily (Leo and Lieber, 1985; Marill *et al.*, 2000; Omdahl *et al.*, 2002).

CYP1α and CYP24 are located in the inner mitochondrial membrane to receive NADPH-reducing equivalents, which are supplied via NADPH to a flavoprotein (ferredoxin reductase, **FR**) then to an iron-sulphur protein (ferredoxin, **FDX**) then to the cytochrome P450 monooxygenase, which catalyses the hydroxylation by utilizing one oxygen atom from O_2 to form hydroxylated vitamin D_3 (**D–OH**) and water (**Figure 1.7.1**) (Jones *et al.*, 1998; Omdahl *et al.*, 2002).

In contrast, CYP26 and other non-specific cytochrome P450 4-hydroxylases present in the liver, which are microsomal P450 enzymes, are located in the membrane of the endoplasmic reticulum of a cell. FAD/FMN-dependent NADPH-cytochrome

P450 oxidoreductase serves as the redox partner for this microsomal P450 enzyme. FAD serves as an electron acceptor from NADPH, and FMN interacts with and reduces the P450 enzymes (Lewis and Hlavica, 2000; Sevrioukova *et al.*, 1999) (**Figure 1.7.2**).

In both situations, a molecule of oxygen is split during the catalytic reactions with one atom used in the hydroxylation step and another atom reduced to water. Hence these P450 enzymes belong to the class of mixed-function oxidase enzymes. The general reaction of this P450 mediated monooxygenation can be represented as follows (Lewis, 2001):

$$\text{R-H} + \mathbf{O_2} \xrightarrow[2H^+,\, 2e^-]{\textbf{P450}} \text{R-}\mathbf{OH} + \mathbf{H_2O}$$

R = 1α,25-$(OH)_2D_3$ or Retinoic acid

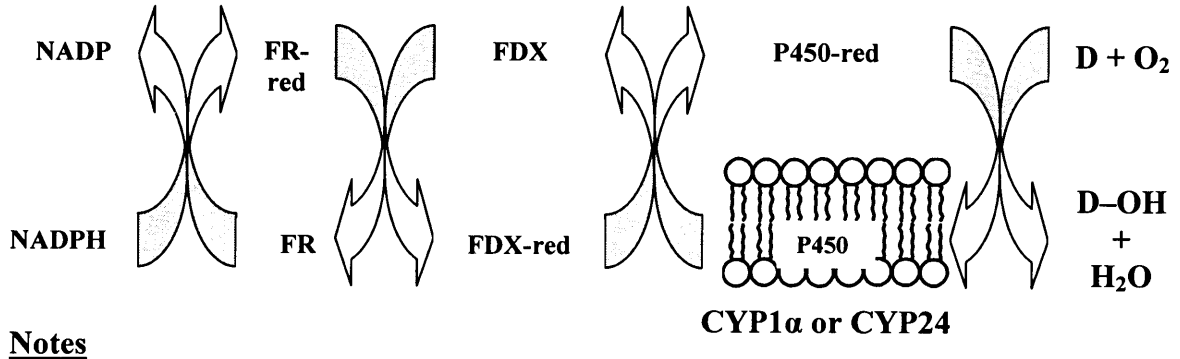

Notes

D = 25-(OH)-D_3 **FR** = Ferrodoxin-reductase (flavoprotein)
FDX = Ferrodoxin **-red** = reduced form

NADPH = Nicotinamide-adenine dinucleotide phosphate (reduced form)

P450 = cytochrome P450 enzyme located in the inner membrane of the mitochondrial

Figure 1.7.1. The enzyme involved in hydroxylation of 25-(OH)-D_3 (**CYP1α** and **CYP24**) is a mitochondrial cytochrome P450 that requires molecular oxygen, NADPH, and two redox carrier proteins, namely, the ferrodoxin-reductase (**FR**) and an iron-sulphur protein redoxin (ferrodoxin, **FDX**).

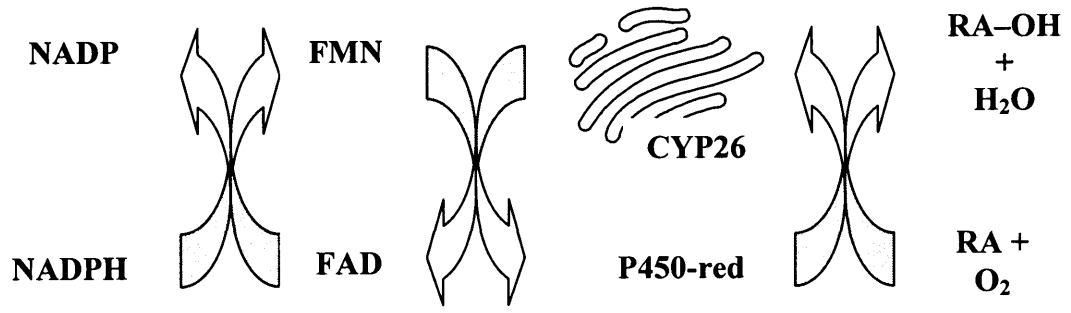

Notes

RA = Retinoic acid
-red = reduced form
FAD = Flavin Adenine dinucleotide
FMN = Flavin Mononucleotide

NADPH = Nicotinamide-adenine dinucleotide phosphate (reduced form)

P450 = cytochrome P450 enzyme located in the endoplasmic reticulum of a cell

Figure 1.7.2. The enzyme involved in hydroxylation of retinoic acid is a cytochrome P450 that requires molecular oxygen, NADPH, and one redox partner, namely the FAD/FMN cofactor.

The heme protein has a porphyrin ring structure (**Figure 1.7.3**) and sits in the interior of the P450 enzyme. The iron atom of the heme protein is involved in the enzyme catalytic reaction (**Figure 1.7.4**). The sulphur atom of the P450 enzyme cysteine residue is ligated to the iron of the heme protein. Whereas, the dioxygen (O_2) is bound to the sixth coordination site of the heme iron (Lewis, 2001) during the P450 catalytic cycle (**Figure 1.7.4**).

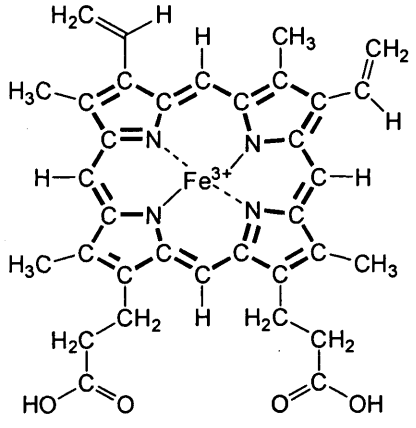

Figure 1.7.3. The porphyrin ring structure of the heme protein.

On addition of carbon monoxide (CO) to the P450 enzyme, it forms a complex which gives a major absorption band at about 450 nm wavelength, hence the name P450.

CYP1α, CYP24 and CYP26 can be found in other tissues, *e.g.* skin, colon, breast and prostate as well as in the kidney and liver as reviewed by Gudas *et al.* (Gudas *et al.*, 1994) and Bouillon *et al.* (Bouillon *et al.*, 1995).

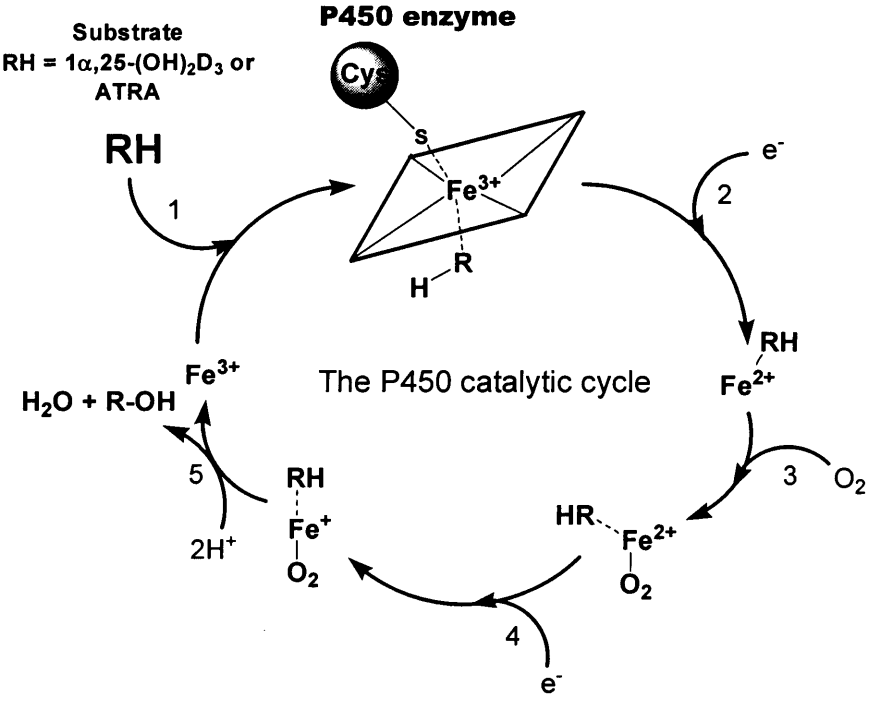

Figure 1.7.4. This catalytic cycle of P450 has been adapted from Lewis (Lewis, 2001). The binding of a substrate (**RH**), such as 1α,25-$(OH)_2$-D_3 in the case of CYP24 or ATRA in the case of CYP26, brings about the displacement of the bound water molecule (H_2O) present in the heme. The substrate becomes oxygenated *via* the activation of molecular O_2 mediated by P450 enzyme. The two electrons (e^-) are provided by the redox carrier protein and the two hydrogen (H^+) from NADPH.

1.7.2 Vitamin D_3 hydroxylases

The important role of vitamin D_3 in many physiological and pathological processes (Bouillon *et al.*, 1995; Ettinger and DeLuca, 1996; Jones *et al.*, 1998) has attracted many researchers in developing new drugs for targeting the key enzymes in the synthesis or metabolism of the active vitamin D_3 hormone, 1α,25-$(OH)_2$-D_3:-

- 25-Hydroxyvitamin D-1α-hydroxylase (CYP1α or CYP27B1) – the key enzymes in the synthesis of the biological active metabolite, 1α,25-$(OH)_2$-D_3.
- 24-Hydroxylases (CYP24) – a multicatalytic enzyme, that causes side-chain oxidative cleavage of 25-$(OH)_2$-D_3 resulting in calcitroic acid formation. CYP24

is a VDR target gene, *i.e.* binding of 1α,25-$(OH)_2$-D_3 to the VDR result in CYP24 gene transcription.

Please note that the term vitamin D_3 hydroxylase enzymes refer to both CYP1α and CYP24. Although human CYP1α and CYP24 enzymes have been purified and cloned (Monkawa *et al.*, 1997; Ohyama *et al.*, 1991; Ohyama and Okuda, 1991), the structural information from X-ray crystallography or NMR analysis is still missing.

1.7.3 Inhibitors of vitamin D_3 hydroxylase enzymes

Various azole compounds *e.g.* ketoconazole and liarozole (**Figure 1.7.5**), have been shown to inhibit cytochrome P450 vitamin D_3 metabolising enzymes. The azole compounds bind directly to the prosthetic heme iron via a lone pair of electrons from the heterocyclic nitrogen and through interaction with other sites in the binding pockets (Schuster *et al.*, 2003). The use of these inhibitors have been shown to slow down the metabolism and depletion of the active vitamin D_3 hormone, 1α,25-$(OH)_2$-D_3 (Ly *et al.*, 1999; Zhao *et al.*, 1996).

SDZ 89-443 and (*R*)-**VID400** (**Figure 1.7.5**) have been identified as potent CYP24 inhibitors and also more selective for CYP24 compared with CYP1α (Schuster and Egger, 1997; Schuster *et al.*, 2001a). These selective inhibitors of CYP24 are used by the Schuster group to study vitamin D_3 metabolism in human keratinocytes.

Posner's group have synthesised potent 1α,25-$(OH)_2$-D_3 analogous with selective CYP24 inhibition properties (Posner *et al.*, 2004). One of the 1α,25-$(OH)_2$-D_3 analogous, CTA018, which is co-developed with Cytochroma Inc., showed dual mechanism of action, *i.e.* with enhanced anti-proliferative and pro-differentiating activities and also potent inhibition of CYP24.

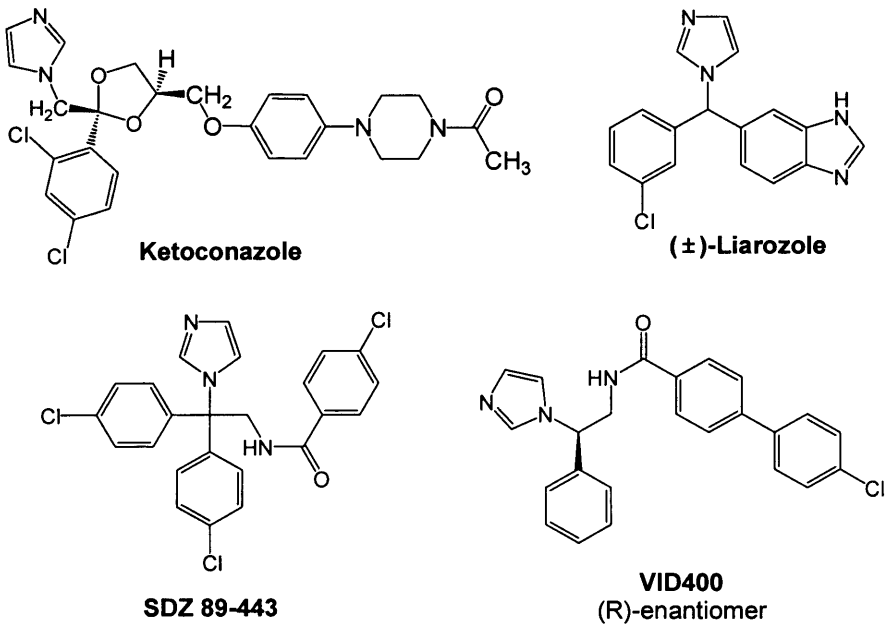

Figure 1.7.5. Azole compounds which show inhibition of CYP24.

1.7.3.1 Vitamin D_3 hydroxylase enzymes inhibitors and prostate cancer

1α,25-$(OH)_2$-D_3 has an effect on modulating the growth and differentiation of prostate cancer cells, and it has been postulated from *in vitro* and *in vivo* studies that inhibitors of vitamin D_3 metabolising enzymes together with 1α,25-$(OH)_2$-D_3 can be useful agents for the treatment of AIPC (Peehl *et al.*, 2001; Peehl *et al.*, 2002). For example, Ly and co-workers (Ly *et al.*, 1999) demonstrated that liarozole could enhanced the half-life of 1α,25-$(OH)_2$-D_3 and up-regulate the vitamin D_3 receptor in androgen-independent DU-145 cell line. Liarozole, is also currently used in Phase II trials for AIPC (Seidmon *et al.*, 1995). There are also promising results from preclinical studies carried out in prostate cancer cells to study the combination of ketoconazole with 1α,25$(OH)_2$-D_3 (Peehl *et al.*, 2001; Peehl *et al.*, 2002).

Inhibition of vitamin D_3 metabolising enzymes (ideally selective CYP24 inhibitor) could be a promising combination therapy together with 1α,25-$(OH)_2$-D_3 for AIPC and in other cancers by sustaining the level of 1α,25-$(OH)_2$-D_3 and in the mean time, the dose of 1α,25-$(OH)_2$-D_3 could be reduced thus reducing the side-effects of 1α,25-$(OH)_2$-D_3. The combination could potentially slow the growth of the prostate cancer cells and restore normal responses to hormonal signaling (Zhao and Feldman, 2001).

1.7.4 Retinoic acid hydroxylase enzymes

In human, in addition to the already mentioned CYP26 (Ray *et al.*, 1997; White *et al.*, 1997), there are several other microsomal cytochrome P450 enzymes that have been identified in the metabolism of ATRA, *i.e.*, CYPs 2C8 (Leo *et al.*, 1989; Nadin and Murray, 1999), 2C9, 3A4 and 3A7 (Chen *et al.*, 2000a; Marill *et al.*, 2000; McSorley and Daly, 2000). As mentioned in section **1.4.1**, CYP26 appears to be specific for 4-hydroxylation of ATRA, as it only recognises ATRA as its substrate, and the expression of CYP26 is induced by ATRA *in vitro* and *in vivo*.

1.7.5 Inhibitors of ATRA hydroxylase enzymes or RAMBAs

Due to the rapid metabolism of retinoic acid in cells, ATRA shows a decrease in plasma concentrations after repeated dosage (Muindi *et al.*, 1994). Many research groups are searching for inhibitors of these cytochrome P450s that mediate the metabolism of RA, *i.e.* retinoic acid metabolism blocking agents (RAMBAs). The use of RAMBAs should delay *in vivo* ATRA metabolism thus resulting in increased endogenous levels (Njar, 2002). Liarozole and ketoconazole are capable of inhibiting the CYP-dependent metabolism of RA by hamster (Njar *et al.*, 2000; Van Wauwe *et al.*, 1990) and rat (Kirby *et al.*, 2003) liver microsomes respectively. Moreover, it has been shown that liarozole with ATRA potentiates the anti-proliferative effect in *in vitro* tumour cell lines (Djikman *et al.*, 1994; Wouters *et al.*, 1992). *In vivo* studies using liarozole has also been studied, showing enhanced plasma levels of ATRA following oral dosing of liarozole in rat (Van Wauwe *et al.*, 1992).

Njar's group have identified azolyl retinoid compounds (**Figure 1.7.6**) which showed interesting activities against RA metabolism enzyme(s) in hamster liver microsomes (IC_{50} = 0.68 – 1.6 μM) (Njar *et al.*, 2000) and in breast and prostate cancer cell lines, which demonstrated enhanced anti-proliferative action compared with ATRA and liarozole (Njar, 2002; Patel *et al.*, 2004).

The selective and potent CYP26 inhibitors, discovered by Janssen Pharmaceutical, are the 2-benzothiazolamine compounds, **R115866** and **R110610** (**Figure 1.7.6**) (Aelterman *et al.*, 2001; Stoppie *et al.*, 2000; Van heusden *et al.*, 2002). In an *in vivo* study, R115866 was able to enhance endogenous RA levels and also to mimic the effects of RA (Stoppie *et al.*, 2000). More recently, OSI Pharmaceuticals Inc. reported potent and selective CYP26 inhibitors, with a naphthyl-based backbone structure, as shown in **Figure 1.7.6** (Mulvihill *et al.*, 2005). The most active compound

showing IC_{50} = 3.3 nM in the assay performed using microsomal preparations from T47D breast cancer cells induced to express CYP26 enzyme (Mulvihill *et al.*, 2005).

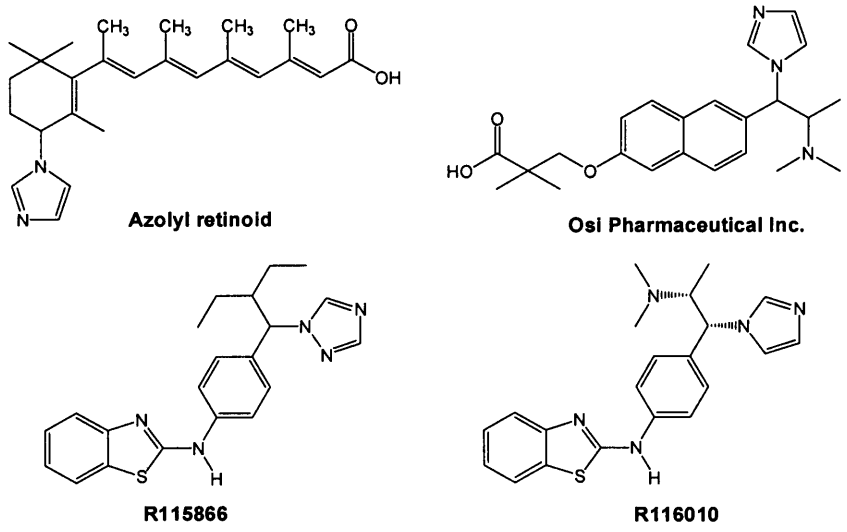

Figure 1.7.6. Examples of some Retinoic Acid Metabolism Blocking Agents (RAMBAs).

1.7.5.1 RAMBAs and prostate cancer

The rationale behind the use of ATRA with RAMBAs in the treatment of acute promyelocytic leukemia (APL) was that the remission duration for patients treated with ATRA was very brief (Chen *et al.*, 1991; Miller *et al.*, 1994). *In vivo* studies have shown that the use of a RAMBAs administered with retinoic acid, *e.g.* ketoconazole or liarozole, increased plasma half-life of retinoic acid and enhanced endogenous retinoic acid plasma levels in rats (Van Wauwe *et al.*, 1990; Van Wauwe *et al.*, 1992). In androgen-dependent and androgen-independent prostate cancer mouse models (R3327 Dunning prostate adenocarcinomas), liarozole, was shown to contribute to its anti-tumoural effect (De Coster *et al.*, 1992; Djikman *et al.*, 1994). Although the combination therapy using liarozole or ketoconazole with ATRA was not used in prostate cancer, the use of these compounds by themselves has had some success in clinical trials, *e.g.* ketoconazole is currently used as second-line treatment in AIPC (Harris and Reese, 2001), whereas, liarozole is in phase II trials for AIPC (Seidmon *et al.*, 1995).

In order to achieve sufficient and non-toxic levels of ATRA in target tissues, the use of a RAMBA could be a new strategy. This allows ATRA to play its role as a differentiation agent at lower doses to achieve effectiveness. The selective CYP26 inhibitor, R115866 and R116010 (**Figure 1.7.6**), have demonstrated strong anti-tumour

effects in androgen-independent rat prostate adenocarcinoma and in oestrogen-independent mouse mammary tumours (Njar, 2002; Stoppie *et al.*, 2000; Van heusden *et al.*, 2002), this suggests that CYP26 inhibitor can be a potential candidate for the treatment of prostate and breast cancer.

CHAPTER 2

Aims of the investigation

2. Aims of the investigation

The aims of the investigation were:

1. To synthesise organic compounds inhibiting the vitamin D_3 and ATRA metabolising enzymes.
2. To study vitamin D_3 and ATRA metabolism in rat kidney mitochondrial and rat liver microsomes respectively.
3. To study vitamin D_3 and ATRA metabolism in cancer cell-lines (MCF-7 and DU-145).
4. To study the inhibition of vitamin D_3 and ATRA metabolism in these *in vitro* assays **2** and **3** above using the synthesised compounds.

Since the X-ray crystal structures of CYP24 and CYP26 are unknown, the design of organic compounds targeting these enzymes is based on intuition. Judging from the structures of (**Figure 2.1**):

- inhibitors of vitamin D_3 and ATRA metabolising enzymes (liarozole and ketoconazole) and the more selective inhibitors for CYP24 (**SDZ 89-443** and **VID 400**); and
- organic compounds synthesised by our group which affect activity of the cytochrome P450 enzymes involved in hormone biosynthesis (Le Lain *et al.*, 2002; Vinh *et al.*, 1999; Vinh *et al.*, 2001) or retinoic acid catabolism (Greer *et al.*, 2003; Kirby *et al.*, 2003; Kirby *et al.*, 2002); as a result, three series of compounds were proposed. The methods will be described in Chapter **3 – 5**.

Series I compounds are based on the 1-(benzofuran-2-yl)phenylmethyl back bone structure described by Vinh *et al.* (Vinh *et al.*, 1999; Vinh *et al.*, 2001) as selective P450 aromatase inhibitors. A lipophilic alkyl chain or phenyl ring attached to the compound as shown in the diagram below may mimic the lipophilic chain structure of ATRA and 1α,25-$(OH)_2$-D_3.

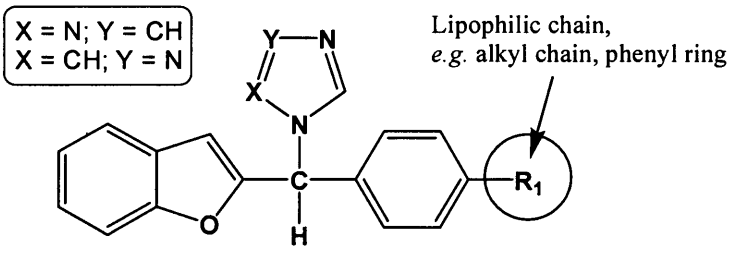

Series I
1- and 4- [Benzofuran-2-yl)phenylmethyl]triazole derivatives

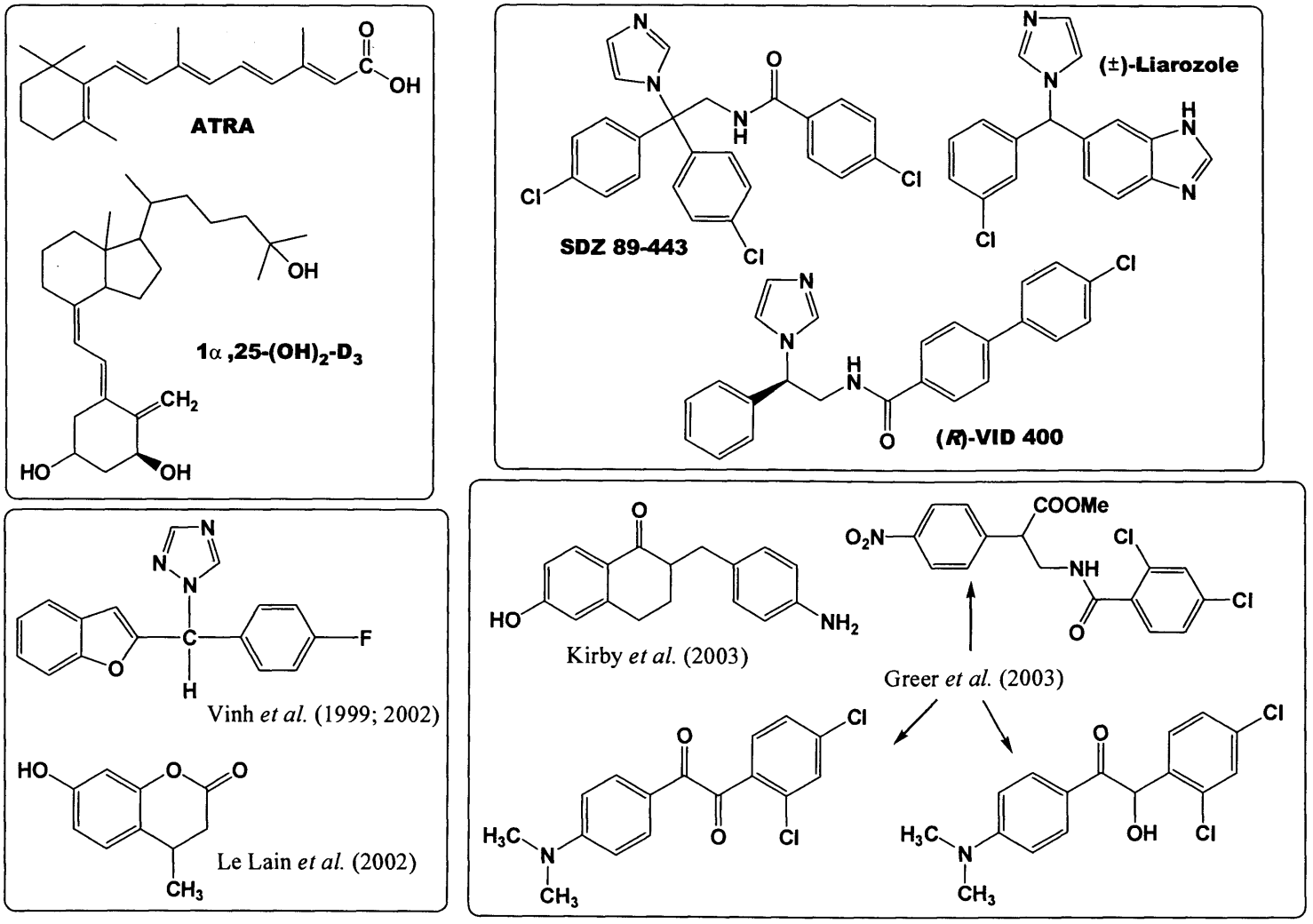

Figure 2.1. Chemical structures of ATRA, 1α,25-$(OH)_2$-D_3, known inhibitors of CYP24 and CYP26 and some chemical structures synthesised by our group

In **Series II**, the amide bond was chosen to link the benzofuran ring with the phenyl methyl ring, as shown below. This mimics the selective inhibitors of CYP24, SDZ 89-443 and VID 400 described by Schuster *et al.* (Schuster *et al.*, 2001a). In addition, our group has also synthesised some 1,2-diphenylpropane compounds (Greer *et al.*, 2003) with an amide bond linkage, which showed comparable inhibition results against retinoic acid metabolising enzymes with ketoconazole.

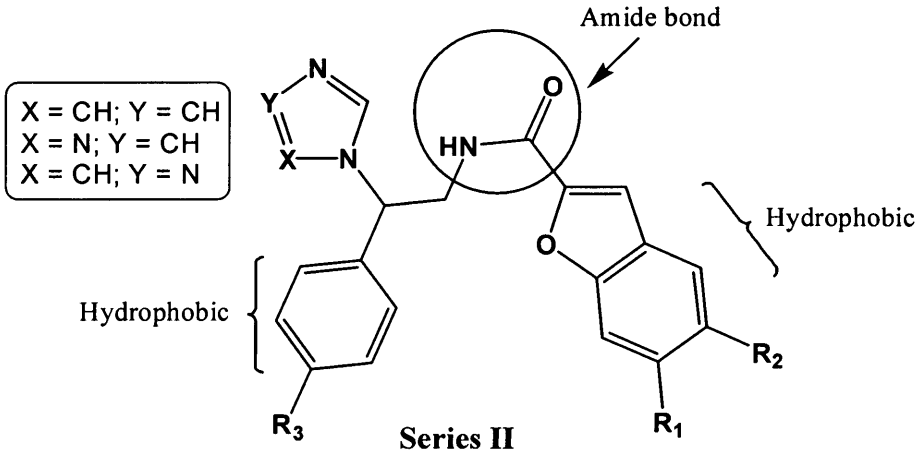

Benzofuran-2-carboxamido ethyl-imidazole and -1,2,4-triazole derivatives

Dietary and epidemiological factors have been implicated in the low rates of breast and prostate cancer in China and Japan (Sasagawa and Nakada, 2001). The population in China and Japan consume a diet rich in soy beans, which are rich in isoflavanoids. Isoflavanoids belong to a group of phytoestrogens and the major constituents of isoflavanoids are genistein and daidzein (**Figure 2.2**).

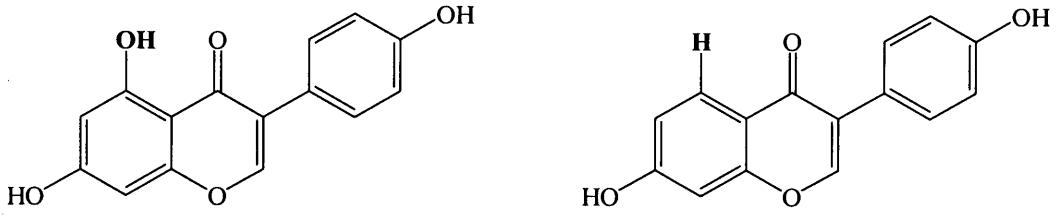

Genistein **Daidzein**

Figure 2.2. The structure of genistein and daidzein.

It has been shown in our own laboratory, that isoflavones and flavones (Le Lain *et al.*, 2001); tetralones (Kirby *et al.*, 2003; Smith *et al.*, 2001); and coumarin (Le Lain et al., 2002) are known to affect the activity of cytochrome P450 enzymes involved in hormone biosynthesis. In view of these facts, it would be interesting to

investigate the inhibition of these compounds against the vitamin D_3 and ATRA metabolising enzyme.

Since it was shown by Kirby *et al.* (Kirby *et al.*, 2003) that 2-(4-aminophenylmethyl)-6-hydroxy-3,4-dihydronaphthalene-1-one (**Figure 2.1**) showed comparable results with ketoconazole in the inhibition of RA metabolising enzymes, a series of tetralone compounds was synthesized (**Series III**). Hydrophobic and/or hydrophilic substituents were chosen to probe the active site of vitamin D_3 and ATRA metabolising enzymes.

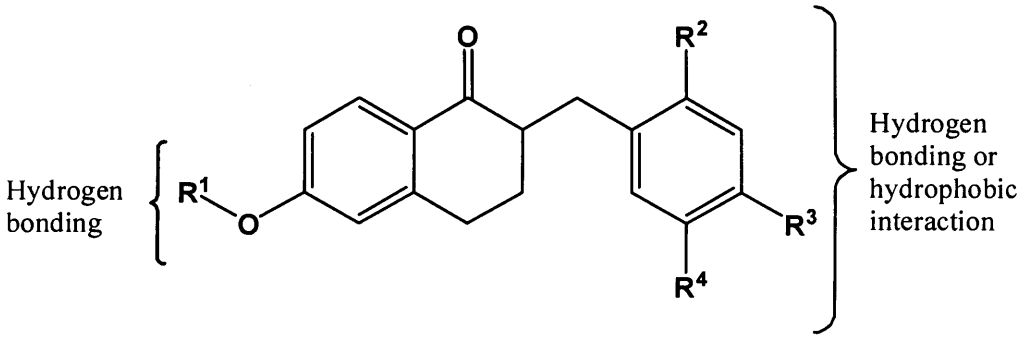

Series III

6-Substituted-2-(phenylmethylene)-3,4-dihydronaphthalene-1-one derivatives

CHAPTER 3

Synthesis of 1- and 4- [(benzo[*b*]furan-2-yl)phenylmethyl]triazoles derivatives

3.1 Synthesis of 1- and 4-[(benzo[*b*]furan-2-yl)phenylmethyl]triazoles

The synthesis of the substituted 1- and 4-[(benzo[*b*]furan-2-yl)phenylmethyl]triazoles was carried out according to a sequence of 5 steps as outlined in **Scheme 3.1.** The reactions shown in **Scheme 3.1)** involve a modification of the procedure described by Pestellini and co-workers (Pestellini *et al.*, 1987).

3.1.1 Synthesis of the phenacyl bromide

A wide range of brominated reagents, for example, $AlCl_3/Br_2$ and phenyltrimethylammonium tribromide (PTT), could be used to brominate aldehydes and ketones in the α-position. 4'-Ethylacetophenone (**1**) was reacted with bromine in the presence of aluminium chloride at 0 °C to give 2-bromo-1-(4-ethyl-phenyl)-ethanone (**2**) (**Scheme 3.1**). $AlCl_3$ acts as a Lewis acid and catalyst to promote bromination. The reaction was stirred for 3.5 h. The low temperature and high dilution with the solvent (THF) may slow down the reaction, to prevent the formation of the di-brominated acetophenone, 2,2-dibromo-1-(4-ethyl-phenyl)-ethanone. Bromine should be added dropwise over a 20 minute period to minimise the formation of 2,2-dibromo-1-(4-ethyl-phenyl)-ethanone.

The presence of the 2-bromo-1-(4-ethyl-phenyl)-ethanone was confirmed by ^1H n.m.r. by the disappearance of the CH_3 singlet at 2.6 ppm which was replaced by a CH_2 singlet observed at 4.4 ppm.

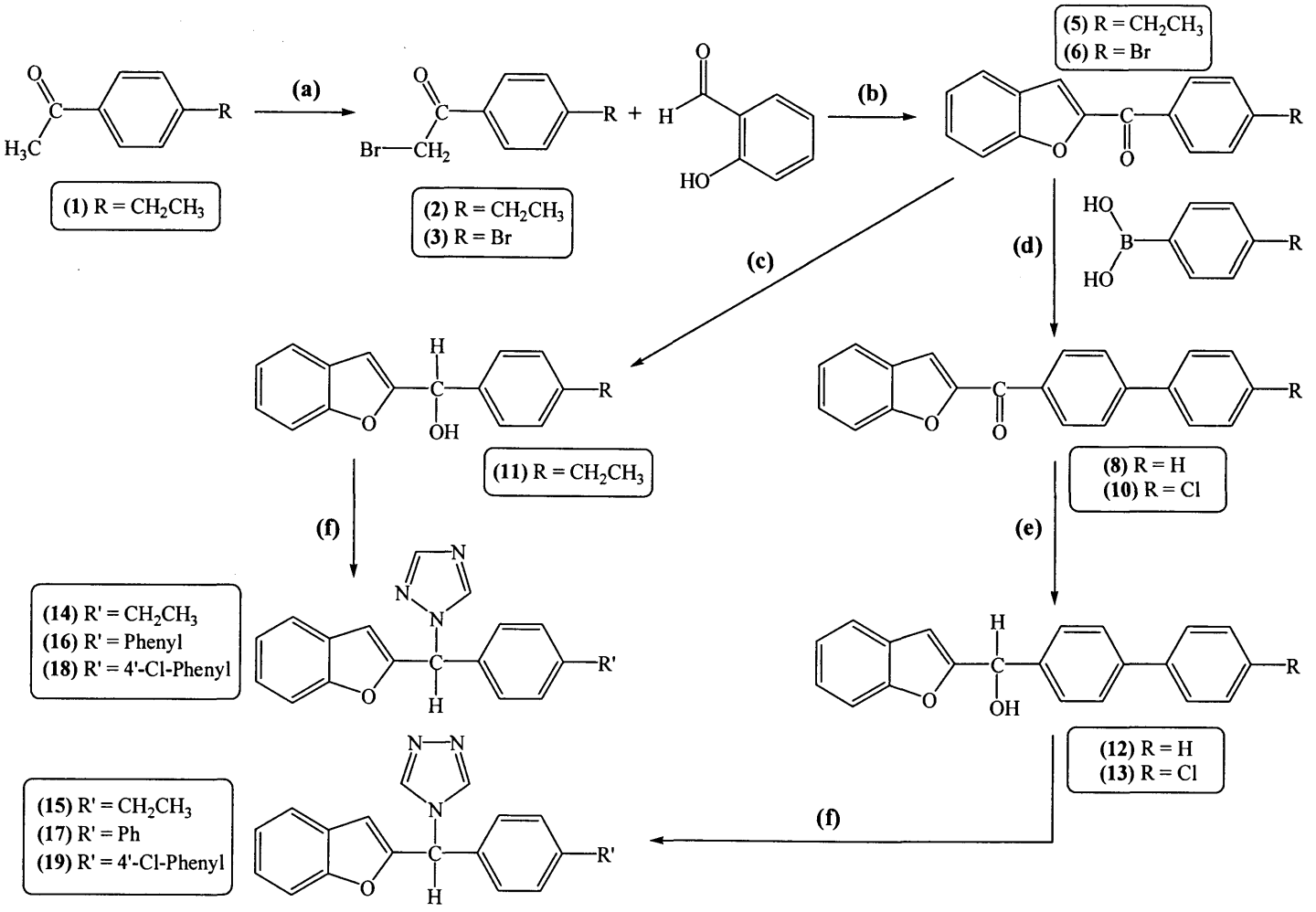

Scheme 3.1. General reaction scheme for the synthesis of substituted 1- and 4- [(benzofuran-2-yl)phenylmethyl]triazoles. Reagents and conditions: **(a)** Br_2, $AlCl_3$, THF, 0 °C, 3.5 h. **(b)** (i) NaH, DMF, 80 °C, 2.5 h, (ii) NaOMe, 80 °C, 1.5 h. **(c)** and **(e)** $NaBH_4$, 1,4-dioxane, 6 h. **(d)** (i) phenylboronic acid or 4-chlorophenylboronic acid, $Pd(PPh_3)_4$, toluene, 100 °C, 4 h (ii) H_2O_2, room temperature, 1 h. **(f)** (i) 1,2,4-triazole, thionyl chloride, acetonitrile, 10 °C, 1 h, (ii) K_2CO_3, room temperature, 4 – 6 days.

3.1.2 Synthesis of the substituted (benzo[*b*]furan-2-yl)-phenyl-methanones

The synthesis of the substituted (benzo[*b*]furan-2-yl)-phenyl-methanones was achieved by the Rap-Stöermer reaction (Stöermer, 1900). This reaction (**Scheme 3.2**) involves two bases, sodium hydride and sodium methoxide.

In **step 1**, sodium hydride (NaH), a strong base, forms a sodium salt of salicylaldehyde with concurrent liberation of hydrogen gas. The resulting phenoxy anion, which acts as a nucleophile, attacks the α-carbon of the phenacyl bromide (**2** or **3**) with the loss of the bromine atom.

In **step 2**, sodium methoxide ($NaOCH_3$), a base, removes the proton in the α-carbon position, resulting in the formation of the carbanion. This carbanion attacks the aldehyde group of the salicylaldehyde, resulting in the formation of a cyclic ring. Protonation then occurs to form the intermediate, finally a molecule of water is lost to form the substituted (benzofuran-2-yl)-phenyl-methanones (**5** or **6**).

The crude product was recrystallised from methanol to give a reasonable yield for product **5** (34 %) and good yield for product **6** (92 %). The presence of impurities in the synthesis of compound **5** made recrystallisation to be difficult and thus a low yield was achieved.

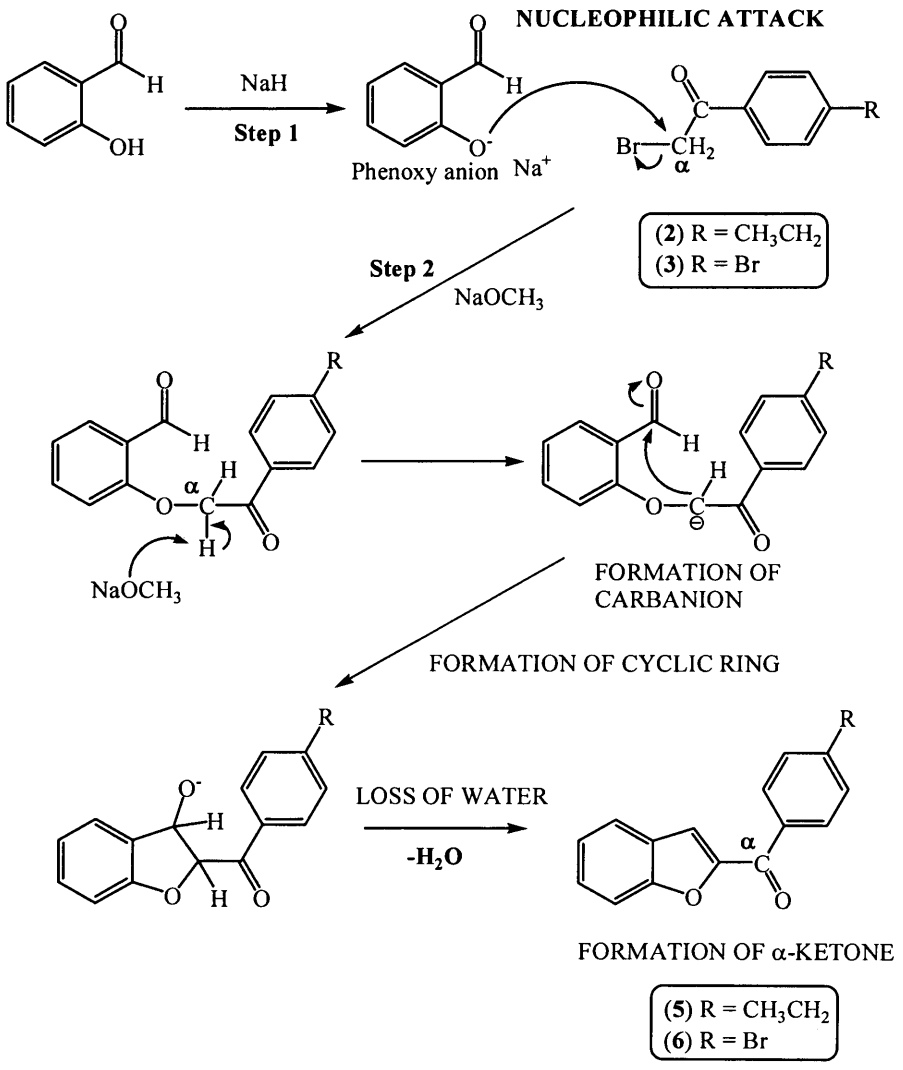

Scheme 3.2. The formation of substituted (benzo[*b*]furan-2-yl)-phenyl-methanones by the Rap-Stöermer reaction. **Step 1** – NaH, DMF, 80 °C, 2.5 h. **Step 2** – $NaOCH_3$, 80 °C, 1.5 h.

3.1.3 Synthesis of the biphenyl ring

The synthesis of the biphenyls (**8** and **10**) was performed by the Suzuki reaction using the commercially available phenylboronic acids (**7** or **9**) [**Scheme 3.4**]. Miyaura *et al.* (Miyaura *et al.*, 1981) reported the cross-coupling reaction of phenylboronic acid (**i**) with aryl bromide (**ii**) in the presence of palladium catalysts and base to provide the corresponding biaryls (**iii**) in good yields (**Scheme 3.3**). After the reaction was complete, 30 % H_2O_2, as an oxidising agent, was added to remove the residual phenyl boronic acid. The Suzuki reaction is tolerant to a wide variety of functional groups, and thus various substituted aromatic rings can be used. It is one of the direct methods for the formation of carbon-carbon bonds. Moreover, arylboronic acid is easy to handle as it is stable at high temperature.

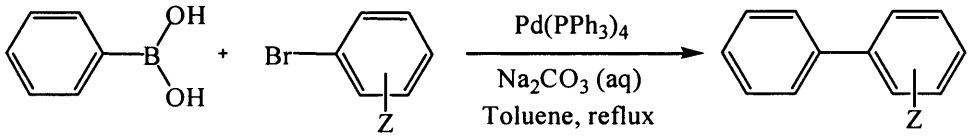

(i) (ii) (iii)

Scheme 3.3. The Suzuki reaction – cross-coupling reaction of phenylboronic acid (**i**) with aryl bromide (**ii**) using palladium catalyst ($Pd(PPh_3)_4$) and Na_2CO_3 base to form biaryls (**iii**).

Phenylboronic acid (**7**) and 4-chloro-phenylboronic acid (**9**) were reacted with benzo[*b*]furan-2-yl-(4-bromo-phenyl)-methanone (**6**) to form (**8**) and (**10**) respectively (**Scheme 3.4**). The Suzuki reaction gives reasonably good yields of products **8** (58 %) and **10** (73 %) after purification by column chromatography and/or recrystallisation.

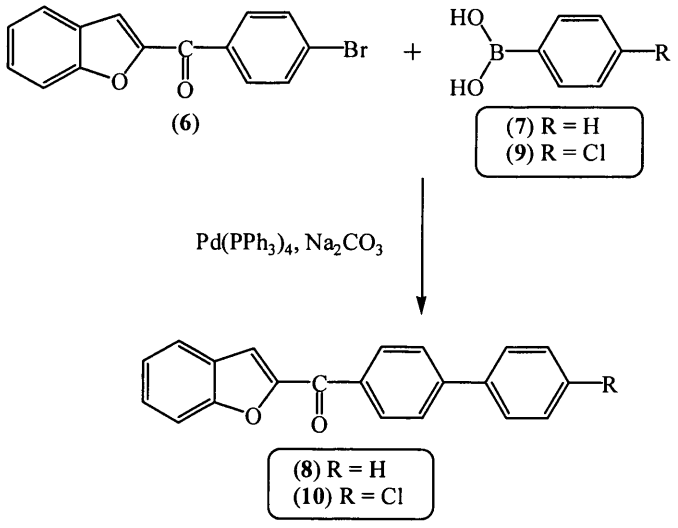

Scheme 3.4. The synthesis of benzo[*b*]furan-2-yl-biphenyl-4-yl-methanone (**8**) and benzofuran-2-yl-(4'-chloro-biphenyl-4-yl)-methanone (**10**) using Suzuki reaction. Reaction conditions: $Pd(PPh_3)_4$, Na_2CO_3 (aq.), toluene, 100 °C, then H_2O_2, r.t., 1 h.

3.1.4 Synthesis of the benzo[*b*]furan-2-yl(4-substituted phenyl)methanol)

The ketone compounds (**5**, **8** and **10**) can be reduced to the secondary alcohols (**11**, **12** and **13** respectively) by the action of the metal hydride $NaBH_4$. $NaBH_4$ is a mild reducing agent, it reduces ketones rapidly at room temperature in 1,4-dioxane solvent. The mechanism of this reaction involved nucleophilic addition (**Scheme 3.5**). The pair of electrons from the boron metal was transferred to the hydrogen to form hydride ion, H^-, which then acts as a nucleophile to attack the carbonyl carbon of the ketone compound.

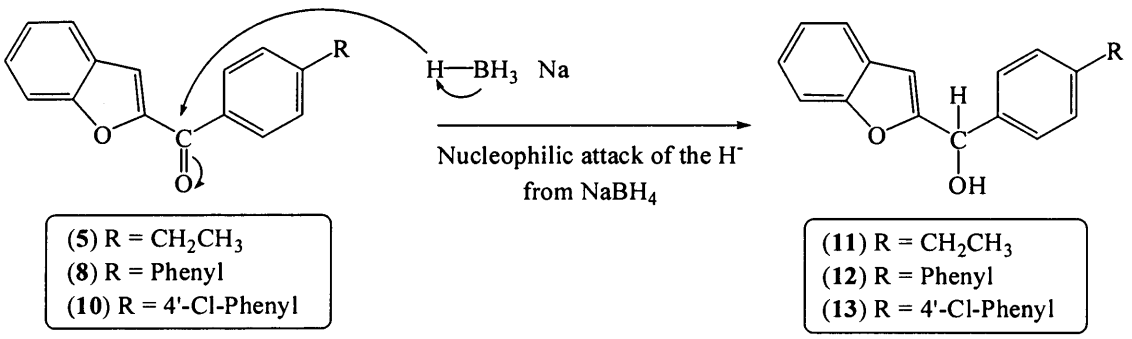

Scheme 3.5. The synthesis of the secondary alcohol compounds (**11**, **12** and **13**). 4 moles of the α-ketone compounds (**5**, **8** or **10**) reacted with 1 mole of $NaBH_4$. Reaction conditions: $NaBH_4$, 1,4-dioxane, r.t., 8 h.

The reduction of the ketone compounds to the secondary alcohol compounds (**11** – **13**) using $NaBH_4$ gave very good yield (75 %, 83 % and 90 % respectively). Moreover, no further recrystallisation or column chromatography was required prior the next reaction step.

3.1.5 Synthesis of the substituted 1- and 4-[(benzo[*b*]furan-2-yl)phenylmethyl]triazoles

Drabel and Regel in 1975 patented a superior method (Draber and Regel, 1975) by reacting thionyl-imidazole with a substituted carbinol (**Scheme 3.6**) to form *N*-(1,1,1-trisubstituted)-methylazoles. The synthesis of the triazole compounds (**14** – **19**) involved the reaction of the carbinol compounds (**11** – **13**) with the *in situ* prepared di-triazole-sulphoxide (**Scheme 3.7**).

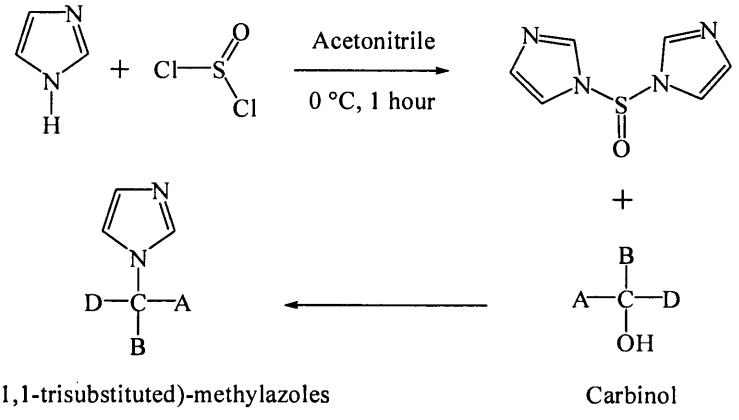

Scheme 3.6. Synthesis of *N*-(1,1,1-trisubstituted)-methylazoles by reacting thionyl-imidazole with substituted carbinol (Draber and Regel, 1975).

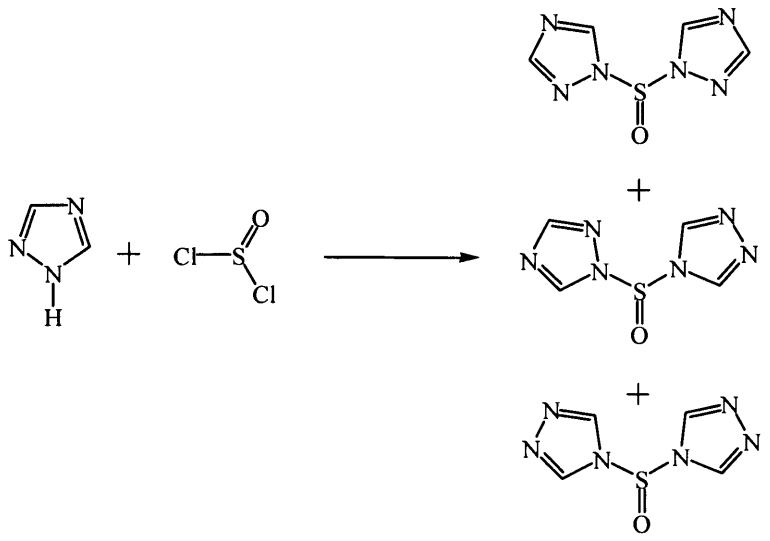

Scheme 3.7. The *in situ* prepared di-triazole-sulphoxide. Reaction conditions: 4:1 = 1,2,4-triazole:$SOCl_2$, acetonitrile, 10 °C, 1 h.

The mechanism of the synthesis of the triazole compounds (**14** – **19**) involved two nucleophilic substitution reactions (**Scheme 3.8**). The carbinol compounds (**11** – **13**) reacted with (**I**) or (**II**) to give the products (**14** – **19**) after undergoing a second nucleophilic substitution (**Scheme 3.8**).

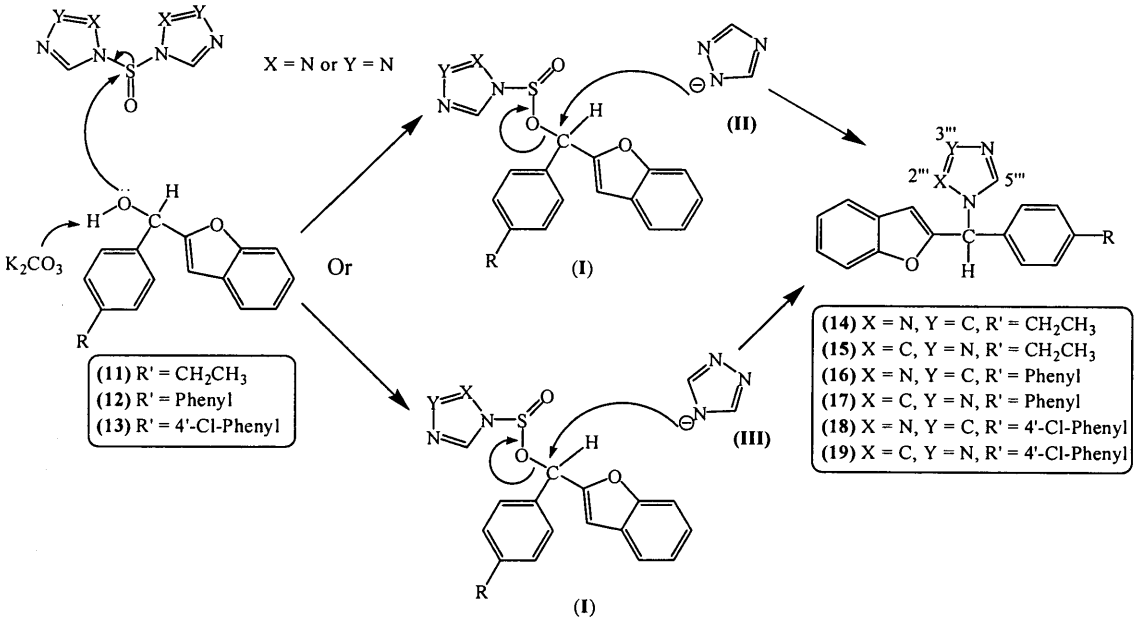

Scheme 3.8. The mechanism of the synthesis of substituted 1- and 4-[(benzo[*b*]furan-2-yl)phenylmethyl]triazoles (**14** – **19**). Reaction conditions: 1,2,4-triazole, $SOCl_2$, acetonitrile, 10 °C, 1h then add K_2CO_3, carbinol compound (**11**, **12** or **13**), r.t., 4 – 6 days.

The above reaction took 4 – 6 days to go to completion (**Table 3.1**). The reaction was purified by flash column chromatography using two different systems, *i.e.* petroleum ether/ethyl acetate and dichloromethane/methanol. The substituted 1-

[(benzo[*b*]furan-2-yl)phenylmethyl]triazoles (**14**, **16** and **18**) elute out before the 4-[(benzo[*b*]furan-2-yl)phenylmethyl]triazoles (**15**, **17** and **19**). The substituted 4-[(benzo[*b*]furan-2-yl)phenylmethyl]triazoles gave a lower yield compared with the substituted 1-[(benzofuran-2-yl)phenylmethyl]triazoles (**Table 3.1**). This shows that the nucleophile (**II**) is more nucleophilic compared with the nucleophile (**III**) to attack the carbon atom of the intermediate (**I**) (**Scheme 3.8**).

The products were confirmed by ^{1}H n.m.r. after purification by flash column chromatograph. The ^{1}H n.m.r. showed the disappearance of the OH group at approximately 2.7 – 2.9 ppm and the presence of the two singlet protons (H-3''' and H-5''') of the triazoles compounds, **14**, **16** and **18**, at approximately 8.1 and 8.2 ppm. The two protons (H-2''' and H-5''') of the triazoles compounds, **15**, **17** and **19** appeared as a singlet at 8.3 ppm. These two protons are symmetrical and thus show only one singlet peak with two proton integration.

Table 3.1. Summary of the synthesis of the substituted 1- and 4- [(benzo[*b*]furan-2-yl)phenylmethyl]triazoles.

Product	Total reaction (days)	Yield (%)	Ratio	Melting point (°C)
14	4	67	5	Semi-solid at r.t.
15		13	1	126 -128
16	6	53	9	130 – 132
17		6	1	56 - 58
18	6	67	5	34 – 36
19		13	1	68 - 70

3.2 General material and method

All reactions were carried out under an atmosphere of nitrogen when necessary. ^{1}H and ^{13}C n.m.r. spectra were recorded on a Bruker Advance DPX300 spectrometer at 300 MHz and 75 MHz respectively. The n.m.r. solvent was $CDCl_3$ for all cases unless mentioned otherwise. Each resonance signal was reported according to the following convention:

- chemical shifts are given in parts per million (ppm) relative to the internal standard tetramethyl silane (Me_4Si).
- coupling constants [J in hertz (Hz)].
- multiplicity are denoted as s (singlet), d (doublet), t (triplet), m (multiplet) or combinations thereof.

Infra red (IR) spectra were recorded on a Perkin-Elmer 1600 (FTIR) spectrophotometer as either films or sodium chloride discs or as solids *via* a diffuse reflectance accessory using a potassium bromide (KBr) disc. Low resolution mass spectra ES (Electrospray) were recorded on Fisions VG Platform Electrospray Mass Spectrometer. Mass spectra were determined under EI (Electron Impact) or CI (Chemical Ionisation) conditions at the EPSRC National Mass Spectrometry Service Centre, University of Wales, Swansea. Accurate mass measurements were also performed at the EPSRC National Mass Spectrometry Service Centre. Microanalysis data were performed by Medac Ltd., Brunel Science Centre, Surrey.

For column chromatography, a glass column was slurry packed in the appropriate eluent with silica gel (Fluka Kieselgel 60). Flash column chromatography was performed with the aid of a pump. Analytical thin layer chromatography (t.l.c.) was carried out on pre-coated silica plates (Merck Kieselgel 60 F_{254}) with visualisation *via* UV light (254 nm) and/or vanillin stain.

Vanillin stain was prepared from the following ingredients:

Vanillin	3 g
Absolute ethanol	250 mL
Concentrated H_2SO_4	5 mL

Melting points were determined using a Gallenkamp melting point apparatus and were uncorrected. All reagents and solvents employed were of general purpose or analytical grade and purchased from Sigma-Aldrich Chemical Company, Fluka or

Agros Chemicals. Solvents were appropriately dried over molecular sieves (3Å) or by distillation when necessary.

3.3 Experimental results for the synthesis of substituted 1- and 4-[(benzo[*b*]furan-2-yl)phenylmethyl]triazoles

The numbering of compounds for n.m.r. characterisation is as follows:

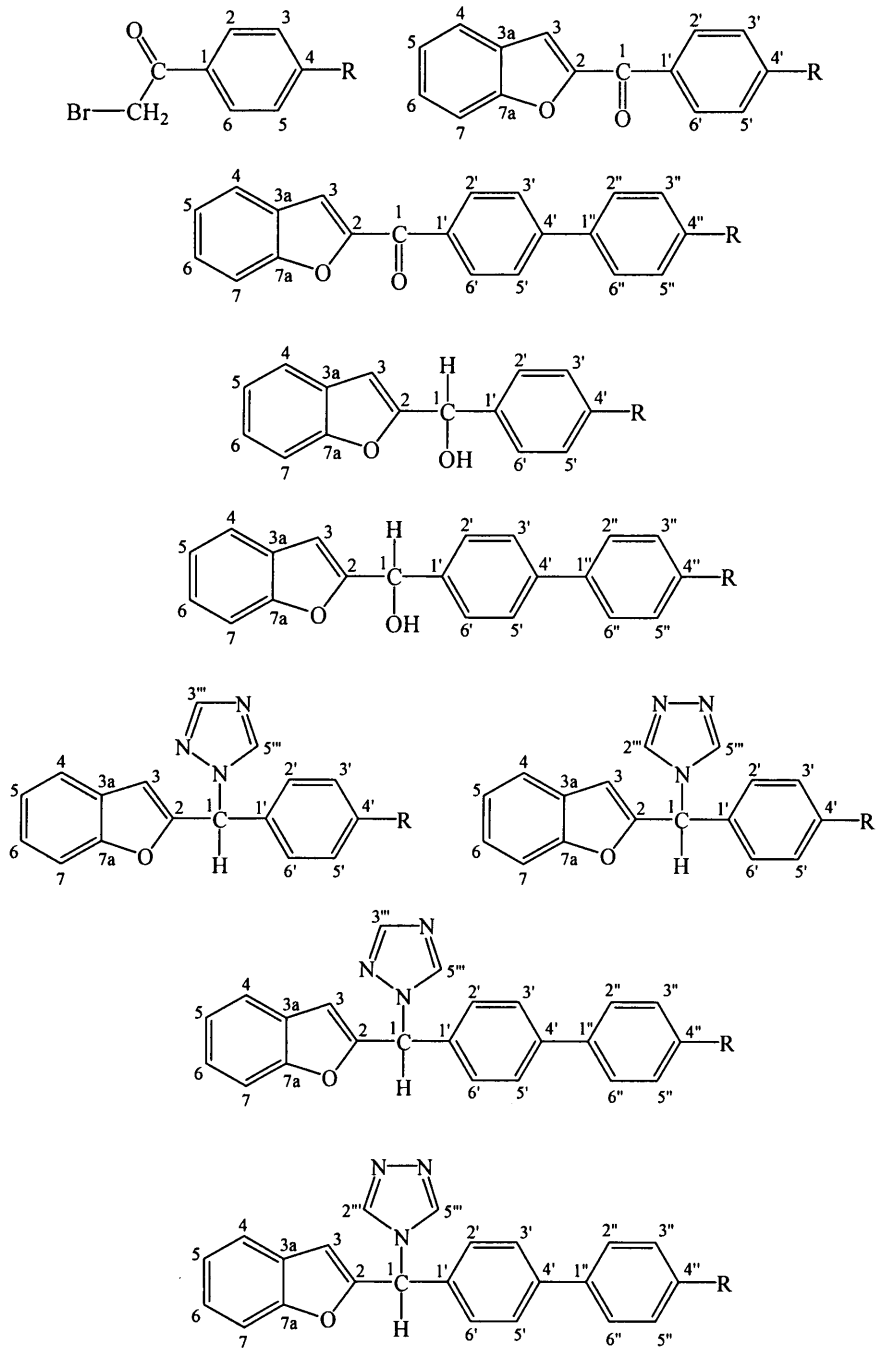

All n.m.r. characterisations were made by comparison with previous n.m.r. spectra of the appropriate structure class and or predictions from ACD/HNMR and ACD/CNMR

(Advanced Chemistry Development Inc., Version 2.51, 1997) and ChemDraw Ultra™ 7.0 (CambridgeSoft).

2-Bromo-1-(4-ethyl-phenyl)-ethanone (**2**) (Mason, 2000)

($C_{10}H_{11}BrO$, MW: 227.100)

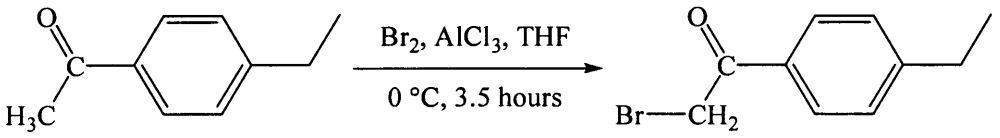

(**1**) (**2**)

To a cooled solution (0 °C) of 4'-ethyl acetophenone (**1**) (2.52 mL, 16.87 mmol) in anhydrous THF (20 mL) was added a catalytic amount of aluminium chloride (0.23 g, 1.7 mmol). Bromine (0.87 mL, 16.87 mmol) was added dropwise to the solution (to give an orange solution) over a period of 20 minutes and the reaction stirred for a further 3.5 hours until the orange solution faded to a yellow colouration. The reaction was then concentrated under reduced pressure. The resulting residue was extracted with CH_2Cl_2 (150 mL) and water (3 x 100 mL). The organic layer was dried with $MgSO_4$, filtered and reduced *in vacuo* to give a dark green solution. Purification by flash column chromatography (petroleum ether – ethyl acetate 100:0 v/v increasing to 97.5:2.5 v/v) gave 2-bromo-1-(4-ethyl-phenyl)-ethanone (**2**) as a dark brown liquid. Yield: 3.56 g (93 %), t. l. c. system: petroleum ether – ethyl acetate 4:1 v/v, R_F: 0.53, stain positive.

^{1}H n.m.r. δ 7.91 (m, 2H, H-2 and H-6), 7.30 (m, 2H, H-3 and H-5), 4.43 (s, 2H, C$\underline{H}_2$-Br), 2.70 (q, J = 7.6 Hz, 2H, C$\underline{H}_2$), 1.26 (t, J = 7.6 Hz, 3H, C$\underline{H}_3$)

^{13}C n.m.r. δ 191.40 (C=O), 151.54 (C, C-4), 132.08 (C, C-1), 129.64 (2 x CH, CH-2 and CH-6), 128.93 (2 x CH, CH-3 and CH-5), 31.48 (CH_2, $\underline{C}H_2$-Br), 29.46 (CH_2, $\underline{C}H_2$-CH_3), 15.54 (CH_3, CH_2-$\underline{C}H_3$).

Synthesis of benzo[*b*]furan-2-yl-phenyl-methanone derivatives (compound **5** and **6**)

Benzo[*b*]furan-2-yl(4-ethylphenyl)methanone (5)

($C_{17}H_{14}O_2$, MW: 250.296)

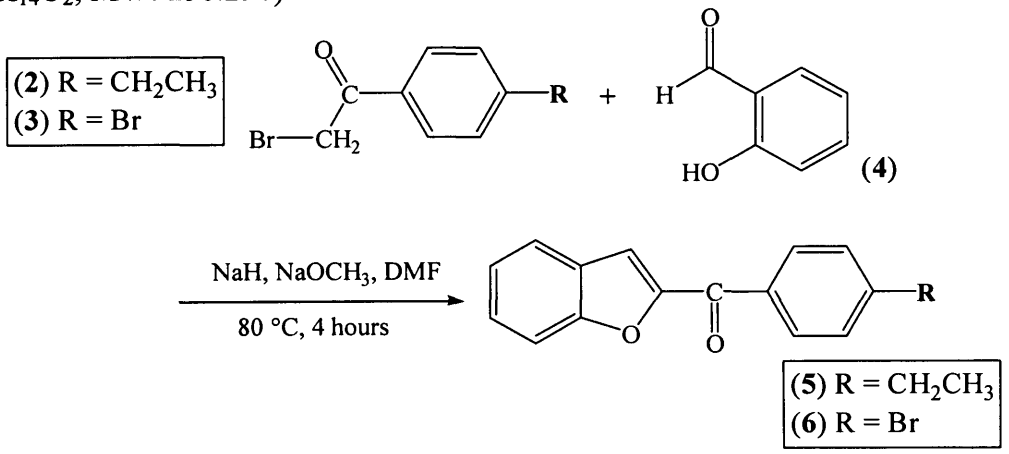

Salicylaldehyde (**4**) (1.68 mL, 15.74 mmol) in anhydrous DMF (2.0 mL), was added dropwise to a stirred solution of sodium hydride (60 % in mineral oil, 0.70 g, 17.31 mmol) in anhydrous DMF (8.0 mL). Hydrogen gas was liberated to give a bright yellow solution of the sodium salt. 2-Bromo-1-(4-ethyl-phenyl)-ethanone (**2**) (3.56 g, 15.74 mmol) in anhydrous DMF (10 mL) was then added dropwise and the resulting solution was stirred at 80 °C for 2.5 hours. Then sodium methoxide (0.26 g, 4.72 mmol) was added and the solution heated for another 1.5 hours at 80 °C. The solvent was then evaporated to about $^1/_3$ its volume to give a brown syrup. The crude product was extracted with CH_2Cl_2 (200 mL) and water (3 x 100 mL). The organic layer was dried with $MgSO_4$, filtered and reduced *in vacuo* to give a yellow oily residue. The oily residue was recrystallised with methanol to yield the brown solid, benzo[*b*]furan-2-yl-(4-ethyl-phenyl)-methanone (**5**). Yield: 1.32 g (34 %), t. l. c. system: petroleum ether – ethyl acetate 5:2 v/v, R_F: 0.43, stained negative. Melting point 60 – 62 °C. Microanalysis: Calculated C = 81.58 %, H = 5.64 %; Found C = 81.44 %, H = 5.84 %.

^{1}H n.m.r. δ 8.05 (d, J = 8.1 Hz, 2H, Ar), 7.78 (d, J = 7.7 Hz, 1H, Ar), 7.70 (d, J = 7.9, 1H, Ar), 7.55 (m, 2H, Ar), 7.37 (m, 3H, Ar), 2.81 (q, J = 7.6 Hz, 2H, C<u>H</u>$_2$), 1.36 (t, J = 7.6 Hz, 3H, C<u>H</u>$_3$).

^{13}C n.m.r. δ 184.56 (C=O), 156.35 (C, C-7a), 152.83 (C, C-4'), 150.43 (C, C-1'), 135.22 (C, C-2), 130.19 (2 x CH, CH-2' and CH-6'), 128.66 (CH, CH-6), 128.52 (2 x CH, CH-3' and CH-5'), 127.48 (C, C-3a), 124.36 (CH, CH-5), 123.70 (CH, CH-4),

116.62 (CH, CH-7), 112.98 (CH, CH-3), 29.46 (CH_2, $\underline{C}H_2$-CH_3), 15.71 (CH_3, CH_2-$\underline{C}H_3$).

I.R. (KBr diffusion): 1643.8 cm^{-1} (C=O).

The following analogue of compound **5** was prepared using the same general method detailed above.

Benzo[*b*]furan-2-yl(4-bromophenyl)methanone (6)

($C_{15}H_9BrO_2$, MW: 301.138)

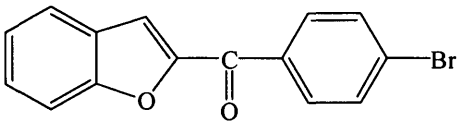

(6)

With benzo[*b*]furan-2-yl-(4-bromophenyl)methanone (**6**), a yellow residue was obtained. Recrystallisation with methanol gave a light yellow solid.

Yield: 5.0 g (92 %), t. l. c. system: petroleum ether – ethyl acetate 4:1 v/v, R_F: 0.55, stain negative. Melting point 155-157 °C [literature: 155 – 157 °C] (Buu-Hoi *et al.*, 1957).

^1H n.m.r. δ 8.00 (dd, J = 1.6, 6.8 Hz, 2H, Ar), 7.74 (m, 4H, Ar), 7.57 (m, 2H, Ar), 7.40 (m, 1H, H-3).

^{13}C n.m.r. δ 183.57 (C=O), 156.45 (C, C-7a), 152.44 (C, C-2), 136.26 (C, C-1'), 132.32 (2 x CH, CH-3' and CH-5'), 131.46 (2 x CH, CH-2' and CH-3'), 129.04 (CH, CH-6), 128.54 (C, C-4'), 127.32 (C, C-3a), 124.57 (CH, CH-5), 123.82 (CH, CH-4), 117.01 (CH, CH-7), 113.01 (CH, CH-3).

Synthesis of benzo[*b*]furan-2-yl-biphenyl-4-yl-methanone derivatives (compound **8** and **10**)

Benzo[*b*]furan-2-yl-biphenyl-4-yl-methanone (8)

($C_{21}H_{14}O_2$, MW: 298.340)

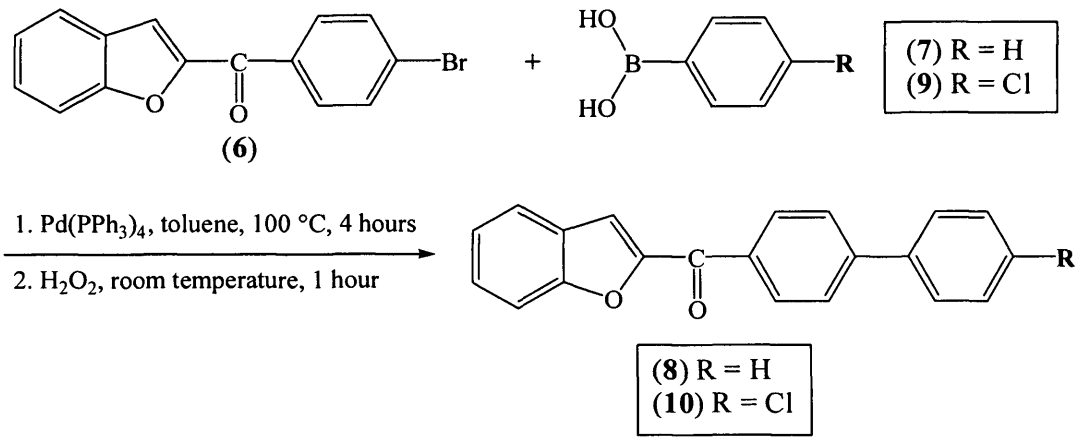

2M aqueous Na_2CO_3 (11.65 mL) was added to a solution of benzo[*b*]furan-2-yl(4-bromophenyl)methanone (**6**) (1.0 g, 3.32 mmol) in toluene (20 mL). The mixture was bubbled with nitrogen for one minute and then $Pd(PPh_3)_4$ (0.20 g, 0.166 mmol) was added to the mixture. Phenylboronic acid (0.81 g, 6.64 mmol) in ethanol (5 mL) was added to the above mixture and the reaction was refluxed at 100 °C for 4 hours. After the reaction was complete, the residual borane was oxidised by the addition of H_2O_2 (30 %, 2.5 mL) at room temperature for 1 hour. The crude product was extracted with CH_2Cl_2 (100 mL) and water (3 x 100 mL). The organic layer was dried with $MgSO_4$, filtered and reduced *in vacuo* to give a light yellow oily residue. Purification by flash column chromatography (petroleum ether – ethyl acetate 95:5 v/v increasing to 80:20 v/v) gave a mixture of the starting material and the product. The mixture was recrystallised with petroleum ether to yield light yellow fine crystals, benzo[*b*]furan-2-yl-biphenyl-4-yl-methanone (**8**). Yield: 0.57 g (58 %), t. l. c. system: petroleum ether – ethyl acetate 1:1 v/v, R_F: 0.63, stain negative. Melting point 150 – 152 °C [literature: 153 – 155 °C (Pestellini *et al.*, 1984)].

^{1}H n.m.r. δ 8.21 (dd, J = 1.6, 8.2 Hz, 2H, Ar), 7.82 (m, 3H, Ar), 7.73 (m, 3H, Ar), 7.65 (s, 1H, H-3), 7.46 (m, 5H, Ar).

^{13}C n.m.r. δ 184.33 (C=O), 156.43 (C, C-7a), 152.80 (C, C-4'), 146.16 (C, C-1''), 140.29 (C, C-1'), 136.31 (C, C-2), 130.58 (2 x CH, CH-2' and CH-6'), 129.46 (2 x CH, CH-3'' and CH-5''), 128.83 (2 x CH, CH-3' and CH–5'), 128.76 (CH, CH-4''),

127.77 (2 x CH, CH-2'' and CH-6''), 127.66 (CH, CH-6), 127.48 (C, C-3a), 124.46 (CH, CH-5), 123.78 (CH, CH-4), 116.83 (CF, CH-7), 113.03 (CH, CH-3).
I.R. (KBr diffusion): 1641 cm^{-1} (C=O) [Literature 1640 cm^{-1}] (Pestellini *et al.*, 1984).

The following analogue of compound **8** was prepared using the same general method detailed above.

Benzo[*b*]furan-2-yl(4'-chlorobiphenyl-4-yl)methanone (10)

($C_{21}H_{13}ClO_2$, MW: 332.785)

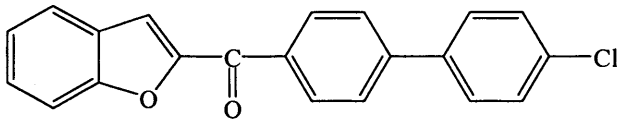

(10)

With benzo[*b*]furan-2-yl(4'-chlorobiphenyl-4-yl)methanone (**10**), a yellow oily residue was obtained. Recrystallisation with petroleum ether yield light yellow solid. Yield: 1.10 g (73 %), t. l. c. system: petroleum ether – ethyl acetate 4:1 v/v, R_F: 0.50, stain negative. Microanalysis: Calculated C = 75.79 %, H = 3.94 %; Found C = 76.14 %, H = 4.00 %. Melting point: 154 – 156 °C.
^1H n.m.r. δ 8.25 (dd, J = 1.7, 6.6 Hz, 2H, Ar), 7.81 (m, 4H, Ar), 7.69 (m, 2H, Ar), 7.52 (m, 5H, Ar).
^{13}C n.m.r. δ 184.18 (C=O), 156.44 (C, C-7a), 152.75 (C, C-4'), 144.82 (C, C-1'), 138.71 (C ,C-2), 136.57 (C, C-1''), 134.96 (C, C-4''), 130.67 (2 x CH, CH-2' and CH-6'), 129.64 (2 x CH, CH-3'' and CH-5''), 128.89 (2 x CH, CH-3' and CH-5'), 128.65 (CH, CH-6), 127.49 (2 x CH, CH-2'' and CH-6''), 127.44 (C, C-3a), 124.49 (CH, CH-5), 123.79 (CH, CH-4), 116.87 (CH, CH-7), 113.02 (CH, CH-3).
I.R. (KBr diffusion): 1644.9 cm^{-1} (C=O).

Synthesis of benzo[*b*]furan-2-yl-phenyl-methanol derivatives (compound **11 – 13**)

Benzo[*b*]furan-2-yl(4-ethylphenyl)methanol (11)

($C_{17}H_{16}O_2$, MW: 252.311)

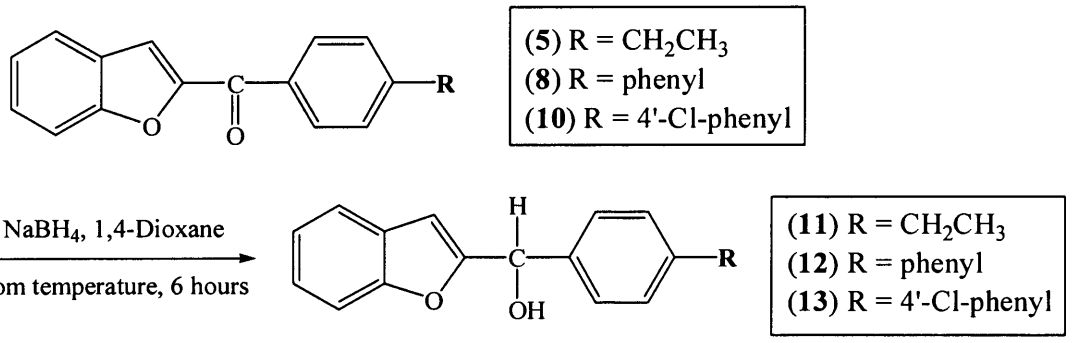

Benzo[*b*]furan-2-yl-(4-ethylphenyl)methanone (**5**) (1.2 g, 4.80 mmol) was dissolved in anhydrous 1,4-dioxane (40 mL). Sodium borohydride (0.18 g, 4.80 mmol) was then added and the mixture stirred under nitrogen at room temperature for 8 hours. The solvent was evaporated *in vacuo* and 1M aqueous hydrochloric acid (25 mL) was added to the residue in order to quench any excess reducing agent. The oil that separated was extracted with diethyl ether (2 x 150 mL), washed with water (3 x 100 mL), then the organic layer was dried with $MgSO_4$, filtered and reduced *in vacuo* to give a white solid, benzo[*b*]furan-2-yl(4-ethylphenyl)methanol (**11**). Yield: 1.0 g (83 %), t. l. c. system: petroleum ether – ethyl acetate 3:2 v/v, R_F: 0.64, stain positive. LRMS (EI^+) *m/z*: 252.1 (M^+). Microanalysis: Calculated C = 80.93 %, H = 6.39 %; Found C = 80.73 %, H = 6.41 %. Melting point: 45 – 47 °C.

^{1}H n.m.r. δ 7.60 (m, 1H, Ar), 7.50 (m, 3H, Ar), 7.32 (m, 4H, Ar), 6.61 (s, 1H, H-3), 5.96 (d, J = 4.6 Hz, 1H, C<u>H</u>-OH), 2.91 (d, J = 4.6 Hz, 1H, OH), 2.76, (q, J = 7.6 Hz, 2H, C<u>H</u>$_2$), 1.34 (t, J = 7.6 Hz, 3H, C<u>H</u>$_3$).

^{13}C n.m.r. δ 160.31 (C, C-2), 159.21 (C, C-7a), 155.54 (C, C-4'), 144.97 (C, C-1'), 138.12 (C, C-3a), 128.58 (2 x CH, CH-3' and CH-5'), 127.34 (2 x CH, CH-2' and CH-6'), 124.67 (CH, CH-6), 123.25 (CH, CH-5), 121.58 (CH, CH-4), 111.81 (CH, CH-7), 104.35 (CH, CH-3), 71.02 (<u>C</u>H-OH), 29.08 (CH_2, <u>C</u>H_2-CH_3), 16.05 (CH_3, CH_2-<u>C</u>H_3).

The following analogues of compound **11** were prepared using the same general method detailed above.

Benzo[*b*]furan-2-yl-biphenyl-4-yl-methanol (12)

($C_{21}H_{16}O_2$, MW: 300.355)

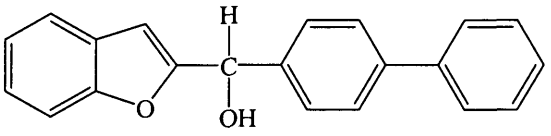

(12)

With benzo[*b*]furan-2-yl-biphenyl-4-yl-methanol (**12**), a white solid was obtained. Yield: 0.51 g (90 %), t. l. c. system: petroleum ether – ethyl acetate 1:1 v/v, R_F: 0.63, stain positive. LRMS (EI^+) *m/z*: 300.1 (M^+). Melting point: 121 – 123 °C [literature: 123 – 125 °C] (Pestellini *et al.*, 1984).

^{1}H n.m.r. δ 7.63 (m, 6H, Ar), 7.46 (m, 4H, Ar), 7.30 (m, 3H, Ar), 6.64 (d, J = 0.6 Hz, 1H, H-3), 6.04 (d, J = 3.1 Hz, 1H, CH-OH), 2.73, (d, J = 3.9 Hz, 1H, OH).

^{13}C n.m.r. δ 158.84 (C, C-2), 155.57 (C, C-7a), 141.76 (C, C-1'), 141.10 (C, C-1''), 139.69 (C, C-4'), 129.28 (2 x CH, CH-3'' and CH-5''), 128.47 (C, C3a-), 127.92 (2 x CH, CH-2' and CH-6'), 127.83 (2 x CH, CH-3' and CH-5'), 127.72 (2 x CH, CH-2'' and CH-6''), 127.60 (CH, CH-4''), 124.82 (CH, CH-6), 123.34 (CH, CH-5), 121.64 (CH, CH-4), 111.83 (CH, CH-7), 104.57 (CH, CH-3), 70.91 (CH-OH).

I.R. (KBr diffusion): 3271.8 cm^{-1} (Broad, OH).

Benzo[*b*]furan-2-yl(4'-chlorobiphenyl-4-yl)methanol (13)

($C_{21}H_{15}ClO_2$, MW: 334.800)

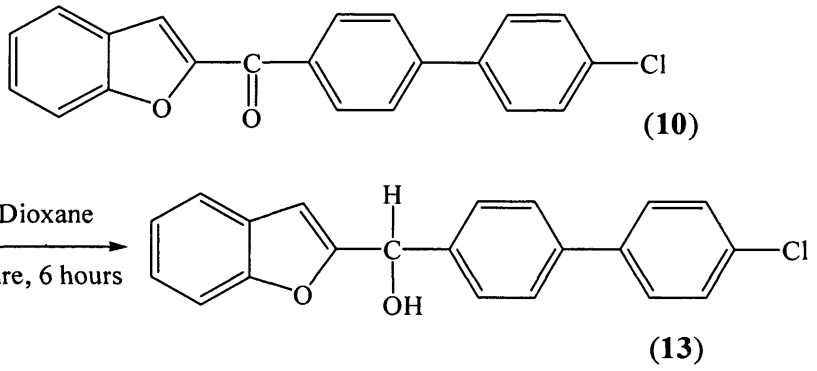

With benzo[*b*]furan-2-yl-(4'-chlorobiphenyl-4-yl)methanol (**13**), a white solid was obtained. Yield: 0.60 g (75 %), t. l. c. system: petroleum ether – ethyl acetate 1:1 v/v,

R_F: 0.60, stain positive. Microanalysis: Calculated C = 75.20 %, H = 4.45 %; Found C = 75.34 %, H = 4.52 %. Melting point: 76 – 78 °C.

^{1}H n.m.r. δ 7.54 (m, 7H, Ar), 7.44 (m, 3H, Ar), 7.25 (m, 2H, Ar), 6.59 (s, 1H, H-3), 6.00 (d, J = 4.5 Hz, 1H, CH-OH), 2.65 (d, J = 4.6 Hz, 1H, OH).

^{13}C n.m.r. δ 158.69 (C, C-2), 155.55 (C, C-7a), 140.48 (C, C-1'), 140.31 (C, C-4'), 139.51 (C, C-1''), 134.02 (C, C-4''), 129.42 (2 x CH, CH-3'' and CH-5''), 128.81 (2 x CH, CH-2'' and CH-6''), 128.41 (C, C-3a), 127.80 (2 x CH, CH-2' and CH-6'), 127.64 (2 x CH, CH-3' and CH-5'), 124.87 (CH, CH-6), 123.36 (CH, CH-5), 121.65 (CH, CH-4), 111.82 (CH, CH-7), 104.59 (CH, CH-3), 70.82 (CH-OH).

I.R. (KBr diffusion): 3317.8 cm^{-1} (Broad, OH).

Synthesis of 1-[benzo[*b*]furan-2-yl-phenylmethyl]-1*H*-[1,2,4]triazole derivatives (compound **14**, **16** and **18**) and **4-[benzo[*b*]furan-2-yl-phenylmethyl]-4*H*-[1,2,4]triazole derivatives** (compound **15**, **17** and **19**)

1-[Benzo[*b*]furan-2-yl-(4-ethylphenyl)methyl]-1*H*-[1,2,4]triazole (**14**) and **4-[Benzo[*b*]furan-2-yl-(4-ethylphenyl)methyl]-4*H*-[1,2,4]triazole** (**15**)

($C_{19}H_{17}N_3O$, MW: 303.362)

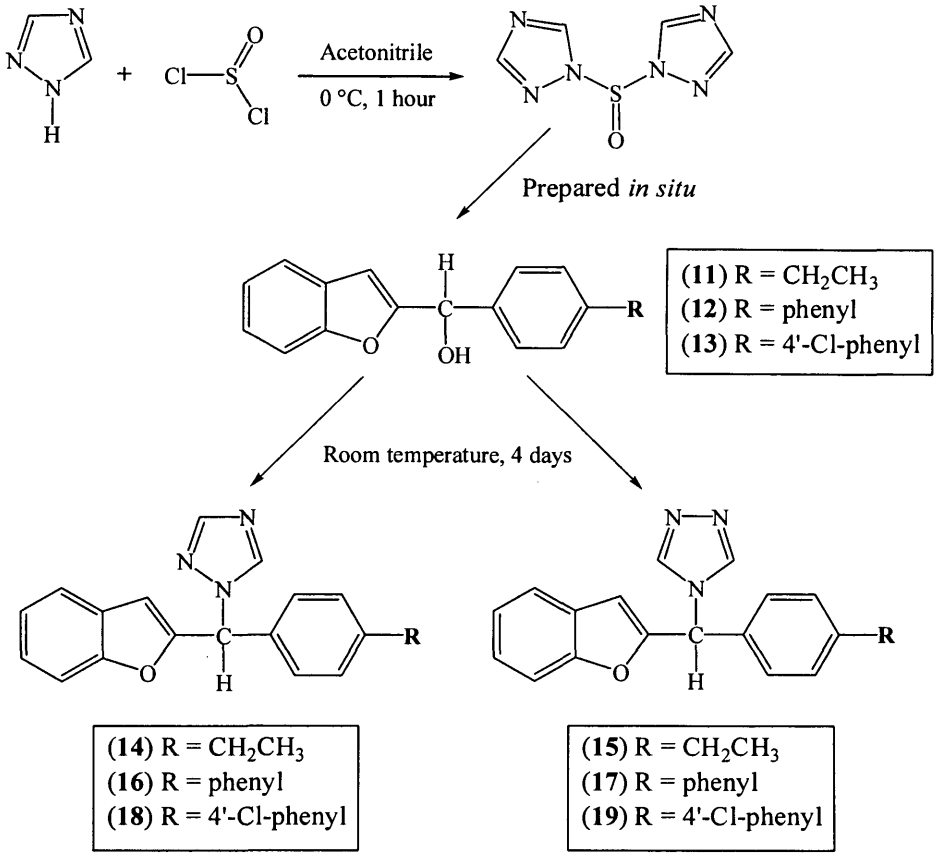

Thionyl chloride (0.47 g, 3.96 mmol) in anhydrous acetonitrile (10.0 mL) was added dropwise to a stirred solution of 1,2,4-triazole (1.09 g, 15.85 mmol) in anhydrous acetonitrile (10.0 mL) at a temperature of 10 °C. The white suspension formed was stirred for 1 h at 10 °C. A solution of benzo[*b*]furan-2-yl-(4-ethylphenyl)methanol (**11**) (1.0 g, 3.96 mmol) in anhydrous acetonitrile (10.0 mL) was added to the mixture followed by activated potassium carbonate (1.10 g, 7.93 mmol). The suspension was stirred under nitrogen at room temperature for 4 days. The resulting suspension was filtered and the filtrate was evaporated *in vacuo* to yield a light brown oil. The oil was extracted with CH_2Cl_2 (150 mL) and water (3 x 100 mL). The organic layer was dried with $MgSO_4$, filtered and reduced *in vacuo* to give a yellow oil. Purification by flash column chromatography (petroleum ether – ethyl acetate 90:10 v/v increasing to 70:30 v/v) gave 1-[benzo[*b*]furan-2-yl-(4-ethylphenyl)methyl]-1*H*-[1,2,4]triazole (**14**) (0.80 g, 67 %) as a yellow syrup. T. l. c. system: petroleum ether – ethyl acetate 1:1 v/v, R_F: 0.42, stain positive. HRMS (EI^+) *m/z* Calculated for $C_{19}H_{17}N_3O$ $(M+H)^+$ 304.1444; Found 304.1442. The flash column chromatography was continued (dichloromethane – methanol 100:0 v/v increasing to 99:1 v/v) to give 4-[benzo[*b*]furan-2-yl-(4-ethylphenyl)methyl]-4*H*-[1,2,4]triazole (**15**) (0.16 g, 13 %) as a white solid. T. l. c. system: dichloromethane – methanol 9:1 v/v, R_F: 0.31, stain positive. Microanalysis: Calculated C = 75.23 %, H = 5.65 %, N = 13.84 %; Found C = 75.19 %, H = 5.74 %, N = 13.61 %. Melting point: 126 – 128 °C.

N.M.R. data for 1-[benzo[*b*]furan-2-yl-(4-ethylphenyl)methyl]-1*H*-[1,2,4]triazole (**14**)

^{1}H n.m.r. δ 8.19 (s, 1H, H-3'''), 8.09 (s, 1H, H-5'''), 7.58 (d, J = 8.4 Hz, 1H, Ar), 7.51 (d, J = 9.3 Hz, 1H, Ar), 7.39 - 7.27 (m, 6H, Ar), 6.89 (s, 1H, H-3), 6.63 (s, 1H, H-1), 2.73 (q, J = 7.6 Hz, 2H, C$\underline{H}_2$), 1.30 (t, J = 7.6 Hz, 3H, C$\underline{H}_3$).

^{13}C n.m.r. δ 155.75 (C, C-2), 153.342 (C, C-7a), 152.65 (CH, CH-5'''), 145.91 (C, C-4'), 143.67 (CH, CH-3'''), 133.20 (C, C-1'), 129.06 (2 x CH, CH-2' and CH-6'), 128.16 (2 x CH, CH-3' and CH-5'), 127.96 (C, C-3a), 125.59 (CH, CH-6), 123.73 (CH, CH-5), 121.93 (CH, CH-4), 111.97 (CH, CH-7), 108.06 (CH, CH-3), 62.51 (CH, CH-1), 28.99 (CH_2), 15.85 (CH_3).

N.M.R. data for 4-[benzo[*b*]furan-2-yl-(4-ethylphenyl)methyl]-4*H*-[1,2,4]triazole (**15**)

^{1}H n.m.r. δ 8.25 (s, 2H, triazole H-2''' and H-5'''), 7.57 (d, J = 6.8 Hz, 1H, Ar), 7.46 (d, J = 8.4 Hz, 1H, Ar), 7.37 – 7.19 (m, 6H, Ar), 6.75 (s, 1H, H-3), 6.62 (s, 1H, H-1), 2.70 (q, J = 7.6 Hz, 2H, C$\underline{H}_2$), 1.26 (t, J = 7.6 Hz, 3H, C$\underline{H}_3$).

^{13}C n.m.r. δ 155.76 (C, C-2), 152.90 (C, C-7a), 146.26 (C, C-4'), 142.95 (2 x CH, CH-2''' and CH-5'''), 132.98 (C, C-1'), 129.27 (2 x CH, CH-2' and CH-6'), 127.89 (2 x CH, CH-3' and CH-5'), 127.67 (C, C-3a), 125.91 (CH, CH-6), 123.94 (CH, CH-5), 122.01 (CH, CH-4), 112.01 (CH, CH-7), 108.04 (CH, CH-3), 58.28 (CH, CH-1), 28.95 (CH_2), 15.83 (CH_3).

The following analogues of compound **14** and **15** were prepared using the same general method detailed above.

1-(Benzo[*b*]furan-2-yl-biphenyl-4-yl-methyl)-1*H*-[1,2,4]triazole (**16**) and **4-(Benzo[*b*]furan-2-yl-biphenyl-4-yl-methyl)-4*H*-[1,2,4]triazole** (**17**)

($C_{23}H_{17}N_3O$, MW: 351.406)

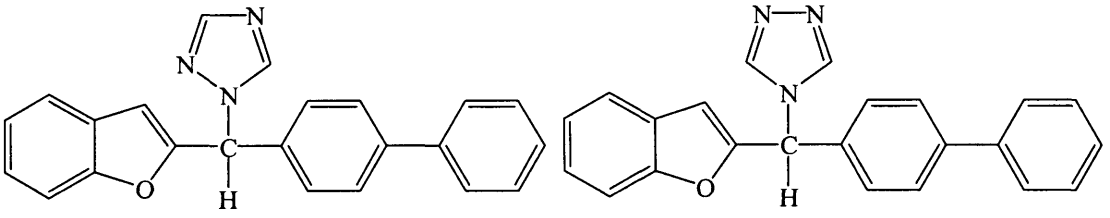

(16) **(17)**

With 1-(benzo[*b*]furan-2-yl-biphenyl-4-yl-methyl)-1*H*-[1,2,4]triazole (**16**), a white solid was obtained after purification by flash column chromatography (petroleum ether – ethyl acetate 90:10 v/v increasing to 65:35 v/v). Yield: 0.34 g (53 %), t. l. c. system: petroleum ether – ethyl acetate 1:1 v/v, R_F: 0.41, stain positive. Microanalysis: Calculated C = 78.61 %, H = 4.88 %, N = 11.95 %; Found C = 78.38 %, H = 4.74 %, N = 11.89 %. Melting point: 130 – 132 °C.

The flash column chromatography was continued (dichloromethane – methanol 100:0 v/v increasing to 99:1 v/v) to give 4-(benzo[*b*]furan-2-yl-biphenyl-4-yl-methyl)-4*H*-[1,2,4]triazole (**17**). Yield: 0.04 g (6.25 %) as a yellow light solid. T. l. c. system: dichloromethane – methanol 9:1 v/v, R_F: 0.31, stain positive. Microanalysis ($C_{23}H_{17}N_3O.0.35H_2O$): Calculated C = 77.29 %, H = 4.98 %, N = 11.81 %; Found C = 77.11 %, H = 4.63 %, N = 11.84 %. Melting point: 56 - 58 °C.

N.M.R. data for 1-(benzo[*b*]furan-2-yl-biphenyl-4-yl-methyl)-1*H*-[1,2,4]triazole (**16**)

^{1}H n.m.r. δ 8.24 (s, 1H, H-3'''), 8.12 (s, 1H, H-5'''), 7.68 (d, J = 8.3 Hz, 2H, Ar), 7.63 (m, 3H, Ar), 7.53 (m, 3H, Ar), 7.45 – 7.31 (m, 5H, Ar), 6.96 (s, 1H, H-3), 6.69 (s, 1H, H-1).

^{13}C n.m.r. δ 155.80 (C, C-2), 152.99 (C, C-7a), 152.78 (CH, CH-5'''), 143.76 (CH, CH-3'''), 142.6.1 (C, C-1''), 140.55 (C, C-1'), 134.92 (C, C-4'), 129.36 (2 x CH, CH-2' and CH-6'), 128.58 (2 x CH, CH-3'' and CH-5''), 128.27 (2 x CH, CH-2'' and CH-6''), 128.23 (2 x CH, CH-3' and CH-5'), 127.92 (C, C-3a), 127.60 (CH, CH-4''), 125.75 (CH, CH-6), 123.83 (CH, CH-5), 122.02 (CH, CH-4), 112.02 (CH, CH-7), 108.34 (CH, CH-3), 62.41 (CH, CH-1).

N.M.R. data for 4-(benzo[*b*]furan-2-yl-biphenyl-4-yl-methyl)-4*H*-[1,2,4]triazole (**17**)

^{1}H n.m.r. δ 8.41 (s, 2H, triazole H-2''' and H-5'''), 7.79 (d, J = 8.4 Hz, 2H, Ar), 7.72 (m, 3H, Ar), 7.61 (m, 3H, Ar), 7.58 – 7.40 (m, 5H, Ar), 6.87 (s, 1H, H-3), 6.79 (s, 1H, H-1).

^{13}C n.m.r. δ 155.85 (C, C-2), 152.44 (C, C-7a), 143.02 (C, C-1''), 142.93 (2 x CH-2''' and CH-5'''), 140.23 (C, C-1'), 134.50 (C, C-4'), 129.42 (2 x CH, CH-2' and CH-6'), 128.51 (2 x CH, CH-3'' and CH-5''), 128.41 (2 x CH, CH-2'' and CH-6''), 128.31 (CH, CH-4''), 127.59 (2 x CH, CH-3' and CH-5' and C, C-3a), 126.12 (CH, CH-6), 124.07 (CH, CH-5), 122.09 (CH, CH-4), 112.10 (CH, CH-7), 108.34 (CH, CH-3), 58.33 (CH, CH-1).

1-[Benzo[*b*]furan-2-yl-(4'-chloro-biphenyl-4-yl)-methyl]-1*H*-[1,2,4]triazole (**18**) and **4-[Benzo[*b*]furan-2-yl-(4'chloro-biphenyl-4-yl)-methyl]-4*H*-[1,2,4]triazole** (**19**)

($C_{23}H_{16}ClN_3O$, MW: 385.852)

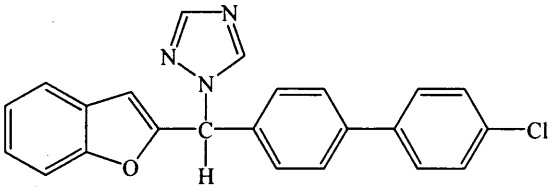

(18)

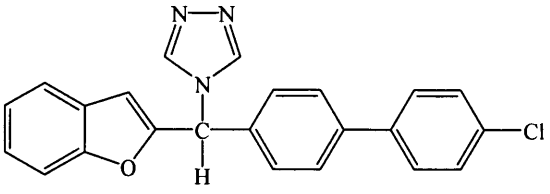

(19)

With 1-[benzo[*b*]furan-2-yl-(4'-chlorobiphenyl-4-yl)methyl]-1*H*-[1,2,4]triazole (**18**), a white solid was obtained after purification by flash column chromatography (petroleum ether – ethyl acetate 90:10 v/v increasing to 65:35 v/v). Yield: 0.38 g (67 %), t. l. c. system: petroleum ether – ethyl acetate 1:1 v/v, R_F: 0.26, stain positive. Microanalysis: Theory C = 71.60 %, H = 4.18 %, N = 10.89 %; Found C = 71.45 %, H = 4.10 %, N = 10.62 %. Melting point: 34 – 36 °C.

The flash column chromatography was continued (dichloromethane – methanol 100:0 v/v increasing to 99:1 v/v) to give 4-[benzo[*b*]furan-2-yl-(4'chlorobiphenyl-4-yl)methyl]-4*H*-[1,2,4]triazole (**19**) (0.075 g, 13 %) as a light yellow solid. T. l. c. system: dichloromethane – methanol 9:1 v/v, R_F: 0.50, stain positive. Microanalysis ($C_{23}H_{16}ClN_3O.0.2H_2O$): Theory C = 71.07 %, H = 4.25 %, N = 10.81 %; Found C = 71.05 %, H = 4.09 %, N = 10.75 %. Melting point: 68 – 70 °C.

N.M.R. data for 1-[benzo[*b*]furan-2-yl-(4'-chlorobiphenyl-4-yl)methyl]-1*H*-[1,2,4]triazole (**18**)

^{1}H n.m.r. δ 8.24 (s, 1H, H-3'''), 8.11 (s, 1H, H-5'''), 7.64 (d, J = 8.3 Hz, 2H, Ar), 7.60 – 7.52 (m, 3H, Ar), 7.49 – 7.29 (m, 7H, Ar), 6.95 (s, 1H, H-3), 6.69 (s, 1H, H-1).
^{13}C n.m.r. δ 155.80 (C, C-2), 152.80 (CH, CH-5''' and C, C-7a), 143.74 (CH, CH-3'''), 141.36 (C, C-1'), 138.97 (C, C-1''), 135.32 (C, C-4'), 134.38 (C, C-4''), 129.52 (2 x CH, CH-2' and CH-6'), 128.83 (2 x CH, CH-3'' and CH-5''), 128.67 (2 x CH, CH-2'' and CH-6''), 128.10 (2 x CH, CH-3' and CH-5'), 127.87 (C, C-3a), 125.80 (CH, CH-6), 123.86 (CH, CH-5, 122.02 (CH, CH-4), 112.02 (CH, CH-7), 108.40 (CH, CH-3), 62.35 (CH, CH-1).

N.M.R. data for 4-[benzo[*b*]furan-2-yl-(4'chlorobiphenyl-4-yl)methyl]-4*H*-[1,2,4]triazole (**19**)

^{1}H n.m.r. δ 8.31 (s, 2H, triazole H-2''' and H-5'''), 7.65 (d, J = 8.3 Hz, 2H, Ar), 7.61 – 7.43 (m, 6H, Ar), 7.41 – 7.31 (m, 4H, Ar), 6.79 (s, 1H, H-3), 6.70 (s, 1H, H-1).
^{13}C n.m.r. δ 155.85 (C, C-2), 152.29 (C, C-7a), 142.89 (2 x CH, CH-2''' and CH-5'''), 141.75 (C, C-1'), 138.66 (C, C-1''), 134.93 (C, C-4'), 134.58 (C, C-4''), 129.59 (2 x CH, CH-2' and CH-6'), 128.82 (2 x CH, CH-3'' and CH-5''), 128.42 (2 x CH, CH-2'' and CH-6''), 128.35 (2 x CH, CH-3' and CH-5'), 127.56 (C, C-3a), 126.16 (CH, CH-6), 124.10 (CH, CH-5), 122.10 (CH, CH-4), 112.10 (CH, CH-7), 108.37 (CH, CH-3), 58.26 (CH, CH-1).

CHAPTER 4

Synthesis of benzo[*b*]furan-2-carboxamido ethyl-imidazole and -1,2,4-triazole derivatives

4.1 Synthesis of benzo[*b*]furan-2-carboxamido ethyl-imidazole and -1,2,4-triazole derivatives

The synthesis of *N*2-[2-phenyl-2-(1*H*-imidazoyl)ethyl]-benzo[*b*]furan-2-carboxamide derivatives (**51** – **55**), *N*2-[2-phenyl-2-(1*H*-1,2,4-triazol-1-yl)ethyl]-benzo[*b*]furan-2-carboxamide derivatives (**56**, **58**, **60**, **62** and **64**), and *N*2-[2-phenyl-2-(4*H*-1,2,4-triazol-4-yl)ethyl]-benzo[*b*]furan-2-carboxamide derivatives (**57**, **58**, **61**, **63** and **65**) involved a 5 step reaction as outlined in **Scheme 4.1**. It involved a modification of the procedure described by Schuster and co-workers (Schuster and Egger, 1997) and Moenius and co-workers (Moenius *et al.*, 1999).

4.1.1 Synthesis of substituted ethyl benzo[*b*]furan-2-carboxylate

The method described in section **3.1.2** was applied to the synthesis of ethyl benzo[*b*]furan-2-carboxylate (**21**), however, the reaction did no go to completion (**Method 1**, **Scheme 4.2**). Purification by flash column chromatography isolated the intermediate compound **22**. The ^{1}H n.m.r. showed one extra singlet peak at 4.78 ppm which referred to two H atoms of the α-CH_2. A singlet peak at 10.58 ppm referred to the H atom of the aldehyde group. This confirmed that the formation of the benzofuran ring had not occurred. The method used by Suzuki's group (Suzuki *et al.*, 1983) was tried in the synthesis of the substituted ethyl benzo[*b*]furan-2-carboxylate (**Method 2**, **Scheme 4.2**). The formation of the products **21**, **32** and **34** was successful using the base, K_2CO_3, as described by Suzuki's group.

After purification by flash chromatography or recrystallisation with petroleum ether, the products were confirmed by ^{1}H n.m.r. by the presence of the H-3 as a doublet at approximately 7.5 ppm (**Scheme 4.2**) and the presence of the C=O in the carbon n.m.r. at approximately 156 to 157 ppm. Overall, this method gave moderate yields (22 % - 53 %).

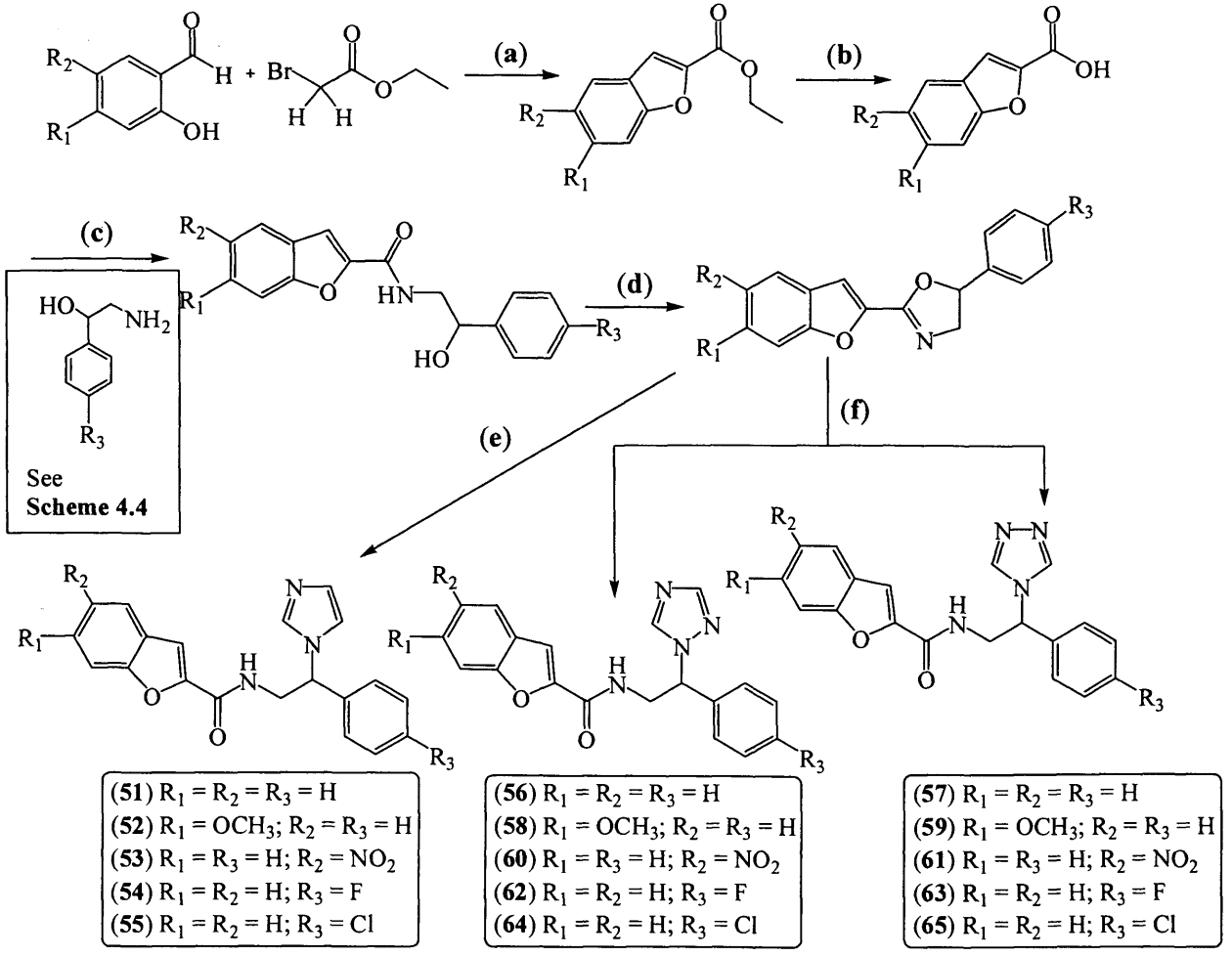

Scheme 4.1. General reaction scheme for the synthesis of *N*2-[2-phenyl-2-(1*H*-imidazoyl)ethyl]-benzo[*b*]furan-2-carboxamide derivatives (**51** – **55**), *N*2-[2-phenyl-2-(1*H*-1,2,4-triazol-1-yl)ethyl]-benzo[*b*]furan-2-carboxamide derivatives (**56**, **58**, **60**, **62** and **64**), and *N*2-[2-phenyl-2-(4*H*-1,2,4-triazol-4-yl)ethyl]-benzo[*b*]furan-2-carboxamide derivatives (**57**, **58**, **61**, **63** and **65**). Reaction conditions: (**a**) K_2CO_3, DMF, 130 °C, 6 h (**b**) 2 M NaOH, methanol, r.t., 20 min (**c**) (i) 1,1'-carbonyl-diimidazole, DMF, r.t., 1 h, (ii) 2-amino-1-phenyl-ethanol, r.t., 12 h. (**d**) $(CH_3SO_2)_2O$, NEt_3, 0 °C, 24 h. (**e**) and (**f**) 1,2,4-triazole or imidazole, isopropyl acetate, 125 - 128 °C, 24 – 72 h.

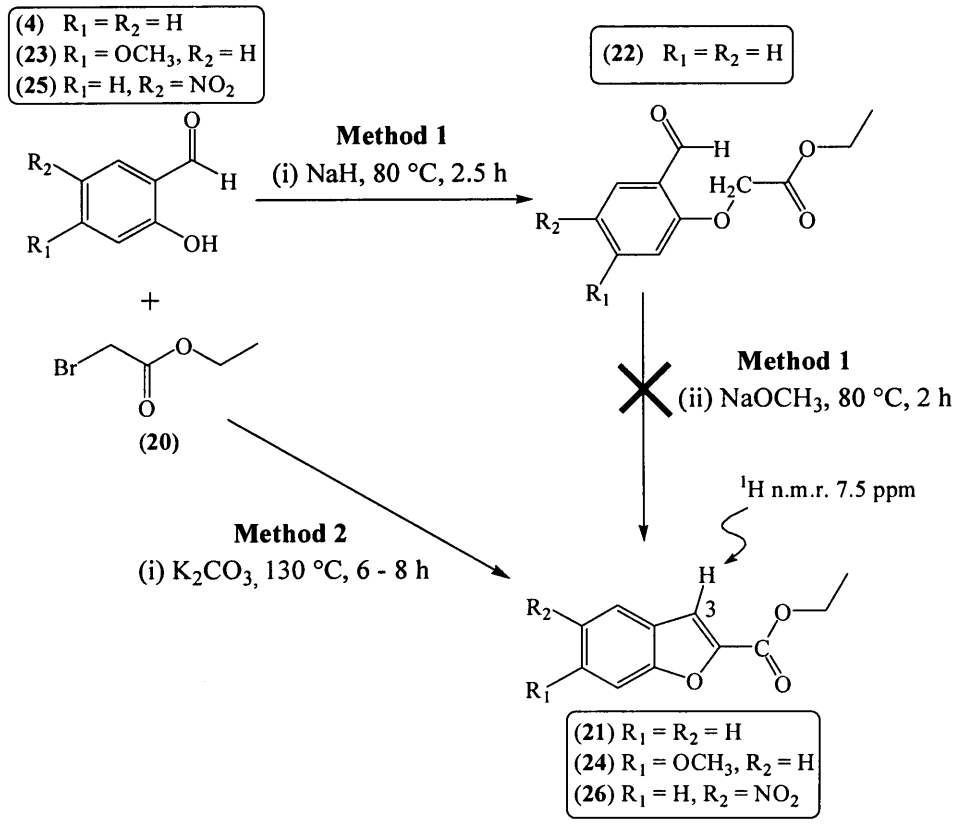

Scheme 4.2. The synthesis of substituted ethyl benzo[*b*]furan-2-carboxylate (**21, 24** and **26**). Reaction conditions, **Method 1**: (i) NaH, DMF, 80 °C, 2.5 h, (ii) NaOMe, 80 °C, 1.5 h. Reaction conditions, **Method 2**: (i) K_2CO_3, DMF, 130 °C, 6 – 7 h. **Method 1** failed to synthesise product **21** and thus **method 2** was used in the synthesis of products **21**, **24** and **26**.

4.1.2 Synthesis of substituted benzo[*b*]furan-2-carboxylic acid

The synthesis of the substituted benzo[*b*]furan-2-carboxylic acid involved base hydrolysis of the substituted ethyl benzo[*b*]furan-2-carboxylate (**Scheme 4.3**). The substituted benzo[*b*]furan-2-carboxylic acid compounds **27** – **29** were confirmed by the disappearance of the CH_2 and CH_3 peaks in the ^1H n.m.r. and ^{13}C n.m.r. The alkaline hydrolysis of the benzo[*b*]furan-2-carboxylic acid ethyl ester compound produced good yields (88 % – 98 %).

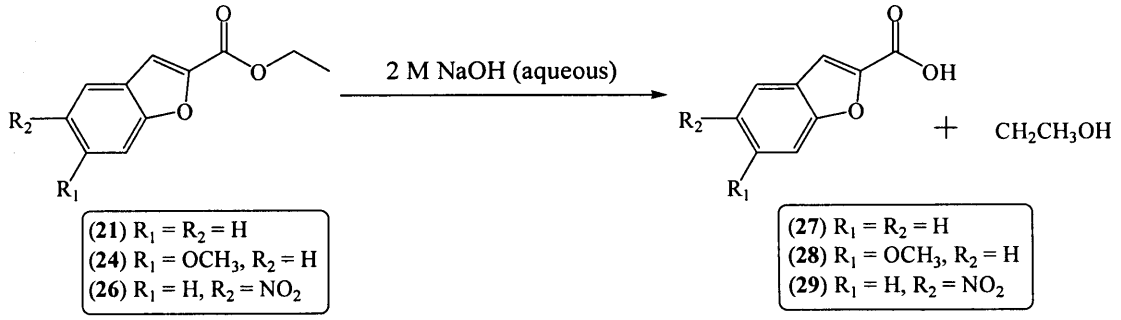

Scheme 4.3. Synthesis of the substituted benzo[*b*]furan-2-carboxylic acid (**27, 28** and **29**). Reaction conditions: 2M NaOH (aq.), CH_3OH, r.t., 20 min., 85 - 98 %.

4.1.3 Synthesis of the substituted 2-amino-1-phenyl-ethanol

The synthesis of the substituted 2-amino-1-phenyl-ethanol derivatives (**35** and **36**) involved two steps as shown in **Scheme 4.4 (a)** and **(b)**. The first step (**Scheme 4.4 (a)**) involved the base catalysed (NaOH) condensation of benzaldehydes, **30** and **33**, with nitromethane in ice-cooled methanol to form the corresponding nitro-alcohol **32** and **34** (Langer *et al.*, 2001). Overall, the condensation of benzaldehyde with nitromethane gave moderate yields (54 % - 74 % respectively) after purification by flash column chromatography.

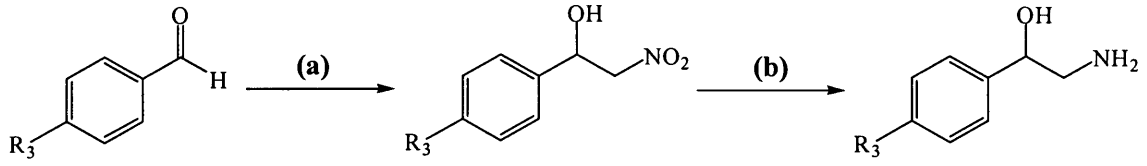

(**30**) R_3 = F
(**33**) R_3 = Cl

(**32**) R_3 = F
(**34**) R_3 = Cl

(**35**) R_3 = F
(**36**) R_3 = Cl

Scheme 4.4. The synthesis of substituted 2-amino-1-phenyl-ethanol (**35** and **36**). **(a)** nitromethane, 10 M NaOH (aq.), acetic acid (aq.) 2 % v/v, methanol, 5 – 10 °C, 8 h. **(b)** Raney nickel, formic acid (aq.) 50 % v/v, 40 psi H_2, room temperature, 24 h.

The next step (**Scheme 4.4 (b)**) involved the reduction of the nitro compound (**32** and **34**) to the corresponding amine compound (**35** and **36**). The most frequently employed method for nitro reduction to form a primary amine is catalytic hydrogenation, for example, palladium catalyst with H_2 gas (Pd/H_2). However, the use of Pd/H_2 in the reduction of 1-(4-fluorophenyl)-2-nitro-1-ethanol (**32**) and 1-(4-chlorophenyl)-2-nitro-1-ethanol (**34**) could result in the cleavage of the halogen atom in **32** and **34**. Raney nickel was used as a catalyst in the hydrogenation of the nitro compound **32** and **34**, as this method is more selective (*i.e.* occurs without dehalogenation) (Gowda *et al.*, 2000; Langer *et al.*, 2001) compared with Pd/H_2 catalytic hydrogenation.

The reaction went to completion after 24 hours and the products **35** and **36** were purified by flash column chromatography using a dichloromethane-methanol-triethylamine eluent system. 5 % of triethylamine was used in the mobile phase system to neutralize the acid in the silica gel as compound **35** and **36** are sensitive to acid.

The purified products were confirmed by ^1H, ^{13}C n.m.r. and compared with the literature (Cho *et al.*, 2002). Referring to **Figure 4.5**, the H atoms of the CH_2, $\mathbf{H_A}$ and $\mathbf{H_B}$, are coupled to each other with the coupling constant, J_{AB} = 12.8 Hz; and they are

each coupled to $\mathbf{H_X}$, with different coupling constants, one large (J_{BX} = 7.5 Hz) and one small (J_{AX} = 4.4 Hz). This is denoted as the ABX system, which involved a partially strongly coupled 3-spin system.

Overall the reduction of the nitro compound **32** and **34** with Raney nickel hydrogenation gave reasonable yields (44 % - 46 % respectively).

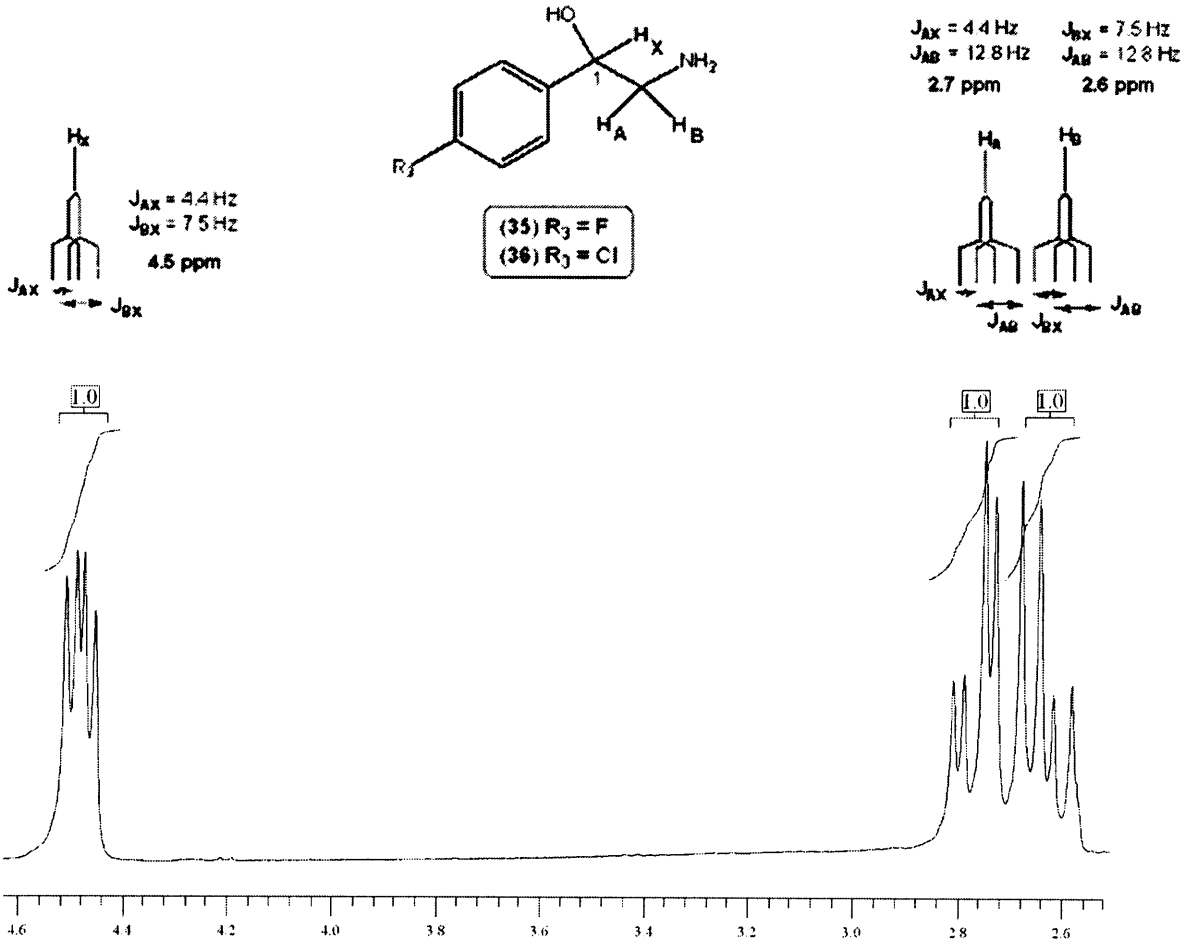

Figure 4.5. The ABX system of the substituted 2-amino-1-phenyl-ethanol (**35** and **36**). Assignment of the peaks for $\mathbf{H_A}$, $\mathbf{H_B}$ and $\mathbf{H_X}$ in the ^{1}H n.m.r. spectra. The ^{1}H n.m.r. spectrum of compound **35** is shown here.

4.1.4 Synthesis of the substituted *N*2-(2-hydroxy-2-phenylethyl)-benzo[*b*]furan-2-carboxamide

The synthesis of the substituted *N*2-(2-hydroxy-2-phenylethyl)-benzo[*b*]furan-2-carboxamide (**39** – **43**) was carried out using the reagent 1,1'-carbonyldiimidazole (CDI) (**37**) with the corresponding substituted 2-amino-1-phenyl-ethanol (**35**, **36** or **38**) (**Scheme 4.6**). CDI is used as a coupling reagent in the synthesis of the amide compound (**39** – **43**). The product was recrystallised from ethanol and ice water to give good purity and yield (72 % - 88 %).

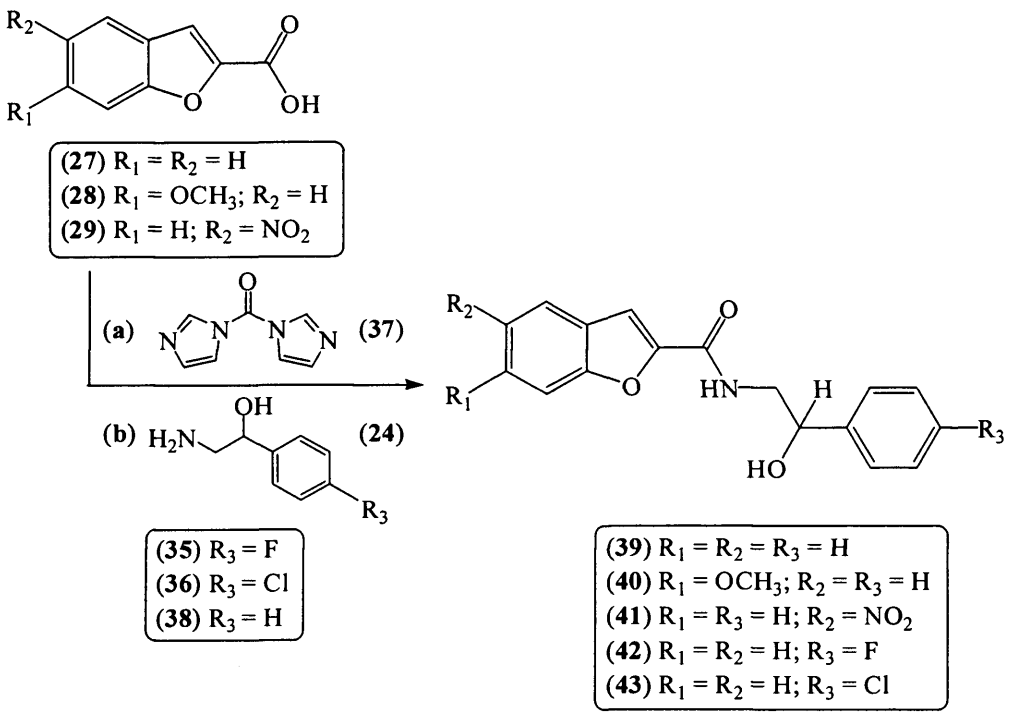

Scheme 4.6. The synthesis of substituted benzofuran-2-carboxylic acid (2-hydroxy-2-phenylethyl)-amide (**39** – **43**). Reaction conditions: (**a**) 1,1'-carbonyldiimidazole (**37**), DMF, r.t., 1h. (**b**) substituted 2-amino-1-phenyl-ethanol (**35**, **36** or **38**), r.t., 12 h., recrystallisation, 72 - 88 %.

4.1.5 Synthesis of the substituted 2-benzo[*b*]furan-2-yl-5-phenyl-4,5-dihydro-1,3-oxazole

This synthesis involved formation of an oxazole ring structure in which the oxazole compounds (**45** – **49**) were prepared by the reaction of the amide-containing compound (**39** – **43**) with methanesulphonic anhydride (**44**) and a base (triethylamine) (Gant and Meyers, 1994; Sund *et al.*, 1987) [**Scheme 4.7**].

The mechanism of this reaction involved nucleophilic attack by the hydroxyl group at the sulphur atom of methanesulphonic anhydride (**44**) to form the intermediate (**44a**). The activation of the carboxyl-oxygen as a nucleophilic centre will then occur as a result of the abstraction of the amido proton by the base, triethylamine (Sund *et al.*, 1987) (**Scheme 4.7**).

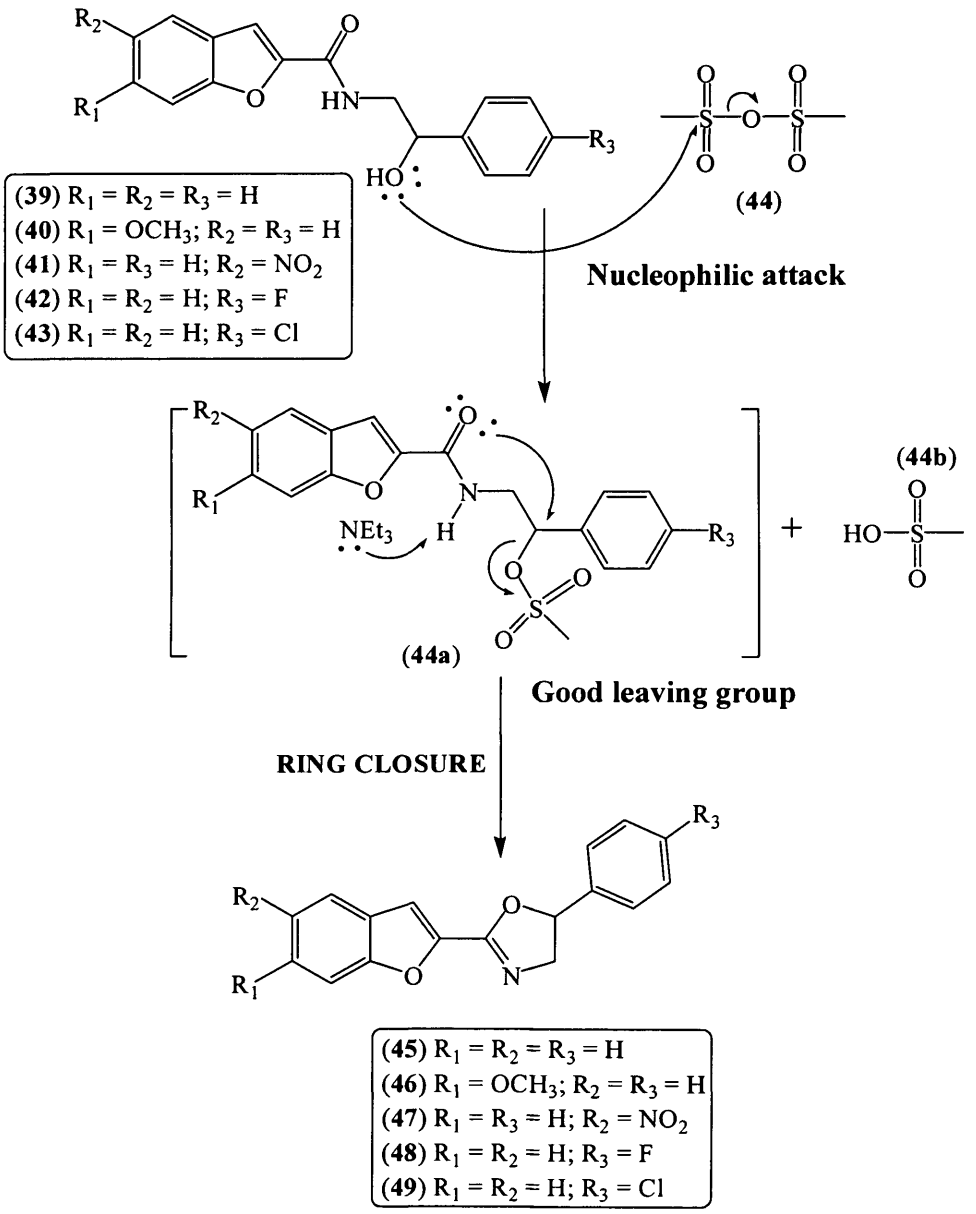

Scheme 4.7. Synthesis of the substituted 2-benzo[*b*]furan-2-yl-5-phenyl-4,5-dihydro-1,3-oxazole (**45** – **49**). Reaction conditions: $(CH_3SO_2)_2O$, NEt_3, 0 °C, 24 h, column chromatograph or recrystallisation, 54 - 67 %.

The presence of the 4,5-dihydro-1,3-oxazole ring structure in the compound (**45** – **49**) was illustrated on the ^1H n.m.r. as an ABX system (**Figure 4.8**). **Figure 4.8** shows the signals of the three carbon-bound protons of the 4,5-dihydro-1,3-oxazole compound (**45** – **49**). The geminal pair, H_A and H_B, are diastereotopic; they are coupled to each other with the largest of the three coupling constants (~15 Hz) and they are each coupled to H_X, with different coupling constants, one large (~10 Hz) and one small (~8 Hz). The H_X signal (~5.8 ppm) in compound (**45** – **49**) is downfield from the H_A and H_B signals (~4.5 and 4.0 ppm).

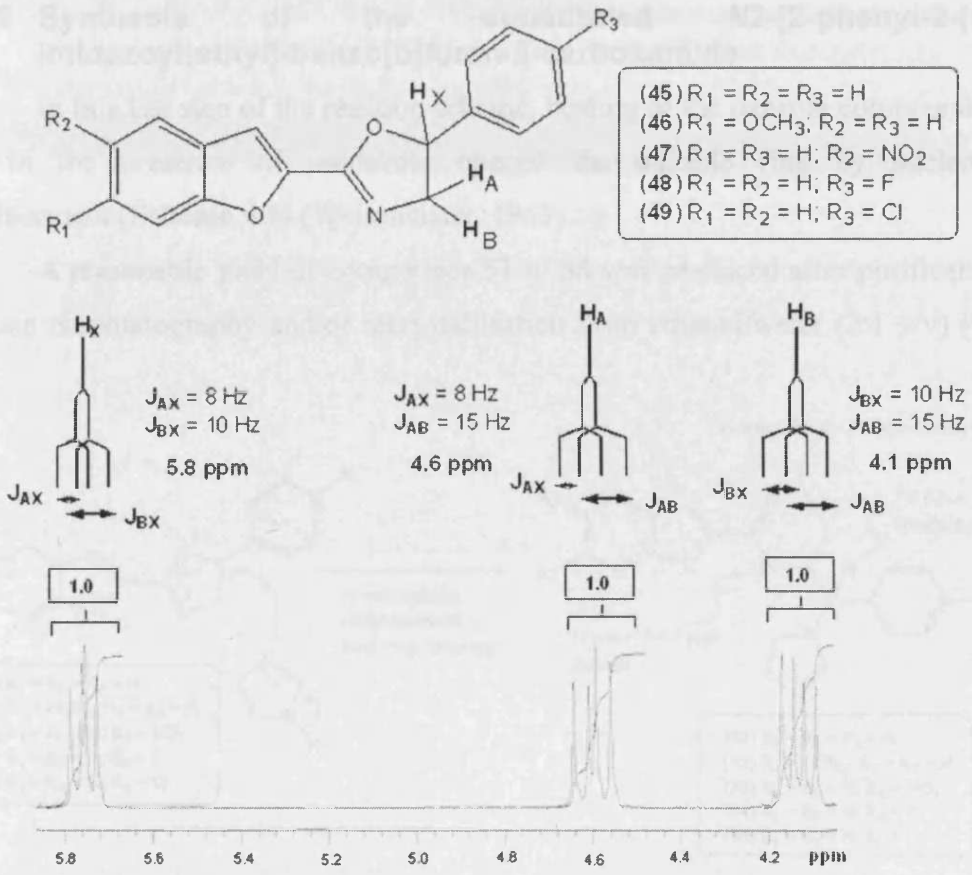

Figure 4.8. The signals of the three protons of the 4,5-dihydro-1,3-oxazole compound (**45 – 49**). The ^{1}H n.m.r. spectrum of compound **45** is shown here.

Overall, the synthesis of the oxazole compounds (**45 – 49**) gave moderate yield after purification by column chromatography or recrystallisation from ethanol (**Table 4.1**). The synthesis of compound **47** is very low, this may due to the presence of the electron withdrawing nitro group which discouraged the ring closure reaction.

Table 4.1. Summary of the synthesis of 2-(substituted-benzofuran-2-yl)-5-phenyl-4,5-dihydro-1,3-oxazole.

Product	Total reaction hours	Yield (%)	Melting point (° C)	Purification methods
45	24	53	79 – 81	Recrystallisation
46	24	67	116 – 118	Column chromatography
47	24	16	159 – 161	Column chromatography
48	24	66	88 – 90	Recrystallisation
49	24	65	103 – 105	Recrystallisation

4.1.6 Synthesis of the substituted *N*2-[2-phenyl-2-(1*H*-1-imidazoyl)ethyl]-benzo[*b*]furan-2-carboxamide

In this last step of the reaction scheme, heating of the oxazole compound (**45** – **49**) in the presence of imidazole opened the oxazole ring by nucleophilic displacement (**Scheme 4.9**) (Wehrmeister, 1963).

A reasonable yield of compounds **51** to **55** was produced after purification by column chromatography and/or recrystallisation from ethanol/water (2:1 v/v) (**Table 4.2**).

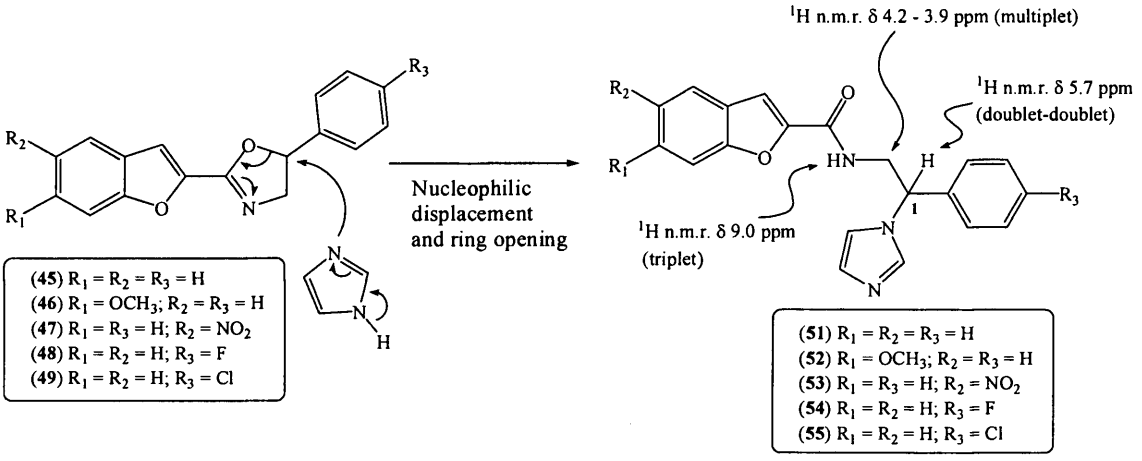

Scheme 4.9. The synthesis of the substituted *N*2-[2-phenyl-2-(1*H*-imidazoyl)ethyl]-benzo[*b*]furan-2-carboxamide (**51** – **55**). Reaction conditions: imidazole, isopropyl acetate, 125 °C, 24 h, recyrstallisation and/or column chromatography, 28 – 72 %.

Table 4.2. The summary of the synthesis of the substituted *N*2-[2-phenyl-2-(1*H*-imidazoyl)ethyl]-benzo[*b*]furan-2-carboxamide (**51** – **55**).

Product	Total reaction hours	Yield (%)	Melting point (° C)	Purification methods
51	24	28	180 – 182	Recrystallisation
52	24	66	110 – 112	Recrystallisation
53	24	33	204 – 206	Column chromatography
54	24	73	198 – 200	Recrystallisation
55	24	72	76 – 78	Recrystallisation

4.1.7 Synthesis of the substituted *N*2-[2-phenyl-2-(1*H*-1,2,4-triazol-1-yl)ethyl]-benzo[*b*]furan-2-carboxamide and the substituted *N*2-[2-phenyl-2-(4*H*-1,2,4-triazol-4-yl)ethyl]-benzo[*b*]furan-2-carboxamide

The synthesis of the substituted *N*2-[2-phenyl-2-(1*H*-1,2,4-triazol-1-yl)ethyl]-benzo[*b*]furan-2-carboxamide **Scheme 4.10** (**i**) and the substituted *N*2-[2-phenyl-2-(4*H*-1,2,4-triazol-4-yl)ethyl]-benzo[*b*]furan-2-carboxamide **Scheme 4.10** (**ii**) was carried out in one reaction.

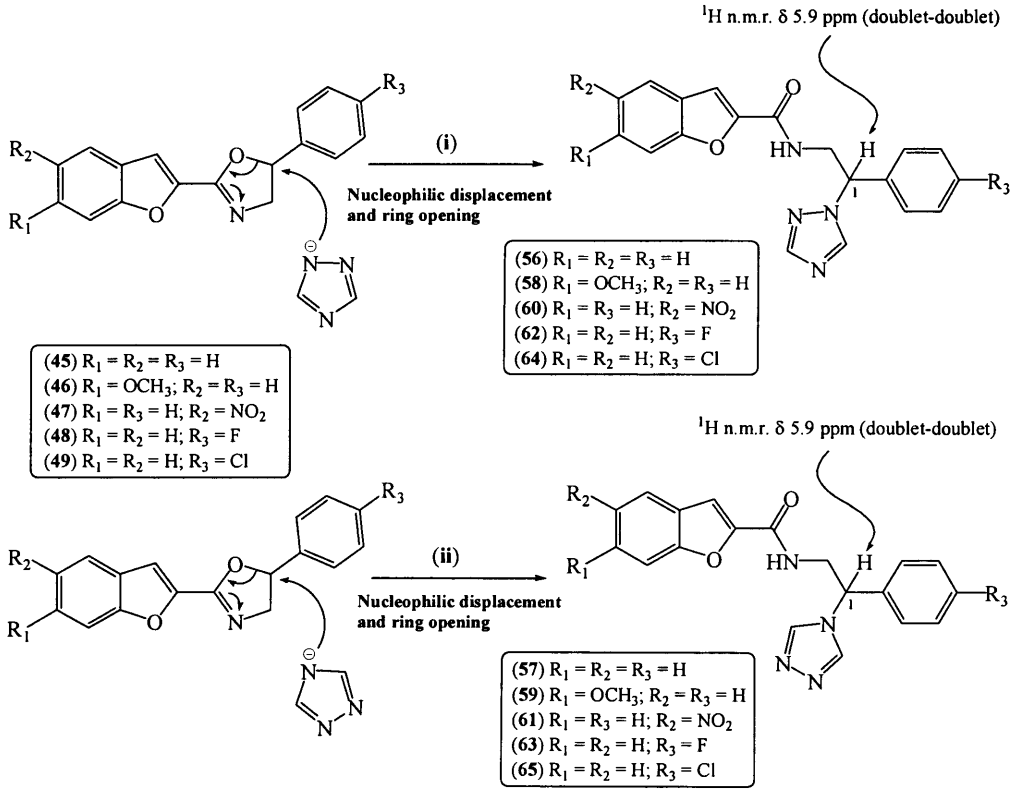

Scheme 4.10. The synthesis of the substituted *N*2-[2-phenyl-2-(1*H*-1,2,4-triazol-1-yl)ethyl]-benzo[*b*]furan-2-carboxamide (**56**, **58**, **60**, **62** and **64**) (**i**) and the substituted *N*2-[2-phenyl-2-(4*H*-1,2,4-triazol-4-yl)ethyl]-benzo[*b*]furan-2-carboxamide (**57**, **59**, **61**, **63** and **65**) (**ii**). Reaction conditions: 1,2,4-triazole, isopropyl acetate, 130 °C, 28 – 36 h.

The mixture of the substituted *N*2-[2-phenyl-2-(1*H*-1,2,4-triazol-1-yl)ethyl]-benzo[*b*]furan-2-carboxamide (**56**, **58**, **60**, **62** and **64**) and the substituted *N*2-[2-phenyl-2-(4*H*-1,2,4-triazol-4-yl)ethyl]-benzo[*b*]furan-2-carboxamide (**57**, **59**, **61**, **63** and **65**) was first recrystallised from toluene and then from methanol/ethanol or with ethanol/water to yield substituted *N*2-[2-phenyl-2-(4*H*-1,2,4-triazol-4-yl)ethyl]-benzo[*b*]furan-2-carboxamide (**57**, **59**, **61**, **63** and **65**). The filtrate from the recrystallisation was purified by flash column chromatography to give the substituted *N*2-[2-phenyl-2-(1*H*-1,2,4-triazol-1-yl)ethyl]-benzo[*b*]furan-2-carboxamide (**56**, **58**,

60, **62** and **64**) [**Table 4.3**]. The very low yield of **60** and **61** is due to difficulty in purification of these products.

Table 4.3. The summary of the synthesis of the substituted *N*2-[2-phenyl-2-(1*H*-1,2,4-triazol-1-yl)ethyl]-benzo[*b*]furan-2-carboxamide (**56**, **58**, **60**, **62** and **64**) and synthesis of the substituted *N*2-[2-phenyl-2-(4*H*-1,2,4-triazol-4-yl)ethyl]-benzo[*b*]furan-2-carboxamide (**57**, **59**, **61**, **63** and **65**).

Reactants	Products	Reaction temperature (°C)/Reaction time (hours)	Yield (%)	Ratio	Melting Point (°C)
45 and 1,2,4-triazole	**56**	130/30	32	3.5	126 – 128
	57		9	1.0	276 – 278
46 and 1,2,4-triazole	**58**	130/28	33	2.3	164 – 166
	59		14	1.0	218 – 220
47 and 1,2,4-triazole	**60**	130/36	6	1.5	60 – 62
	61		4	1.0	125 – 127
48 and 1,2,4-triazole	**62**	130/30	22	1.8	174 – 176
	63		12	1.0	252 – 254
49 and 1,2,4-triazole	**64**	130/30	28	2.3	200 – 202
	65		12	1.0	221 – 223

The synthesis of compound **56** was tried using the method described in section **3.1.5**, however this reaction was not successful (**Scheme 4.11**). A product with a higher R_F value compared with the starting material (**39**) was isolated by column chromatography. The ^1H n.m.r. showed absence of the OH peak and the ^{13}C n.m.r. gave the same number of carbon atoms as compound **39**. The Electron Spray (ES^+) showed a molecular weight peak of 322.1. This could be the formation of *N*2-(2-chloro-2-phenylethyl)benzofuran-2-carboxamide (**39a**, 66 % yield) which gives a peak at 322.1 [M+Na] (**Scheme 4.11**) and microanalysis of compound **39a** confirmed the structure of **39a**. Microanalysis ($C_{17}H_{14}ClNO_2$): Calculated C = 68.12 %, H = 4.71

%, N = 4.67 %; Found C = 68.00 %, H = 4.69 %, N = 4.69 %. The unreacted $SOCl_2$ in the mixture could have reacted with compound **39** to form the product **39a**.

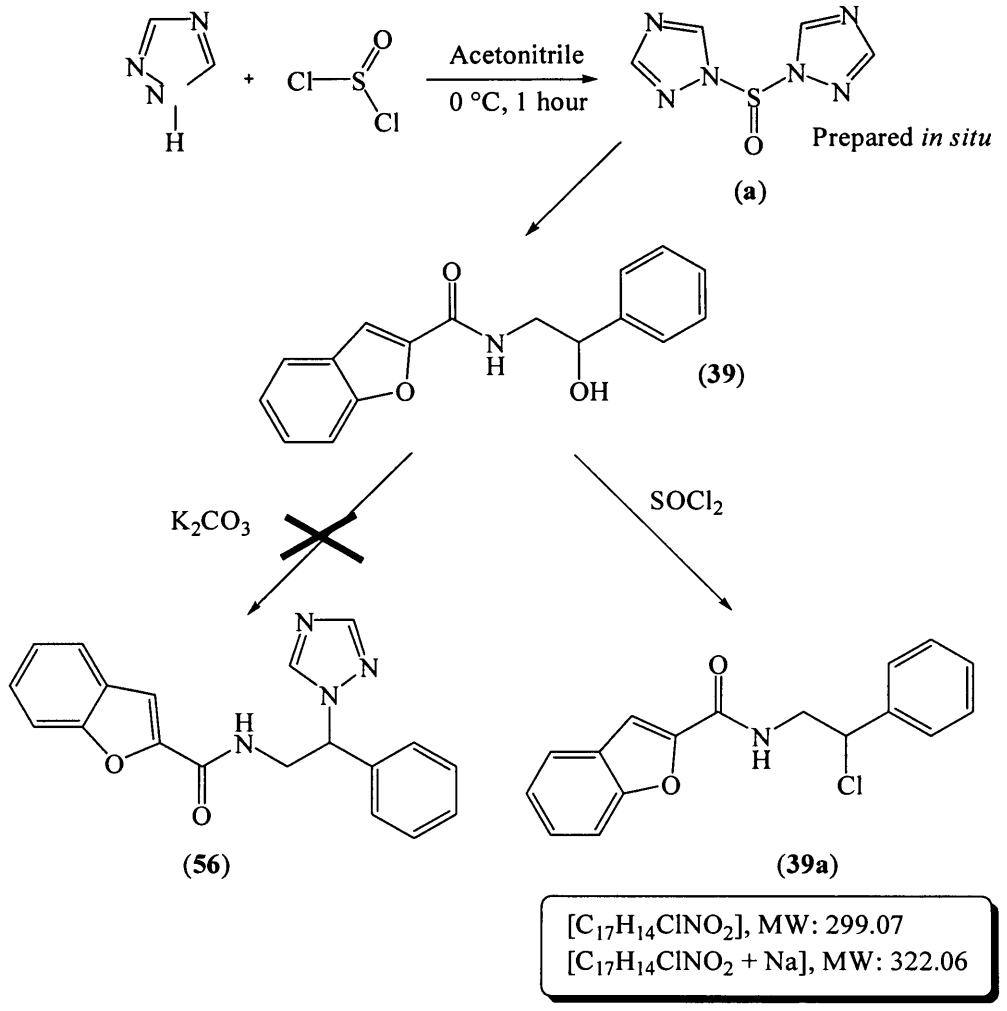

Scheme 4.11. Formation of compound **39a** from compound **39** using the method described in section **3.1.5**. Reaction conditions: 1,2,4-triazole, $SOCl_2$, acetonitrile, 10 °C, 1h then add K_2CO_3, compound **39**, r.t., 24 h.

4.2 Experimental results for the synthesis of benzofuran-2-carboxamido ethyl–imidazole and –1,2,4-triazole derivatives

The numbering of compounds for n.m.r. characterisation is as follows:

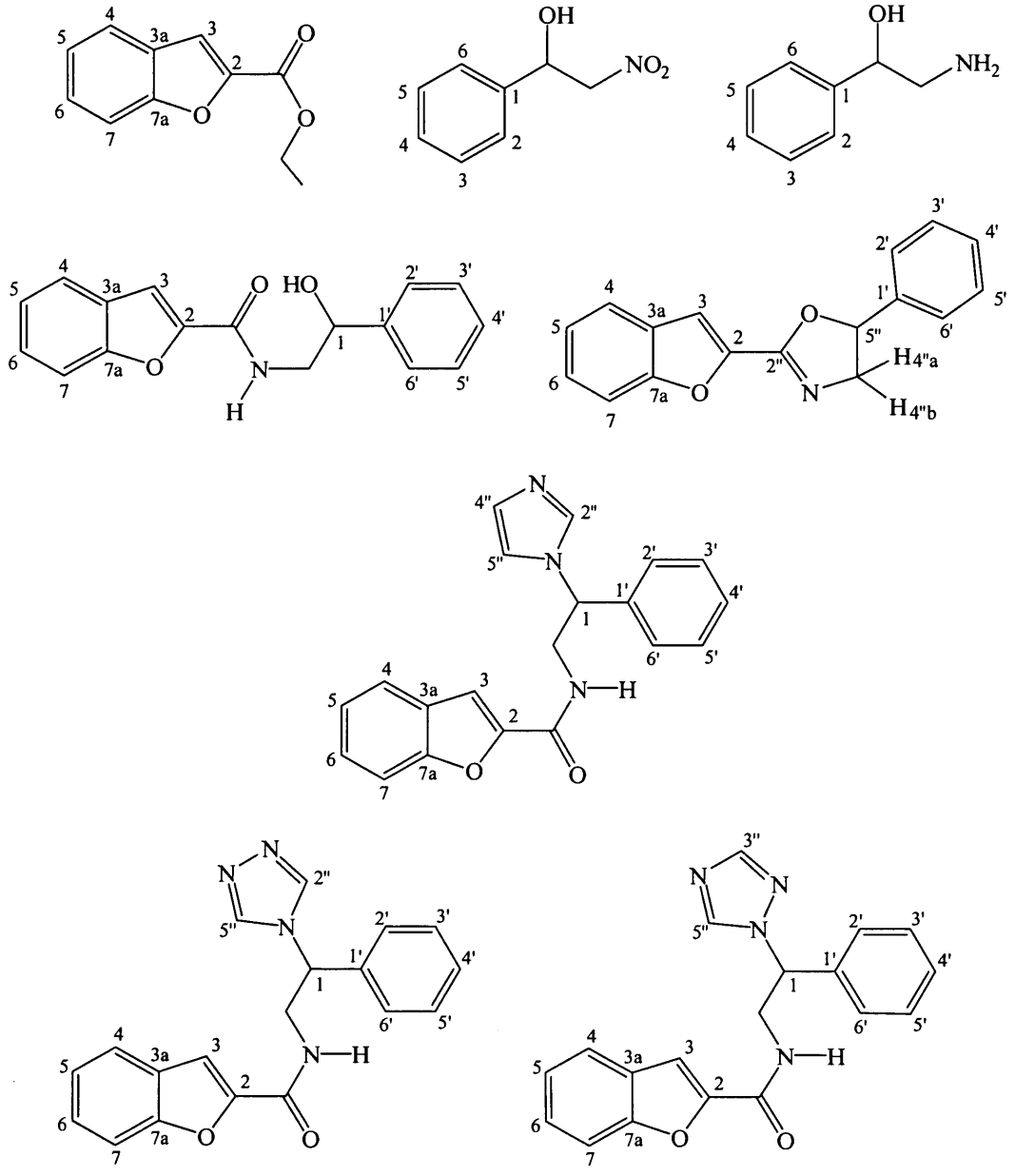

All n.m.r. characterisations were made by comparison with previous n.m.r. spectra of the appropriate structure class and or predictions from ACD/HNMR and ACD/CNMR (Advanced Chemistry Development Inc., Version 2.51, 1997) and ChemDraw Ultra™ 7.0 (CambridgeSoft).

Synthesis of ethyl benzo[*b*]furan-2-carboxylate derivatives (compounds **21**, **24** and **26**)

Ethyl benzo[*b*]furan-2-carboxylate (**21**) (Suzuki *et al.*, 1983)

($C_{11}H_{10}O_3$, MW: 190.197)

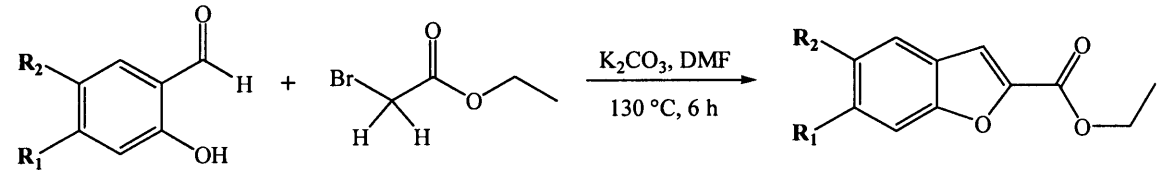

(**4**) $R_1 = R_2 = H$
(**23**) $R_1 = OCH_3$; $R_2 = H$
(**25**) $R_1 = H$; $R_2 = NO_2$

(**20**)

(**21**) $R_1 = R_2 = H$
(**24**) $R_1 = OCH_3$; $R_2 = H$
(**26**) $R_1 = H$; $R_2 = NO_2$

Activated potassium carbonate (16.55 g, 119.75 mmol) was added to a stirred solution of salicylaldehyde (**4**) (7.31 g, 59.88 mmol) in anhydrous DMF (15 mL). Ethyl bromoacetate (**20**) (10.0 g, 59.88 mmol) in anhydrous DMF (20 mL) was then added to the above mixture and the reaction was stirred at 130 °C for 6 hours. The solvent was then evaporated to about $^1/_3$ its volume to give a brown syrup. The crude product was extracted with CH_2Cl_2 (200 mL) and water (3 x 100 mL). The organic layer was dried with $MgSO_4$, filtered and reduced *in vacuo* to give a yellow residue. The residue was purified by flash column chromatography (petroleum ether – ethyl acetate 100:0 v/v increasing to 95:5 v/v) to give ethyl benzo[*b*]furan-2-carboxylate (**21**) as a yellow solid. Yield: 6.0 g (53 %), t. l. c. system: petroleum ether – ethyl acetate 3:1 v/v, R_F: 0.71, stain negative. Melting point: 40 – 42 °C. [Suzuki *et al.*, 1983 did not purify this compound prior next reaction, therefore, literature melting point is not available.]

^{1}H n.m.r. δ 7.70 (ddd, J = 0.5, 1.2, 8.4 Hz, 1H, H-4), 7.62 (dd, J = 0.8, 8.4 Hz, 1H, H-7), 7.55 (d, J = 0.9 Hz, 1H, H-3), 7.45 (m, 1H, H-6), 7.33 (m, 1H, H-5), 4.48 (q, 2H, J = 7.1 Hz, CH_2), 1.50 (t, 3H, J = 7.1 Hz, CH_3).

^{13}C n.m.r. δ 159.95 (C, C-7a), 156.09 (C=O), 146.13 (C, C-2), 127.95 (CH, CH-6), 127.37 (C, C-3a), 124.15 (CH, CH-5), 123.19 (CH, CH-4), 114.15 (CH, CH-3), 112.72 (CH, CH-7), 61.87 (CH_2), 14.73 (CH_3).

The following analogues of compound **21** were prepared using the same general method detailed above.

Ethyl 6-methoxybenzo[*b*]furan-2-carboxylate (24)

($C_{12}H_{12}O_4$, MW: 220.223)

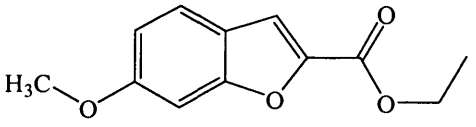

(24)

With ethyl 6-methoxybenzo[*b*]furan-2-carboxylate (**24**), yellow residue was obtained. Purification by flash column chromatography gave brown solid.

Yield: 6.6 g (53 %), t. l. c. system: petroleum ether – ethyl acetate 3:1 v/v, R_F: 0.55, stain positive. Microanalysis: Calculated C = 65.45 %, H = 5.49 %; Found C = 65.32 %, H = 5.53 %. Melting point: 66 - 68 °C.

^{1}H n.m.r. δ 7.63 (d, J = 8.7 Hz, 1H, H-4), 7.57 (d, J = 0.9 Hz, 1H, H-3), 7.17 (d, J = 1.8 Hz, 1H, H-7), 7.03 (dd, J = 2.2, 8.7 Hz, 1H, H-5), 4.53 (q, J = 7.1 Hz, 2H, CH_2), 3.97 (s, 3H, OCH_3), 1.52 (t, J = 7.1 Hz, 3H, CH_3).

^{13}C n.m.r. δ 160.93 (C, C-7a), 160.01 (C-6), 157.53 (C, C=O), 145.41 (C, C-2), 123.42 (CH, CH-4), 120.67 (C, C-3a), 114.45 (CH, CH-3), 114.39 (CH, CH-5), 96.16 (CH, CH-7), 61.67 (CH_2), 56.09 (CH_3, -OCH_3), 14.79 (CH_3).

I.R. (KBr diffusion): 1714 cm^{-1} (ester).

Ethyl 5-nitrobenzo[*b*]furan-2-carboxylate (26)

($C_{11}H_9NO_5$, MW: 235.194)

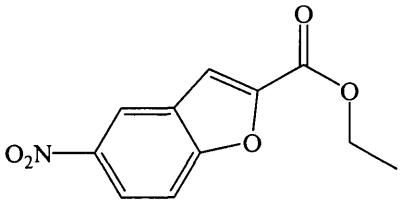

(26)

With ethyl 5-nitrobenzo[*b*]furan-2-carboxylate (**26**), a brown residue was obtained. Purification by flash column chromatography gave yellow solid.

Yield: 3.1 g (22 %), t. l. c. system: petroleum ether – ethyl acetate 4:1 v/v, R_F: 0.60, stain negative. Microanalysis: Calculated C = 56.17 %, H = 3.86 %, N = 5.95 %; Found C = 56.38 %, H = 3.90 %, N = 5.88 %. Melting point: 139 - 141 °C.

^{1}H n.m.r. δ 8.69 (d, J = 2.3 Hz, 1H, H-4), 8.42 (dd, J = 2.3, 9.1 Hz, 1H, H-6), 7.75 (d, J = 9.1 Hz, 1H, H-7), 7.70 (s, 1H, H-3), 4.53 (q, 2H, J = 7.1 Hz, CH_2), 1.50 (t, 3H, J = 7.1 Hz, CH_3).

^{13}C n.m.r. δ 159.04 (C, C-7a), 158.42 (C=O), 149.14 (C, C-2), 145.23 (C, C-5), 127.69 (C, C-3a), 123.34 (CH, CH-6), 119.89 (CH, CH-4), 114.32 (CH, CH-3), 113.39 (CH, CH-7), 62.56 (CH_2), 14.69 (CH_3).

I.R. (KBr diffusion): 1720 cm^{-1} (ester).

Synthesis of ethyl benzo[*b*]furan-2-carboxylic acid derivatives (compounds **27** – **29**)

Benzo[*b*]furan-2-carboxylic acid (**27**) (Suzuki *et al.*, 1983)

($C_9H_6O_3$, MW: 162.143)

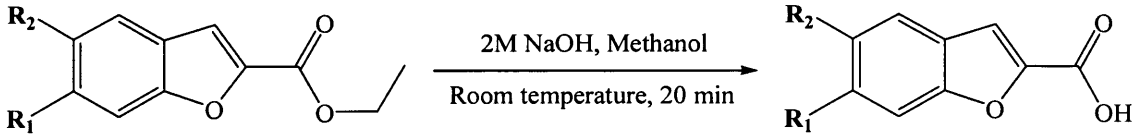

(**21**) $R_1 = R_2 = H$
(**24**) $R_1 = OCH_3$; $R_2 = H$
(**26**) $R_1 = H$; $R_2 = NO_2$

(**27**) $R_1 = R_2 = H$
(**28**) $R_1 = OCH_3$; $R_2 = H$
(**29**) $R_1 = H$; $R_2 = NO_2$

A solution of ethyl benzo[*b*]furan-2-carboxylate (**21**) (6 g, 31.55 mmol) in methanol (100 mL) was treated with 2M aqueous sodium hydroxide (50 mL) and warmed gently on a steam bath. Progress of the reaction was monitored by observing the disappearance of ethyl benzo[*b*]furan-2-carboxylate by t. l. c. After hydrolysis was complet (*ca.* 30 min.), the reaction solution was cooled and acidified to pH 1 by the dropwise addition of concentrated HCl. The solution was then extracted with diethyl ether (3 x 150 mL) and the organic layer dried with $MgSO_4$, filtered and reduced *in vacuo* to give a crude yellow solid. The crude yellow solid was washed with water, collected and dried under vacuum with phosphorus pentoxide to give pure benzo[*b*]furan-2-carboxylic acid (**27**). Yield: 5.0 g (98 %), t. l. c. system: petroleum ether – ethyl acetate 1:1 v/v, R_F: 0.0, stain negative. Melting point: 190 – 192 °C [Literature: 192 – 193 °C (Suzuki *et al.*, 1983)].

^{1}H n.m.r. (Acetone-d_6) δ 7.73 (split d, J = 0.7, 7.9 Hz, 1H, H-4), 7.58 (split d, J = 1.7, 7.6, 1H, H-7), 7.57 (d, J = 0.8 Hz, H-3), 7.49 (m, 1H, H-6), 7.32 (m, 1H, H-5).

^{13}C n.m.r. (Acetone-d_6) δ 162.94 (C=O), 157.53 (C, C-7a), 147.78 (C, C-2), 129.15 (CH, CH-6), 128.88 (C, C-3a), 125.31 (CH, CH-5), 124.45 (CH, CH-4), 115.28 (CH, CH-3), 113.35 (CH, CH-7).

I.R. (KBr diffusion): 1670 and 940 cm^{-1} (-COOH). [Literature found: 1680 and 943 cm^{-1} (Suzuki *et al.*, 1983)].

The following analogues of compound **27** were prepared using the same general method detailed above.

6-Methoxybenzo[*b*]furan-2-carboxylic acid (28)

($C_{10}H_8O_4$, MW: 192.169)

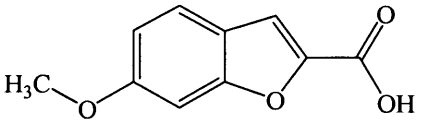

(28)

With 6-methoxybenzo[*b*]furan-2-carboxylic acid (**33**), a yellow solid was obtained after drying under vacuum at 80 °C.

Yield: 5.4 g (88 %), t. l. c. system: petroleum ether – ethyl acetate 1:1 v/v, R_F: 0.0, stain positive. Microanalysis: Calculated C = 62.50 %, H = 4.20 %; Found C = 62.49 %, H = 4.19 %. Melting point: 194 – 196 °C.

^{1}H n.m.r. (DMSO-d_6) δ 13.36 (s, 1H, COO<u>H</u>), 7.67 (d, J = 8.7 Hz, 1H, H-4), 7.61 (s, 1H, H-3), 7.31 (s, 1H, H-7), 6.99 (split d, J = 2.1, 8.6 Hz, H-5), 3.85 (s, 3H, OC<u>H</u>$_3$).

^{13}C n.m.r. (DMSO-d_6) δ 160.41 (C=O and C, C-7a), 156.85 (C, C-6), 145.64 (C, C-2), 123.70 (CH, CH-4), 120.32 (C, C3a), 114.17 (CH, CH-3), 114.13 (CH, CH-5), 96.22 (CH, CH-7), 56.08 (CH_3, -O<u>C</u>H$_3$).

I.R. (KBr diffusion): 1689 and 930 cm^{-1} (-COOH).

5-Nitrobenzo[*b*]furan-2-carboxylic acid (29)

($C_9H_5NO_5$, MW: 207.140)

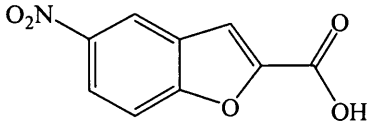

(29)

With 5-nitrobenzo[*b*]furan-2-carboxylic acid (**29**), yellow solid was obtained after dried under vacuum at 80 °C.

Yield: 2.5 g (95 %), t. l. c. system: petroleum ether – ethyl acetate 1:1 v/v, R_F: 0.0, stain positive. Microanalysis: Calculated C = 52.19 %, H = 2.43 %, N = 6.76 %; Found C = 52.30 %, H = 2.43 %, N = 6.68 %. Melting point: 268 – 270 °C.

^{1}H n.m.r. (DMSO-d_6) δ 14.00 (s, 1H, COOH), 8.75 (d, J = 2.2 Hz, 1H, H-4), 8.36 (dd, J = 2.2, 9.2 Hz, 1H, H-4), 7.97 (d, J = 9.2 Hz, 1H, H-7), 7.85 (s, 1H, H-3).

^{13}C n.m.r. (DMSO-d_6) δ 159.79 (C, C-7a), 157.90 (C=O), 149.40 (C, C-5), 144.54 (C, C-2), 127.77 (C, C-3a), 123.06 (CH, CH-6), 120.18 (CH, CH-4), 114.49 (CH, CH-3), 113.58 (CH, CH-7).

1-(4-Fluorophenyl)-2-nitro-1-ethanol (32)

($C_8H_8FNO_3$, MW: 185.153)

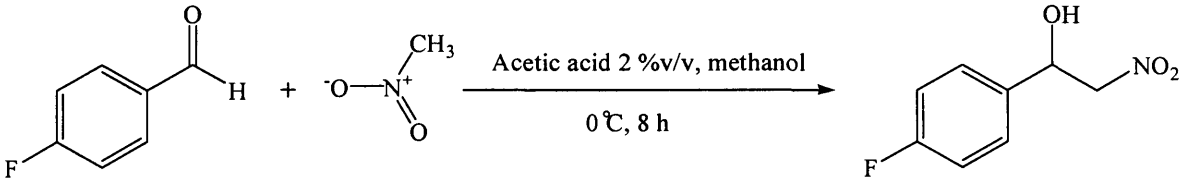

(30) **(31)** **(32)**

Nitromethane (**31**) (9.84 g, 161.15 mmol) and aqueous NaOH (10M, 80.57 mmol) were added to a solution of 4-fluorobenzaldehyde (**30**) (10.0 g, 80.57 mmol) in methanol (150 mL). The resulting solution was stirred at 0 °C for 8 h. Aqueous acetic acid (2 % v/v, 80.57 mmol) was added to the above reaction mixture and was stirred at room temperature for another 30 min. The methanol was removed under vacuum and the aqueous phase extracted with CH_2Cl_2 (2 x 150 mL). The combined organic layers were washed with brine (2 x 100 mL), dried with $MgSO_4$, filtered and reduced *in vacuo* to give a brown residue. The residue was purified by flash column chromatography (petroleum ether – ethyl acetate 100:0 v/v increasing to 85:15 v/v) to give 1-(4-fluorophenyl)-2-nitro-1-ethanol (**32**) as a brown syrup. Yield: 8.0 g (54 %), t. l. c. system: petroleum ether – ethyl acetate 4:1 v/v, R_F: 0.33, stain positive.

^{1}H n.m.r. δ 7.44 (m, 2H, H-2 and H-6), 7.15 (m, 2H, H-3 and H-5), 5.51 (m, 1H, CH-OH), 4.64 (dd, J = 9.3, 13.3 Hz, 1H, CHHNO$_2$), 4.54 (dd, J = 3.4, 13.3 Hz, 1H, CHHNO$_2$), 3.10 (d, J = 3.4 Hz, 1H, OH). [Literature ^{1}H n.m.r. from Watanabe *et al.* (Watanabe *et al.*, 2002)].

^{13}C n.m.r. δ 164.98 and 161.70 (C, C-4), 134.40 and 134.36 (C, C-1), 128.28 and 128.17 (CH, CH-2 and CH-6), 116.58 and 116.29 (CH, CH-3 and CH-5), 81.56 (CH_2), 70.77 (CH-OH).

1-(4-Chlorophenyl)-2-nitro-1-ethanol (34)

($C_8H_8ClNO_3$, MW: 201.608)

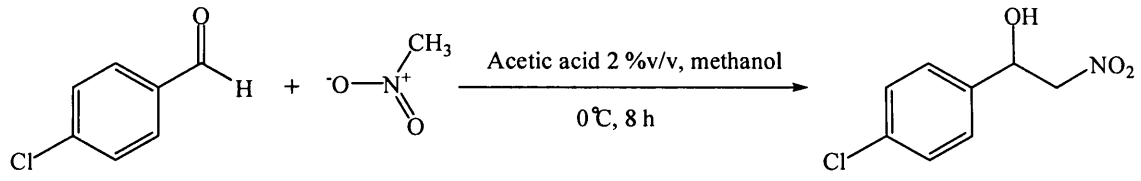

(33) **(31)** **(34)**

Nitromethane (17.37 g, 284.56 mmol) and aqueous NaOH (10M, 142.28 mmol) were added to a solution of 4-chlorobenzaldehyde (20.0 g, 142.28 mmol) in methanol (150 mL). The resulting solution was stirred at 0 °C for 8 h. Aqueous acetic acid (2 % v/v, 142.28 mmol) was added to the above reaction mixture and was stirred at room temperature for another 30 min. The methanol was removed under vacuum and the aqueous phase extracted with CH_2Cl_2 (2 x 150 mL). The combined organic layers were washed with brine (2 x 100 mL), dried with $MgSO_4$, filtered and reduced *in vacuo* to give a brown residue. The residue was purified by flash column chromatography (petroleum ether – ethyl acetate 100:0 v/v increasing to 85:15 v/v) to give 1-(4-chlorophenyl)-2-nitro-1-ethanol as a yellow syrup. Yield: 21.23 g (74 %), t. l. c. system: petroleum ether – ethyl acetate 4:1 v/v, R_F: 0.34, stain positive.

^{1}H n.m.r. δ 7.50 – 7.42 (m, 4H, Ar), 5.48 (m, 1H, C<u>H</u>-OH), 4.68 (dd, J = 9.3, 13.3 Hz, 1H, C<u>H</u>HNO$_2$), 4.59 (dd, J = 3.6, 13.3 Hz, 1H, CH<u>H</u>NO$_2$), 3.31 (d, J = 3.6 Hz, 1H, OH). [Literature ^{1}H n.m.r. from Choudary *et al.* (Choudary *et al.*, 2001)].

^{13}C n.m.r. δ 137.05 (C, C-1), 135.22 (C, C-4), 129.64 (2 x CH, CH-2 and CH-6), 127.80 (2 x CH, CH-3 and CH-5), 81.43 (CH_2), 70.74 (<u>C</u>H-OH).

2-Amino-1-(4-fluorophenyl)-1-ethanol (35)

($C_8H_{10}FNO$, MW: 155.171)

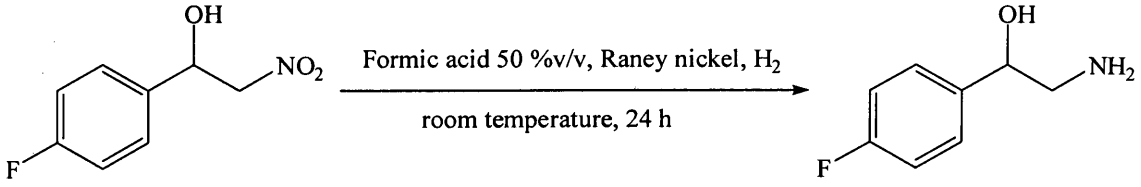

(32) **(35)**

Raney nickel (50 % slurry in H_2O, 6 mL) was added to a solution of 1-(4-fluorophenyl)-2-nitro-1-ethanol (**32**) (7.0 g, 37.83 mmol) in methanol (100 mL) and aqueous formic acid (50 % v/v, 8 mL). The reaction flask was then degassed and

purged with hydrogen. The reaction was carried out under 40 psi H_2 atmosphere using a Paar hydrogenator. The reaction flask was shaken at room temperature for 24 hours until all starting material had been consumed. After removal of hydrogen the reaction mixture was filtered, and the methanol was removed *in vacuo*. The aqueous residue was made alkaline with NH_4OH (28 %) and extracted with ethyl acetate (2 x 100 mL). The organic layer was then washed with brine (2 x 50 mL), dried with $MgSO_4$, filtered and reduced *in vacuo* to give 2-amino-1-(4-fluorophenyl)-1-ethanol (**35**) as a green residue. The residue was purified by flash column chromatography (dichloromethane – methanol - triethylamine 100:0:0.05 v/v increasing to 95:5:0.05 v/v) to give the product as a yellow solid. Yield: 2.60 g (44 %), t. l. c. system: dichloromethane – methanol 9:1 v/v, R_F: 0.08, stain positive. Melting point: 59 - 61 °C [Literature: 63 – 65 °C (Cho *et al.*, 2002)].

^{1}H n.m.r. (DMSO-d_6) δ 7.37 (m, 2H, Ar), 7.14 (m, 2H, Ar), 4.87 (dd, J = 4.5, 7.3 Hz, 1H, C<u>H</u>-OH), 2.76 (dd, J = 4.3, 12.8 Hz, 1H, C<u>H</u>HNH$_2$), 2.63 (dd, J = 7.6, 12.8 Hz, 1H, CH<u>H</u>NH$_2$), 2.18 (brs, 3H, NH_2 and OH).

^{13}C n.m.r. (DMSO-d_6) δ 163.09 and 159.89 (C, C-4), 140.97 and 140.93 (C, C-1), 128.18 and 128.08 (CH, CH-2 and CH-6), 115.07 and 114.79 (CH, CH-3 and CH-5), 74.18 (CH-OH), 50.52 (CH_2).

I.R. (KBr diffusion): 3352, 2998, 2886, 1609, 1499 cm $^{-1}$. [Literature: 3357, 2998, 2878, 1603, 1501 cm $^{-1}$ (Cho *et al.*, 2002)].

<u>2-Amino-1-(4-chlorophenyl)-1-ethanol</u> (36)

($C_8H_{10}ClNO$, MW: 171.626)

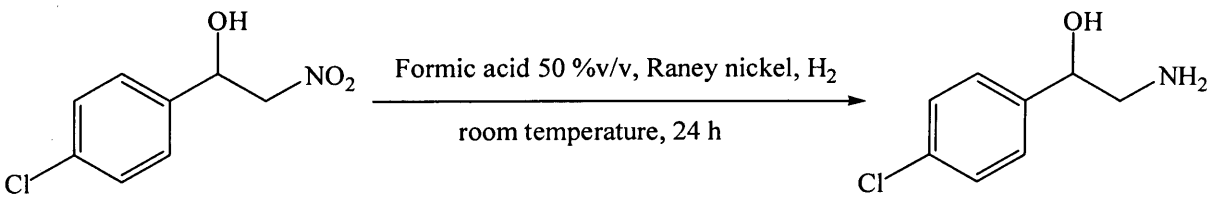

(34) **(36)**

Raney nickel (50 % slurry in H_2O, 8 mL) was added to a solution of 1-(4-chlorophenyl)-2-nitro-1-ethanol (**34**) (13.84 g, 68.65 mmol) in methanol (100 mL) and aqueous formic acid (50 % v/v, 10 mL). The reaction flask was then degassed and purged with hydrogen. The reaction was carried out under 40 psi H_2 atmosphere using a Paar hydrogenator. The reaction flask was shaken at room temperature for 24 hours

until all starting material had been consumed. After removal of hydrogen the reaction mixture was filtered, and the methanol was removed *in vacuo*. The aqueous residue was made alkaline with NH_4OH (28 %) and extracted with ethyl acetate (2 x 100 mL). The organic layer was then washed with brine (2 x 50 mL), dried with $MgSO_4$, filtered and reduced *in vacuo* to give a brown residue. The residue was purified by flash column chromatography (dichloromethane – methanol - triethylamine 100:0:0.05 v/v increasing to 95:5:0.05 v/v) to give 2-amino-1-(4-chlorophenyl)-1-ethanol (**36**) as a white solid. Yield: 5.40 g (46 %), t. l. c. system: dichloromethane – methanol 9:1 v/v, R_F: 0.10, stain positive. Melting point: 93 - 95 °C [Literature: 95 – 97 °C (Cho *et al.*, 2002)].

^{1}H n.m.r. (DMSO-d_6) δ 7.41 (m, 4H, Ar), 4.51 (dd, J = 4.4, 7.4 Hz, 1H, C<u>H</u>-OH), 2.71 (dd, J = 4.4, 12.9 Hz, 1H, C<u>H</u>HNH$_2$), 2.61 (dd, J = 7.5, 12.9 Hz, 1H, CH<u>H</u>NH$_2$), 2.20 (brs, 3H, NH_2 and OH).

^{13}C n.m.r. (DMSO-d_6) δ 143.83 (C, C-1), 131.50 (C, C-4), 128.20 (2 x CH, CH-2 and CH-6), 128.16 (2 x CH, CH-3 and CH-5), 74.19 (<u>C</u>H-OH), 50.46 (CH_2).

I.R. (KBr diffusion): 3348, 3236, 3104, 2975, 2834, 1611, 1493 cm $^{-1}$. [Literature: 3357, 3214, 3104, 2964, 2853, 1595, 1491 cm $^{-1}$ (Cho *et al.*, 2002)].

Synthesis of *N*2-(2-hydroxy-2-phenylethyl)benzo[*b*]furan-2-carboxamide derivatives (compounds 39 – 43)

<u>*N*2-(2-Hydroxy-2-phenylethyl)benzo[*b*]furan-2-carboxamide</u> (39)

($C_{17}H_{15}NO_3$, MW: 281.309)

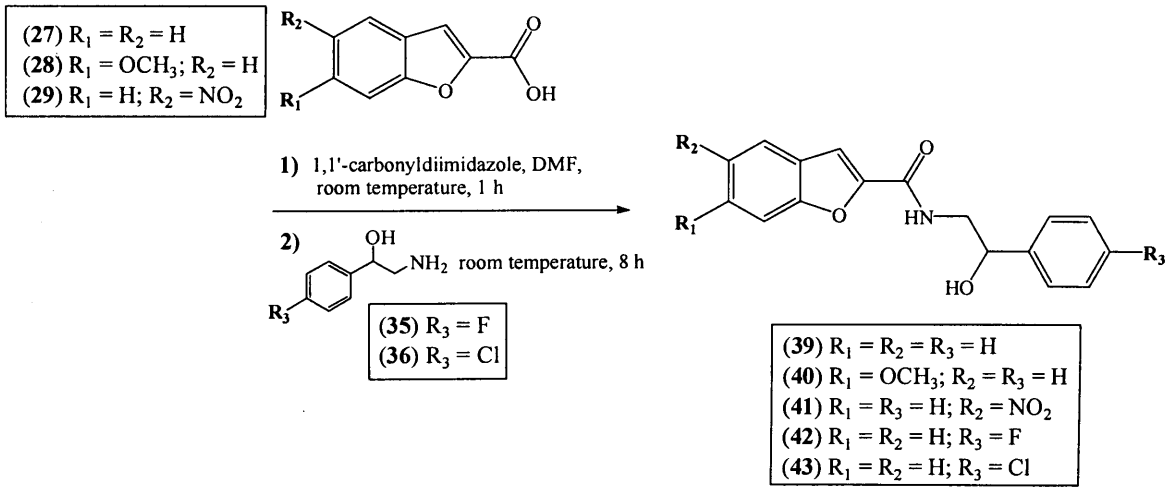

To a suspension of benzo[*b*]furan-2-carboxylic acid (**27**) (4.50 g, 27.75 mmol) in anhydrous DMF (30 mL) was added of 1,1'-carbonyl-diimidazole (4.50 g, 27.75

mmol) and the reaction stirred at room temperature for 1 hr. The reaction was cooled to 0 °C and subsequently combined with a solution of 2-amino-1-phenyl-ethanol (3.81 g, 27.75 mmol) in DMF (10 mL). The mixture was stirred at room temperature for 8 h. After the reaction was complete, an aliquot amount of ice was poured into the flask to precipitate out the product which was then filtered and washed with 10 mL of ethanol to give the white solid, *N*-(2-hydroxy-2-phenylethyl)benzo[*b*]furan-2-carboxamide (**39**). The product was then collected and dried under vacuum with phosphorus pentoxide. Yield: 5.63 g (72 %), t. l. c. system: petroleum ether – ethyl acetate 3:2 v/v, R_F: 0.45, stain positive. Microanalysis: Theory C = 72.58 %, H = 5.37 %, N = 4.98 %; Found C = 72.44 %, H = 5.32 %, N = 4.88 %. Melting point: 140 - 142 °C.

^{1}H n.m.r. (DMSO-d_6) δ 8.67 (t, J = 5.6 Hz, 1H, NH), 7.78 (d, J = 7.7 Hz, 1H, Ar), 7.67 (d, J = 8.3 Hz, 1H, Ar), 7.56 (s, 1H, H-3), 7.47 (m, 1H, Ar), 7.41-7.24 (m, 5H, Ar), 5.60 (d, J= 4.4 Hz, 1H, OH), 4.83 (m, 1H, H-1), 3.58-3.34 (m, 2H, CH_2).

^{13}C n.m.r. (DMSO-d_6) δ 158.53 (C=O), 154.54 (C, C-7a), 149.51 (C, C-2), 143.89 (C, C-1'), 128.41 (2 x CH, CH-3' and CH-5'), 127.53 (C, C-3a), 127.45 (CH, CH-4'), 127.10 (CH, CH-6), 126.35 (2 x CH, CH-2' and CH-6'), 124.02 (CH, CH-5), 123.08 (CH, CH-4), 112.12 (CH, CH-7), 109.66 (CH, CH-3), 71.28 (CH, CH1-OH), 47.35 (CH_2).

The following analogues of compound **39** were prepared using the same general method detailed above.

<u>*N*2-(2-Hydroxy-2-phenylethyl)-6-methoxybenzo[*b*]furan-2-carboxamide</u> (40)

($C_{18}H_{17}NO_4$, MW: 311.335)

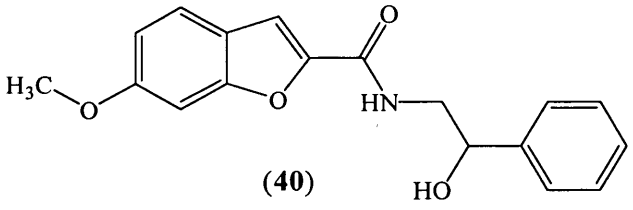

(40)

With *N*2-(2-hydroxy-2-phenylethyl)-6-methoxybenzo[*b*]furan-2-carboxamide (**40**), a light brown powder was obtained after drying under vacuum at 80 °C.

Yield: 6.38 g (88 %), t. l. c. system: petroleum ether – ethyl acetate 3:2 v/v, R_F: 0.40, stain positive. Microanalysis: Theory C = 69.44 %, H = 5.50 %, N = 4.50 %; Found C = 69.47 %, H = 5.46 %, N = 4.37 %. Melting point: 147 - 149 °C.

^{1}H n.m.r. (DMSO-d_6) δ 8.45 (t, J = 5.7 Hz, 1H, NH), 7.62 (d, J = 8.7 Hz, 1H, Ar), 7.46 (d, J = 0.8 Hz, 1H, H-3), 7.39-7.30 (m, 4H, Ar), 7.27-7.20 (m, 2H, Ar), 6.95 (dd, J = 2.2, 8.6 Hz, 1H, Ar), 5.58 (d, J= 4.4 Hz, 1H, OH), 4.79 (m, 1H, H-1), 3.82 (s, 3H, $OC\underline{H}_3$), 3.55-3.30 (m, 2H, $C\underline{H}_2$).

^{13}C n.m.r. (DMSO-d_6) δ 159.77 (C, C-6), 158.62 (C=O), 155.89 (C, C-7a), 148.73 (C, C-2), 143.91 (C, C-1'), 128.44 (2 x CH, CH-3' and CH-5'), 127.47 (CH, CH-4'), 126.37 (2 x CH, CH-2' and CH-6'), 123.34 (CH, CH-4), 120.65 (C, C-3a), 113.54 (CH, CH-5), 109.83 (CH, CH-3), 96.25 (CH, CH-7), 71.46 (CH, CH1-OH), 56.05 ($O\underline{C}H_3$), 47.29 (CH_2).

<u>*N*2-(2-Hydroxy-2-phenylethyl)-5-nitrobenzo[*b*]furan-2-carboxamide</u> (41)

($C_{17}H_{14}N_2O_5$, MW: 326.306)

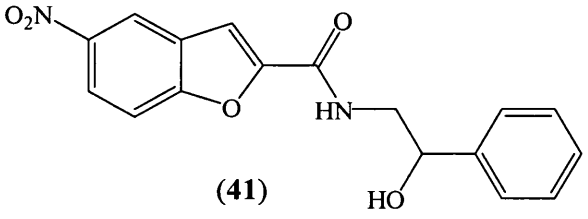

(41)

With *N*2-(2-hydroxy-2-phenylethyl)-5-nitrobenzo[*b*]furan-2-carboxamide (**41**), a light yellow solid was obtained after drying under vacuum at 80 °C.

Yield: 3.47 g (88 %), t. l. c. system: petroleum ether – ethyl acetate 3:2 v/v, R_F: 0.59, stain positive. Microanalysis: Theory C = 62.57 %, H = 4.32 %, N = 8.58 %; Found C = 62.42 %, H = 4.21 %, N = 8.59 %. Melting point: 174 - 176 °C.

^{1}H n.m.r. (DMSO-d_6) δ 8.92 (t, J = 5.6 Hz, 1H, NH), 8.80 (d, J = 2.1 Hz, 1H, H-4), 8.35 (dd, J = 2.0, 9.1 Hz, 1H, H-6), 7.93 (d, J = 9.1 Hz, 1H, H-7), 7.79 (s, 1H, H-3), 7.44-7.26 (m, 5H, Ar), 5.62 (d, J= 2.9 Hz, 1H, OH), 4.85 (m, 1H, H-1), 3.59-3.37 (m, 2H, $C\underline{H}_2$).

^{13}C n.m.r. (DMSO-d_6) δ 157.80 (C, C=O), 157.23 (C, C-7a), 152.26 (C, C-2), 144.51 (C, C-5), 143.81 (C, C-1'), 128.46 (2 x CH, CH-3' and CH-5'), 128.14 (C, C-3a), 127.51 (CH, CH-4'), 126.37 (2 x CH, CH-2' and CH-6'), 122.44 (CH, CH-4), 119.87 (CH, CH-6), 113.21 (CH, CH-7), 110.42 (CH, CH-3), 71.31 (CH, CH1-OH), 47.47 (CH_2).

***N*2-[2-(4-Fluorophenyl)-2-hydroxyethyl]benzo[*b*]furan-2-carboxamide (42)**

($C_{17}H_{14}FNO_3$, MW: 299.300)

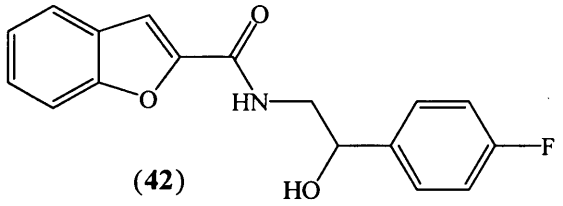

(**42**)

With *N*2-[2-(4-fluorophenyl)-2-hydroxyethyl]benzo[*b*]furan-2-carboxamide (**42**), a white solid was obtained after drying under vacuum at 80 °C.

Yield: 3.60 g (85 %), t. l. c. system: petroleum ether – ethyl acetate 3:2 v/v, R_F: 0.41, stain positive. Microanalysis: Theory C = 68.22 %, H = 4.71 %, N = 4.68 %; Found C = 68.27 %, H = 4.67 %, N = 4.66 %. Melting point: 172 - 174 °C.

^{1}H n.m.r. (DMSO-d_6) δ 8.69 (t, J = 5.7 Hz, 1H, NH), 7.79 (d, J = 7.7 Hz, 1H, Ar), 7.68 (d, J = 8.3 Hz, 1H, Ar), 7.58 (s, 1H, Ar), 7.51 – 7.27 (m, 4H, Ar), 7.18 (t, J = 8.9 Hz, 2H, Ar), 5.68 (d, J = 4.5 Hz, 1H, OH), 4.85 (m, 1H, C<u>H</u>-OH), 3.57-3.37 (m, 2H, C<u>H</u>$_2$).

^{13}C n.m.r. (DMSO-d_6) δ 163.31 (C=O), 160.11 and 158.57 (C, C-4'), 154.56 (C, C-7a), 149.48 (C, C-2), 140.06 and 140.02 (C, C-1'), 128.37 and 128.26 (2 x CH, CH-2' and CH-6'), 127.54 (C, C-3a), 127.14 (CH, CH-6), 124.05 (CH, CH-5), 123.10 (CH, CH-4), 115.28 and 114.99 (2 CH, CH-3' and CH-5'), 112.15 (CH, CH-3), 109.74 (CH, CH-7), 70.78 (CH, CH1-OH), 47.24 (CH_2).

***N*2-[2-(4-Chlorophenyl)-2-hydroxyethyl]benzo[*b*]furan-2-carboxamide (43)**

($C_{17}H_{14}ClNO_3$, MW: 315.754)

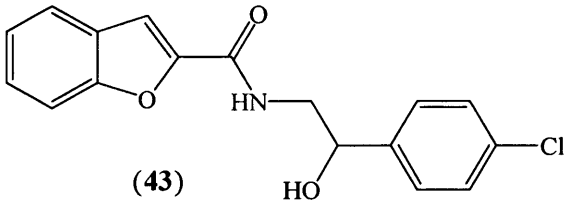

(**43**)

With *N*2-[2-(4-chlorophenyl)-2-hydroxyethyl]benzo[*b*]furan-2-carboxamide (**43**), a white solid was obtained after drying under vacuum at 80 °C.

Yield: 3.25 g (84 %), t. l. c. system: petroleum ether – ethyl acetate 3:2 v/v, R_F: 0.47, stain positive. Microanalysis: Theory C = 64.67 %, H = 4.47 %, N = 4.43 %; Found C = 64.58 %, H = 4.51 %, N = 4.44 %. Melting point: 189 - 191 °C.

^{1}H n.m.r. (DMSO-d_6) δ 8.69 (t, J = 5.7 Hz, 1H, NH), 7.79 (d, J = 7.8 Hz, 1H, Ar), 7.68 (d, J = 8.3 Hz, 1H, Ar), 7.57 (s, 1H, Ar), 7.51 – 7.33 (m, 6H, Ar), 5.71 (d, J = 4.5 Hz, 1H, OH), 4.84 (ddd, J = 4.9, 7.2, 12.1 Hz, 1H, C<u>H</u>-OH), 3.56-3.37 (m, 2H, C<u>H</u>$_2$). ^{13}C n.m.r. (DMSO-d_6) δ 158.56 (C=O), 154.56 (C, C-7a), 149.45 (C, C-2), 142.88 (C, C-1'), 128.39 (2 x CH, CH-3' and CH-5'), 128.30 (2 x CH, CH-2' and CH-6'), 127.53 (C, C-3a), 127.15 (CH, CH-6), 124.05 (CH, CH-5), 123.11 (CH, CH-4), 112.15 (CH, CH-7), 109.75 (CH, CH-3), 70.75 (CH, CH1-OH), 47.11 (CH_2).

Synthesis of 2-benzo[*b*]furan-2-yl-5-phenyl-4,5-dihydro-1,3-oxazole derivatives (compounds **45** – **49**)

<u>2-Benzo[*b*]furan-2-yl-5-phenyl-4,5-dihydro-1,3-oxazole</u> (45)

($C_{17}H_{13}NO_2$, MW: 263.294)

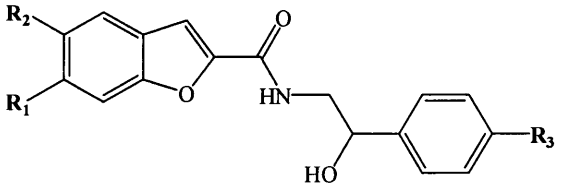

(**39**) $R_1 = R_2 = R_3 = H$
(**40**) $R_1 = OCH_3$; $R_2 = R_3 = H$
(**41**) $R_1 = R_3 = H$; $R_2 = NO_2$
(**42**) $R_1 = R_2 = H$; $R_3 = F$
(**43**) $R_1 = R_2 = H$; $R_3 = Cl$

1) Methanesulphonic anhydride, Triethylamine, THF, 0 °C, 24 hours
2) NH_3 (aq.) 28%, room temparature, 15 minutes

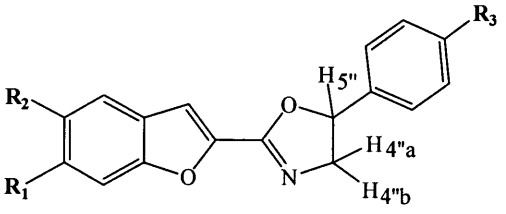

(**45**) $R_1 = R_2 = R_3 = H$
(**46**) $R_1 = OCH_3$; $R_2 = R_3 = H$
(**47**) $R_1 = R_3 = H$; $R_2 = NO_2$
(**48**) $R_1 = R_2 = H$; $R_3 = F$
(**49**) $R_1 = R_2 = H$; $R_3 = Cl$

To a solution of *N*-(2-hydroxy-2-phenylethyl)benzo[*b*]furan-2-carboxamide (**39**) (2.0 g, 7.11 mmol) in anhydrous THF (15 mL) was added methanesulphonic anhydride (1.86 g, 10.66 mmol) dissolved in anhydrous THF (5 mL). The homogenous mixture was stirred at 0 °C for 15 minutes, then triethylamine (3.0 mL, 21.33 mmol) was added dropwise to the above mixture. After keeping the homogenous mixture in the fridge at 0 °C for 24 hours the reaction went to completion. The mixture was quenched by the addition of aqueous ammonia solution (28 %, 1 mL). After stirring at room temperature for 15 minutes the mixture was concentrated *in vacuo* and finally

distributed between ethyl acetate (150 mL) and aqueous $NaHCO_3$ solution (2 x 100 mL). After repeated extraction the organic phases were dried and evaporated *in vacuo*. Purification of the resulting residue by recrystallisation from ethanol yielded 2-benzo[*b*]furan-2-yl-5-phenyl-4,5-dihydro-1,3-oxazole (**45**) (1.0 g, 54 %) as a yellow solid, t. l. c. system: petroleum ether – ethyl acetate 1:1 v/v, R_F: 0.57, stain positive. LRMS (ES^+) *m/z*: 286.1 $(M+Na)^+$. Microanalysis ($C_{17}H_{13}NO_2.0.1H_2O$): Calculated C = 77.02 %, H = 5.02 %, N = 5.28 %; Found C = 77.05 %, H = 4.95 %, N = 5.25 %. Melting point: 79 – 81 °C.

^{1}H n.m.r. δ 7.71 (d, J = 7.8 Hz, 1H, Ar), 7.45 (d, J = 8.4 Hz, 1H, Ar), 7.49-7.32 (m, 8H, Ar), 5.75 (dd, $J_{5'',4''a}$ = 8.1 Hz, $J_{5'',4''b}$ = 10.0 Hz, 1H, $C\underline{H_{5''}}CH_{4''a}CH_{4''b}$), 4.60 (dd, $J_{4''b,5''}$ = 10.1Hz, $J_{4''b,4''a}$ = 15.1 Hz, 1H, $CH_{5''}CH_{4''a}C\underline{H_{4''b}}$), 4.14 (dd, $J_{4''a,5''}$ = 8.0 Hz, $J_{4''a,4''b}$ = 15.1 Hz, 1H, $CH_{5''}C\underline{H_{4''a}}CH_{4''b}$).

^{13}C n.m.r. δ 157.28 (C, C-2''), 156.15 (C, C-7a), 144.59 (C, C-2), 140.69 (C, C-1'), 129.33 (2 x CH, CH-3' and CH-5'), 129.00 (CH, CH-4'), 127.75 (C, C-3a), 127.15 (CH, CH-6), 126.32 (2 x CH, CH-2' and CH-6'), 124.04 (CH, CH-5), 122.68 (CH, CH-4), 112.52 (CH, CH-7), 111.19 (CH, CH-3), 82.08 (CH- CH-5''), 63.60 (CH_2).

The following analogues of compound **45** were prepared using the same general method detailed above.

2-(6-Methoxybenzo[*b*]furan-2-yl)-5-phenyl-4,5-dihydro-1,3-oxazole (46)

($C_{18}H_{15}NO_3$, MW: 293.320)

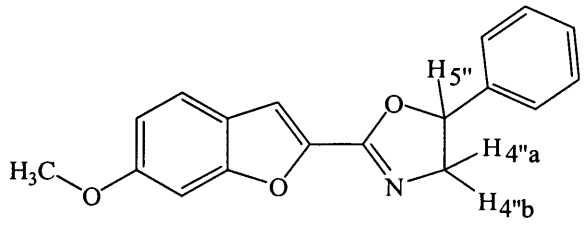

(46)

With 2-(6-methoxybenzo[*b*]furan-2-yl)-5-phenyl-4,5-dihydro-1,3-oxazole (**46**), a light yellow solid was obtained after purification by flash column chromatography (petroleum ether – ethyl acetate 90:10 v/v increasing to 50:50 v/v).

Yield: 3.17 g (67 %). t. l. c. system: petroleum ether – ethyl acetate 3:2 v/v, R_F: 0.30, stain positive. Microanalysis: Calculated C = 73.71 %, H = 5.15 %, N = 4.77 %; Found C = 73.52 %, H = 5.03 %, N = 4.72 %. Melting point: 116 – 118 °C.

^{1}H n.m.r. δ 7.65 (d, J = 8.7 Hz, 1H, Ar), 7.50 (d, J = 0.5 Hz, 1H, Ar), 7.47-7.33 (m, 6H, Ar), 7.00 (d, J = 2.2, 8.7 Hz, 1H, Ar), 5.82 (dd, $J_{5'',4''a}$ = 7.5 Hz, $J_{5'',4''b}$ = 10.0 Hz, 1H, $C\underline{H}_{5''}CH_{4''a}CH_{4''b}$), 4.49 (dd, $J_{4''b,5''}$ = 10.0 Hz, $J_{4''b,4''a}$ = 15.1 Hz, 1H, $CH_{5''}CH_{4''a}C\underline{H}_{4''b}$), 3.89 (dd, $J_{4''a,5''}$ = 7.5 Hz, $J_{4''a,4''b}$ = 15.1 Hz, 1H, $CH_{5''}C\underline{H}_{4''a}CH_{4''b}$), 3.86 (s, 3H, $OC\underline{H}_3$).

^{13}C n.m.r. δ 159.90 (C, C-6), 156.71 (C, C-2''), 155.67 (C, C-7a), 143.35 (C, C-2), 141.07 (C, C-1'), 129.15 (2 x CH, CH-3' and CH-5'), 128.65 (CH, CH-4'), 126.15 (2 x CH-2' and CH-6'), 123.14 (CH, CH-4), 120.48 (C, C-3a), 113.81 (CH, CH-5), 111.35 (CH, CH-3), 96.26 (CH, CH-7), 80.64 (CH- CH-5''), 62.93 (CH_2), 56.08 (CH_3).

2-(5-Nitrobenzo[*b*]furan-2-yl)-5-phenyl-4,5-dihydro-1,3-oxazole (47)

($C_{17}H_{12}N_2O_4$, MW: 308.291)

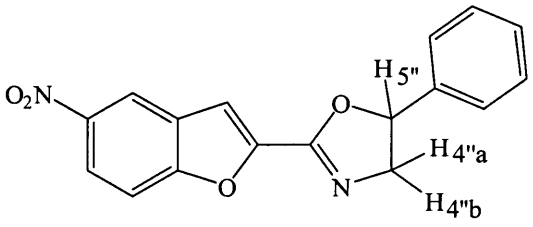

(47)

With 2-(5-nitrobenzo[*b*]furan-2-yl)-5-phenyl-4,5-dihydro-1,3-oxazole (**47**), a white solid was obtained after purification by flash column chromatography (petroleum ether – ethyl acetate 90:10 v/v increasing to 60:40 v/v).

Yield: 0.50 g (16 %), t. l. c. system: petroleum ether – ethyl acetate 3:2 v/v, R_F: 0.30, stain positive. Microanalysis: Calculated C = 66.23 %, H = 3.92 %, N = 9.08 %; Found C = 66.09 %, H = 3.89 %, N = 9.06 %. Melting point: 159 – 161 °C.

^{1}H n.m.r. (DMSO-d_6) δ 8.75 (d, J = 2.3 Hz, H-4), 8.36 (dd, J = 2.4, 9.1 Hz, H-6), 7.99 (d, J = 9.1 Hz, 1H, H-7), 7.79 (s, 1H, H-3), 7.48 – 7.36 (m, 5H, Ar), 5.89 (dd, $J_{5'',4''a}$ = 7.8 Hz, $J_{5'',4''b}$ = 10.0 Hz, 1H, $C\underline{H}_{5''}CH_{4''a}CH_{4''b}$), 4.55 (dd, $J_{4''a,5''}$ = 10.0 Hz, $J_{4''a,4''b}$ = 15.5 Hz, 1H, $CH_{5''}C\underline{H}_{4''a}CH_{4''b}$), 3.96 (dd, $J_{4''a,5''}$ = 7.8 Hz, $J_{4''a,4''b}$ = 15.5 Hz, 1H, $CH_{5''}CH_{4''a}C\underline{H}_{4''b}$).

^{13}C n.m.r. (DMSO-d_6) δ 157.94 (C, C-2''), 155.03 (C, C-7a), 147.08 (C, C-5), 144.64 (C, C-1'), 140.64 (C, C-2), 129.20 (2 x CH, CH-2' and CH-6'), 128.83 (CH, CH-4'), 128.04 (C, C-3a), 126.30 (2 x CH, CH-3' and CH-5'), 122.62 (CH, CH-6), 119.59

(CH, CH-4), 113.27 (CH, CH-3), 111.96 (CH, CH-7), 81.24 (CH, CH-1), 62.94 (CH_2).

2-Benzo[*b*]furan-2-yl-5-(4-fluorophenyl)-4,5-dihydro-1,3-oxazole (48)

($C_{17}H_{12}FNO_2$, MW: 281.285)

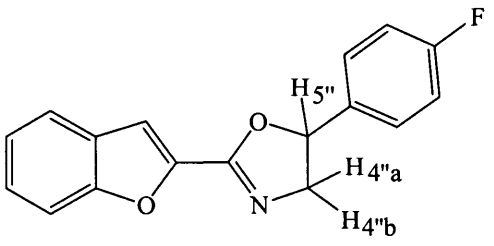

(48)

With 2-benzo[*b*]furan-2-yl-5-(4-fluorophenyl)-4,5-dihydro-1,3-oxazole (**48**), a yellow solid was obtained after recrystallisation from ethanol.

Yield: 2.0 g (66 %), t. l. c. system: petroleum ether – ethyl acetate 3:2 v/v, R_F: 0.74, stain positive. Microanalysis: Calculated C = 72.59 %, H = 4.30 %, N = 4.98 %; Found C = 72.40 %, H = 4.28 %, N = 4.90 %. Melting point: 88 - 90 °C.

^{1}H n.m.r. (DMSO-d_6) δ 7.78 (d, J = 7.8 Hz, 1H, Ar), 7.72 (d, J = 8.3 Hz, 1H, Ar), 7.59 (s, 1H, Ar), 7.52 – 7.45 (m, 3H, Ar), 7.39 – 7.33 (m, 1H, Ar), 7.27 (t, J = 8.9 Hz, 2H), 5.86 (dd, $J_{5'',4''a}$ = 7.8 Hz, $J_{5'',4''b}$ = 9.9 Hz, 1H, $C\underline{H_{5''}}CH_{4''a}CH_{4''b}$), 4.50 (dd, $J_{4''b,5''}$ = 9.9 Hz, $J_{4''b,4''a}$ = 15.3 Hz, 1H, $CH_{5''}CH_{4''a}C\underline{H_{4''b}}$), 3.92 (dd, $J_{4''a,5''}$ = 7.8 Hz, $J_{4''a,4''b}$ = 15.3 Hz, 1H, $CH_{5''}C\underline{H_{4''a}}CH_{4''b}$).

^{13}C n.m.r. (DMSO-d_6) δ 163.98 (C, C-4'), 160.74 (C, C-2''), 155.57 (C, C-4'), 155.29 (C, C-7a), 144.20 (C, C-2), 137.15 (C, C-2''), 137.11 (C, C-1'), 128.59 (2 x CH, CH-3' and CH-5'), 128.48 (2 x CH, CH-2' and CH-6'), 127.37 (C, C-3a), 127.28 (CH, CH-6), 124.21 (CH, CH-5), 122.94 (CH, CH-4), 116.15 (2 x CH, CH-3' and CH-5'), 115.86 (2 x CH-3' and CH-5'), 112.13 (CH, CH-7), 111.26 (CH, CH-2), 80.22 (CH, CH-5''), 62.86 (CH_2).

2-Benzo[*b*]furan-2-yl-5-(4-chlorophenyl)-4,5-dihydro-1,3-oxazole (49)

($C_{17}H_{12}ClNO_2$, MW: 297.740)

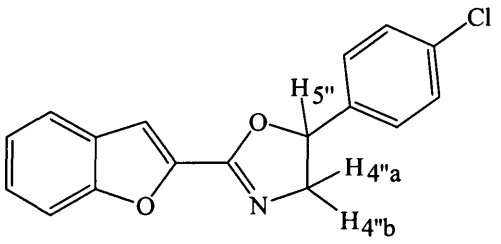

(49)

With 2-benzo[*b*]furan-2-yl-5-(4-chlorophenyl)-4,5-dihydro-1,3-oxazole (**49**), a light yellow solid was obtained by recrystallisation from ethanol.

Yield: 1.85 g (65 %), t. l. c. system: petroleum ether – ethyl acetate 3:2 v/v, R_F: 0.62, stain positive. Microanalysis: Calculated C = 68.58 %, H = 4.06 %, N = 4.70 %; Found C = 68.56 %, H = 3.97 %, N = 4.72 %. Melting point: 103 - 105 °C.

^{1}H n.m.r. (DMSO-d_6) δ 7.70 (d, J = 7.7 Hz, 1H, Ar), 7.74 (d, J = 8.3 Hz, 1H, Ar), 7.62 (s, 1H, Ar), 7.54 – 7.36 (m, 6H, Ar), 5.88 (dd, $J_{5'',4''a}$ = 7.5 Hz, $J_{5'',4''b}$ = 10.0 Hz, 1H, $C\underline{H_{5''}}CH_{4''a}CH_{4''b}$), 4.53 (dd, $J_{4''b,5''}$ = 10.0 Hz, $J_{4''b,4''a}$ = 15.3 Hz, 1H, $CH_{5''}CH_{4''a}C\underline{H_{4''b}}$), 3.92 (dd, $J_{4''a,5''}$ = 7.5 Hz, $J_{4''a,4''b}$ = 15.3 Hz, 1H, $CH_{5''}C\underline{H_{4''a}}CH_{4''b}$).

^{13}C n.m.r. (DMSO-d_6) δ 155.57 (C, C-2''), 155.30 (C, C-7a), 144.11 (C, C-2), 139.96 (C, C-1'), 133.27 (C, C-4'), 129.17 (2 x CH, CH-3' and CH-5'), 128.10 (2 x CH-2' and CH-6'), 127.36 (C, C-3a), 127.32 (CH, CH-6), 124.23 (CH, CH-5), 122.96 (CH, CH-4), 112.14 (CH, CH-7), 111.34 (CH, CH-3), 80.03 (CH, CH-5''), 62.91 (CH_2).

Synthesis of *N*2-(2-phenyl-2-(1*H*-1-imidazoyl)ethyl)-benzo[*b*]furan-2-carboxamide derivatives (compounds 51 – 55)

*N*2-(2-Phenyl-2-(1*H*-1-imidazoyl)ethyl)-benzo[*b*]furan-2-carboxamide (51)

($C_{20}H_{17}N_3O_2$, MW: 331.372)

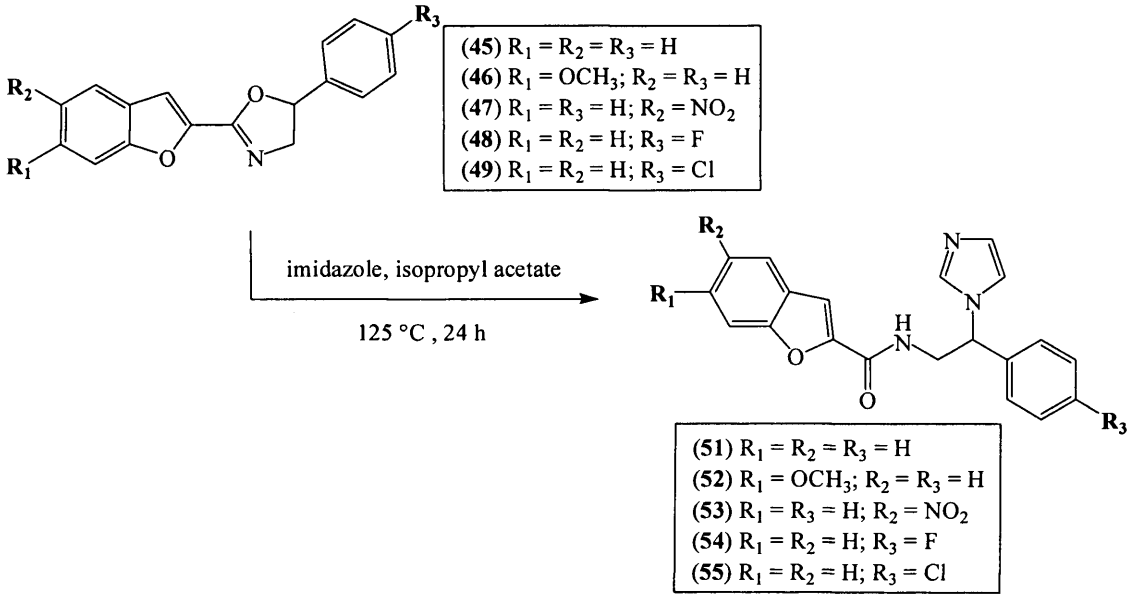

A mixture of 2-benzo[*b*]furan-2-yl-5-phenyl-4,5-dihydro-1,3-oxazole (**45**) (0.33 g, 1.25 mmol) and imidazole (1.71 g, 25.07 mmol) dissolved in isopropyl acetate (3 mL) was heated at 125 °C for 24 hours. After completion of the reaction the mixture was partitioned between water (100 mL) and ethyl acetate (150 mL). The organic layer was washed three times with water (3 x 100 mL), dried over magnesium sulphate and concentrated *in vacuo*. The residue was recrystallised from ethanol to yield the white solid, *N*2-(2-phenyl-2-(1*H*-1-imidazolyl)-ethyl)-benzo[*b*]furan-2-carboxamide (**51**). Yield: 0.114 g (28 %), t. l. c. system: dichloromethane – methanol 9:1 v/v, R_F: 0.74, stain negative. LRMS (ES^+) *m/z*: 332.13 $(M+H)^+$. Microanalysis ($C_{20}H_{17}N_3O_2.0.4H_2O$): Calculated: C = 71.00 %, H = 5.30 %; N = 12.42 %; Found: C = 71.08 %, H = 5.40 %, N = 12.21 %. Melting point: 180 – 182 °C.

^{1}H n.m.r. (DMSO-d_6) δ 9.04 (t, J = 5.4 Hz, 1H, NH), 7.90 (s, 1H, H-2''), 7.79 (d, J = 7.7 Hz, 1H, Ar), 7.66 (d, J = 8.3 Hz, 1H, Ar), 7.56 (s, 1H, H-3), 7.52-7.33 (m, 8H, Ar and imidazole), 6.95 (s, 1H, H-imidazole), 5.75 (dd, J = 5.6, 9.3 Hz, 1H, H-1), 4.23-3.98 (m, 2H, $C\underline{H}_2$).

^{13}C n.m.r. (DMSO-d_6) δ 158.75 (C=O), 154.54 (C, C-7a), 149.00 (C, C-2), 139.52 (CH, CH-2''), 137.14 (C, C-1'), 129.11 (2 x CH, CH-3' and CH-5'), 128.92 (CH,

CH-6), 128.49 (CH, CH-5''), 127.40 (C, C-3a), 127.31 (CH, CH-4'), 127.17 (2 x CH, CH2' and CH-6'), 124.11 (CH, CH-5), 123.16 (CH, CH-4), 118.73 (CH, CH-4''), 112.11 (CH, CH-7), 110.20 (CH, CH-3), 59.83 (CH, CH-1), 43.24 (CH_2).

<u>*N*2-[2-Phenyl-2-(1*H*-1-imidazoyl)ethyl]-6-methoxybenzo[*b*]furan-2-carboxamide</u> (52)

($C_{21}H_{19}N_3O_3$, MW: 361.398)

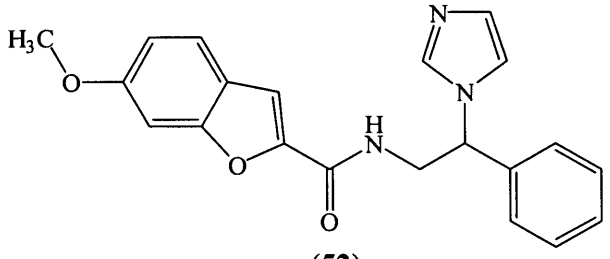

(52)

With *N*2-[2-phenyl-2-(1*H*-1-imidazoyl)ethyl]-6-methoxybenzo[*b*]furan-2-carboxamide (**52**), a brown solid was obtained after recrystallisation from ethanol/water (2:1 v/v).

Yield: 0.41 g (66 %), t. l. c. system: dichloromethane – methanol 9:1 v/v, R_F: 0.63, stain negative. Microanalysis ($C_{21}H_{19}N_3O_3.0.1H_2O$): Calculated: C = 69.45 %, H = 5.33 %; N = 11.60 %; Found: C = 69.43 %, H = 5.41 %, N = 11.54 %. Melting point: 110 – 112 °C.

^{1}H n.m.r. (DMSO-d_6) δ 8.83 (t, J = 5.5 Hz, 1H, NH), 7.87 (s, 1H, H-2''), 7.62 (d, J = 8.6 Hz, 1H, Ar), 7.45 (s, 1H, H-3), 7.38 - 7.29 (m, 6H, Ar and imidazole), 7.16 (d, J = 1.8 Hz, 1H), 6.96 (dd, J = 1.8, 8.7 Hz, 1H, Ar), 6.92 (s, 1H, H-imidazole), 5.70 (dd, J = 5.7, 9.4 Hz, 1H, H-1), 4.17 - 3.94 (m, 2H, C<u>H$_2$</u>), 3.82 (s, 3H, CH_3).

^{13}C n.m.r. (DMSO-d_6) δ 158.75 (C=O), 154.54 (C, C-7a), 149.00 (C, C-2), 139.52 (CH, CH-2''), 137.14 (C, C-1'), 129.11 (2 x CH, CH-3' and CH-5'), 128.92 (CH, CH-6), 128.49 (CH, CH-5''), 127.40 (C, C-3a), 127.31 (CH, CH-4'), 127.17 (2 x CH, CH2' and CH-6'), 124.11 (CH, CH-5), 123.16 (CH, CH-4), 118.73 (CH, CH-4''), 112.11 (CH, CH-7), 110.20 (CH, CH-3), 59.83 (CH, CH-1), 43.24 (CH_2).

***N*2-[2-Phenyl-2-(1*H*-1-imidazoyl)ethyl)-5-nitrobenzo[*b*]furan-2-carboxamide (53)**

($C_{20}H_{16}N_4O_4$, MW: 376.369)

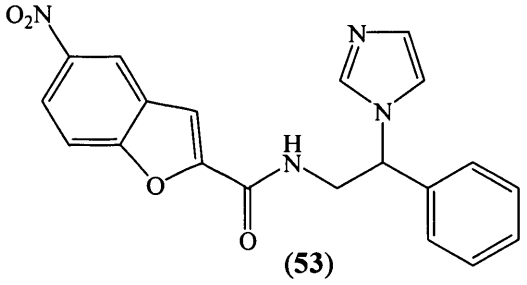

(53)

With *N*2-[2-phenyl-2-(1*H*-1-imidazoyl)ethyl)-5-nitrobenzo[*b*]furan-2-carboxamide (**53**), a brown solid was obtained after recrystallisation from ethanol/water (2:1 v/v). Further purification by flash column chromatography (dichloromethane – methanol 100:0 v/v increasing to 95:5 v/v) gave white solid.

Yield: 80 mg (33 %), t. l. c. system: dichloromethane – methanol 9:1 v/v, R_F: 0.23, stain negative. Microanalysis ($C_{20}H_{16}N_4O_4.0.3H_2O$): Calculated C = 62.92 %, H = 4.38 %, N = 14.68 %; Found C = 62.72 %, H = 4.13 %, N = 14.50 %. Melting point: 204 - 206 °C.

^{1}H n.m.r. (DMSO-d_6) δ 9.23 (t, J = 5.6 Hz, 1H, NH), 8.79 (d, J = 2.4 Hz, 1H, H-4), 8.33 (dd, J = 2.4, 9.1 Hz, 1H, H-6), 7.90 (d, J = 8.6 Hz, 2H, Ar), 7.75 (s, 1H, H-2''), 7.42 – 7.33 (m, 6H, Ar), 6.93 (s, 1H, H-3), 5.71 (dd, J = 5.6, 9.3 Hz, 1H, H-1), 4.22 – 3.98 (m, 2H, CH_2).

^{13}C n.m.r. (DMSO-d_6) δ 158.05 (C=O), 157.24 (C, C-7a), 151.68 (C, C-2), 144.56 (C, C-1'), 139.43 (C, C-5), 137.15 (CH, CH-2''), 129.14 (2 x CH, CH-3' and CH-5'), 128.96 (2 x CH, CH-2' and CH-6'), 128.54 (CH, CH-4'), 128.02 (C, C-3a), 127.12 (CH, CH-4''), 122.62 (CH, CH-6) 119.98 (CH, CH-4), 118.72 (CH, CH-5''), 113.26 (CH, CH-3), 110.96 (CH, CH-7), 59.77 (CH, CH-1), 43.35 (CH_2).

<u>*N*2-[2-(4-Fluorophenyl)-2-(1*H*-1-imidazoyl)ethyl]-benzo[*b*]furan-2-carboxamide</u>
(54)

($C_{20}H_{16}FN_3O_2$, MW: 349.363)

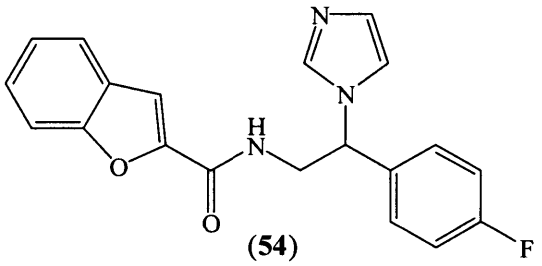

(54)

With *N*2-[2-(4-fluorophenyl)-2-(1*H*-1-imidazoyl)ethyl]-benzo[*b*]furan-2-carboxamide (**54**) a brown solid was obtained after recrystallisation from ethanol/water (2:1 v/v). Yield: 0.64 g (73 %), t. l. c. system: dichloromethane – methanol 9:1 v/v, R_F: 0.38, stain negative. Microanalysis: Calculated: C = 68.76 %, H = 4.62 %; N = 12.02 %; Found: C = 68.56 %, H = 4.62 %, N = 12.11 %. Melting point: 198 – 200 °C.

^{1}H n.m.r. (DMSO-d_6) δ 9.00 (t, J = 5.5 Hz, 1H, NH), 7.88 (s, 1H, H-2''), 7.78 (d, J = 7.7 Hz, 1H, Ar), 7.54 (s, 1H, H-3), 7.65 (d, J = 8.3 Hz, 1H, Ar), 7.48 (m, 3H, Ar), 7.35 (m, 2H, Ar), 7.23 (t, J = 8.8 Hz, 2H, Ar), 6.93 (s, 1H, H-4''), 5.73 (dd, J = 6.2, 8.9 Hz, 1H, H-1), 4.18 – 3.96 (m, 2H, CH_2).

^{13}C n.m.r. (DMSO-d_6) δ 163.77 (C=O), 160.53 (C, C-4'), 158.77 (C, C-4'), 154.55 (C, C-7a), 148.99 (C, C-2), 137.09 (CH, CH-2''), 135.76 (C, C-1'), 135.53 (C, C-1'), 129.52 (CH, CH-2' or CH-6'), 129.41 (CH, CH-2' or CH-6'), 129.03 (CH, CH-5''), 127.40 (C, C-3a), 127.33 (CH, CH-6), 124.13 (CH, CH-5), 123.19 (CH, CH-4''), 118.63 (CH, CH-4), 116.05 (CH, CH-3' or CH-5'), 115.76 (CH, CH-3' or CH-5'), 112.13 (CH, CH-3), 110.25 (CH, CH-7), 59.08 (CH, CH-1), 43.20 (CH_2).

<u>*N*2-[2-(4-Chlorophenyl)-2-(1*H*-1-imidazoyl)ethyl]-benzo[*b*]furan-2-carboxamide</u>
(55)

($C_{20}H_{16}ClN_3O_2$, MW: 365.818)

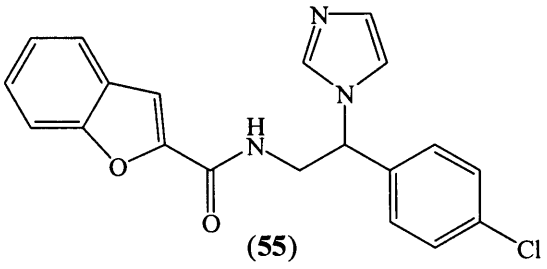

(55)

With *N*2-[2-(4-chlorophenyl)-2-(1*H*-1-imidazoyl)ethyl]-benzo[*b*]furan-2-carboxamide (**55**), a brown residue was obtained after recyrstallisation from ethanol/water (2:1 v/v). Further purification by flash column chromatography (dichloromethane – methanol 100:0 v/v increasing to 96:4 v/v) gave a light yellow solid.

Yield: 0.44 g (72 %), t. l. c. system: petroleum ether – ethyl acetate 3:2 v/v, R_F: 0.16, stain negative. Microanalysis ($C_{20}H_{16}ClN_3O_2.0.2H_2O$): Calculated: C = 65.03 %, H = 4.47 %; N = 11.37 %; Found: C = 64.93 %, H = 4.35 %, N = 11.36 %. Melting point: 76 - 78 °C.

^{1}H n.m.r. (DMSO-d_6) δ 9.00 (t, J = 5.4 Hz, 1H, NH), 7.88 (s, 1H, H-2''), 7.76 (d, J = 7.7 Hz, 1H, Ar), 7.63 (d, J = 8.3 Hz, 1H, Ar), 7.53 (s, 1H), 7.49 – 7.31 (m, 7H, Ar), 6.91 (s, 1H,), 5.73 (dd, J = 6.2, 8.8 Hz, 1H, H-1), 4.16 – 3.95 (m, 2H, CH_2).

^{13}C n.m.r. (DMSO-d_6) 158.82 (C=O), 154.56 (C, C-7a), 148.98 (C, C-2), 138.48 (C, C-1), 137.19 (CH, CH-2''), 133.20 (C, C-4'), 129.20 (2 x CH, CH-2' and CH-6'), 129.08 (2 x CH, CH-3' and CH-5'), 127.41 (C, C-3a), 127.32 (CH, CH-5''), 124.11 (CH, CH-6), 123.17 (2 x CH, CH-5 and CH-4''), 118.71 (CH, CH-4), 112.12 (CH, CH-7), 110.30 (CH, CH-3), 59.13 (CH, CH-1), 43.10 (CH_2).

Synthesis of *N*2-[2-phenyl-2-(1*H*-1,2,4-triazol-1-yl)ethyl]-benzo[*b*]furan-2-carboxamide derivatives (compounds **56**, **58**, **60**, **62** and **64**) and ***N*2-[2-phenyl-2-(4*H*-1,2,4-triazol-4-yl)ethyl]-benzo[*b*]furan-2-carboxamide derivatives** (**57**, **59**, **61**, **63** and **65**)

***N*2-[2-Phenyl-2-(1*H*-1,2,4-triazol-1-yl)ethyl]-benzo[*b*]furan-2-carboxamide** (**56**) and ***N*2-[2-Phenyl-2-(4*H*-1,2,4-triazol-4-yl)ethyl]-benzo[*b*]furan-2-carboxamide** (**57**)

($C_{19}H_{16}N_4O_2$, MW: 332.360)

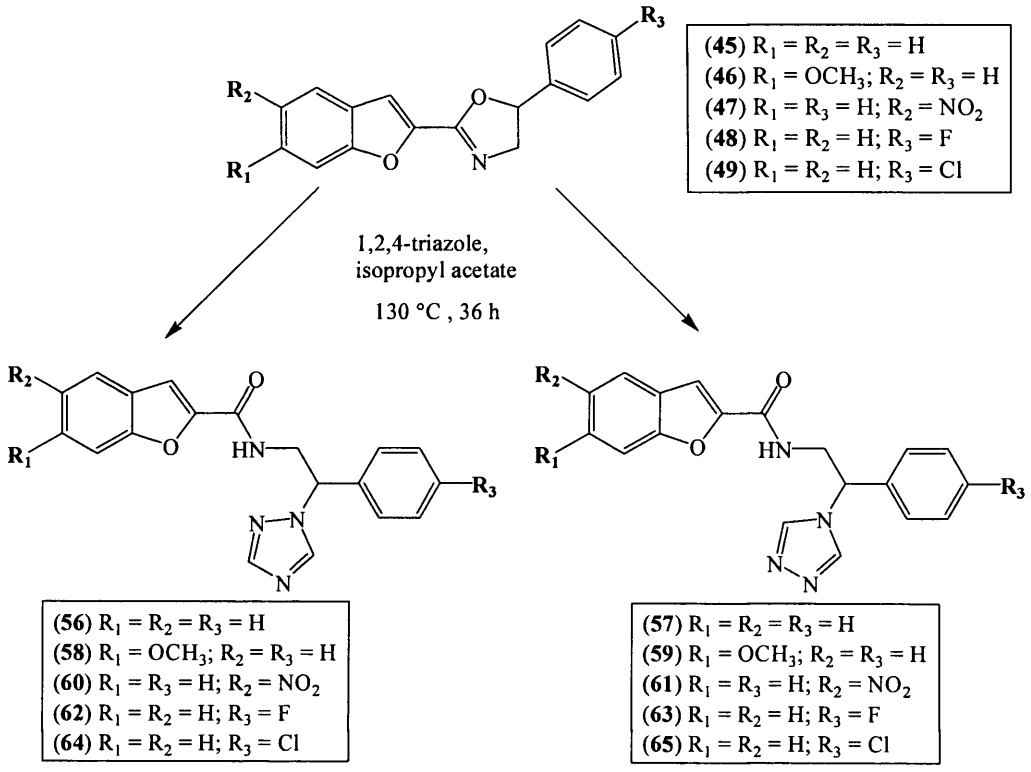

A mixture of 2-benzo[*b*]furan-2-yl-5-phenyl-4,5-dihydro-1,3-oxazole (**45**) (0.40 g, 1.52 mmol) and imidazole (2.10 g, 30.38 mmol) dissolved in isopropyl acetate (5 mL) was heated at 128 °C for 30 hours. After completion, the reaction the mixture was partitioned between water (100 mL) and ethyl acetate (150 mL). The organic layer was washed three times with water (3 x 100 mL), dried over magnesium sulphate and concentrated *in vacuo*. The residue was recrystallised from toluene to yield the light yellow solid which contained a mixture of two compounds as observed by t.l.c. system: petroleum ether – ethyl acetate 2:3 v/v, R_F: 0.18, stain negative and R_F: 0.0, stain negative. A second recrystallisation was carried out with methanol to yield the white solid *N*2-[2-phenyl-2-(4*H*-1,2,4-triazol-4-yl)ethyl]-benzo[*b*]furan-2-carboxamide (**57**). Yield: 0.055 g (9 %), t. l. c. system: dichloromethane – methanol 9:1 v/v, R_F: 0.50, stain negative. Microanalysis ($C_{19}H_{16}N_4O_2$): Calculated: C = 68.66

%, H = 4.85 %; N = 16.85 %; Found: C = 68.53 %, H = 4.93 %, N = 16.65 %. Melting point: 276 – 278 °C.

The filtrate from the second recrystallisation was purified by flash column chromatography (petroleum ether – ethyl acetate 90:10 v/v increasing to 25:75 v/v) to give *N*2-[2-phenyl-2-(1*H*-1,2,4-triazol-1-yl)ethyl]-benzo[*b*]furan-2-carboxamide (**56**) (0.20 g, 32 %) as a white solid. T. l. c. system: petroleum ether – ethyl acetate 2:3 v/v, R_F: 0.18, stain negative. HRMS (ES^+) calculated for $C_{19}H_{16}N_4O_2$ $(M+H)^+$ 333.1346; Found 333.1346. Melting point: 126 – 128 °C.

N.M.R. data for *N*2-[2-phenyl-2-(1*H*-1,2,4-triazol-1-yl)ethyl]-benzo[*b*]furan-2-carboxamide (**56**)

^{1}H n.m.r. (DMSO-d_6) δ 9.00 (t, J = 5.5 Hz, 1H, NH), 8.80 (s, 1H, H-3''), 8.08 (s, 1H, H-5''), 7.78 (d, J = 7.8 Hz, 1H, Ar), 7.65 (d, J = 8.3 Hz, 1H, Ar), 7.55 (s, 1H, H-3), 7.51-7.33 (m, 7H, Ar), 5.99 (dd, J = 5.5, 9.1 Hz, 1H, H-1), 4.26-4.02 (m, 2H, CH_2).

^{13}C n.m.r. (DMSO-d_6) δ 158.84 (C=O), 154.55 (C, C-7a), 152.05 (CH, CH-5''), 148.94 (C, C-2), 144.48 (CH, CH-3''), 138.14 (C, C-1'), 129.04 (2 x CH, CH-3' and CH-5'), 128.69 (CH, CH-6), 127.57 (2 x CH, CH-2' and CH-6'), 127.38 (C, C-3a), 127.30 (CH, CH-4'), 124.10 (CH, CH-5), 123.16 (CH, CH-4), 112.13 (CH, CH-7), 110.17 (CH, CH-3), 62.10 (CH, CH-1), 43.25 (CH_2).

N.M.R. data for *N*2-[2-phenyl-2-(4*H*-1,2,4-triazol-4-yl)ethyl]-benzo[*b*]furan-2-carboxamide (**57**)

^{1}H n.m.r. (DMSO-d_6) δ 9.10 (t, J = 5.6 Hz, 1H, NH), 8.79 (s, 2H, triazole H-2'' and H-5''), 7.78 (d, J = 7.4 Hz, 1H, Ar), 7.65 (dd, J = 0.7, 8.3 Hz, 1H, Ar), 7.54 (d, J = 0.8 Hz, 1H, H-3), 7.51-7.32 (m, 7H, Ar), 5.81 (dd, J = 5.1, 9.7 Hz, 1H, H-1), 4.25 - 3.98 (m, 2H, CH_2).

^{13}C n.m.r. (DMSO-d_6) δ 157.36 (C=O), 153.09 (C, C-7a), 147.41 (C, C-2), 142.88 (2 x CH, CH-2'' and CH-5''), 141.40 (C, C-1'), 137.00 (C, C-3a), 129.33 (2 x CH, CH-3' and CH-5'), 128.58 (CH, CH-6), 127.58 (2 x CH, CH-2' and CH-6'), 127.29 (CH, CH-4'), 124.16 (CH, CH-5), 123.24 (CH, CH-4), 112.15 (CH, CH-7), 110.37 (CH, CH-3), 58.85 (CH, CH-1), 43.15 (CH_2).

The following analogues of compound **56** and **57** were prepared using the same general method detailed above.

<u>*N*2-[2-Phenyl-2-(1*H*-1,2,4-triazol-1-yl)ethyl]-6-methoxybenzo[*b*]furan-2-carboxamide</u> (**58**) and **<u>*N*2-[2-phenyl-2-(4*H*-1,2,4-triazol-4-yl)ethyl]-6-methoxybenzo[*b*]furan-2-carboxamide</u>** (**59**)

($C_{20}H_{18}N_4O_3$, MW: 362.386)

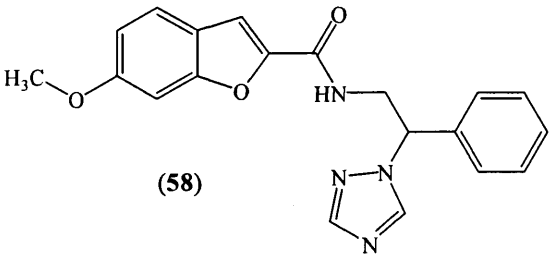

(58)

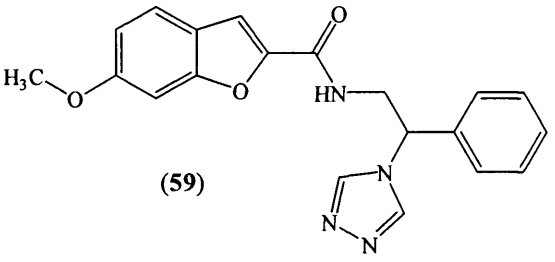

(59)

A mixture of 2-(6-methoxybenzo[*b*]furan-2-yl)-5-phenyl-4,5-dihydro-oxazole (**46**) (1.0 g, 3.41 mmol) and triazole (4.71 g, 68.18 mmol) dissolved in isopropyl acetate (5 mL) was heated at 130 °C for 30 hours. After completion of the reaction the mixture was partitioned between water (100 mL) and ethyl acetate (150 mL). The organic layer was washed three times with water (3 x 100 mL), dried over magnesium sulphate and concentrated *in vacuo*. The residue was recrystallised from toluene and then a second recrystallisation from ethanol to yield the light brown solid, *N*2-[2-phenyl-2-(4*H*-1,2,4-triazol-4-yl)ethyl]-6-methoxybenzo[*b*]furan-2-carboxamide (**59**). Yield: 0.18 g (14 %), t. l. c. system: dichloromethane – methanol 9:1 v/v, R_F: 0.40, stain positive. Microanalysis ($C_{20}H_{18}N_4O_3$): Calculated: C = 66.29 %, H = 5.01 %; N = 15.45 %; Found: C = 66.54 %, H = 5.14 %, N = 15.45 %. Melting point: 218 – 220 °C.

The filtrate from the recrystallisation was purified by flash column chromatography (petroleum ether – ethyl acetate 90:10 v/v increasing to 20:80 v/v) to give *N*2-[2-phenyl-2-(1*H*-1,2,4-triazol-1-yl)ethyl]-6-methoxybenzo[*b*]furan-2-carboxamide (**58**) (0.41 g, 33 %) as a light yellow solid. T. l. c. system: petroleum ether – ethyl acetate 1:3 v/v, R_F: 0.21, stain positive. Microanalysis ($C_{20}H_{18}N_4O_3.0.1H_2O$): Calculated: C = 65.96 %, H = 5.04 %; N = 15.38 %; Found: C = 65.96 %, H = 5.02 %, N = 15.12 %. Melting point: 164 – 166 °C.

N.M.R. data for *N*2-[2-phenyl-2-(1*H*-1,2,4-triazol-1-yl)ethyl]-6-methoxybenzo[*b*]furan-2-carboxamide (**58**)

^{1}H n.m.r. (DMSO-d_6) δ 8.84 (t, J = 5.5 Hz, 1H, NH), 8.81 (s, 1H, H-3''), 8.09 (s, 1H, H-5''), 7.68 (d, J = 8.6 Hz, 1H, Ar), 7.50-7.37 (m, 6H, Ar), 7.22 (d, J = 1.7 Hz, 1H, Ar), 7.00 (dd, J = 1.7, 8.6 Hz, 1H, Ar), 5.99 (dd, J = 5.5, 9.0 Hz, 1H, H-1), 4.25-4.02 (m, 2H, CH_2), 3.88 (s, 3H, CH_3).

^{13}C n.m.r. (DMSO-d_6) δ 161.08 (C=O), 160.08 (C, C-7a), 157.08 (C, C-6), 153.24 (CH, CH-5''), 149.36 (C, C-2), 145.67 (CH, CH-3''), 139.37 (C, C-1'), 130.24 (2 x CH, CH-3' and CH-5'), 129.87 (CH, CH-4'), 128.74 (2 x CH, CH-2' and CH-6'), 124.62 (CH, CH-4), 121.69 (C, C-3a), 114.82 (CH, CH-3), 111.49 (CH, CH-5), 97.40 (CH, CH-7), 63.33 (CH, CH-1), 57.24 (CH_3), 44.40 (CH_2).

N.M.R. data for *N*2-[2-phenyl-2-(4*H*-1,2,4-triazol-4-yl)ethyl]-6-methoxybenzo[*b*]furan-2-carboxamide (**59**)

^{1}H n.m.r. (DMSO-d_6) δ 8.93 (t, J = 5.6 Hz, 1H, NH), 8.79 (s, 2H, triazole H-2'' and H-5''), 7.64 (d, J = 8.7 Hz, 1H, Ar), 7.47 - 7.36 (m, 5H, Ar), 7.18 (d, J = 1.7 Hz, 1H, H-3), 6.97 (dd, J = 2.2, 8.7 Hz, 1H, Ar), 5.80 (dd, J = 5.2, 9.7 Hz, 1H, H-1), 4.23 - 3.97 (m, 2H, CH_2), 3.84 (s, 3H, CH_3).

^{13}C n.m.r. (DMSO-d_6) δ 158.70 (C=O), 157.68 (C, C-7a), 154.68 (C, C-6), 146.90 (C, C-2), 141.64 (2 x CH, CH-2'' and CH-5''), 137.27 (C, C-1'), 129.32 (2 x CH, CH-3' and CH-5'), 128.70 (CH, CH-4'), 127.28 (2 x CH, CH-2' and CH-6'), 123.48 (CH, CH-4), 119.29 (C, C-3a), 112.41 (CH, CH-3), 109.09 (CH, CH-5), 94.99 (CH, CH-7), 57.69 (CH, CH-1), 54.83 (CH_3), 41.90 (CH_2).

<u>*N*2-[2-Phenyl-2-(1*H*-1,2,4-triazol-1-yl)ethyl]-5-nitrobenzo[*b*]furan-2-carboxamide</u> (**60**) and **<u>*N*2-[2-phenyl-2-(4*H*-1,2,4-triazol-4-yl)ethyl]-5-nitrobenzo[*b*]furan-2-carboxamide</u>** (**61**)

($C_{19}H_{15}N_5O_4$, MW: 377.357)

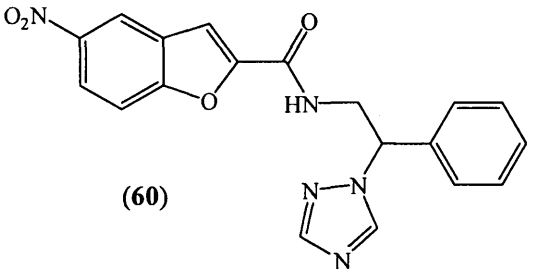

(**60**)

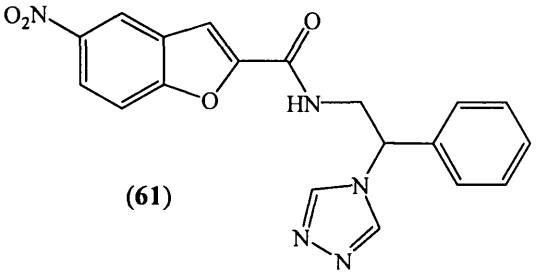

(**61**)

A mixture of 2-(5-nitrobenzo[*b*]furan-2-yl)-5-phenyl-4,5-dihydro-1,3-oxazole (**47**) (0.20 g, 0.65 mmol) and triazole (0.90 g, 12.97 mmol) dissolved in isopropyl acetate (3 mL) was heated at 130 °C for 36 hours. After completion of the reaction the mixture was partitioned between water (100 mL) and ethyl acetate (150 mL). The organic layer was washed three times with water (3 x 100 mL), dried over magnesium sulphate and concentrated *in vacuo*. The residue was recrystallised from toluene and then a second recrystallisation from ethanol to yield white solid, *N*2-[2-phenyl-2-(4*H*-1,2,4-triazol-4-yl)ethyl]-5-nitrobenzo[*b*]furan-2-carboxamide (**61**). Yield: 9 mg (4 %), t. l. c. system: dichloromethane – methanol 9:1 v/v, R_F: 0.23, stain positive. Melting point: 125 – 127 °C. [Booked for HRMS – Nov 2003]

The filtrate from the recrystallisation was purified by flash column chromatography (petroleum ether – ethyl acetate 90:10 v/v increasing to 20:80 v/v) to give crude *N*2-[2-phenyl-2-(1*H*-1,2,4-triazol-1-yl)ethyl]-5-nitrobenzo[*b*]furan-2-carboxamide as a yellow solid. The crude solid was further purified again by flash column chromatography (dichloromethane – methanol 100:0 v/v increasing to 95:5 v/v) to give a pure *N*2-[2-phenyl-2-(1*H*-1,2,4-triazol-1-yl)ethyl]-5-nitrobenzo[*b*]furan-2-carboxamide (**60**) (15 mg, 6 %) as a light yellow solid. T. l. c. system: petroleum ether – ethyl acetate 1:3 v/v, R_F: 0.21, stain positive. Melting point: 60 – 62 °C. HRMS (EI^+) *m/z* Calculated for $C_{19}H_{15}N_5O_4$ (M^+) 377.1119; Found 377.1122.

<u>N.M.R. data for *N*2-[2-phenyl-2-(1*H*-1,2,4-triazol-1-yl)ethyl]-5-nitrobenzo[*b*]furan-2-carboxamide</u> (**60**)

^{1}H n.m.r. (DMSO-d_6) δ 9.23 (t, J = 5.5 Hz, 1H, NH), 8.83 (d, J = 2.4 Hz, 1H, H-4), 8.82 (s, 1H, H-5''), 8.38 (dd, J = 2.5, 9.2 Hz, 1H, H-6), 8.10 (s, 1H, H-3''), 7.95 (d, J

= 9.2 Hz, 1H, H-7), 7.78 (s, 1H, H-3), 7.52 – 7.36 (m, 5H, Ar), 5.99 (dd, J = 5.5, 9.1 Hz, 1H, H-1), 4.29 – 4.05 (m, 2H, CH_2).

^{13}C n.m.r. (DMSO-d_6) δ 158.13 (C=O), 157.25 (C, C-7a), 152.07 (CH, CH-5''), 151.62 (C, C-2), 144.56 (C, C-5), 144.52 (CH, CH-3''), 138.07 (C, C-1'), 129.07 (2 x CH, CH-2' and CH-6'), 128.74 (CH, CH-4'), 128.00 (C, C-3a), 127.57 (2 x CH, CH-3' and CH-5'), 122.62 (CH, CH-6), 119.99 (CH, CH-4), 113.27 (CH, CH-7), 110.93 (CH, CH-3), 62.01 (CH, CH-1), 43.36 (CH_2).

N.M.R. data for *N*2-[2-phenyl-2-(4*H*-1,2,4-triazol-4-yl)ethyl]-5-nitrobenzo[*b*]furan-2-carboxamide (**61**)

^{1}H n.m.r. (DMSO-d_6) δ 9.29 (t, J = 5.5 Hz, 1H, NH), 8.80 (s, 3H, triazole H-2'' and H-5'', and H-4), 8.34 (dd, J = 2.4, 9.1 Hz, 1H, H-6), 7.91 (d, J = 9.1 Hz, 1H, H-7), 7.76 (s, 1H, H-3), 7.48 – 7.37 (m, 5H, Ar), 5.81 (dd, J = 5.1, 9.7 Hz, 1H, H-1), 4.27 – 4.01 (m, 2H, CH_2).

^{13}C n.m.r. (DMSO-d_6) δ 158.15 (C=O), 157.26 (C, C-7a), 151.56 (C, C-2), 144.57 (C, C-5), 142.85 (2 x CH, CH-2'' and CH-5''), 138.36 (C, C-1'), 129.33 (2 x CH-2' and CH-6'), 128.92 (CH, CH-4'), 128.01 (C, C-3a), 127.30 (2 x CH, CH-3' and CH-5'), 122.67 (CH, CH-6), 120.02 (CH, CH-4), 113.27 (CH, CH-7), 111.09 (CH, CH-3), 58.97 (CH, CH-1), 43.27 (CH_2).

_N_2-[2-(4-Fluorophenyl)-2-(1*H*-1,2,4-triazol-1-yl)ethyl]benzo[*b*]furan-2-carboxamide (62) and _N_2-[2-(4-fluorophenyl)-2-(4*H*-1,2,4-triazol-4-yl)ethyl]benzo[*b*]furan-2-carboxamide (63)

($C_{19}H_{15}FN_4O_2$, MW: 350.351)

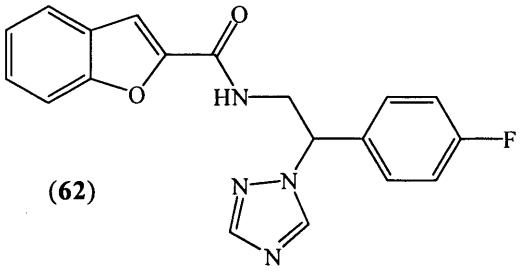

(62)

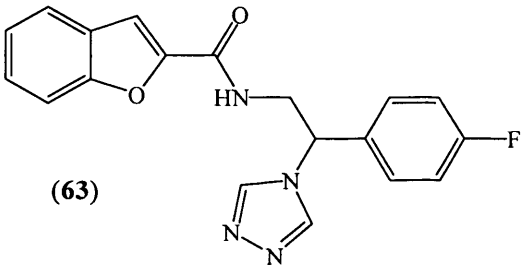

(63)

A mixture of 2-benzo[*b*]furan-2-yl-5-(4-fluorophenyl)-4,5-dihydro-1,3-oxazole (**48**) (1.10 g, 3.91 mmol) and triazole (5.40 g, 78.21 mmol) dissolved in isopropyl acetate (5 mL) was heated at 130 °C for 30 hours. After completion of the reaction the mixture was partitioned between water (100 mL) and ethyl acetate (150 mL). The organic layer was washed two times with water (2 x 100 mL), dried over magnesium sulphate and concentrated *in vacuo*. The residue was recrystallised from ethanol/water

(2:1) to yield a mixture of *N*2-[2-(4-fluorophenyl)-2-(1*H*-1,2,4-triazol-1-yl)ethyl]benzo[*b*]furan-2-carboxamide (**62**) and *N*2-[2-(4-fluorophenyl)-2-(4*H*-1,2,4-triazol-4-yl)ethyl]benzo[*b*]furan-2-carboxamide (**63**). A second recrystallisation from dichloromethane/methanol (1:1) to yield *N*2-[2-(4-fluorophenyl)-2-(4*H*-1,2,4-triazol-4-yl)ethyl]benzo[*b*]furan-2-carboxamide (**63**) as a white solid (0.16 g, 12 %). T. l. c. system: dichloromethane – methanol 9:1 v/v, R_F: 0.29, stain positive. Microanalysis ($C_{19}H_{15}FN_4O_2.0.1H_2O$): Calculated: C = 64.80 %, H = 4.35 %; N = 15.91 %; Found: C = 64.80 %, H = 4.29 %, N = 15.87 %. Melting point: 252 – 254 °C.

The residue from the second recrystallisation was purified by flash column chromatography (petroleum ether – ethyl acetate 90:10 v/v increasing to 30:70 v/v) to give *N*2-[2-(4-fluorophenyl)-2-(1*H*-1,2,4-triazol-1-yl)ethyl]benzo[*b*]furan-2-carboxamide (**62**) (0.31 g, 22 %) as a white solid. T. l. c. system: dichloromethane – methanol 9:1 v/v, R_F: 0.48, stain positive. Microanalysis ($C_{19}H_{15}FN_4O_2.0.5H_2O$): Calculated: C = 63.50 %, H = 4.48 %; N = 15.59 %; Found: C = 63.78 %, H = 4.33 %, N = 15.29 %. Melting point: 174 – 176 °C.

N.M.R. data for *N*2-[2-(4-fluorophenyl)-2-(1*H*-1,2,4-triazol-1-yl)ethyl]benzo[*b*]furan-2-carboxamide (**62**)

^{1}H n.m.r. (DMSO-d_6) δ 8.99 (t, J = 5.6 Hz, 1H, NH), 8.78 (s, 1H, H-3''), 8.07 (s, 1H, H-5''), 7.73 (d, J = 7.7 Hz, 1H, Ar), 7.60 (d, J = 8.3 Hz, 1H, Ar), 7.52 (m, 3H, Ar), 7.42 (m, 1H, Ar), 7.29 (m,1H, Ar), 7.20 (t, J = 8.8 Hz, 2H), 5.99 (dd, J = 5.8, 8.7 Hz, 1H), 4.22 – 3.99 (m, 2H, CH_2).

^{13}C n.m.r. (DMSO-d_6) δ 163.92 (C=O), 160.68 (C, C-4'), 158.89 (C, C-4'), 154.57 (C, C-7a), 152.18 (CH, CH-5''), 148.92 (C, C-2), 144.51 (CH, CH-3''), 134.33 (C, C-1'), 134.29 (C, C-1'), 129.97 (CH, CH-2' or CH-6'), 129.85 (CH, CH-2' or CH-6'), 127.39 (C, C-3a), 127.30 (CH, CH-6), 124.09 (CH, CH-5), 123.16 (CH, CH-4), 115.99 (CH, CH-3' or CH-5'), 115.72 (CH, CH-3' or CH-5'), 112.12 (CH, CH-3), 110.25 (CH, CH-7), 61.32 (CH, CH-1), 43.28 (CH_2).

N.M.R. data for *N*2-[2-(4-fluorophenyl)-2-(4*H*-1,2,4-triazol-4-yl)ethyl]benzo[*b*]furan-2-carboxamide (**63**)

^{1}H n.m.r. (DMSO-d_6) δ 9.11 (t, J = 5.4 Hz, 1H, NH), 8.80 (s, 2H, triazole H-2'' and H-5''), 7.78 (d, J = 7.6 Hz, 1H, Ar), 7.64 (d, J = 8.4 Hz, 1H, Ar), 7.57 - 7.46 (m, 4H, Ar), 7.37 – 7.31 (m, 1H, Ar), 7.27 (t, J = 8.8 Hz, 2H, Ar), 5.83 (dd, J = 5.4, 9.5 Hz, 1H, CH-1), 4.22 – 4.15 (m, 2H, CH_2).

^{13}C n.m.r. (DMSO-d_6) δ 163.97 (C=O), 160.72 (C, C-4'), 158.85 (C, C-4'), 154.56 (C, C-7a), 148.84 (C, C-2), 142.78 (2 x CH, CH-2'' and CH-5''), 134.70 (C, C-1'), 134.66 (C, C-1'), 129.73 (CH, CH-2' or CH-6'), 129.62 (CH, CH-2' or CH-6'), 127.40 (CH, CH-6), 127.38 (C, C-3a), 124.16 (CH, CH-5), 123.22 (CH, CH-4), 116.29 (CH, CH-3' or CH-5'), 116.00 (CH, CH-3' or CH-5'), 112.14 (CH, CH-3), 110.38 (CH, CH-7), 58.08 (CH, CH-1), 43.07 (CH_2).

_N_2-[2-(4-Chlorophenyl)-2-(1_H_-1,2,4-triazol-1-yl)ethyl]benzo[_b_]furan-2-carboxamide and (**64**) **_N_2-[2-(4-chlorophenyl)-2-(4_H_-1,2,4-triazol-4-yl)ethyl]benzo[_b_]furan-2-carboxamide** (**65**)

($C_{19}H_{15}ClN_4O_2$, MW: 366.805)

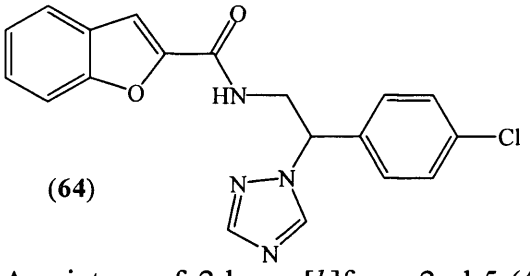

(64)

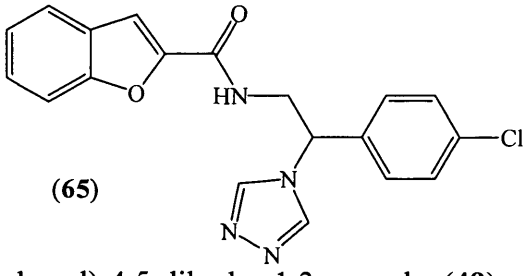

(65)

A mixture of 2-benzo[*b*]furan-2-yl-5-(4-chlorophenyl)-4,5-dihydro-1,3-oxazole (**49**) (1.0 g, 3.37 mmol) and triazole (4.65 g, 67.33 mmol) dissolved in isopropyl acetate (5 mL) was heated at 130 °C for 30 hours. After completion of the reaction the mixture was partitioned between water (100 mL) and ethyl acetate (150 mL). The organic layer was washed two times with water (2 x 100 mL), dried over magnesium sulphate and concentrated *in vacuo*. The residue was recrystallised from ethanol/water (2:1) to yield a mixture of *N*2-[2-(4-chlorophenyl)-2-(1*H*-1,2,4-triazol-1-yl)ethyl]benzo[*b*]furan-2-carboxamide (**64**) and *N*2-[2-(4-chlorophenyl)-2-(4*H*-1,2,4-triazol-4-yl)ethyl]benzo[*b*]furan-2-carboxamide (**65**). The mixture was purified by flash column chromatography (petroleum ether-ethyl acetate 80:20 v/v increasing to 30:70 v/v) to give *N*2-[2-(4-chlorophenyl)-2-(1*H*-1,2,4-triazol-1-yl)ethyl]benzo[*b*]furan-2-carboxamide (**64**) as a white solid (0.35 g, 28 %). T. l. c. system: dichloromethane – methanol 9.5:0.5 v/v, R_F: 0.45, stain negative. Microanalysis ($C_{19}H_{15}ClN_4O_2$): Calculated: C = 62.22 %, H = 4.12 %; N = 15.27 %; Found: C = 62.22 %, H = 4.17 %, N = 15.26 %. Melting point: 200 – 202 °C. The flash column chromatography was continued (dichloromethane – methanol 100:0 v/v increasing to 95:5 v/v) to give *N*2-[2-(4-chlorophenyl)-2-(4*H*-1,2,4-triazol-4-yl)ethyl]benzo[*b*]furan-2-carboxamide (**65**) (0.15 g, 12 %) as white solid. T. l. c.

system: dichloromethane – methanol 9.5:0.5 v/v, R_F: 0.28, stain negative. Microanalysis $C_{19}H_{15}ClN_4O_2.0.3H_2O$): Calculated C = 61.42 %, H = 4.08 %, N = 14.98 %; Found C = 61.31 %, H = 4.22 %, N = 15.05 %. Melting point: 221 – 223 °C.

N.M.R. data for *N*2-[2-(4-chlorophenyl)-2-(1*H*-1,2,4-triazol-1-yl)ethyl]benzo[*b*]furan-2-carboxamide (**64**)

^{1}H n.m.r. (DMSO-d_6) δ 9.00 (t, J = 5.3 Hz, 1H, NH), 8.79 (s, 1H, H-3''), 8.09 (s, 1H, H-5''), 7.78 (d, J = 7.7 Hz, 1H, Ar), 7.65 (d, J = 8.3 Hz, 1H, Ar), 7.54 (s, 1H, H-3), 7.55 – 7.45 (m, 5H, Ar), 7.34 (t, J = 7.5 Hz, 1H, Ar), 5.99 (dd, J = 6.1, 8.3 Hz, 1H), 4.21 – 4.01 (m, 2H, CH_2).

^{13}C n.m.r. (DMSO-d_6) δ 158.85 (C=O), 154.57 (C, C-7a), 152.22 (CH, CH-5''), 148.89 (C, C-2), 144.60 (CH, CH-3''), 137.04 (C, C1'), 133.42 (C, C-4'), 129.62 (2 x CH, CH-2' and CH6'), 129.05 (2 x CH, CH-3' and CH-5'), 127.39 (C, C-3a), 127.34 (CH, CH-6), 124.13 (CH, CH-5), 123.19 (CH, CH-4), 112.15 (CH, CH-7), 110.25 (CH, CH-3), 61.27 (CH, CH-1), 43.14 (CH_2).

N.M.R. data for *N*2-[2-(4-chlorophenyl)-2-(4*H*-1,2,4-triazol-4-yl)ethyl]benzo[*b*]furan-2-carboxamide (**65**)

^{1}H n.m.r. (DMSO-d_6) δ 9.15 (t, J = 5.4 Hz, 1H, NH), 8.84 (s, 2H, triazole H-2'' and H-5''), 7.80 (d, J = 7.7 Hz, 1H, Ar), 7.67 (d, J = 8.3 Hz, 1H, Ar), 7.57 (s, 1H, H-3), 7.56 - 7.47 (m, 5H, Ar), 7.36 (t, J = 7.5 Hz, 1H, Ar), 5.87 (dd, J = 5.6, 9.3 Hz, 1H, CH-1), 4.26 – 4.03 (m, 2H, CH_2).

^{13}C n.m.r. (DMSO-d_6) δ 158.87 (C=O), 154.57 (C, C-7a), 148.84 (C, C-3a), 142.84 (2 x CH, CH-2'' and CH-5''), 137.37 (C, C-1'), 133.59 (C, C-4'), 129.36 (2 x CH, CH-2' and CH-6'), 129.29 (2 x CH, CH-3' and CH-5'), 127.38 (C, C-3a and CH, 6), 124.15 (CH, CH-5), 123.22 (CH, CH-4), 112.14 (CH, CH-7), 110.41 (CH, CH-3), 58.09 (CH, CH-1), 42.98 (CH_2).

CHAPTER 5

Synthesis of 6-substituted-2-(phenylmethylene)-3,4-dihydronaphthalene-1-one (tetralone) derivatives

5.1 Synthesis of 6-substituted-2-(phenylmethylene)-3,4-dihydronaphthalene-1-one (tetralone) derivatives

All the synthesis of 6-substituted-2-(phenylmethylene)-3,4-dihydronaphthalene-1-one (tetralone) derivatives were performed by the general methods outlined in **Scheme 5.1.** (**a**), (**b**) and (**c**). The synthesis was based on the procedure described by our group (Kirby *et al.*, 2003; Maharlouie, 1996).

One of the methods for the preparation of 2-(phenylmethylene)-3,4-dihydronapthalene-1-one derivatives is by direct condensation of tetralone and the appropriate benzaldehyde in 4 % ethanolic KOH. This general method is successfully used in the absence of the hydroxyl group on tetralone or benzaldehyde. The presence of hydroxyl group will form a salt complex with the 4 % ethanolic KOH. To overcome this problem, one of the solutions is to protect the hydroxyl group using a protecting group that will be stable under the alkaline conditions of this condensation reaction.

Scheme 5.1 (a)

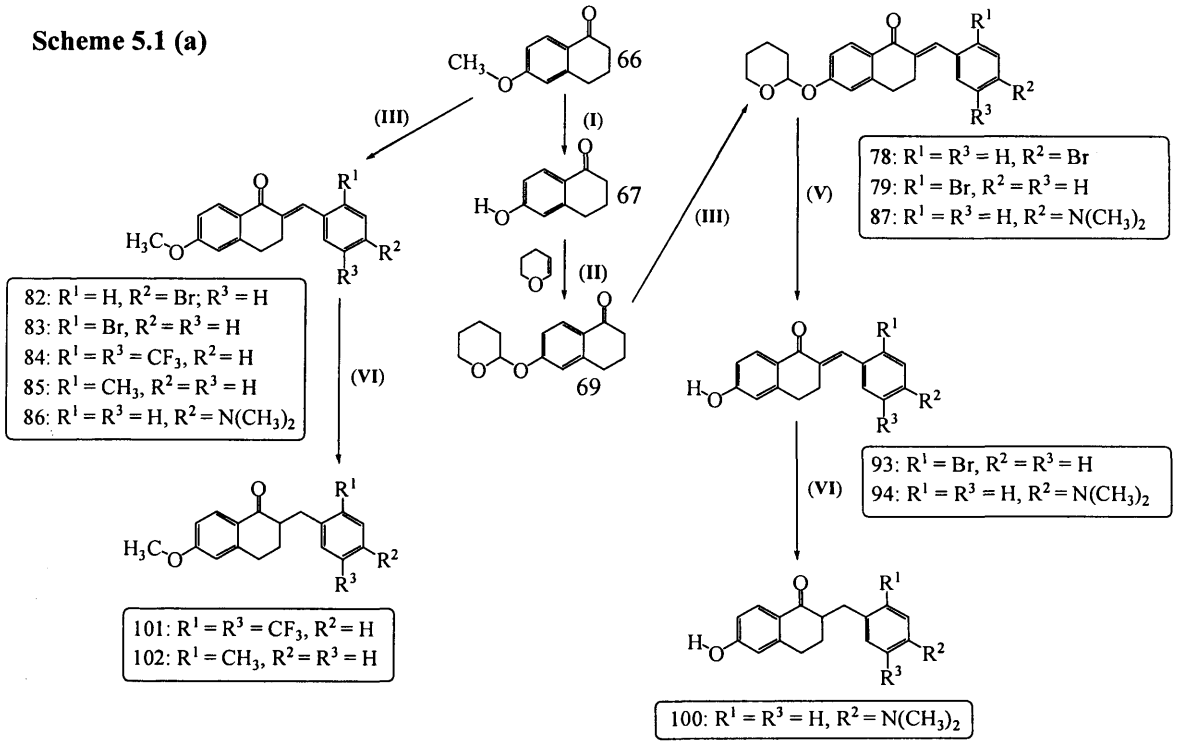

Scheme 5.1 (b)

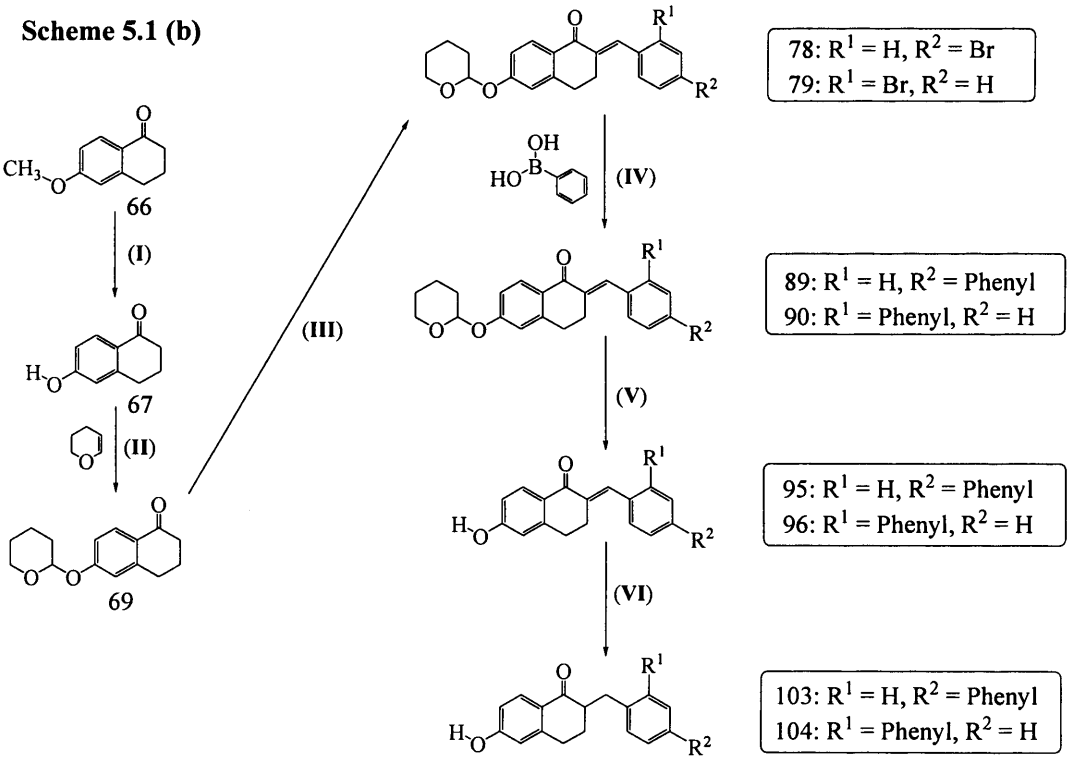

Scheme 5.1 (c)

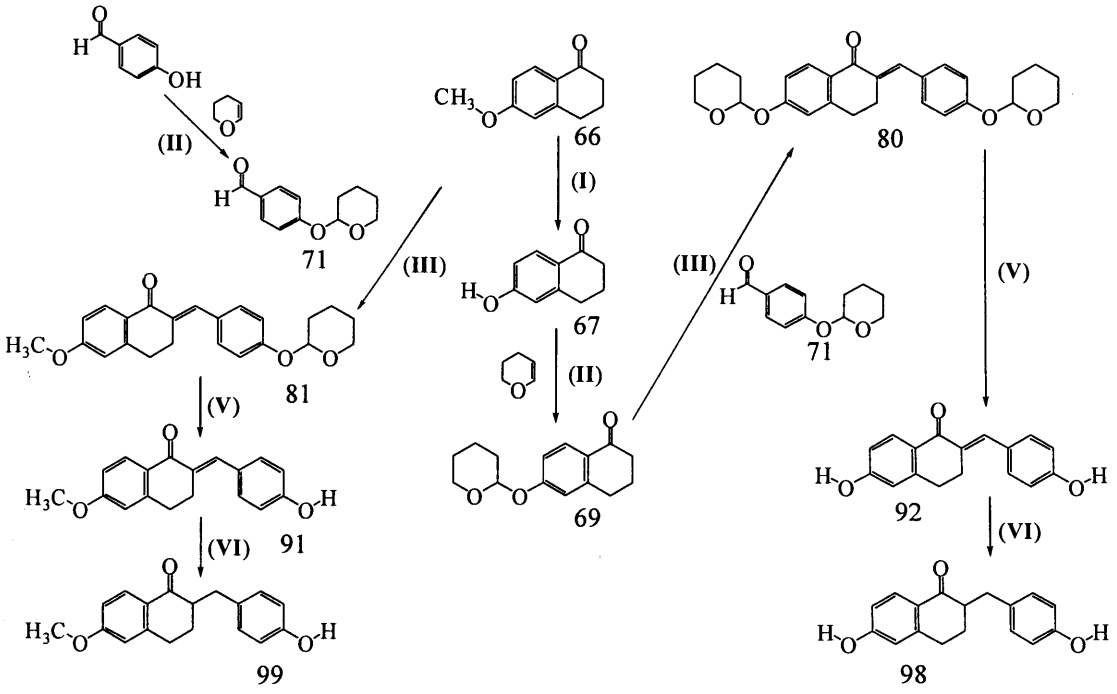

Scheme 5.1 (**a**), (**b**) and (**c**). Synthesis of 6-substituted-2-(phenylmethylene)-3,4-dihydronaphthalene-1-one derivatives. Structures of the compounds and their corresponding numbers synthesised are listed in the scheme. Reagents and conditions: (**I**) 48 % HBr (aq.), reflux, 8 h. (**II**) 3,4-dihydro-2*H*-pyran, PTSA, acetic anhydride, diethyl ether, 2.5 h. (**III**) Corresponding substituted benzaldehyde, 4 % ethanolic KOH, 2 – 72 h. (**IV**) (i) Phenylboronic acid, $Pd(PPh_3)_4$, toluene, 100 °C, 5 h (ii) H_2O_2, room temperature, 1 h. (**V**) 2 M HCl (aq.), ethyl acetate/2-butanone (1/1 v/v), reflux, 1 h. (**VI**) Pd/C 10 %, methanol, 1 h.

In order to synthesise the 6-hydroxy-2-(phenylmethylene)-3,4-dihydronaphthalene-1-one derivatives, the commercially available 6-methoxy tetralone (**66**) was demethylated by refluxing in 48 % aqueous HBr. This reaction did not go to completion even after refluxing at 100 °C for 10 hours. The dark brown residue was then recrystallised from water. The desired product, 6-hydroxy tetralone (**67**) crystallised out in cold water to give a 36 % yield.

3,4-Dihydropyran is a useful reagent for the protection of primary, secondary, and tertiary alcohols to give tetrahydropyranyl ethers (**69**) which are stable to basic media (Bolitt *et al.*, 1988; Smith and March, 2001). *Para*-toluensulphonic acid (PTSA) was used as an acid catalyst with an excess of 3,4-dihydropyran. It was found that the addition of a few drops of acetic anhydride to the mixture increased the yield possibly by preventing the hydrolysis reaction which can occur in the presence of water (Maharlouie, 1996). The yield reported here is 61 % after recrystallisation with ethanol.

Rapson and Shuttleworth reported the condensation of aromatic aldehydes with various cyclic ketone including tetralone in 4 % ethanolic KOH (Rapson and Shuttleworth, 1940). The mechanism is illustrated in **Scheme 5.2**. In this base-catalysed condensation between two carbonyl compounds, the hydroxide ion (from KOH) abstracts a proton from the α-carbon of the tetralone to from the carbanion (Morrison and Boyd, 1987). The carbanion, which is the nucleophilic species, attacks the electrophilic carbonyl carbon atom of the benzaldehyde to gives the unstable alkoxide. The alkoxide abstracts a hydrogen ion from water to form the intermediary aldol. The elimination of water from the aldol will form a carbon-carbon double bond which is conjugated to the aromatic ring, giving stability to the molecule (Maharlouie, 1996). The product will precipitate out so that it can be filtered and recrystallised before the next step. Some of the reactions required longer reaction times (12 – 72 h) until the product precipitated out (yield 25 % - 87 %). Some reactions required the product to be purified by flash column chromatography and hence the yield was lower.

The tetrahydropyranyl ether (**69**) underwent mild acid-catalysed hydrolysis (Smith and March, 2001a) to give the corresponding alcohol compound in good yield (90 % – 99 %). 2-Butanone was used as a co-solvent to facilitate the dispersion of the hydrochloric acid in an ethyl acetate solution (Maharlouie, 1996).

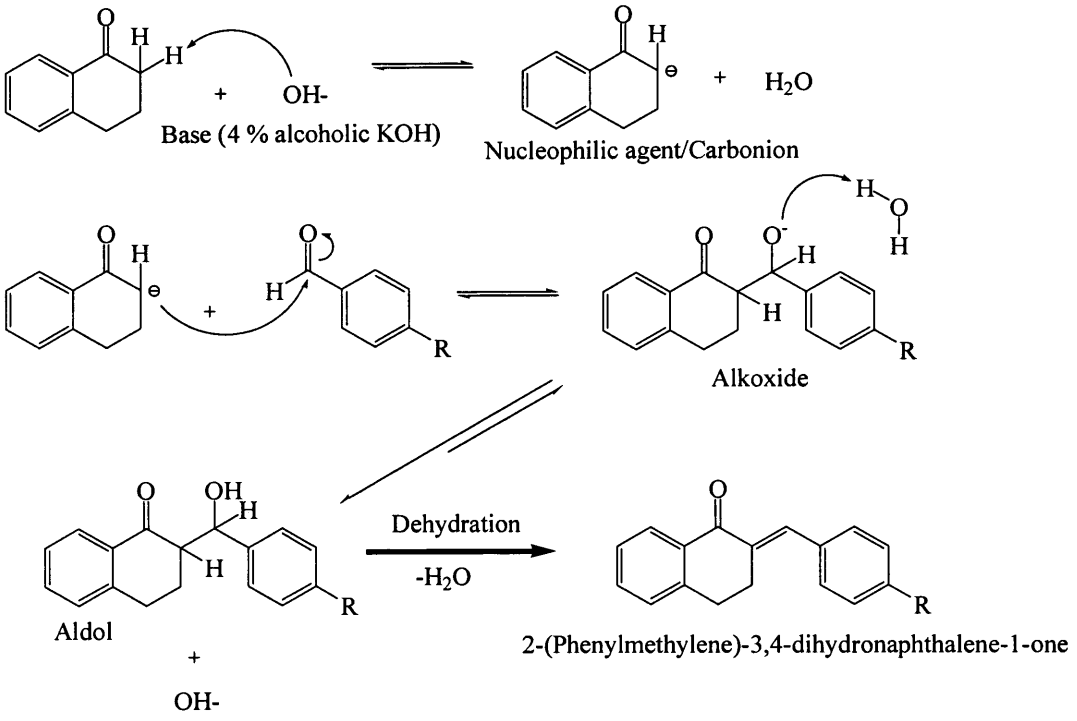

Scheme 5.2. General mechanism for the synthesis of 2-phenylmethylene-3,4-dihydronapthalen-1-one. The scheme is modified from Maharlouie (Maharlouie, 1996).

Hassner and co-workers (Hassner *et al.*, 1958) reported the use of concentrated sulphuric acid in the condensation of benzaldehyde with tetralone to form the 2-phenylmethylene-3,4-dihydronapthalen-1-one. This method (Yoshihama et al., 1999) was employed in the synthesis of 2-[1-(4-hydroxyphenyl)methylidene]-6-methoxy-3,4-dihydronapthalen-1-one (**92**) which only involved a one step synthesis (**Scheme 5.3**). Whereas, the based-catalysed condensation involved three steps: firstly to protect the 4-hydroxy-benzaldehyde with 3,4-dihydropyran, then the based catalysed condensation with 4 % ethanolic KOH and finally deprotection of the pyran protecting group to form **92** (**Scheme 5.1 (c)**).

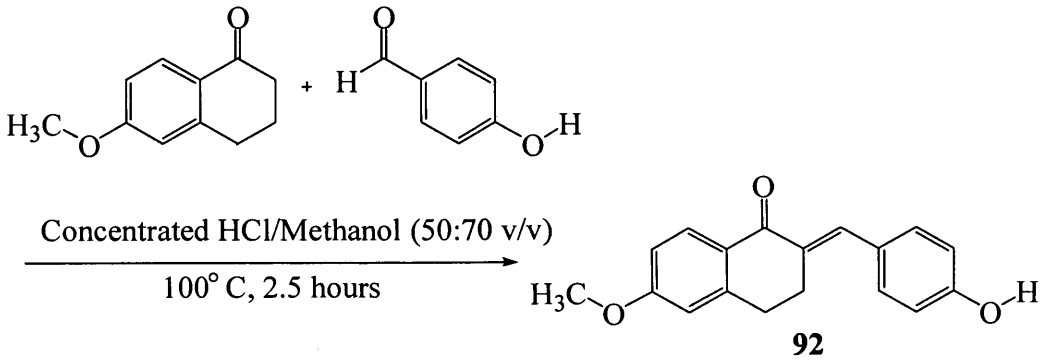

92

Scheme 5.3. The use of concentrated hydrochloric acid in methanol in the synthesis of 2-[1-(4-hydroxyphenyl)methylidene]-6-methoxy-3,4-dihydronapthalen-1-one.

The synthesis of the saturated tetralone involved the catalytic hydrogenation of the C=C bond in the 2-phenylmethylene-3,4-dihydronapthalen-1-one derivatives in methanol using H_2 and 10 % palladium on charcoal as catalyst at room temperature for 1 h. When the reaction was left under H_2 for 2 h at room temperature, the carbonyl (**92**) was reduced to methylene (**97**) in 63 % yield (**Scheme 5.4**). The ^{1}H n.m.r. showed the two H atoms of the CH_2 as a doublet at 2.61 ppm and the ^{13}C n.m.r. showed an extra CH_2 peak at 35.6 ppm. It has been reported by Augustine (Augustine, 1965) that hydrogenolysis of the aryl ketone to the methylene by palladium catalyst at room temperature for 1 – 2 h. Therefore in order to prevent the carbonyl group of the tetralone compound being reduced to methylene, the reaction was stopped after 1 h.

Generally, the yield of the saturated tetralone derivative was quite good (57 – 83 %) after trituration with acetone. There were a few compounds where the yields were as low as 6 %, this was due to the higher polarity of the product that made the purification by flash column chromatography difficult.

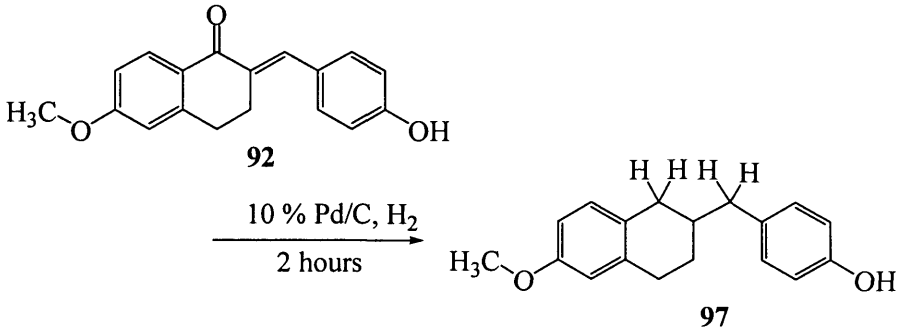

Scheme 5.4. The reduction of the C=C bond and carbonyl to methylene by 10 % palladium on charcoal with H_2 at room temperature for 2 h.

An unexpected result was observed in the ^{1}H n.m.r. spectra for the compounds **79**, **83** and **93** (**Figure 5.5**). There was one singlet peak corresponding to 4 H atoms at around 2.5 ppm in all these three compounds (**Figure 5.7**). These four H atoms corresponded to the hydrogen atoms of carbon 3 and 4 of the tetralone. However, on the DEPT-^{13}C n.m.r., the two CH_2 at carbon 3 and 4 appeared as two separate CH_2 peaks. Normally, these H atoms are expected to appear as two separate multiplet peaks at around 3.0 ppm and 2.5 ppm in the ^{1}H n.m.r. From these n.m.r. data, we could possibly ask two questions, firstly, is it an accidental degeneracy that these four H atoms give similar ppm; secondly, is the 2-bromobenzaldehyde attached to the β-carbon instead of the α-carbon of the tetralone?

To find out the answers, the structure of compound **83** was determined using a 400 MHz NMR (kindly carried out by Dr. M.P. Coogan of the Chemistry Department of Cardiff University) to carry out ^{1}H n.m.r., HSQC (Heteronuclear Single Quantum Coherence) and HMBC (Heteronuclear Multiple Bond Coherence).

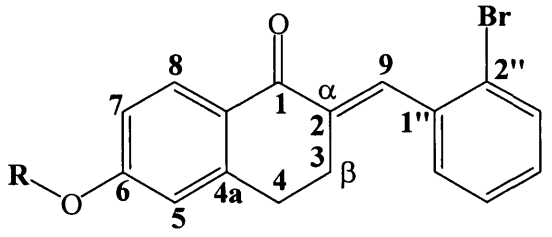

79: R = pyran
83: R = CH_3
93: R = OH

Figure 5.5. Compounds **79**, **83** and **93** produced unexpected results on ^{1}H n.m.r.

The 400 MHz ^{1}H n.m.r. (**Figure 5.7**) showed that the base of the broad singlet at 2.95 ppm widened out and showed distinct shoulders, *i.e.* approximately 10 Hz at each side of the singlet. This broad shoulder showed that the four H atoms at carbon 3 and 4 co-incidentally have similar ppm values.

A HSQC experiment is used to correlate the chemical shift of the protons with the chemical shift of the directly bonded carbon (Reynolds and Enriquez, 2001). This experiment utilises one-bond coupling. Only the directly bonded hydrogen and carbons will give cross peaks, and it will look like a series of concentric ellipses on the spectra. The quaternary carbons are not seen in the spectra. The HSQC spectrum (**Figure 5.8**) showed that the two CH_2 peaks at 27 ppm and 29 ppm (^{13}C n.m.r., Y-axis) corresponded to the broad singlet peak at 2.95 ppm (^{1}H n.m.r., X-axis).

A HMBC experiment is used to determine the multiple-bond couplings over two or three bonds (Reynolds and Enriquez, 2001). The cross peaks shown on the spectrum (**Figure 5.9**) are between protons and carbons that are two or three bonds away. The results from HMBC (**Figure 5.9**) highlighted a few major points:-

- Both CH_2 at 27 and 29 ppm correlated the four H atoms of the broad singlet.
- The CH_2 at 27 ppm correlated to the H atom of the alkene (H-9) (**Figure 5.5**).
- The CH_2 at 29 ppm correlated to the H-5 (6.6 ppm).
- If the 2-bromobenzaldehyde was attached to the β-carbon instead of α-carbon of the tetralone, the two CH_2 should be correlated to H-9. Therefore, it is

conclusive that the product is 2-[1-(2-bromophenyl)methylidene]-6-methoxy-3,4-dihydronaphthale-1-one (**83**).

- The H atom of the alkene (H-9, 7.8 ppm) correlated to the C=O (187 ppm). In this case, the carbonyl is 3 bonds away from H-9. If the 2-bromobenzaldehyde is attached to the β-carbon of the tetralone, the carbonyl will be 4 bonds away from the H-9, and it will not be observed in the HMBC.

A crystal structure of 2-[1-(2-bromophenyl)methylidene]-6-methoxy-3,4-dihydronaphthale-1-one (**83**) was obtained to confirm the structure (**Figure 5.6**). Full crystal data for compound **83** can be seen in **Appendix 1**. Therefore, we could conclude that the four H atoms from the two CH_2 at carbon 3 and 4 appear as one broad singlet peak is due to accidental degeneracy.

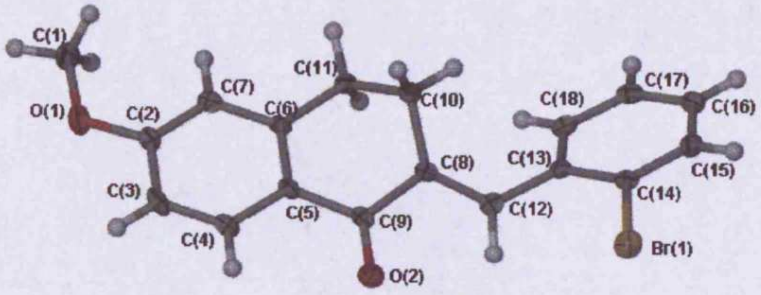

Figure 5.6. The crystal structure of compound **83**.

Figure 5.7. ^{1}H n.m.r. (400 MHz) for compound **83**.

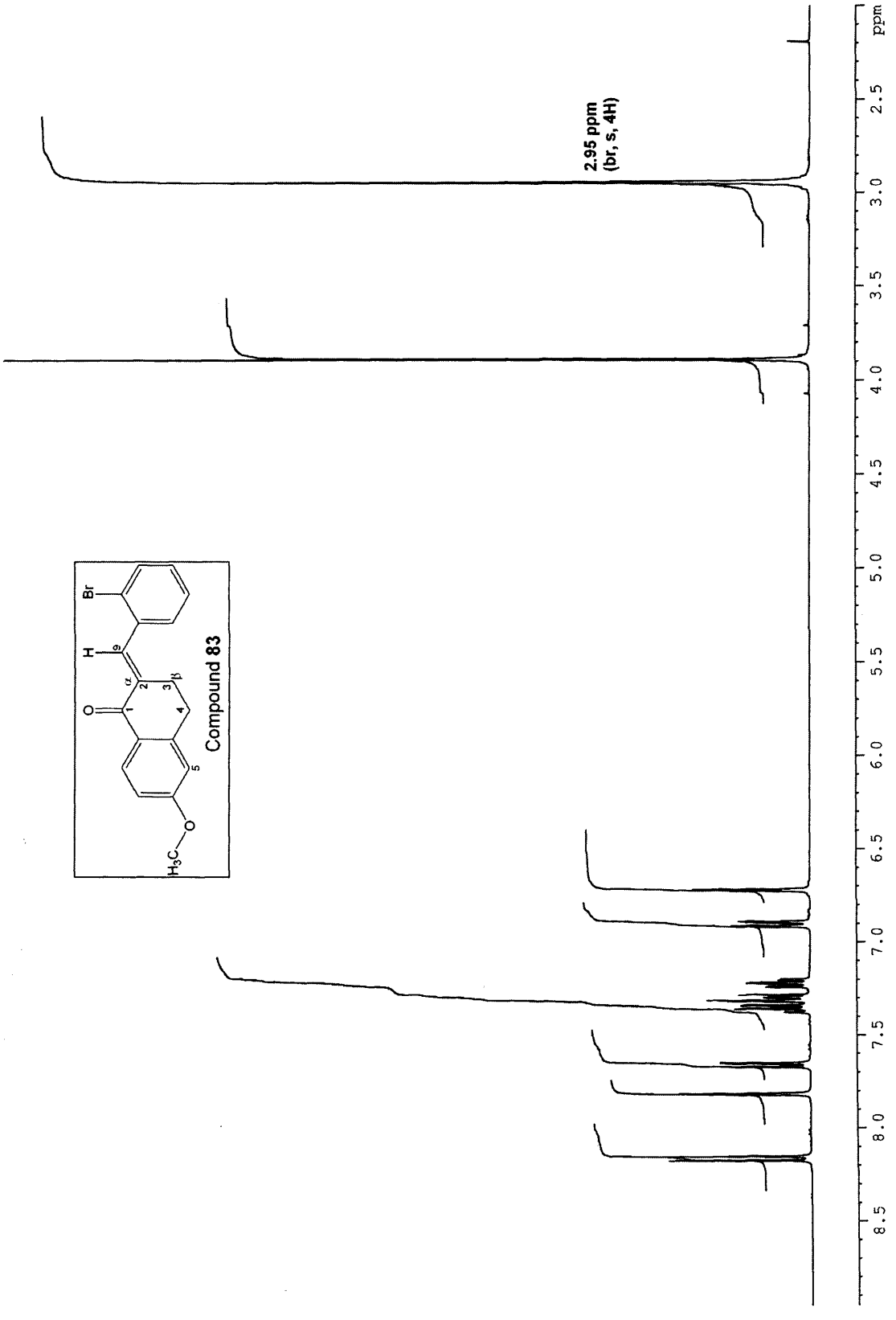

Figure 5.8. HSQC spectrum for compound **83**.

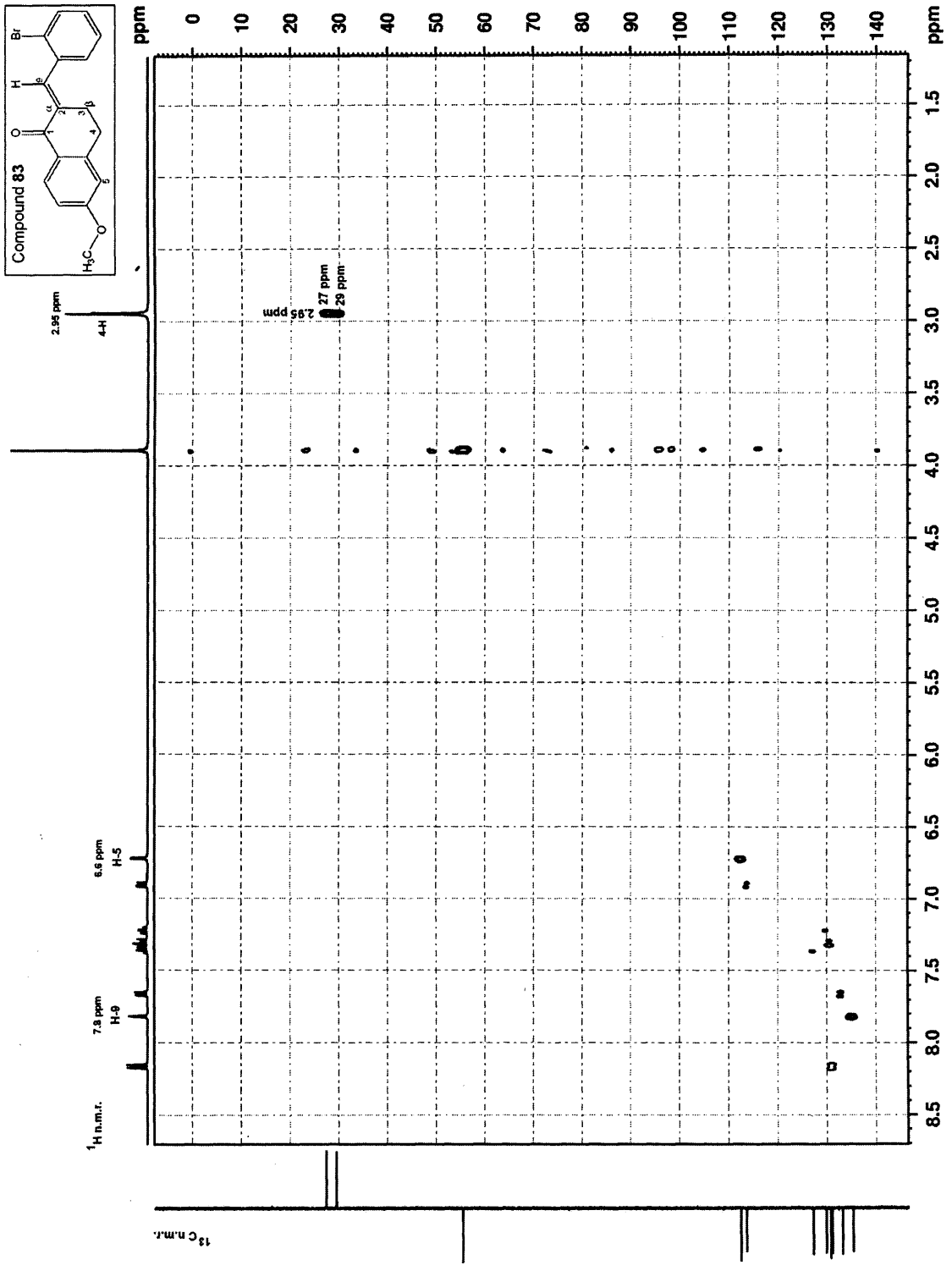

Figure 5.9. HMBC spectrum for compound **83**.

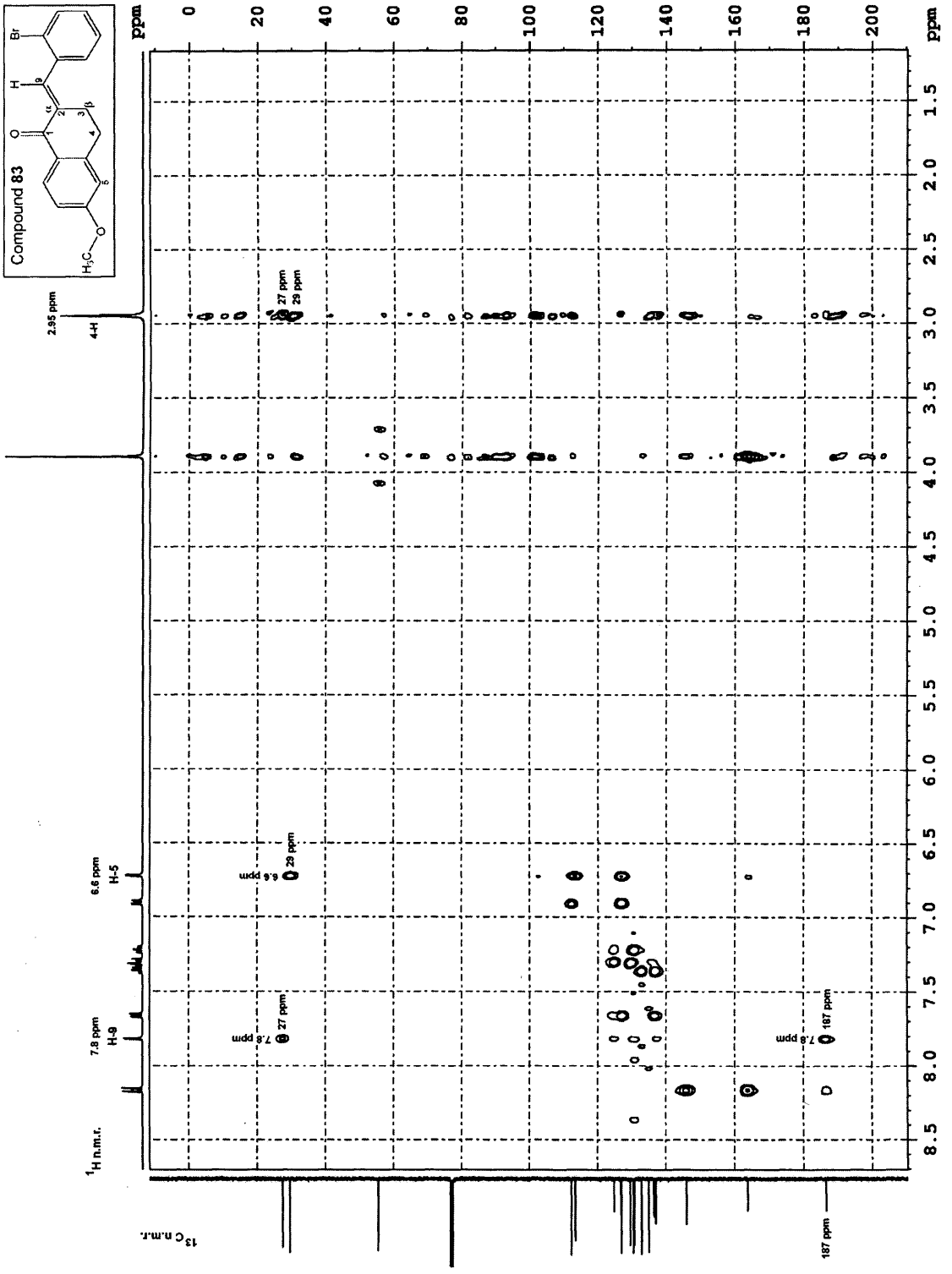

5.2 Experimental results for the synthesis of 6-substituted-2-(phenylmethylene)-3,4-dihydronaphthalene-1-one derivatives

The numbering of compounds for n.m.r. characterisation is as follows:

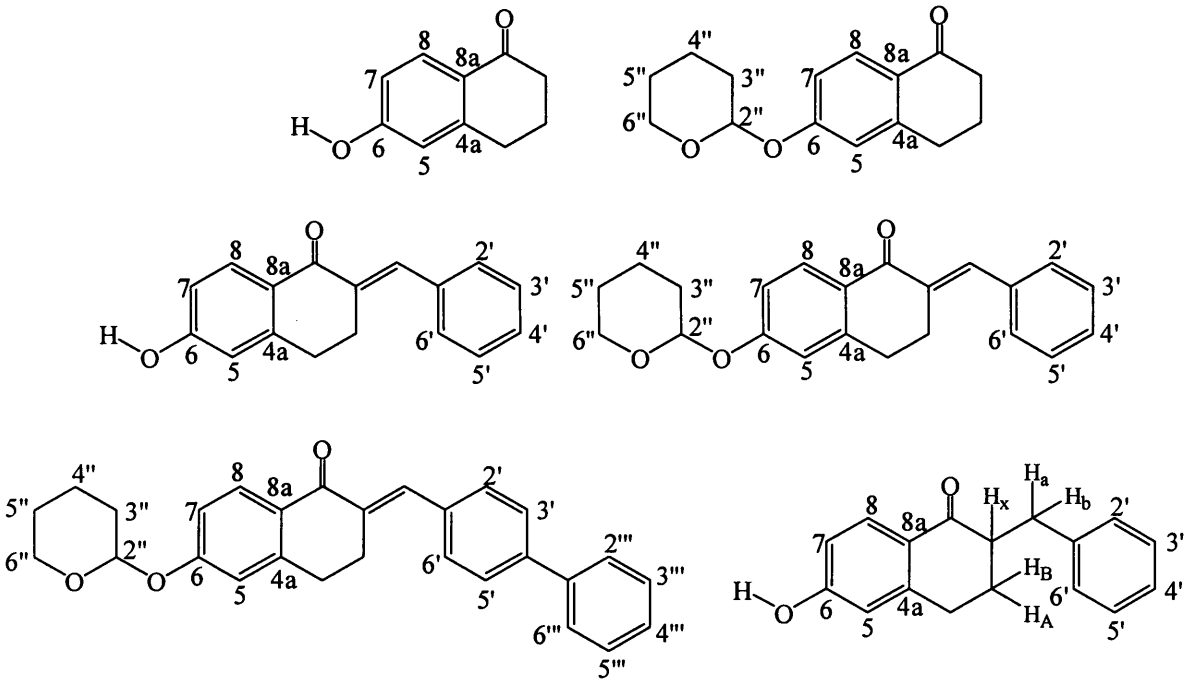

6-Hydroxy-3,4-dihydro-2*H*-naphthalen-1-one (**67**) (Kirby *et al.*, 2003)

($C_{10}H_{10}O_2$, MW: 162.19)

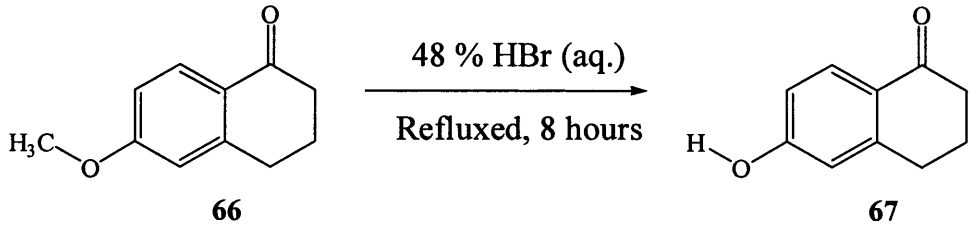

66 **67**

A solution of 6-methoxy-3,4-dihydro-2*H*-naphthalen-1-one (**66**) (20.0 g, 123.31 mmol) in 48 % HBr was heated under reflux for 8 hours. The aqueous layer was then evaporated to about $^1/_3$ its volume. The precipitate formed was then recrystallised from water to give light brown solid, 6-hydroxy-3,4-dihydro-2*H*-naphthalen-1-one (**67**). Yield: 6.56 g (36 %), t.l.c. system petroleum ether – ethyl acetate 3:1 v/v, R_F: 0.32, stain positive. Melting point: 154 – 156 °C [literature: 156 – 157 °C] (Kirby *et al.*, 2003).

^{1}H n.m.r. (DMSO-d_6) δ 10.25 (s, br, 1H, OH), 7.73 (d, J = 8.5 Hz, 1H, H-8), 6.70 (d, J = 8.5 Hz, 1H, H-7), 6.64 (s, 1H, H-5), 2.81 (t, J = 5.9 Hz, 2H, –CH_2-CH_2-$C\underline{H_2}$-C=O), 2.47

(t, J = 6.2 Hz, 2H, –C<u>H</u>$_2$-CH$_2$-CH$_2$-C=O), 1.97 (quintet, J = 6.1 Hz, 2H, –CH$_2$-C<u>H</u>$_2$-CH$_2$-C=O).

^{13}C n.m.r. (DMSO-d_6) δ 198.14 (C=O), 162.29 (C, C-6), 148.21 (C, C-8a), 129.55 (CH, <u>C</u>H-8), 124.72 (C, C-4a), 114.64 (CH, <u>C</u>H-5), 114.61 (CH, <u>C</u>H-7), 38.56 (CH$_2$, –CH$_2$-CH$_2$-<u>C</u>H$_2$-C=O), 29.40 (CH$_2$, –<u>C</u>H$_2$-CH$_2$-CH$_2$-C=O), 23.15 (CH$_2$, –CH$_2$-<u>C</u>H$_2$-CH$_2$-C=O).

<u>6-(Tetrahydro-pyran-2-yloxy)-3,4-dihydro-2*H*-naphthalen-1-one</u> (**69**) (Kirby *et al.*, 2003)

(C$_{15}$H$_{18}$O$_3$, MW: 246.30)

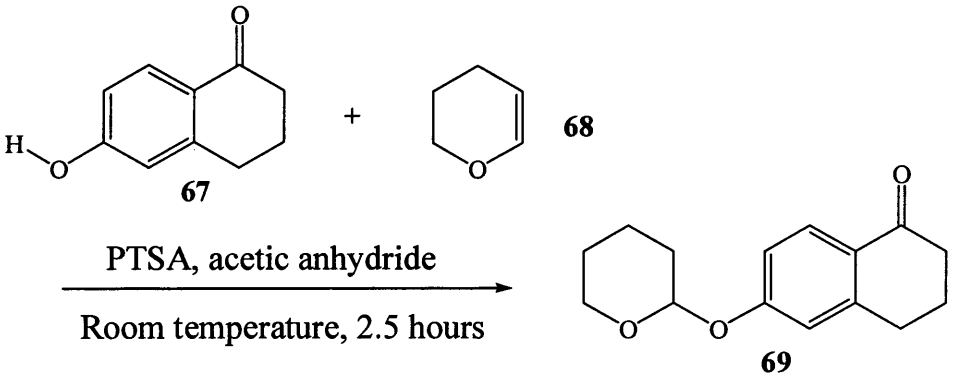

A mixture of 6-hydroxy-3,4-dihydro-2*H*-naphthalen-1-one (**67**) (6.0 g, 36.99 mmol), 3,4-dihydro-2*H*-pyran (**68**) (7.47 g, 88.78 mmol), acetic anhydride (0.5 mL) and *p*-toluensulfonic acid (60 mg) in diethyl ether (150 mL) was stirred at room temperature for 2.5 hours. The resulting brown suspension turned into a clear brown solution on stirring at room temperature. The organic layer was then washed with 2 % KOH (2 × 50 mL) and water (2 × 50 mL), dried with MgSO$_4$, filtered and reduced *in vacuo* to give a brown residue. The residue was recrystallised from ethanol to give, off-white solid, 6-(tetrahydro-pyran-2-yloxy)-3,4-dihydro-2*H*-naphthalen-1-one (**69**). Yield: 5.56 g (61 %), t.l.c. system petroleum ether – ethyl acetate 3:1 v/v, R_F: 0.60, stain positive. Melting point: 88 – 90 °C [literature: 90 – 92 °C] (Kirby et al., 2003).

^{1}H n.m.r. δ 7.98 (d, J = 8.7 Hz, 1H, H-8), 6.94 (dd, J = 2.2, 8.7 Hz, 1H, H-7), 6.88 (s, 1H, H-5), 5.50 (t, J = 2.8 Hz, 1H, C<u>H</u>-2''), 3.83 (m, 1H, <u>H$_a$H$_b$</u>-6''), 3.61 (m, 1H, H$_a$<u>H$_b$</u>-6''), 2.91 (t, J = 6.0 Hz, 2H, –CH$_2$-CH$_2$-C<u>H$_2$</u>-C=O), 2.58 (t, J = 6.2 Hz, 2H, –C<u>H$_2$</u>-CH$_2$-CH$_2$-C=O), 2.09 (quintet, J = 6.3 Hz, 2H, –CH$_2$-C<u>H$_2$</u>-CH$_2$-C=O), 1.98 (m, 1H, <u>H$_a$H$_b$</u>-3''), 1.86 (quintet, J = 3.2 Hz, 2H, C<u>H$_2$</u>-5''), 1.79 – 1.57 (m, 3H, C<u>H$_2$</u>-4'' and H$_a$<u>H$_b$</u>-3'').

^{13}C n.m.r. δ 197.48 (C=O), 161.43 (C, C-6), 147.32 (C, C-8a), 129.93 (CH, C<u>H</u>-8), 127.24 (C, C-4a), 115.47 (CH, C<u>H</u>-5), 115.34 (CH, C<u>H</u>-7), 96.29 (CH, C<u>H</u>-2''), 62.37 (CH_2, C<u>H</u>$_2$-6''), 39.31 (CH_2, –CH_2-CH_2-C<u>H</u>$_2$-C=O), 30.49 (2 x CH_2, –C<u>H</u>$_2$-CH_2-CH_2-C=O and C<u>H</u>$_2$-3''), 25.47 (CH_2, C<u>H</u>$_2$-5''), 23.78 (CH_2, –CH_2-C<u>H</u>$_2$-CH_2-C=O), 18.86 (CH_2, C<u>H</u>$_2$-4'').

<u>4-(Tetrahydro-pyran-2-yloxy)-benzaldehyde</u> (71)

($C_{12}H_{14}O_3$, MW: 206.238)

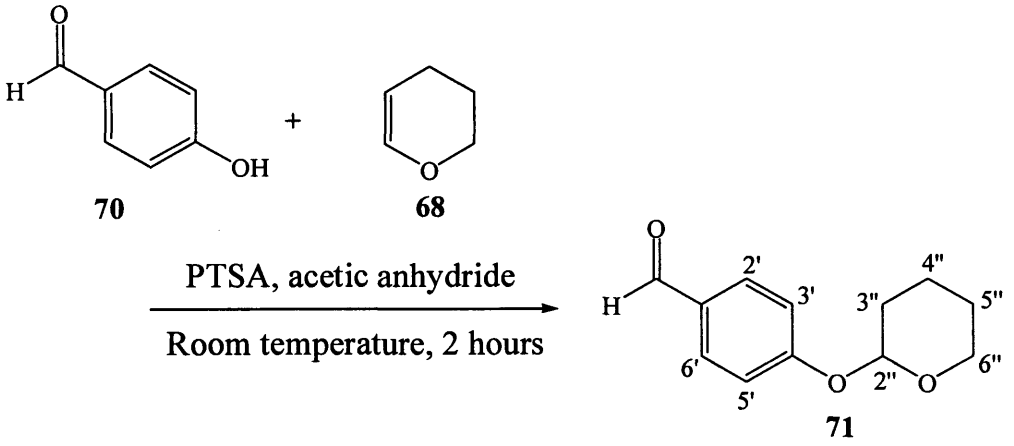

A mixture of 4-hydroxy-benzaldehyde (**70**) (5.0 g, 40.94 mmol), 3,4-dihydro-2*H*-pyran (**68**) (8.27 g, 98.26 mmol), acetic anhydride (1 mL) and *p*-toluensulfonic acid (50 mg) in diethyl ether (150 mL) was stirred at room temperature for 2 hours. The resulting light brown suspension turned into a clear brown solution on stirring at room temperature. The organic layer was then washed with 2 % KOH (2 × 100 mL) and water (2 × 100 mL), dried with $MgSO_4$, filtered and reduced *in vacuo* to give as a yellow residue. Purification by flash column chromatography (petroleum ether – ethyl acetate 100:0 v/v increasing to 87.5:12.5 v/v) gave 4-(tetrahydro-pyran-2-yloxy)-benzaldehyde (**71**) as colourless syrup. Yield: 6.37 g (76 %), t.l.c. system petroleum ether – ethyl acetate 3:1 v/v, R_F: 0.55, stain positive. LRMS (ES^+) *m/z* Calculated for $C_{12}H_{14}O_3$ $[M+Na]^+$ 230.1; Found 229.1.

^1H n.m.r. δ 9.86 (s, 1H, O=C<u>H</u>), 7.79 (dt, J = 1.9 Hz, 8.7 Hz, 2H, H-2' and H-6'), 7.12 (dt, J = 1.8, 8.7 Hz, 2H, H-3' and H-5'), 5.51 (t, J = 2.9 Hz, 1H, C<u>H</u>-2''), 3.81 (m, 1H, C<u>H$_a$</u>H$_b$-6''), 3.59 (m, 1H, CH$_a$<u>H$_b$</u>-6''), 2.00 – 1.89 (m, 1H, C<u>H$_a$</u>H$_b$-4''), 1.85 (m, 2H, CH$_a$<u>H$_b$</u>-4'' and C<u>H$_a$</u>H$_b$-3''), 1.75 – 1.53 (m, 3H, CH$_a$<u>H$_b$</u>-3'' and C<u>H$_2$</u>-5'').

^{13}C n.m.r. δ 191.36 (C=O), 162.57 (C, C-4'), 132.25 (2 x CH, CH-2' and CH-6'), 130.88 (C, C-1), 116.92 (2 x CH, CH-3' and CH-5'), 96.54 (CH, CH-2''), 62.49 (CH_2, CH_2-6''), 30.47 (CH_2, CH_2-3''), 25.44 (CH_2, CH_2-5''), 18.84 (CH_2, CH_2-4'').

Synthesis of 2-benzylidene-3,4-dihydro-2*H*-naphthalen-1-one (unsaturated tetralone) derivatives (compound 78 – 96)

2-(4-Bromo-benzylidene)-6-(tetrahydro-pyran-2-yloxy)-3,4-dihydro-2*H*-naphthalen-1-one (78)

($C_{22}H_{21}O_3Br$, MW: 413.30)

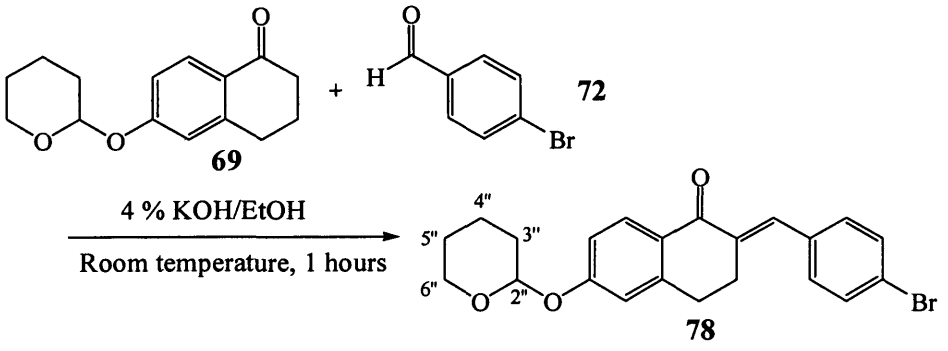

A mixture of the 6-(tetrahydro-pyran-2-yloxy)-3,4-dihydro-2*H*-naphthalen-1-one (**69**) (5.0 g, 21.43 mmol) and 4-bromobenzaldehyde (**72**) (3.97 g, 21.43 mmol) in 4 % ethanolic KOH was stirred at room temperature for 1 h. The resulting precipitate was collected, washed with water and finally recrystalised from ethanol to give 2-(4-bromo-benzylidene)-6-(tetrahydro-pyran-2-yloxy)-3,4-dihydro-2*H*-naphthalen-1-one (**78**) as white solid. Yield: 4.55 g (51 %), t.l.c. system petroleum ether – ethyl acetate 3:1 v/v, R_F: 0.61, stain positive. Microanalysis ($C_{22}H_{21}BrO_3.0.5H_2O$): Calculated C = 62.57 %, H = 5.25 %; Found C = 62.84 %, H = 5.02 %. Melting point: 165 - 167 °C.

^1H n.m.r. δ 8.06 (d, J = 8.7 Hz, 1H, H-8), 7.70 (s, 1H, –CH_2-CH_2-C=C<u>H</u>–Phenyl), 7.49 (d, J = 8.4 Hz, 2H, H-3' and H-5'), 7.25 (d, J = 8.4 Hz, 2H, H-2' and H-6'), 6.97 (dd, J = 2.4, 8.7 Hz, 1H, H-7), 6.84 (d, J = 2.2 Hz, 1H, H-5), 5.50 (t, J = 2.9 Hz, 1H, C<u>H</u>-2''), 3.83 (m, 1H, <u>H_a</u>H_b-6''), 3.60 (m, 1H, H_a<u>H_b</u>-6''), 3.02 (m, 2H, –C<u>H_2</u>-CH_2-C=CH–Phenyl), 2.88 (m, 2H, –CH_2-C<u>H_2</u>-C=CH–Phenyl), 1.96 (m, 1H, <u>H_a</u>H_b- 3''), 1.84 (quintet, J = 3.5 Hz, 2H, C<u>H_2</u>-5''), 1.71 – 1.55 (m, 3H, C<u>H_2</u>-4'' and H_a<u>H_b</u>- 3'').

^{13}C n.m.r. δ 186.98 (C=O), 161.62 (C, C-6), 145.95 (C, C-4a), 136.72 (C, C-2), 135.34 (C, C-1'), 135.01 (CH, –CH_2-CH_2-C=<u>C</u>H–Phenyl), 132.05 (2 x CH, <u>C</u>H-3' and <u>C</u>H-5'), 131.75 (2 x CH, <u>C</u>H-2' and <u>C</u>H-6'), 131.05 (CH, CH-8), 127.85 (C, C-8a), 122.93 (C,

C-4'), 116.01 (CH, CH-5), 114.93 (CH, CH-7), 96.38 (CH, CH-2''), 62.48 (CH_2, CH_2-6''), 30.53 (CH_2, CH_2-3''), 29.58 (CH_2, $-CH_2$-CH_2-CH_2-C=O), 27.66 (CH_2, CH_2-5''), 25.50 (CH_2, $-CH_2$-CH_2-CH_2-C=O), 18.89 (CH_2, CH_2-4'').

The following derivatives of 2-benzylidene-3,4-dihydro-2*H*-naphthalen-1-one (unsaturated tetralone) (**79** – **87**) were prepared using the same general method detailed above.

2-[1-(2-bromophenyl)methylidene]-6-(tetrahydro-pyran-2-yloxy)-3,4-dihydro-2*H*-naphthalen-1-one (**79**)

($C_{22}H_{21}BrO_3$, MW: 413.304)

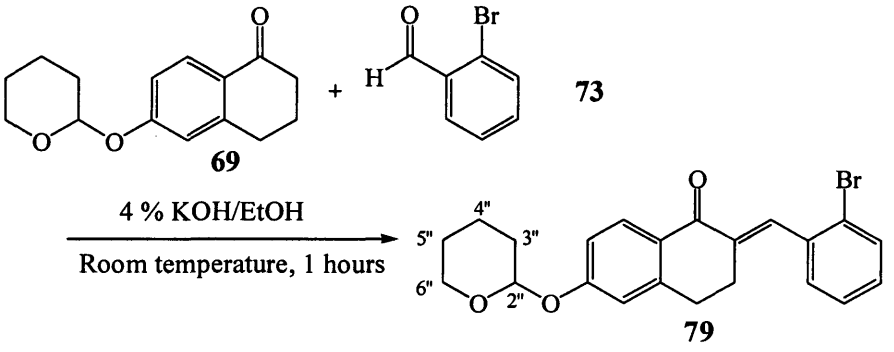

With 2-[1-(2-bromophenyl)methylidene]-6-(tetrahydro-pyran-2-yloxy)-3,4-dihydro-2*H*-naphthalene-1-one (**79**), a white solid was obtained. Yield: 7.60 g (87 %), t.l.c. system petroleum ether – ethyl acetate 3:1 v/v, R_F: 0.66, stain positive. Microanalysis ($C_{22}H_{21}BrO_3.0.5H_2O$): Calculated C = 62.57 %, H = 5.25 %; Found C = 62.32 %, H = 4.98 %. Melting point 76 – 78 °C.

^{1}H n.m.r. δ 8.19 (d, J = 8.1 Hz, 1H, H-8), 7.85 (s, 1H, $-CH_2$-CH_2-C=CH–Phenyl), 7.70 (d, J = 8.0 Hz, 1H, CH-3'), 7.28 (m, 2H, phenyl), 7.27 (m, 2H, phenyl), 7.07 (dd, 1H, J = 2.4, 8.7 Hz, H-7), 6.94 (d, J = 2.3 Hz, H-5), 5.59 (t, J = 2.8 Hz, CH-2''), 3.92 (m, 1H, CH_aH_b-6''), 3.69 (m, 1H, CH_aH_b-6''), 2.98 (s, br, 4H, $-CH_2$-CH_2-C=CH–Phenyl and $-CH_2$-CH_2-C=CH–Phenyl), 2.12 – 1.98 (m, 1H, CH_aH_b-3''), 1.85 (m, 2H, CH_2-5''), 1.75 – 1.53 (m, 3H, CH_aH_b-3'' and CH_2-4'').

^{13}C n.m.r. δ 186.98 (C=O), 161.65 (C, C-6), 146.27 (C, C-4a), 137.54 (C, $-CH_2$-CH_2-C=CH–Phenyl), 136.96 (C, C-1'), 135.39 (CH, $-CH_2$-CH_2-C=CH–Phenyl), 133.33 (CH, CH-3'), 131.05 (CH, CH-4'), 130.88 (CH, CH-6'), 129.99 (CH, CH-8), 127.84 (C, C-8a), 127.40 (CH, CH-5'), 125.31 (C, C-2'), 116.01 (CH, CH-7), 115.00 (CH, CH-5), 96.36 (CH, CH-2''), 62.47 (CH_2, CH_2-6''), 30.53 (CH_2, CH_2-3''), 29.84 (CH_2, $-CH_2$-CH_2-C=CH–Phenyl), 27.78 (CH_2, $-CH_2$-CH_2-C=CH–Phenyl), 25.50 (CH_2, CH_2-5'') and 18.88 (CH_2, CH_2-4'').

6-(Tetrahydro-pyran-2-yloxy-2-{1-[4-(tetrahydro-pyran-2-yloxy)phenyl]methylidene}-3,4-dihydro-2*H*-naphthalen-1-one (80)

($C_{27}H_{30}O_5$, MW: 434.524)

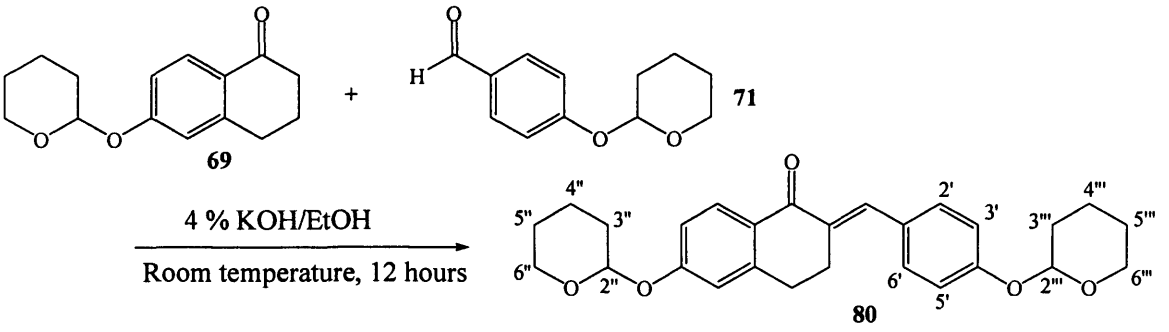

Reaction was stirred at room temperature for 12 h. With 6-(tetrahydro-pyran-2-yloxy)-2-{1-[4-(tetrahydro-pyran-2-yloxy)phenyl]methylidene}-3,4-dihydro-2*H*-naphthalen-1-one (**80**), a colourless syrup was obtained after purification by column chromatography with petroleum ether – ethyl acetate 100:0 v/v increasing to 87:13 v/v. Yield: 1.00 g (41 %), t.l.c. system petroleum ether – ethyl acetate 4:1 v/v, R_F: 0.51, stain positive. HRMS (ES^+) *m/z* Calculated for $C_{27}H_{30}O_5$ $[M+H]^+$ 435.2166; Found 435.2165.

^{1}H n.m.r. δ 8.06 (d, J = 8.7 Hz, 1H, H-8), 7.77 (s, 1H, –CH_2-CH_2-C=C<u>H</u>–Phenyl), 7.36 (d, J = 8.7 Hz, 2H, H-3' and H-5'), 7.05 (d, J = 8.7 Hz, 2H, H-2' and H-6'), 6.96 (dd, J = 2.3, 8.7 Hz, 1H, H-7), 6.84 (d, J = 2.3 Hz, 1H, H-5), 5.49 (t, J = 2.9 Hz, 1H, C<u>H</u>-2''), 5.44 (t, J = 3.1 Hz, 1H, C<u>H</u>-2'''), 3.85 (m, 2H, <u>H_a</u>H_b-6'' and <u>H_a</u>H_b-6'''), 3.59 (m, 2H, H_a<u>H_b</u>-6'' and H_a<u>H_b</u>-6'''), 3.08 (m, 2H, –C<u>H_2</u>-CH_2-C=CH–Phenyl), 2.86 (m, 2H, –CH_2-C<u>H_2</u>-C=CH–Phenyl), 1.95 (m, 2H, <u>H_a</u>H_b-3'' and <u>H_a</u>H_b-3'''), 1.84 (m, 4H, C<u>H_2</u>-5'' and C<u>H_2</u>-5'''), 1.73 – 1.55 (m, 6H, C<u>H_2</u>-4'', H_a<u>H_b</u>-3'', C<u>H_2</u>-4''' and H_a<u>H_b</u>-3''').

^{13}C n.m.r. δ 187.30 (C=O), 161.38 (C, C-6), 157.70 (C, C-4'), 145.89 (C, C-4a), 136.42 (CH, –CH_2-CH_2-C=C<u>H</u>–Phenyl), 134.40 (C, C-2), 131.92 (2 x CH, CH-2' and CH-6'), 130.91 (CH, CH-8), 129.78 (C, C-8a), 128.17 (C, C-1'), 116.71 (2 x CH, CH-3' and CH-5'), 115.83 (CH, CH-7), 114.86 (CH, CH-5), 96.66 (CH, CH-2''), 96.37 (CH, CH-2'''), 62.50 (CH_2, CH_2-6''), 62.47 (CH_2, CH_2-6'''), 30.69 (CH_2, CH_2-3''), 30.60 (CH_2, CH_2-3'''), 29.63 (CH_2, –<u>C</u>H_2-CH_2-C=CH–Phenyl), 27.69 (CH_2, –CH_2-<u>C</u>H_2-C=CH–Phenyl), 25.59 (CH_2, CH_2-5''), 25.52 (CH_2, CH_2-5'''), 19.12 (CH_2, CH_2-4''), 18.92 (CH_2, CH_2-4''').

6-Methoxy-2-{1-[4-(tetrahydro-pyran-2-yloxy)phenyl]methylidene}-3,4-dihydro-2*H*-naphthalen-1-one (81)

($C_{23}H_{24}O_4$, MW: 364.434)

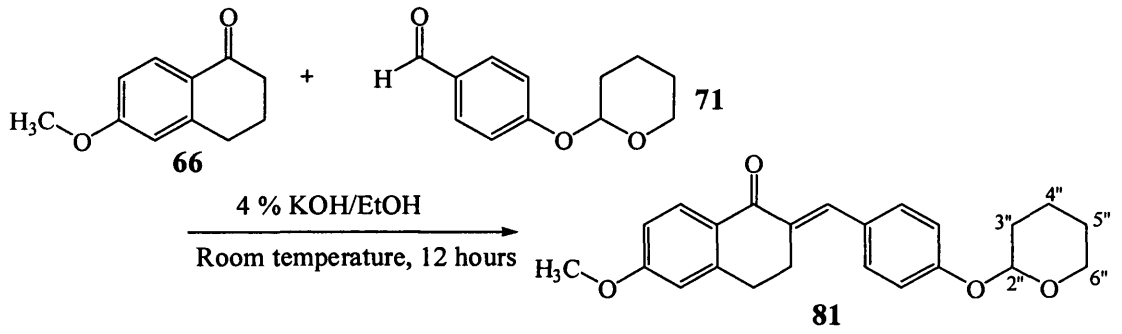

Reaction was stirred at room temperature for 12 h. With 6-methoxy-2-{1-[4-(tetrahydro-pyran-2-yloxy)phenyl]methylidene}-3,4-dihydro-*2H*-naphthalen-1-one (**81**), a light brown solid was obtained. Yield: 3.00 g (42 %), t.l.c. system petroleum ether – ethyl acetate 3:1 v/v, R_F: 0.47, stain positive. Microanalysis ($C_{23}H_{24}O_4$.): Calculated C = 75.80 %, H = 6.64 %; Found C = 75.63 %, H = 6.67 %. Melting point 100 – 102 °C.

^{1}H n.m.r. δ 8.15 (d, J = 8.7 Hz, 1H, H-8), 7.85 (s, 1H, –CH_2-CH_2-C=C<u>H</u>–Phenyl), 7.44 (d, J = 8.7 Hz, 2H, H-3' and H-5'), 7.14 (d, J = 8.7 Hz, 2H, H-2' and H-6'), 6.92 (dd, J = 2.5, 8.7 Hz, 1H, H-7), 6.75 (d, J = 2.4 Hz, 1H, H-5), 5.52 (t, J = 3.0 Hz, 1H, C<u>H</u>-2''), 3.97 (m, 1H, <u>H_a</u>H_b-6''), 3.91 (s, 3H, –O-CH_3), 3.77 (m, 1H, H_a<u>H_b</u>-6''), 3.16 (m, 2H, –C<u>H_2</u>-CH_2-C=CH–Phenyl), 2.95 (m, 2H, –CH_2-C<u>H_2</u>-C=CH–Phenyl), 2.05 (m, 1H, <u>H_a</u>H_b-3''), 1.93 (m, 2H, C<u>H_2</u>-5''), 1.81 – 1.63 (m, 3H, H_a<u>H_b</u>-3'' and C<u>H_2</u>-4'').

^{13}C n.m.r. δ 187.22 (C=O), 163.88 (C, C-6), 157.71 (C, C-4'), 146.02 (C, C-4a), 136.42 (CH, –CH_2-CH_2-C=C<u>H</u>–Phenyl), 134.34 (C, C-2), 131.92 (2 x CH, CH-2' and CH-6'), 131.10 (CH, CH-8), 129.76 (C, C-8a), 127.62 (C, C-1'), 116.72 (2 x CH, CH-3' and CH-5'), 113.67 (CH, CH-7), 112.65 (CH, CH-5), 96.65 (CH, CH-2''), 62.51 (CH_2, CH_2-6''), 55.87 (CH_3, –O-CH_3), 30.69 (CH_2, CH_2-3''), 29.67 (CH_2, –<u>C</u>H_2-CH_2-C=CH–Phenyl), 27.68 (CH_2, –CH_2-<u>C</u>H_2-C=CH–Phenyl), 25.59 (CH_2, CH_2-5''), 19.12 (CH_2, CH_2-4'').

2-[1-(4-Bromophenyl)methylidene]-6-methoxy-3,4-dihydro-2*H*-naphthalen-1-one (82)

($C_{18}H_{15}BrO_2$, MW: 343.214)

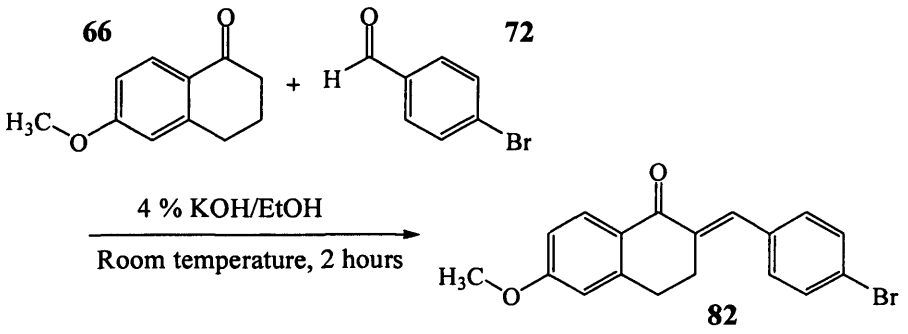

With 2-[1-(4-bromophenyl)methylidene]-6-methoxy-3,4-dihydro-2*H*-naphthalen-1-one (**82**), a light yellow solid was obtained. Yield: 2.5 g (63 %), t.l.c. system petroleum ether – ethyl acetate 3:1 v/v, R_F: 0.6, stain positive. Microanalysis ($C_{18}H_{15}BrO_2$): Calculated C = 62.99 %, H = 4.40 %; Found C = 62.79 %, H = 4.54 %. Metlting point 126 – 128 °C.

^{1}H n.m.r. δ 8.13 (d, J = 8.7 Hz, 1 H, H-8), 7.76 (s, 1H, -CH_2-CH_2-C=C<u>H</u>-Phenyl), 7.56 (d, J = 8.4 Hz, 2H, H-3' and H-5'), 7.31 (d, J = 8.3 Hz, 2H, H-2' and H-6'), 6.90 (dd, J = 2.3, 8.7 Hz, 1H, H-7), 6.73 (d, J = 2.1 Hz, 1H, H-5), 3.89 (s, 3H, -O-C<u>H</u>$_3$), 3.08 (m, 2H, –C<u>H</u>$_2$-CH_2-C=CH–Phenyl), 2.94 (m, 2H, –CH_2-C<u>H</u>$_2$-C=CH–Phenyl).

^{13}C n.m.r. δ 186.47 (C=O), 163.70 (C, C-6), 145.66 (C, C-4a), 136.25 (C, C-2), 134.92 (CH, –CH_2-CH_2-C=C<u>H</u>–Phenyl), 134.92 (C, C-1'), 131.64 (2 x CH, CH-2' and CH-6'), 131.33 (2 x CH, CH-3' and CH-5'), 130.83 (CH, CH-8), 126.91 (C, C-8a), 122.52 (C, C-4'), 113.45 (CH, CH-7), 112.32 (CH, CH-5), 55.49 (CH_3, -O-CH_3), 29.20 (CH_2, –<u>C</u>H_2-CH_2-C=CH–Phenyl), 27.23 (CH_2, –CH_2-<u>C</u>H_2-C=CH–Phenyl).

2-[1-(2-Bromophenyl)methylidene]-6-methoxy-3,4-dihydro-2*H*-naphthalen-1-one (83)

($C_{18}H_{15}BrO_2$, MW: 343.214)

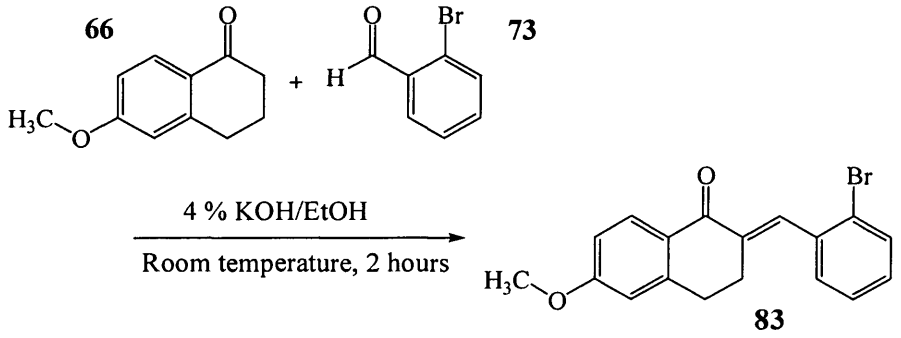

With 2-[1-(2-bromophenyl)methylidene]-6-methoxy-3,4-dihydro-*2H*-naphthalen-1-one (**83**), a white crystal was obtained. Yield: 3.22 g (68 %), t.l.c. system petroleum ether – ethyl acetate 3:1 v/v, R_F: 0.62, stain positive. Microanalysis ($C_{18}H_{15}BrO_2$): Calculated C = 62.99 %, H = 4.40 %; Found C = 63.19 %, H = 4.41 %. Melting point 78 – 80 °C.

^{1}H n.m.r. δ 8.19 (d, J = 8.7 Hz, 1H, H-8), 7.85 (s, 1H, –CH_2-CH_2-C=C<u>H</u>–Phenyl), 7.69 (d, J = 7.9, 1H, H-3''), 7.37 (m, 2H, Ar), 7.25 (m, 1H, Ar), 6.93 (dd, J = 2.4, 8.7 Hz, 1H, H-7), 6.75 (d, J = 2.3 Hz, 1H, H-5), 3.92 (s, 3H, -O-CH_3), 2.92 (s, br, 4H, –C<u>H</u>$_2$-CH_2-C=CH–Phenyl and –CH_2-C<u>H</u>$_2$-C=CH–Phenyl).

^{13}C n.m.r. δ 186.87 (C=O), 164.15 (C, C-6), 146.40 (C, C-4a), 137.47 (C, C-2), 136.94 (C, C-1'), 135.38 (CH, –CH_2-CH_2-C=C<u>H</u>–Phenyl), 133.34 (CH, CH-3'), 131.23 (CH, CH-6'), 130.88 (CH, CH-4'), 130.02 (CH, CH-8), 127.42 (CH, CH-5'), 127.30 (C, C-8a), 125.31 (C, C-2'), 113.91 (CH, CH-7), 112.78 (CH, CH-5), 55.92 (CH_3, -O-CH_3), 29.86 (CH_2, –<u>C</u>H_2-CH_2-C=CH–Phenyl), 27.77 (CH_2, –CH_2-<u>C</u>H_2-C=CH–Phenyl).

2-{1-[2,5-Di(trifluoromethyl)phenyl]methylidene}-6-methoxy-3,4-dihydro-*2H*-naphthalen-1-one (84)

($C_{20}H_{14}F_6O_2$, MW: 400.314)

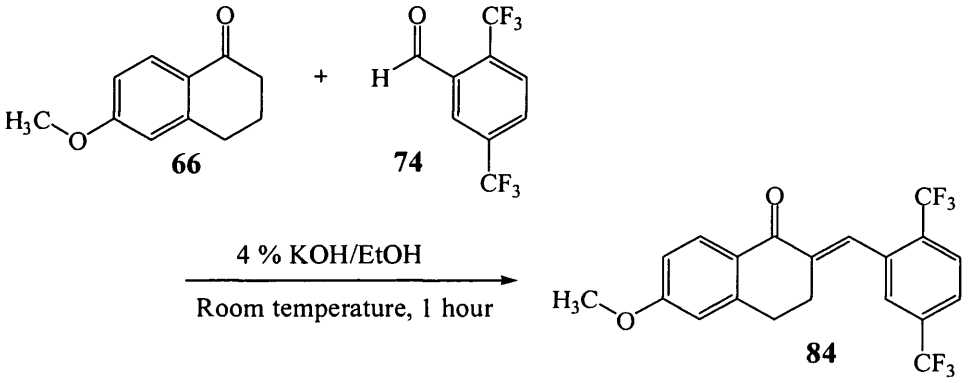

With 2-{1-[2,5-di(trifluoromethyl)phenyl]methylidene}-6-methoxy-3,4-dihydro-2*H*-naphthalen-1-one (**84**), a white solid was obtained. Yield: 0.40 g (24 %), t.l.c. system petroleum ether – ethyl acetate 3:1 v/v, R_F: 0.69, stain positive. Melting point: 98 – 100 °C. Microanalysis ($C_{20}H_{14}F_6O_2$): Calculated C = 60.01 %, H = 3.52 %, Found C = 59.93 %, H = 3.48 %.

^{1}H n.m.r. δ 8.22 (d, J = 8.8 Hz, 1H, H-8), 7.96 (d, J = 8.3 Hz, 2H, H-3' and H-6'), 7.81 (d, J = 8.2 Hz, 1H, H-4'), 7.67 (s, 1H, –CH_2-CH_2-C=C<u>H</u>–Phenyl), 6.99 (d, J = 2.5, 8.8 Hz, 1H, H-7), 6.79 (d, J = 2.4 H, 1H, H -5), 3.97 (s, 3H, –O-CH_3), 3.01 (m, 2H, –C<u>H_2</u>-CH_2-C=CH–Phenyl), 2.92 (m, 2H, –CH_2-C<u>H_2</u>-C=CH–Phenyl).

^{13}C n.m.r. δ 186.12 (C=O), 164.39 (C, C-6), 146.35 (C, C-4a), 139.94 (C, C-1'), 136.81 (C, C-2), 134.35, 132.68 (C, C-2'), 131.37 (CH, CH-8), 130.84 (CH, –CH_2-CH_2-C=C<u>H</u>–Phenyl), 127.83, 127.78 (CH, CH-6'), 127.42, 127.21 (CH, CH-4'), 126.94 (C, C-5'), 125.43 (C, C-8a), 125.26, 125.22 (CH, CH-3'), 121.80 (C, CF_3), 114.10 (CH, CH-7), 112.85 (CH, CH-5), 55.92 (CH_3), 29.69 (CH_2, –C<u>H_2</u>-CH_AH_B-CH_x-(C=O)), 27.80 (CH_2, –CH_2-C<u>H_A</u>H_B-CH_x-(C=O)).

^{19} F n.m.r. δ -61.72, -63.59 ppm.

6-Methoxy-2-[1-(2-methylphenyl)methylidene]-3,4-dihydro-2*H*-naphthlalen-1-one (85)

($C_{19}H_{18}O_2$, MW: 278.345)

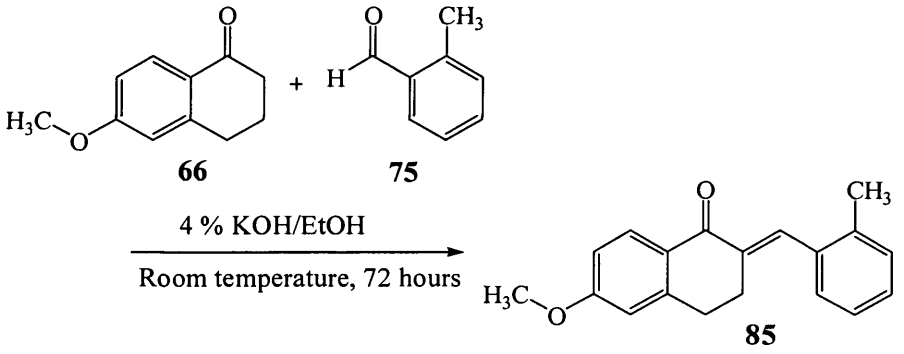

Reaction was stirred at room temperature for 72 h. The brown residue obtained was then purified by column chromatography with petroleum ether – ethyl acetate 100:0 v/v increasing to 87:13 v/v to give 6-methoxy-2-[1-(2-methylphenyl)methylidene]-3,4-dihydro-*2H*-naphthlalen-1-one (**85**) as a yellow solid. Yield: 1.57 g (71 %), t.l.c. system petroleum ether – ethyl acetate 3:1 v/v, R_F: 0.65, stain positive. Microanalysis ($C_{19}H_{18}O_2$): Calculated C = 81.99 %, H = 6.52 %; Found C = 81.77 %, H = 6.55 %.

^{1}H n.m.r. δ 8.21 (d, J = 8.7 Hz, 1H, H-8), 7.94 (s, 1H, –CH_2-CH_2-C=C<u>H</u>–Phenyl), 7.30 (m, 4H, Ar), 6.95 (dd, J = 2.4, 8.7 Hz, 1H, H-7), 6.76 (d, J = 2.2 Hz, 1H, H-5), 3.93 (s, 3H, –O-C<u>H</u>$_3$), 2.98 (m, 4H, –C<u>H</u>$_2$-CH_2-C=CH–Phenyl and –CH_2-C<u>H</u>$_2$-C=CH–Phenyl), 2.40 (s, 3H, CH_3).

^{13}C n.m.r. δ 187.30 (C=O), 164.05 (C, C-6), 146.45 (C, C-4a), 138.16 (C, C-2'), 136.51 (C, C-2), 135.66 (C, C-1'), 135.45 (CH, –CH_2-CH_2-C=C<u>H</u>–Phenyl), 131.18 (CH, CH-3'), 130.63 (CH, CH-6'), 129.33 (CH, CH-4'), 128.76 (CH, CH-8), 127.48 (C, C-8a), 125.90 (CH, CH-5'), 113.82 (CH, CH-5), 112.77 (CH, CH-7), 55.89 (CH_3, -O-CH_3), 30.07 (CH_2, –<u>C</u>H_2-CH_2-C=CH–Phenyl), 27.74 (CH_2, –CH_2-<u>C</u>H_2-C=CH–Phenyl), 20.50 (CH_3).

2-{1-[4-(Dimethylamino)phenyl]methylidene}-6-methoxy-3,4-dihydro-2*H*-naphthalen-1-one (86)

($C_{20}H_{21}NO_2$, MW: 307.386)

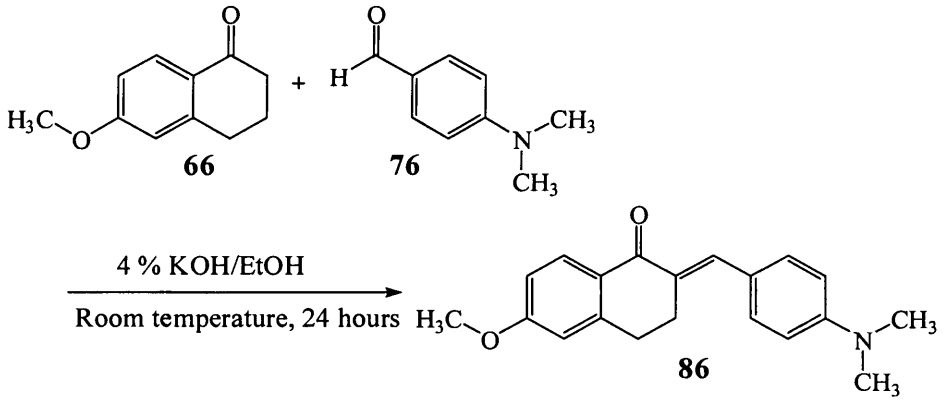

Reaction was stirred at room temperature for 24 h. With 2-{1-[4-(dimethylamino)phenyl]methylidene}-6-methoxy-3,4-dihydro-2*H*-naphthalen-1-one (**86**), an orange crystal was obtained. Yield: 0.38 g (7 %), t.l.c. system petroleum ether – ethyl acetate 3:1 v/v, R_F: 0.32, stain positive. Melting point: 146 – 148 °C. Microanalysis ($C_{20}H_{21}NO_2$.): Calculated C = 78.15 %, H = 6.89 %, N = 4.55 %; Found C = 78.26 %, H = 6.95 %, N = 4.53 %.

^{1}H n.m.r. δ 8.16 (d, J = 8.7 Hz, 1H, H-8), 7.89 (s, 1H, –CH_2-CH_2-C=C<u>H</u>–Phenyl), 7.47 (d, J = 8.8 Hz, 2H, H-3' and H-5'), 6.92 (dd, J = 2.5, 8.7 Hz, 1H, H-7), 6.77 (m, 3H, H-2', H-6' and H-5), 3.91 (s, 3H, -O-CH_3), 3.21 (t, J = 6.2 Hz, 2H, –C<u>H</u>$_2$-CH_2-C=CH–Phenyl), 2.95 (t, J = 6.2 Hz, 2H, –CH_2-C<u>H</u>$_2$-C=CH–Phenyl).

^{13}C n.m.r. δ 187.18 (C=O), 163.65 (C, C-6), 150.90 (C, C-4'), 145.86 (C, C-4a), 137.60 (CH, –CH_2-CH_2-C=C<u>H</u>–Phenyl), 132.50 (2 x CH, CH-2' and CH-4'), 131.66 (C, C-2), 130.91 (CH, CH-8), 127.94 (C, C-8a), 124.17 (C, C-1'), 113.52 (CH, CH-7), 112.57 (CH, CH-5), 112.08 (2 x CH, CH-3' and CH-5'), 55.85 (CH_3, –O-CH_3), 40.60 (2 x CH_3, –N(CH_3)CH_3), 29.62 (CH_2, –<u>C</u>H_2-CH_2-C=CH–Phenyl), 27.82 (CH_2, –CH_2-<u>C</u>H_2-C=CH–Phenyl).

2-{1-[4-(Dimethylamino)phenyl]methylidene}-6-(tetrahydro-pyran-2-yloxy)-3,4-dihydro-2*H*-naphthalen-1-one (87)

($C_{24}H_{27}NO_3$, MW: 377.476)

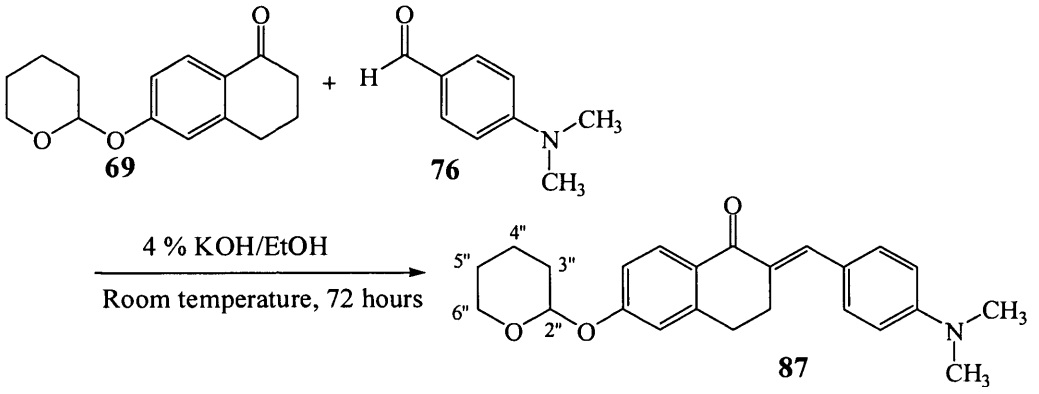

Reaction was stirred at room temperature for 72 h. The brown residue obtained was purified by column chromatography with dichloromethane – methanol 100:0 v/v increasing to 99:1 v/v to give 2-{1-[4-(dimethylamino)phenyl]methylidene}-6-(tetrahydro-pyran-2-yloxy)-3,4-dihydro-2*H*-naphthalen-1-one (**87**) as a orange solid. Yield: 1.72 g (35 %), t.l.c. system petroleum ether – ethyl acetate 3:1 v/v, R_F: 0.59, stain positive. Microanalysis ($C_{24}H_{27}NO_3$): Calculated C = 76.36 %, H = 7.21 %, N = 3.71 %; Found C = 76.12 %, H = 7.23 %, N = 3.57 %.

^{1}H n.m.r. δ 8.14 (d, J = 8.7 Hz, 1H, H-8), 7.88 (s, 1H, –CH_2-CH_2-C=C<u>H</u>–Phenyl), 7.47 (d, J = 8.8 Hz, 2H, H-3' and H-5'), 7.05 (dd, J = 2.4, 8.7 Hz, 1H, H-7), 6.93 (d, J = 2.3 Hz, 1H, H-5), 6.77 (d, J = 8.8 Hz, 2H, H-2' and H-6'), 5.58 (t, J = 3.0 Hz, 1H, C<u>H</u>-2''), 3.94 (m, 1H, <u>H_a</u>H_b-6''), 3.69 (m, 1H, H- H_a<u>H_b</u>-6''), 3.21 (m, 2H, –C<u>H_2</u>-CH_2-C=CH–Phenyl), 3.08 (s, 6H, –N(C<u>H_3</u>)C<u>H_3</u>), 2.95 (m, 2H, –CH_2-C<u>H_2</u>-C=CH–Phenyl), 2.06 (m, 1H, <u>H_a</u>H_b- 3''), 1.94 (m, 2H, –CH_2-C<u>H_2</u>-C=CH–Phenyl), 1.82 – 1.65 (m, 3H, C<u>H_2</u>-4'' and H_a<u>H_b</u>- 3'').

^{13}C n.m.r. δ 187.28 (C=O), 161.13 (C, C-6), 150.89 (C, C-4'), 145.70 (C, C-4a), 137.59 (CH, –CH_2-CH_2-C=<u>C</u>H–Phenyl), 132.36 (2 x CH, CH-3' and CH-5'), 131.77 (C, C-2), 130.76 (CH, CH-8), 128.52 (C, C-8a), 124.24 (C, C-1'), 115.68 (CH, CH-7), 114.78 (CH, CH-5), 112.08 (2 x CH, CH-2' and CH-6'), 96.38 (CH, <u>C</u>H-2''), 62.48 (CH_2, CH_2-6''), 40.62 (2 x CH_3, –N(CH_3)CH_3), 30.59 (CH_2, CH_2-3''), 29.61 (CH_2, –<u>C</u>H_2-CH_2-C=CH–Phenyl), 27.83 (CH_2, –CH_2-<u>C</u>H_2-C=CH–Phenyl), 25.55 (CH_2, CH_2-5''), 18.96 (CH_2, CH_2-4'').

2-Biphenyl-4-ylmethylene-6-(tetrahydro-pyran-2-yloxy)-3,4-dihydro-2*H*-naphthalen-1-one (89)

($C_{28}H_{26}O_3$, MW: 410.50)

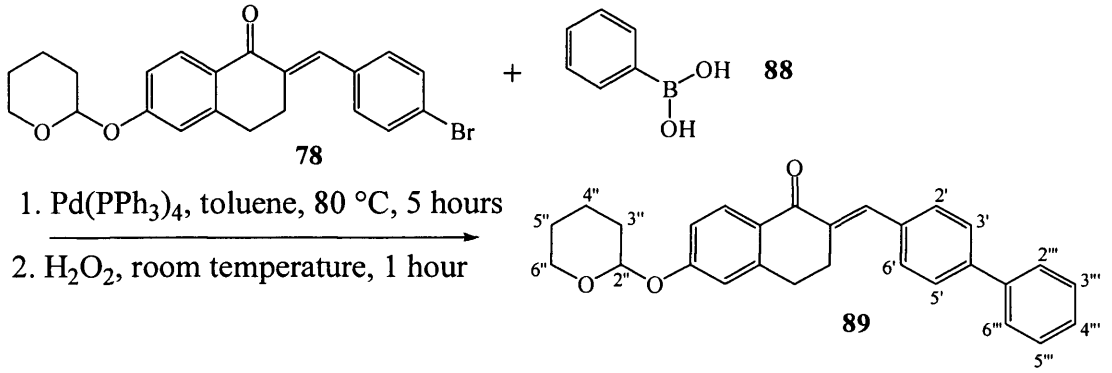

2M aqueous Na_2CO_3 (8.50 mL) was added to a solution of 2-(4-bromo-benzylidene)-6-(tetrahydro-pyran-2-yloxy)-3,4-dihydro-2*H*-naphthalen-1-one (**78**) (1.0 g, 2.42 mmol) in toluene (20 mL). The mixture was bubbled with nitrogen for one minute and then $Pd(PPh_3)_4$ (0.14 g, 0.12 mmol) was added to the mixture. Phenylboronic acid (**88**) (0.59 g, 4.84 mmol) in ethanol (5 mL) was added to the above mixture and the reaction was refluxed at 100 °C for 5 hours. After the reaction was complete, the residual borane was oxidised by the addition of H_2O_2 (30 %, 2.5 mL) at room temperature for 1 hour. The crude product was extracted with CH_2Cl_2 (100 mL) and water (3 x 100 mL). The organic layer was dried with $MgSO_4$, filtered and reduced *in vacuo* to give a light yellow oily residue. Purification by flash column chromatography (dichloromethane – methanol 100:0 v/v increasing to 99:1 v/v) gave a yellow residue. The residue was recrystallised with methanol to yield light yellow solid, 2-biphenyl-4-ylmethylene-6-(tetrahydropyran-2yloxy)-3,4-dihydro-2*H*-naphthalen-1-one (**89**). Yield: 0.50 g (50 %), t. l. c. system: petroleum ether – ethyl acetate 3:1 v/v, R_F: 0.62, stain positive. Microanalysis ($C_{28}H_{26}O_3$): Calculated C = 81.92 %, H = 6.38 %; Found C = 81.95 %, H = 6.37 %. Melting point 116 – 118 °C.

^{1}H n.m.r. δ 8.17 (d, J = 8.7 Hz, 1H, H-8), 7.94 (s, 1H, –CH_2-CH_2-C=C<u>H</u>–Phenyl), 7.71 (m, 3H, Ar), 7.55 (m, 3H, Ar), 7.43 (m, 1H, Ar), 7.30 (m, 1H, Ar), 7.08 (dd, J = 2.4, 8.7 Hz, 1H, H-7), 6.96 (d, J = 2.4 Hz, 1H, H-5), 6.94 (m, 1H, Ar), 5.61 (t, J = 2.9 Hz, 1H, C<u>H</u>-2''), 3.94 (m, 1H, <u>H_a</u>H_b-6''), 3.70 (m, 1H, H- H_a<u>H_b</u>-6''), 3.23 (m, 2H, –CH_2-C<u>H_2</u>-C=CH–Phenyl), 3.00 (m, 2H, –C<u>H_2</u>-CH_2-C=CH–Phenyl), 2.08 (m, 1H, <u>H_a</u>H_b- 3''), 1.95 (m, 2H, C<u>H_2</u>-5''), 1.84 – 1.66 (m, 3H, C<u>H_2</u>-4'' and H_a<u>H_b</u>- 3'').

^{13}C n.m.r. δ 187.23 (C=O), 161.53 (C, C-6), 146.01 (C, C-4a), 141.61 (C, –CH_2-CH_2-C=CH–Phenyl), 140.88 (C, C-1'''), 136.12 (C, C-4'), 136.07 (CH, –CH_2-CH_2-C=CH–Phenyl), 135.46 (C, C-1'), 131.03 (CH, CH-4'''), 130.85 (2 x CH, Ar), 130.07 (2 x CH, Ar), 129.31 (CH, CH-8), 128.06 (CH, C-8a), 127.50 (4 x CH, Ar), 115.74 (CH, CH-7), 114.91 (CH, CH-5), 96.39 (CH, CH-2''), 62.49 (CH_2, CH_2-6''), 30.55 (CH_2, CH_2-3''), 29.69 (CH_2, –CH_2-CH_2-C=CH–Phenyl), 27.81 (CH_2, –CH_2-CH_2-C=CH–Phenyl), 25.52 (CH_2, CH_2-5''), 18.90 (CH_2, CH_2-4'').

2-Biphenyl-2-ylmethylene-6-(tetrahydro-pyran-2-yloxy)-3,4-dihydro-2*H*-naphthalen-1-one (90)

($C_{28}H_{26}O_3$, MW: 410.504)

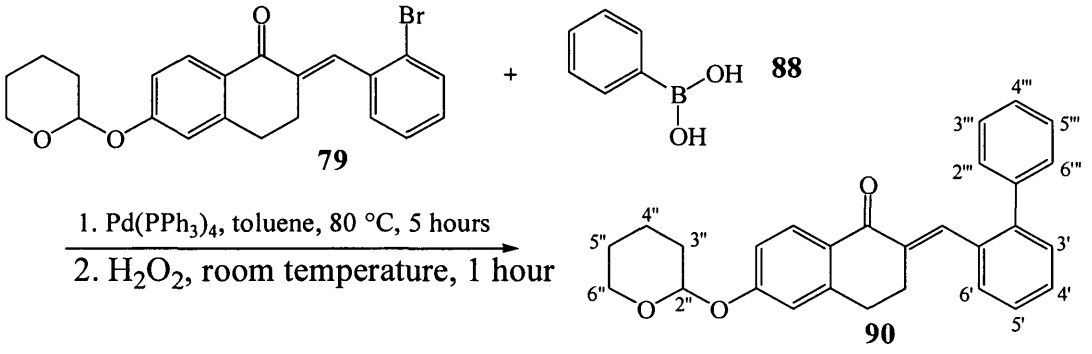

2-biphenyl-2-ylmethylene-6-(tetrahydro-pyran-2-yloxy)-3,4-dihydro-2*H*-naphthalen-1-one (**90**) was prepared using the same method detailed above (compound **89**). A light yellow solid was obtained. Yield: 1.30 g (87 %), t. l. c. system: petroleum ether – ethyl acetate 3:1 v/v, R_F: 0.64, stain positive. Microanalysis ($C_{28}H_{26}O_3.0.2H_2O$): Calculated C = 81.21 %, H = 6.43 %; Found C = 81.22 %, H = 6.37 %. Melting point 158 – 160 °C.

^{1}H n.m.r. δ 8.15 (d, J = 8.7 Hz, 1H, H-8), 7.79 (s, 1H, –CH_2-CH_2-C=C<u>H</u>–Phenyl), 7.54 – 7.32 (m, 9H, Ar), 7.06 (dd, J = 2.2, 8.7 Hz, 1H, H-5), 6.94 (d, J = 2.2 Hz, 1H, H-7), 5.59 (t, J = 2.8 Hz, 1H, C<u>H</u>-2''), 3.93 (m, 1H, C<u>H$_a$H$_b$</u>-6''), 3.70 (m, 1H, CH$_a$<u>H$_b$</u>-6''), 2.97 (m, 2H, –C<u>H$_2$</u>-CH_2-C=CH–Phenyl), 2.88 (m, 2H, –CH_2-C<u>H$_2$</u>-C=CH–Phenyl), 2.13 – 2.02 (m, 1H, C<u>H$_a$H$_b$</u>-3''), 1.93 (m, 2H, C<u>H$_2$</u>-5''), 1.84 – 1.65 (m, 3H, CH$_a$<u>H$_b$</u>-3'' and C<u>H$_2$</u>-4'').

^{13}C n.m.r. δ 187.08 (C=O), 161.51 (C, C-6), 146.28 (CH, Ar), 142.85 (C, C-2'), 141.05 (C, C-1'''), 136.68 (CH, –CH_2-CH_2-C=CH–Phenyl), 136.20 (C, C-4a), 134.69 (C, C-1'), 130.97 (CH, Ar), 130.60 (C, C-2), 130.22 (CH, Ar), 130.04 (CH, CH-Ar), 129.94 (2 x CH, CH-2''' and CH-6'''), 128.93 (CH, Ar), 128.67 (2 x CH, CH-3''' and CH-5'''), 128.32 (CH, Ar), 127.98 (C, C-8a), 127.80 (CH, CH-8), 127.35 (CH, CH-3'), 115.93

(CH, CH-5), 114.99 (CH, CH-7), 96.37 (CH, CH-2''), 62.47 (CH_2, CH_2-6''), 30.56 (CH_2, CH_2-3''), 29.78 (CH, –$\underline{C}H_2$-CH_2-C=CH–Phenyl), 27.86 (CH_2, –CH_2-$\underline{C}H_2$-C=CH–Phenyl), 25.54 (CH_2, CH_2-5''), 18.92 (CH_2, CH_2-4'').

2-[1-(4-Hydroxyphenyl)methylidene]-6-methoxy-3,4-dihydro-2*H*-naphthalen-1-one (91)

($C_{18}H_{16}O_3$, MW: 280.318)

Method 1

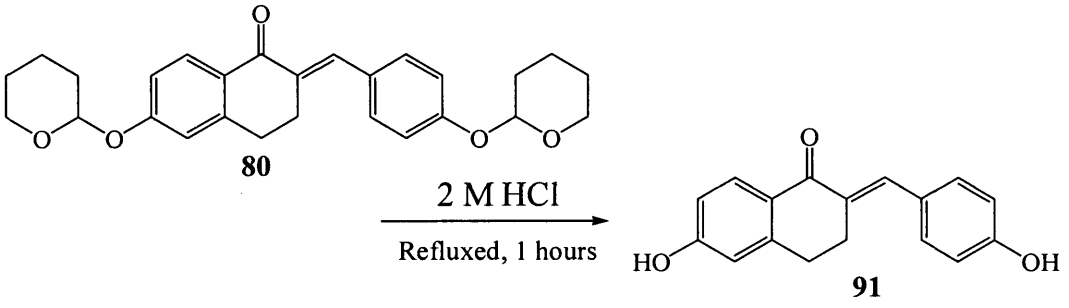

Aqueous hydrochloric acid (2 M, 15 mL) was added to a solution of 6-methoxy-2-{1-[4-(tetrahydro-pyran-2-yloxy)phenyl]methylidene}-3,4-dihydro-2*H*-naphthalen-1-one (**81**) (2 g, 5.49 mmol), in 2-butanone-ethyl acetate (1/1 v/v, 40 mL), and the mixture stirred at 100 °C for 1 h. The yellow solution was evaporated *in vacuo* and the resulting yellow solid was washed with water-methanol (2/1 v/v, 40 mL) to give 2-[1-(4-hydroxyphenyl)methylidene]-6-methoxy-3,4-dihydro-2*H*-naphthalen-1-one (**91**), as yellow powder. Yield: 1.39 g (90 %), t. l. c. system: petroleum ether – ethyl acetate 3:1 v/v, R_F: 0.22, stain positive. Microanalysis ($C_{18}H_{16}O_3.0.5H_2O$): Calculated C = 74.55 %, H = 5.66 %; Found C = 74.72 %, H = 5.92 %.

^{1}H n.m.r. (DMSO-d_6) δ 9.92 (s, br, 1H, OH), 7.92 (d, J = 8.6 Hz, 1H, H-8), 7.62 (s, 1H, –CH_2-CH_2-C=C$\underline{H}$–Phenyl), 7.40 (d, J = 8.4 Hz, 2H, Ar), 6.93 (m, 2H, Ar), 6.86 (d, J = 8.3 Hz, 2H, H-7 and H-5), 3.85 (s, 3H, CH_3), 3.06 (t, J = 6.0 Hz, 2H, –$C\underline{H}_2$-CH_2-C=CH–Phenyl), 2.90 (t, J = 3.0 Hz, 2H, –CH_2-$C\underline{H}_2$-C=CH–Phenyl).

^{13}C n.m.r. (DMSO-d_6) δ 185.72 (C=O), 163.43 (C, C-6), 158.58 (C, C-4'), 146.06 (C, C-4a), 135.89 (CH, –CH_2-CH_2-C=C$\underline{H}$–Phenyl), 132.87 (C, C-2), 132.32 (2 x CH, CH-2' and CH-6'), 130.13 (CH, CH-8), 126.88 (C, C-8a), 126.57 (C, C-1'), 115.84 (2 x CH, CH-3' and CH-5'), 113.93 (CH, CH-7), 112.57 (CH, CH-5), 55.86 (CH_3, -O-CH_3), 28.59 (CH_2, –$\underline{C}H_2$-CH_2-C=CH–Phenyl), 27.09 (CH_2, –CH_2-$\underline{C}H_2$-C=CH–Phenyl).

Method 2 (Yoshihama et al., 1999)

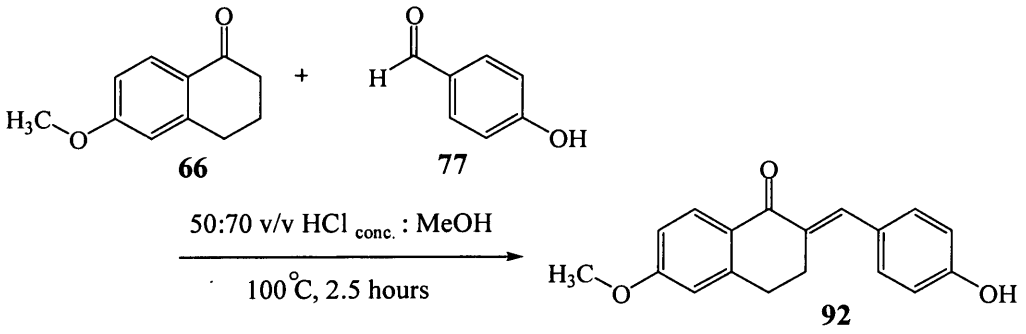

After a mixture of concentrated hydrochloric acid (50 mL) and methanol (70 mL) were added to a mixture of 6-methoxy-3,4-dihydro-2*H*-naphthalen-1-one (**66**) (1.50 g, 8.51 mmol) and 4-hydroxybenzaldehyde (**77**) (1.10 g, 9.00 mmol), the mixture was refluxed for 2.5 hours and cooled to room temperature. 100 mL of water was added and allowed to stand for one hour. The precipitated solid was filtered. The solid was then recrystallised from acetone to yield 2-[1-(4-hydroxyphenyl)methylidene]-6-methoxy-3,4-dihydro-*2H*-naphthalen-1-one (**91**) as yellow solid. Yield: 0.63 g (26 %). t. l. c. system: petroleum ether – ethyl acetate 3:1 v/v, R_F: 0.22, stain positive.

^{1}H n.m.r. data same as above.

The following derivatives of 2-benzylidene-3,4-dihydro-2*H*-naphthalen-1-one (unsaturated tetralone) (**92** – **96**) were prepared using the same general method detailed in ***method 1*** for compound **91**.

6-Hydroxy-2-[1-(4-hydroxyphenyl)methylidene]-3,4-dihydro-*2H*-naphthalen-1-one (92)

($C_{17}H_{14}O_3$, MW: 266.291)

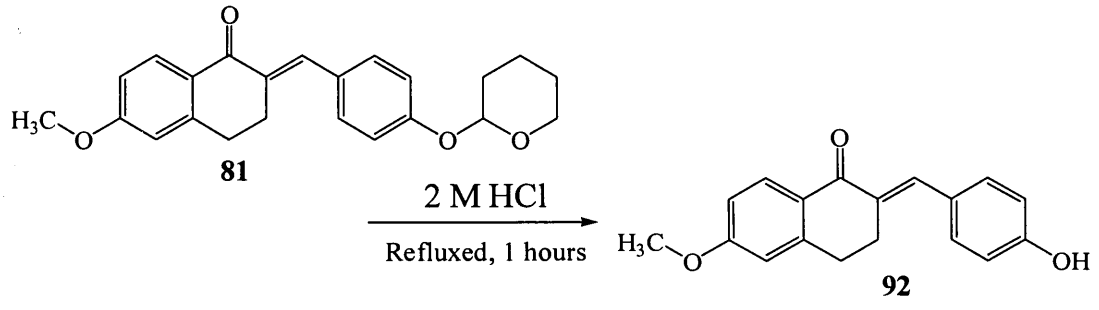

With 6-hydroxy-2-[1-(4-hydroxyphenyl)methylidene]-3,4-dihydro-*2H*-naphthalen-1-one (**92**), a yellow powder was obtained. Yield: 0.67 g (55 %), t. l. c. system: petroleum ether – ethyl acetate 3:1 v/v, R_F: 0.05, stain positive. Microanalysis ($C_{17}H_{14}O_3.0.1H_2O$): Calculated C = 76.04 %, H = 5.29 %; Found C = 76.16 %, H = 5.34 %. Melting point: 260 – 262 °C.

^{1}H n.m.r. (DMSO-d_6) δ 10.38 (s, 1H, OH), 9.90 (s, 1H, OH), 7.85 (d, J = 8.5 Hz, 1H, H-8), 7.59 (s, 1H, –CH_2-CH_2-C=C<u>H</u>–Phenyl), 7.38 (d, J = 8.4 Hz, 2H, Ar), 6.86 (d, J = 8.3 Hz, 2H, Ar), 6.78 (dd, J = 1.7, 8.5 Hz, 1H, H-7), 6.68 (s, br, 1H, H-5), 3.04 (m, 2H, –C<u>H$_2$</u>-CH_2-C=CH–Phenyl), 2.83 (m, 2H, –CH_2-C<u>H$_2$</u>-C=CH–Phenyl).

^{13}C n.m.r. (DMSO-d_6) δ 185.57 (C=O), 162.38 (C, C-6), 158.47 (C, C-4'), 146.10 (C, C-4a), 135.47 (CH, –CH_2-CH_2-C=<u>C</u>H–Phenyl), 133.15 (C, –CH_2-CH_2-<u>C</u>=CH–Phenyl), 132.23 (2 x CH, CH-3' and CH-5'), 130.49 (CH, CH-8), 126.67 (C, C-8a), 125.68 (C, C-1'), 115.82 (2 x CH, CH-2' and CH-6'), 114.96 (CH, CH-7), 114.20 (CH, CH-5), 28.53 (CH_2, –<u>C</u>H_2-CH_2-C=CH–Phenyl), 27.12 (CH_2, –CH_2-<u>C</u>H_2-C=CH–Phenyl).

<u>2-[1-(2-Bromophenyl)methylidene]-6-hydroxy-3,4-dihydro-*2H*-naphthalen-1-one</u> (**93**)

($C_{17}H_{13}BrO_2$, MW: 329.188)

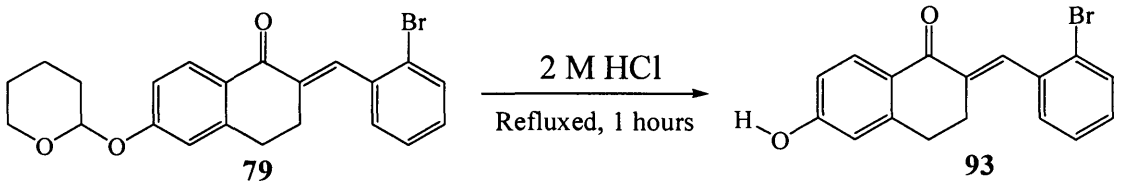

79 **93**

With 2-[1-(2-bromophenyl)methylidene]-6-hydroxy-3,4-dihydro-*2H*-naphthalen-1-one (**93**), a white solid was obtained. Yield: 0.60 g (63 %), t. l. c. system: petroleum ether – ethyl acetate 3:1 v/v, R_F: 0.20, stain positive. Microanalysis ($C_{17}H_{13}BrO_2$): Calculated C = 62.03 %, H = 3.98 %; Found C = 62.03 %, H = 4.05 %. Melting point: 178 – 180 °C.

^{1}H n.m.r. (DMSO-d_6) δ 10.51 (s, 1H, OH), 7.90 (d, J = 8.5 Hz, 1H, H-8), 7.74 (d, J = 7.7 Hz, 1H, Ar), 7.60 (s, 1H, –CH_2-CH_2-C=C<u>H</u>–Phenyl), 7.47 (d, J = 2.3, 2H, Ar), 7.34 (s, br, 1H, Ar), 6.81 (d, J = 8.5 Hz, 1H, H-7), 6.69 (s, br, 1H, H-5), 2.87 (s, br, 4H, –C<u>H$_2$</u>-CH_2-C=CH–Phenyl and –CH_2-C<u>H$_2$</u>-C=CH–Phenyl).

^{13}C n.m.r. (DMSO-d_6) δ 185.37 (C=O), 162.87 (C, C-6), 146.66 (C, C-4a), 137.72 (C, –CH_2-CH_2-<u>C</u>=CH–Phenyl), 135.88 (C, C-1'), 133.44 (CH, –CH_2-CH_2-C=<u>C</u>H–Phenyl), 133.08 (CH, CH-3'), 131.15 (CH, CH-4'), 130.74 (CH, CH-6'), 130.63 (CH, CH-8), 127.97 (CH, CH-5'), 125.23 (C, C-8a), 124.56 (C, C-2'), 115.27 (CH, CH-7), 114.42 (CH, CH-5), 28.66 (CH_2, –<u>C</u>H_2-CH_2-C=CH–Phenyl), 27.04 (CH_2, –CH_2-<u>C</u>H_2-C=CH–Phenyl).

2-{1-[4-(Dimethylamino)phenyl]methylidene}-6-hydroxy-3,4-dihydro-*2H*-naphthalen-1-one (94)

($C_{19}H_{19}NO_2$, MW: 293.360)

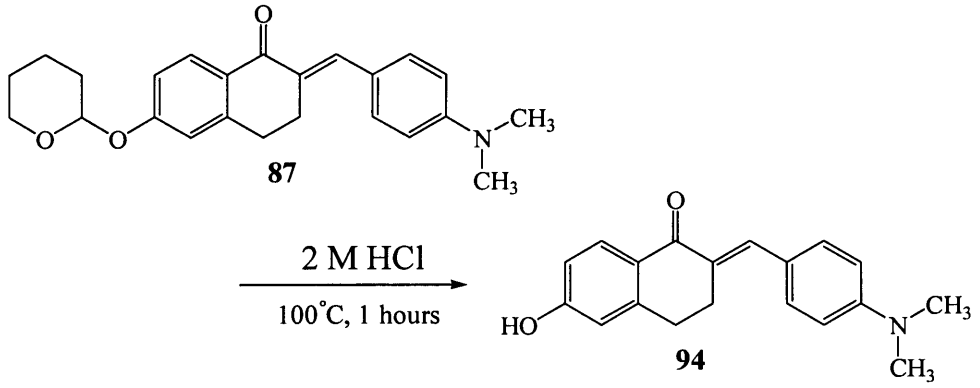

With 2-{1-[4-(dimethylamino)phenyl]methylidene}-6-hydroxy-3,4-dihydro-*2H*-naphthalen-1-one (**94**), a yellow solid was obtained. Yield: 0.82 g (70 %), t. l. c. system: petroleum ether – ethyl acetate 3:1 v/v, R_F: 0.05, stain positive. Melting point: 210 – 212 °C.

^{1}H n.m.r. (DMSO-d_6) δ 9.03 (s, br, 1H, OH), 7.84 (d, J = 8.6 Hz, 1H, H-8), 7.61 (s, 1H, –CH_2-CH_2-C=C<u>H</u>–Phenyl), 7.56 (d, J = 8.6 Hz, 2H, Ar), 7.44 (s, br, 2H, Ar), 6.81 (dd, J = 2.3, 8.6 Hz, 1H, H-7), 6.70 (d, J = 2.1 Hz, 1H, H-5), 3.08 (s, 6H, 2 x CH_3), 3.01 (m, 2H, –C<u>H$_2$</u>-CH_2-C=CH–Phenyl), 2.82 (m, 2H, –CH_2-C<u>H$_2$</u>-C=CH–Phenyl) (Yoshihama et al., 1999).

^{13}C n.m.r. (DMSO-d_6) δ 185.41 (C=O), 162.65 (C, C-6), 146.17 (2 x C, C-4a and C-4'), 134.38 (CH, –CH_2-CH_2-C=<u>C</u>H–Phenyl), 133.38 (C, –CH_2-CH_2-<u>C</u>=CH–Phenyl), 131.76 (2 x CH, Ar), 130.51 (CH, CH-8), 125.48 (C, C-8a), 123.8 (C, C-1'), 117.50 (2 x CH, Ar), 115.11 (CH, CH-5), 114.26 (CH, CH-7), 43.36 (2 x CH_3), 28.52 (CH_2, –<u>C</u>H_2-CH_2-C=CH–Phenyl), 27.12 (CH_2, –CH_2-<u>C</u>H_2-C=CH–Phenyl).

2-Biphenyl-4-ylmethylene-6-hydroxy-3,4-dihydro-2*H*-naphthalen-1-one (95)

($C_{23}H_{18}O_2$, MW: 326.388)

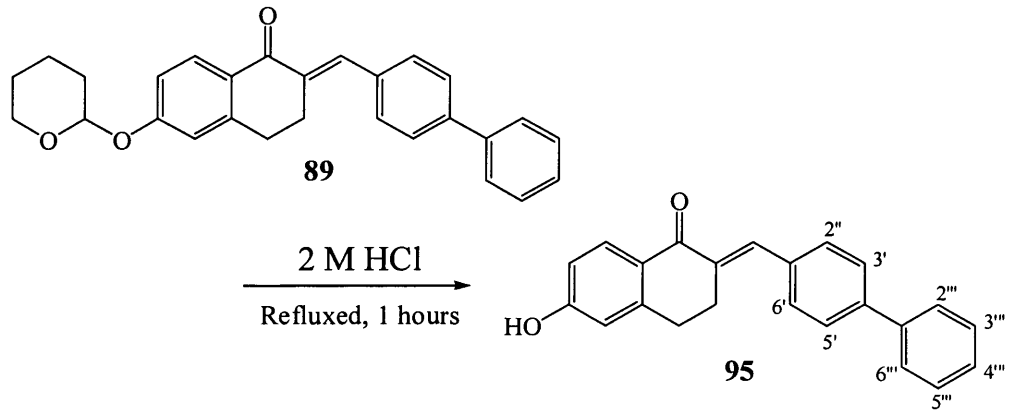

With 2-biphenyl-4-ylmethylene-6-hydroxy-3,4-dihydro-2*H*-naphthalen-1-one (**95**), a yellow solid was obtained. Yield: 0.38 g (95 %), t. l. c. system: petroleum ether – ethyl acetate 3:1 v/v, R_F: 0.05, stain positive. Microanalysis ($C_{23}H_{18}O_2$): Calculated C = 84.64 %, H = 5.56 %; Found C = 84.71 %, H = 5.51 %. Melting point: 258 – 260 °C.

^{1}H n.m.r. (DMSO-d_6) δ 10.47 (s, br, 1H, OH), 7.89 (d, J = 8.5 Hz, 1H, H-8), 7.75 (m, 4H, Ar), 7.62 (d, J = 8.1 Hz, 2H, Ar), 7.50 (m, 2H, Ar), 7.41 (m, 1H, Ar), 6.80 (dd, J = 1.7, 8.6 Hz, 1H, H-7), 6.70 (s, br, 1H, H-5), 3.10 (t, J = 5.9 Hz, 2H, –C$\underline{H_2}$-CH_2-C=CH–Phenyl), 2.87 (t, J = 6.1 Hz, 2H, –CH_2-C$\underline{H_2}$-C=CH–Phenyl).

^{13}C n.m.r. (DMSO-d_6) δ 185.54 (C=O), 162.68 (C, C-6), 146.39 (C, C-1'''), 140.48 (C, C-2'''), 139.79 (C, C-4a), 136.34 (C, –CH_2-CH_2-$\underline{C}$=CH–Phenyl), 134.98 (C, C-1'') 134.44 (CH, –CH_2-CH_2-C=$\underline{C}$H–Phenyl), 130.86 (2 x CH, CH-3''' and CH-5'''), 130.65 (CH, Ar), 129.39 (2 x CH, CH-2''' and CH-6'''), 128.16 (CH, Ar), 127.04 (CH, CH-8), 127.04 (2 x CH, CH-3'' and CH-5''), 125.46 (C, C-8a), 115.14 (CH, CH-5), 114.30 (CH, CH-7), 28.58 (CH_2, –$\underline{C}H_2$-CH_2-C=CH–Phenyl), 27.23 (CH_2, –CH_2-$\underline{C}H_2$-C=CH–Phenyl).

2-Biphenyl-2-ylmethylene-6-hydroxy-3,4-dihydro-2*H*-naphthalen-1-one (96)

($C_{23}H_{18}O_2$, MW: 326.388)

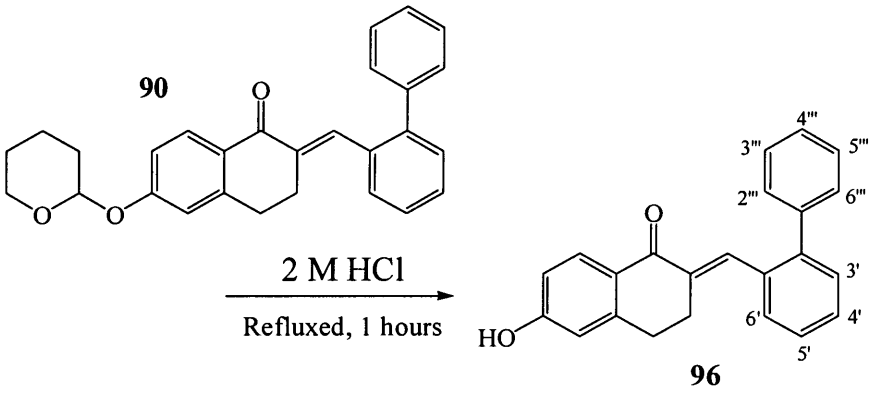

96

With 2-biphenyl-2-ylmethylene-6-hydroxy-3,4-dihydro-2*H*-naphthalen-1-one (**96**), a yellow solid was obtained. Yield: 0.86 g (91 %), t. l. c. system: petroleum ether – ethyl acetate 3:1 v/v, R_F: 0.05, stain positive. Microanalysis ($C_{23}H_{18}O_2$): Calculated C = 84.64 %, H = 5.56 %; Found C = 84.44 %, H = 5.51 %. Melting point: 221 – 223 °C.

^{1}H n.m.r. (DMSO-d_6) δ 10.46 (s, br, 1H, OH), 7.81 (d, J = 8.5 Hz, 1H, H-8), 7.41 (m, 10H, Ar), 6.78 (dd, J = 1.5, 8.5 Hz, 1H, H-7), 6.68 (s, 1H, H-5), 2.88 (m, 2H, –C<u>H$_2$</u>-CH$_2$-C=CH–Phenyl), 2.80 (m, 2H, –CH$_2$-C<u>H$_2$</u>-C=CH–Phenyl).

^{13}C n.m.r (DMSO-d_6) δ 185.48 (C=O), 162.69 (C, C-6), 146.60 (C, C-2'), 142.09 (C, C-1'''), 140.48 (C, C-4a), 136.15 (C, C-1'), 134.77 (CH, –CH$_2$-CH$_2$-C=<u>C</u>H–Phenyl), 133.84 (C, –CH$_2$-CH$_2$-<u>C</u>=CH–Phenyl), 130.60 (CH, Ar), 130.29 (2 x CH, CH-2''' and CH-6'''), 130.02 (CH, Ar), 129.82 (CH, Ar), 129.09 (CH, Ar), 128.63 (2 x CH, CH-3''' and CH-5'''), 127.77 (CH, Ar), 127.57 (CH, CH-8), 125.34 (C, C-8a), 115.12 (CH, CH-5), 114.34 (CH, CH-7), 28.66 (CH$_2$, –<u>C</u>H$_2$-CH$_2$-C=CH–Phenyl), 27.21 (CH$_2$, –CH$_2$-<u>C</u>H$_2$-C=CH–Phenyl).

4-[(6-Methoxy-3,4-dihydro-2*H*-naphthalenyl)methyl]phenol (97)

($C_{18}H_{20}O_2$, MW: 268.35)

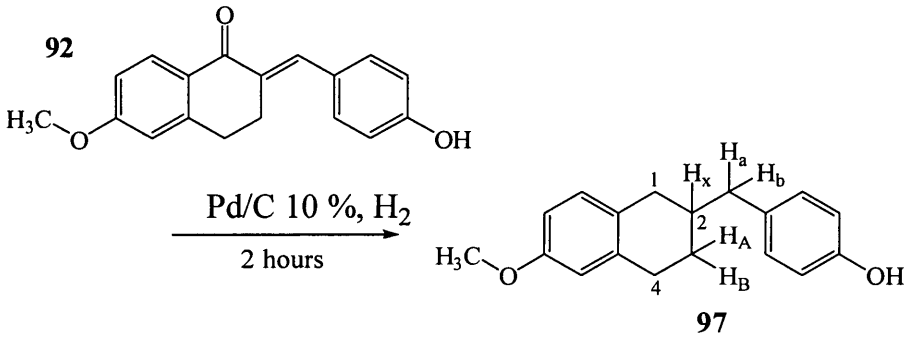

A mixture of 2-[1-(4-hydroxyphenyl)methylidene]-6-methoxy-3,4-dihydro-*2H*-naphthalen-1-one (**91**) (1.0 g, 3.56 mmol) and 10 % palladium on charcoal (75 mg) in methanol (200 mL), was shaken in an atmosphere of hydrogen at room temperature for 2 h. Palladium was removed by filtration over a bed of celite and the filtrate was concentrated *in vacuo* to give 4-[(6-methoxy-3,4-dihydro-2*H*-naphthalenyl)methyl]phenol (**97**), as white solid. Yield: 0.60 g (63 %), t. l. c. system: petroleum ether – ethyl acetate 3:1 v/v, R_F: 0.61, stain positive. Melting point: 84 – 86 °C. Microanalysis ($C_{18}H_{20}O_2$): Calculated C = 80.56 %, H = 7.51 %; Found C = 80.27 %, H = 7.51 %.

^{1}H n.m.r. δ 7.09 (d, J = 8.3 Hz, 2H, Ar), 6.96 (d, J = 8.3 Hz, 1H, H-8), 6.80 (d, J = 8.3 Hz, 2H, Ar), 6.69 (dd, J = 2.6, 8.3 Hz, 1H, H-7), 6.64 (d, J = 2.3 Hz, 1H, H-7), 3.79 (s, 3H, –O-CH_3), 2.78 (m, 3H, –$C\underline{H_2}$-CH_AH_B-CH_x-CH_aH_b-Phenyl and CH_2-CH_AH_B-CH_x-$C\underline{H_a}H_b$-Phenyl), 2.75 – 2.70 (s, br, 1H, OH), 2.61 (d, J = 7.1 Hz, 2H, –$C\underline{H_2}$-1), 2.40 (dd, J = 10.5, 16.1 Hz, 1H, –CH_2-CH_AH_B-CH_x-$CH_a\underline{H_b}$-Phenyl), 2.02 – 1.92 (m, 2H, –CH_2-CH_AH_B-$C\underline{H_x}$-CH_aH_b-Phenyl and –CH_2-$C\underline{H_A}H_B$-CH_x-CH_aH_b-Phenyl), 1.45 (m, 1H, –CH_2-$CH_A\underline{H_B}$-CH_x-CH_aH_b-Phenyl).

^{13}C n.m.r. δ 157.79 (C, C-6), 154.19 (C, C-4'), 138.40 (C, C-4a), 133.41 (C, C-1'), 130.74 (2 x CH, CH-2' and CH-6'), 130.36 (CH, CH-8), 129.48 (C, C-8a), 115.70 (2 x CH, CH-3' and CH-5'), 114.06 (CH, CH-5), 112.42 (CH, CH-7), 55.87 (CH_3, –O-CH_3), 42.47 (CH_2, –CH_2-CH_AH_B-CH_x-$\underline{C}H_aH_b$-Phenyl), 37.10 (CH, $\underline{C}H_x$), 35.62 (CH_2, –$\underline{C}H_2$-1), 29.92 (CH_2, –$\underline{C}H_2$-CH_AH_B-CH_x-CH_aH_b-Phenyl), 29.50 (CH_2, –CH_2-$\underline{C}H_AH_B$-CH_x-CH_aH_b-Phenyl).

Sythesis of saturated 3,4-dihydro-2*H*-naphthalen-1-one (saturated tetralone) derivatives (compound **98** – **104**)

6-(Hydroxy-2-(4-hydroxybenzyl)-3,4-dihydro-*2H*-naphthalen-1-one (98)

($C_{17}H_{16}O_3$, MW: 268.307)

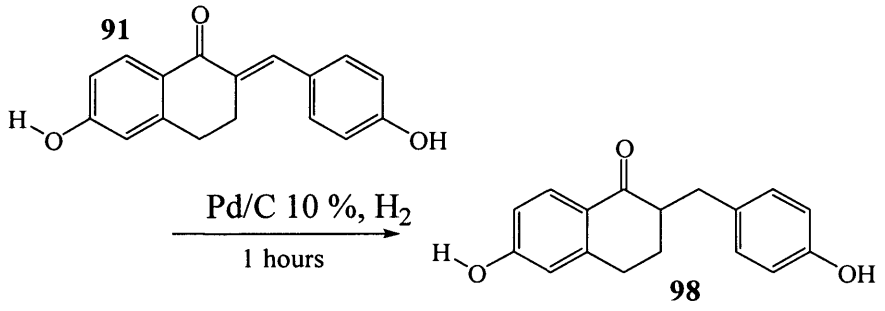

A mixture of 6-hydroxy-2-[1-(4-hydroxyphenyl)methylidene]-3,4-dihydro-*2H*-naphthalen-1-one (**92**) (0.50 g, 1.88 mmol) and 10 % palladium on charcoal (50 mg) in methanol (150 mL), was shaken in an atmosphere of hydrogen at room temperature for 1 hour. Palladium was removed by filtration over a bed of celite and the filtrate was concentrated *in vacuo* to give yellow syrup which was fractionated on a column of dry silica with dichloromethane – methanol 100:0 v/v increasing to 97:3 v/v. The fraction was evaporated to give crude white fluffy solid. The white fluffy solid was then triturated with acetone to give 6-(hydroxy-2-(4-hydroxybenzyl)-3,4-dihydro-2*H*-naphthalen-1-one (**98**) as a light brown solid. Yield: 30 mg (6 %), t. l. c. system: petroleum ether – ethyl acetate 1:1 v/v, R_F: 0.05, stain positive. Microanalysis ($C_{17}H_{16}O_3$.): Calculated C = 76.10 %, H = 6.01 %; Found C = 76.18 %, H = 6.07 %. Melting point: 189 – 191 °C.

^{1}H n.m.r. (DMSO-d_6) δ 10.27 (s, br, 1H, OH), 10.22 (s, br, 1H, OH), 7.80 (d, J = 8.6 Hz, 1H, H-8), 7.02 (d, J = 8.4 Hz, 2H, H-3' and H-5'), 6.74 (dd, J = 2.4, 8.6 Hz, 1H, H-7), 6.70 (d, J = 8.4 Hz, 2H, H-2' and H-6'), 6.63 (d, J = 2.4 Hz, 1H, H-5), 3.15 (dd, J = 4.0, 13.2 Hz, 1H, –CH_2-CH_AH_B-CH_x-CH_aH_b-Phenyl), 2.83 (m, 2H, –CH_2-CH_AH_B-CH_x-(C=O)), 2.69-2.59 (m, 1H, –CH_2-CH_AH_B-CH_x-(C=O)), 2.53 (m, 1H, –CH_2-CH_AH_B-CH_x-CH_aH_b-Phenyl), 1.97 – 1.89 (m, 1H, –CH_2-CH_AH_B-CH_x-(C=O)), 1.67 – 1.54 (m, 1H, –CH_2-CH_AH_B-CH_x-(C=O)).

^{13}C n.m.r. (DMSO-d_6) δ 197.51 (C=O), 162.33 (C, C-6), 155.84 (C, C-4'), 147.16 (C, C-4a), 130.43 (2 x CH, CH-2' and CH-6'), 130.26 (C, C-1'), 129.73 (CH, CH-8), 124.71 (C, C-8a), 115.36 (2 x CH, CH-3' and CH-5'), 114.70 (CH, CH-5), 114.45 (CH,

CH-7), 48.63 (CH, $-CH_2-CH_2-\underline{C}H_x-(C=O)$), 34.63 ($CH_2$, $-\underline{C}H_2-CH_2-CH_x-(C=O)$), 28.31 ($CH_2$, $-CH_2-\underline{C}H_2-CH_x-(C=O)$), 27.53 ($CH_2$, $-CH_2-CH_2-CH_x-\underline{C}H_2$-Phenyl).

The following derivatives of saturated 3,4-dihydro-2*H*-naphthalen-1-one (saturated tetralone) (compound **99** – **104**) were prepared using the same general method detailed above.

2-(4-Hydroxybenzyl)-6-methoxy-3,4-dihydro-2*H*-naphthalen-1-one (**99**)

($C_{18}H_{16}O_3$, MW: 280.318)

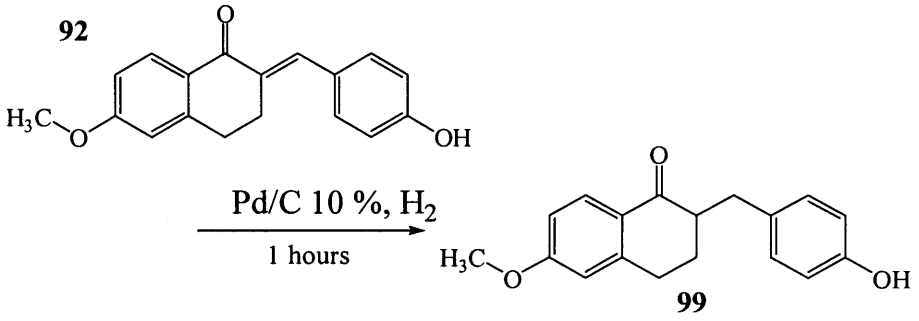

With 2-(4-hydroxybenzyl)-6-methoxy-3,4-dihydro-2*H*-naphthalen-1-one (**99**), a hygroscopic solid was obtained after trituration with acetone. Yield: 0.34 g (57 %), t. l. c. system: petroleum ether – ethyl acetate 1:1 v/v, R_F: 0.30, stain positive. Microanalysis ($C_{18}H_{16}O_3.0.3H_2O$): Calculated C = 75.27 %, H = 6.36 %; Found C = 75.14 %, H = 6.52 %.

^{1}H n.m.r. δ 8.06 (d, J = 8.8 Hz, 1H, H-8), 7.08 (d, 2H, J = 8.4 Hz, Ar), 6.83 (m, 3H, Ar and OH), 6.68 (d, J = 2.3 Hz, 1H, H-7), 6.49 (s, br, 1H, H-5), 3.86 (s, 3H, $-O-CH_3$), 3.37 (dd, J = 3.1, 12.9 Hz, 1H, $-CH_2-CH_AH_B-C\underline{H}_x-(C=O)$), 2.90 (m, 2H, $-CH_2-CH_AH_B-CH_x-C\underline{H}_a\underline{H}_b$-Phenyl), 2.65 (m, 2H, $-C\underline{H}_2-CH_AH_B-CH_x-(C=O)$), 2.17 – 2.04 (m, 1H, $-CH_2-C\underline{H}_AH_B-CH_x-(C=O)$), 1.83 – 1.72 (m, 1H, $-CH_2-CH_A\underline{H}_B-CH_x-(C=O)$).

^{13}C n.m.r. δ 199.78 (C=O), 164.10 (C, C-6), 154.85 (C, C-4'), 147.27 (C, C-4a), 132.02 (C, C-1'), 130.74 (2 x CH, CH-2' and CH-6'), 130.53 (CH, CH-8), 126.40 (C, C-8a), 115.80 (2 x CH, CH-3' and CH-5'), 113.72 (CH, CH-5), 112.94 (CH, CH-7), 55.73 (CH, $-CH_2-CH_2-\underline{C}H_x-(C=O)$), 49.64 ($CH_3$), 35.30 ($CH_2$, $-CH_2-CH_2-CH_x-\underline{C}H_2$-Phenyl), 29.17 ($CH_2$, $-\underline{C}H_2-CH_2-CH_x-(C=O)$), 27.89 ($CH_2$, $-CH_2-\underline{C}H_2-CH_x-(C=O)$).

2-[4-(Dimethylamino)benzyl]-6-hydroxy-3,4-dihydro-*2H*-naphthalen-1-one (100)

($C_{19}H_{21}NO_2$, MW: 295.38)

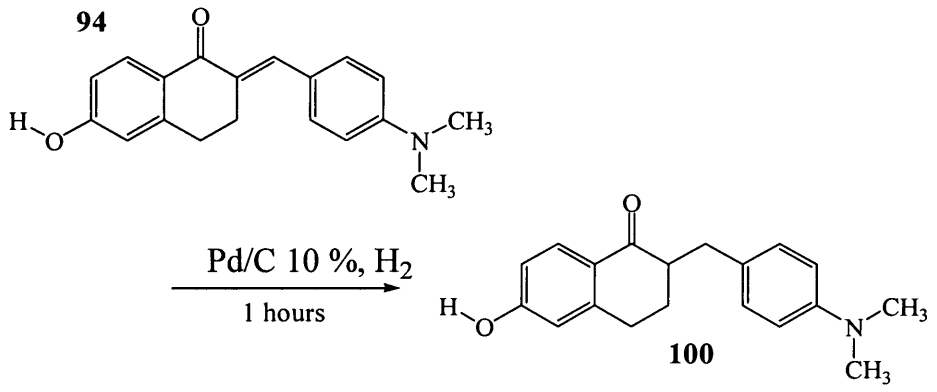

With 2-[4-(dimethylamino)benzyl]-6-hydroxy-3,4-dihydro-*2H*-naphthalen-1-one (**100**), a brown solid was obtained after trituration with acetone. Yield: 42 mg (6 %), t. l. c. system: petroleum ether – ethyl acetate 3:1 v/v, R_F: 0.10, stain positive. Melting point: 200 – 202 °C. Microanalysis ($C_{19}H_{21}NO_2.0.1H_2O$): Calculated C = 76.85 %, H = 7.25 %, N = 4.62 %; Found C = 76.79 %, H = 7.19 %, N = 4.71 %.

^{1}H n.m.r. (DMSO-d_6) δ 10.20 (s, br, 1H, OH), 7.78 (d, J = 8.6 Hz, 1H, H-8), 7.04 (d, J = 8.6 Hz, 2H, H-3' and H-5'), 6.72 (dd, J = 2.4, 8.6 Hz, 1H, H-7), 6.66 (d, J = 8.7 Hz, 2H, H-2' and H-6'), 6.61 (d, J = 2.3 Hz, 1H, H-5), 3.12 (dd, J = 3.7, 13.0 Hz, 1H, –CH_2-CH_AH_B-$C\underline{H}_x$-(C=O)), 2.85 (s, 6H, 2 x CH_3, –N($C\underline{H}_3$)$_2$), 2.81 (m, 2H, –$C\underline{H}_2$-CH_AH_B-CH_x-(C=O)), 2.66 – 2.57 (m, 1H, –CH_2-CH_AH_B-CH_x-$C\underline{H}_aH_b$-Phenyl), 2.54 – 2.49 (m, 1H, –CH_2-CH_AH_B-CH_x-$CH_a\underline{H}_b$-Phenyl), 1.97 – 1.88 (m, 1H, –CH_2-$C\underline{H}_AH_B$-CH_x-(C=O)), 1.66 – 1.55 (m, 1H, –CH_2-$CH_A\underline{H}_B$-CH_x-(C=O)).

^{13}C n.m.r. (DMSO-d_6) δ 197.58 (C=O), 162.31 (C, C-6), 149.26 (C, C-4'), 147.16 (C, C-4a), 129.95 (2 x CH, CH-3' and CH-5'), 129.73 (CH, CH-8), 127.10 (C, C-8a), 124.74 (C, C-1'), 114.69 (CH, CH-7), 114.44 (CH, CH-5), 112.94 (2 x CH, CH-2' and CH-6'), 48.73 (CH, –CH_2-CH_2-$\underline{C}H_x$-(C=O)), 40.70 (2 x CH_3, –N($\underline{C}H_3$)$_2$), 34.50 (CH_2, –CH_2-CH_2-CH_x-$\underline{C}H_2$-Phenyl), 28.29 (CH_2, –$\underline{C}H_2$-CH_2-CH_x-(C=O)), 27.51 (CH_2, –CH_2-$\underline{C}H_2$-CH_x-(C=O)).

2-[2,5-Di(trifluoromethyl)benzyl]-6-methoxy-3,4-dihydro-*2H*-naphthalen-1-one (101)

($C_{20}H_{16}F_6O_2$, MW: 402.330)

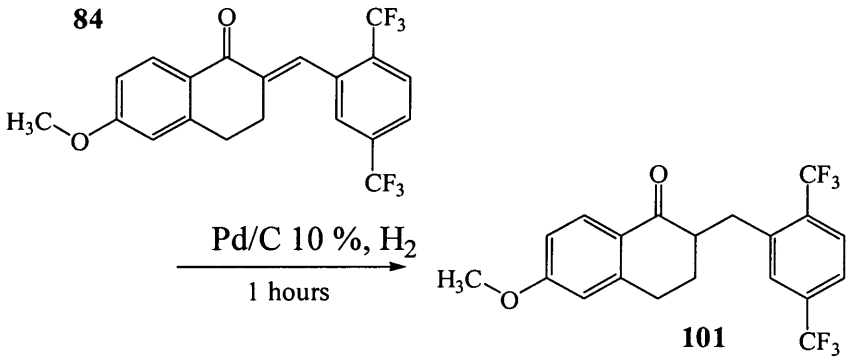

The resulting residue was purified by column chromatography with petroleum ether – ethyl acetate 100:0 v/v increasing to 87.5:12.5 v/v to give white residue with two close spots on t. l. c. plate. The impure compound was further purified using preparative t. l. c. to give 2-[2,5-di(trifluoromethyl)benzyl]-6-methoxy-3,4-dihydro-*2H*-naphthalen-1-one (**101**) as white solid. Yield: 19 mg (6 %), t. l. c. system: petroleum ether – ethyl acetate 1:1 v/v, R_F: 0.72, stain positive. HRMS (ES^+) *m/z* Calculated for $C_{20}H_{16}F_6O_2$ $[M+H]^+$ 403.1127; Found 435.1121. Melting point: 48 – 50 °C.

^{1}H n.m.r. δ 8.05 (d, J = 8.8 Hz, 1H, H-8), 7.80 (d, J = 8.3 Hz, 1H, H-3'), 7.69 (s, 1H, H-6'), 7.60 (d, J = 8.2 Hz, 1H, H-4'), 6.85 (d, J = 2.5, 8.8 Hz, 1H, H-7), 6.68 (d, J = 2.5 H, 1H, H -5), 3.86 (s, 3H, –O-CH_3), 3.82 (m, 1H, –CH_2-CH_AH_B-$C\underline{H}_x$-(C=O)), 2.93 (m, 2H, –CH_2-CH_AH_B-CH_x-$C\underline{H_aH_b}$-Phenyl), 2.87 – 2.74 (m, 2H, –$C\underline{H_2}$-CH_AH_B-CH_x-(C=O)), 2.02 (m, 1H, –CH_2-$C\underline{H_A}H_B$-CH_x-(C=O)), 1.88 (m, 1H, –CH_2-$CH_A\underline{H_B}$-CH_x-(C=O)).

^{13}C n.m.r. δ 197.43 (C=O), 164.07 (C, C-6), 146.65 (C, C-4a), 141.32 (C, C-1'), 134.35, 133.92 (C, C-2'), 130.53 (CH, CH-8), 128.98, 128.93 (CH, CH-6'), 127.47, 127.26 (CH, CH-4'), 126.30, 126.03 (C, C-5'), 125.61 (C, C-8a), 123.68, 123.59 (CH, CH-3'), 122.39 (C, CF_3), 121.99 (C, CF_3), 113.75 (CH, CH-7), 112.89 (CH, CH-5), 55.87 (CH_3), 49.27 (CH, –CH_2-CH_2-$C\underline{H}_x$-(C=O)), 32.82 (CH_2, –CH_2-CH_2-CH_x-$C\underline{H}_2$-Phenyl), 29.83 (CH_2, –$C\underline{H}_2$-CH_2-CH_x-(C=O)), 28.83 (CH_2, –CH_2-$C\underline{H}_2$-CH_x-(C=O)).

6-Methoxy-2-(2-methylbenzyl)-3,4-dihydro-2*H*-naphthalen-1-one (102)

($C_{19}H_{20}O_2$, MW: 280.361)

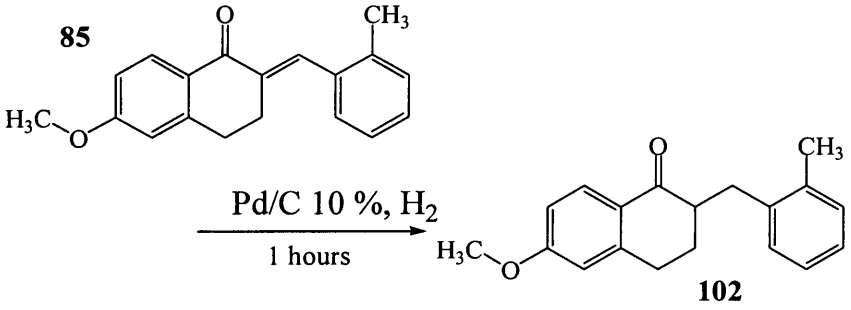

The resulting residue was purified by column chromatography with petroleum ether – ethyl acetate 100:0 v/v increasing to 80:20 v/v to give 6-methoxy-2-(2-methylbenzyl)-3,4-dihydro-2*H*-naphthalen-1-one (**102**) as yellow syrup. Yield: 0.43 g (77 %), t. l. c. system: petroleum ether – ethyl acetate 3:1 v/v, R_F: 0.71, stain positive. Microanalysis ($C_{19}H_{20}O_2.0.1H_2O$): Calculated C = 80.88 %, H = 7.22 %; Found C = 80.98 %, H = 7.07 %.

^{1}H n.m.r. δ 8.07 (d, J = 8.8 Hz, 1H, H-8), 7.15 (m, 4H, Ar), 6.85 (dd, J = 2.5, 8.7 Hz, 1H, H-7), 6.64 (d, J = 2.4 Hz, 1H, H-5), 3.86 (s, 3H, –O-C$\underline{H}_3$), 3.64 (dd, J = 3.4, 13.8 Hz, –CH_2-CH_AH_B-CH_x-C$\underline{H}_a\underline{H}_b$-Phenyl), 2.89 (m, 2H, –C$\underline{H}_2$-CH_AH_B-CH_x-(C=O)), 2.66 (m, 1H, –CH_2-CH_AH_B-C$\underline{H}_x$-(C=O)), 2.53 (dd, J = 10.38, 13.8 Hz, 1H, –CH_2-CH_AH_B-CH_x-$CH_a\underline{H}_b$-Phenyl), 2.36 (s, 3H, CH_3), 2.05 – 2.14 (m, 1H, –CH_2-C$\underline{H}_A$$H_B$-$CH_x$-(C=O)), 1.78 – 1.88 (m, 1H, –CH_2-$CH_A\underline{H}_B$-CH_x-(C=O)).

^{13}C n.m.r. δ 198.66 (C=O), 163.91 (C, C-6), 146.96 (C, C-4a), 138.96 (C, C-1'), 136.92 (C, C-2'), 130.88 (CH, CH-3'), 130.50 (CH, CH-8), 130.43 (CH, CH-6'), 126.68 (CH, CH-4'), 126.56 (C, C-8a), 126.24 (CH, CH-5'), 113.64 (CH, CH-5), 112.87 (CH, CH-7), 55.86 (CH_3, –O-$\underline{C}H_3$), 48.40 (CH, –CH_2-CH_2-$\underline{C}H_x$-(C=O)), 33.45 (CH_2, –$\underline{C}H_2$-CH_2-CH_x-(C=O)), 29.62 (CH_2, –CH_2-$\underline{C}H_2$-CH_x-(C=O)), 28.36 (CH_2, –CH_2-CH_2-CH_x-$\underline{C}H_2$-Phenyl), 19.96 (CH_3).

2-Biphenyl-4-ylmethyl-6-hydroxy-3,4-dihydro-2*H*-naphthalen-1-one (103)

($C_{23}H_{20}O_2$, MW: 328.404)

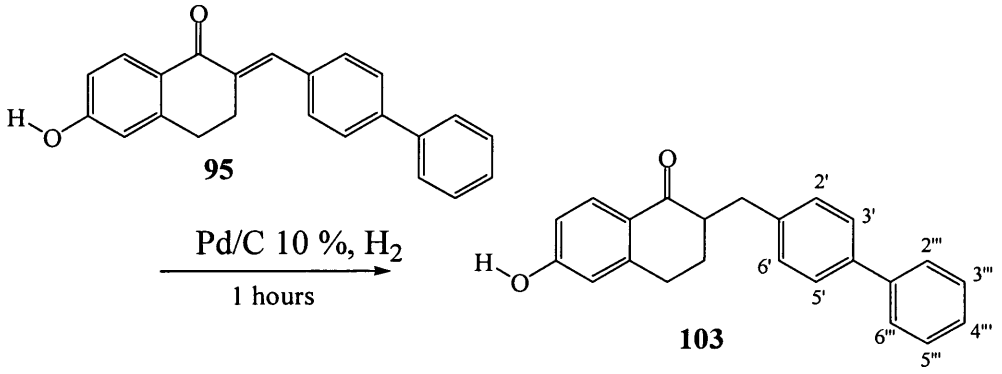

With 2-biphenyl-4-ylmethyl-6-hydroxy-3,4-dihydro-2*H*-naphthalen-1-one (**103**), a white solid was obtained after trituration with methanol. Yield: 0.20 g (63 %), t. l. c. system: petroleum ether – ethyl acetate 1:1 v/v, R_F: 0.32, stain positive. Microanalysis ($C_{23}H_{20}O_2$): Calculated C = 84.12 %, H = 6.14 %; Found C = 84.06 %, H = 6.14 %. Melting point: 220 – 222 °C.

^{1}H n.m.r. (DMSO-d_6) δ 10.45 (s, br, 1H, OH), 7.82 (d, J = 8.6 Hz, 1H, H-8), 7.65 (m, 2H, Ar), 7.58 (m, 2H, Ar), 7.45 (m, 2H, Ar), 7.34 (m, 3H, Ar), 6.74 (dd, J = 2.2, 8.6Hz, 1H, H-7), 6.63 (d, J = 1.9 Hz, H-5), 3.31 (dd, J = 3.9, 13.3 Hz, 1H, –CH_2-CH_AH_B-CH_x-CH_aH_b-Phenyl), 2.88 – 2.74 (m, 2H, –CH_2-CH_AH_B-CH_x-(C=O)), 2.66 (dd, J = 9.2, 13.3 Hz, 1H, –CH_2-CH_AH_B-CH_x-CH_aH_b-Phenyl), 2.51 (m, 1H, –CH_2-CH_AH_B-CH_x-(C=O)), 1.96 (m, 1H, –CH_2-CH_AH_B-CH_x-(C=O)), 1.73 – 1.59 (m, 1H, –CH_2-CH_AH_B-CH_x-(C=O)).

^{13}C n.m.r. (DMSO-d_6) δ 197.29 (C=O), 162.40 (C, C-6), 147.19 (C, C-4a), 140.42 (C, C-1'), 139.81 (C, C-1'''), 138.20 (C, C-4'), 130.11 (2 x CH, phenyl), 129.80 (CH, CH-8), 129.25 (2 x CH, phenyl), 127.54 (CH, CH-4'''), 126.88 (2 x CH, phenyl), 126.85 (2 x CH, phenyl), 124.68 (C, C-8a), 114.75 (CH, CH-5), 114.48 (CH, CH-7), 48.37 (CH, –CH_2-CH_2-CH_x-CH_2-Phenyl), 35.18 (CH_2, –CH_2-CH_2-CH_x-CH_2-Phenyl), 28.46 (CH_2, –CH_2-CH_2-CH_x-(C=O)), 27.83 (CH_2, –CH_2-CH_2-CH_x-(C=O)).

2-Biphenyl-2-ylmethyl-6-hydroxy-3,4-dihydro-2*H*-naphthalen-1-one (104)

($C_{23}H_{20}O_2$, MW: 328.404)

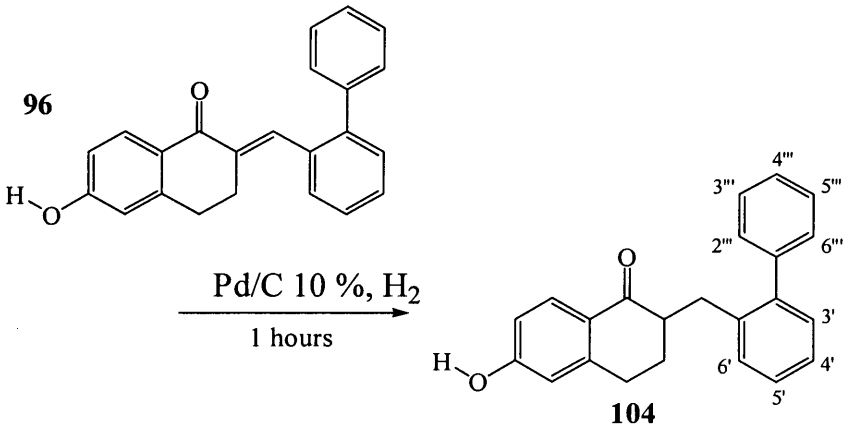

104

The resulting residue was purified by column chromatography with petroleum ether – ethyl acetate 90:10 v/v increasing to 65:35 v/v to give 2-biphenyl-2-ylmethyl-6-hydroxy-3,4-dihydro-2*H*-naphthalen-1-one (**104**) as light brown semi-solid. Yield: 0.50 g (83 %), t. l. c. system: petroleum ether – ethyl acetate 1:1 v/v, R_F: 0.05, stain positive. Microanalysis ($C_{23}H_{20}O_2.0.3H_2O$): Calculated C = 82.76 %, H = 6.22 %; Found C = 82.93 %, H = 6.14 %. Melting point: 38 – 40 °C.

^{1}H n.m.r. δ 8.35 (s, br, 1H, OH), 8.00 (d, J = 8.6 Hz, 1H, H-8), 7.47 – 7.31 (m, 9H, Ar), 6.85 (dd, J = 2.4, 8.6 Hz, 1H, H-7), 6.71 (d, J = 2.3 Hz, 1H, H-5), 3.66 (dd, J = 4.3, 14.0 Hz, 1H, –CH_2-CH_AH_B-CH_x-CH_aH_b-Phenyl), 2.79 (dd, J = 10.7, 14.0 Hz, 1H, –CH_2-CH_AH_B-CH_x-CH_aH_b-Phenyl), 2.71 (m, 2H, –CH_2-CH_AH_B-CH_x-(C=O)), 2.60 (m, 1H, –CH_2-CH_AH_B-CH_x-(C=O), 1.96 – 1.87 (m, 1H, –CH_2-CH_AH_B-CH_x-(C=O)), 1.66 – 1.54 (m, 1H, –CH_2-CH_AH_B-CH_x-(C=O)).

^{13}C n.m.r. δ 200.60 (C=O), 162.05 (C, C-6), 147.97 (C, C-4a), 143.04 (C, C-1'), 142.13 (C, C-2'), 137.88 (C, C-1'''), 130.96 (CH, Ar), 130.78 (CH, Ar), 130.54 (CH, Ar), 129.77 (2 x CH, Phenyl), 128.76 (2 x CH, Phenyl), 128.01 (CH, Ar), 127.48 (CH, Ar), 126.79 (CH, CH-8), 125.66 (C, C-8a), 115.23 (CH, CH-5), 114.99 (CH, CH-7), 48.90 (CH, –CH_2-CH_2-CH_x-(C=O)), 33.33 (CH_2, –CH_2-CH_2-CH_x-(C=O)), 28.97 (CH_2, –CH_2-CH_2-CH_x-(C=O)), 27.91 (CH_2, –CH_2-CH_2-CH_x-CH_2-Phenyl).

CHAPTER 6

Inhibition of vitamin D_3 and all-*trans* retinoic acid metabolism in rat kidney mitochondria and rat liver microsomes

6. Inhibition of vitamin D_3 and all-*trans* retinoic acid metabolism in rat kidney mitochondria and rat liver microsomes

6.1 Vitamin D_3 metabolism study

25-Hydroxyvitamin D_3 (25-(OH)-D_3), synthesised in the liver, is then oxidised in the kidney to:

- 1α,25-dihydroxyvitamin D_3 (1α,25-$(OH)_2$-D_3), the active metabolite, by cytochrome P450 1α-hydroxylase (CYP1α); and
- 24-hydroxyvitamin D_3 (24,25-$(OH)_2$-D_3), inactive metabolite, by cytochrome P450 24-hydroxylase (CYP24). This enzyme can also oxidised the active metabolite 1α,25-$(OH)_2$-D_3 to 1α,24,25-trihydroxyvitamin D_3 (1α,24,25-$(OH)_3$-D_3).

It was found by Omdahl *et al.* (Omdahl *et al.*, 1972) that isolated kidney mitochondria from low calcium-fed animals metabolised 25-(OH)-D_3 to 1α,25-$(OH)_2$-D_3; whereas, those isolated from high calcium-fed animals metabolised 25-(OH)-D_3 to a 24,25-$(OH)_2$-D_3 as identified by Holick *et al.* (Holick *et al.*, 1972).

A few research groups have carried out the investigation of vitamin D_3 metabolism studies in mitochondria of the:

- chick kidney (Burgos-Trinidad *et al.*, 1986; Burgos-Trinidad *et al.*, 1990);
- rat kidney (Ohyama and Okuda, 1991; Vieth and Fraser, 1979; Warner, 1982)
- pig kidney (Araya *et al.*, 2003).

Ohyama *et al.* have developed a method for the purification of 24-hydroxylase from rat kidney mitochondria by solubilising the enzyme from the kidney mitochondria with cholate and then subjected the soluble fraction to the column chromatography (Ohyama *et al.*, 1989; Ohyama *et al.*, 1997; Ohyama and Okuda, 1991).

Since the amino acid sequence of the human (Chen *et al.*, 1993) and rat (Ohyama and Okuda, 1991) CYP24 have been identified, Sakaki's group employed the *Escherichia coli* expression system to reveal CYP24-dependent metabolism of vitamin D_3 in rat (Kusudo *et al.*, 2003; Sakaki *et al.*, 1999) and human (Kusudo *et al.*, 2003; Sakaki *et al.*, 2000).

6.2 All-*trans* retinoic acid metabolism study

The liver is recognised as an important site for P450-mediated oxidation of retinoic acid in the rat (Ahmad *et al.*, 2000). The microsomal cytochrome P450 isozyme system is involved in the 4-hydroxylation of retinoic acid (RA) (Raner *et al.*, 1996). The different P450 isozymes that are able to catalyse the 4-hydroxylation of RA are, for example:

- rat liver P450s 2B1, 2C7 (Leo and Lieber, 1985) and 3A4 (Martini and Murray, 1993)
- rabbit liver P450s 1A2 and 2B4 (Roberts *et al.*, 1992)
- human liver P450s 2C8, 2C9, 3A4 (Leo *et al.*, 1989; McSorley and Daly, 2000; Nadin and Murray, 1999), 3A7 (Marill *et al.*, 2000) and 26 (Ray *et al.*, 1997; White *et al.*, 1997).

The search for the inhibitors of the CYP-mediated metabolism of RA, *i.e.* retinoic acid metabolism blocking agents (RAMBAs) is actively pursued by many research groups. Liarozole and ketoconazole are capable of inhibiting the CYP-dependent metabolism of RA by hamster (Van Wauwe *et al.*, 1990) and rat (Kirby *et al.*, 2003) liver microsomes respectively. The use of human CYP26 expressed in *Candida albicans* and other expression systems has been developed by some research groups to investigate the ATRA metabolism *in vitro* (Chithalen *et al.*, 2002; Stoppie *et al.*, 2000).

6.3 Aims and objectives

The aims of this study were:

- To develop a method for the vitamin D_3 metabolism study and to evaluate the inhibition of vitamin D_3 metabolism using crude mitochondria cytochrome P450s extract from rat kidney.
- To follow on the method described by our group (Ahmad *et al.*, 2000; Kirby *et al.*, 2003) to evaluate the inhibition of ATRA metabolism by the synthesized compounds using microsomal preparations of rat liver.

6.4 Materials and equipments

The following materials and equipments were used in the vitamin D_3 metabolism assay in rat kidney mitochondria and ATRA metabolism assay in rat liver microsomes:

Material/Chemical	Source
25-Hydroxy-[26,27-methyl-^{3}H]-vitamin D_3 (0.925 MBq, 500 μCi)	Amersham Biosciences (Bucks, UK)
25-Hydroxyvitamin D_3	Fluka Chemicals (Dorset, UK)
[^{3}H-11,12]-All trans retinoic acid (9.25 MBq, 250 μCi)	PerkinElmer Life Science Ltd. (Massachusetts, USA)
All-*trans* retinoic acid (ATRA)	Sigma Chemicals (Dorset, UK)
1 % Calcium and Vitamin D_3 special feed	Special Diets Services, Essex, UK
Ketoconazole	Sigma Chemicals (Dorset, UK)
HPLC grade solvents e.g. acetonitrile, methanol. butylated-hydroxyanisole, ethyl acetate, ethanol, ammonium acetate	Fisher Scientific (Leicestershire, UK)
Nicotinamide-adenine dinucleotide phosphate (reduced form) (NADPH) – cofactor	Sigma Chemicals (Dorset, UK)
All buffer (see preparation below)	Aldrich Chemicals, UK
OptiFlow Safe 1 liquid scintillation cocktail	Fisions Chemicals, UK
Borosilicate tubes (12 x 75 mm and 13 x 100 mm)	Corning (New York, USA)

Equipment	Source
Centrifuge	MSE Harrier 18/80, Sanyo, Japan
Ultracentrifuge (high speed 2000 – 64,000 rpm) and centrifuge tubes	Sorvall centrifuge, Dupont, USA
Potter-Elvejhem homogeniser (TRI-R STR-R model S63C) and homogeniser tubes	TRI-R Instruments, Inc., USA
10 μm C_{18} μBondapak® 3.9 x 300 mm column	Waters, UK
5 μm ODS EXSIL® 4.6 x 200 mm column	Jones Chromatography, UK
Beta-RAM online scintillation detector	LKB Wallace 1217 Rackbeta
Pump	Milton-Roy
Water bath with shaker	Grant, UK
Rotating evaporator	Christ Alpha RVC (Germany)
Computer	Compaq™
Laura data acquisition and analysis software	Lablogic Ltd.

- *Preparation of 25-hydroxy-[26,27-methyl-^{3}H]-vitamin D_3 stock solution*

  50 µL of 0.5 mM 25-hydroxyvitamin D_3 in EtOH was diluted with 850 µL of ^{i}PrOH:EtOH 1:1 v/v. To this was added 100 µL of 25-hydroxy[26,27-methyl-^{3}H]-vitamin D_3 (0.925 MBq, 500 µCi).

  - 1 mL of the above stock solution contains 100/500 x 0.925 MBq = 0.185 MBq.
  - 10 µL of the stock solution contains 0.01 µCi x 0.185 MBq/0.037 MBq = 0.05 µCi.

- *Preparation of [^{3}H-11,12]-all-trans retinoic acid stock solution*

  100 µL of 1.2 mM ATRA in EtOH was diluted with 900 µL of ^{i}PrOH:EtOH 1:1 v/v. To this was added 10 µL of [^{3}H-11,12]-ATRA(9.25 MBq, 250 µCi).

  - 1 mL of the above stock solution contains 10/250 x 9.25 MBq = 0.37 MBq.
  - 10 µL of the stock solution contains 0.01 µCi x 0.37 MBq/0.037 MBq = 0.10 µCi.

- *Preparation of phosphate buffer (50 mM, pH 7.4)*

  To prepare 1000 mL of phosphate buffer (50 mM, pH 7.4), 6.68 g of disodium hydrogen orthophosphate dehydrate was dissolved in 750 mL of water and 1.95 g of monosodium dihydrogen orthophosphate dihydrate was dissolved in 250 mL of water. This mixture was then titrated to pH 7.4 with aqueous NaOH (5 M). To prepare 500 mL of phosphate/sucrose buffer (250 mM), 42.75 g of sucrose made up to 500 mL with phosphate buffer prepared above.

- *Preparation of Tris-acetate buffer (15 mM, pH 7.4)*

  To prepare 1000 mL of 15 mM Tris-acetate buffer, 1.82 g TRIS (tris(hydroxymethyl)methylamine) was dissolved in 1000 mL of water and titrated to pH 7.4 with 5 M aqueous acetic acid. To prepare 500 mL of Tris-acetate/sucrose buffer (250 mM), 42.75 g of sucrose made up to 500 mL with Tris-acetate buffer prepared above.

6.5 Pharmacological preparation of the rat kidney mitochondria and rat liver microsome

The pharmacological preparation of the rat kidney mitochondria for the study of 25-hydroxyvitamin D_3 metabolism was based on a modification of the procedures described by DeLuca's group (Burgos-Trinidad *et al.*, 1986).

Whereas, the pharmacological preparation of the rat liver microsome for the study of all-*trans* retinoic acid metabolism was based on the assay previously set up by our group (Ahmad *et al.*, 2000; Kirby *et al.*, 2003).

6.5.1 Method for the preparation of the rat kidney mitochondria

1. Three male Wistar rats (250 g) were bought in from Harlan and were fed with calcium and vitamin D replete diet (calcium carbonate was added to the feed to achieve a 1 % calcium level and vitamin D_3 was added to achieve 2200 iu/kg in the feed). The rats were fed for two weeks to reach the weight of 300 g.
2. The rats were killed by cervical dislocation, and the kidneys were removed. The kidneys were washed with ice-cold phosphate buffer (50 mM, pH 7.4) containing 0.25 mM sucrose, to remove excess blood. The kidney was stored in the – 80 °C freezer for 5 days.
3. The kidney was defrosted in ice-cold Tris-acetate buffer (15 mM, pH 7.4) with 0.25 mM sucrose. The connective tissues were removed and the buffer was drained off.
4. The kidney was cut in to smaller pieces using scissors. The tissues were homogenized with four times their weight of Tris-acetate buffer (15 mM, pH 7.4). The Potter-Elvejhem homogeniser was used by moving the pestle up and down to create a uniform, stable emulsion (the homogenate). [**NOTE**: Do not move the pestle up and down more than four times, to minimise degradation of tissue enzymes.] The homogenising tube was immersed in an ice bucket at all times.
5. The above homogenate was decanted into centrifuge tubes and the homogenate was then centrifuged at 2000 rpm for 20 min at 3 °C to remove nuclei and cell debris. The supernatant was retained.
6. The pellet from **5** was resuspended in the sucrose medium and was centrifuged at 2000 rpm for 20 min at 3 °C.

7. The supernatant from **5** and **6** above were combined and centrifuged at 10, 000 rpm for 20 min at 3 °C.
8. The supernatant was decanted and the pellet containing the mitochondria was washed with the sucrose medium and resuspended in ice-cold 20 % glycerol and 15 mM Tris-acetate pH 7.4, containing 0.6 % sodium cholate.
9. This 20 % w/w homogenate was stirred on ice for 1 h and the homogenate was centrifuged at 12, 000 rpm for 1 h.
10. Aliquots of the above supernatant were placed into 1.5 mL capped eppendorfs and snapped frozen in liquid N_2 and stored in a – 80 °C freezer.

6.5.2 Method for the preparation of the rat liver microsome

1. Three male Wistar rats (275 g) were bought in from Harlan.
2. The rats were killed by cervical dislocation, and the livers were removed. The livers were washed with ice-cold phosphate buffer (50 mM, pH 7.4) containing 0.25 mM sucrose, to remove excess blood. The connective tissues were removed and the buffer was drained off.
3. The liver was cut in to smaller pieces using scissors. The tissues were homogenized with four times their weight of the above ice-cold phosphate buffer. The Potter-Elvejhem homogeniser was used by moving the pestle up and down to create a uniform, stable emulsion (the homogenate). [**NOTE**: Do not move the pestle up and down more than four times, to minimise degradation of tissue enzymes.] The homogenising tube was immersed in an ice bucket at all times.
4. The above homogenate was decanted into the centrifuge tubes and the homogenate was then centrifuged at 12000 rpm for 20 min at 3 °C. The pellet (solid at the bottom of the centrifuge tube which contains unwanted connective tissues, cell membranes, *etc.*) was discarded.
5. The above supernatant was centrifuged at 37, 000 rpm for 1h at 3 °C.
6. The supernatant was decanted and the pellet containing the microsome was washed with the sucrose medium and resuspended in ice-cold phosphate buffer (50 mM, pH 7.4) and homogenised with the Potter-Elvejhem homogeniser.
7. Aliquots of the above homogenate were placed into 1.5 mL capped eppendorfs and snapped frozen in liquid N_2 and stored in a – 80 °C freezer.

6.6 General assay for the inhibition studies of vitamin D_3 in rat kidney mitochondria and all-*trans* retinoic acid in rat liver microsome

The procedures for the general assay for the metabolism of vitamin D_3 and all-*trans* retinoic acid are summarised in the following steps. The experiments were performed in duplicate:

1. 10 μL of the [^{3}H]-25-(OH)-D_3 or [^{3}H-11,12]-ATRA stock solution was added to each test tube.
2. 10 μL ethanol or acetonitrile as control or synthesised compound (at various concentrations) was added to each test tube.
3. All test tubes were diluted with phosphate buffer (50 mM, pH 7.4) to make up the final volume, after addition of enzyme and co-factor, of 500 μL.
4. Enzyme which was stored at – 80 °C was defrosted prior to use. 30 μL of rat kidney mitochondria or 20 μL of rat liver microsomes was added to each test tube.
5. NADPH (16 mM, 50 μL, in pH 7.4 phosphate buffer) was added to each test tube and vortexed.
6. The reaction mixture was incubated in a shaking water bath at 37 °C.
7. After 30 mins, the reaction was stopped by the addition of 100 μL 2 % acetic acid, and the mixture was extracted from 2 mL of ethyl acetate containing butylated-hydroxyanisole 0.05 %.
8. The top organic layer was removed, and then evaporated to dryness.
9. The residue left in the test tube was redissolved in 60 μL methanol, and then subjected to HPLC analysis.

6.6.1 Set up of the high performance liquid chromatography (HPLC)

The assay used was to measure the effect of the novel compounds on the rate of conversion of radiolabelled 25-hydroxyvitamin D_3 or all-*trans* retinoic acid to their respective metabolites.

The HPLC system was equipped with a high pressure pump (Milton-Roy pump), injector with a 50 μL loop connected to a beta-RAM radioactivity detector, connected to a Compaq™ computer running Laura® data acquisition and analysis software. This enabled on-line detection and quantification of radioactive peaks. The 5 μm ODS EXSIL® 4.6 x 200 mm column (for vitamin D_3 assay) or 10 μm C_{18} μBondapak® 3.9 x 300 mm column (for ATRA assay) operating at room temperature was used to separate

the metabolites which were eluted with 750 mL acetonitrile/250 mL 1 % ammonium acetate in water/1 mL acetic acid at a flow rate of 1.5 mL/min (for vitamin D_3 assay) or 1.9 mL/min (for ATRA assay).

6.7 Biological results and discussions

6.7.1 Metabolism of vitamin D_3 in rat kidney mitochondria

The special diet which were fed to the male Wistar rats has enhanced the activity of the metabolism of [^{3}H]-25-(OH)-D_3. In the control set up, 40 ± 5 % of [^{3}H]-25-(OH)-D_3 was converted into metabolites by using 30 µL of the crude enzyme of the special diet rats (section **6.5.1**). Compared to 20 ± 8 % of [^{3}H]-25-(OH)-D_3 was converted into metabolites using 50 µL of the crude enzyme in normal diet rats. This result was similar to the observation by Warner (Warner, 1982).

The HPLC separation of the [^{3}H]-25-(OH)-D_3 metabolites were based on a modification of the method described by Kang *et al.* (Kang *et al.*, 1997). The three possible metabolites of 25-(OH)-D_3 metabolism in rat kidney mitochondria are 1α,25-$(OH)_2$-D_3, 24,25-$(OH)_2$-D_3 and 1α,24,25-$(OH)_3$-D_3 (Ohyama *et al.*, 1997; Warner, 1982). Due to the high cost of the radiolabelled metabolites, the 25-(OH)-D_3 metabolites were identified by matching their elution rate to the retention time of the known standards, 1α,25-$(OH)_2$-D_3, 24,25-$(OH)_2$-D_3 and 1α,24,25-$(OH)_3$-D_3, (generous gifts from Dr. L. Binderup, Leo Pharma, Denmark) by using a photodiode array detector to monitor UV absorption at 265 nm [**Figure 6.1** (**C**)]. Following the same conditions described in **Figure 6.1** (**A**), known standards of the vitamin D_3 metabolites were injected into the HPLC and the elution order detected by photodiode array detector is 1α,24,25-$(OH)_3$-D_3 (retention time: 2.5 min); 24,25-$(OH)_2$-D_3 (retention time: 3.8 min); 1α,25-$(OH)_2$-D_3 (retention time: 4.5 min) followed by 25-(OH)-D_3 (retention time 10.5 min) [**Figure 6.1** (**C**)].

The separated [^{3}H]-metabolites were quantitatively calculated from the areas under the curves. The approximate percentage metabolites of the individual [^{3}H]-metabolites of 25-(OH)-D_3 are as following:

- 20 % of [^{3}H]-1α,24,25-$(OH)_3$-D_3
- 10 % of [^{3}H]-24,25-$(OH)_2$-D_3
- 10 % of [^{3}H]-1α,25-$(OH)_2$-D_3

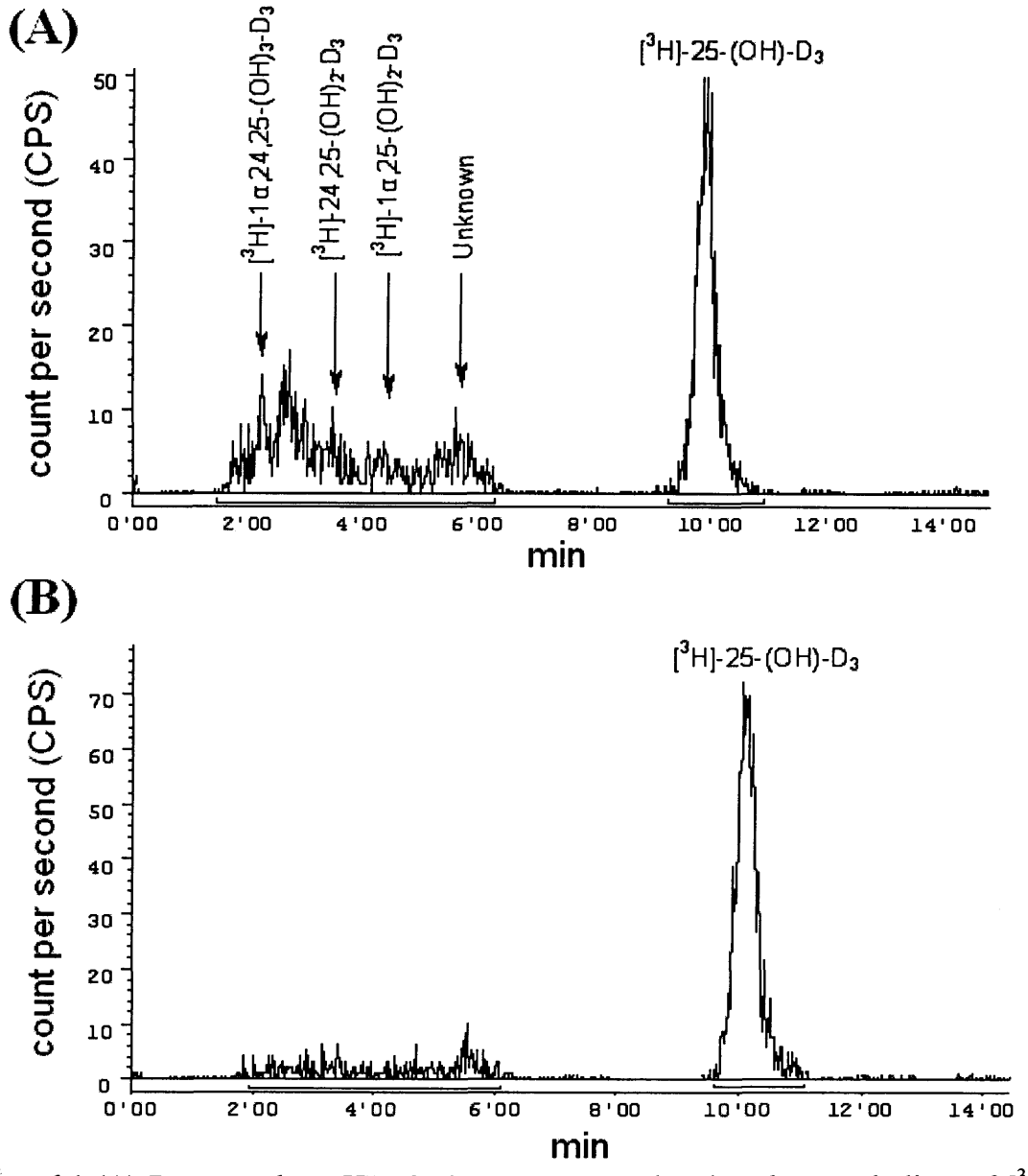

Figure 6.1 (**A**) Reverse-phase HPLC chromatograms showing the metabolism of [^{3}H]-25-(OH)-D_3 in the presence of (**A**) rat kidney mitochondria and ethanol with NADPH. 35 ± 5 % of [^{3}H] 25-(OH)-D_3 was converted into metabolites by using 30 µL of the crude kidney mitochondria enzyme from rats fed with special diet. (**B**) Same as (**A**) but with 100 µM ketoconazole. HPLC column: 5 µm ODS EXSIL® 4.6 x 200 mm; Mobile phase: 75:25:0.1 = acetonitrile:1 % w/v ammonium acetate in water:acetic acid at a flow rate of 1.5 mL/min. Retention time for [^{3}H]-25-(OH)-D_3 = 10.5 min.

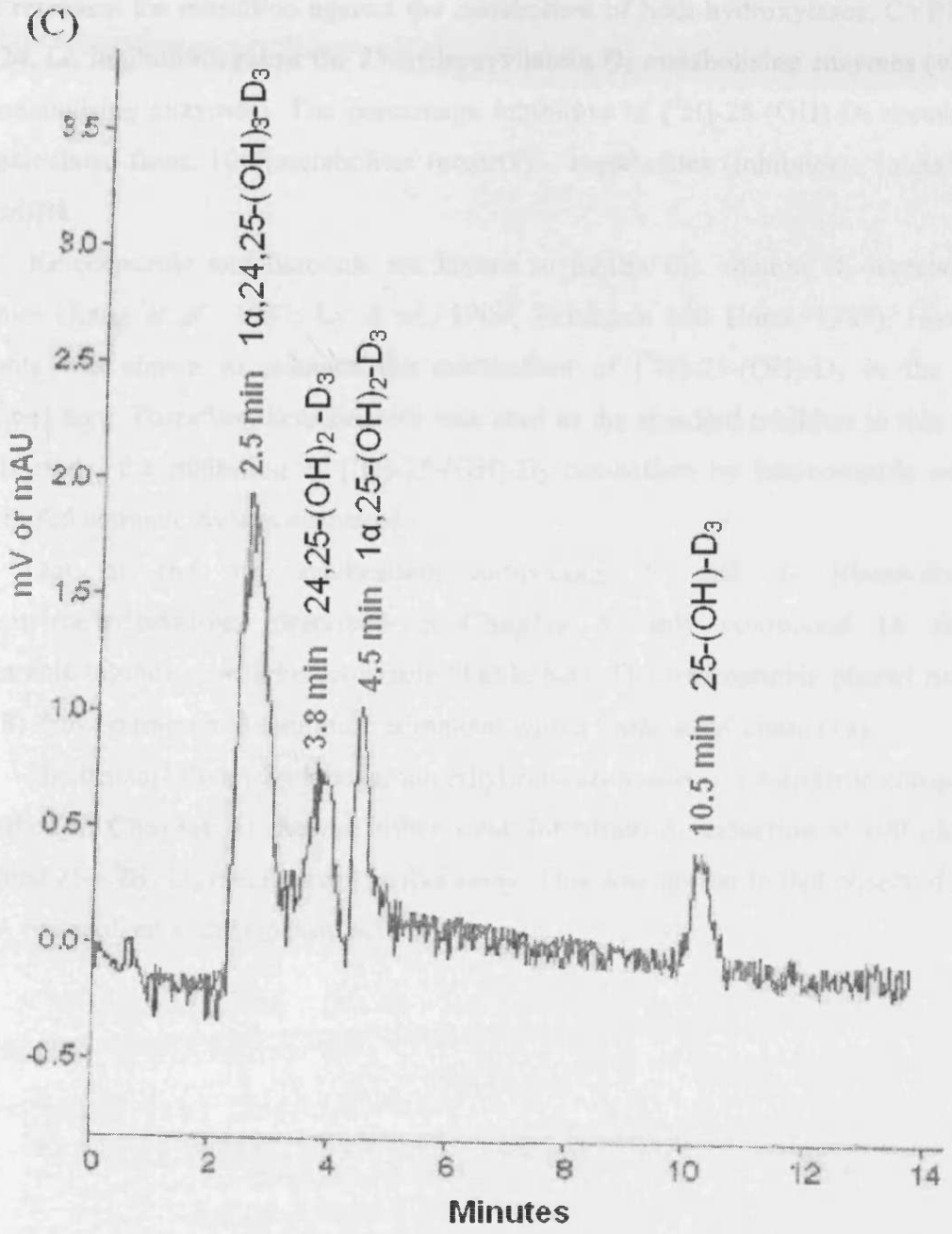

Figure 6.1 (**C**) The retention time of approximately 10 μM of the vitamin D_3 metabolites, 1α,25-$(OH)_2$-D_3, 24,25-$(OH)_2$-D_3, 1α,24,25-$(OH)_3$-D_3, and 25-(OH)-D_3 by using a photodiode array detector to monitor UV absorption at 265 nm. Column: 5 μm ODS EXSIL® 4.6 x 200 mm; Mobile phase: 75:25:0.1 = acetonitrile:1 % w/v ammonium acetate in water:acetic acid at a flow rate of 1.5 mL/min.

Ideally, the synthesised compounds should be more selective against CYP24 than CYP1α, as CYP24 is responsible for metabolism of the biologically active hormone, 1α,25$(OH)_2D_3$. Due to the low level of the individual metabolites, it was not possible to study the inhibition against the specific hydroxylases enzymes, CYP1α and CYP24 present in the rat kidney mitochondria. Therefore the IC_{50} values reported in **Table 6.1**

– **6.2** represent the inhibition against the metabolism of both hydroxylases, CYP1α and CYP24, *i.e.* inhibition against the 25-hydroxyvitamin D_3 metabolising enzymes (vitamin D_3 metabolising enzymes). The percentage inhibition of [^{3}H]-25-(OH)-D_3 metabolism was calculated from: 100[(metabolites (control) – metabolites (inhibitor) / (metabolites control)]%.

Ketoconazole and liarozole are known to inhibit the vitamin D_3 metabolising enzymes (Kang *et al.*, 1997; Ly *et al.*, 1999; Reinhardt and Horst, 1989). However, liarozole was shown to enhance the metabolism of [^{3}H]-25-(OH)-D_3 in the assay described here. Therefore, ketoconazole was used as the standard inhibitor in this assay. In this study, the inhibition of [^{3}H]-25-(OH)-D_3 catabolism by ketoconazole and the synthesised compounds was evaluated.

Out of the six synthesised compounds 1- and 4- [(benzofuran-2-yl)phenylmethyl]triazoles described in **Chapter 3**, only compound **16** showed comparable inhibition with ketoconazole (**Table 6.1**). The hydrophobic phenyl ring (**16** and **18**) showed improved inhibition compared with a linear alkyl chain (**14**).

The benzo[*b*]furan-2-carboxamidoethyl-imidazole and -1,2,4-triazole compounds (described in **Chapter 4**) showed either weak inhibition or induction at 100 μM (*i.e.* enhanced 25-(OH)-D_3 metabolism) in this assay. This was similar to that observed in the ATRA metabolism assay (section **6.7.2**).

Table 6.1. Inhibition of 25-(OH)-D_3 metabolism using rat kidney mitochondria homogenate. The IC_{50} values were the mean of two experiments (± 5 %). These values for inhibition of [^{3}H]-25-(OH)-D_3 metabolism were measured using 0.5 μM 25-(OH)-D_3 with 0.05 μCi [^{3}H]-25-(OH)-D_3 as substrate.

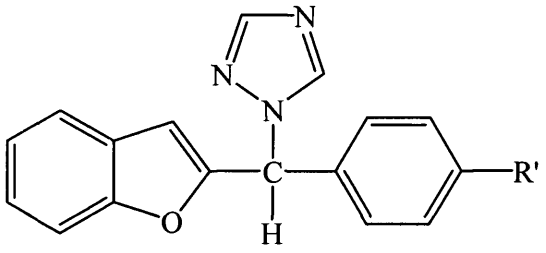

(14) R' = CH_2CH_3
(16) R' = Phenyl
(18) R' = Phenyl-Cl

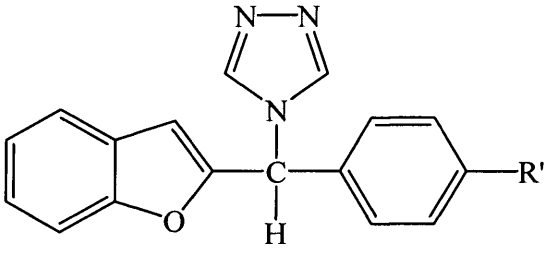

(15) R' = CH_2CH_3
(17) R' = Phenyl
(19) R' = Phenyl-Cl

Compound	IC_{50} (μM)
14	> 100
15	> 100
16	10 – 20
17	> 50
18	20 – 40
19	> 50
Ketoconazole	20

The saturated form of the 6-substituted-2-(phenylmethylene)-3,4-dihydro naphthalene-1-one derivatives (**Box 6.1**) showed good inhibition compared with the standard inhibitor, ketoconazole (**Table 6.2**).

The saturated tetralone and tetralin compounds show greater inhibition activity compared with the unsaturated tetralone. The rigid structure of the unsaturated tetralone could affect the flexibility of the compound to interact with the enzyme active site. Among the saturated tetralone compounds, **102** and **104** showed better inhibition against the vitamin D_3 metabolising enzymes. From here, we can predict that there may be a hydrophobic pocket at the second position of the phenyl ring. By comparing compound **97**, **98** and **99**, it tells us that:

- a methoxy group at the 6-position of the tetralone, might be indicative of a hydrophilic interaction between the inhibitor and the enzyme at this position
- the oxo group in position-1 of the tetralones is not essential for P450 inhibitor activity.

Box 6.1

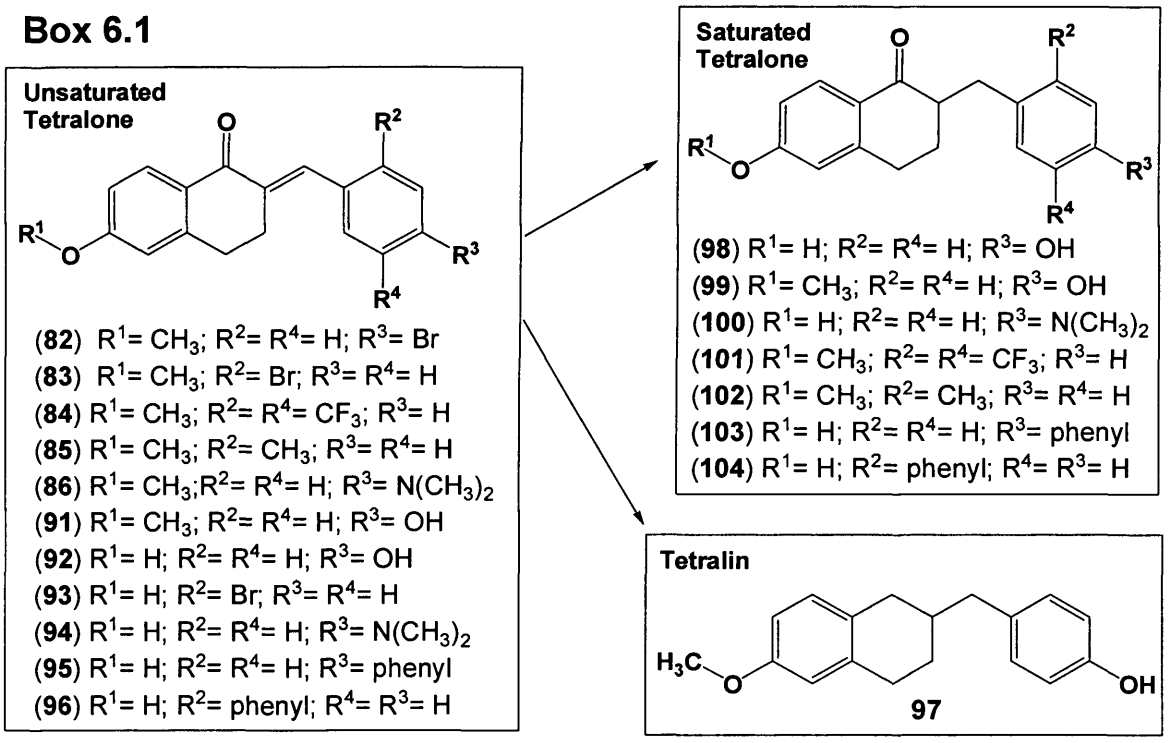

Table 6.2. Inhibition of 25-(OH)-D_3 metabolism using rat kidney mitochondria homogenate. The IC_{50} values were the mean of two experiments. These values for inhibition of [^{3}H]-25-(OH)-D_3 metabolism were measured using 0.5 μM 25-(OH)-D_3 with 0.05 μCi [^{3}H]-25-(OH)-D_3 as substrate and was determined from dose-response curves (Yee and Simons, 2004).

Compound	IC_{50} (μM)
All unsaturated tetralone	> 20
98	8.9
99	3.5
100	18
101	4.5
102	0.9
103	0.8
104	2.1
97	2.6
Ketoconazole	20

6.7.2 Metabolism of all-*trans* retinoic acid in rat liver microsome

Figure 6.2 (**A**) shows a representative chromatogram of the radioactivity profile obtained by HPLC analysis of metabolites of [^{3}H]-ATRA metabolism in rat liver microsome. ATRA was converted into two prominent metabolites, mainly the 4-keto-ATRA (retention time: 1.5 min) and 4-hydroxy-ATRA (retention time: 2.5 min) and other polar metabolites which eluted at the same positions as the two prominent metabolites. This result was in agreement with the previous results reported by our group (Mason, 2000). The separated [^{3}H]-metabolites were quantitatively calculated from the areas under the curves. The percentage inhibition was calculated from: 100[(metabolites (control) – metabolites (inhibitor)/(metabolites control)]%. Typically in a control set up, 60 ± 10 % of [^{3}H]-ATRA was converted into metabolites.

The synthesised compounds 1- and 4-[(benzo[*b*]furan-2-yl)phenylmethyl]triazoles (**Chapter 3**) showed poor activity (IC_{50} > 100 μM). Moreover, the synthesised compounds benzo[*b*]furan-2-carboxamidoethyl-imidazole and -1,2,4-triazole (**Chapter 4**) either showed weak inhibition or induction at 100 μM (*i.e.* enhanced ATRA metabolism) in this assay. In addition, liarozole which is a well-known inhibitor against retinoic acid metabolism (Freyne *et al.*, 1998), showed induction of ATRA metabolism in this assay, which was also observed by another group (Stoppie *et al.*, 2000). Therefore, ketoconazole was used as the standard inhibitor in this assay.

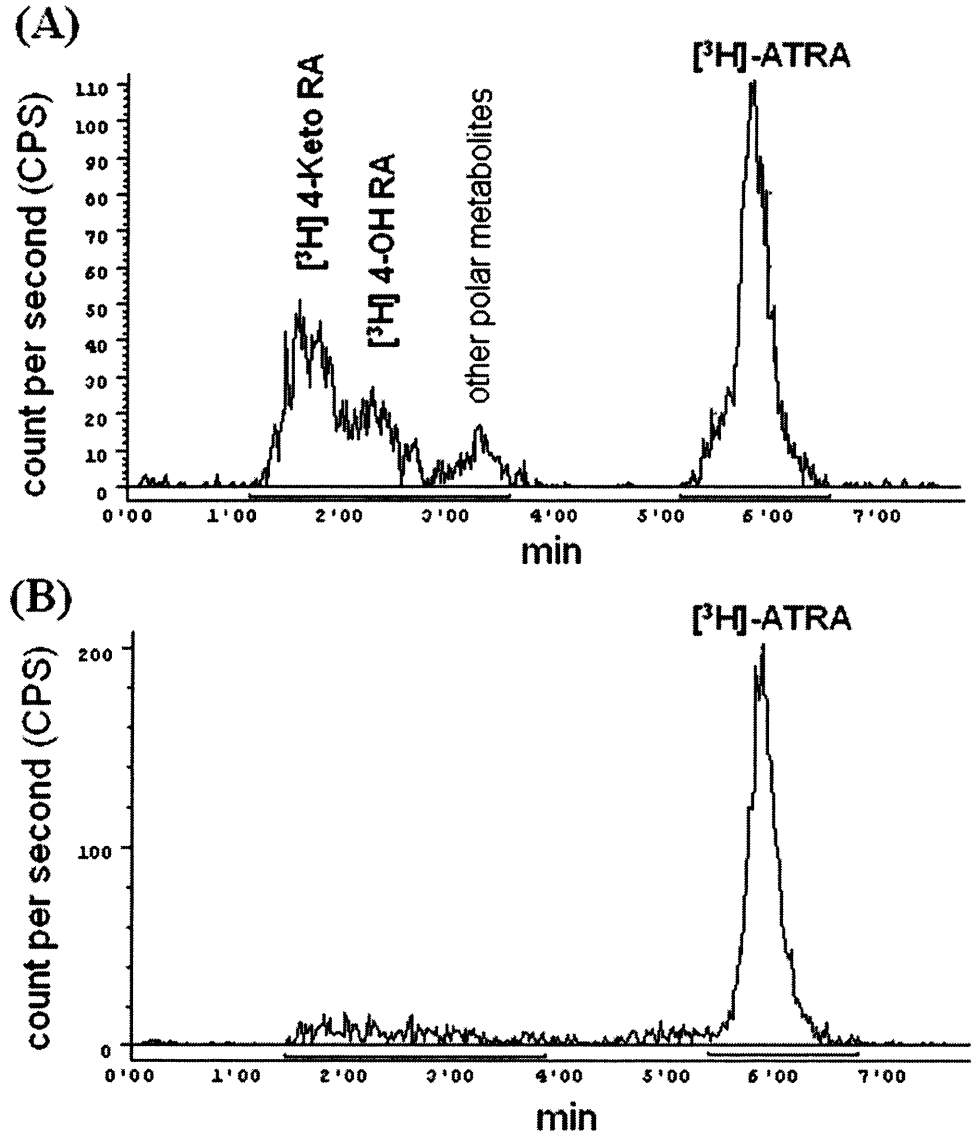

Figure 6.2. Reverse-phase HPLC chromatograms showing the metabolism of [^{3}H]-ATRA in the presence of (**A**) liver microsomes and acetonitrile with NADPH and (**B**) liver microsomes and 100 μM ketoconazole with NADPH. Column: 10 μm C_{18} μBondapak® 3.9 x 300 mm; Mobile phase: 75:25:0.1 = acetonitrile:1 % w/v ammonium acetate in water:acetic acid at a flow rate of 1.9 mL/min. Retention time of [^{3}H]-ATRA = 5.5 min.

The synthesised compounds of the 6-substituted-2-(phenylmethylene)-3,4-dihydro naphthalene-1-one derivatives (**Chapter 5**), as summarised in **Box 6.1**, were evaluated for inhibition of ATRA metabolism (**Table 6.3**).

Generally, the reduced tetralone compounds and tetralin showed improved inhibition of ATRA metabolism (except for **101**) compared with the unsaturated tetralone compounds (IC_{50}> 20 μM) and ketoconazole (IC_{50} = 18 μM). The tetralin compound (**97**) also showed comparable inhibition result with the saturated tetralone.

Table 6.3. Inhibition of ATRA metabolism in rat liver microsome. The IC_{50} values were mean of two experiments. These values for inhibition of ATRA metabolism were measured using 2.4 μM ATRA with 0.1 μCi [^{3}H]-ATRA as substrate and were determined from dose-response curves (Yee *et al.*, 2005).

Compound	IC_{50} (μM)
93	2.4
All unsaturated tetralone except 93	> 20
98	1.5
99	0.4
100	1.2
101	18
102	1.8
103	> 20
104	0.5
97	2.2
Ketoconazole	18

6.8 General conclusions

A novel method to study the metabolism of [^{3}H]-25-(OH)-D_3 using crude enzyme from rat kidney mitochondria has been developed. An on-line radioactivity detector and reverse-phase HPLC was used to analyse the [^{3}H]-25-(OH)-D_3 metabolites. The limitation of this assay is that it only allows the study of inhibition of both vitamin D_3 metabolising enzymes, CYP1α and CYP24 rather than the individual enzymes, as the level of metabolites formed from CYP1α and CYP24 are insufficient to allow determination of the IC_{50} against each enzyme.

The preparation of rat liver microsomes to evaluate the inhibition of ATRA metabolism by the synthesised compounds was carried out with slight modifications from the methods described earlier from our group (Kirby *et al.*, 2003).

Generally, the synthesised reduced tetralone compounds and tetralin showed improved inhibition compared with ketoconazole against the ATRA and 25-(OH)-D_3 metabolism, as summarised in **Table 6.4**. The *in vitro* evaluation of the tetralone compounds and tetralin revealed that compounds **97**, **99**, **102** and **104** exhibited good inhibition against both ATRA and 25-(OH)-D_3 metabolism. This showed that a hydroxyl

group at the 4-position and a hydrophobic group at the 2-position of the phenyl ring form hydrophilic interaction and hydrophobic interactions respectively at both the enzyme active sites.

The methods described above for the inhibition studies of the 25-(OH)-D_3 or ATRA metabolising enzymes are more rapid and facile assays in identifying potential inhibitors compared with the inhibition studies carried out using intact cell-lines or using yeast or bacterial cell systems that expressed specific enzyme.

Table 6.4. The IC_{50} of the tetralone, tetralin and ketoconazole compounds against ATRA metabolism by rat liver microsome and against 25-(OH)-D_3 metabolism by rat kidney mitochondria.

Compound	Inhibition of 25-(OH)-D_3 metabolism IC_{50}, μM	Inhibition of ATRA metabolism IC_{50}, μM
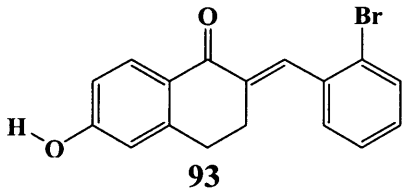 **93**	>100	2.4
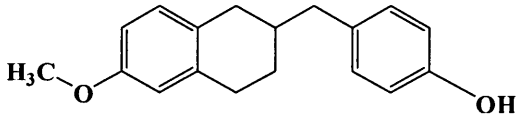 **97**	**2.6**	**2.2**
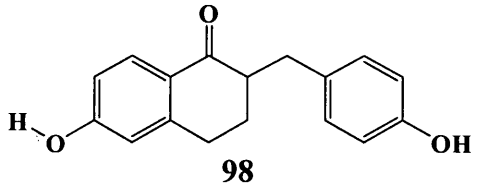 **98**	8.9	1.5
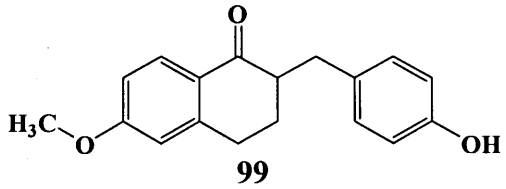 **99**	**3.5**	**0.4**

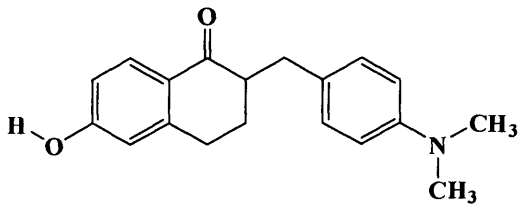 **100**	18.0	1.2
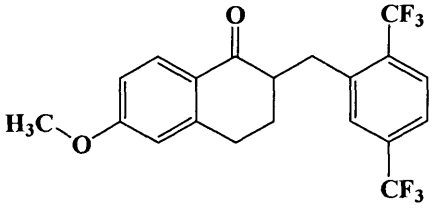 **101**	4.5	18
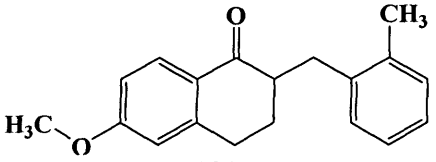 **102**	**0.9**	**1.8**
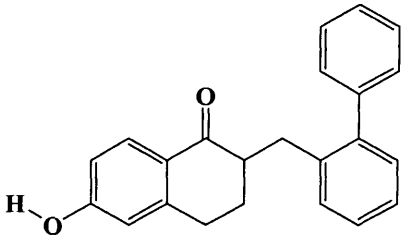 **104**	**2.1**	**0.5**
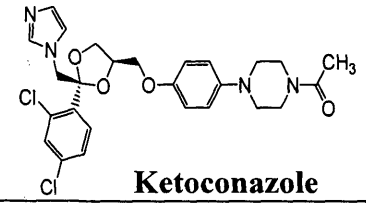 **Ketoconazole**	20.0	18.0

CHAPTER 7

In vitro cell culture studies of vitamin D_3 and all-*trans* retinoic acid metabolism

7. *In vitro* cell culture studies of vitamin D_3 and all-*trans* retinoic acid metabolism

1α,25-$(OH)_2$-D_3 and ATRA have been shown to have pro-differentiation and anti-proliferation effects in both breast cancer and prostate cancer cell lines, namely the MCF-7, LNCaP, PC-3 and DU-145 cell lines (Campbell *et al.*, 1997; Campbell *et al.*, 1998; de Vos *et al.*, 1997; Guo *et al.*, 2002; Guo *et al.*, 2000; James *et al.*, 1995; Koshiuka *et al.*, 2000; Krekels *et al.*, 1997; Wang *et al.*, 2001).

In vitro cell line studies of 25-(OH)-D_3 and ATRA metabolism have been studies by various groups, to name a few examples:

- The use of human keratinocytes for vitamin D_3 metabolism (Kang *et al.*, 1997; Schuster *et al.*, 2001a; Schuster *et al.*, 2001b).
- The use of human colon cancer cells (Bareis *et al.*, 2001) and human non-small cell lung cancer cells (Jones *et al.*, 1999) for vitamin D_3 metabolism.
- The use of prostate cancer cells (DU-145, PC-3 and LNCaP) for the vitamin D_3 or all-*trans* retinoic acid metabolism (Farhan *et al.*, 2002; Farhan *et al.*, 2003; Guo *et al.*, 2002).
- The use of breast cancer cells (MCF-7, T47D) for the ATRA metabolism (Krekels *et al.*, 1997; Patel *et al.*, 2004; Van heusden *et al.*, 2002).
- The use of microsomal preparations from T47D breast cancer cells induced to express CYP26 enzyme (Mulvihill *et al.*, 2005; Stoppie *et al.*, 2000).

7.1 Aims and objectives

DU-145 and MCF-7 cell lines were chosen for the studies of *in vitro* metabolism of 25-(OH)-D_3 and ATRA. The MCF-7 cell line was routinely cultured at the Tenovus Cancer Research Centre at the Welsh School of Pharmacy. Whereas, DU-145 cell line was kindly donated by Dr. Moray J. Campbell (Institute of Biomedical Research, University of Birmingham) and cultured at the Tenovus Cancer Research Centre.

The aims of these studies were:

- To establish the methods and to investigate the metabolism of 25-(OH)-D_3 and ATRA in DU-145 and MCF-7 cell-lines.
- To evaluate the inhibition of 25-(OH)-D_3 and ATRA metabolism by the synthesized compounds using this *in vitro* cell culture based assay.

- To compare the metabolism of 25-(OH)-D_3 and ATRA in the two cell-lines with the metabolism of 25-(OH)-D_3 and ATRA in the rat kidney mitochondria and rat liver microsomes respectively.

7.2 Overview

7.2.1 Tissue culture

The equipments and materials used in tissue culture are as following:

Disposable materials used in tissue culture	Source
Sterile disposable pipettes (1 mL, 5 mL and 10 mL)	Corning (New York, USA)
Sterile syringe (1 mL and 10 mL)	Becton Dickinson (BD®) UK Ltd.
25 mL Universal tube	L.I.P. (Equipment and Services Ltd.)
Sterile needles (BD microbalance™ 25 G 0.5 x 16 mm or 23 G 0.6 x 25 mm)	Becton Dickinson UK Ltd.
Tissue culture plates (6 wells) and flasks (25 cm^2 and 72 cm^2)	Corning (New York, USA)

Media and supplements	Source
Tissue culture media (RPMI 1640, RPMI 1640 phenol red-free)	All from Gibco Europe Ltd. (Paisley, Scotland)
0.25 % Trypsin-EDTA	
Streptomycin/Penicillin	
Fungizone	
Foetal calf serum (FCS)	
L-glutamine	

Chemicals and Equipment	Source
Trypan blue	Sigma Chemical (Dorset, UK)
Phosphate Buffer Saline (PBS) tablets (50 mM, pH 7.4)	Sigma Chemical (Dorset, UK)
Class II biological safety cabinet	(Sorvall, Kendro Laboratory Products, Germany)
Incubator (37 °C, 5 % CO_2)	Sanyo (Japan)
Haemocytometer	Neubauer (Germany)
Phase contrast microscope	Leitz Wetzlar (Germany)
Liarozole and R115866	Gift from Stiefel Laboratories, High Wycombe, UK

7.2.2 Cell-lines used

The two cell lines used in this research were:

1. The oestrogen responsive MCF-7 human mammary-carcinoma cell line which is oestrogen receptor-positive. This cell line is also known as the wild-type MCF-7 cell line. This cell was routinely grown in phenol-red free RPMI medium (wRPMI), supplemented with 5 % (v/v) steroid-depleted foetal calf serum (S-FCS), antibiotics (streptomycin and penicillin) and fungizone at the same concentration of 10 iU/mL.

Note: Phenol-red has been shown to have oestrogenic properties. Therefore MCF-7 cells were cultured in the absence of unwanted oestrogenic factors by using phenol-red free RPMI. In addition, it is necessary to grow the cells in the absence of steroid with the steroid-depleted foetal-calf serum (S-FCS).

2. The DU-145 human prostate cancer cell line which is androgen receptor-negative. This cell was routinely grown in RPMI medium, supplemented with 10 % (v/v) foetal calf serum (FCS), antibiotics (streptomycin and penicillin) and fungizone at the same concentration of 10 iU/mL.

7.2.3 Methods of tissue culture

7.2.3.1 Cells passaging

The MCF-7 and DU-145 cells were routinely cultured in 75 cm^2 sterile flasks. Cells were passaged approximately every 5 – 7 days when the cells in the flasks reached confluency. Cells passaging were carried out as follows:

1. The medium in the flask was removed by an aspirating pump.
2. The monolayer was washed with PBS and was then removed.
3. 2 mL of trypsin (0.25 % trypsin-EDTA) was added to allow the cells in the flask to detach. Trypsin should not be left in the flask for longer than 5 minutes.
4. When cells were detached, 8 mL of the medium was added to the flask. The mixture was then transferred into a 25 mL universal tube and centrifuged at 1000 rpm for 5 min at room temperature.
5. The supernatant was removed by an aspirating pump.
6. The cells (pellet) were resuspended in 10 mL of medium by pipetting through a 10 mL sterile disposable pipette until no cell lumps could be seen.

7. 1 mL of the cell suspension above was seeded in 15 mL medium in a 75 cm^2 culture flask.
8. The culture flask was then kept in an incubator (5 % CO_2 at 37 °C) until needed.

7.2.3.2 Settting up of cells for vitamin D_3 and all-*trans* retinoic acid metabolism studies

The MCF-7 and DU-145 cell lines were seeded at 3 x 10^6 cells and 1.5 x 10^6 cells per well-plate (12 wells) respectively. MCF-7 cells are smaller in size compared with DU-145. Each of the cell lines was set up as follows:

1. The medium in the 75 cm^2 culture flask was removed by an aspirating pump and replaced by 2 mL of trypsin (0.25 % trypsin-EDTA).
2. When cells were detached (no longer than 5 minutes), 8 mL of medium was added to the flask. The mixture was then transferred into a 25 mL universal tube and centrifuged at 1000 rpm for 5 min at room temperature.
3. The supernatant was removed by an aspirating pump.
4. The cells (pellet) were resuspended in 10 mL of medium and were aspirated through a 10 mL sterile syringe attached to a 25 G 0.5 x 16 mm needle (for DU-145 a 23 G 0.6 x 25 mm needle was used instead) and then the cells were pushed through so that the cells could be separated from each other rather than forming clumps of cells when seeded on the well-plates.
5. A viable cell count was performed using a haemocytometer.
6. An adequate volume containing the appropriate number of cells needed was then mixed with the medium and seeded in the well-plates.

7.3 General assay for metabolism of vitamin D_3 and all-*trans* retinoic acid in cell based assay

The materials and equipments used in the general assay of vitamin D_3 and ATRA metabolism in cell culture were the same as described in section **6.4**.

7.3.1 Methods

The methods described below were based on a modification of the method of Jarno (Jarno, 2003) and Kirby *et al.* (Kirby *et al.*, 2003).

1. The MCF-7 cell lines were seeded at 3 x 10^6 cells per well (12 wells) in the medium and left to settle for 24 h. The DU-145 cell line was seeded at 1.5 x 10^6 cells per well (12 wells) in the medium and left to settle for 48 h.

2. After 24 h, the medium of the wild-type MCF-7 cells were removed and washed with 1 mL of PBS before being replaced by fresh medium plus various treatments.
3. After 48 h, the medium of the DU-145 cells were removed and washed with 1 mL of PBS before being replaced by the medium plus various treatments.
4. These treatments in each well contained either cold 25-hydroxyvitamin D_3 (10^{-8} M) plus 0.05 μCi 25-hydroxy-[26,27-methyl-^{3}H]-vitamin D_3 or ATRA (10^{-7} or 10^{-8} M) plus 0.10 μCi [^{3}H-11,12]-ATRA plus control (ethanol or acetonitrile) or inhibitor.
5. Tissue culture plates were wrapped in aluminum foil during the incubation time to prevent metabolism of the substrate.
6. Each treatment was performed in duplicate.
7. The incubation with the respective substrate was stopped by the addition of 2 % v/v acetic acid (100 μL/well).
8. The medium and acetic acid from each well was then removed and transferred to borosilicate glass tubes (13 x 100 mm) which contained 2 mL solution of ethyl acetate with 0.05 % (w/v) butylated-hydroxyanisole.
9. Distilled water (200 μL) was subsequently added to each well plate and the cells were scrapped off using the rubber end of a 1 mL syringe insert.
10. The cell suspension from each tube was transferred to the respective glass tubes.
11. Finally, each well was rinsed with distilled water (400μL) and then transferred to the respective glass tubes.
12. The glass tubes were centrifuged (3000 rpm for 15 min at room temperature).
13. The top organic layer containing the substrate and metabolites was transferred into respective borosilicate glass tubes (12 x 75 mm).
14. The medium was re-extracted with 2 mL of ethyl acetate with 0.05 % (w/v) butylated-hydroxyanisole. Steps **12** and **13** above were then repeated.
15. The tubes were placed in a rotating evaporator for 50 – 60 min.
16. The residue in each tube was redissolved in 60 μL methanol, then analysed using an on-line radioactive detector connected to a HPLC as described before under section **6.61**.

7.4 Biological results and discussions

7.4.1 Metabolism of vitamin D_3 in MCF-7 and DU-145 cell-lines

After 3, 12 or 24 h incubation time, the peaks for the [^{3}H]-25-(OH)-D_3 metabolites were not significant in both cell lines. Attempt to incubate the cells with 10^{-8} M 1α,25-$(OH)_2D_3$ to enhance the level of CYP24 enzyme was carried out. After 12 – 48 h of pre-incubation time with 1α,25-$(OH)_2D_3$, the medium was removed and replaced with 25-hydroxyvitamin D_3 (10^{-8} M) plus 0.05 μCi 25-hydroxy-[26,27-methyl-^{3}H]-vitamin D_3 in medium. The cells were then incubated for another 3, 12 or 24 h. However, the peaks for the [^{3}H]-25-(OH)-D_3 metabolites were not significant (less than 15 % 25-(OH)-D_3 metabolites) in both cell lines. This could be due to the absence of the hydroxylase enzymes in the cells which resulted in the absence of 25-(OH)-D_3 metabolites.

A RT-PCR (reverse-transcriptase polymerase chain reaction) analysis was carried out, as described in **chapter 8.2**, to identify the presence of CYP24 mRNA. Since high level of CYP24 mRNA was expressed in DU-145 cells as shown in the PCR (see **chapter 8.2**), another method was tried to investigate the metabolism of 25-(OH)-D_3 in DU-145 cells based on the modification of various literatures (Bareis *et al.*, 2001; Ma *et al.*, 2004; Miller *et al.*, 1995). DU-145 cells at approximately 80 % confluence were trypsinised to detach the cells from a 75 cm^2 sterile flask. 1 x 10^6 cells in 200 μL of RMPI + 1 % FBS media were transferred into 12 x 75 mm borosilicate glass tubes. To each glass tube was added 1 μM 25-(OH)-D_3 plus 0.05 μCi 25-hydroxy-[26,27-methyl-^{3}H]-vitamin D_3 with or without inhibitor prior to the addition of 1 x 10^6 cells/200μL medium. The glass tubes were then incubated for 30 min at 37 °C in a shaking water bath. The reaction was stopped by adding 620 μL of chloroform:methanol (1:2) into each glass tubes. After each glass tubes was vortexed, the tubes were left standing at room temperature for 45 min. The tubes were then centrifuged at 1000 rpm for 15 min. The supernatant was then transferred into respective glass tubes containing 200 μL of chloroform and 100 μL of distilled water. After vortexing, the tubes were centrifuged at 1000 rpm for 15 min. The lower organic phase was transferred into another clean glass tube, whereas the water phase was re-extracted with 200 μL chloroform. The combined organic phases in the tubes were placed in a rotating evaporator for 20 min. The percentage of the peaks for the 25-(OH)-D_3 metabolites were 25 – 28 % in the absence of inhibitor (**Figure 7.1A**), compared with 10 – 11 % metabolites in the presence of the

inhibitor, (50 μM of compound **99**) (**Figure 7.1B**). The inhibition studies of the 25-(OH)-D_3 metabolisms using the synthesised compounds were not carried out due to the low amount of metabolites in the control.

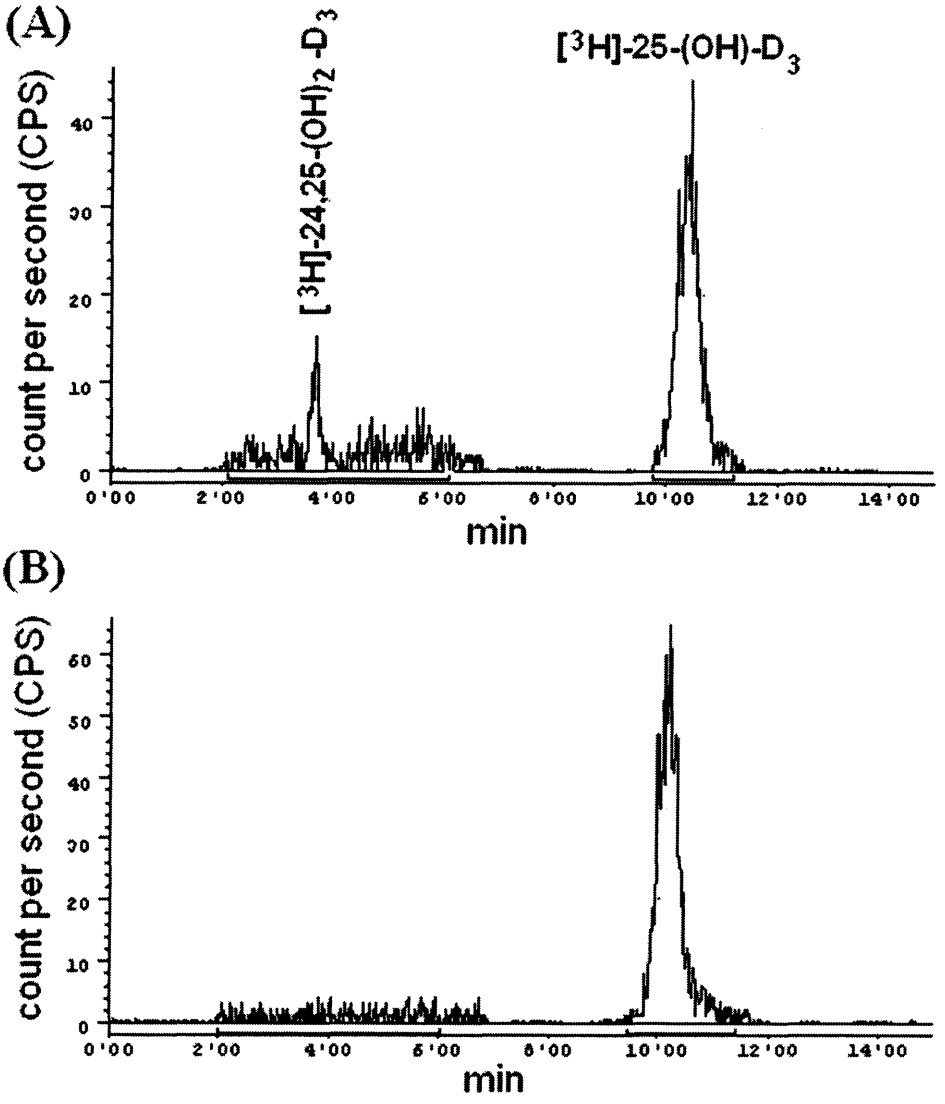

Figure 7.1 (**A**) Reverse-phase HPLC chromatograms showing the metabolism of [^{3}H] 25-(OH)-D_3 in the presence of (**A**) suspension of DU-145 cells in RPMI and 1 % FBS medium (control) (**B**) suspension of DU-145 cells in RPMI and 1 % FBS medium plus 50 μM compound **99**. Column: 5 μm ODS EXSIL® 4.6 x 200 mm; Mobile phase: 75:25:0.1 = acetonitrile:1 % w/v ammonium acetate in water:acetic acid at a flow rate of 1.5 mL/min. Retention time for [^{3}H] 24,25-(OH)-D_3 = 3.8 min, [^{3}H] 25-(OH)-D_3 = 10.5 min.

7.4.2 Metabolism of all-*trans* retinoic acid in MCF-7 cell-line

After 9 h incubation time, approximately 60 ± 10 % [^{3}H]-ATRA was metabolised in the MCF-7 cell-line (**Figure 7.2**). Addition of 100 µM liarozole reduced the metabolism of all-trans retinoic acid to 13 % in the wild-type MCF-7 cells. This result was consistent with the result reported by Jarno (Jarno, 2003).

A RT-PCR analysis was carried out, as described in **section 8.2**, to identify the presence of CYP26A1 isozyme. CYP26A1 is only present after MCF-7 cells are induced with 10^{-7} M ATRA for 9 hours. This shows that this MCF-7 cell based assay is more relevant being a measure of human ATRA metabolism by the specific CYP26A1 enzyme.

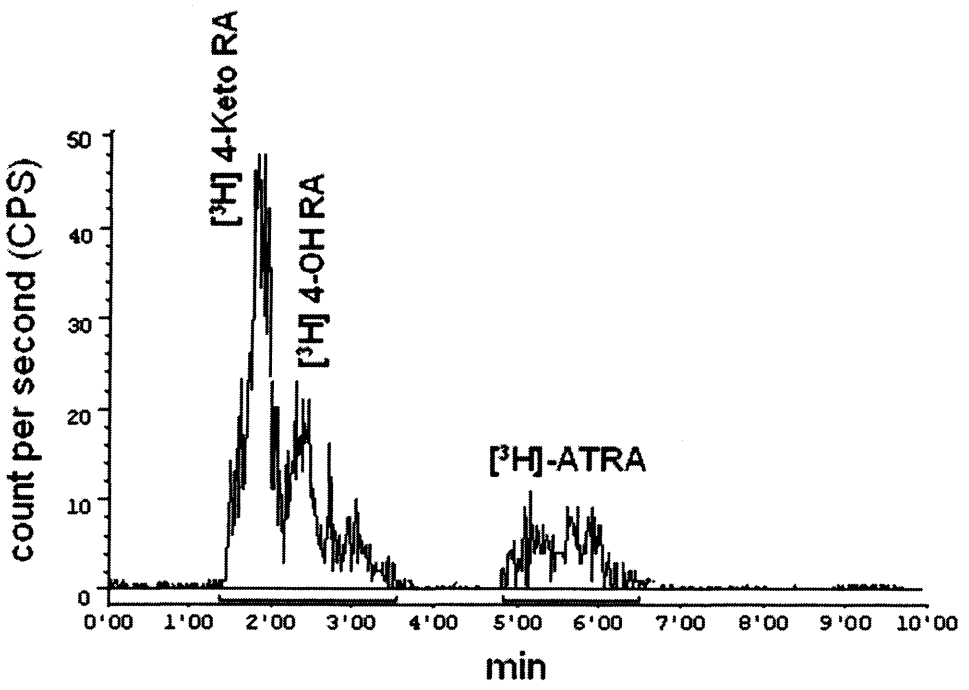

Figure 7.2. HPLC of an incubation extract of 10^{-7} M all-*trans* retinoic acid plus 0.1 µCi [^{3}H-11,12] all-*trans* retinoic acid with MCF-7 cell-line. HPLC column: 10 µM C18 µBondapak© 300 x 3.9 mm column; mobile phase: 75:25:1 = Acetonitrile: 1 % w/v ammonium acetate in water: acetic acid. Pump rate: 1.9 mL/min. Retention time: 4-keto-retinoic acid and 4-hydroxy-retinoic acid (1.5 min – 3.5 min) and all-trans retinoic acid (5.5 min).

7.4.2.1 Inhibition of all-*trans* retinoic acid metabolism in MCF-7 cell-line

Inhibition of ATRA metabolising enzyme in MCF-7 cells was studied using the synthesised compounds described in **chapter 3 – 5**. Ketoconazole, liarozole and the selective CYP26 inhibitor, R115866, were used as the standard inhibitors. The IC_{50} of the inhibition of ATRA metabolising enzyme in the MCF-7 cell line are illustrated in **Table 7.1 – 7.4**. The IC_{50} values were the mean of two experiments. These values for inhibition of ATRA metabolism was measured using 10^{-7} M ATRA with 0.1 μCi [^{3}H]-ATRA as substrate.

Table 7.1. Inhibition of ATRA metabolising enzyme in MCF-7 cells.

Compound	IC_{50}	Compound	IC_{50}
14 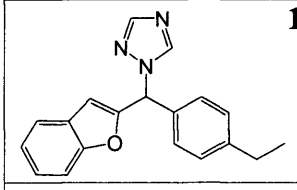	4.5 μM	**15** 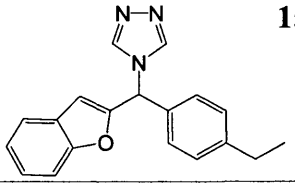	5 μM
16 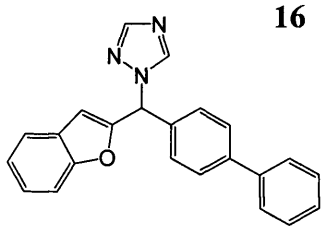	7 μM	**17** 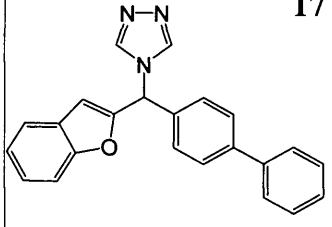	9 μM
18 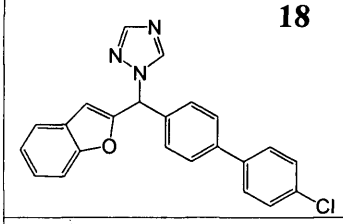	20 – 40 μM	**19** 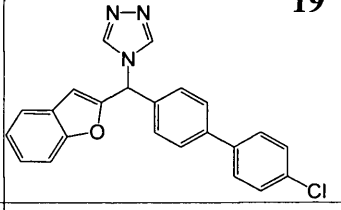	20 – 40 μM
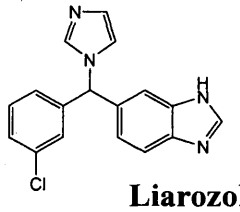 **Liarozole**	7 μM	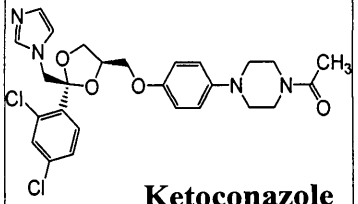 **Ketoconazole**	10 – 20 μM
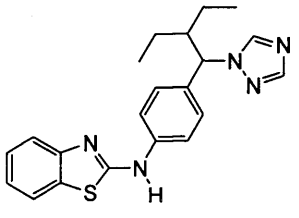 **R115866**	0.005 μM		

Table 7.2. Inhibition of ATRA metabolising enzyme in MCF-7 cells.

Compound	IC_{50}
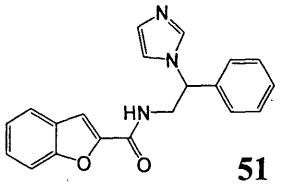 **51**	25 – 50 μM
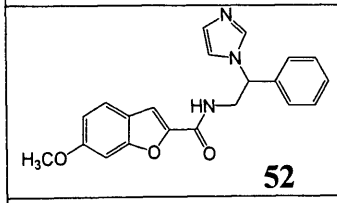 **52**	10 – 20 μM
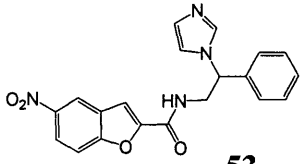 **53**	25 – 50 μM
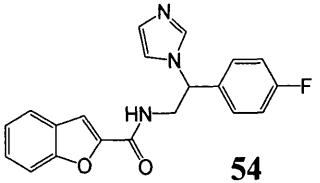 **54**	25 – 50 μM
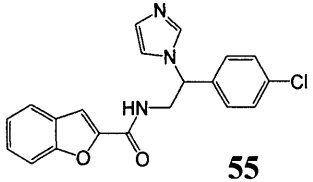 **55**	10 – 20 μM

Compound	IC_{50}
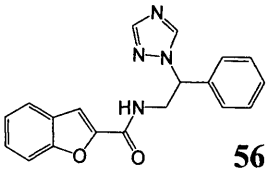 **56**	> 100 μM
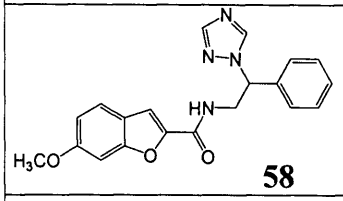 **58**	50 – 100 μM
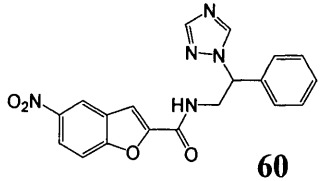 **60**	> 100 μM
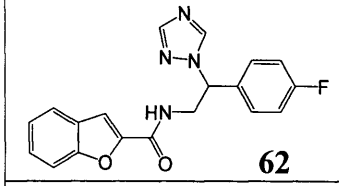 **62**	50 – 100 μM
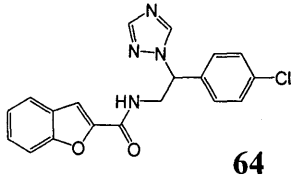 **64**	25 – 50 μM

Compound	IC_{50}
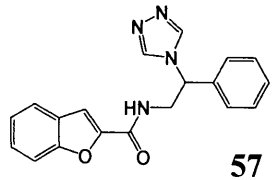 **57**	> 100 μM
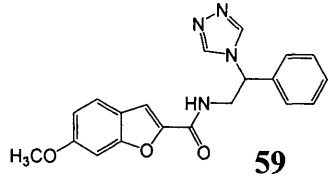 **59**	50 – 100 μM
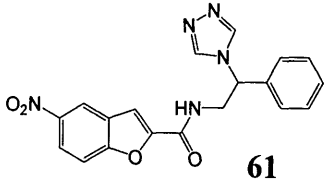 **61**	> 100 μM
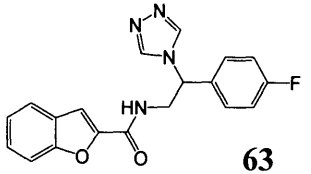 **63**	> 100 μM
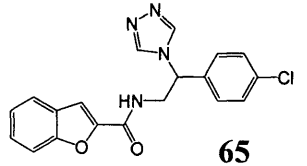 **65**	50 – 100 μM

Table 7.3. Comparing the unsaturated and saturated tetralone compounds for inhibition of ATRA metabolising enzyme in MCF-7 cells (Yee *et al.*, 2005).

Compound (Unsaturated tetralone)	IC_{50}	Compound (Saturated tetralone)	IC_{50}
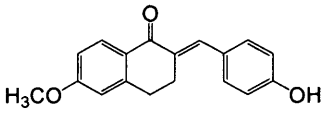 **91**	7 μM	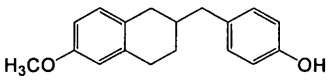 **97**	25 – 50 μM
		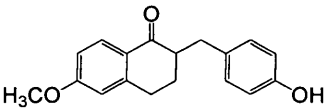 **99**	5 μM
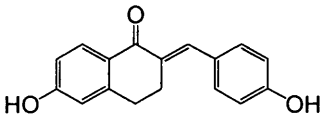 **92**	9 μM	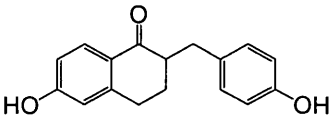 **98**	20 – 40 μM
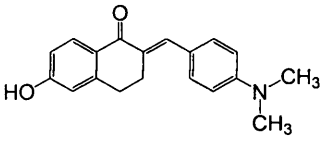 **94**	50 – 100 μM	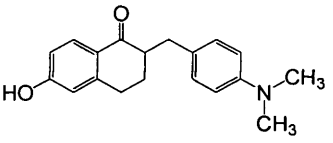 **100**	25 – 50 μM
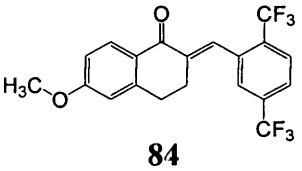 **84**	50 – 100 μM	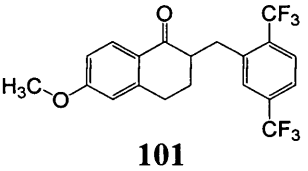 **101**	50 – 100 μM
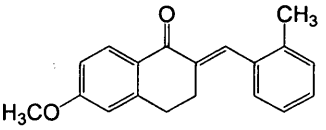 **85**	20 – 40 μM	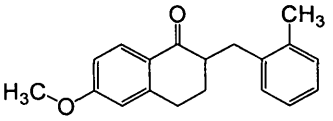 **102**	20 – 40 μM
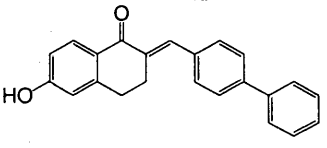 **95**	50 – 100 μM	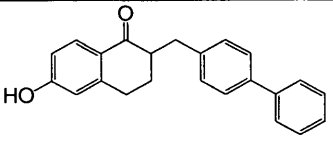 **103**	10 – 20 μM
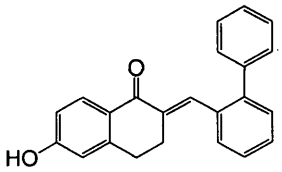 **96**	20 – 40 μM	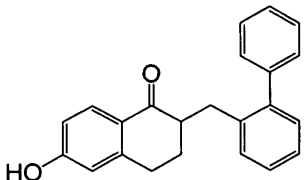 **104**	10 – 20 μM

Table 7.4. Inhibition of ATRA metabolising enzyme in MCF-7 cells.

Compound (Unsaturated tetralone)	IC_{50}	Compound (Unsaturated tetralone)	IC_{50}
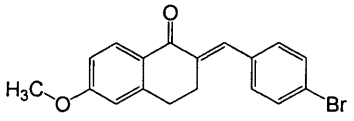 **82**	50 – 100 μM	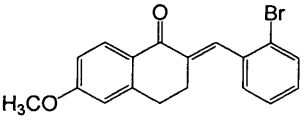 **83**	9 μM
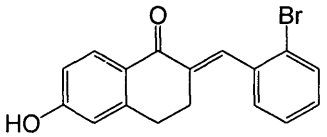 **93**	20 – 40 μM	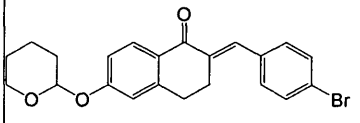 **78**	50 – 100 μM
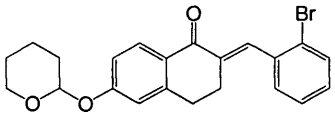 **79**	50 – 100 μM	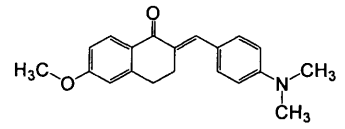 **86**	25 – 50 μM
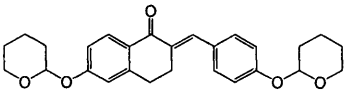 **80**	50 – 100 μM	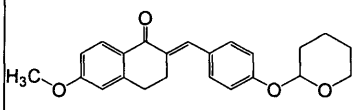 **81**	25 – 50 μM

Table 7.1 and **7.2** show two series of compounds which have either imidazole or triazole ring moieties. The first series of compounds (**14** – **17**) illustrated in **Table 7.1** shows comparable IC_{50} results to liarozole. Introduction of a chloro atom at the 4-position of the bi-phenyl ring (compounds **18** and **19**) reduces the inhibition. This may indicate that the size of the enzyme active site is not favourable for bulky groups.

However, when introducing an amide linkage between the benzofuran and the phenyl ring (**Table 7.2**, compounds **51** – **65**), this reduces the IC_{50} results compared with liarozole, except for compounds **52** and **55** which were comparable with ketoconazole (10 μM – 20 μM). This indicates that there may be a hydrogen-bonding interaction between the $-OCH_3$ (compound **52**) and the amino acid of the enzyme active site and there may be a hydrophobic interaction between the Cl atom (compound **55**) at the enzyme active site.

Derivatives of unsaturated and saturated tetralones were synthesised (described in chapter **5**) and reported here to be less potent or equipotent with standard inhibitors, ketoconazole and liarozole, in MCF-7 cells (**Table 7.3** and **7.4**). Compounds **91**, **92**, **99** (**Table 7.3**) and compound **83** (**Table 7.4**) are equipotent to liarozole, whereas compounds **103** and **104** (**Table 7.3**) are equipotent to ketoconazole.

Our group (Kirby *et al.*, 2003) have demonstrated that 2-(4-aminophenylmethyl)-6-hydroxy-3,4-dihydro-2*H*-naphthalen-1-one (**105**) (**Figure 7.3**) to have moderate inhibition of ATRA-metabolising enzymes in mammalian cadaverous tissue microsomes and homogenates as well as ATRA-induced enzymes in cultured human genital fibroblasts and HaCat cells (transformed keratinocytes), as summarised in **Table 7.5**. In view of this, the compounds (+) and (-) 2-(4-aminophenylmethyl)-6-hydroxy-3,4-dihydro-2*H*-naphthalen-1-one, (±) **105**, were tested using the above MCF-7 cell assay (**Table 7.5**). But they are less active than ketoconazole and liarozole.

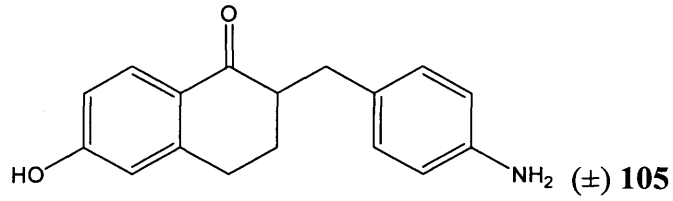

(±) **105**

Figure 7.3. Chemical structure of 2-(4-aminophenylmethyl)-6-hydroxy-3,4-dihydro-2*H*-naphthalen-1-one, (±) **105**.

Table 7.5. IC_{50} (μM) of compound (±) **105** against ATRA metabolising enzymes in different assay systems.

Assay	Compound	IC_{50} (μM)
Rat liver microsomes (Kirby *et al.*, 2003)	(±)-**105**	13
	(+)-**105**	18
	(-)-**105**	10
Human liver microsomes (Kirby *et al.*, 2003)	(±)-**105**	66 % at 100 μM
	(+)-**105**	61 % at 100 μM
	(-)-**105**	54 % at 100 μM
ATRA-induced genital fibroblast cells (Kirby *et al.*, 2003)	(±)-**105**	19 ± 5
ATRA-induced HaCat cells (Kirby *et al.*, 2003)	(±)-**105**	16 ± 8
MCF-7 cells	(+)-**105**	43
	(-)-**105**	39

The synthesised saturated and unsaturated tetralone derivatives evalua ted for their retinoic acid metabolism inhibitory activity using rat liver microsomes were described in chapter **6**. A summary of their inhibitory activity using rat liver microsomes and the MCF-7 cell based assay is described here in **Table 7.6**.

Table 7.6. A summary of the tetralone derivatives evaluated for their retinoic acid metabolism inhibitory activity using MCF-7 cell assay and rat liver microsomes. Ketoconazole, liarozole and R115866 were used as standards for comparison (Yee *et al.*, 2005).

Compound	MCF-7 IC_{50}, μM	Rat liver microsomes IC_{50}, μM
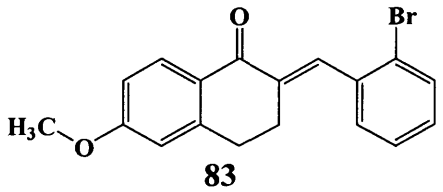 **83**	9	> 20
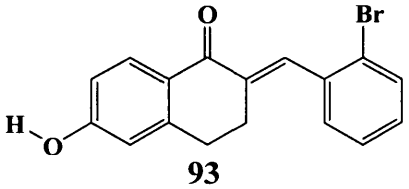 **93**	20-40	2.4
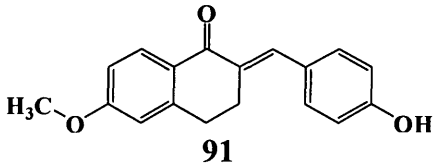 **91**	7	> 20
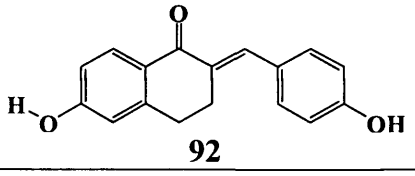 **92**	9	> 20
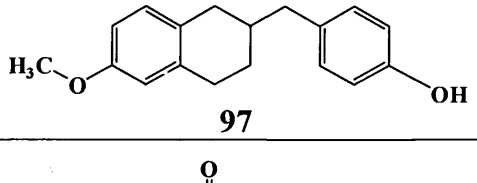 **97**	25 – 50	2.2
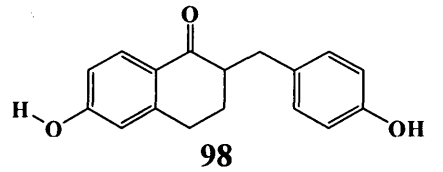 **98**	20 – 40	1.5
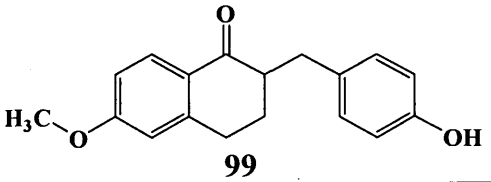 **99**	5	0.4
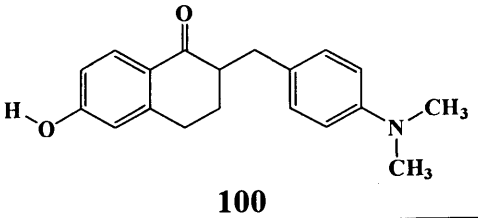 **100**	25 – 50	1.2

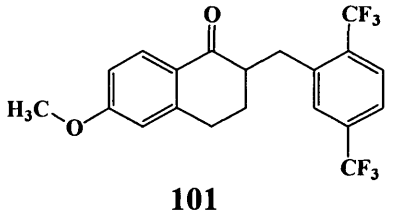 **101**	> 50	18
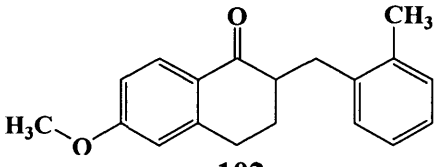 **102**	20 – 40	1.8
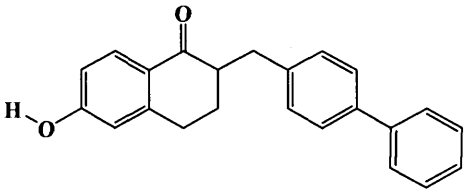 **103**	10 – 20	>20
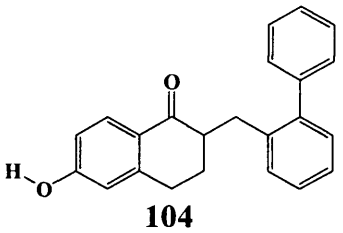 **104**	10 – 20	0.5
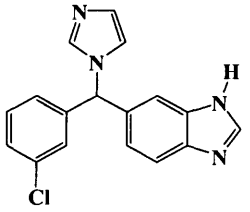 **Liarozole**	7	> 100
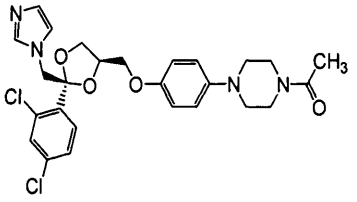 **Ketoconazole**	10 – 20	18
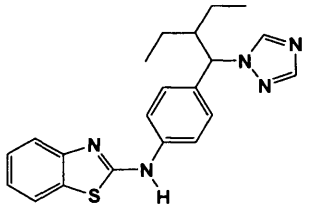 **R115866**	0.005	10

The inhibitory activity using the two assay systems, as summarised in **Table 7.6** did not generally correlate. This is because, the ATRA metabolism in the rat liver microsomes involves non-specific liver CYPs whereas the ATRA metabolism in MCF-7 cells involves the ATRA-inducible CYP26. In terms of selectivity, the unsaturated tetralone compounds **83**, **91** and **92** (IC_{50}: rat liver microsomes, > 20 μM; MCF-7 cells, 7 – 9 μM) would appear to be more specific for CYP26A1. In contrast, compound **99** shows good inhibitory activity in both assays (IC_{50}: rat liver microsomes, 0.4 μM; MCF-7 cells, 5 μM). Two research groups, Johnson & Johnson Pharmaceutical Research group (Stoppie *et al.*, 2000; Van heusden *et al.*, 2002) and OSI Pharmaceuticals Inc. (Mulvihill *et al.*, 2005) have shown compounds with high selectivity of CYP26 compared with different CYP isoforms found in liver. However, it seems that both the non-specific liver CYPs and the ATRA-inducible CYP26 would need to be inhibited. This is because it is necessary to have initial ATRA accumulation by the inhibition of non-specific CYPs in the liver to allow induction of CYP26 (Njar *et al.*, 2000; Patel *et al.*, 2004).

7.4.2.2 Molecular docking

Cytochrome P450 is a superfamily of enzymes comprising a large range of proteins with diverse functions. The 3-dimensional structures of P450s are of scientific interest. Although the sequences of different P450s proteins are known, only five crystallographic structures of P450s were identified by 2002. Four of the P450s are from bacterial sources and one from a mammalian source, they are:

- $P450_{cam}$ (CYP101) derived from *Pseudomonas putida* camphor P450 (Poulos *et al.*, 1987)
- $P450_{BM-3}$ (CYP102) derived from *Bacillus megaterium* P450 (Ravichandran *et al.*, 1993)
- $P450_{eryF}$ (CYP107) derived from *Saccharaopolyspora erythreae* erythromycin F P450 (Cupp-Vickery and Poulos, 1995)
- $P450_{terp}$ (CYP108) derived from *Pseudomonas putida* α-terpineol P450 (Hasemann *et al.*, 1994)
- P450 2C5/3LVdH derived from modification to the residues and modifications to the C- and N-terminal transmembrane domain of the rabbit cytochrome P450 2C5 (to increase solubility and to promote crystallisation) (Williams *et al.*, 2000)

In July 2003, P.A. Williams's group reported the first crystal structure of human cytochrome P450, which is the CYP2C9 (Williams *et al.*, 2003). This was then followed by two other crystal structures of human P450 enzymes, namely, CYP2C8 (Schoch *et al.*, 2004) and CYP3A4 (Yano *et al.*, 2004). Our group recently used comparative modelling to construct models of CYP26A1 using the three-dimensional structure of these three recent human cytochrome P450 as templates, *i.e.* CYPs 2C8 (PDB code: 1PQ2), 2C9 (1R90) and 3A4 (1TQN). The three models were generated by the available software packages (i) Molecular Operating Environment (MOE) (Molecular Operating Environment 2003.04) and (ii) SYBYL (SYBYL 7.0).

7.4.2.3 Docking studies

The FlexX programme (Rarey *et al.*, 1996) interfaced with SYBYL 7.0 and the MOE-Dock programme (MOE-Dock 2003.04) were used to dock the substrate (ATRA) and CYP26A1 inhibitor (R115866) inside the active site of these three generated CYP26A1 models. The docking studies showed that the CYP26A1 model using the CYP3A4 as template gave the best active site fitting for both ATRA and CYP26A1 inhibitor after performing molecular dynamics and further active site optimisation (**Figure 7.4**). **Figure 7.4** shows the ATRA substrate at the active site of this CYP26A1 model based on CYP3A4 as template. The carboxylic acid group of ATRA is H-bonded to the SER126 and ASN127 residues and the cyclohexyl ring of ATRA lies close to the heme (**Figure 7.4**). The C-4 atom of the ATRA is positioned at a distance of 4.85 Å directly above the heme iron to allow hydroxylation at the C-4 position by a water molecule. ATRA is held within the hydrophobic tunnel *via* multiple hydrophobic interactions with amino acid residues at the active site TRP112, PHE299, THR304, PHE374 and VAL370.

The nitrogen atom of the imidazole or triazole group of the inhibitors, *R*- and *S*-liarozole and R115866, coordinate with the heme iron transition metal, at a distance of 2.2 – 3.2 Å. H-bonding and multiple hydrophobic interactions between the inhibitor and the active site hold the inhibitor within the active site. For example, H-bonding interactions between the nitrogen atom of the liarozole benzimidazole ring and the peptide carbonyl of VAL480 and PRO113 for the *R*- and *S*-enantiomer respectively [**Figure 7.5** (**A**) and (**B**)]. Similarly to ATRA, *R*- and *S*-liarozole is also held within the hydrophobic tunnel. The main amino acid residues at the active site, TRP112, PHE299, PRO113, THR304, PHE374, ALA114, VAL116 and THR118 contributed to the

hydrophobic interactions with *R*- and *S*-liarozole [**Figure 7.5** (**A**) and (**B**)]. *R*- and *S*-R115866 form a H-bonding interaction with the peptide carbonyl of PRO113 in the model (**Figure 7.6**), as well as hydrophobic interactions with the side chains of TRP112, PHE374, THR304, VAL370, PHE84, PHE299, VAL116 and GLY300.

Docking of the synthesised compounds has been carried out using FlexX. The triazole ring of compounds **14** – **19** showed a co-ordination with the transition metal, as seen with liarozole, at the active site and only hydrophobic interactions between the inhibitor and the amino acid side-chains. Similarly, the series II compounds, **51** – **65** also form hydrophobic interactions with the side-chain amino acids and co-ordination with the heme iron transition metal. The nitrogen atom of the amide bond in compounds **51** – **65** does not form a H-bonding with the amino acid unlike R115866. This may explain why these compounds displayed poor IC_{50} values compared with R115866.

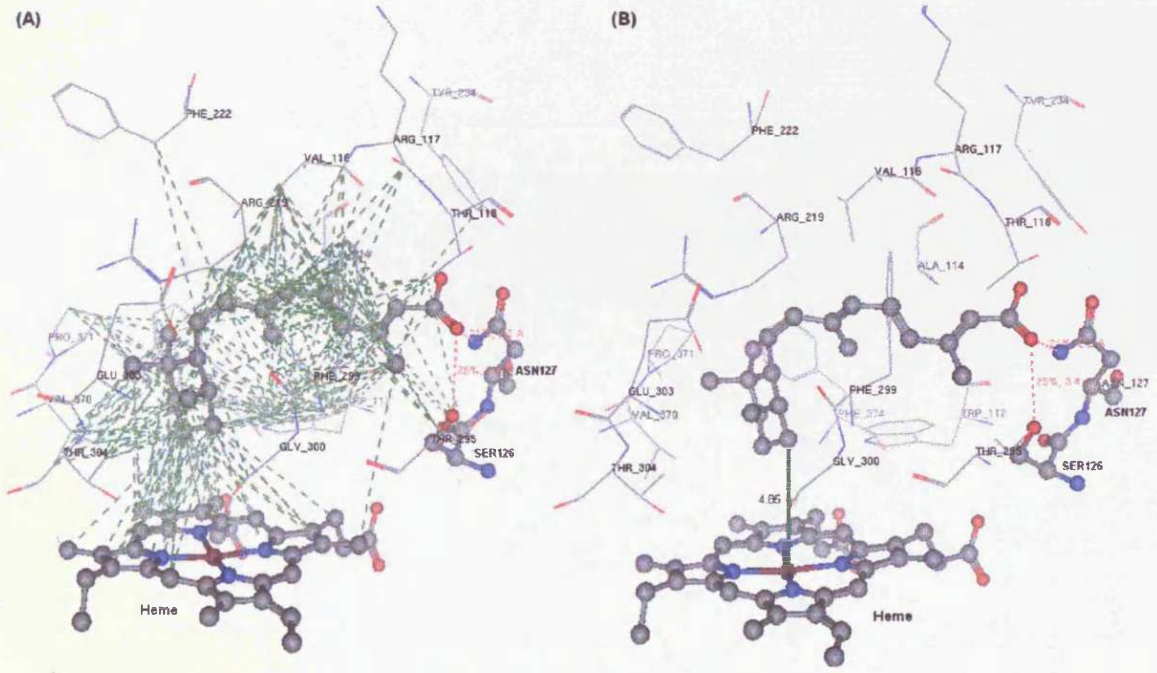

Figure 7.4. Diagram showing ATRA docked at the active site of the CYP26A1 model based on CYP3A4 as template. (**A**) Hydrogen bonding and hydrophobic interactions are shown as red and green dashed lines respectively. (**B**) The distance between the C-4 atom of ATRA and the heme iron is shown as dark green line. Colour coding of the atoms: grey=carbon; red=oxygen; blue=nitrogen, brown=iron, yellow=sulphur.

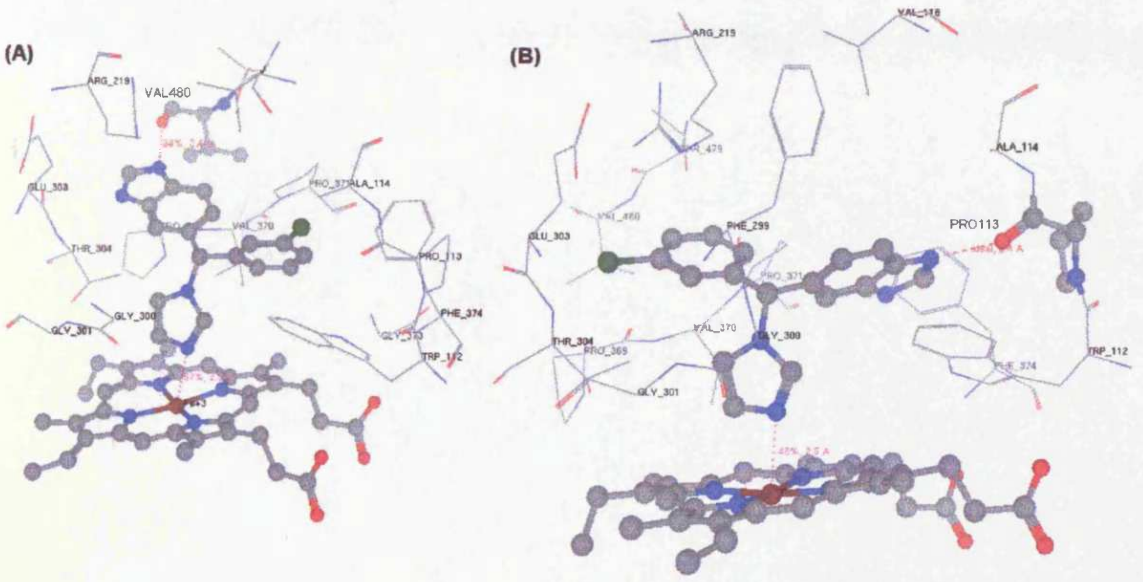

Figure 7.5. Diagram showing the inhibitor (**A**) *R*-liarozole and (**B**) *S*-liarozole docked at the active site region of CYP26A1 model based on CYP3A4 as template. Hydrogen bonding interactions are shown as red dashed lines and co-ordination with the transition metal is indicated with a purple line. Colour coding of the atoms: grey=carbon; red=oxygen; blue=nitrogen, brown=iron, yellow=sulphur.

Docking of the tetralone compounds have been carried out. The docking results show that the 4-hydroxyphenyl of compounds **91**, **92**, **97** – **99** forms H-bonding interaction with GLY300 and/or co-ordination with the transition metal at the active site (**Figure 7.6**). In addition, the 6-hydroxy group of compound **92** forms H-bonding interaction with SER115 and ASP227 besides co-ordination of the 4-hydroxy group of the phenyl ring with the transition metal at the active site (**Figure 7.6**). Similarly to liarozole and R115866, these compounds also form hydrophobic interactions with the side chains.

These H-bonding, hydrophobic interactions and co-ordination with the transition metal at the active site resulted in good inhibition of CYP26A1 by compounds **91**, **92** and **99** in MCF-7 cells (IC_{50}: 5 – 9 μM). Although compounds **97** and **98** also form these interactions at the active site, they demonstrate poor IC_{50} (> 20 μM). Overall, this CYP26A1 model has led to a better understanding of the key binding mode between the ligand or inhibitor with the amino acid residues at the active site.

(*S*)-R115866

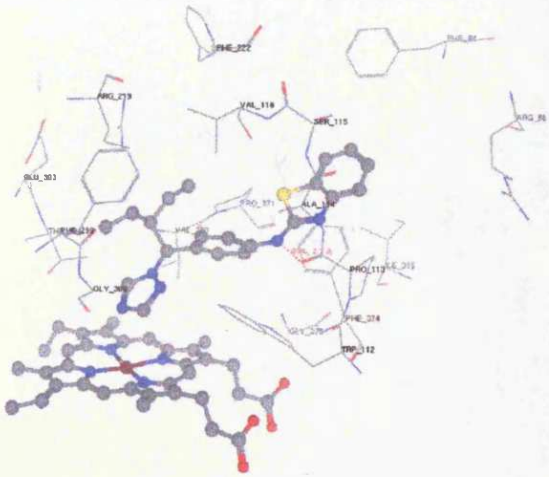

Compound 91

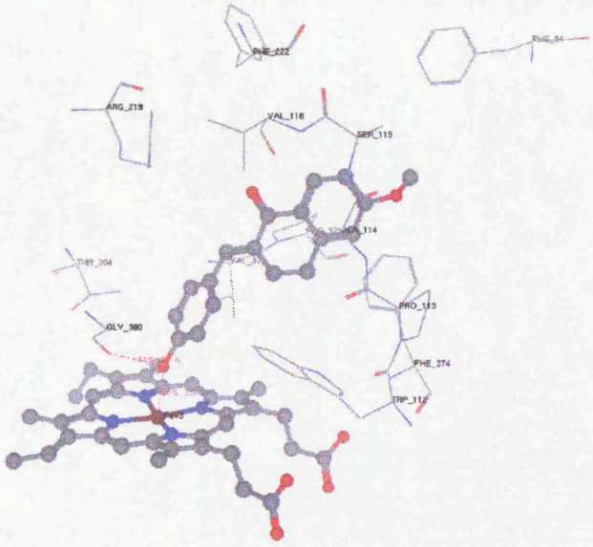

Compound 92

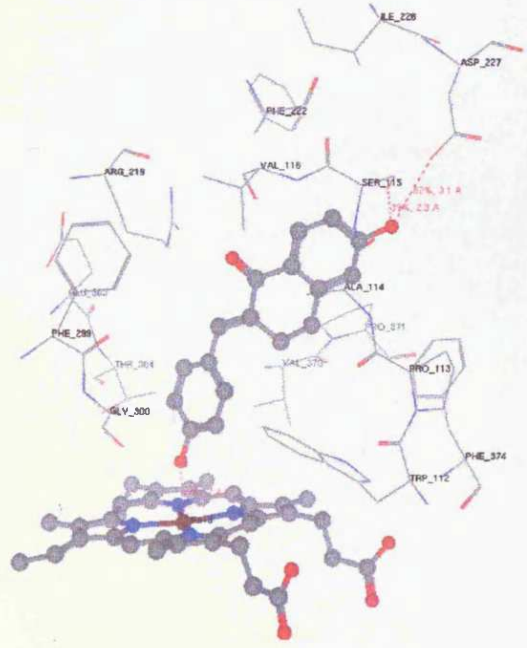

Compound (*S*)-99

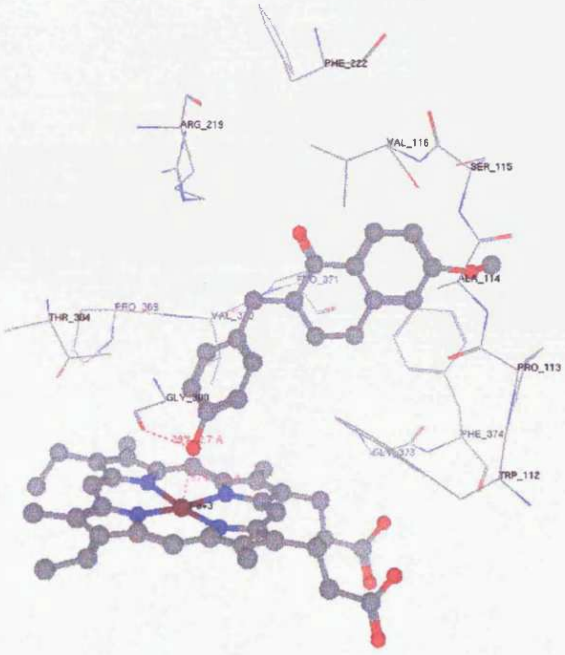

Figure 7.6. The H-bonding interactions between the inhibitors and the side-chains at the active site as shown in red dashed line. Colour coding of the atoms: grey=carbon; red=oxygen; blue=nitrogen, brown=iron, yellow=sulphur.

7.4.3 Metabolism of all-*trans* retinoic acid in DU-145 cell-line

After 24 h incubation time, only 15 – 18 % of the [^{3}H]-ATRA were metabolised in the DU-145 cell-lines. Attempt to incubate the cells with 10^{-7} M ATRA to enhance the level of CYP26 enzyme was carried out. After 24 h of incubation time with ATRA, the medium was removed and being replaced with ATRA (10^{-7} M) plus 0.10 μCi [^{3}H]-ATRA in medium. The cells were then incubated for another 12, 24 or 48 h. After 12, 24 or 48 h incubation time, approximately 20±5 %, 40±2 % and 60±5 % of [^{3}H]-ATRA were metabolised respectively (**Figure 7.4**).

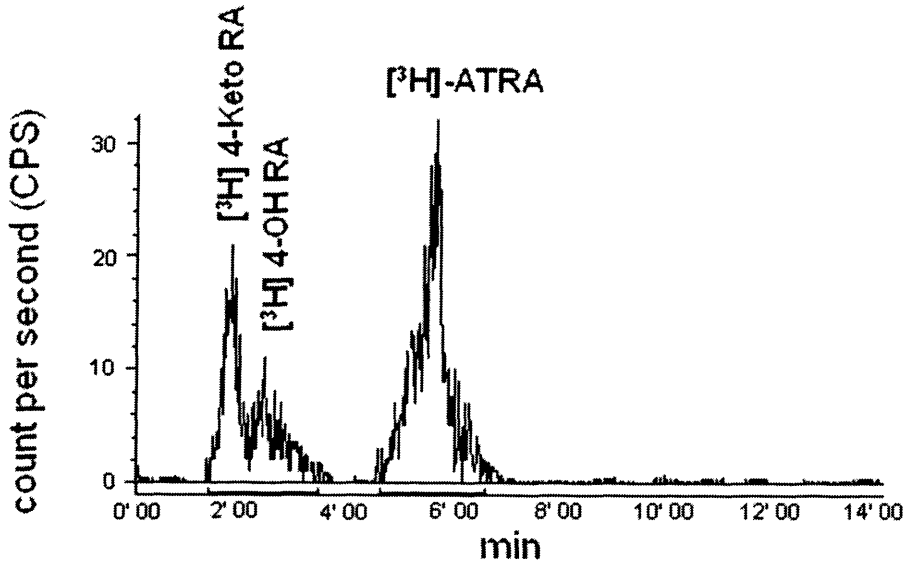

Figure 7.4. HPLC of an incubation extract of 10^{-7} M ATRA plus 0.1 μCi [^{3}H]-ATRA with DU-145 cell-line. HPLC column: 10 μM C18 μBondapak© 300 x 3.9 mm column; mobile phase: 75:25:1 = Acetonitrile: 1 % w/v ammonium acetate in water: acetic acid. Pump rate: 1.9 mL/min. Retention time: 4-keto-retinoic acid and 4-hydroxy-retinoic acid (1.5 min – 3.5 min) and ATRA (5.5 min). DU-145 cells were incubated with 10^{-7} M ATRA for 24 h before addition of 10^{-7} M ATRA plus 0.1 μCi [^{3}H]-ATRA for a further 24 h.

Due to time constraints, only 4 compounds (**14**, **15**, **91** and **99**) and two standard inhibitors (liarozole and R115866) at 10 μM were tested for inhibition of ATRA metabolism in DU-145 cells. The % inhibitions of ATRA metabolism in DU-145 cells using 10 μM of tested compounds are shown in **Table 7.7**. Unlike the inhibition of ATRA metabolism in MCF-7 cells, the percentage inhibition of the synthesised compounds (**14**, **15**, **91** and **99**) and liarozole at 10 μM did not show above 50 % inhibition. The differences could be due to the different susceptibility of the inhibitor to DU-145 cells and the different accessibility of the inhibitor to the target enzymes compared with MCF-7 cells.

Table 7.7. % Inhibition of ATRA metabolism in DU-145 cells using 10 μM of the tested compounds and 10^{-7} M ATRA plus 0.1 μCi [^{3}H]-ATRA. DU-145 cells were incubated with 10^{-7} M ATRA for 24 h before addition of 10^{-7} M ATRA plus 0.1 μCi [^{3}H-11,12] ATRA and the following inhibitors for a further 24 h.

Compound	% Inhibition	Compound	% Inhibition
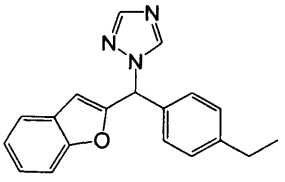 **14**	44	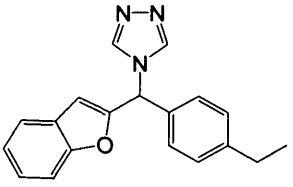 **15**	41
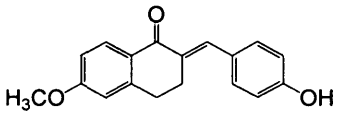 **91**	39	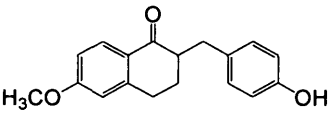 **99**	37
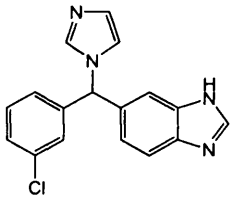 **Liarozole**	42	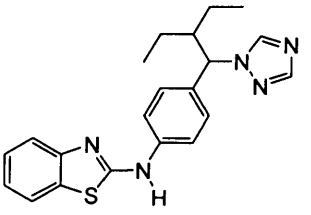 **R115866**	80

7.5 General conclusions

Despite the fact that DU-145 cells expressed a high level of CYP24 mRNA (as demonstrated by RT-PCR analysis, section **8.2**), only a small amount of [^{3}H]-25-(OH)-D_3 metabolites (10 – 15 %) were observed by HPLC analysis. Even though DU-145 cells were pre-treated with 10 nM 1α,25-$(OH)_2$-D_3 for 24 h to induce a higher level of CYP24 enzyme, the amount of [^{3}H]-25-(OH)-D_3 metabolites were still low (20 – 25 %), unlike the rat kidney mitochondria assay, where 40 ± 5 % of [^{3}H]-25-(OH)-D_3 metabolites were formed (section **6.7.1**). The rate of metabolism and the rate of transport of [^{3}H]-25-(OH)-D_3 in these two systems could be very different and resulted in the lower [^{3}H]-25-(OH)-D_3 metabolites formed in DU-145 cells.

A novel method to study the metabolism of ATRA in MCF-7 and DU-145 cells has been described here. In the MCF-7 and DU-145 cell assays, the ATRA metabolising enzyme, CYP26A1 is induced by ATRA (10^{-7} M). The RT-PCR analysis (section **8.2**) showed the presence of CYP26A1 mRNA only after 9 h and 24 h incubation with ATRA (10^{-7} M) in MCF-7 and DU-145 cells respectively. DU-145 cells required a longer incubation time with ATRA (up to 48 h) to produce the same amount of [^{3}H]-

ATRA metabolites as in MCF-7 cells (9 h). As a result, the IC_{50} of the synthesised compounds were only evaluated in the MCF-7 cells.

Compared with the rat liver microsome assay (section **6.7.2**), the enzyme activity in the MCF-7 and DU-145 cell assays is more relevant being a measure of human ATRA metabolism by the specific CYP26A1 enzyme. Some of the synthesised compounds described in **Table 7.6** inhibited both enzyme activities in both assays, whereas, some compounds were more selective against the non-specific CYPs in the rat liver microsomes. As mentioned earlier, it is necessary to inhibit the non-specific CYPs in the liver microsomes in order to have a sufficient level of ATRA to induce the CYP26A1 enzyme.

A molecular model for CYP26A1 based on the CYP3A4 template was constructed by our group recently. Molecular docking using the substrate, ATRA and inhibitors (standard inhibitors and some of the synthesised compounds) was carried out to identify the key interactions between the substrate and inhibitors with the enzyme residues at the active site.

CHAPTER 8

Further studies and investigations

8. Further studies and investigations

Since the DU-145 prostate cancer cells did not express significant level of 25-(OH)-D_3 metabolites after incubation of [^{3}H]-25-(OH)-D_3 at various time point and after pre-treatment with 1,25-$(OH)_2$-D_3 (section **7.4.1**), further investigations were pursued. The analysis that could be carried out to determine whether the DU-145 cells that were used express the CYP24 enzyme are western blotting, immunohistochemistry and reverse-transcriptase polymerase chain reaction (RT-PCR). Due to its simplicity and the available facilities, RT-PCR was used to look at the expression of CYP24 and CYP26A1 mRNA in the DU-145 and MCF-7 cells that were used in the assays described in **Chapter 7**. RT-PCR was carried out (section **8.2**) under the supervision of Dr. Bronwen Evans and Mrs. Carole Elford at the Department of Child Health, Heath Hospital, Cardiff.

Dr. Moray J. Campbell (Institute of Biomedical Research, Birmingham University) who has done considerable research in studying vitamin D_3 receptor and vitamin D_3 gene targets in breast and prostate cancer (Campbell *et al.*, 1997; Campbell and Koeffler, 1997; Ma *et al.*, 2004), allowed me to spend some time in his laboratory. The aim and objectives of the work in Campbell's laboratory were:

- To quantify the expression level of CYP24 in DU-145 with or without inhibitors using real-time quantitative RT-PCR method.
- To investigate whether co-treatment with the inhibitor and 1α,25-$(OH)_2$-D_3 will enhance the proliferation of the DU-145 cells compared with 1α,25-$(OH)_2$-D_3 treated prostate cancer cells.

8.1 Introduction to RT-PCR and real-time quantitative RT-PCR

Polymerase chain reaction (PCR) has a great variety of application in forensic sciences and in molecular biology (White, 1996). It is a method by which millions of DNA or genes can be made in a couple of hours. This method (Mullis and Fuloona, 1987) was invented by Dr. Kary B. Mullis in 1983, for which he received the Nobel Prize in Chemistry in 1993.

In this section, a brief introduction to the principle of the PCR will be discussed using CYP24 as the example of the mRNA of interest.

In order to run a PCR, cDNA is required. Total RNA from the cells (*e.g.* DU-145 cells) is first isolated and then all the RNA in the cells is reverse transcribed to cDNA by the enzyme reverse transcriptase (RT). Following the reverse transcription

step, PCR is then carried out with the amplification of the target cDNA (*i.e.* CYP24 as example) using CYP24 forward and reverse primers (**Figure 8.1**). In the PCR reaction, only the cDNA of interest will be amplified, as specific primers of the specific cDNA are used here. Since both strands of the cDNA are copied during the PCR (**Step 2, Figure 8.1**), there is an exponential increase in the number of copies of the gene. The forward and reverse primers that are chosen have to be very specific for the cDNA of interest, and it is usually 19-25 base pair long. *Taq* Polymerase enzyme, which was originally isolated from *Thermus aquaticus* (Eom *et al.*, 1996; Saiki *et al.*, 1988), can now be supplied as a recombinant enzyme from *Escherichia coli* (Lawyer *et al.*, 1989), and is an important enzyme in the annealing of the primer to the cDNA (**Step 2**) and allow extension of the chain (**Step 3, Figure 8.1**).

The next step is the verification and detection of PCR product at the end of the PCR reaction on agarose gel. This is to check whether the cDNA is formed and whether it is of the right size.

Before introducing the quantitative real-time PCR technique, it is important to understand what happens during PCR reaction. PCR reaction is broken down to 3 phases (**Figure 8.2**):

- **Exponential** phase: Doubling of the product occurs every cycle.
- **Linear** phase: Reaction is slowing down since reaction components are being consumed.
- **Plateau** phase (End-point): The reaction begins to slow down and stops all together. The PCR products will degrade if the reaction is left longer.

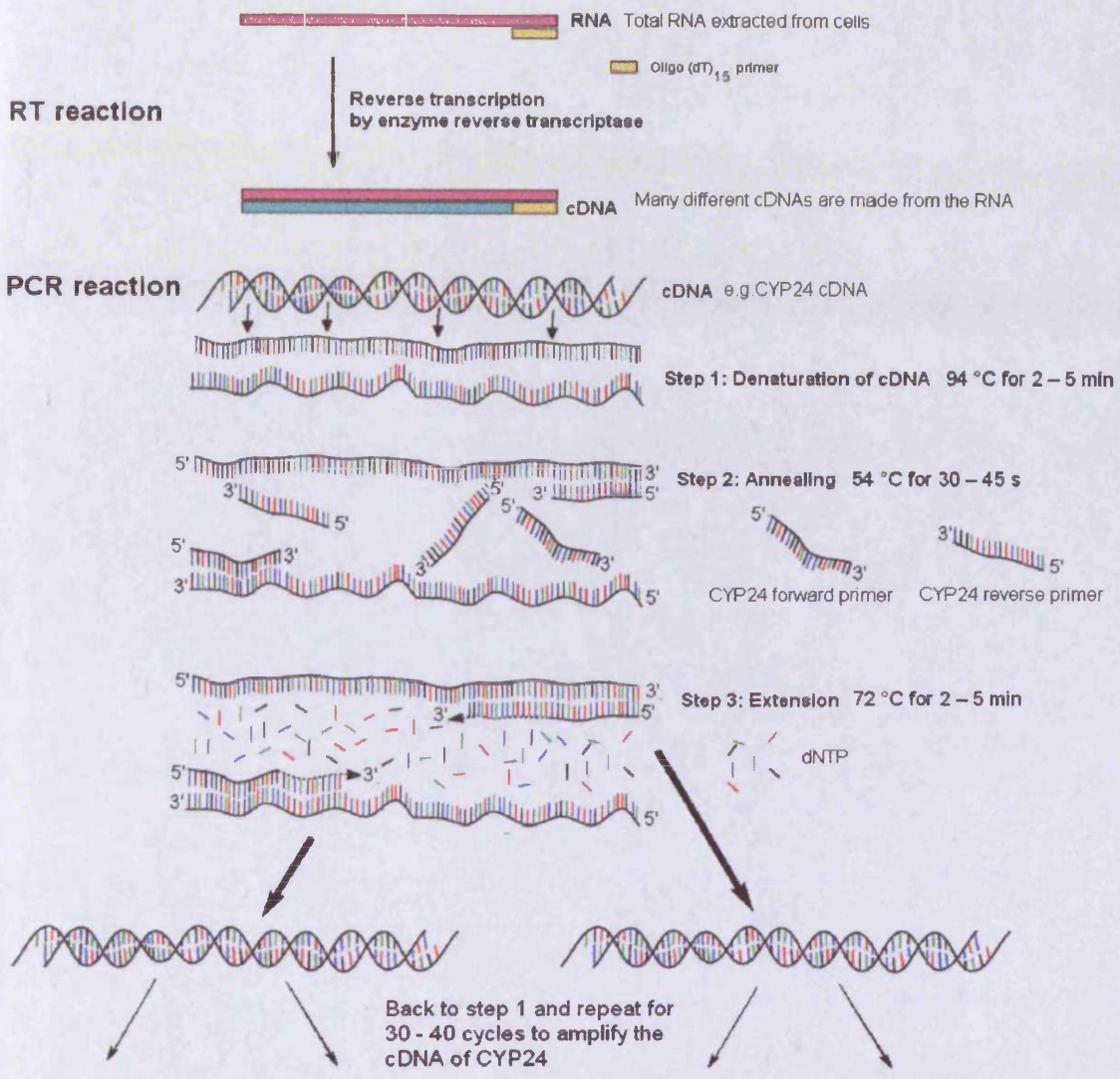

Figure 8.1. The diagram shows the steps involved in the reverse-transcriptase polymerase chain reaction (RT-PCR). The RT reaction converts the total RNA in the cells into cDNA. In the PCR reaction, only the specific cDNA of interest (*e.g.* CYP24 cDNA) is amplified.

In the traditional PCR, agarose gel is used to detect the amount of the target at the **plateau phase**, which would not truly represent the initial amounts of the target. In real-time PCR, a Sequence Detection Systems (SDS) instrument is used to measure the amount of the target during the amplification cycle of the PCR (as shown in **Figure 8.2**). This technique is revolutionised by the use of a fluorescence dye in the reaction. The higher the starting copy number of the target (*e.g.* CYP24), the sooner an increase in fluorescence is observed, and thus giving a lower threshold cycle (Ct) value. Ct value is the cycle number at which logarithmic PCR plots cross a calculated threshold-line (**Figure 8.2**).

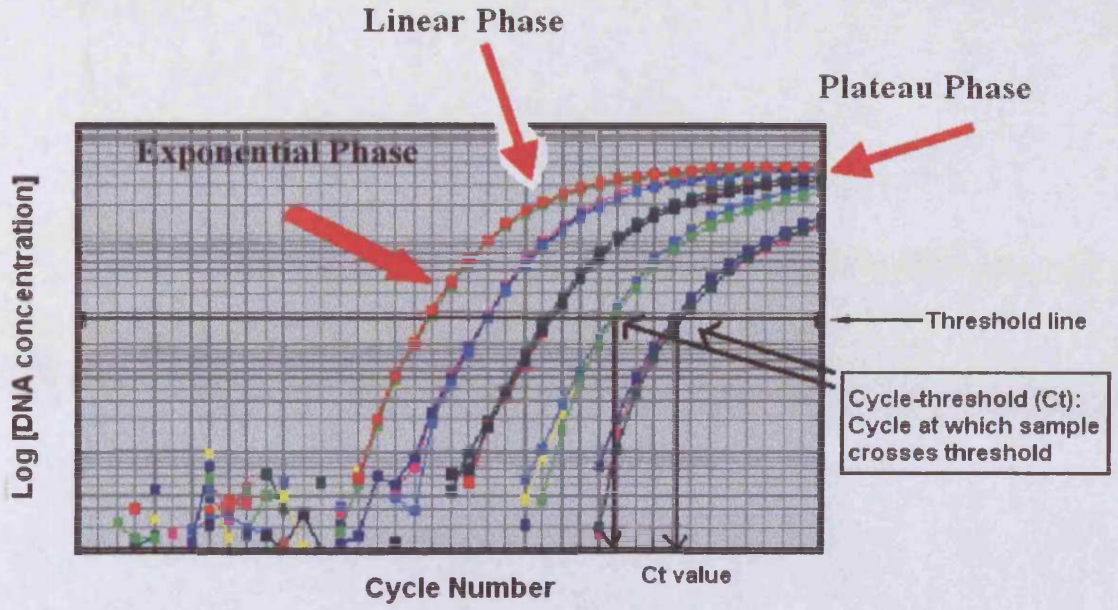

Figure 8.2. The three phases in a PCR reaction. The different colours of the dashed lines indicate different cDNA sample, for example, cDNAs of DU-145 cells treated at different time point with 1α,25-$(OH)_2$-D_3. The diagram is modified from the Applied Biosystems "Application tools and tutorials" which can be downloaded from the website www.appliedbiosystems.com.

There are two types of fluorescence dye that are used to detect PCR products using SDS instrument, namely fluorogenic 5' nuclease chemistry and SYBR Green I dye chemistry. Fluorogenic 5' nuclease chemistry involves a fluorogenic probe, while SYBR Green I dye chemistry involves a highly specific, double-stranded DNA binding dye, to enable the detection of the PCR product as it accumulates during the PCR cycles. Fluorogenic probe was chosen for the quantitation of the PCR products due to its specificity, sensitivity and the ability to multiplex reactions. The following diagram (**Figure 8.3**) demonstrates the steps that are involved in the fluorogenic 5' nuclease chemistry.

The SDS instrument will capture the fluorescence emitted by the reporter signal. The amount of reporter signal increase is proportional to the amount of product being produced for a given sample (Applied Biosystems). As a result, you will get a plot as shown in **Figure 8.2**. Real-time PCR provides fast, precise and accurate results for DNA or RNA quantitation. This makes the real-time PCR able to detect as little as a 2-fold change.

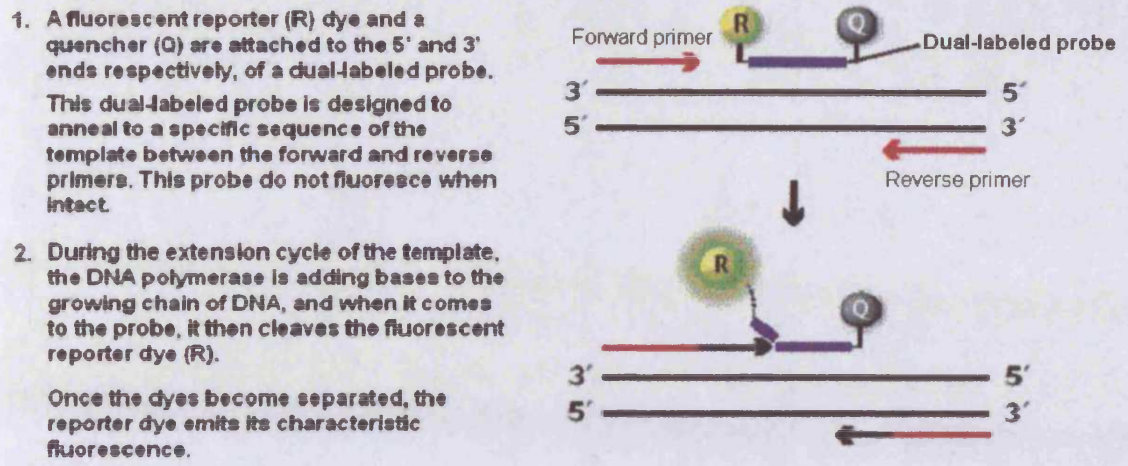

Figure 8.3. The steps that are involved in the quantitation of the PCR products using the fluorogenic probe (dual-labeled probe). The figure has been adapted from Applied Biosystem's website (Applied Biosystems).

The objectives of using real-time RT-PCR in this study were:

- To quantify the expression level of CYP24 mRNA in DU-145 and PC-3 androgen-independent prostate cancer cell-lines with or without 1α,25-$(OH)_2$-D_3.
- To quantify the expression level of CYP24 mRNA in DU-145 and PC-3 cells treated with 1α,25-$(OH)_2$-D_3 and inhibitor, *e.g.* ketoconazole or inhibitor alone.

1α,25-$(OH)_2$-D_3 inhibits growth and stimulates differentiation of cancer cells, by regulating the expression of specific genes. Two of the genes that are involved in cell growth and cell differentiation are $p21^{waf1/cip1}$ and GADD45α genes. Previous work has demonstrated that $p21^{waf1/cip1}$ gene, encoding the cyclin-dependent kinase inhibitor, is a target of 1α,25-$(OH)_2$-D_3 (Prudencio *et al.*, 2001). The magnitude of $p21^{waf1/cip1}$ induction varies among different cell types (Prudencio *et al.*, 2001). The expression of GADD45α (growth-arrest and DNA-damage) gene is overexpressed in cells that are associated with growth arrest (Prudencio *et al.*, 2001). It would be interesting to investigate by the real-time PCR whether the level of $p21^{waf1/cip1}$ and GADD45α mRNA are affected by 1α,25-$(OH)_2$-D_3 alone or with inhibitor.

8.2 RT-PCR analysis

The following traditional RT-PCR analysis was carried out under the supervision of Dr. Bronwen Evans and Mrs. Carole Elford at the Department of Child Health, Heath Hospital, Cardiff.

DU-145 (gift from Dr. M.J. Campbell) and MCF-7 cells cultured at Tenovus Cancer Research Centre, Cardiff University, were both seeded at 1.5 x 10^6 cells in a T75 flask. Cells at approximately 70 % confluence were then used for isolation of total RNA using Tri Reagent (Sigma-Aldrich) following the manufacturer's instructions. Total RNA amounts were quantified by measuring absorbance at 260 nm. The A_{260}/A_{280} nm absorption ratio was greater than 1.7. Total RNA was used to synthesise cDNA using the manufacturer's protocol provided with an AMV reverse transcriptase (Promega, Madison, Wisconsin) and performed in a thermocycler (Perkin Elmer). Total RNA (2 μg) in the presence of 8 μL of $MgCl_2$ (25 mM), 2 μL of oligo$(dT)_{15}$ primer (500 ng/μL), 4 μL of Reverse Transcription 10 x buffer, 4 μL of dNTP mix (10 mM), 1 μL of Recombinant RNasin® Ribonuclease Inhibitor, 1.6 μL AMV reverse transcriptase and nuclease-free water (to give a total reaction volume of 40 μL) was incubated at 42 °C for 60 min in a thermocycler. The newly synthesised cDNA was then used for PCR analysis. The RNA and cDNA were stored at – 20 °C when not used.

PCR amplification kit by Promega (Promega, Madison, Wisconsin) was used for the PCR reaction. The PCR reaction mixture for CYP24 contained 2 μL of cDNA, 2.5 μL of 10 x PCR reaction buffer, 1 μL forward primer (50 pmol/μL), 1 μL reverse primer (50 pmol/μL), 0.5 μL dNTP mix (10 mM), 0.2 μL *Taq* DNA polymerase (5U/μL) and nuclease-free water (to give a total reaction volume of 25 μL). Reactions were cycled as follows: 94 °C for 5 min, 59 °C for 30 s, 72 °C for 1 min, then 28 cycles at 94 °C for 15 s, 59 °C for 30 s, 72 °C for 1 min.

The PCR reaction mixture for CYP26A1 or β-actin contained 2.5 μL of cDNA, 2.5 μL of 10 x Reverse Transcription 10 x buffer, 0.25 μL forward primer (100 μM), 0.25 μL reverse primer (100 μM), 0.5 μL dNTP mix (10 mM), 0.2 μL *Taq* DNA polymerase (5U/μL) and nuclease-free water (to give a total reaction volume of 25 μL). *Taq* DNA polymerase was activated at 94 °C for 5 min. The mixtures were then subjected to 30 cycles of amplification. Each cycle conditions: 94 °C for 1 min, 55 °C for 1 min and 72 °C for 2 min. An extra extension step was included (72 °C for 10 min) at the end of the incubation. β-Actin was used as the endogenous control.

Negative control of cDNA synthesis was carried out under the same experimental conditions, but in the absence of AMV reverse transcriptase. The sequences of the forward and reverse primers are listed in **Table 8.1**. 20 μL of the PCR products were separated on a 1.5 % (w/v) agarose gel containing ethidium bromide and separated at 100 V. The bands were visualized under UV light illumination (**Figure 8.4**).

Table 8.1. The sequences of the forward and reverse primers for the specific mRNAs.

Primers	**Sequence**
CYP24 forward primer CYP24 reverse primer (507 base pair segment)	5'-CCCACTAGCACCTCGTACCAAC-3' 5'-CGTAGCCTTCTTTGCGGTAGTC-3' (Bareis *et al.*, 2001; Farhan *et al.*, 2003)
CYP26A1 forward primer CYP26A1reverse primer (184 base pair segment)	5'-GCTGAAGAGTAAGGGTTTAC-3' 5'-CTTGGGAATCTGGTATCCAT-3' (Van heusden *et al.*, 2002)
β-actin forward primer β-actin reverse primer (800 base pair segment)	5'-CCCAGCCATGTACGTTGCTA-3' 5'-AGGGCATACCCCTCGTAGATG-3'

The results showed that DU-145 cells expressed significant level of CYP24 but MCF-7 cells did not express the CYP24 enzyme, in untreated condition [**Figure 8.4, (A)**]. Enhanced level of CYP24 mRNA is observed in both DU-145 and MCF-7 cells in the presence of 10 nM 1α,25-$(OH)_2$-D_3 for 6 h as demonstrated from the real-time quantitative RT-PCR (data not shown here).

CYP26A1 is not expressed in untreated DU-145 and MCF-7 cells, however, CYP26A1 is expressed after treatment with 10^{-7} M ATRA for 24 and 9 h respectively [**Figure 8.4, (B)**]. This demonstrated that in the MCF-7 and DU-145 cell assays (described in section **7.4.2** and **7.4.3**), expression of the ATRA metabolising enzyme, CYP26A1 is induced by ATRA (10^{-7} M), therefore the inhibition enzyme studies in the MCF-7 and DU-145 cell assays is more relevant being a measure of the human CYP26A1.

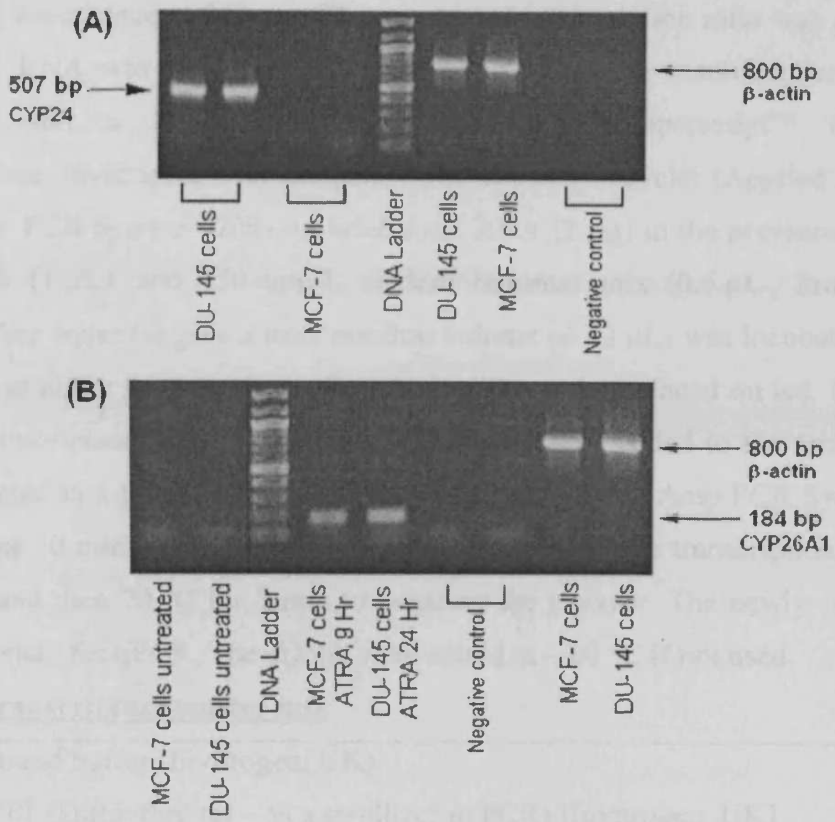

Figure 8.4. RT-PCR analysis of (**A**) CYP24 and (**B**) CYP26A1 mRNA expression in MCF-7 and DU-145 cancer cells. Total RNA was isolated and subjected to RT-PCR. Amplified products were separated on an agarose gel containing ethidium bromide by electrophoresis.

8.3 Real-time quantitative RT-PCR analysis (qPCR)

The following experiments described below were carried out in Dr. Moray J. Campbell's laboratory at the Institute Biomedical Research, Birmingham University.

The prostate cancer cell lines PC-3 and DU-145 were obtained from the American Type Culture Collection (ATCC, Rockville, MD, USA). The cells were maintained in RPMI 1640 medium (Gibco-BRL, Paisley), supplemented with 10 % fetal calf serum (Gibco-BRL), 100 units/mL penicillin and 100 μg/mL streptomycin. The cells were passaged by trypsinising with 0.25 % trypsin-EDTA (Gibco-BRL). The cells were grown at 37 °C in a humidified atmosphere of 5 % CO_2 in air.

DU-145 and PC-3 cells were both seeded at 3.5 x 10^5 cells/well in a 6-well plate. Cells at approximately 70 % confluence were then used for isolation of total RNA using Tri Reagent (Sigma-Aldrich) following the manufacturer's instructions. The cells were also treated with various treatments for certain amounts of time before total RNA isolation was carried out. Total RNA amounts were quantified by

measuring absorbance at 260 nm. The A_{260}/A_{280} nm absorption ratio was greater than 1.7. Total RNA was used to synthesise cDNA using the manufacturer's protocol provided with a M-MLV reverse transcriptase (Superscript™ II Reverse Transcriptase, Invitrogen, UK) and performed in a thermocycler (Applied Biosystems Gene Amp PCR System 9700). In brief, total RNA (2 μg) in the presence of 10 mM dNTP mix (1 μL) and 250 ng/μ L random hexamer mix (0.5 μL , Promega) and nuclease-free water (to give a total reaction volume of 12 μL) was incubated at 68 °C for 5 min to allow for annealing of random primers, then placed on ice. 8 μL of the reverse transcriptase master mix (table below) was then added to the mixture above and incubated in a thermocycler (Applied Biosystems Gene Amp PCR System 9700) at 25 °C for 10 min, then 42 °C for 90 min to enable reverse transcription elongation to occur, and then 70 °C for 5 min to denature the enzyme. The newly synthesised cDNA is ready for qPCR. The cDNA were stored at – 20 °C if not used.

Reverse transcriptase master mix

5X First-strand buffer (Invitrogen, UK)	4 μL
0.1 mM DTT (Dithiothreitol – as a stabilizer in PCR) [Invitrogen, UK]	2 μL
40 units/μL recombinant ribonuclease inhibitor (RNaseOUT™, Invitrogen, UK)	1 μL
2000 units/μL M-MLV reverse transcriptase (Superscript™ II Reverse Transcriptase, Invitrogen, UK).	1 μL

The expression of the specific mRNAs (*i.e.* CYP24, $p21^{waf1/cip1}$ and GADD45α) was quantitated using the ABI PRISM 7700 Sequence Detection System. The sequences of the forward and reverse primers and the probe are listed in **Table 8.2**. Each sample was amplified in triplicate wells in 20 μL volumes containing 19 μL of the following qPCR master mix and 1 μL of the cDNA made. All-reactions were multiplexed with pre-optimised control primers and VIC labeled probe for 18S ribosomal RNA (TaqMan® Ribosomal RNA control reagents, Applied Biosystems, Warrington, UK). Reactions were cycled as follows: 50 °C for 2 min, 95 °C for 10 min (for activation of the QuickGoldStar DNA polymerase); then 44 cycles for 95 °C for 15s and 60 °C for 1 min (Gommersall *et al.*, 2004; Ma *et al.*, 2004).

qPCR master mix

2X qPCR™ QuickGoldStar MasterMix (5mM $MgCl_2$, dNTPs, QuickGoldStar DNA polymerase, Uracil-N-glycosylase) [Eurogentec Ltd., Belgium]	10 µL
1.25 pmol/µL FAM-labeled TaqMan probe (Eurogentec Ltd., Belgium)	2 µL
9 pmol/µL forward primer (Alta Bioscience, Birmingham, UK)	2 µL
9 pmol/µL reverse primer (Alta Bioscience, Birmingham, UK)	2 µL
18S ribosomal RNA forward primer (Applied Biosystems, Warrington, UK)	0.1 µL
18S ribosomal RNA reverse primer (Applied Biosystems, Warrington, UK)	0.1 µL
18S ribosomal RNA VIC labeled probe (Applied Biosystems, Warrington, UK)	0.1 µL
Nuclease-free water	2.7 µL

Table 8.2. The sequences of the forward and reverse primers and the FAM-labelled TaqMan probe used for the specific mRNAs.

Primers and probe	**Sequence**
CYP24 forward primer	5'-CAAACCGTGGAAGGCCTATC-3'
CYP24 reverse primer	5'-AGTCTTCCCCTTCCAGGATCA-3'
CYP24 probe	5'-ACTACCGCAAAGAAGGCTACGGGCTGT-3'
$p21^{waf1/cip1}$ forward primer	5'-GCAGACCAGCATGACAGATTTC-3'
$p21^{waf1/cip1}$ reverse primer	5'-GGATTAGGGCTTCCTCTTGGA-3'
$p21^{waf1/cip1}$ probe	5'-CCACTCCAAACGCCGGCTGATCTTT-3'
GADD45α forward primer	5'-AAGACCGAAAGGATGGATAAGGT-3'
GADD45α reverse primer	5'-GTGATCGTGCGCTGACTCA-3'
GADD45α probe	5'-TGCTGAGCACTTCCTCCAGGGCAT-3'

Data were expressed as, Ct values (see **Figure 8.2**) and used to determine δCt values. δCt = Ct of the target gene minus Ct of the housekeeping gene. The housekeeping gene is the 18S ribosomal RNA. The data was transformed through the equation $2^{-\delta\delta Ct}$ to give fold changes in gene expression (Gommersall *et al.*, 2004; Ma *et al.*, 2004). δδCt = δCt of the target gene from treated cells minus δCt of the target gene from non-treated (control) cells (Livak and Schmittgen, 2001). To exclude potential bias due to averaging of data all statistics were performed with δCt values. Measurements were carried out at least two times each in triplicate wells.

8.3.1 Results and discussions of the qPCR analysis

Initial studies have focused on the effect of the inhibitors of vitamin D_3 metabolising enzymes, *i.e.* ketoconazole and compound **99** (2-(4-hydroxybenzyl)-6-methoxy-3,4-dihydro-2*H*-naphthalen-1-one), for the qPCR study to measure the regulation of the known VDR target genes, CYP24, $p21^{waf1/cip1}$ and GADD45α in response to the following treatment conditions (**1** – **4**) in DU-145 and PC-3 cells.

1. DMSO solvent (control).
2. 10 nM 1α,25-$(OH)_2$-D_3 for 7 h.
3. Ketoconazole (100 μM) or compound **99** (100 μM) throughout the treatment.
4. For treatment with inhibitor plus 1α,25-$(OH)_2$-D_3, the cells were pre-treated with the inhibitor, ketoconazole (100 μM) or compound **99** (100 μM) for overnight (16 h) before the addition of this combination mixture for further 7 h.

However, it was found later from cell-proliferation assay (MTT assay, section **8.4**) and direct cell-counting (by haemocytometer) that the concentration of the inhibitors used (100 μM) had direct anti-proliferative effect. Therefore, lower concentration of the inhibitors was used that do not have direct anti-proliferative effect to the cells. Due to time factor, the qPCR analysis was repeated following the above same treatment conditions (**1** – **4**) however using lower concentration of the inhibitors (*i.e.* 7.5 μM ketoconazole or 10 μM compound **99**) in DU-145 cells only.

Compound **99** was chosen among all the other synthesised compounds, as it was shown to have good inhibition compared with ketoconazole and other compounds in the *in vitro* inhibition of 25-(OH)-D_3 metabolism in rat kidney mitochondria (**Table 6.2**); and ATRA metabolism in rat liver microsomes (**Table 6.3**) and MCF-7 cell culture assay (**Table 7.3**).

Each data point in the graphs here (**Graphs 8.1** – **8.3**) represent the mean of three separate experiments (only two separate experiments for the DU-145 cells treated with 7.5 μM ketoconazole and 10 μM compound **99** with or without 1α,25-$(OH)_2$-D_3) each measured in triplicate wells. The CYP24, $p21^{waf1/cip1}$ and GADD45α mRNA levels of all samples shown in the graphs are normalized to 18S RNA and compared with the cells treated with DMSO only, which was arbitrarily set to 1. The error bars in the graphs represent ± standard error mean (SEM). All statistical analyses were performed using the Student's *t*-test, $p < 0.05$ was considered statistically significant.

8.3.1.1 Regulation of CYP24 mRNA in DU-145 and PC-3

The untreated DU-145 and PC-3 cells expressed undetectable to low level of CYP24 mRNA. However, when the cells were treated with 10 nM 1α,25-$(OH)_2$-D_3 for 7 h, DU-145 cells showed 1999-fold induction, while PC-3 cells showed 1100-fold induction in CYP24 mRNA relative to the untreated cells (**Graph 8.1**). Ketoconazole (at 100 and 7.5 μM) or compound **99** (at 100 and 10 μM) alone did not have significant effect on the CYP24 mRNA level in DU-145 and PC-3 cells.

Ketoconazole (100 μM), when combined with 10 nM 1α,25-$(OH)_2$-D_3 reduced the CYP24 mRNA to 362-fold change and 266-fold change in DU-145 and PC-3 cells respectively, relative to the cells treated with 10 nM 1α,25-$(OH)_2$-D_3 alone. However, 7.5 μM ketoconazole when combined with 10 nM 1α,25-$(OH)_2$-D_3 synergistically increased the CYP24 mRNA transcription level (5340-fold change) in DU-145 compared to DU-145 treated with 1α,25-$(OH)_2$-D_3 alone (1999-fold change), as shown in **Graph 8.1**.

On the other hand, combination treatment with compound **99** (100 or 10 μM) and 10 nM 1α,25-$(OH)_2$-D_3 in DU-145 significantly enhanced the CYP24 mRNA (> 10000-fold change) compared to the cells treated with 1α,25-$(OH)_2$-D_3 alone (1999-fold change). However, combination treatment with compound **99** (100 μM) and 10 nM 1α,25-$(OH)_2$-D_3 in PC-3 cells (2242-fold change) did not show statistically significant difference to the PC-3 cells treated with 1α,25-$(OH)_2$-D_3 alone (1100-fold change) ($p < 0.1$).

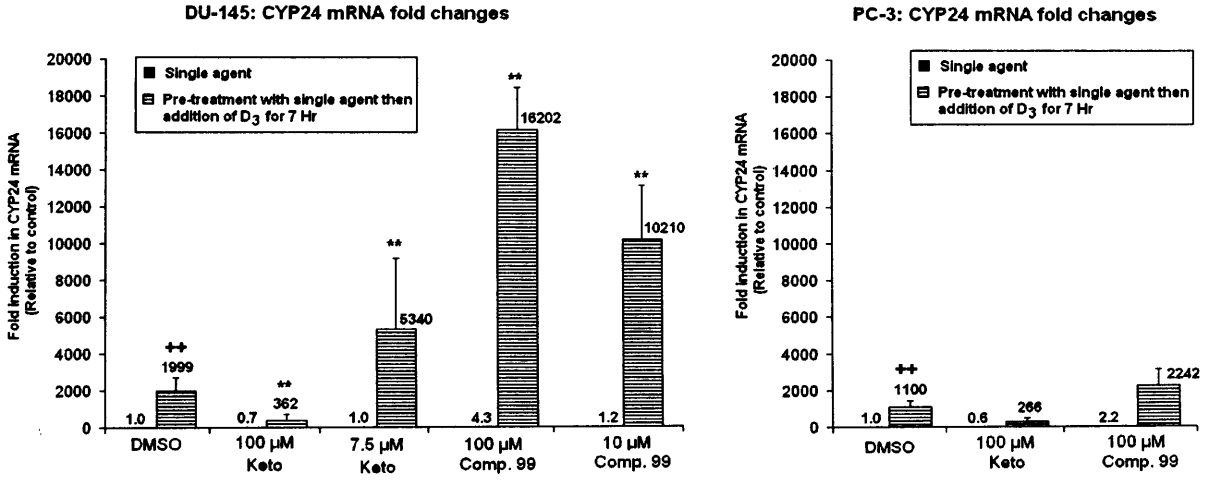

Graph 8.1. Determinations of CYP24 mRNA fold changes in DU-145 and PC-3 cells by quantitative real-time RT-PCR. Values are given as mean ± S.E.M (n = 2 or 3). $^{++}$ $p < 0.05$ when compared to control and ** $p < 0.05$ when compared to cells treated with 1α,25-$(OH)_2$-D_3 alone.

It is known from various studies that ketoconazole inhibits the activity of vitamin D_3 metabolising enzymes, *i.e.* both CYP1α and CYP24 enzymes (Kang *et al.*, 1997; Peehl *et al.*, 2001) and thus prevents the conversion of active metabolite, 1α,25-$(OH)_2$-D_3, to inactive metabolites. Farhan's group (Farhan *et al.*, 2002; Farhan *et al.*, 2003) has shown that 50 μM of genistein alone reduces CYP24 mRNA expression to more than 40 % after 8 h dosing in DU-145. The group used the conventional RT-PCR and the densitometer to semi-quantitatively measured the intensity of the band on the agarose gel. In contrast, Kang's group demonstrated using northern blot analysis that addition of ketoconazole to 1α,25-$(OH)_2$-D_3 on normal healthy human skin for 2 days, caused synergistic increase of the CYP24 mRNA level (RNA extracted from the normal healthy human skin biopsy specimen) (Kang *et al.*, 1997). Recently, Feldman's group (Swami *et al.*, 2005) used real-time RT-PCR and demonstrated significant increase in CYP24 mRNA in DU-145 co-treated with 10 μM genistein and 10 nM 1α,25-$(OH)_2$-D_3.

The results here showed that compound **99** (at 100 μM and 10 μM) and ketoconazole (at 7.5 μM) enhanced the 1α,25-$(OH)_2$-D_3-mediated induction of CYP24 mRNA in DU-145. In the rat kidney mitochondria assay (section **6.6.1**, **Table 6.2**), ketoconazole and compound **99** showed inhibition of 25-(OH)-D_3 metabolising enzymes activity. As a result, this prolongs the half-life of 1α,25-$(OH)_2$-D_3 and enhances the genomic actions of 1α,25-$(OH)_2$-D_3 to induce the VDR target genes including CYP24 gene as measured by the increased in CYP24 mRNA expression as shown in here (**Graph 8.1**).

However, the reduced CYP24 mRNA level in DU-145 and PC-3 caused by combination treatment of ketoconazole (100 μM) with 10 nM 1α,25-$(OH)_2$-D_3 (**Graph 8.1**) could be due to the direct anti-proliferative effect of ketoconazole (at 100 μM) which resulted in a decreased in the number of cells, and thus reduced the level of CYP24 mRNA.

8.3.1.2 Regulation of $p21^{waf1/cip1}$ mRNA in DU-145 and PC-3

The effects of the inhibitor alone or with 1α,25-$(OH)_2$-D_3 and the effect of 1α,25-$(OH)_2$-D_3 alone on expression of $p21^{waf1/cip1}$ mRNA were investigated here. Studies in cancer cell-lines have shown that transcriptional induction of $p21^{waf1/cip1}$ mRNA facilitates the induced differentiation of the cell-lines (Hager *et al.*, 2001; Liu *et al.*, 1996). The $p21^{waf1/cip1}$ protein , a cell-cycle regulatory protein, inhibits the

activity of cyclin-dependent kinases in the G_0/G_1 cell-cycle phase, for example, resulting in cell-cycle arrest in response to 1α,25-$(OH)_2$-D_3 in prostate cancer cells (Campbell *et al.*, 1997).

However, the degree of $p21^{waf1/cip1}$ induction varies among different cell types (Prudencio *et al.*, 2001). There were conflicting results from various studies related to the degree of $p21^{waf1/cip1}$ expression. Some studies found that 1α,25-$(OH)_2$-D_3 had no effect on $p21^{waf1/cip1}$ mRNA expression, others found that 1α,25-$(OH)_2$-D_3 downregulated $p21^{waf1/cip1}$ mRNA, while others found that the anti-proliferative effect of 1α,25-$(OH)_2$-D_3 is linked to the over expression of $p21^{waf1/cip1}$ protein (Hager *et al.*, 2004).

The results here showed that treatment with 10 nM 1α,25-$(OH)_2$-D_3 alone had no significant effect on $p21^{waf1/cip1}$ mRNA expression in DU-145 and PC-3 cells compared to untreated cells (**Graph 8.2**). However, when both cell-lines were treated with inhibitor alone (at 100 μM) or combination treatment of inhibitor and 1α,25-$(OH)_2$-D_3, these enhanced the $p21^{waf1/cip1}$ mRNA significantly ($p < 0.005$). There were no significant difference when comparing the cells treated with inhibitor alone (at 100 μM) to the cells treated with both inhibitor and 1α,25-$(OH)_2$-D_3. This observation indicated that the inhibitor itself at 100 μM has a significant effect on $p21^{waf1/cip1}$ mRNA.

Eichenberger et. al. (Eichenberger *et al.*, 1989) showed that ketoconazole (1 – 50 μg/mL) has a direct anti-proliferative effect on the prostate cancer cells (DU-145 and PC-3). Moreover, the cell proliferation and cell viability assay (MTT assay, described in section **8.4**) showed that ketoconazole (at 10 – 25 μM) or compound **99** (at 25 μM) alone in DU-145 and PC-3, showed anti-proliferative effect compared to untreated cells (**Graph 8.4**). This direct anti-proliferative effect by ketoconazole (100 μM) or compound **99** (100 μM) could result in induction of $p21^{waf1/cip1}$ mRNA as observed in the qPCR here.

At lower concentration of the inhibitor alone (10 μM compound **99**), this did not have an effect on the $p21^{waf1/cip1}$ mRNA level in DU-145 (0.7-fold change). However, ketoconazole (7.5 μM) alone caused slightly enhanced $p21^{waf1/cip1}$ mRNA (2-fold change) compared to untreated cells. It is interesting to observe the synergistic enhanced $p21^{waf1/cip1}$ mRNA level in DU-145 cells co-treated with compound **99** (10 μM) and 1α,25-$(OH)_2$-D_3 compared to the cells treated with compound **99** or 1α,25-$(OH)_2$-D_3 alone (**Graph 8.2**).

However, this co-operative enhancement of $p21^{waf1/cip1}$ mRNA level was not observed in combination treatment with ketoconazole (7.5 μM) and 1α,25-$(OH)_2$-D_3, as ketoconazole (at 7.5 μM) alone also caused significant enhanced induction of $p21^{waf1/cip1}$ mRNA (2.0-fold change, **Graph 8.2**).

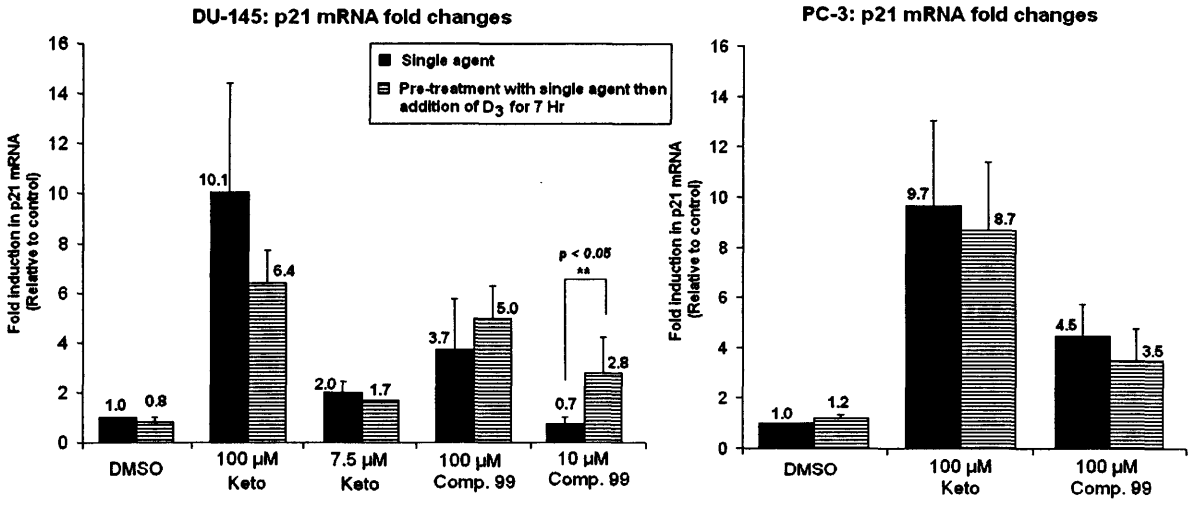

Graph 8.2. Determinations of $p21^{waf1/cip1}$ mRNA fold changes in DU-145 and PC-3 cells by quantitative real-time RT-PCR (qPCR). Values are given as mean ± S.E.M. (*n* = 2 or 3).

8.3.1.3 Regulation of GADD45α mRNA in DU-45 and PC-3

Campbell's group and others have demonstrated using cDNA microarray analysis that GADD45α is a vitamin D_3 receptor (VDR) target gene in 1α,25-$(OH)_2$-D_3-sensitive cell lines (Akutsu *et al.*, 2001; Gommersall *et al.*, 2004; Khanim *et al.*, 2004). Over expression of GADD45α inhibits cell proliferation and it is induced by various agents that damage DNA and arrest cell growth (Akutsu *et al.*, 2001). Induction of GADD45α contributes to the growth-inhibitory effects of 1α,25-$(OH)_2$-D_3 in 1α,25-$(OH)_2$-D_3-sensitive cell lines (Akutsu *et al.*, 2001).

After 7 h treatment with 10 nM 1α,25-$(OH)_2$-D_3 alone, there is no significant elevated levels of GADD45α mRNA (1.3- and 1.7-fold change in DU-145 and PC-3 respectively compared to untreated cells) [**Graph 8.3**]. This showed that 1α,25-$(OH)_2$-D_3 alone had limited effect on GADD45α in DU-145 and PC-3 cells. This is similar to the reported studies by Campbell's group (Gommersall *et al.*, 2004).

However, when DU-145 and PC-3 were treated with inhibitor alone (at 100 μM) or combination treatment of inhibitor (at 100 μM) with 1α,25-$(OH)_2$-D_3, there is a strong induction of GADD45α mRNA ($p < 0.05$) (> 3-fold changes). There

were no significant difference when comparing the cells treated with inhibitor alone (at 100 μM) to the cells co-treated with inhibitor (at 100 μM) and 1α,25-$(OH)_2$-D_3. This indicated that the inhibitor alone at 100 μM significantly elevated the GADD45α mRNA in DU-145 and PC-3. The induction of GADD45α mRNA observed here could be due to the direct anti-proliferative effect in the presence of high concentration of the inhibitor (100 μM).

The synergistic enhanced GADD45α mRNA in DU-145 cells treated with compound **99** (10 μM) and 1α,25-$(OH)_2$-D_3 was observed here (**Graph 8.3**). However, this synergistic enhanced of GADD45α mRNA level was not observed in combination treatment with ketoconazole (7.5 μM) and 1α,25-$(OH)_2$-D_3, as ketoconazole (at 7.5 μM) alone also caused induction of GADD45α mRNA (1.9-fold change, **Graph 8.3**).

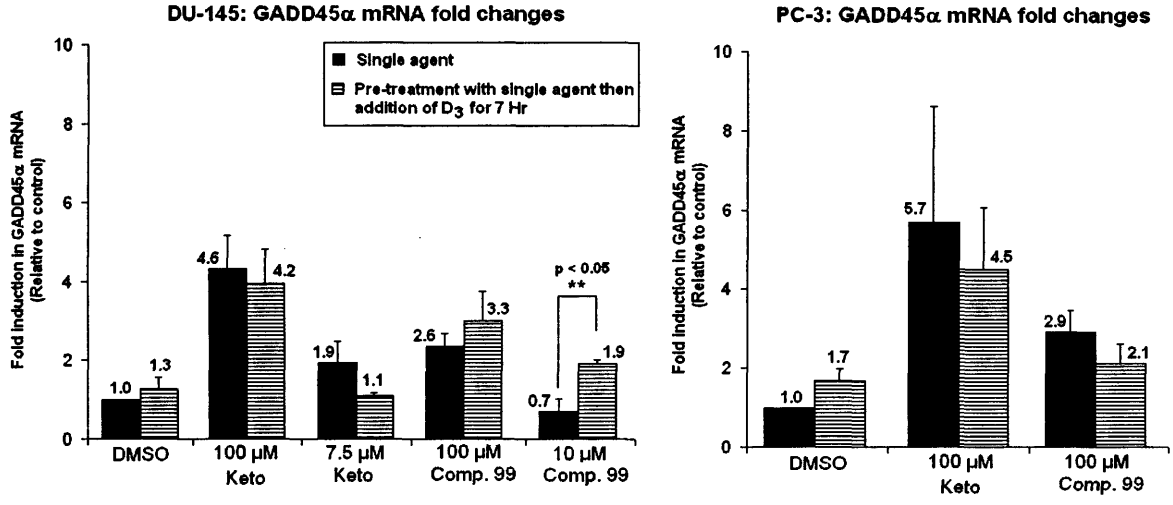

Graph 8.3. Determinations of GADD45α mRNA fold changes in DU-145 and PC-3 cells by quantitative real-time RT-PCR (qPCR). Values are given as mean ± S.E.M. (*n* = 2 or 3).

8.3.1.4 Summary of the qPCR results

Ketoconazole (7.5 μM) or compound **99** (100 and 10 μM) alone did not alter the basal CYP24 mRNA level, however, the combination of the inhibitor with 1α,25-$(OH)_2$-D_3 (10 nM) synergistically increased the CYP24 mRNA transcription level in DU-145 and/or PC-3 (**Graph 8.1**) by impeding the inactivation of 1α,25-$(OH)_2$-D_3 (*i.e.* by inhibiting the CYP24 enzyme activity).

Ketoconazole or compound **99** (at 100 μM) alone or with 1α,25-$(OH)_2$-D_3 (10 nM) caused significant anti-proliferative effect which resulted in the enhanced level of $p21^{waf1/cip1}$ and GADD45α mRNA in DU-145 and PC-3 (**Graph 8.2** and **8.3**).

Compound **99** (at 10 μM) did not alter the $p21^{waf1/cip1}$ and GADD45α mRNA level, however, compound **99** (at 10 μM) with 1α,25-$(OH)_2$-D_3 (10 nM) synergistically increased the $p21^{waf1/cip1}$ and GADD45α mRNA level in DU-145 (**Graph 8.2** and **8.3**). These observations co-relate well with the result from the cell proliferation assay [section **8.4**, **Graph 8.4 (b)**], which showed that the addition of compound **99** (at 10 μM) to 1α,25-$(OH)_2$-D_3 (10 nM) significantly reduced the growth of DU-145 cells.

8.4 Cell proliferation and cell viability assay (MTT assay)

MTT (3-[4,5-dimethylthiazol-2-yl]-2,5-diphenyltetrazolium bromide) assay is commonly used to study cell viability and proliferation in cell populations. This assay can be carried out in a microplate (96-well plates), thus reduces the amount of culture medium and number of cells required.

MTT assay is developed based on the detection of cell viability and cell proliferation (Mossman, 1983). The MTT is reduced to a blue-magenta coloured formazan precipitate only by reductase enzyme present only in metabolically active cell's mitochondrial dehydrogenases (cofactor NADPH) (**Figure 8.5**). Moreover, this assay is also for the determination of cell proliferation since proliferating cells are metabolically more active than non-proliferating (resting) cells. Quantitation of MTT reduction measured directly in the microplate using an absorbance microplate reader.

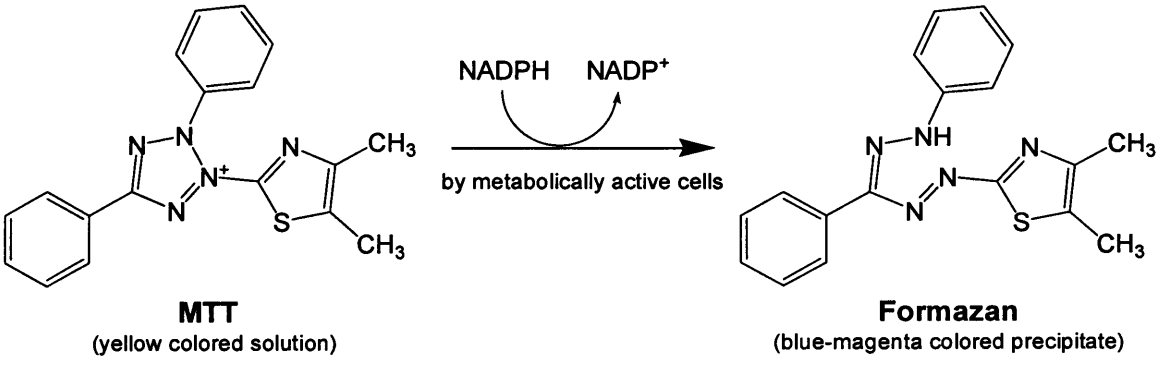

Figure 8.5. Chemical structure of MTT and its corresponding formazan product.

8.4.1 Methods for MTT assay

Cells were plated in 96-well plates (Appleton Woods, Birmingham, UK). Both the DU-145 and PC-3 cells were seeded at 2 x 10^3 cells per well. Cells were allowed to attach (left at least 7 h), and treated with growth media containing varying concentrations of the inhibitor alone, varying concentrations of the inhibitor with 10 nM 1α,25-$(OH)_2$-D_3, or 10 nM 1α,25-$(OH)_2$-D_3 alone, resulting in a final volume of 100 μL per well. The plates were incubated for 96 h, with re-dosing after 48 h. After

93 h incubation, 20 μL of MTT solution (5 mg/mL in distilled water and filtered to sterilise and to remove small amount of insoluble residue present) [Sigma-Aldrich, Dorset, UK] were added to each well and the cells were left for 3 h in the incubator (37 °C and 5 % CO_2) [So in total 96 h incubation time]. The 120 μL of MTT-containing cells and medium were removed without disturbing the blue precipitate attached to the well. 100 μL of DMSO (Sigma-Aldrich, Dorset, UK) were added into each well and incubated for 15 min at room temperature. Finally, the absorption was measured at 550 nm using the absorbance microplate reader (EMax®, Molecular Devices Corporation). The growth inhibition was expressed as a percentage of control.

8.4.2 Results and discussions from the MTT assay

The action of the individual inhibitor alone (ketoconazole or compound **99**) and in combination with 10 nM 1α,25-$(OH)_2$-D_3, or with 10 nM 1α,25-$(OH)_2$-D_3 alone in both DU-145 and PC-3 cells was examined using this MTT assay. The results are shown in **Graphs 8.4 (a) – (d)**.

DU-145 and PC-3 cells responded minimally to the anti-proliferative effect of 1α,25-$(OH)_2$-D_3 (at 10 nM), i.e. only 5 % - 7 % growth inhibition after 96 h [**Graphs 8.5 (a) – (b)**]. In DU-145 cells, ketoconazole and compound **99** showed significant anti-proliferation effect at > 10 μM (> 20 % growth inhibition). However, the combination treatment with 5 μM ketoconazole or 10 μM compound **99** with 10 nM 1α,25-$(OH)_2$-D_3 caused more than 30 % growth inhibition in DU-145 [**Graphs 8.4 (a) – (b)**].

In contrast, PC-3 cells are not only recalcitrant to 1α,25-$(OH)_2$-D_3 (at 10 nM) but also did not show significant anti-proliferation when the inhibitor and 1α,25-$(OH)_2$-D_3 were used together [**Graphs 8.4 (c) – (d)**]. Ketoconazole and compound **99** alone showed significant anti-proliferation effects at, ≥ 10 μM and > 25 μM, respectively in PC-3.

The potentiation of the anti-proliferative effect of 1α,25-$(OH)_2$-D_3 by ketoconazole and compound **99** in DU-145 could be due to the inhibition of 1α,25-$(OH)_2$-D_3 metabolism in the cells. However, this potentiation of the anti-proliferative effect of 1α,25-$(OH)_2$-D_3 is not significant in PC-3 cells.

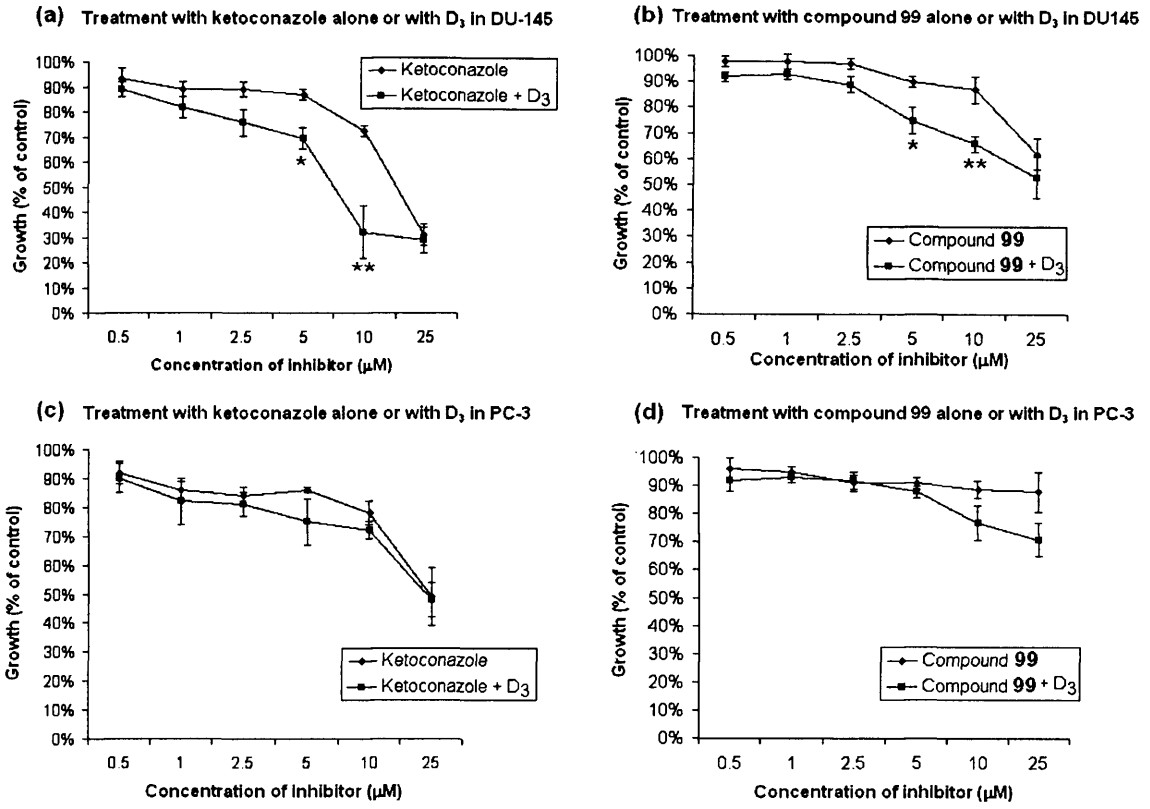

Graphs 8.4 (a) – (d). The effects of the inhibitor (ketoconazole or compound **99** at various concentrations) with or without 10 nM 1α,25-$(OH)_2$-D_3 on the proliferation of DU-145 (**a** – **b**) and PC-3 cells (**c** – **d**) was assessed by MTT assay after 96 h, with a re-dose after 48 h. Each data point represents the mean of three separate experiments undertaken in triplicate wells (± S.E.M). * Indicates $p < 0.05$ and ** indicates $p < 0.01$ when samples were compared to samples treated with the inhibitor alone.

From the above preliminary data, further MTT assays were carried out to study the anti-proliferative effect of other inhibitors alone and in combination with 10 nM 1α,25-$(OH)_2$-D_3 in DU-145 and PC-3. A total of four other tetralone analogues (compounds **91**, **102**, **98** and **104**) and four azole compounds (compounds **14**, **16**, **55** and liarozole) at 20 μM, 10 μM and 2 μM concentration with or without 1α,25-$(OH)_2$-D_3 were used in this proliferation assay [**Graphs 8.5 (a) – (d)**].

Generally, the inhibitors (at 20 μM and 10 μM) with 10 nM 1α,25-$(OH)_2$-D_3 showed synergistic anti-proliferative effect in both DU-145 and PC-3 cells. Among the azole compounds, compound **14** maintained synergistic anti-proliferative effect with 10 nM 1α,25-$(OH)_2$-D_3 even at 2 μM concentration in both cell-lines, whereas, 2 μM liarozole with 1α,25-$(OH)_2$-D_3 only showed synergistic effect in PC-3 [**Graphs 8.5 (a)** and **(b)**].

Unlike the tetralone analogues, the azole compounds alone generally showed anti-proliferative effect at 10 and 20 μM. The potentiation of the anti-proliferative

effect of 1α,25-$(OH)_2$-D_3 by these tetralone analogues is more significant in DU-145 than in PC-3. However, this potentiation effect was lost when low concentration of the inhibitor (2 μM) was used together with 10 nM 1α,25-$(OH)_2$-D_3.

In conclusion, the azole compounds and the tetralone analogues (at 10 – 20 μM) with 1α,25-$(OH)_2$-D_3 (at 10 nM) showed strong combinatorial inhibition of proliferation in DU-145 and PC-3. Some inhibitors with 1α,25-$(OH)_2$-D_3 showed more significant anti-proliferation in DU-145 compared to PC-3. This shows that the enhancement of anti-proliferative activity of 1α,25-$(OH)_2$-D_3 by the inhibitor is cell-type specific, which was also observed by Zhao *et al.* (Zhao *et al.*, 1996). A number of cell-proliferation assay have been carried out by other research groups which demonstrated that ketoconazole or liarozole showed synergistic growth inhibition with 1α,25-$(OH)_2$-D_3 (1 – 10 nM) in various cancer cell lines, *e.g.* HL60, MCF-7, MDA-MB-231 and DU-145 (Ly *et al.*, 1999; Peehl *et al.*, 2002; Rashid *et al.*, 2001; Wang *et al.*, 1997; Zhao *et al.*, 1996). This showed that ketoconazole, liarozole or other potential vitamin D_3 metabolising enzymes inhibitor could potentially be used together with 1α,25-$(OH)_2$-D_3 for the treatment of various cancer, including prostate cancer. This combination treatment allowed the used of lower dose of 1α,25-$(OH)_2$-D_3 and thus the reducing the undesirable side-effects of 1α,25-$(OH)_2$-D_3, *e.g.* hypercalcemia.

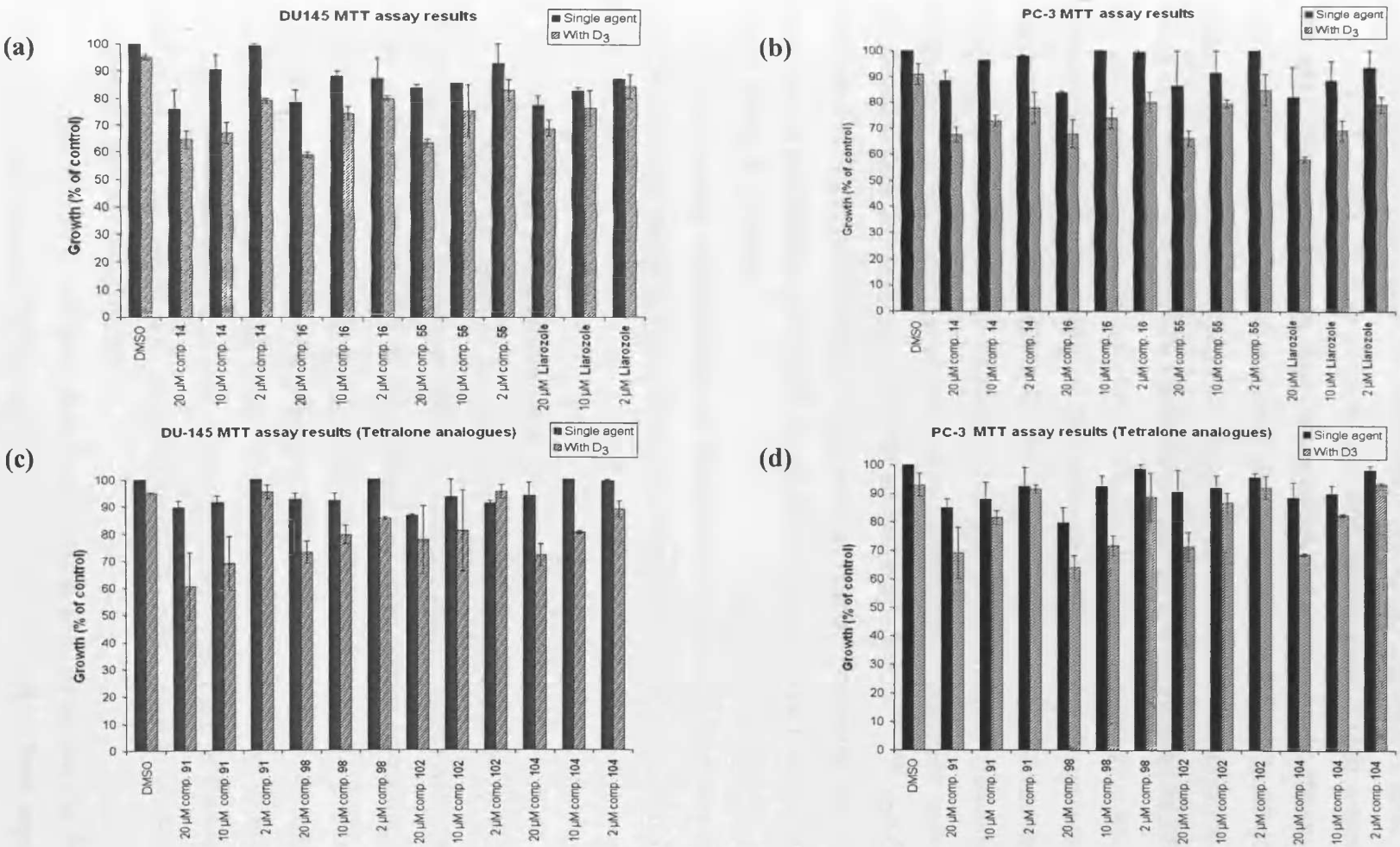

Graphs 8.5 (a) – (d). The effects of the inhibitor (azole compounds and tetralone analogues at 20, 10 and 2 µM concentrations) with or without 10 nM 1α,25-$(OH)_2$-D_3 on the proliferation of DU-145 and PC-3 cells was assessed by MTT assay after 96 h, with a re-dose after 48 h. Each data point represents the mean of two separate experiments undertaken in triplicate wells (± S.E.M).

8.5 General conclusions

The conventional RT-PCR and real-time quantitative RT-PCR analysis demonstrated that the presence of 1α,25-$(OH)_2$-D_3 and ATRA induced the expression of CYP24 and CYP26A1 mRNA respectively in DU-145 and MCF-7 cells.

1α,25-$(OH)_2$-D_3 is an effective anti-proliferative agent at high concentration (> 100 nM), however, its use at high concentration is limited by side-effects in human, *e.g.* hypercalcemia and hypercalciuria. Moreover, the half-life of 1α,25-$(OH)_2$-D_3 is limited by the induction of CYP24 enzyme. Therefore, the combination treatment using an inhibitor of vitamin D_3 metabolising enzymes with low dose 1α,25-$(OH)_2$-D_3 (10 nM) could increase the half-life of 1α,25-$(OH)_2$-D_3. The cell-proliferation assay demonstrated that the sensitivity of DU-145 and/or PC-3 cells to the growth inhibitory actions of low dose 1α,25-$(OH)_2$-D_3 (10 nM) is increased by co-treatment with an inhibitor of vitamin D_3 metabolising enzymes (ketoconazole, liarozole and the synthesised tetralone analogues and azole compounds). Consistent with this cell-proliferation data, the expression of VDR target genes, *i.e.* $p21^{waf1/cip1}$ and GADD45α, associated with growth arrest showed significant increase following the combination treatment of an inhibitor of vitamin D_3 metabolising enzymes (compound **99**) with 1α,25-$(OH)_2$-D_3 (10 nM).

It is possible that inhibitors of vitamin D_3 metabolising enzymes or selective CYP24 inhibitors can be used as combination therapies or as single agents in AIPC or other cancers.

8.6 Antifungal and antileishmanial evaluations

Dr. Marc Le Borgne and his group at the Department of Organic and Medicinal Chemistry, Faculty of Pharmacy, Nantes, France, have synthesised several series of imidazole and triazole compounds that have shown interesting antifungal and/or antileishmanial activities (Marchand *et al.*, 2002; Na *et al.*, 2003; Na *et al.*, 2004; Pagniez *et al.*, 2002). His group has collaborated with us to test some of their imidazole compounds for inhibition of retinoic acid metabolism in our rat liver microsomal enzyme assay. In return, his group at the Department of Parasitology, has performed the antifungal and antileishmanial *in vitro* activity of some of the compounds described in **chapter 4**.

Amphotericin B and the conazole compounds (*e.g.* ketoconazole, fluconazole, itraconazole and miconazole) are currently used in the market for both superficial and

systemic fungal infections. The function of the conazoles is to inhibit the cytochrome P-450-dependent 14α-lanosterol demethylase in the fungi and *Leishmania* species. This enzyme is responsible for the synthesis of the ergosterols (a component of the fungal and *Leishmania* cell membrane) via three sequential hydroxylations to remove the methyl group on C-14 (Aoyama *et al.*, 1989).

A total of seven compounds **51 – 55**, **58** and **64** (**chapter 4**) were selected to be evaluated against *Candida albicans* and *Aspergillus fumigatus*, the two most clinically important fungi responsible for the majority of systemic fungal infections; and these seven compounds were also tested against *Leishmania mexicana* promastigotes *in vitro*. The methods for the *in vitro* antifungal activity was carried out by the method based on the fluorometric properties of alamar Blue described by Le Borgne's co-workers (Pagniez and Le Pape, 2001). The *in vitro* antileishmanial activity involved measuring the antiproliferative effect of the inhibitor against the *L. mexicana* promastigotes using a colorimetric method as described by Le Borgne's group (Marchand *et al.*, 2002; Na *et al.*, 2004). Amphotericin B, ketoconazole, fluconazole and itraconazole were used as positive controls.

Among the seven compounds tested, compounds **51**, **52**, **54** and **55** showed activity against *Candida albicans* (IC_{80} < 5 μM) and *Leishmania mexicana* promastigotes (IC_{50} 38 – 62 μM) [**Table 8.3**] but no activity against *Aspergillus fumigatus*. Compounds **52** and **55** were the most active compounds among the seven compounds tested. The introduction of a methoxy group at 6-position of the benzofuran ring (compound **52**) and chlorine atom at 4-position of the phenyl ring (compound **55**) improved the activity slightly. Introduction of the nitro group at the 5-position of benzofuran group (compound **53**) resulted in a loss of activity. The results also showed that the triazole compounds (**58** and **64**) were less active than the imidazole compounds. Although none of these compounds were as active as the positive controls these results will be useful for future reference in rational design of azole compounds to improve the potency against the fungal and/or leishmania species.

Table 8.3. *In vitro* antifungal and antileishmanial activity of benzofuran-2-carboxamido ethyl-imidazole and -triazole derivatives (**51** – **55**, **58** and **64**)

Compound	Antifungal activity MIC (=IC_{80})		Antileishmanial activity IC_{50}
	Candida albicans (CA980001)	*Aspergillus fumigatus* (AF980003)	*Leishmania mexicana promastigotes*
	µM	µM	µM
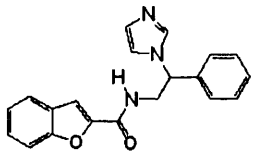 **51**	9.6 ± 0.8	> 100	52.7 ± 0.7
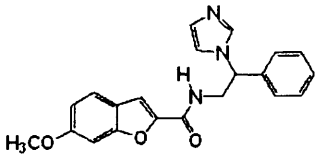 **52**	**1.8 ± 0.7**	> 100	54.4 ± 1.0
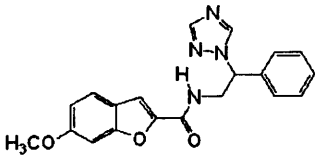 **58**	62.3 ± 0.6	> 100	61.5 ± 1.6
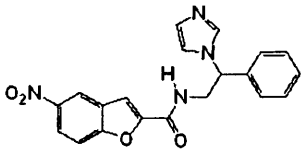 **53**	> 100	> 100	> 100
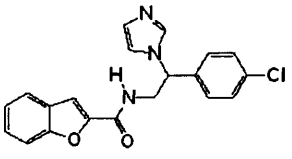 **55**	**2.8 ± 0.7**	> 100	**38.7 ± 1.7**
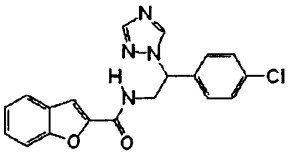 **64**	> 100	> 100	> 100
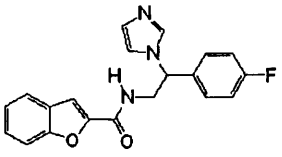 **54**	7.8 ± 0.2	> 100	52.1 ± 1.3
Amphotericin B	**0.12 ± 0.01**		**0.15 ± 0.04**
Fluconazole	**0.07 ± 0.001**		-
Itraconazole	-		**0.6 ± 0.06**
Ketoconazole	**0.0094**		-

CHAPTER 9

References

Abrahamsson PA (2001) Treatment of locally advanced prostate cancer: a new role for antiandrogen monotherapy? *European Urology*, **39**, 22-28.

Abu-Abed SS, Beckett BR, Chiba H, Chithalen JV, Jones G, Metzger D, Chambon P and Petkovich M (1998) Mouse P450RAI (CYP26) expression and retinoic acid-inducible retinoic acid metabolism in F9 cells are regulated by retinoic acid receptor gamma and retinoid X receptor alpha. *Journal of Biological Chemistry*, **273**, 2409-2415.

Adlercreutz H (2002) Phyto-oestrogens and cancer. *Lancet Oncology*, **3**, 364-373.

Aelterman W, Lang Y, Willemsens B, Vervest I, Leurs S and De Knaep F (2001) Conversion of the laboratory synthetic route of the *N*-aryl-2-benzothiazolamine R116010 to a manufacturing method. *Organic Process Research & Development*, **5**, 467-471.

Ahmad M, Ahmadi M, Nicholls PJ and Smith HJ (2000) In-vitro metabolism of retinoic acid by different tissues from male rats. *Journal of Pharmacy and Pharmacology*, **52**, 511-515.

Akutsu N, Lin R, Bastien Y, Bestawros A, Enepekides DJ, Black M and White JH (2001) Regulation of gene expression by 1α,25-dihydroxyvitamin D_3 and its analog EB1089 under growth-inhibitory conditions in squamous carcinoma cells. *Molecular Endocrinology*, **15**, 1127-1139.

Allenby G, Bocquel M-T, Saunders M, Kazmer S, Speck J, Rosenberg M, Lovey A, Kastner P, Grippo JF, Chambon P and Levin AA (1993) Retinoic acid receptors and retinoid x receptors: interations with endogenous retinoic acids. *Proceedings of the National Academy of Sciences of the United States of America*, **90**, 30-34.

American Joint Committee on Cancer (1992) *AJCC Manual for staging of cancer* 4th ed., Lippincott-Raven, Philadelphia.

Anon (2005) *British National Formulary 49 March 2005* British Medical Association and Royal Pharmaceutical Society of Great Britain, London.

Aoyama Y, Yoshida Y, Sonoda Y and Sato Y (1989) Deformylation of 32-oxo-24,25-dihydrolanosterol by the purified cytochrome P-450_{14DM} (Lanosterol 14α-demethylase) from yeast evidence confirming the intermediate step of lanosterol 14α-demethylation. *Journal of Biological Chemistry*, **264**, 18502-18505.

Applied Biosystems. URL: http://www.appliedbiosystems.com. Last Updated: 2005 <Date Access: 05 May 2005>.

Araya Z, Hosseinpour F, Bodin K and Wikvall K (2003) Metabolism of 25-hydroxyvitamin D_3 by microsomal and mitochondrial vitamin D_3 25-hydroxylases (CYP2D25 and CYP27A1): a novel reaction by CYP27A1. *Biochimica Et Biophysica Acta*, **1632**, 40-47.

Augustine RL (1965) Chapter 5: Hydrogenation of functional group II: aldehydes and ketones, in *Catalytic hydrogenation. Techniques and applications in organic synthesis* (Augustine RL ed, 1st Ed.) pp 81-123, Marcel Dekker, Inc., New York.

Bagga D, Capone S, Wang HJ, Heber D, Lill M, Chap L and Glaspy JA (1997) Dietary modulation of omega-3-omega-6 polyunsaturated fatty acid ratios in patients with breast cancer. *Journal of the National Cancer Institute*, **89**, 1123-1131.

Baggiolini EG, Iacobelli JA, Hennessy BM, Batcho AD, Sereno JF and Uskokovic MR (1986) Stereocontrolled total synthesis of 1alpha,25-dihydroxycholecalciferol and 1alpha,25-dihydroxyergocalciferol. *Journal of Organic Chemistry*, **51**, 3098-3108.

Baggiolini EG, Iacobelli JA, Hennessy BM and Uskokovic MR (1982) Stereoselective total synthesis of 1alpha,25-dihydroxycholecalciferol. *Journal of the American Chemical Society*, **104**, 2945-2948.

Baker AR, McDonnell DP, Hughes M, Crisp TM, Mangelsdorf DJ, Haussler MR, Pike JW, Shine J and Omalley BW (1988) Cloning and expression of full-length cDNA-encoding human vitamin-D receptor. *Proceedings of the National Academy of Sciences of the United States of America*, **85**, 3294-3298.

Bareis P, Bises G, Bischof MG, Cross HS and Peterlik M (2001) 25-Hydroxyvitamin D metabolism in human colon cancer cells during tumour progression. *Biochemical and Biophysical Research Communications*, **285**, 1012-1017.

Barton DHR, Hesse RH, Pechet MM and Rizzardo E (1973) A convenient synthesis of 1α-hydroxyvitamin D_3. *Journal of the American Chemical Society*, **95**, 2748-2749.

Beer TM (2003) Development of weekly high-dose calcitriol based therapy for prostate cancer. *Urologic Oncology: Seminars and Original Investigations*, **21**, 399-405.

Berrevoets CA, Umar A and Brinkmann AO (2002) Antiandrogens: selective androgen receptor modulators. *Molecular and Cellular Endocrinology*, **198**, 97-103.

Berry WR (2005) The evolving role of chemotherapy in androgen-independent (hormone-refractory) prostate cancer. *Urology*, **65**, 2-7.

Bhandari MS, Petrylak DP and Hussain M (2005) Clinical trials in metastatic prostate cancer - has there been real progress in the past decade? *European Journal of Cancer*, **41**, 941-953.

Blaner WS and Olson JA (1994) Retinol and retinoic acid metabolism, in *The retinoids: biology, chemistry and medicine* (Sporn MB, Roberts AB and Goodman DS eds, 2nd Ed.) pp 229-255, Raven Press, Ltd., New York.

Blomhoff R, Green MH and Norum KR (1992) Vitamin A: Physiological and biochemical processing. *Annual Review of Nutrition*, **12**, 37-57.

Blutt SE, Allegretto EA, Pike JW and Weigel NL (1997) 1,25-Dihydroxyvitamin D_3 and 9-*cis*-retinoic acid act synergistically to inhibit the growth of LNCaP prostate cells and cause accumulation of cells in G(1). *Endocrinology*, **138**, 1491-1497.

Blutt SE, McDonnell TJ, Polek TC and Weigel NL (2000a) Calcitriol-induced apoptosis in LNCaP cells is blocked by overexpression of Bcl-2. *Endocrinology*, **141**, 10-17.

Blutt SE, Polek TC, Stewart LV, Kattan MW and Weigel NL (2000b) A calcitriol analogue, EB1089, inhibits the growth of LNCaP tumors in nude mice. *Cancer Research*, **60**, 779-782.

Bolitt V, Mioskowski C, Shin D and Falck JR (1988) Triphenylphosphine hydrobromide: A mild and efficient catalyst for tetrahydropyranylation of tertiary alcohols. *Tetrahedron Letters*, **29**, 4583-4586.

Boring CC, Squires TS and Tong T (1992) Cancer statistics, 1992. *Ca-a Cancer Journal for Clinicians*, **42**, 19-38.

Bouillon R, Okamura WH and Norman AW (1995) Structure-function-relationships in the vitamin-D endocrine system. *Endocrine Reviews*, **16**, 200-257.

Bray F, Sankila R, Ferlay J and Parkin DM (2002) Estimates of cancer incidence and mortality in Europe in 1995. *European Journal of Cancer*, **38**, 99-166.

Brinkmann AO (2001) Molecular basis of androgen insensitivity. *Molecular and Cellular Endocrinology*, **179**, 105-109.

Burgos-Trinidad M, Brown AJ and DeLuca HF (1986) Solubilization and reconstitution of chick renal mitochondrial 25-hydroxyvitamin D_3 24-hydroxylase. *Biochemistry*, **25**, 2692-2696.

Burgos-Trinidad M, Brown AJ and DeLuca HF (1990) A rapid assay for 25-hydroxyvitamin D and 1,25-dihydroxyvitamin D 24-hydroxylase. *Analytical Biochemistry*, **190**, 102-107.

Buu-Hoi NP, Bisagni E, Royer R and Routier C (1957) Oxygen heterocycles. Part VII. Spasmolytic ketones in the benzofuran series, and related compounds. *Journal of the Chemical Society*, 625-627.

Campbell MJ, Elstner E, Holden S, Uskokovic M and Koeffler HP (1997) Inhibition of proliferation of prostate cancer cells by a 19-*nor*-hexafluoride vitamin D_3 analogue involves the induction of p21(waf1), p27(kip1) and E-cadherin. *Journal of Molecular Endocrinology*, **19**, 15-27.

Campbell MJ and Koeffler HP (1997) Toward therapeutic intervention of cancer by vitamin D compounds. *Journal of the National Cancer Institute*, **89**, 182-185.

Campbell MJ, Park S, Uskokovic M, Dawson MI and Koeffler HP (1998) Expression of retinoic acid receptor-β sensitizes prostate cancer cells to growth inhibition mediated by combinations of retinoids and a 19-*nor*-hexafluoride vitamin D_3 analog. *Endocrinology*, **139**, 1972-1980.

Catalona WJ, Carvalhal GF, Mager DE and Smith DS (1999) Potency, continence and complication rates in 1,870 consecutive radical retropubic prostatectomies. *Journal of Urology*, **162**, 433-438.

Chamberlain J, Melia J, Moss S and Brown J (1997a) Treatment of advanced prostate cancer. *Health Technology Assessment*, **1**, 35-39.

Chamberlain J, Melia J, Moss S and Brown J (1997b) Treatment of localised prostate cancer. *Health Technology Assessment*, **1**, 29-34.

Chambon P (1996) A decade of molecular biology of retinoic acid receptors. *The FASEB Journal*, **10**, 940-954.

Chen ZX, Xue YQ, Zhang R, Tao RF, Xia XM, Li C, Wang W, Zu WY, Yao XZ and Ling BJ (1991) A clinical and experimental study on all-*trans* retinoic acid-treated acute promyelocytic leukemia patients. *Blood*, **78**.

Chen KS, Prahl JM and DeLuca HF (1993) Isolation and expression of human 1,25-dihydroxyvitamin D_3 24-hydroxylase cDNA. *Proceedings of the National Academy of Sciences of the United States of America*, **90**, 4543-4547.

Chen H, Fantel AG and Juchau MR (2000a) Catalysis of the 4-hydroxylation of retinoic acids by CYP3A7 in human fetal hepatic tissues. *Drug Metabolism and Disposition*, **28**, 1051-1057.

Chen H, Howald WN and Juchau MR (2000b) Biosynthesis of all-*trans*-retinoic acid from all-*trans*-retinol: catalysis of all-*trans*-retinol oxidation by human P-450 cytochromes. *Drug Metabolism and Disposition*, **28**, 315-322.

Chen TC, Schwartz GG, Burnstein KL, Lokeshwar BL and Holick MF (2000c) The *in vitro* evaluation of 25-hydroxyvitamin D_3 and 19-*nor*-1alpha,25-dihydroxyvitamin D_2 as therapeutic agents for prostate cancer. *Clinical Cancer Research*, **6**, 901-908.

Chithalen JV, Luu L, Petkovich M and Jones G (2002) HPLC-MS/MS analysis of the products generated from all-*trans*-retinoic acid using recombinant human CYP26A. *Journal of Lipid Research*, **43**, 1133-1142.

Cho BT, Kang SK and Shin SH (2002) Application of optically active 1,2-diol monotosylates for synthesis of β-azido and β-amino alcohols with very high enantiomeric purity. Synthesis of enantiopure (*R*)-octopamine, (*R*)-tembamide and (*R*)-aegeline. *Tetrahedron: Asymmetry*, **13**, 1209-1217.

Choudary BM, Kantam ML and Kavita B (2001) Synthesis of 2-nitroalkanols by Mg---Al---*O-t*-Bu hydrotalcite. *Journal of Molecular Catalysis A: Chemical*, **169**, 193-197.

Christie Hospital NHS Trust. (2003). Cystectomy for men. URL: http://www.christie.man.ac.uk/patientinfo/booklets/textbooklets/cystectomy/cystectomy_men.htm. Last Updated: 7 February 2003. <Date Access: 3 March 2003>.

Coetzee GA and Ross RK (1994) Prostate cancer and the androgen receptor. *Journal of the National Cancer Institute*, **86**, 872-873.

Cohen JH, Kristal AR and Stanford JL (2000) Fruit and vegetable intakes and prostate cancer risk. *Journal of the National Cancer Institute*, **92**, 61-68.

Cook LS, Goldoft M, Schwartz SM and Weiss NS (1999) Incidence of adenocarcinoma of the prostate in Asian immigrants to the United States and their descendants. *Journal of Urology*, **161**, 152-155.

Cross HS, Huber C and Peterlik M (1991) Antiproliferative effect of 1,25-dihydroxyvitamin D_3 and its analogs on human colon adenocarcinoma cells (Caco-2): influence of extracellular calcium. *Biochemical and Biophysical Research Communications*, **179**, 57-62.

Culine S, Kramar A, Droz JP and Theodore C (1999) Phase II study of all-*trans* retinoic acid administered intermittently for hormone refractory prostate cancer. *The Journal of Urology*, **161**, 173-175.

Cupp-Vickery JR and Poulos TL (1995) Structure of cytochrome $P450_{eryF}$ involved in erythromycin biosynthesis. *Natural Structural Biology*, **2**, 144-153.

Dai HY and Posner GH (1994) Synthetic approaches to vitamin D. *Synthesis-Stuttgart*, **12**, 1383-1398.

Dalesio O, van Tinteren H, Clarke M, Peto R, Schroder FH, Dechering I, Evans V, Godwin J, Blumenstein BA, Crawford ED, Denis L, Hall R, Hill C, Iversen P, Shipley WU, Soloway M and Sylvester R (2000) Maximum androgen blockade in advanced prostate cancer: an overview of the randomised trials. *Lancet*, **355**, 1491-1498.

Dawson MI and Hobbs PD (1994) The synthetic chemistry of retinoids, in *The retinoids: Biology, chemistry and medicine* (Sporn MB, Roberts AB and Goodman DS eds, 2nd Ed.) pp 5-178, Raven Press Ltd., New York.

De Coster R, Wouters W, Vanginckel R, End D, Krekels M, Coene MC and Bowden C (1992) Experimental studies with Liarozole (R-75251) - an antitumoral agent which inhibits retinoic acid breakdown. *Journal of Steroid Biochemistry and Molecular Biology*, **43**, 197-201.

de Vos S, Dawson MI, Holden S, Le J, Wang A, Cho S, Chen D and Koeffler HP (1997) Effects of retinoic X receptor (RXR)-class-selective ligands on prostate cancer cell proliferation. *Prostate*, **32**, 115-121.

Debes JD and Tindall DJ (2002) Mini review: The role of androgens and the androgen receptor in prostate cancer. *Cancer Letters*, **187**, 1-7.

DeLuca HF (1988) The vitmain-D story - a collaborative effort of basic science and clinical medicine. *The FASEB Journal*, **2**, 224-236.

DeMarzo AM, Nelson WG, Isaacs WB and Epstein JI (2003) Pathological and molecular aspects of prostate cancer. *Lancet*, **361**, 955-954.

Djikman GA, Van Moorselaar RJA, Van Ginckel R, Van Stratum P, Wouters L, Debruyne FMJ, Schalken JA and De Coster R (1994) Antitumoral effects of liarozole in androgen-dependent and independent R3327-Dunning prostate adenocarcinomes. *Journal of Urology*, **151**, 217-222.

Dodds EC, Goldberg L, Lawson W and Robinson R (1938) Estrogenic activity of certain synthetic compounds. *Nature*, **141**, 247-249.

Dowling CR and Risbridger GP (2000) The role of inhibins and activins in prostate cancer pathogenesis. *Endocrine-Related Cancer*, **7**, 243-256.

Draber W and Regel E (1975) Process for the production of N-(1,1,1-trisubstituted)-methylazoles. Germany, US 3,897,438.

Eichenberger T, Trachtenberg J, Toor P and Keating A (1989) Ketoconazole: a possible direct cytotoxic effect on prostate carcinoma cells. *Journal of Urology*, **141**, 190-191.

Eisenberger MA, Blumenstein BA, Crawford ED, Miller G, McLeod DG, Loehrer PJ, Wilding G, Sears K, Culkin DJ, Thompson IM, Bueschen AJ and Lowe BA (1998) Bilateral orchiectomy with or without flutamide for metastatic prostate cancer. *New England Journal of Medicine*, **339**, 1036-1042.

Elstner E, Campbell MJ, Munker R, Shintaku P, Binderup L, Heber D, Said J and Koeffler HP (1999) Novel 20-*epi*-vitamin D_3 analog combined with 9-*cis*-retinoic acid markedly inhibits colony growth of prostate cancer cells. *Prostate*, **40**, 141-149.

Eom SH, Wang J and Steitz TA (1996) Structure of Taq polyerase with DNA at the polymerase active site. *Nature*, **382**, 278-281.

Ettinger RA and DeLuca HF (1996) The Vitamin D endocrine system and its therapeutic potential. *Advances in Drug Research.*, **28**, 269-312.

Evans RM (1988) The steroid and thyroid-hormone receptor superfamily. *Science*, **240**, 889-895.

Farhan H, Wahala K, Adlercreutz H and Cross HS (2002) Isoflavonoids inhibit catabolism of vitamin D in prostate cancer cells. *Journal of Chromatography B*, **777**, 261-268.

Farhan H, Wahala K and Cross HS (2003) Genistein inhibits vitamin D hydroxylase CYP24 and CYP27B1 expression in prostate cells. *Journal of Steroid Biochemistry and Molecular Biology*, **84**, 423-429.

Feldman BJ and Feldman D (2001) The development of androgen-independent prostate cancer. *Nature Reviews*, **1**, 34-45.

Fiorella PD and Napoli JL (1991) Expression of cellular retinoic acid binding protein (CRABP) in *Escherichia coli*. *Journal of Biological Chemistry*, **266**, 16572-16579.

Fisher GJ and Voorhees JJ (1996) Molecular mechanisms of retinoid actions in skin. *The FASEB Journal*, **10**, 1002-1013.

Fletcher SG and Theodorescu D (2005) Surgery or radiation: what is the optimal management for locally advanced prostate cancer? *Canadian Journal of Urology*, **12**, 58-61.

Fong CJ, Sutkowski DM, Braun EJ, Bauer KD, Sherwood ER, Lee C and Kozlowski JM (1993) Effect of retinoic acid on the proliferation and secretory activity of androgen-responsive prostatic carcinoma cells. *Journal of Urology*, **149**, 1190-1194.

Frankel S, Smith GD, Donovan J and Neal D (2003) Screening for prostate cancer. *Lancet*, **361**, 1122-1128.

Freedman LP (1999) Transcriptional targets of the vitamin D_3 receptor-mediated cell cycle arrest and differentiation. *Journal of Nutrition*, **129**, 581S-586S.

Freyne E, Raeymaekers A, Venet M, Sanz G, Wouters W, De Coster R and Van Wauwe J (1998) Synthesis of LIAZAL^{TM}, a retinoic acid metabolism blocking agent (RAMBA) with potential clinical applications in oncology and dermatology. *Bioorganic & Medicinal Chemistry Letters*, **8**, 267-272.

Galbraith SM and Duchesne GM (1997) Androgens and prostate cancer: biology, pathology and hormonal therapy. *European Journal of Cancer*, **33**, 545-554.

Gamblin GT, Liberman UA, Eil C, Downs RW, DeGrange DA and Marx SJ (1985) Vitamin D-dependent rickets type II. Defective induction of 25-hydroxyvitamin D_3-24-hydroxylase by 1,25-dihydroxyvitamin D_3 in cultured skin fibroblast. *Journal of Clinical Investigation*, **75**, 954-960.

Gann PH, Hennekens CH, Sacks FM, Grodstein F, Giovannucci EL and Stampfer MJ (1994) Prospective-study of plasma fatty-acids and risk of prostate cancer. *Journal of the National Cancer Institute*, **86**, 281-286.

Gant TG and Meyers AI (1994) The chemistry of 2-oxazolines (1985-present). *Tetrahedron*, **50**, 2297-2360.

Gao M, Ossowski L and Ferrari AC (1999) Activation of Rb and decline in androgen receptor protein precede retinoic acid-induced apoptosis in androgen-dependent LNCaP cells and their androgen-independent derivative. *Journal of Cellular Physiology*, **179**, 336-346.

Garnick MB (1993) Prostate cancer - screening, diagnosis, and management. *Annals of Internal Medicine*, **118**, 804-818.

Ghazarian JG, Schnoes HK and DeLuca HF (1973) Mechanism of 25-hydroxycholecalciferol 1-hydroxylation. Incorporation of oxygen-18 into the 1 position of 25-hydroxycholecalciferol. *Biochemistry*, **12**, 2555-2558.

Ghazarian JG, Jefcoate CR, Knutson JC, Orme-Johnson WH and DeLuca HF (1974) Mitochondrial cytochrome P450. A componene of chick kidney 25-hydrocholecalciferol-1alpha-hydroxylase. *Journal of Biological Chemistry*, **249**, 3026-3033.

Giguere V, Ong ES, Segui P and Evans RM (1987) Identification of a receptor for the morphogen retinoic acid. *Nature*, **330**, 624-629.

Giovannucci E, Stampfer MJ, Krithivas K, Brown M, Brufsky A, Talcott J, Hennekens CH and Kantoff PW (1997) The CAG repeat within the androgen receptor gene and its relationship to prostate cancer. *Proceedings of the National Academy of Sciences of the United States of America*, **94**, 3320-3323.

Giovannucci E (1999) Tomatoes, tomato-based products, lycopene, and cancer: Review of the epidemiologic literature. *Journal of the National Cancer Institute*, **91**, 317-331.

Giuliano AR, Franceschi RT and Wood RJ (1991) Characterization of the vitamin D receptor from Caco-2 human colon carcinoma cell line: Effect of cellular differentiation. *Archives of Biochemistry and Biophysics*, **285**, 261-269.

Goldgar DE, Easton DF, Cannonalbright LA and Skolnick MH (1994) Systematic population-based assessment of cancer risk in first-degree relatives of cancer probands. *Journal of the National Cancer Institute*, **86**, 1600-1608.

Gollnick H, Ehlert R, Rinck G and Organos CE (1990) Retinoids: An overview of pharmacokinetics and therapeutic value. *Methods in enzymology*, **190**, 291-304.

Gommersall LM, Khanim FL, Peehl DM, Doherty AH and Campbell MJ (2004) Epigenetic repression of transcription by the vitamin D_3 receptor in prostate cancer cells. *Journal of Steroid Biochemistry and Molecular Biology*, **89-90**, 251-256.

Goodman DS (1984) Vitamin A and retinoids in health and disease. *New England Journal of Medicine*, **310**, 1023-1031.

Goodman HM (1994a) Adrenal glands, in *Basic Medical Endocrinology* (Goodman HM ed, 2nd Ed.) pp 71-112, Lippincott-Raven, Philadelphia.

Goodman HM (1994b) Pituitary gland, in *Basic Medical Endocrinology* (Goodman HM ed, 2nd Ed.) pp 28-45., Lippincott-Raven, Philadelphia.

Gowda DC, Gowda ASP, Baba AR and Gowda S (2000) Nickel-catalyzed formic acid reductions. A selective method for the reduction of nitro compounds. *Synthetic Communications*, **30**, 2889-2895.

Greer VP, Mason P, Kirby AJ, Smith HJ, Nicholls PJ and Simons C (2003) Some 1,2- and 1,3-diphenylethane derivatives as inhibitors of retinoic acid-metabolising enzymes. *Journal of Enzyme Inhibition and Medicinal Chemistry*, **18**, 431-443.

Griffin JE (2000) Male reproductive function, in *Textbook of Endocrine Physiology* (Griffin JE and Ojeda SR eds, 4th Ed.) pp 243-264, Oxford University Press, New York.

Gross C, Stamey T, Hancock S and Feldman D (1998) Treatment of early recurrent prostate cancer with 1,25- dihydroxyvitamin D3 (calcitriol). *Journal of Urology*, **159**, 2035-2039.

Gudas LJ, Sporn MB and Roberts AB (1994) Cellular biology and biochemistry of the retinoids, in *The retinoids: biology, chemistry and medicine* (Sporn MB, Roberts AB and Goodman DS eds, 2nd Ed.) pp 443-520, Raven Press Ltd., New York.

Guo Y, Strugnell SA, Back DW and Jones GW (1993) Transfected human liver cytochrome P-450 hydroxylates vitamin D analogs at different side-chain positions. *Proceedings of the National Academy of Sciences of the United States of America*, **90**, 8668-8672.

Guo X, Ruiz A, Rando RR, Bok D and Gudas LJ (2000) Esterification of all-*trans*-retinol in normal human epithelial cell strains and carcinoma lines from oral cavity, skin and breast: reduced expression of lecithin:retinol acyltransferase in carcinoma lines. *Carcinogenesis*, **21**, 1925-1933.

Guo X, Knudsen BS, Peehl DM, Ruiz A, Bok D, Rando RR, Rhim JS, Nanus D and Gudas LJ (2002) Retinol metabolism and lecithin:retinoc acyltransferase levels are reduced in cultured human prostate cancer cells and tissue specimens. *Cancer Research*, **62**, 1654-1661.

Guzey M, Kitada S and Reed JC (2002) Apoptosis induction by 1alpha,25-dihydroxyvitamin D_3 in prostate cancer. *Molecular Cancer Therapeutics*, **1**, 667-677.

Habuchi T, Suzuki T, Sasaki R, Wang LZ, Sato K, Satoh S, Akao T, Tsuchiya N, Shimoda N, Wada Y, Koizumi A, Chihara J, Osamu OA and Kato T (2000) Association of vitamin D receptor gene polymorphism with prostate cancer and benign prostatic hyperplasia in a Japanese population. *Cancer Research*, **60**, 305-308.

Hager G, Formanek M, Gedlicka C, Thurnher D, Knerer B and Kornfehl J (2001) $1,25(OH)_2$ vitamin D_3 induces elevated expression of the cell cycle-regulating genes P21 and P27 in squamous carcinoma cell lines of the head and neck. *Acta Oto-Laryngologica*, **121**, 103-109.

Hager G, Kornfehl J, Knerer B, Weigel G and Formanek M (2004) Molecular analysis of p21 promoter activity isolated from squamous carcinoma cell lines of the head and neck under the influence of $1,25(OH)_2$ vitamin D_3 and its analogs. *Acta Oto-Laryngologica*, **124**, 90-96.

Hanchette CL and Schwartz GG (1992) Geographic patterns of prostate cancer mortality - Evidence for a protective effect of ultraviolet-radiation. *Cancer*, **70**, 2861-2869.

Hanlon AL and Hanks GE (2000) Failure patterns and hazard rates for failure suggest the cure of prostate cancer by external beam radiation. *Urology*, **55**, 725-729.

Harper ME, Pike A, Peeling WB and Griffith D (1974) Steroids of adrenal origin metabolised by human prostatic tissue *in vivo* and *in vitro*. *Journal of Endocrinology*, **60**, 117-125.

Harris KA and Reese DM (2001) Treatment options in hormone-refractory prostate cancer: current and future approaches. *Drugs*, **61**, 2177-2192.

Hartley-Asp B (1984) Estramustine-induced mitotic arrest in 2 human prostatic-carcinoma cell-lines DU-145 and PC-3. *Prostate*, **5**, 93-100.

Harvei S, Bjerve KS, Tretli S, Jellum E, Robsahm TE and Vatten L (1997) Prediagnostic level of fatty acids in serum phospholipids: omega-3 and omega-6 fatty acids and the risk of prostate cancer. *International Journal of Cancer*, **71**, 545-551.

Hasemann CA, Ravichandran KG, Peterson JA and Deisenhofer J (1994) Crystal structure and refinement of cytochrome $P450_{terp}$ at 2.3 Å resolution. *Journal of Molecular Biology*, **236**, 1169-1185.

Hassner A, Cromwell NH and Davis SJ (1958) The chemistry of derivatives of 2-benzaltetralone. I. A novel rearrangement leading to 2-substituted-1-naphthols. *Journal of the American Chemical Society*, **79**, 230-234.

Haussler MR, Whitfield GK, Haussler CA, Hsieh J-C, Thompson PD, Selznick SH, Dominguez CE and Jurutka PW (1998) The nuclear vitamin D receptor: Biological and molecular regulatory properties revealed. *Journal of Bone and Mineral Research.*, **13**, 325-349.

Heinonen OP, Albanes D, Virtamo J, Taylor PR, Huttunen JK, Hartman AM, Haapakoski J, Malila N, Rautalahti M, Ripatti S, Maenpaa H, Teerenhovi L, Koss L, Virolainen M and Edwards BK (1998) Prostate cancer and supplementation with alpha-tocopherol and beta-carotene: incidence and mortality in a controlled trial. *Journal of the National Cancer Institute*, **90**, 440-446.

Heshmat MY, Kaul L, Kovi J, Jackson MA, Jackson AG, Jones GW, Edson M, Enterline JP, Worrell RG and Perry SL (1985) Nutrition and prostate cancer - a case control study. *Prostate*, **6**, 7-17.

Heyman RA, Mangelsdorf DJ, Dyck JA, Stein RB, Eichele G, Evans RM and Thaller C (1992) 9-*Cis* retinoic acid is a high affinity ligand for the retinoid X receptor. *Cell*, **68**, 397-406.

Hill DL and Grubbs CJ (1992) Retinoids and cancer prevention. *Annual Review of Nutrition*, **12**, 161-181.

Hisatake J, Kubota T, Hisatake Y, Uskokovic M, Tomoyasu S and Koeffler HP (1999) 5,6-*trans*-16-*ene*-Vitamin D_3: A new class of potent inhibitors of proliferation of prostate, breast, and myeloid leukemic cells. *Cancer Research*, **59**, 4023-4029.

Holick MF, Garabedian M and DeLuca HF (1972) 1,25-dihydroxycholecalciferol: metabolite of vitamin D_3 active on bone in anephric rats. *Science*, **176**, 1146-1147.

Holick MF, Kleiner-Bossaller A, Schnoes HK, Kasten PM, Boyle IT and DeLuca HF (1973) 1,24,25-Trihydroxyvitamin D_3. A metabolites of vitamin D_3 effective on intestine. *Journal of Biological Chemistry*, **248**, 6691-6696.

Huang ME, Ye YC, Chen SR, Chai JR, Lu JX, Zhoa L, Gu LJ and Wang ZY (1988) Use of all-*trans*-retinoic acid in the treatment of acute promyelocytic leukemia. *Blood*, **72**, 567-572.

Huggins C, Stevens RE and and Hodges CW (1941) Studies on prostatic carcinoma. II. The effects of castration on advanced carcinoma of the prostate gland. *Archive surgery*, **43**, 209-211.

Hughes MR and Haussler MR (1978) 1,25-Dihydroxyvitamin D_3 receptors in parathyroid glands. Preliminary characterization of cytoplasmic and nuclear binding components. *Journal of Biological Chemistry*, **252**, 1065-1073.

Igawa M, Tanabe T, Chodak GW and Rukstalis DB (1994) *N*-(4-Hydroxyphenyl) retinamide induces cell cycle specific growth inhibition in PC-3 cells. *Prostate*, **24**.

Ingles SA, Ross RK, Yu MC, Irvine RA, LaPera G, Haile RW and Coetzee GA (1997) Association of prostate cancer risk with genetic polymorphisms in

vitamin D receptor and androgen receptor. *Journal of the National Cancer Institute*, **89**, 166-170.

Irvine RA, Yu MC, Ross RK and Coetzee GA (1995) The CAG and GGC microsatellites of the androgen receptor gene are in linkage disequilibrium in men with prostate cancer. *Cancer Research*, **55**, 1937-1940.

Iversen P, Tyrrell CJ, Kaisary AV, Anderson JB, Van Poppel H, Tammela TLJ, Chamberlain M, Carroll K and Melezinek I (2000) Bicalutamide monotherapy compared with castration in patients with nonmetastatic locally advanced prostate cancer: 6.3 years of followup. *Journal of Urology*, **164**, 1579-1582.

Jacobsen BK, Knutsen SF and Fraser GE (1998) Does high soy milk intake reduce prostate cancer incidence? The Adventist Health Study (United States). *Cancer Causes & Control*, **9**, 553-557.

James SY, Mackay AG and Colston KW (1995) Vitamin D derivatives in combination with 9-*cis* retinoic acid promote active cell death in breast cancer cells. *Journal of Molecular Endocrinology*, **14**, 391-394.

Jani AB and Hellman S (2003) Early prostate cancer: clinical decision-making. *Lancet*, **361**, 1045-1053.

Jarno L (2003) PhD thesis: Studies of the action and metabolism of retinoic acid in MCF-7 human breast cancer cells, in *Welsh School of Pharmacy*, Cardiff University, Cardiff.

Jemal A, Murray T, Ward E, Samuels A, Tiwari RC, Ghafoor A, Feuer EJ and Thun MJ (2005) Cancer statistics, 2005. *Ca-a Cancer Journal for Clinicians*, **55**, 10-30.

John EM, Dreon DM, Koo J and G.G. S (2004) Residential sunlight exposure is associated with decreased risk of prostate cancer. *Journal of Steroid Biochemistry and Molecular Biology*, **89-90**, 549-552.

Johnson CS, Hershberger PA, Bernardi RJ, Mcguire TF and Trump DL (2002) Vitamin D receptor: a potential target for intervention. *Urology*, **60**, 123-130.

Jones GW, Strugnell SA and DeLuca HF (1998) Current understanding of the molecular actions of vitamin D. *Physiological Review*, **78**, 1193-1231.

Jones G, Ramshaw H, Zhang A, Cook R, Byford V, White J and Petkovich M (1999) Expression and activity of vitamin D-metabolizing cytochrome P450s (CYP1α and CYP24) in human nonsmall cell lung carcinomas. *Endocrinology*, **140**, 3303-3310.

Kagechika H, Kawachi E, Hashimoto Y, Himi T and Shudo K (1988) Retinobenzoic acids. 1. Structure-activity relationships of aromatic amides with retinoidal activity. *Journal of Medicinal Chemistry*, **31**, 2182-2192.

Kagechika H, Kawachi E, Hashimoto Y and Shudo K (1989) Retinobenzoic acids. 2. Structure-activity relationships of chalcone-4-carboxylic acids and flavone-4'-carboxylic acids. *Journal of Medicinal Chemistry*, **32**, 834-840.

Kang S, Li X-Y, Duell EA and Voorhees JJ (1997) The Retinoid X receptor agonist 9-*cis*-Retinoic acid and the 24-hydroxylase inhibitor ketoconazole increase activity of 1,25-dihydroxyvitamin D_3 in human skin *in vivo*. *Journal of Investigative Dermatology*, **108**, 513-518.

Karmali RA (1987) Fatty acids: inhibition. *American Journal of Clinical Nutrition*, **45**, 225-229.

Kelly WK, Osman I, Reuter VE, Curley T, Heston WD, Nanus DM and Scher HI (2000) The development of biologic end points in patients treated with differentiation agents: An experience of retinoids in prostate cancer. *Clinical Cancer Research*, **6**, 838-846.

Khanim FL, Gommersall LM, Wood VHJ, Smith KL, Montalvo L, O'Neill LP, Xu Y, Peehl DM, Stewart PM, Turner BM and Campbell MJ (2004) Altered SMRT levels disrupt vitamin D_3 receptor signalling in prostate cancer cells. *Oncogene*, **23**, 6712-6725.

Kirby AJ, Le Lain R, Mason P, Maharlouie F, Nicholls PJ, Smith HJ and Simons C (2002) Some 3-(4-aminophenyl) pyrrolidine-2,5-diones as all-*trans*-retinoic acid metabolising enzyme inhibitors (RAMBAs). *Journal of Enzyme Inhibition*, **17**, 321-327.

Kirby AJ, Le Lain R, Maharlouie F, Mason P, Nicholls PJ, Smith HJ and Simons C (2003) Inhibition of retinoic acid metabolising enzymes by 2-(4-aminophenylmetyl)-6-hydroxy-3,4-dihydronaphthalene-1(2*H*)-one and related compounds. *Journal of Enzyme Inhibition and Medicinal Chemistry*, **18**, 27-33.

Kivineva M, Blauer M, Syvala H, Tammela T and Tuohimaa P (1998) Localization of 1,25-hydroxyvitamin D_3 receptor (VDR) expression in human prostate. *Journal of Steroid Biochemistry and Molecular Biology*, **66**, 121-127.

Klein EA (2005) Chemoprevention of prostate cancer. *Critical Reviews in Oncology/Hematology*, **54**, 1-10.

Koike M, Elstner E, Campbell MJ, Aso H, Uskokovic M and Koeffler HP (1997) 19-*nor*-Hexafluoride analogs of vitamin D_3: a novel class of potent inhibitors of proliferation of human breast cancer cell lines. *Cancer Research*, **57**, 4545-4550.

Koike M, Koshizuka K, Kawabata H, Yang R, Taub HE, Said J, Uskokovic M, Tsuruoka N and Koeffler HP (1999) 20-Cyclopropyl-cholecalciferol vitamin D_3 analogs: A unique class of potent inhibitors of proliferation of human prostate, breast and myeloid leukemia cell lines. *Anticancer Research*, **19**, 1689-1697.

Kolonel LN, Hankin JH and Yoshizawa CN (1987) Vitamin A and prostate cancer in elderly men: enhancement of risk. *Cancer Research*, **47**, 2982-2985.

Kolvenbag GJ, Iversen P and Newling DW (2001) Antiandrogen monotherapy: a new form of treatment for patients with prostate cancer. *Urology*, **58**, 16-23.

Koper PCM, Stroom JC, van Putten WLJ, Korevaar GA, Heijmen BJM, Wijnmaalen A, Jansen PP, Hanssens PEJ, Griep C, Krol ADG, Samson MJ and Levendag PC (1999) Acute morbidity reduction using 3DCRT for prostate carcinoma: A randomized study. *International Journal of Radiation Oncology Biology Physics*, **43**, 727-734.

Koshiuka K, Elstner E, Williamson JW, Said JW, Tada Y and Koeffler HP (2000) Novel therapeutic approach: organic arsenical (melarsoprol) alone or with *all-trans*-retinoic acid markedly inhibit growth of human breast and prostate cancer cells in vitro and in vivo. *British Journal of Cancer*, **82**, 452-458.

Kraus S, Naor Z and Seger R (2005) Gonadotropin-releasing hormone in apoptosis of prostate cancer cells. *Cancer Letters*, article in press.

Krekels MDWG, Verhoeven A, van Dun J, Cools W, Van Hove C, Dillen L, Coene M-C and Wouters W (1997) Induction of the oxidative catabolism of retinoic acid in MCF-7 cells. *British Journal of Cancer*, **75**, 1098-1104.

Krishnan AV, Peehl DM and Feldman D (2003) The role of vitamin D in prostate cancer. *Recent Results in Cancer Research*, **164**, 205-221.

Kurlandsky SB, Duell EA, Kang S, Voorhees JJ and Fisher GJ (1996) Auto-regulation of retinoic acid biosynthesis through regulation of retinol esterification in human keratinocytes. *Journal of Biological Chemistry*, **271**, 15346-15352.

Kusudo T, Sakaki T, Abe D, Fujishima T, Kittaka A, Takayama H, Ohta M and Inouye K (2003) Metabolism of 20-epimer of 1α,25-dihydroxyvitamin D_3 by CYP24: species-based difference between humans and rats. *Biochemical and Biophysical Research Communications*, **309**, 885-892.

Langer O, Dolle F, Valette H, Halldin C, Vaufrey F, Fruseau C, Coulon C, Ottaviani M, Nagren K, Bottlaender M, Maziere B and Crouzel C (2001) Synthesis of high-specific-radioactivity 4- and 6-[^{18}F]fluorotaraminol- PET tracers for the andrenergic nervous system of the heart. *Bioorganic & Medicinal Chemistry*, **9**, 677-694.

Lawyer FC, Stoffel S, Saiki RK, Myambo K, Drummond R and Gelfand DH (1989) Isolation, characterization, and expression in *Escherichia coli* of the DNA polymerase gene from *Thermus aquaticus*. *Journal of Biological Chemistry*, **264**, 6427-6437.

Le Lain R, Nicholls PJ, Smith HJ and Maharlouie FH (2001) Inhibitors of human and rat testes microsomal 17β-hydroxysteroid dehydrogenase (17β-HSD) as potential agents for prostatic cancer. *Journal of Enzyme Inhibition*, **16**, 35-45.

Le Lain R, Barrell KJ, Saeed GS, Nicholls PJ, Simons C, Kirby AJ and Smith HJ (2002) Some coumarins and triphenylethene derivatives as inhibitors of human testes microsomal 17β-hydroxysteroid dehydrogenase (17β-HSD Type 3): Further studies with tamoxifen on the rat testes microsomal enzyme. *Journal of Enzyme Inhibition and Medicinal Chemistry*, **17**, 93-100.

Leo MA and Lieber CS (1985) New pathway for retinol metabolism in liver microsomes. *Journal of Biological Chemistry*, **260**, 5228-5231.

Leo MA, Lasker JM, Raucy JL, Kim CI, Black M and Lieber CS (1989) Metabolism of retinol and retinoic acid by human liver cytochrome P4502C8. *Archives of Biochemistry and Biophysics*, **269**, 305-312.

Lepor H, Nieder AM and Ferrandino MN (2001) Intraoperative and postoperative complications of radical retropubic prostatectomy in a consecutive series of 1,000 cases. *Journal of Urology*, **166**, 1729-1733.

Lewis DFV and Hlavica P (2000) Interactions between redox partners in various cytochrome P450 systems: functional and structural aspects. *Biochimica Et Biophysica Acta*, **1460**, 353-374.

Lewis DFV (2001) *Guide to cytochromes P450 structure and function*, Taylor and Francis, London.

Liang JY, Fontana JA, Rao JN, Ordonez JV, Dawson MI, Shroot B, Wilber JF and Feng P (1999) Synthetic retinoid CD437 induces S-phase arrest and apoptosis in human prostate cancer cells LNCaP and PC-3. *Prostate*, **38**, 228-236.

Limonta P, Marelli MM and Moretti RM (2001) LHRH analogues as anticancer agents: pituitary and extrapituitary sites of action. *Expert Opinion on Investigational Drugs*, **10**, 709-720.

Liu M, Lee MH, Cohen M, Bommakanti M and Freedman LP (1996) Transcriptional activation of the Cdk inhibitor p21 by vitamin D_3 leads to the induced differentiation of the myelomonocytic cell line U937. *Genes & Development*, **10**, 142-153.

Liu G, Oettel K, Ripple G, Staab MJ, Horvath D, Alberti D, Arzoomanian R, Marnocha R, Bruskewitz R, Mazess R, Bishop C, Bhattacharya A, Bailey H and Wilding G (2002) Phase I trial of 1α-hydroxyvitamin D_2 in patients with hormone refractory prostate cancer. *Clinical Cancer Research*, **8**, 2820-2827.

Liu G, Wilding G, Staab MJ, Horvath D, Miller K, Dresen A, Alberti D, Arzoomanian R, Chappell R and Bailey H (2003) Phase II study of 1α-hydroxyvitamin D_2 in the treatment of advanced androgen-independent prostate cancer. *Clinical Cancer Research*, **9**, 4077-4083.

Livak KJ and Schmittgen TD (2001) Analysis of relative gene expression data using real-time quantitative PCR and the 2(-Delta Delta *C*(T)) method. *Methods*, **25**, 402-408.

Lodish H, Berk A, Matsudaira P, Kaiser CA, Krieger M, Scott MP, Zipursky SL and Darnell J (2003) Transcriptional control of gene expression, in *Molecular cell biology* (Lodish H, Berk A, Matsudaira P, Kaiser CA, Krieger M, Scott MP, Zipursky SL and Darnell J eds, 5th Ed.) pp 447-491, W.H. Freeman and Company, New York.

Lotan R (1980) Effects of vitamin A and its analogs (retinoids) on normal and neoplastic cells. *Biochimica Et Biophysica Acta*, **605**, 33-91.

Lou YR, Laaksi I, Syvala H, Blauer M, Tammela TLJ, Ylikomi T and Tuohimaa P (2003) 25-Hydroxyvitamin D_3 is an active hormone in human primary prostatic stromal cells. *The FASEB Journal*, **18**, 332-334.

Luscombe CJ, Fryer AA, French ME, Liu S, Saxby MF, Jones PW and Strange RC (2001) Exposure to ultraviolet radiation: association with susceptibility and age at presentation with prostate cancer. *Lancet*, **358**, 641-642.

Ly LH, Zhao XY, Holloway L and Feldman D (1999) Liarozole acts synergistically with 1 alpha,25-dihydroxyvitamin D_3 to inhibit growth of DU145 human prostate cancer cells by blocking 24-hydroxylase activity. *Endocrinology*, **140**, 2071-2076.

Lythgoe B (1980) Simonsen Lecture. Synthetic approaches to vitmain D and its relatives. *Chemical Society Review*, **9**, 449-475.

Ma JF, Nonn L, Campbell MJ, Hewison M, Feldman D and Peehl DM (2004) Mechanisms of decreased vitamin D 1α-hydroxylase activity in prostate cancer cells. *Molecular and Cellular Endocrinology*, **221**, 67-74.

Maharlouie FH (1996) Design and synthesis of inhibitors of steroid sulphate and 17 beta-hydroxysteroid dehydrogenase as potential agents in the treatment of breast cancer., in *Welsh School of Pharmacy*, Cardiff University, Cardiff.

Malkowicz SB (2001) The role of diethylstilbestrol in the treatment of prostate cancer. *Urology*, **58**, 108-113.

Mangelsdorf DJ, Ong ES, Dyck JA and Evans RM (1990) Nuclear receptor that identifies a novel retinoic acid response pathway. *Nature*, **345**, 224-229.

Mangelsdorf DJ and Evans RM (1995) The RXR heterodimers and orphan receptors. *Cell*, **83**, 841-850.

Mangelsdorf DJ, Thummel C, Beato M, Herrlich P, Schutz G, Umesono K, Blumberg B, Kastner P, Mark M, Chambon P and Evans RM (1995) The nuclear receptor superfamily - the 2nd decade. *Cell*, **83**, 835-839.

Marchand P, Le Borgne M, Na Y-M, Pagniez F, Abdala H, Le Baut G and Le Pape P (2002) Synthesis of antileishmanial activity of 3-(α-azolylbenzyl)indoles. *Journal of Enzyme Inhibition and Medicinal Chemistry*, **17**, 353-358.

Marill J, Cresteil T, Lanotte M and Chabot GG (2000) Identification of human cytochrome P450s involved in the formation of all-*trans*-retinoic acid principal metabolites. *Molecular Pharmacology*, **58**, 1341-1348.

Martinez AA, Pataki I, Edmundson G, Sebastian E, Brabbins D and Gustafson G (2001) Phase II prospective study of the use of conformal high-dose- rate brachytherapy as monotherapy for the treatment of favorable stage prostate cancer: A feasibility report. *International Journal of Radiation Oncology Biology Physics*, **49**, 61-69.

Martini R and Murray M (1993) Participation of P4503A4 enzymes in rat hepatic microsomal retinoic acid 4-hydroxylation. *Archives of Biochemistry and Biophysics*, **303**, 17-66.

Mason P (2000) PhD thesis: Studies on inhibitors of cytochrome P450 enzymes as potential anti-cancer agents, in *Welsh School of Pharmacy*, Cardiff University, Cardiff.

McLeod DG (2003) Hormonal therapy: Historical perspective to future directions. *Urology*, **61**, 3-7.

McSorley LC and Daly AK (2000) Identification of human cytochrome P450 isoforms that contribute to all-*trans*-retinoic acid 4-hydroxylation. *Biochemical and Pharmacology*, **60**, 517-526.

Merrick GS, Butler WM, Dorsey AT, Galbreath RW, Blatt H and Lief JH (2000) Rectal function following prostate brachytherapy. *International Journal of Radiation Oncology Biology Physics*, **48**, 667-674.

Merrick GS, Wallner K, Butler WM, Lief JH and Sutlief S (2001) Short-term sexual function after prostate brachytherapy. *International Journal of Cancer*, **96**, 313-319.

Mettlin C, Selenskas S, Natarajan N and Huben R (1989) Beta-carotene and animal fats and their relationship to prostate cancer risk - a case control study. *Cancer*, **64**, 605-612.

Miller VA, Francis PA, Rigas JR, Muindi JRF, Tong WP, Kris MG and Warrell RP (1994) The cytochrome P-450 inhibitors, ketoconazole and liarozole, modulate all-*trans* retinoic acid metabolism. In: 8th NCI/EORTC Symposium on New Drugs in Cancer Therapy, Amsterdam, March 15-18.

Miller GJ, Stapleton GE, Hedlund TE and Moffatt KA (1995) Vitamin D receptor expression, 24-hydroxylase activity, and inhibition of growth by 1alpha,25-dihydroxyvitamin D_3 in seven human prostatic carcinoma cell lines. *Clinical Cancer Research*, **1**, 997-1003.

Mills PK, Beeson WL, Phillips RL and Fraser GE (1989) Cohort study of diet, life-style, and prostate cancer in Adventist men. *American Journal of Epidemiology*, **130**, 829-829.

Miyaura N, Yanagi T and Suzuki A (1981) The palladium-catalyzed cross-coupling reaction of phenylboronic acid with haloarenes in the presence of bases. *Synthetic Communications*, **11**, 513-519.

Miyaura C, Abe E, Suda T and Kuroki T (1985) Alternative differentiation of human promyelocytic leukemia cells (HL-60) induced selectively by retinoic acid and 1alpha,25-dihydroxyvitamin D_3. *Cancer Research*, **45**, 4244-4248.

MOE-Dock 2003.04. Chemical Computing Group, Inc., Montreal, Quebec, Canada. URL: http://www.chemcomp.com.

Moenius T, Burtscher P, Egger H, Bovermann G and Oberer L (1999) C-14 labelling of NVPVID400 - a specific vitamin D_3- hydroxylase inhibitor. *Journal of Labelled Compounds & Radiopharmaceuticals*, **42**, 1053-1060.

Molecular Operating Environment 2003.04. Chemical Computing Group, Inc., Montreal, Quebec, Canada. URL: http://www.chemcomp.com.

Monkawa T, Yoshida T, Wakino S, Shinki T, Anazawa H, DeLuca HF, Suda T, Hayashi M and Saruta T (1997) Molecular cloning of cDNA and genomic DNA for human 25-hydroxyvitamin D_3 1alpha-hydroxylase. *Biochemical and Biophysical Research Communications*, **239**, 527-533.

Montie JE and Pienta KJ (1994) Review of the role of androgenic hormones in the epidemiology of benign prostatic hyperplasia and prostate cancer. *Urology*, **43**, 892-899.

Moon RC, Mehta RG and Rao KVN (1994) Retinoids and cancer in experimental animals, in *The retinoids: Biology, chemistry and medicine* (Sporn MB, Roberts AB and Goodman DS eds, 2nd Ed.) pp 573-595, Raven Press Ltd., New York.

Mooradian AD, Morley JE and Korenman SG (1987) Biological actions of androgens. *Endocrine Reviews*, **8**, 1-28.

Moore MJ, Osoba D, Murphy K, Tannock IF, Armitage A, Findlay B, Coppin C, Neville A, Venner P and Wilson J (1994) Use of palliative end-points to evaluate the effects of mitoxantrone and low-dose prednisone in patients with hormonally resistant prostate cancer. *Journal of Clinical Oncology*, **12**, 689-694.

Moraga D, Rivasberrios A, Farias G, Wallin M and Maccioni RB (1992) Estramustine-phosphate binds to a tubulin binding domain on microtubule-associated proteins MAP-2 and TAU. *Biochimica Et Biophysica Acta*, **1121**, 97-103.

Morris MJ and Scher HI (2002) Novel therapies for the treatment of prostate cancer: current clinical trials and development strategies. *Surgical Oncology-Oxford*, **11**, 13-23.

Morrison RT and Boyd RN (1987) Carbonions 1, Aldol and Claisen condensation, in *Organic Chemistry* (Morrison RT and Boyd RN eds, 1st Ed.) pp 905-929, Allyn and Bacon Inc., Massachusette.

Mossman T (1983) Rapid colorimetric assay for cellular growth and survival: Application to proliferation and cytotoxicity assays. *Journal of Immunological Methods*, **65**, 55-63.

Muindi JR, Young CW and Warrell JRP (1994) Clinical pharmacology of all-*trans* retinoic acid. *Leukemia*, **8**, 1807-1812.

Muir CS, Nectoux J and Staszewski J (1991) The epidemiology of prostatic cancer - geographical distribution and time trends. *Acta Oncologica*, **30**, 133-140.

Mullis KB and Fuloona FA (1987) Specific synthesis of DNA in vitro via polymerase-catalyzed chain reaction. *Methods in enzymology*, **155**, 335-350.

Mulvihill MJ, Kan JL, Beck P, Bittner M, Cesario C, Cooke A, Keane DM, Nigro AI, Nilson C, Smith V, Srebernak M, Sun F-L, Vrkljan M, Winski SL, Castelhano AL, Emerson D and Gibson N (2005) Potent and selective [2-imidazol-1-yl-2-(6-alkoxy-naphthalen-2-yl)-1-methyl-ethyl]-dimethyl-amines as retinoic acid metabolic blocking agents (RAMBAs). *Bioorganic & Medicinal Chemistry Letters*, **15**, 1669-1673.

Na Y-M, Le Borgne M, Pagniez F, Le Baut G and Le Pape P (2003) Synthesis and antifungal activity of new 1-halogenobenzyl-3-imidazolylmethylindole derivatives. *European Journal of Medicinal Chemistry*, **38**, 75-87.

Na Y-M, Lebouvier N, Le Borgne M, Pagniez F, Alvarez N, Le Pape P and Le Baut G (2004) Synthesis and antileishmanial activity of 3-imidazolylalkylindoles. Part I. *Journal of Enzyme Inhibition and Medicinal Chemistry*, **19**, 451-457.

Nadin L and Murray M (1999) Participation of CYP2C8 in retinoic acid 4-hydroxylation in human hepatic microsomes. *Biochemical Pharmacology*, **58**, 1201-1208.

Napoli JL (1996) Retinoic acid biosynthesis and metabolism. *The FASEB Journal*, **10**, 993-1001.

Njar VCO, Nnane IP and Brodie AMH (2000) Potent inhibition of retinoic acid metabolism enzyme(s) by novel azolyl retinoids. *Bioorganic & Medicinal Chemistry Letters*, **10**, 1905-1908.

Njar VCO (2002) Cytochrome P450 retinoic acid 4-hydroxylase inhibitors: potential agents for cancer therapy. *Mini Reviews in Medicinal Chemistry*, **2**, 261-269.

Oh WK and Kandoff PW (1998) Management of hormone refractory prostate cancer: current standards and future prospects. *Journal of Urology*, **160**, 1220-1229.

Ohori M, Wheeler TM, Kattan MW, Goto Y and Scardino PT (1995) Prognostic-significance of positive surgical margins in radical prostatectomy specimens. *Journal of Urology*, **154**, 1818-1824.

Ohyama Y, Hayashi S and Okuda K (1989) Purification of 25-hydroxyvitamin D_3 24-hydroxylase from rat kidney mitochondria. *FEBS Letter*, **255**, 405-408.

Ohyama Y and Okuda K (1991) Isolation and characterization of a cytochrome P-450 from rat kidney mitochondria that catalyzes the 24-hydroxylation of 25-hydroxyvitamin D_3. *Journal of Biological Chemistry*, **266**, 8690-8695.

Ohyama Y, Noshiro M and Okuda K (1991) Cloning and expression of cDNA encoding 25-hydroxyvitamin D_3 24-hydroxylase. *FEBS Letter*, **278**, 195-198.

Ohyama Y, Hayashi S, Usui E, Noshiro M and Okuda K-I (1997) Assay of vitamin D derivatives and purification of vitamin D hydroxylases. *Methods in Enzymology*, **282**, 186-199.

Ojeda SR and McCann SM (2000) The anterior pituitary and hypothalamus, in *Textbook of Endocrine Physiology* (Griffin JE and Ojeda SR, 4th) pp 128-162., Oxford University Press, New York.

Omdahl JL, Gray RW, Boyle IT, Knutson JC and DeLuca HF (1972) Regulation of metabolism of 25-hydroxycholecalciferol by kidney tissue in vitro by dietary calcium. *Nature - New Biology.*, **237**, 63-64.

Omdahl JA, Morris HA and May BK (2002) Hydroxylase enzymes of the vitamin D pathway: expression, function and regulation. *Annual Review of Nutrition*, **22**, 139-166.

Omdahl JA, Bobrovnikova EV, Annalora A, Chen P and Serda R (2003) Expression, structure-function, and molecular modeling of vitamin D P450s. *Journal of Cellular Biochemistry*, **88**, 356-362.

Ong DE (1994) Cellular transport and metabolism of vitamin A: roles of the cellular retinoid-binding proteins. *Nutrition Review*, **52**, S24-S31.

Osborne JL, Schwartz GG, Smith DC, Bahnson R, Day R and Trump DL (1995) Phase II trial of oral 1,25-dihydroxyvitamin D (Calcitriol) in hormone refractory prostate cancer. *Urologic Oncology*, **1**, 195-198.

Pagniez F and Le Pape P (2001) Possible new fluorometric screening test for antifungal drugs. *Journal de Mycologie Medicale*, **11**, 73-78.

Pagniez F, Le Borgne M, Marchand P, Na Y-M, Le Baut G, Robert-Piessard S and Le Pape P (2002) *In vitro* activity of a new antifungal azolyl-substituted indole

against *Aspergillus fumigatus*. *Journal of Enzyme Inhibition and Medicinal Chemistry*, **17**, 425-429.

Parkin DM (2004) International variation. *Oncogene*, **23**, 6329-6340.

Pasquali D, Thaller C and Eichele G (1996) Abnormal level of retinoic acid in prostate cancer tissues. *Journal of Clinical Endocrinology and Metabolism*, **81**, 2186-2191.

Patel JB, Huynh CK, Handratta VD, Gediya LK, Brodie AMH, Goloubeva OG, Clement OO, Nanne IP, Soprano DR and Njar VCO (2004) Novel retinoic acid metabolism blocking agents endowed with multiple biological activities are efficient growth inhibitors of human breast and prostate cancer cells in vitro and a human breast tumor xenograft in nude mice. *Journal of Medicinal Chemistry*, **47**, 6716-6729.

Peck GL (1982) Retinoids: therapeutic use in dermatology. *Drugs*, **24**, 342-351.

Peck GL and DiGiovanna JJ (1994) Synthetic retinoids in dermatology, in *The retinoids: Biology, chemistry and medicine* (Sporn MB, Roberts AB and Goodman DS eds, 2nd Ed.) pp 631-658, Raven Press Ltd., New York.

Peehl DM, Wong ST and Stamey T (1993) Vitamin A regulates proliferation and differentiation of human prostatic epithelial cells. *Prostate*, **23**, 69-78.

Peehl DM, Skowronski RJ, Leung GK, Wong ST, Stamey TA and Feldman D (1994) Antiproliferative effects of 1,25-dihydroxyvitamin D_3 on primary cultures of human prostatic cells. *Cancer Research*, **54**, 805-810.

Peehl DM, Wong ST, Cramer SD, Gross C and Feldman D (1995) Suramin, hydrocortisone and retinoic acid modify inhibitory effects of 1,25-dihydroxyvitamin D_3 on prostatic epithelial cells. *Urologic Oncology: Seminars and Original Investigations*, **1**, 188-194.

Peehl DM, Seto E and Feldman D (2001) Rationale for combination ketoconazole/vitamin D treatment of prostate cancer. *Urology*, **58**, 123-126.

Peehl DM, Seto E, Hsu JY and Feldman D (2002) Preclinical activity of ketoconazole in combination with calcitriol or the vitamin D analogue EB 1089 in prostate cancer cells. *Journal of Urology*, **168**, 1583-1588.

Peehl DM, Shinghal R, Nonn L, Seto E, Krishnan AV, Brooks JD and Feldman D (2004) Molecular activity of 1,25-dihydroxyvitamin D_3 in primary cultures of human prostatic epithelial cells revealed by cDNA microarray analysis. *Journal of Steroid Biochemistry and Molecular Biology*, **92**, 131-141.

Pestellini V, Ghelardoni M, Maggi CA, Roncucci G and Meli A (1984) *N*-[(Benzofuran-2-yl)(phenyl)methyl]-alkylene diamines useful in treating arrhythmic, histaminic and tussive conditions. Italy, US 4,485,112.

Pestellini V, Giannotti D, Giolitti A, Fanto N, Riviera L and Bellotti MG (1987) New benzofuran-imidazoles as antimycotic agents. 1. Synthesis and characterization. *Chemioterapia*, **6**, 269-271.

Petkovich M, Brand NJ, Krust A and Chambon P (1987) A human retinoic acid receptor which belongs to the family of nuclear receptors. *Nature*, **330**, 444-450.

Petrylak DP, Tangen CM, Hussain MHA, Lara PNJ, Jones JA, Taplin ME, Burch PA, Berry D, Moinpour C, Kohli M, Benson MC, Small EJ, Raghavan D and Crawford ED (2004) Docetaxel and estramustine compared with mitoxantrone and prednisone for advanced refractory prostate cancer. *New England Journal of Medicine*, **351**, 1513-1520.

Pienta KJ and Esper PS (1993) Risk factors for prostate cancer. *Annals of Internal Medicine*, **118**, 793-803.

Pienta KJ, Nguyen NM and Lehr JE (1993) Treatment of prostate cancer in rat with the synthetic retinoid fenretinide. *Cancer Research*, **53**, 224-226.

Pollack A, Zagars GK, Smith LG, Lee JJ, von Eschenbach AC, Antolak JA, Starkschall G and Rosen I (2000) Preliminary results of a randomized radiotherapy dose-escalation study comparing 70 Gy with 78 Gy for prostate cancer. *Journal of Clinical Oncology*, **18**, 3904-3911.

Pollard M, Luckert PH and Sporn MB (1991) Prevention of primary prostate cancer in Lobund-Wistar rats by *N*-(4-hydroxyphenyl)retinamide. *Cancer Research*, **51**, 3610-3611.

Ponchon G, Kennan AL and DeLuca HF (1969) "Activation" of vitamin D by the liver. *Journal of Clinical Investigation*, **48**, 2032-2037.

Posner GH, Crawford KR, Yang HW, Kahraman M, Jeon HB, Li H, Lee JK, Suh BC, Hatcher MA, Labonte T, Usera A, Dolan PM, Kensler TW, Peleg S, Jones G, Zhang A, Korczak B, Saha U and Chuang SS (2004) Potent, low-calcemic, selective inhibitors of CYP24 hydroxylase: 24 sulfone analogs of the hormone 1α,25-dihydroxyvitamin D_3. *Journal of Steroid Biochemistry and Molecular Biology*, **89-90**, 5-12.

Potters L, Torre T, Fearn PA, Leibel SA and Kattan MW (2001) Potency after permanent prostate brachytherapy for localized prostate cancer. *International Journal of Radiation Oncology Biology Physics*, **50**, 1235-1242.

Poulos TL, Finzel BC and Howard AJ (1987) High-resolution crystal structure of cytochrome $P450_{cam}$. *Journal of Molecular Biology*, **195**, 687-700.

Preslock JP (1980) Steroidogenesis in the mammalian testis. *Endocrine Reviews*, **1**, 132-139.

Prudencio J, Akutsu N, Benlimame N, Wang T, Bastien Y, Lin R, Black MJ, Alaoui-Jamali MA and White JH (2001) Action of low calcemic 1α,25-dihydroxyvitamin D_3 analogue EB1089 in head and neck squamous cell carcinoma. *Journal of the National Cancer Institute*, **93**, 745-753.

Ralhan R and Kaur J (2003) Retinoids as chemopreventive agents. *Journal of Biological Regulators & Homeostatic Agents*, **17**, 66-91.

Raner GM, Vaz AD and Coon MJ (1996) Metabolism of all-*trans*, 9-*cis*, and 13-*cis* isomers of retinal by purified isozymes of microsomal cytochrome P450 and mechanism-based inhibition of retinoid oxidation by citral. *Molecular Pharmacology*, **49**, 515-522.

Rapson WS and Shuttleworth RGJ (1940) The production of polycyclic aromatic types through the cyclodehydration of unsaturated ketones. *Journal of the Chemical Society*, 636-641.

Rarey M, Kramer B, Lengauer T and Kleber G (1996) A fast flexible docking method using an incremental construction algorithm. *Journal of Molecular Biology*, **261**, 470-489.

Rashid SF, Mountford JC, Gombart AF and Campbell MJ (2001) 1α,25-Dihydroxyvitamin D_3 displays divergent growth effects in both normal and malignant cells. *Steroids*, **66**, 433-440.

Ravichandran KG, Boddupalli SS, Hasermann CA, Peterson JA and Deisenhofer J (1993) Crystal structure of hemoprotein domain of $P450_{BM-3}$, a prototype for microsomal P450's. *Science*, **261**, 731-736.

Ray WJ, Bain G, Yao M and Gottlieb DI (1997) CYP26, a novel mammalian cytochrome P450, is induced by retinoic acid and defines a new family. *Journal of Biological Chemistry*, **272**, 18702-18708.

Reichel H, Koeffler HP and Norman AW (1989) The role of the vitamin D endocrine system in health and disease. *New England Journal of Medicine*, **320**, 980-991.

Reinhardt TA and Horst RL (1989) Ketoconazole inhibits self-induced metabolism of 1,25-dihydroxyvitamin D_3 and amplifies 1,25-dihydroxyvitamin D_3 receptor up-regulation in rat osteosarcoma cells. *Archives of Biochemistry and Biophysics*, **272**, 459-465.

Reynolds WF and Enriquez RG (2001) Gradient-selected versus phase-cycled HMBC and HSQC: pros and cons. *Magnetic Resonance in Chemistry*, **39**, 531-538.

Richter F, Joyce A, Fromowitz F, Wang SL, Watson J, Watson R, Irwin RJ and Huang HFS (2002) Immunohistochemical localization of the retinoic acid receptors in human prostate. *Journal of Andrology*, **23**, 830-838.

Roberts AB, Nichols MD, Newton DL and Sporn MB (1979) In vitro metabolism of retinoic acid in hamster intestine and liver. *Journal of Biological Chemistry*, **254**, 6296-6302.

Roberts ES, Vaz ADN and Coon MJ (1992) Role of isozymes of rabbit microsomal cytochrome P-450 in the metabolism of retinoic acid, retinol and retinal. *Molecular Pharmacology*, **41**, 427-433.

Robertson CN, Roberson KM, Padilla GM, O'Brien ET, Cook JM, Kim CS and Fine RL (1996) Induction of apoptosis by diethylstilbestrol in hormone-insensitive prostate cancer cells. *Journal of the National Cancer Institute*, **88**, 908-917.

Rose DP, Boyar AP and Wynder EL (1986) International comparisons of mortality-rates for cancer of the breast, ovary, prostate, and colon, and per-capita food-consumption. *Cancer*, **58**, 2363-2371.

Rosenberger M (1982) Retinoic acid metabolites. 1. Total synthesis of 4-hydroxy- and 4-oxo-retinoic acid. *Journal of Organic Chemistry*, **47**, 1698-1701.

Ross AC, Zolfaghari R and Weisz J (2001) Vitamin A: recent advances in the biotransformation, transport, and metabolism of retinoids. *Current Opinions in Gastroenterology*, **17**, 184-192.

Ross AC (2003) Retinoid production and catabolism: role of diet in regulating retinol esterification and retinoic acid oxidation. *Journal of Nutrition*, **133**, 291S-296S.

Rowe A (1997) Retinoid X Receptors. *International Journal of Biochemistry and Cell Biology*, **29**, 275-278.

Russell PJ, Bennett S and Sticker P (1998) Growth factor involvement in progression of prostate cancer. *Clinical Chemistry*, **44**, 705-723.

Saiki RK, Gelfand DH, Stoffel S, Scharf SJ, Higuchi R, Horn GT, Mullis KB and Erlich HA (1988) Primer-directed enzymatic amplification of DNA with a thermostable DNA polymerase. *Science*, **239**, 487-491.

Sakaki T, Sawada N, Nonaka Y, Ohyama Y and Inouye K (1999) Metabolic studies using recombinant *Escherichia coli* cells producing rat mitochondrial CYP24. *European Journal of Biochemistry*, **262**, 43-48.

Sakaki T, Sawada N, Komai K, Shiozawa S, Yamada S, Yamamoto K, Ohyama Y and Inouye K (2000) Dual metabolic pathway of 25-hydroxyvitamin D_3 catalyzed by human CYP24. *European Journal of Biochemistry*, **267**, 6158-6165.

Sasagawa I and Nakada T (2001) Epidemiology of prostatic cancer in East Asia. *Archives of Andrology*, **47**, 195-201.

Schally AV, Comaru-Schally AM, Plonowski A, Nagy A, Halmos G and Rekasi Z (2000) Peptide analogs in the therapy of prostate cancer. *Prostate*, **45**, 158-166.

Schellhammer PF (2001) Luteinizing hormone-releasing hormone monotherapy: a viable option for treatment of prostate cancer? *Urology*, **58**, 10-15.

Scherr D, Pitts WR, Jr. and Vaughn ED, Jr. (2002) Diethylstilbesterol revisited: androgen deprivation, oesteoporosis and prostate cancer. *Journal of Urology*, **167**, 535-538.

Scherr D, Swindle PW and Scardino PT (2003) National comprehensive cancer network guidelines for the management of prostate cancer. *Urology*, **61**, 14-24.

Schoch GA, Yano JK, Wester MR, Griffin KJ, Stout CD and Johnson EF (2004) Structure of human microsomal cytochrome P450 2C8. *Journal of Biological Chemistry*, **279**, 9497-9503.

Schuster I and Egger H (1997) Acylated aminoalkanimidazoles and -triazoles. Austria, US 5,622,982.

Schuster I, Egger H, Astecker N, Herzig G, Schussler M and Vorisek G (2001a) Selective inhibitors of CYP24: mechanistic tools to explore vitamin D metabolism in human keratinocytes. *Steroids*, **66**, 451-462.

Schuster I, Egger H, Bikle DD, Herzig G, Reddy GS, Stuetz A and Stuetz P (2001b) Selective inhibition of vitamin D hydroxylases in human keratinocytes. *Steroids*, **66**, 409-422.

Schuster I, Egger H, Nussbaumer P and Kroemer RT (2003) Inhibitors of vitamin D hydroxylases: structure-activity relationships. *Journal of Cellular Biochemistry*, **88**, 372-380.

Schwartz GG and Hulka BS (1990) Is vitamin D deficiency a risk factor for prostate cancer - (hypothesis). *Anticancer Research*, **10**, 1307-1311.

Schwartz GG, Whitlatch LW, Chen TC, Lokeshwar BL and Holick MF (1998) Human prostate cells synthesize 1,25-dihydroxyvitamin D_3 from 25-hydroxyvitamin D_3. *Cancer Epidemiology Biomarkers & Prevention*, **7**, 391-395.

Seidenfeld J, Samson DJ, Hasselblad V, Aronson N, Albertsen PC, Bennett CL and Wilt TJ (2000) Single-therapy androgen suppression in men with advanced prostate cancer: A systematic review and meta-analysis. *Annals of Internal Medicine*, **132**, 566-577.

Seidmon EJ, Trump DL, Kreis W, hall SW, Kurman MR, Ouyang P, Wu JM and Kremer AB (1995) Pharse I/II dose escalation study of liarozole in patients

with stage D, hormone refractory carcinoma of the prostate. *Annals of Surgical Oncology.*, **2**, 550-556.

Selley S, Donovan J, Faulkner A, Coast J and Gillatt D (1997a) Diagnosis. *Health Technology Assessment*, **1**, 11-29.

Selly S, Donovan J, Faulkner A, Coast J and Gillatt D (1997b) Staging systems and methods. *Health Technology Assessment*, **1**, 31-35.

Selley S, Donovan J, Faulkner A, Coast J and Gillatt D (1997c) Diagnosis, management and screening of early localised prostate cancer. *Health Technology Assessment*, **1**, 1.

Sevrioukova IF, Li H, Zhang H, Peterson JA and Poulos TL (1999) Structure of a cytochrome P450-redox partner electron-transfer complex. *Biochemistry*, **96**, 1863-1868.

Sharp RM, Bello-DeOcampo D, Quader ST and Webber MM (2001) *N*-(4-hydroxyphenyl)retinamide (4-HPR) decreases neoplastic properties of human prostate cells: an agent for prevention. *Mutation Research*, **496**, 163-170.

Shen JC, Wang TT, Chang S and Hursting SD (1999) Mechanistic studies of the effects of the retinoid *N*-(4-hydroxyphenyl)retinamide on prostate cancer cell growth and apoptosis. *Molecular Carcinogenesis*, **24**, 160-168.

Shipley WU, Thames HD, Sandler HM, Hanks GE, Zietman AL, Perez CA, Kuban DA, Hancock SL and Smith CD (1999) Radiation therapy for clinically localized prostate cancer - A multi-institutional pooled analysis. *JAMA-Journal of the American Medical Association*, **281**, 1598-1604.

Shirai T, Asamoto M, Takahashi S and Imaida K (2002) Diet and prostate cancer. *Toxicology*, **181-182**, 89-94.

Skladanowski A and Konopa J (2000) Mitoxantrone and ametantrone induce interstrand cross-links in DNA of tumour cells. *British Journal of Cancer*, **82**, 1300-1304.

Slattery ML, Schumacher MC, West DW, Robison LM and French TK (1990) Food-consumption trends between adolescent and adult years and subsequent risk of prostate-cancer. *American Journal of Clinical Nutrition*, **52**, 752-757.

Slawin K, Kadmon D, Park SH, Scardino PT, Anzano M, Sporn MB and Thompson TC (1993) Dietary fenretinide, a synthetic retinoid, decreases the tumor incidence and the tumor mass of ras+myc-induced carcinomas in the mouse prostate reconstitution model system. *Cancer Research*, **53**, 4461-4465.

Smith JR, Freije D, Carpten JD, Gronberg H, Xu JF, Isaacs SD, Brownstein MJ, Bova GS, Guo H, Bujnovszky P, Nusskern DR, Damber JE, Bergh A, Emanuelsson M, Kallioniemi OP, WalkerDaniels J, BaileyWilson JE, Beaty TH, Meyers DA, Walsh PC, Collins FS, Trent JM and Isaacs WB (1996) Major susceptibility locus for prostate cancer on chromosome 1 suggested by a genome-wide search. *Science*, **274**, 1371-1374.

Smith MB and March J (2001) Addition to carbon-carbon multiple bonds, in *March's advanced organic chemistry. reactions, mechanisms and structure* (Smith MB and March J eds, 5th Ed.) pp 970-1171, John Wiley and Sons, Inc., New York.

Smith MB and March J (2001a) Aliphatic nucleophilic substitution, in *March's advanced organic chemistry. reactions, mechanisms and structure* (Smith MB and March J eds, 5th Ed.) pp 389-674, John Wiley and Sons, Inc., New York.

Smith HJ, Mason P, Ahmadi M, Nicholls PJ and Greer V (2001) Benzyl tetralins, formulations and uses thereof. Great Britain, WO 01/42181 A1.

Snowdon DA, Phillips RL and Choi W (1984) Diet, obesity, and risk of fatal prostate cancer. *American Journal of Epidemiology*, **120**, 244-250.

Sonneveld E, van den Brink CE, van der Leede BM, Schulkes RK, Petkovich M, van der Burg B and van der Saag PT (1998) Human retinoic acid (RA) 4-hydroxylase (CYP26) is highly specific for all-trans-RA and can be induced through RA receptors in human breast and colon carcinoma cells. *Cell Growth and Differentiation*, **9**, 629-637.

Stanford JL, Feng ZD, Hamilton AS, Gilliland FD, Stephenson RA, Eley JW, Albertsen PC, Harlan LC and Potosky AL (2000) Urinary and sexual function after radical prostatectomy for clinically localized prostate cancer - The prostate cancer outcomes study. *JAMA-Journal of the American Medical Association*, **283**, 354-360.

Stege R (2000) Potential side-effects of endocrine treatment of long duration in prostate cancer. *Prostate*, **10**, 38-42.

Steinberg GD, Carter BS, Beaty TH, Childs B and Walsh PC (1990) Family history and the risk of prostate cancer. *Prostate*, **17**, 337-347.

Stöermer R (1900) Synthesen und abbaureactionen in der cumaronreihe. *Annalen der Chemie*, **312**, 237.

Stoppie P, Borgers M, Borghgraef P, Dillen L, Goossens J, Sanz G, Szel H, Van Hove C, Van Nyen G, Nobels G, Vanden Bossche H, Venet M, Willemsens G and Van Wauwe J (2000) R115866 inhibits all-*trans*-retinoic acid metabolism and exerts retinoidal effects in rodents. *The Journal of Pharmacology and Experimental Therapeutics*, **293**, 304-312.

Sun SY, Yue P and Lotan R (1999) Induction of apoptosis by *N*-(4-hydroxyphenyl)retinamide and its association with reactive oxygen species,

nuclear retinoic acid receptors, and apoptosis-related genes in human prostate carcinoma cells. *Molecular Pharmacology*, **55**, 403-410.

Sund C, Ylikoski J and Kwiatkowski M (1987) A new simple and mild synthesis of 2-substituted 2-oxazolines. *Synthesis-Stuttgart*853-854.

Suzuki T, Horaguchi T, Shimizu T and Abe T (1983) Benzofuran derivatives.1. On the effects of substituents in benzofuran synthesis. *Bulletin of the Chemical Society of Japan*, **56**, 2762-2767.

Swami S, Krishnan AV, Peehl DM and Feldman D (2005) Genistein potentiates the growth inhibitor effects of 1,25-dihydroxyvitamin D_3 in DU145 human prostate cancer cells: Role of the direct inhibition of CYP24 enzyme activity. *Molecular and Cellular Endocrinology*, **241**, 49-61.

SYBYL 7.0. Tripos Inc., 1699 South Hanley Road, St. Louis, Missouri, 63144, USA. URL: http://www.tripos.com.

Taimi M, Helvig C, Wisniewski J, Ramshaw H, White J, Amad M, Korczak B and Petkovich M (2004) A novel human cytochrome P450, CYP26C1, involved in metabolism of 9-*cis* and all-*trans* isomers of retinoic acid. *Journal of Biological Chemistry*, **279**, 77-85.

Tang G and Russell RM (1990) 13-*cis* Retinoic acid is an endogenous compound in human serum. *Journal of Lipid Research*, **30**, 175-182.

Tangpricha V, Flanagan JN, Whitlatch LW, Tseng CC, Chen TC, Holt PR, Lipkin MS and Holick MF (2001) 25-Hydroxyvitamin D-1α-hydroxylase in normal and malignant colon tissue. *Lancet*, **357**, 1673-1674.

Tannock IF, Wit de R, Berry WR, Horti J, Plunzanska A, Chi KN, Oudard S, Theodore C, James ND, Turesson I, Rosenthal MA and Eisenberger MA (2004) For the TAX 327 investigators. Docetaxel plus prednisone or mitoxantrone plus prednisone for advanced prostate cancer. *New England Journal of Medicine*, **351**, 1502-1512.

Taylor JA, Hirvonen A, Watson M, Pittman G, Mohler JL and Bell DA (1996) Association of prostate cancer with vitamin D receptor gene polymorphism. *Cancer Research*, **56**, 4108-4110.

Terry P, Lichenstein P, Feychting M, Ahlbom A and Wolk A (2001) Fatty fish consumption and risk of prostate cancer. *Lancet*, **357**, 1764-1766.

Trump DL, Smith DC, Stiff D, Adedoyin A, Day R, Bahnson RR, Hofacker J and Branch RA (1997) A phase II trial of all-*trans*-retinoic acid in hormone-refractory prostate cancer: a clinical trial with detailed pharmacokinetic analysis. *Cancer Chemotherapy and Pharmacology*, **39**, 349-356.

Trump DL, Hershberger PA, Bernardi RJ, Ahmed S, Muindi J, Fakih M, Yu W-D and Johnson CS (2004) Anti-tumor activity of calcitriol: pre-clinical and clinical

studies. *Journal of Steroid Biochemistry and Molecular Biology*, **89-90**, 519-526.

van der Poel HG (2004) Smart drugs in prostate cancer. *European Urology*, **45**, 1-17.

van der Spek PJ, Kremer A, Murry L and Walker MG (2003) Are gene expression microarray analyses reliable? A review of studies of retinoic acid responsive genes. *Genomics, Proteomics and Bioinformatics*, **1**, 9-14.

Van heusden J, Van Ginckel R, Bruwiere H, Moelans P, Janssen B, Floren W, van der Leede BJ, van Dun J, Sanz G, Venet M, Dillen L, Van Hove C, Willemsens G, Janicot M and Wouters W (2002) Inhibition of all-*TRANS*-retinoic acid metabolism by R116010 induces antitumour activity. *British Journal of Cancer*, **86**, 605-611.

Van Wauwe J, Coene MC, Goossens J, Cools W and Monbaliu J (1990) Effects of cytochrome P450 inhibitors on the *in vivo* metabolism of all-*trans*-retinoic acid in rats. *Journal of Pharmacology and Experimental Therapeutics*, **252**, 365-369.

Van Wauwe J, Vannyen G, Coene MC, Stoppie P, Cools W, Goossens J, Borghgraef P and Janssen PAJ (1992) Liarozole, an Inhibitor of retinoic acid metabolism, exerts retinoid-mimetic effects *in vivo*. *Journal of Pharmacology and Experimental Therapeutics*, **261**, 773-779.

Vicini FA, Kini VR, Edmundson G, Gustafson GS, Stromberg J and Martinez A (1999) A comprehensive review of prostate cancer brachytherapy: Defining an optimal technique. *International Journal of Radiation Oncology Biology Physics*, **44**, 483-491.

Vieth R and Fraser D (1979) Kinetic behaviour of 25-hydroxyvitamin D-1-hydroxylase and -24-hydroxylase in rat kidney mitochondria. *Journal of Biological Chemistry*, **254**, 12455-12460.

Vinh TK, Ahmadi M, Lopez Delgado PO, Fernandez Perez S, Walters HM, Smith HJ, Nicholls PJ and Simons C (1999) 1-[(Benzofuran-2-yl)phenylmethyl]-triazoles and -tetrazoles - potent competitive inhibitors of aromatase. *Bioorganic & Medicinal Chemistry Letters*, **9**, 2105-2108.

Vinh TK, Yee SW, Kirby AJ, Nicholls PJ and Simons C (2001) 1- (Benzofuran-2-yl) phenylmethyl triazoles as steroidogenic inhibitors: synthesis and in vitro inhibition of human placental CYP19 aromatase. *Anti-Cancer Drug Design*, **16**, 217-225.

Wang X, Gardner JP, Kheir A, Uskokovic MR and Studzinski GP (1997) Synergistic induction of HL60 cell differentiation by ketoconazole and 1-desoxy analogues of vitamin D_3. *Journal of the National Cancer Institute*, **89**, 1199-1206.

Wang Q, Lee D, Sysounthone V, Chandraratna RAS, Christakos S, Korah R and Wieder R (2001) 1,25-Dihydroxyvitamin D_3 and retinoic acid analogues induce differentiation in breast cancer cells with function- and cell-specific additive effects. *Breast Cancer Research and Treatment*, **67**, 157-168.

Wang J, Eltoum I and Lamartiniere C (2002) Dietary genistein suppresses chemically induced prostate cancer in Lobund-Wistar rats. *Cancer Letters*, **186**, 11.

Warner M (1982) Catalytic activity of partially purified renal 25-hydroxyvitamin D hydroxylases from vitamin D-deficient and vitamin D-replete rats. *Journal of Biological Chemistry*, **257**, 12995-13000.

Watanabe M, Murata K and Ikariya T (2002) Practical synthesis of optically active amino alcohols via asymmetric transfer hydrogenation of functionalized aromatic ketones. *Journal of Organic Chemistry*, **67**, 1712-1715.

Wehrmeister HL (1963) Reactions of aromatic thiols with oxazolines. *Journal of Organic Chemistry*, **28**, 2587-2588.

White TJ (1996) The future of PCR technology: diversification of technologies and applications. *Trends Biotechnology*, **14**, 478-483.

White JA, Guo YD, Baetz K, Beckett-Jones B, Bonasoro J, Hsu KE, Dilworth J, Jones G and Petkovich M (1996) Identification of the retinoic acid-inducible all-*trans*-retinoic acid 4-hydroxylase. *Journal of Biological Chemistry*, **271**, 29922-29927.

White JA, Beckett-Jones B, Guo YD, Dilworth J, Bonasoro J, Jones G and Petkovich M (1997) cDNA cloning of human retinoic acid-metabolizing enzyme (hP450RAI) identifies a novel family of cytochromes P450 (CYP26). *Journal of Biological Chemistry*, **272**, 18538-18541.

White JH (2004) Profiling 1,25-dihydroxyvitamin D_3-regulated gene expression by microarray analysis. *Journal of Steroid Biochemistry and Molecular Biology*, **89-90**, 239-244.

Wilding G (1995) Endocrine control of prostate cancer. *Cancer Surveys*, **23**, 43-62.

Williams PA, Cosme J, Sridhar V, Johnson EF and McRee DE (2000) Mammalian microsomal cytochrome P450 monooxygenase: structural adaptations for membrane binding and functional diversity. *Molecular Cell*, **5**, 121-131.

Williams PA, Cosme J, Ward A, Angove HC, Vinkovic DM and Jhoti H (2003) Crystal structure of human cytochrome P450 2C9 with bound warfarin. *Nature*, **424**, 464-468.

Willis MS and Wians Jr. FH (2003) The role of nutrition in preventing prostate cancer: a review of the proposed mechanism of action of various dietary substances. *Clinica Chimica Acta*, **330**, 57-83.

Wit de R (2005) Shifting paradigms in prostate cancer; docetaxel plus low-dose prednisone - finally an effective chemotherapy. *European Journal of Cancer*, **41**, 502-507.

Wouters W, van Dun J, Dillen A, Coene M-C, Cools W and De Coster R (1992) Effects of liarozole, a new antitumoral compound, on retinoic acid-induced metabolism in MCF-7 human breast cancer cells. *Cancer Research*, **52**, 2841-2846.

Yang ES and Burnstein KL (2003) Vitamin D inhibits G1 to S progression in LNCaP prostate cancer cells through $p21^{kip1}$ stablization and Cdk2 mislocalization to the cytoplasm. *Journal of Biological Chemistry*, **278**, 46862-46868.

Yano JK, Wester MR, Schoch GA, Griffin KJ, Stout CD and Johnson EF (2004) The structure of human microsomal cytochrome P450 3A4 determined by X-ray crystallography to 2.05-Å resolution. *Journal of Biological Chemistry*, **279**, 38091-38094.

Yee SW and Simons C (2004) Synthesis and CYP24 inhibitory activity of 2-substituted-3,4-dihydro-2*H*-naphthalen-1-one (tetralone) derivatives. *Bioorganic & Medicinal Chemistry Letters*, **14**, 5651-5654.

Yee SW, Jarno L, Gomaa MS, Elford C, Ooi LL, Coogan MP, McClelland R, Nicholson RI, Evans BAJ, Brancale A and Simons C (2005) Novel tetralone-derived retinoic acid metabolism blocking agents (RAMBAs): Synthesis and *in vitro* evaluation with liver microsomal and MCF-7 CYP26A1 cell assays. *Journal of Medicinal Chemistry*, accepted for publication.

Ylikomi T, Laaksi I, Lou YR, Martikainen P, Pennanen P, Purmonen S, Syvala H, Vienonen A and Tuohimaa P (2002) Antiproliferative action of vitamin D. *Vitamin Hormone*, **64**, 357-406.

Yoshihama M, Nakakoshi M, Nakamura J and Nakayama S (1999) Novel tetralone or benzopyranone derivatives and process for producing the same. Japan, EP0902003A1.

Yu H, Harris RE, Gao YT, Gao RN and Wynder EL (1991) Comparative epidemiology of cancers of the colon, rectum, prostate and breast in Shanghai, China versus the United States. *International Journal of Epidemiology*, **20**, 76-81.

Zagars GK, Johnson DE, Voneschenbach AC and Hussey DH (1988) Adjuvant estrogen following radiation-therapy for Stage C adenocarcinoma of the prostate - long-term results of a prospective randomized study. *International Journal of Radiation Oncology Biology Physics*, **14**, 1085-1091.

Zagars GK, Pollack A and vonEschenbach AC (1997) Prognostic factors for clinically localized prostate carcinoma - Analysis of 938 patients irradiated in the prostate specific antigen era. *Cancer*, **79**, 1370-1380.

Zelefsky MJ, Fuks Z, Hunt M, Lee HJ, Lombardi D, Ling CC, Reuter VE, Venkatraman ES and Leibel SA (2001) High dose radiation delivered by intensity modulated conformal radiotherapy improves the outcome of localized prostate cancer. *Journal of Urology*, **166**, 876-881.

Zhang QY, Dunbar D and Kaminsky L (2000) Human cytochrome P-450 metabolism of retinals to retinoic acids. *Drug Metabolism and Disposition*, **28**, 292-297.

Zhao J, Tan BK, Marcelis S, Verstuyf A and Bouillon R (1996) Enhancement of antiproliferative activity of 1alpha,25-dihydroxyvitamin D_3 (analogs) by cytochrome P450 enzyme inhibitors is compound- and cell-type specific. *Journal of Steroid Biochemistry and Molecular Biology*, **57**, 197-202.

Zhao X-Y, Ly LH, Peehl DM and Feldman D (1999) Induction of androgen receptor by 1alpha,25-dihydroxyvitamin D_3 and 9-*cis* retinoic acid in LNCaP human prostate cancer cells. *Endocrinology*, **140**, 1205-1212.

Zhao X-Y and Feldman D (2001) The role of vitamin D in prostate cancer. *Steroids*, **66**, 293-300.

Zhuang SH and Burnstein KL (1998) Antiproliferative effect of 1alpha,25-dihydroxyvitamin D_3 in human prostate cancer cell line LNCaP involves reduction of cyclin-dependent kinase 2 activity and persistent G1 accumulation. *Endocrinology*, **139**, 1197-1207.

Zietman AL, Coen JJ, Dallow KC and Shipley WU (1995) The treatment of prostate-cancer by conventional radiation therapy - an analysis of long-term outcome. *International Journal of Radiation Oncology Biology Physics*, **32**, 287-292.

APPENDIX 1

X-ray crystal data

Table 1. Crystal data and structure refinement for compound **83**.

Identification code	Compound **83**	
Empirical formula	$C_{18}H_{15}BrO_2$	
Formula weight	343.21	
Temperature	150(2) K	
Wavelength	0.71073 Å	
Crystal system	Monoclinic	
Space group	P 21/a	
Unit cell dimensions	a = 12.1499(4) Å	α = 90°.
	b = 7.2410(3) Å	β = 107.5780(10)°.
	c = 17.2445(8) Å	γ = 90°.
Volume	1446.29(10) $Å^3$	
Z	4	
Density (calculated)	1.576 Mg/m^3	
Absorption coefficient	2.844 mm^{-1}	
F(000)	696	
Crystal size	0.20 x 0.20 x 0.15 mm^3	
Theta range for data collection	3.07 to 27.51°.	
Index ranges	-15<=h<=15, -9<=k<=9, -20<=l<=22	
Reflections collected	9753	
Independent reflections	3300 [R(int) = 0.0608]	
Completeness to theta = 27.51°	99.3 %	
Absorption correction	Semi-empirical from equivalents	
Max. and min. transmission	0.707 and 0.687	
Refinement method	Full-matrix least-squares on F^2	
Data / restraints / parameters	3300 / 0 / 191	
Goodness-of-fit on F^2	1.093	
Final R indices [I>2sigma(I)]	R1 = 0.0528, wR2 = 0.1038	
R indices (all data)	R1 = 0.0788, wR2 = 0.1114	
Largest diff. peak and hole	0.586 and -0.452 $e.Å^{-3}$	

Table 2. Atomic coordinates (x 10^4) and equivalent isotropic displacement parameters ($Å^2$x 10^3) for compound **83**. U(eq) is defined as one third of the trace of the orthogonalized U^{ij} tensor.

	x	y	z	U(eq)
C(1)	230(4)	-7527(6)	717(3)	31(1)
C(2)	1557(3)	-4998(6)	930(3)	21(1)
C(3)	2483(4)	-4170(6)	738(3)	26(1)
C(4)	2914(3)	-2535(6)	1095(3)	23(1)
C(5)	2455(3)	-1664(6)	1657(2)	19(1)
C(6)	1524(3)	-2505(5)	1850(2)	18(1)
C(7)	1077(3)	-4169(6)	1480(3)	22(1)
C(8)	2459(3)	914(5)	2660(2)	18(1)
C(9)	2924(3)	146(6)	2012(2)	20(1)
C(10)	1927(4)	-480(6)	3078(3)	23(1)
C(11)	1007(4)	-1624(6)	2455(3)	23(1)
C(12)	2580(3)	2730(5)	2815(3)	20(1)
C(13)	2158(3)	3752(5)	3408(2)	17(1)
C(14)	2862(3)	5015(5)	3951(2)	17(1)
C(15)	2496(4)	5938(6)	4534(3)	23(1)
C(16)	1366(4)	5709(6)	4549(3)	25(1)
C(17)	630(3)	4554(6)	3994(3)	23(1)
C(18)	1010(3)	3586(6)	3431(3)	21(1)
O(1)	1176(3)	-6627(4)	540(2)	32(1)
O(2)	3651(3)	979(4)	1787(2)	28(1)
Br(1)	4368(1)	5506(1)	3892(1)	30(1)

Table 3. Bond lengths [Å] and angles [°] for compound **83**.

	[Å]		[°]
C(1)-O(1)	1.433(5)	C(3)-C(4)-C(5)	121.5(4)
C(2)-O(1)	1.368(5)	C(4)-C(5)-C(6)	118.9(4)
C(2)-C(7)	1.390(6)	C(4)-C(5)-C(9)	119.9(4)
C(2)-C(3)	1.401(6)	C(6)-C(5)-C(9)	121.2(4)
C(3)-C(4)	1.364(6)	C(7)-C(6)-C(5)	119.6(4)
C(4)-C(5)	1.405(5)	C(7)-C(6)-C(11)	119.7(4)
C(5)-C(6)	1.410(5)	C(5)-C(6)-C(11)	120.7(4)
C(5)-C(9)	1.486(6)	C(2)-C(7)-C(6)	120.0(4)
C(6)-C(7)	1.395(6)	C(12)-C(8)-C(10)	127.2(4)
C(6)-C(11)	1.512(6)	C(12)-C(8)-C(9)	117.9(4)
C(8)-C(12)	1.341(5)	C(10)-C(8)-C(9)	115.0(3)
C(8)-C(10)	1.496(6)	O(2)-C(9)-C(5)	121.7(4)
C(8)-C(9)	1.503(6)	O(2)-C(9)-C(8)	121.5(4)
C(9)-O(2)	1.227(5)	C(5)-C(9)-C(8)	116.8(3)
C(10)-C(11)	1.537(6)	C(8)-C(10)-C(11)	110.8(3)
C(12)-C(13)	1.475(6)	C(6)-C(11)-C(10)	110.1(3)
C(13)-C(14)	1.400(5)	C(8)-C(12)-C(13)	126.1(4)
C(13)-C(18)	1.412(5)	C(14)-C(13)-C(18)	116.5(4)
C(14)-C(15)	1.387(6)	C(14)-C(13)-C(12)	121.4(3)
C(14)-Br(1)	1.897(4)	C(18)-C(13)-C(12)	122.0(4)
C(15)-C(16)	1.392(6)	C(15)-C(14)-C(13)	122.3(4)
C(16)-C(17)	1.378(6)	C(15)-C(14)-Br(1)	118.3(3)
C(17)-C(18)	1.385(6)	C(13)-C(14)-Br(1)	119.4(3)
		C(14)-C(15)-C(16)	119.3(4)
O(1)-C(2)-C(7)	124.0(4)	C(17)-C(16)-C(15)	119.7(4)
O(1)-C(2)-C(3)	115.4(4)	C(16)-C(17)-C(18)	120.7(4)
C(7)-C(2)-C(3)	120.6(4)	C(17)-C(18)-C(13)	121.2(4)
C(4)-C(3)-C(2)	119.4(4)	C(2)-O(1)-C(1)	117.5(3)

Table 4. Anisotropic displacement parameters ($Å^2 x\ 10^3$) for compound **83**. The anisotropic displacement factor exponent takes the form: $-2\pi^2[\ h^2 a^{*2} U^{11} + ... + 2\ h\ k\ a^*\ b^*\ U^{12}\ ]$.

	U^{11}	U^{22}	U^{33}	U^{23}	U^{13}	U^{12}
C(1)	32(2)	29(2)	33(3)	-8(2)	12(2)	-9(2)
C(2)	20(2)	24(2)	19(2)	-3(2)	7(2)	1(2)
C(3)	25(2)	37(3)	21(2)	-8(2)	12(2)	4(2)
C(4)	23(2)	31(2)	18(2)	0(2)	9(2)	1(2)
C(5)	22(2)	21(2)	17(2)	1(2)	11(2)	5(2)
C(6)	22(2)	20(2)	14(2)	5(2)	8(2)	7(2)
C(7)	21(2)	24(2)	20(2)	4(2)	9(2)	4(2)
C(8)	18(2)	22(2)	16(2)	3(2)	6(2)	2(2)
C(9)	21(2)	24(2)	15(2)	1(2)	6(2)	5(2)
C(10)	30(2)	19(2)	22(2)	2(2)	14(2)	2(2)
C(11)	29(2)	18(2)	28(2)	-1(2)	18(2)	-2(2)
C(12)	17(2)	18(2)	23(2)	3(2)	4(2)	2(2)
C(13)	19(2)	14(2)	19(2)	4(2)	6(2)	2(2)
C(14)	15(2)	19(2)	19(2)	5(2)	6(2)	3(2)
C(15)	28(2)	19(2)	21(2)	2(2)	6(2)	0(2)
C(16)	34(2)	19(2)	25(2)	5(2)	16(2)	8(2)
C(17)	20(2)	24(2)	28(2)	6(2)	13(2)	1(2)
C(18)	19(2)	19(2)	26(2)	5(2)	7(2)	-1(2)
O(1)	30(2)	34(2)	34(2)	-16(2)	15(1)	-9(2)
O(2)	28(2)	28(2)	34(2)	-3(1)	20(1)	-3(1)
Br(1)	21(1)	32(1)	38(1)	-6(1)	11(1)	-6(1)

Table 5. Hydrogen coordinates (x 10^4) and isotropic displacement parameters ($Å^2$ x 10^3) for compound **83**.

	x	y	z	U(eq)
H(1A)	446	-7824	1298	46
H(1B)	38	-8667	398	46
H(1C)	-443	-6705	576	46
H(3)	2809	-4743	362	32
H(4)	3539	-1971	960	28
H(7)	445	-4736	1603	26
H(10A)	1568	159	3448	27
H(10B)	2535	-1312	3409	27
H(11A)	705	-2596	2740	27
H(11B)	356	-815	2165	27
H(12)	2975	3423	2514	24
H(15)	3013	6718	4919	28
H(16)	1102	6346	4941	30
H(17)	-146	4421	3997	27
H(18)	489	2796	3053	25

APPENDIX 2

Conference abstracts and publications

Appendix 2
Poster presentation: GP2A conference 2003, France

DESIGN AND SYNTHESIS OF BENZOFURAN DERIVATIVES AS CYP24 INHIBITORS FOR ANDROGEN-INDEPENDENT PROSTATE CANCER

S.W. Yee and C. Simons

Welsh School of Pharmacy, Cardiff University, Cathays Park, CF10 3XF

Prostate cancer is the most common malignancy among males in the US, with 220,900 new cases and 28,900 deaths for the year 2003 alone[1]. Androgen ablation via hormonal therapy and surgical castration has a prominent role in the treatment of advanced prostate cancer. It is aimed at inhibiting prostate growth by suppressing endogenous androgen production or blocking androgen action[2]. Unfortunately, hormonal therapy is not capable of producing durable responses in the majority of patients with advanced disease. Once the patient develops hormone-refractory prostate cancer (HRPC), his outlook is poor, with a median survival time of 9 months[3]. Clearly, new effective treatment strategies are needed for the treatment of HRPC. One of the new therapeutic strategies is to employ a differentiating agent to suppress prostate cancer cell proliferation[4]. 1α,25-Dihydroxyvtamin D_3 (1α,25$(OH)_2D_3$), a member of the steroid hormone superfamily, is involved in regulating cellular proliferation and differentiation in various target tissues that possess vitamin D receptors[5].

Numerous studies have shown that 1α,25$(OH)_2D_3$ and vitamin D_3 analogues increase differentiation and decrease proliferation of the prostate cancer cells[6]. However, the use of 1α,25$(OH)_2D_3$ and vitamin D_3 analogues for prostate cancer is limited by the risk of hypercalcemia and hypercalciuria[7]. 25-Hydroxyvitamin D_3-24-hydroxylase (CYP24) is responsible for degradation of the active vitamin D metabolite 1α,25$(OH)_2D_3$. CYP24 has been shown to be expressed in some prostate cancer cell lines[6]. This suggest that the expression of CYP24 can abolish the growth regulatory effect of 1α,25$(OH)_2D_3$. Identification of potent inhibitors of CYP24 may be a new strategy for the treatment of androgen-independent prostate cancer.

Schuster and co-workers have identified SDZ 89-443 and VID400 as selective CYP24 inhibitor[8]. Based on these structures, we have synthesised benzofuran-2-carboxamido ethyl-imidazole and -1,2,4-triazole derivatives. Biological assessment of CYP24 inhibition by these synthesised compounds will be established in the near future.

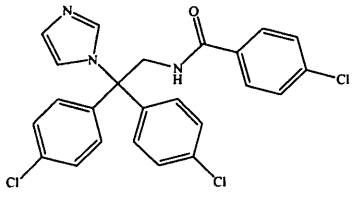

SDZ 89-443

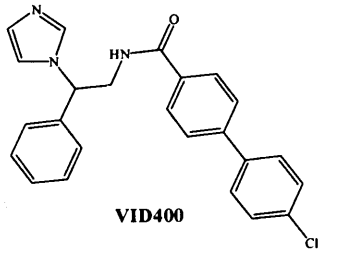

VID400

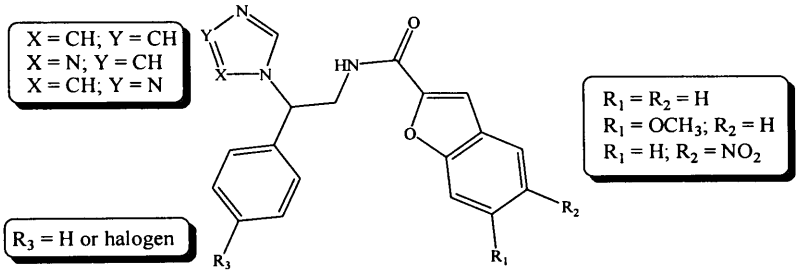

Benzofuran-2-carboxamido ethyl-imidazole and -1,2,4-triazole derivatives

1. Jemal A *et al.* (2003) *Ca-a Cancer Journal for Clinicians* 53:5-26. **2.** Smith HJ *et al.* (2001) *Expert Opinion on Therapeutic Patents* 11: 789-824. **3.** Hussain M *et al.* (1994) *Journal of Clinical Oncology* 12: 1868-1875. **4.** Zhao X-Y and Feldman D (2001) *Steroids* 66: 293-300. **5.** Haussler MR *et al.* (1998) *Journal of Bone and Mineral Research* 13:325-349. **6.** Miller GJ *et al.* (1995) *Clinical Cancer Research* 1: 997-1003. **7.** Gross C *et al.* (1998) *Journal of Urology* 159:2035-2039. **8.** Schuster I *et al.* (2001) *Steroids* 66: 409-422.

Design and synthesis of P450 enzymes inhibitors as differentiating agent for androgen-independent prostate cancer

Sook Wah Yee and Claire Simons

Department of Medicinal Chemistry, Welsh School of Pharmacy, Cardiff University, King Edward Avenue VII, Cardiff, UK

Prostate cancer is the most common malignancy among males in the US, with 220,900 new cases and 28,900 deaths for 2003 alone [1]. Hormonal therapy and surgical castration have prominent roles in the treatment of advanced prostate cancer. Unfortunately, hormonal therapy is not capable of producing durable responses in the majority of patients with advanced disease. Once the patient develops hormone-refractory prostate cancer (HRPC), his outlook is poor, with a median survival time of 9 months. Clearly, new effective treatment strategies are needed for the treatment of HRPC.

One of the new therapeutic strategies is to employ a differentiating agent to suppress prostate cancer cell proliferation. Vitamin D and retinoic acid have antiproliferative and differentiating effect on prostate cancer cells [2]. The P450 enzymes that are responsible for the metabolism of vitamin D and retinoic acid are cytochrome 24 (CYP24) and 26 (CYP26) respectively.

CYP 24 has been shown to be expressed in some prostate cancer cell lines [3]. Liarozole, the inhibitor of CYP26 has shown promising data in the treatment of HRPC [4]. Identification of potent inhibitors of CYP24 and CYP26 may be a new strategy for the treatment of androgen-independent prostate cancer.

Based on the known structures of liarozole and CYP24 inhibitors [5], we have synthesised a series of benzofuran and tetralone derivatives. Biological assessment of the inhibition of these P450 enzymes is being carried out in our laboratory, with promising inhibitory activity observed.

Homology models of CYP24 and CYP26 have been constructed using various templates, and molecular docking studies of substrate and inhibitors have been carried out to broaden the understanding of enzyme/inhibitor interactions.

[1] Jemal, A. et. al. Cancer statistics, 2003. Ca-a Cancer Journal for Clinicians 2003; 53: 5-26.

[2] Peehl, D. M. and D. Feldman. The role of vitamin D and retinoids in controlling prostate cancer progression. Endocrine-Related Cancer 2003; 10: 131-140.

[3] Miller, G. J. et al. Vitamin D receptor expression, 24-hydroxylase activity, and inhibition of growth by 1 alpha,25-dihydroxyvitamin D-3 in seven human prostatic carcinoma cell lines. Clinical Cancer Research 1995; 1: 997-1003.

[4] Debruyne, F.J.M et al. Liarozole - A novel treatment approach for advanced prostate cancer: Results of a large randomized trial versus cyproterone acetate. Urology 1998; 52: 72-81.

[5] Schuster, I. et al. Selective inhibition of vitamin D hydroxylases in human keratinocytes. Steroids 2001; 66: 409-422.

Synthesis and evaluation of tetralone derivatives: P450 enzyme inhibitors as differentiating agents for the treatment of hormone-refractory prostate cancer

S.W. Yee and C. Simons

Department of Medicinal Chemistry, Welsh School of Pharmacy, Cardiff University, King Edward Avenue VII, Cardiff, UK.

E-mail: yeesw@cardiff.ac.uk

Prostate cancer is the most common malignancy among males in the US, with 230,110 estimated new cases and 29,900 deaths for 2004 alone (Jemal et al 2004). Hormonal therapy and surgical castration have prominent roles in the treatment of advanced prostate cancer. Unfortunately, hormonal therapy is not capable of producing durable responses in the majority of patients with advanced disease. Once the patient develops hormone-refractory prostate cancer, his outlook is poor, with a median survival time of 9 months. Clearly, new effective treatment strategies are needed for the treatment of HRPC.

One of the new therapeutic strategies is to employ a differentiating agent to suppress prostate cancer cell proliferation. Vitamin D and retinoic acid have anti-proliferative and differentiating effect on prostate cancer cells (Peehl & Feldman 2003). The P450 enzymes that are responsible for the metabolism of vitamin D and retinoic acid are cytochrome 24 (CYP24) and 26 (CYP26) respectively.

CYP 24 has been shown to be expressed in some prostate cancer cell lines. Liarozole and ketoconazole, the inhibitors of CYP26 have shown promising data in the treatment of HRPC. Identification of potent inhibitors of CYP24 and CYP26 may be a new strategy for the treatment of androgen-independent prostate cancer. It has been shown in our own laboratory, that isoflavones and flavones, tetralones (Kirby et al 2003) and coumarins are known to affect the activity of a variety of cytochrome P450 enzymes involved in hormone biosynthesis. In view of these facts, it was of interest to investigate the inhibitory activity of these compounds against CYP24 and CYP26.

The biochemical evaluation of the synthesised tetralone compounds was undertaken using a modification of the method of Kirby et al (2003). The incubation mixtures (0.5 mL) containing NADPH generating system (50 μL) and substrate (10 μL, either [11,12-^{3}H] retinoic acid or 25-hydroxy[26,27-methyl-^{3}H]-vitamin D) in phosphate buffer (pH 7.4) and enzyme suspension (20 μL liver microsomal or 50 μL kidney mitochondrial fractions) were incubated at 37 °C for 30 min in a shaking water bath. The solutions were quenched by the addition of 1 % acetic acid v/v (200 μL). Then ethyl acetate containing 0.02 % butylated hydroxy anisole (2 mL) was added and the tube vortexed for 15 s. The organic layer (1.5 mL) was transferred into a clear tube and the solvent evaporated using a centrifuge connected to a vacuum pump and a multitrap at – 80 °C. The residue was reconstituted in methanol (50 μL) and was injected into a reverse-phase HPLC connected to an online scintillation detector. The separated [^{3}H]-metabolites were quantitatively calculated from the areas under the curves. The percentage inhibition was calculated from: 100[(metabolites (control) – metabolites (inhibitor)/(metabolites control)]%.

The results showed that the synthesised tetralone compounds (at 100 μM and 20 μM) displayed greater or similar inhibitory activity than the standard compound for CYP24 and CYP26, namely ketoconazole.

Homology models of CYP24 and CYP26 have been constructed using various templates, and molecular docking studies of substrate and inhibitors have been carried out to broaden the understanding of enzyme/inhibitor interactions.

Jemal, A. et al (2004) Ca Cancer J. Clin. **54**: 8-29.
Kirby, A.J. et al (2003) J. Enz. Inhib. Med. Chem. **18**: 27-33.
Peehl, D. M. and D. Feldman (2003) Endocr-Relat. Cancer **10**: 131-140.

Appendix 2
Oral presentation: ACS 2005, San Diego, USA

Synthesis and evaluation of retinoic acid metabolism blocking agents (RAMBAs) as indirect differentiating agents for cancer therapeutics

Sook Wah Yee[†], Laëtitia Jarno[*], Claire Simons[†], Andrea Brancale[†], Rob Nicholson[*]

[†] Department of Medicinal Chemistry, Welsh School of Pharmacy, Cardiff University, King Edward VII Avenue, Cardiff, UK.
[*] Tenovus Cancer Research, Welsh School of Pharmacy, Cardiff University, King Edward VII Avenue, Cardiff, UK.

Differentiating agents are one of the new therapeutic strategies in treating solid tumours *e.g.* breast and prostate cancers. All-trans retinoic acid (ATRA), derived from vitamin A, is able to inhibit cell proliferation and to restore normal differentiation of various cancer cells. However, the use of ATRA is limited by the induction of the cytochrome P-450 enzymes that are involved in the metabolism of ATRA. In addition to CYP26, which only recognises ATRA as its substrate, different P-450 isozymes, namely CYP2C8, CYP2C9, CYP3A4 are able to catalyze this reaction.
A drug which can prolong the action of endogenous retinoic acid by inhibiting the P-450 retinoic acid metabolizing enzymes could have potential use as an anti-cancer agent. The synthesis of three new series of novel compounds with improved activities compared with Ketoconazole and Liarozole in two different biological assay systems will be discussed in relation to the SAR studies and molecular docking studies using homology models of CYP26.

DESIGN AND ASSESSMENT OF NOVEL INHIBITORS OF CYP24 TO ENHANCE VDR SIGNALLING IN ANDROGEN-INDEPENDENT PROSTATE CANCER CELLS

Sook Wah Yee[†], Moray J. Campbell[*] and Claire Simons[†]

[†] Department of Medicinal Chemistry, Welsh School of Pharmacy, Cardiff University, Cardiff, UK.
[*] Department of Medical Science, Institute of Biomedical Research, Birmingham University, Birmingham, UK.

Epidemiological, polymorphism and *in vitro* studies support an antiproliferative role for the VDR in the prostate, and have justified an ongoing series of clinical trials of $1,25(OH)_2D_3$, either alone or in combination with other chemotherapies. Enhanced autocrine $1,25(OH)_2D_3$ metabolism via the cytochrome P450 enzyme, CYP24 (itself a VDR target gene) limits efficacy. Thus CYP24 inhibitors are therapeutically attractive.

Isoflavones, flavones and tetralones inhibit a variety of cytochrome P450 enzymes with broad spectrum. We therefore synthesised a series of tetralone derivatives to investigate the inhibition of CYP24, compared with the broad spectrum P450 inhibitor, ketoconazole. Of these tetralone derivatives 2-(4-hydroxybenzyl)-6-methoxy-3,4-dihydro-2*H*-naphthalen-1-one, (compound YSW87) showed potent inhibition of the metabolism of $[^3H]$-25-(OH)-D_3 in the rat kidney mitochondrial assay (IC_{50} = 3.5 μM, compared to ketoconazole, IC_{50} = 20 μM). This compound was subsequently screened in proliferation and gene regulatory actions in androgen-independent prostate cancer cell lines, PC-3 and DU-145, which are recalcitrant to$1,25(OH)_2D_3$.

Antiproliferative screens revealed that YSW87 alone was minimally active compared to ketoconazole, possibly reflecting the more selective targeting of CYP24. However when DU-145 cells were pre-treated with YSW87 prior to $1,25(OH)_2D_3$ treatment there was a strong combinatorial inhibition of proliferation. Equally we demonstrated a combinatorial enhancement VDR gene regulation by examining CYP24 and $p21^{(waf1/cip1)}$ mRNA levels after individual and co-treatment of YSW87 and $1,25(OH)_2D_3$.

These data identify a novel series of therapeutically attractive tetralone analogs as potent selective inhibitors of CYP24.

Available online at www.sciencedirect.com
SCIENCE DIRECT®
Bioorganic & Medicinal Chemistry Letters
ELSEVIER
Bioorganic & Medicinal Chemistry Letters 14 (2004) 5651–5654

Synthesis and CYP24 inhibitory activity of 2-substituted-3,4-dihydro-2*H*-naphthalen-1-one (tetralone) derivatives

Sook Wah Yee and Claire Simons*

Welsh School of Pharmacy, Cardiff University, King Edward VII Avenue, Cardiff CF10 3XF, UK

Received 6 July 2004; revised 17 August 2004; accepted 18 August 2004
Available online 17 September 2004

Abstract—The synthesis of novel 2-benzyl- and 2-benzylidene-3,4-dihydro-2*H*-naphthalen-1-one (tetralone) derivatives and their inhibitory activity versus kidney mitochondrial 25-hydroxyvitamin D_3 24-hydroxylase (CYP24) is described. The 2-benzylidenetetralone derivatives were found to be very weak inhibitors (IC_{50} 20 >100 μM), whereas the 2-benzyltetralone derivatives showed promising inhibitory activity (IC_{50} 0.9 μM for the most active derivative) compared with ketoconazole (IC_{50} 20 μM).

Prostate cancer, being the second leading cause of cancer death in human males, is a major disease for therapeutic intervention.[1] Androgens play an important role in the development, growth and progression of prostate cancer,[2] therefore androgen ablation therapy by gonadotropin suppression and androgen receptor blockade are current methods of treatment.[3] Although most patients respond well to this therapy, eventually many tumours recur as a result of transition of the cancer cells to androgen-independent growth.[4] Owing to the lack of effective treatments for androgen-independent metastatic prostate cancer, alternative strategies, such as 'differentiation therapy' may be useful.[5] Pro-differentiating agents of interest include retinoic acid (vitamin A) and vitamin D_3 (and their analogues).

1α,25$(OH)_2D_3$ (calcitriol) is the hormonally active metabolite of vitamin D_3, which functions as an antiproliferative and pro-differentiating agent, especially in epithelial and hematopoietic cells.[6] The use of vitamin D analogues (VDR agonists) as differentiating agents has been studied,[6] however the overall therapeutic activity of such analogues is uncertain owing to additional pharmacological effects such as transcaltachia (elevation of intracellular calcium activation of intestinal calcium uptake).[7] In addition the natural substrate calcitriol, and derivative VDR agonists, are rapidly metabolised into less active metabolites by the 24-hydroxylase (CYP24) resulting in a very limited use for either calcitriol or its derivatives as differentiating agents.[8] Therefore, compounds capable of inhibiting CYP24, the cytochrome P450 enzyme that initiates calcitriol metabolism, would have the effect of increasing endogenous levels of calcitriol so enhancing its differentiating capabilities.

Known inhibitors of CYP24 include (i) the CYP26 and CYP17 (P450 17, 17,20-lyase) inhibitor liarozole[9] and (ii) ketoconazole, the nonspecific competitive inhibitor of cytochrome P450-catalysed reactions, which inhibit both CYP24 and 1α-hydroxylase.[10] More selective CYP24 inhibitors have been described such as SDZ 89-443 and VID400.[11] All these inhibitors have a characteristic nitrogen heterocyclic moiety capable of coordinating to the Fe^{3+}-haem component of the P450 active site.

We have recently demonstrated the CYP26 inhibitory activity of a series of 2-(4-aminophenylmethyl)-tetralone derivatives,[12] therefore tetralones with varying substituents in both naphthalene and 2-aryl moieties were synthesised and evaluated for CYP24 inhibitory activity.

Keywords: 2-Substituted-3,4-dihydro-2*H*-naphthalen-1-one (tetralone) derivatives; Enzyme inhibition; 24-Hydroxylase (CYP24); Differentiating therapy.
* Corresponding author. Tel.: +44 02920 876307; fax: +44 02920 874149; e-mail: simonsc@cardiff.ac.uk

0960-894X/$ - see front matter © 2004 Elsevier Ltd. All rights reserved.
doi:10.1016/j.bmcl.2004.08.040

The method employed for the preparation of the 6-methoxy-2-(phenylmethylidene)-3,4-dihydro-2*H*-naphthalen-1-one derivatives (**2a–d**) involved direct condensation of the commercially available tetralone (**1**) with the appropriate benzaldehyde in ethanolic KOH solution.[13] This method was successfully used in the absence of a hydroxyl group on the tetralone or benzaldehyde (Scheme 1).

The synthesis of hydroxyl derivatives (**5**, **8** and **14**) required initial protection of one or both benzaldehyde and tetralone hydroxyl groups (see Schemes 2–4, respectively) with the tetrahydropyran (THP) protecting group, which was stable under the basic ethanolic KOH condensation conditions.

The 6-biphenyl substituted derivatives (**11a–b**) were prepared by Suzuki coupling with phenylboronic acid in the presence of $Pd(PPh_3)_4$ catalyst[14] (Scheme 3). The reduced 2-(benzyl)-3,4-dihydro-2*H*-naphthalen-1-one derivatives (**3a–b**, **6**, **9**, **12a–b** and **15**) were readily obtained by hydrogenation with 10% Pd/C catalyst for 1 h, at approximately 30 psi (Parr hydrogenator). When the hydrogenation reaction was allowed to proceed for 2 h, deoxygenation at C1 was found to occur (**7**, Scheme 2).

The dihydroxy derivative **15** was prepared from the corresponding THP protected tetralone and benzaldehyde (Scheme 4).

The nine 2-(benzylidene)-(**2a–d**, **5**, **8**, **11a**, **11b** and **14**) and eight 2-(benzyl)-tetralone (**3a–b**, **6**, **7**, **9**, **12a–b** and **15**) derivatives were evaluated for their inhibitory activity versus CYP24 using rat kidney mitochondria. The assay performed was based on a modification of the general

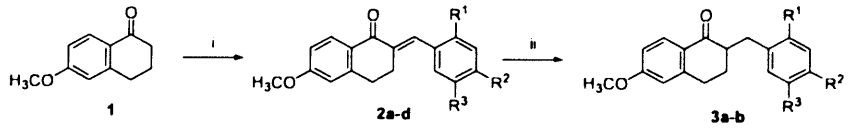

Scheme 1. Reagents and conditions: (i) R–C_6H_4CHO, 4% KOH/EtOH, rt, 1–72 h; (ii) 10% Pd/C, H_2, MeOH, rt, 1 h [**a**, $R^1 = R^3 = CF_3$, $R^2 = H$; **b**, $R^1 = CH_3$, $R^2 = R^3 = H$; **c**, $R^2 = NMe_2$, $R^1 = R^2 = H$; **d**, $R^1 = Br$, $R^2 = R^3 = H$].

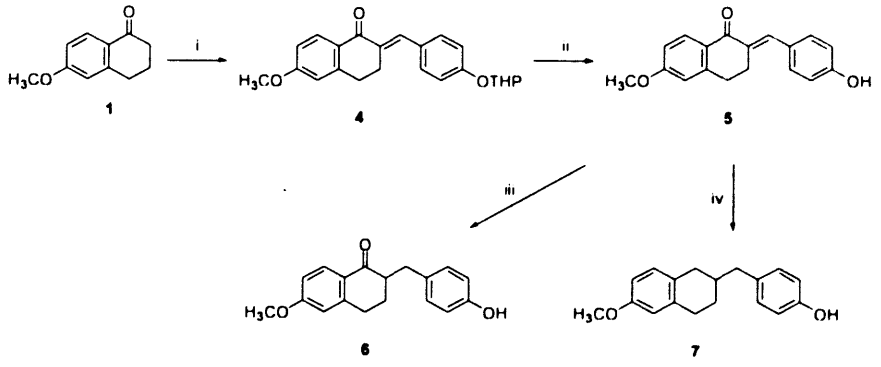

Scheme 2. Reagents and conditions: (i) THPO–C_6H_4CHO, 4% KOH/EtOH, rt, 12 h; (ii) 2 M HCl (aq), EtOAc/2-butanone (1:1 v/v), reflux, 1 h; (iii) 10% Pd/C, H_2, MeOH, rt, 1 h; (iv) 10% Pd/C, H_2, MeOH, rt, 2 h.

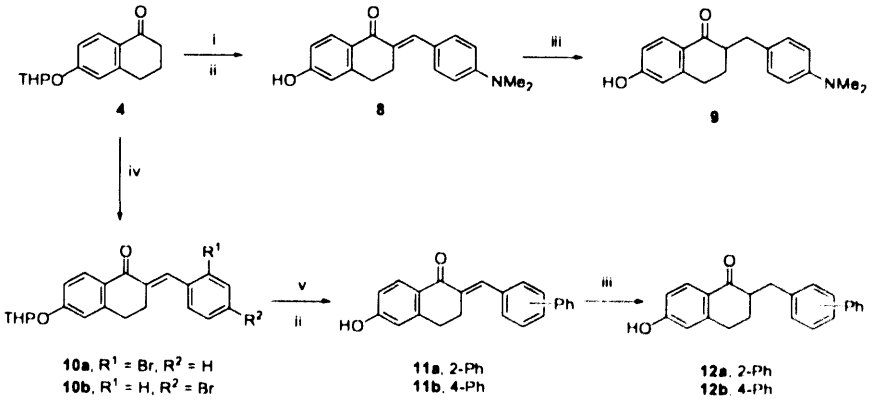

Scheme 3. Reagents and conditions: (i) Me_2N–C_6H_4CHO, 4% KOH/EtOH, rt, 72 h; (ii) 2 M HCl (aq), EtOAc/2-butanone (1:1 v/v), reflux, 1 h; (iii) 10% Pd/C, H_2, MeOH, rt, 1 h; (iv) Br–C_6H_4CHO, 4% KOH/EtOH, rt, 1–4 h; (v) phenylboronic acid, $Pd(PPh_3)_4$, toluene, 100 °C, 5 h

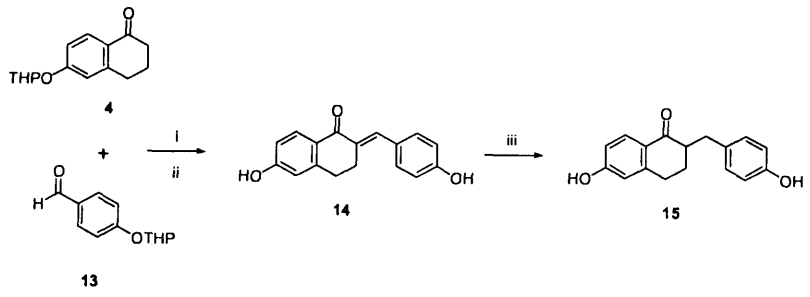

Scheme 4. Reagents and conditions: (i) 4% KOH/EtOH, rt, 1 h; (ii) 2 M HCl (aq), EtOAc/2-butanone (1:1 v/v), reflux, 1 h; (iii)10% Pd/C, H_2, MeOH, rt, 1 h.

procedure previously described for CYP26,[15] using [26,27-methyl-^{3}H]-25-hydroxyvitamin D_3 (from a stock mixture containing 100 μL of [26,27-methyl-^{3}H]-25-hydroxyvitamin D_3 and 1 mL of unlabelled 25-hydroxyvitamin D_3 (25 μM), with a total of 5 μCi of radioactivity in the 1 mL of stock mixture), NADPH, inhibitor (varying concentrations using acetonitrile as solvent) and phosphate buffer (pH 7.4). After incubation in a shaking water bath for 30 min at 37 °C, the vitamin D metabolites were obtained by extraction with ethyl acetate. After evaporation of the organic solvent, the residue was analysed by a HPLC system connected to a β-RAM online scintillation detector, connected to a Compaq PC running Laura data acquisition and analysis software (Lab-Logic Ltd). The separated [^{3}H]-metabolites were quantitatively calculated from the areas under the curves. Using a control with acetonitrile instead of inhibitor, these results were expressed as 'percentage inhibition relative to control' = 100[metabolites (control)−metabolites (inhibitor)/(metabolites control)]%. Ketoconazole was used as a standard for comparison (Table 1).

The benzylidene derivatives were all poor inhibitors of CYP24, perhaps indicating the requirement for flexibility at the C2 position for optimal structure conformation with respect to interaction at the enzyme active site. In the 2-benzyltetralone series, introduction of an alkyl or aryl substituent at the 2-benzyl position, for example, 2-(2-methylbenzyl)- and 2-(2-biphenyl)-derivatives **3b** and **12a** (IC_{50} 0.9 and 2.1 μM, respectively), resulted in good activity, whereas introduction of an aryl substituent at the 4-benzyl position, for example, 2-(4-biphenyl)-derivative **12b** (IC_{50} >20 μM) substantially reduced activity. Introduction of a hydroxyl group at the 4-benzyl position was tolerated, for example **6** and **7** (IC_{50} 3.5 and 2.6 μM, respectively), however introduction of a more bulky moiety, for example, *N*,*N*-dimethyl in compound **9** (IC_{50} 18 μM) was not tolerated. These preliminary results suggest that the compounds may be orientated in the active site with a hydrophobic region or large pocket above the 2-position of the benzyl ring, and a small pocket containing an amino-acid residue capable of forming a hydrogen bond at the 4-benzyl position.

There would appear to be a slight preference for a 6-methoxy rather than a 6-hydroxy substitutent in the naphthalene ring (cf. **6** and **15**, IC_{50} 3.5 and 8.9 μM, respectively). However, no significant difference in inhibitory activity was noted for the tetralone and 1,2,3,4-tetrahydro-naphthalene structures (cf. **6** and **7**, IC_{50} 3.5 and 2.6 μM, respectively). Compared with ketoconazole, potent inhibitory activity was observed for the 2-(2-methylbenzyl)tetralone derivatives **3b**, which may

Table 1. IC_{50} data for the novel benzylidene and benzyl tetralone derivatives

Benzylidene tetralones

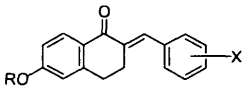

Benzyl tetralones

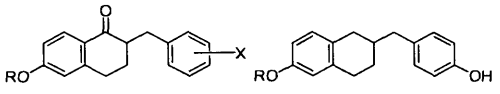

Compound	IC_{50} (μM)	Compound	IC_{50} (μM)
2a	>100	**3a**	4.5
2b	>20	**3b**	0.9
2c	>100	**6**	3.5
2d	100	**7**	2.6
5	>20	**9**	18
8	>100	**12a**	2.1
11a	>100	**12b**	>20
11b	>100	**15**	8.9
14	>20	Ketoconazole	20

IC_{50} values are the mean of two experiments.

be a useful lead compound for further development of potent CYP24 inhibitors.

Acknowledgements

Miss Sook Wah Yee would like to acknowledge the ORS Awards Scheme for a United Kingdom Scholarship.

References and notes

1. Greenlee, R. T.; Murray, T.; Bolden, S.; Wingo, P. A. *CA-Cancer J. Clin.* **2000**, *50*, 7–33.
2. Jarman, M.; Smith, H. J.; Nicholls, P. J.; Simons, C. *Nat. Prod. Rev.* **1998**, *15*, 495–512.
3. Smith, H. J.; Nicholls, P. J.; Simons, C.; LeLain, R. *Exp. Opin. Ther. Pat.* **2001**, *11*, 789–824.
4. Isaacs, J. T. *Urol. Clin. N. Am.* **1999**, *26*, 263–273.
5. Zhao, X.-Y.; Feldman, D. *Steroids* **2001**, *66*, 293–300.
6. Bikle, D. D. *Endocrine Rev.* **1992**, *13*, 765–784.
7. Baran, D. T. Nongenomic Rapid Effects of Vitamin D. In *Vitamin D: Molecular Biology, Physiology, and Clinical Applications*; Horlick, M. F., Ed.; Humana: Totowa, NJ, 1999; pp 195–205.
8. Jones, G.; Strugnell, A. S.; DeLuca, H. F. *Physiol. Rev.* **1998**, *78*, 1193–1231.
9. Zhao, J.; Tan, B. K.; Marcelis, S.; Verstuyf, A.; Bouillon, R. *J. Steroid Biochem.* **1996**, *57*, 197–202.
10. Reinhardt, T. A.; Horst, R. L. *Arch. Biochem. Biophys.* **1989**, *272*, 459–465.
11. Schuster, I.; Egger, H.; Bikle, D.; Herzig, G.; Reddy, G. S.; Stuetz, A.; Stuetz, P.; Vorisek, G. *Steroids* **2001**, *66*, 409–422.
12. Kirby, A. J.; LeLain, R.; Mason, P.; Maharbouie, F.; Nicholls, P. J.; Smith, H. J.; Simons, C. *J. Enzym. Inhib. Med. Chem.* **2003**, *18*, 27–33.
13. Rapson, W. S.; Shuttleworth, R. G. *J. Chem. Soc.* **1940**, 636–641.
14. Weskamp, T.; Bohm, V. P. W.; Herrmann, W. A. *J. Organomet. Chem.* **1999**, *585*, 348–352.
15. Kirby, A. J.; LeLain, R.; Mason, P.; Maharbouie, F.; Nicholls, P. J.; Smith, H. J.; Simons, C. *J. Enzym. Inhib. Med. Chem.* **2002**, *17*, 321–327.